

Smart Innovation, Systems and Technologies 200

Steffen G. Scholz  
Robert J. Howlett  
Rossi Setchi *Editors*



# Sustainable Design and Manufacturing 2020

Proceedings of the 7th International  
Conference on Sustainable Design and  
Manufacturing (KES-SDM 2020)



 Springer

# **Smart Innovation, Systems and Technologies**

Volume 200

## **Series Editors**

Robert J. Howlett, Bournemouth University and KES International,  
Shoreham-by-sea, UK

Lakhmi C. Jain, Faculty of Engineering and Information Technology,  
Centre for Artificial Intelligence, University of Technology Sydney,  
Sydney, NSW, Australia

The Smart Innovation, Systems and Technologies book series encompasses the topics of knowledge, intelligence, innovation and sustainability. The aim of the series is to make available a platform for the publication of books on all aspects of single and multi-disciplinary research on these themes in order to make the latest results available in a readily-accessible form. Volumes on interdisciplinary research combining two or more of these areas is particularly sought.

The series covers systems and paradigms that employ knowledge and intelligence in a broad sense. Its scope is systems having embedded knowledge and intelligence, which may be applied to the solution of world problems in industry, the environment and the community. It also focusses on the knowledge-transfer methodologies and innovation strategies employed to make this happen effectively. The combination of intelligent systems tools and a broad range of applications introduces a need for a synergy of disciplines from science, technology, business and the humanities. The series will include conference proceedings, edited collections, monographs, handbooks, reference books, and other relevant types of book in areas of science and technology where smart systems and technologies can offer innovative solutions.

High quality content is an essential feature for all book proposals accepted for the series. It is expected that editors of all accepted volumes will ensure that contributions are subjected to an appropriate level of reviewing process and adhere to KES quality principles.

**\*\* Indexing: The books of this series are submitted to ISI Proceedings, EI-Compendex, SCOPUS, Google Scholar and Springerlink \*\***

More information about this series at <http://www.springer.com/series/8767>

Steffen G. Scholz · Robert J. Howlett ·  
Rossi Setchi  
Editors

# Sustainable Design and Manufacturing 2020

Proceedings of the 7th International  
Conference on Sustainable Design  
and Manufacturing (KES-SDM 2020)

 Springer

*Editors*

Steffen G. Scholz  
Karlsruhe Institute of Technology  
Karlsruhe, Germany

Rossi Setchi  
Cardiff University  
Cardiff, UK

Robert J. Howlett  
Bournemouth University  
Poole, UK

KES International Research  
Shoreham-by-sea, UK

ISSN 2190-3018

ISSN 2190-3026 (electronic)

Smart Innovation, Systems and Technologies

ISBN 978-981-15-8130-4

ISBN 978-981-15-8131-1 (eBook)

<https://doi.org/10.1007/978-981-15-8131-1>

© The Editor(s) (if applicable) and The Author(s), under exclusive license to Springer Nature Singapore Pte Ltd. 2021, corrected publication 2021

This work is subject to copyright. All rights are solely and exclusively licensed by the Publisher, whether the whole or part of the material is concerned, specifically the rights of translation, reprinting, reuse of illustrations, recitation, broadcasting, reproduction on microfilms or in any other physical way, and transmission or information storage and retrieval, electronic adaptation, computer software, or by similar or dissimilar methodology now known or hereafter developed.

The use of general descriptive names, registered names, trademarks, service marks, etc. in this publication does not imply, even in the absence of a specific statement, that such names are exempt from the relevant protective laws and regulations and therefore free for general use.

The publisher, the authors and the editors are safe to assume that the advice and information in this book are believed to be true and accurate at the date of publication. Neither the publisher nor the authors or the editors give a warranty, expressed or implied, with respect to the material contained herein or for any errors or omissions that may have been made. The publisher remains neutral with regard to jurisdictional claims in published maps and institutional affiliations.

This Springer imprint is published by the registered company Springer Nature Singapore Pte Ltd. The registered company address is: 152 Beach Road, #21-01/04 Gateway East, Singapore 189721, Singapore

# International Programme Committee

Prof. Emmanuel Adamides, University of Patras, Greece  
Dr Y.W.R. Amarasinghe, University of Moratuwa, Sri Lanka  
Dr. Anna Aminoff, Hanken School of Economics, Finland  
Prof. Peter Ball, University of York, UK  
Prof. Nadia Bhuiyan, Concordia University, Canada  
Dr. Jeremy Bonvoisin, University of Bath, UK  
Dr. Yuri Borgianni, Free University of Bozen-Bolzano, Italy  
Dr. Marco Bortolini, University of Bologna, Italy  
Prof. Leszek Borzowski, Wrocław University of Technology, Poland  
Dr. Lucia Botti, University of Modena and Reggio Emilia, Italy  
Prof. Kai Cheng, Brunel University, UK  
Dr. Wai Ming Cheung, Northumbria University, UK  
Dr. James Colwill, Loughborough University, UK  
Dr. John Cosgrove, Limerick Institute of Technology, Ireland  
Prof. Michele Dassisti, University of Bari, Italy  
Assoc. Prof. Dzung Dao, Griffith University, Australia  
Prof. Samir Dani, University of Huddersfield, UK  
Dr. Agnieszka Deja, Maritime University of Szczecin, Poland  
Assist. Prof. Mia Delic, University of Zagreb, Croatia  
Dr. Ahmed Elkaseer, Karlsruhe Institute of Technology (KIT), Germany  
Prof. Waguih ElMaraghy, University of Windsor, UK  
Dr. Daniel Eyers, Cardiff University, UK  
Prof. Anna Maria Ferrari, University of Modena and Reggio, Italy  
Prof. Andrew Fleming, Newcastle University, Australia  
Dr. Francesco Gabriele Galizia, University of Bologna, Italy  
Prof. Loris Giorgini, University of Bologna, Italy  
Prof. Quanquan Han, Shandong University, China  
Prof. Chris Hinde, Loughborough University, UK  
Dr. Maria Holgado, University of Sussex, UK  
Prof. Takamichi Hosoda, Aoyama Gakuin University, Japan  
Prof. Haihong Huang, Hefei University of Technology, China

Prof. Steve Gill, Cardiff Metropolitan University, UK  
Assist. Prof. Giuseppe Ingarao, University of Palermo, Italy  
Dr. Alessio Ishizaka, NEOMA Business School, France  
Dr. Jian Jin, Beijing Normal University, China  
Prof. Dr.-Ing. Stefan Junk, University of Applied Sciences Offenburg, Germany  
Prof. Dr. ONG Soh Khim, National University of Singapore, Singapore  
Dr. Edwin Koh, National University of Singapore, Singapore  
Prof. Kari Koskinen, Tampere University, Finland  
Prof. Tomasz Krolkowski, Koszalin University of Technology, Poland  
Dr. Chi Hieu Le, University of Greenwich, UK  
Prof. Jacquetta Lee, University of Surrey, UK  
Prof. Fiona Lettice, University of East Anglia, UK  
Dr. Soon Chong Johnson Lim, UTHM, Malaysia  
Prof. Zakaria Maamar, Zayed University, UAE  
Prof. Jillian MacBryde, University of Strathclyde, UK  
Prof. Alison McKay, University of Leeds, UK  
Dr. Esmiralda Moradian, Stockholm University, Sweden  
Dr. Piotr Nikonczuk, West Pomeranian University of Technology, Poland  
Dr. Mohamed Osmani, Loughborough University, UK  
Dr. Michael Packianather, Cardiff University, UK  
Dr. Emanuele Pagone, Cranfield University, UK  
Prof. Paulo Pecas, Instituto Superior Técnico, Universidade de Lisboa, Portugal  
Prof. Stefan Pickl, University der Bundeswehr Munchen, Germany  
Assist. Prof. Paolo C. Priarone, Politecnico di Torino, Italy  
Mr. Paul Prickett, Cardiff University, UK  
Prof. Hefin Rowlands, University of South Wales, UK  
Prof. Davide Russo, University of Bergamo, Italy  
Dr. Konstantinos Salonitis, Cranfield University, UK  
Dr. Steffen G. Scholz, Karlsruhe Institute of Technology (KIT), Germany  
Prof. Rossi Setchi, Cardiff University, UK  
Prof. Luca Settineri, Politecnico di Torino, Italy  
Dr. Cristian Spreafico, University of Bergamo, Italy  
Prof. Qian Tang, Chongqing University, China  
Dr. Yuchun Xu, Aston University, UK  
Prof. Hua Zhang, Wuhan University of Science and Technology, China  
Assoc. Prof. Zhinan Zhang, Shanghai Jiao Tong University, China  
Prof. Gang Zhao, Wuhan University of Science and Technology, China

# Preface

Given the rate of expansion of recent advanced design and manufacturing technologies, there exists a real need for parallel sustainability development for these technologies. Especially, these hi-tech technologies are considered to be key enablers for the modern industry with the ability to revolutionize manufacturing with new processes, materials and applications. Their growth is driven by and plays a significant part in driving the enthusiastic demand for a more sustainable and competitive economy. However, enhancing the business atmosphere in the three dimensions of sustainability (social, environmental and economic) will enable to unleash the full potential of these technologies. In this context, the SDM-20 provided excellent opportunities for the presentation of interesting new research results and discussion about the thematic topic “sustainable design and manufacturing”, leading to knowledge exchange and the generation of new ideas.

KES International and I would like to welcome you to this volume, which forms the proceedings of the 7th KES International Conference on Sustainable Design and Manufacturing (SDM-20), organized by KES International as an online conference between 9 and 11 of September 2020. The conference was originally planned to take place in Split, Croatia. However, due to the Covid-19 crisis, and with the idea of keeping our attendees safe, the decision to conduct a virtual conference was taken. Hopefully next year, we will see each other once again for SDM-21.

SDM conferences have always attracted excellent contributions, for which we are grateful and we are also pleased to see so many new contributors to SDM-20 even though it was only a virtual conference. We welcome you all and hope that you can be part of the growing body of academics pursuing sustainability research and would like to contribute to the organization of future conferences. We hope that the format still allowed the building of new relationships that further promote future academic and professional collaborations.

This virtual conference nevertheless proved an excellent stage for the presentation of the state-of-the-art research and for conducting deep scientific discussions about the latest progresses being made regarding the theory and applications of sustainability in design and manufacturing, contributing to greater knowledge sharing and ideation of new innovative solutions for our problems of today. The



topics included both the aspect of sustainability in design and the development of sustainable products and processes through advanced manufacturing. The fields of applications included progress being made in all steps of a product lifecycle, including right from product ideation, design, the complete process chain, as well as modelling, simulations and end of life assessment; therefore, a holistic approach to sustainable production is being made.

This conference builds on the successes of the previous six conferences held so far led by Cardiff University, Wales, UK (2014); University of Seville, Spain (2015); University of Crete, Greece (2016); University of Bologna, Italy (2017); Griffith University, Gold Coast, Australia (2018); and the University of York, York, UK, and held in Budapest, Hungary (2019).

Once again, the conference was comprised of a general tracks chaired by leading experts in the fields of sustainable design, innovation and services; sustainable manufacturing processes and technology; sustainable manufacturing systems and enterprises and decision support for sustainability. The topic of sustainability is one of the most dynamic fields of research and that is reflected by the diverse nature of technical- and management-related papers presented at SDM 20. The trend shows that combining both these aspects shows great promise for the future development of sustainable design and manufacturing.

We also thank our Programme Committee members, chairs of general tracks and our special invited sessions, authors and reviewers for their unwavering commitment to ensure the quality of the work submitted, revised and accepted to SDM-20 was of the high standard required by Springer Nature proceedings.

Karlsruhe, Germany  
Shoreham-by-sea, UK  
Cardiff, UK

Prof. Dr. Steffen G. Scholz  
Prof. Robert J. Howlett  
Prof. Rossi Setchi  
SDM-20 Conference Chairs

# Contents

<b>Bringing Success and Value in Sustainable Product Development: The Eco-design Guidelines</b> . . . . .	1
Lorenzo Maccioni and Yuri Borgianni	
<b>The Identification and Selection of Good Quality Data Using Pedigree Matrix</b> . . . . .	13
Xiaobo Chen and Jacquetta Lee	
<b>Understanding Customer Preference: Outline of a New Approach to Prioritise Sustainability Product Information</b> . . . . .	27
Sze Yin Kwok, Sophie I. Hallstedt, and Veselka Boeva	
<b>Sustainable Supply Chain Management in Fast-Moving Consumer Goods Organizations</b> . . . . .	41
Yang Chen and Luisa Huaccho Huatuco	
<b>Test Stand for Metamaterials Dynamic Properties Examination</b> . . . . .	53
Knitter Remigiusz, Blazejewski Andrzej, Krolikowski Tomasz, Zmuda Trzebiatowski Piotr, and Zuchniewicz Jerzy	
<b>An Association Rule-Based Approach for Storing Items in an AS/RS</b> . . . . .	61
Sara Antomarioni, Maurizio Bevilacqua, and Filippo Emanuele Ciarapica	
<b>Infrastructure Sharing Model as a Support for Sustainable Manufacturing</b> . . . . .	71
Joanna Helman, Maria Rosienkiewicz, Mateusz Molasy, and Mariusz Cholewa	
<b>A Correlation Study Between Weather Conditions and the Control Strategy of a Solar Water Heating System</b> . . . . .	81
Znaczkowski Paweł, Kamiński Kazimierz, and Zuchniewicz Jerzy	

<b>Industry 4.0—Supporting Industry in Design Solutions—All-in-One Computer Cover</b> .....	93
Krolkowski Tomasz, Knitter Remigiusz, Blazejewski Andrzej, Zmuda Trzebiatowski Piotr, Zuchniewicz Jerzy, and Bak Aleksander	
<b>Development of a Robotic System with Stand-Alone Monocular Vision System for Eco-friendly Defect Detection in Oil Transportation Pipelines</b> .....	107
Amith Mudugamuwa, Chathura Jayasundara, Han Baokun, and Ranjith Amarasinghe	
<b>Analysis and Assessment of Bottom-Up Models Developed in Central Europe for Enhancing Open Innovation and Technology Transfer in Advanced Manufacturing</b> .....	119
Maria Rosienkiewicz, Joanna Helman, Mariusz Cholewa, Mateusz Molasy, and Grit Krause-Juettler	
<b>A Simplified TRIZ Approach Involving Technology Transfer for Reducing Product Energy Consumption</b> .....	129
Davide Russo, Christian Spreafico, and Matteo Spreafico	
<b>Calculating Domestic Environmental Impacts: Challenging and Solutions for an Interactive Configurator</b> .....	139
Christian Spreafico and Davide Russo	
<b>Additive Manufacturing of Continuous Carbon Fiber-Reinforced Plastic Components</b> .....	149
Stefan Junk, Manuel Dorner, and Claus Fleig	
<b>Scalability Analysis in Industry 4.0 Manufacturing</b> .....	161
Riccardo Accorsi, Marco Bortolini, Francesco Gabriele Galizia, Francesco Gualano, and Marcella Olini	
<b>An Investigation of the Porosity Effects on the Mechanical Properties and the Failure Modes of Ti-6Al-4V Schwarz Primitive Structures</b> ...	173
Shuai Ma, Qian Tang, Qixiang Feng, Jun Song, Ying Liu, and Rossitza Setchi	
<b>Including Ergonomic Principles in the Design and Management of Reconfigurable Manufacturing Systems</b> .....	183
Marco Bortolini, Lucia Botti, Emilio Ferrari, Francesco Gabriele Galizia, and Cristina Mora	
<b>Non-conventional Warehouses: Comparison of the Handling Performances</b> .....	193
Marco Bortolini, Francesco Gabriele Galizia, Mauro Gamberi, Francesco Gualano, and Ludovica Diletta Naldi	

**Saving Lives and Saving the Planet: The Readiness of Ireland’s Healthcare Manufacturing Sector for the Circular Economy** . . . . . 205  
 Carla Gaberščik, Sinéad Mitchell, and Audrey Fayne

**Effect of Milling Speed and Time on Graphene-Reinforced AA2024 Powder** . . . . . 215  
 Mulla Pekok, Rossitza Setchi, Michael Ryan, and Quanquan Han

**Mechanical Behavior of NiTi-Based Circular Tube Chiral Structure Manufactured by Selective Laser Melting** . . . . . 227  
 Chenglong Ma, Dongdong Gu, Jie Gao, Wei Chen, Yingjie Song, and Rossitza Setchi

**Energy Utilization Analysis and Optimization of Corrective Insoles Manufactured by 3D Printing** . . . . . 239  
 M. J. Kirby, Rachel Johnson, A. Rees, and C. A. Griffiths

**Effect of Remelting Process on Surface Quality and Tensile Behaviour of a Maraging Steel Manufactured by Selective Laser Melting** . . . . . 251  
 Jun Song, Qian Tang, Qixiang Feng, Shuai Ma, Quanquan Han, and Rossitza Setchi

**Event-Driven Knowledge Engineering as Enabling Technology Towards Configuration of Assistance Systems in Industrial Assembly** . . . . . 261  
 Matthias Plasch, Sharath Chandra Akkaladevi, Michael Hofmann, Christian Wögerer, and Andreas Pichler

**Computational Validation of Injection Molding Tooling by Additive Layer Manufacture to Produce EPDM Exterior Automotive Seals** . . . . . 273  
 I. Evans, A. Rees, C. A. Griffiths, and Rachel Johnson

**Impact of Nonplanar 3D Printing on Surface Roughness and Build Time in Fused Filament Fabrication** . . . . . 285  
 Ahmed Elkaseer, Tobias Müller, Dominik Rabsch, and Steffen G. Scholz

**In-Process Digital Monitoring of Additive Manufacturing: Proposed Machine Learning Approach and Potential Implications on Sustainability** . . . . . 297  
 Amal Charles, Mahmoud Salem, Mandaná Moshiri, Ahmed Elkaseer, and Steffen G. Scholz

**Stakeholder-Driven Conceptualization of Open Innovation Approaches in the SYNERGY Project** . . . . . 307  
 Janin Fauth, Clarissa Marquardt, Giulia Di Bari, Nicola Raule, Johanna Lisa Ronco, and Steffen G. Scholz

<b>An Empirical Study of Visual Comfort in Office Buildings</b> . . . . .	319
Isilay Tekce, Deniz Artan, and Esin Ergen	
<b>Heterogeneous Dual-Frequency IoT Network for Vital Data Acquisition</b> . . . . .	333
Mahmoud Salem, Islam El-Maddah, Khaled Youssef, Ahmed Elkaseer, Steffen Scholz, and Hoda Mohamed	
<b>Sustainability Assessment of Rapid Sand Mould Making Using Multi-criteria Decision-Making Mapping</b> . . . . .	345
Emanuele Pagone, Prateek Saxena, Michail Papanikolaou, Konstantinos Salonitis, and Mark Jolly	
<b>NeoPalea: Compostable Composite Material for Packaging Applications</b> . . . . .	357
Leonardo Conti, Federico Rotini, Matteo Barbari, Marco Togni, and Giuseppe Rossi	
<b>Using FFF and Topology Optimisation to Increase Crushing Strength in Equestrian Helmets</b> . . . . .	369
Shwe Soe, Michael Robinson, Khaled Giasin, Rhosslyn Adams, Tony Palkowski, and Peter Theobald	
<b>Polish Public Transport Fire Safety Study</b> . . . . .	379
R. Dobrzyńska	
<b>The Effect of Heat Treatment of AlSi<sub>10</sub>Mg on the Energy Absorption Performance of Surface-Based Structures</b> . . . . .	395
Michael Robinson, Quanquan Han, Heng Gu, Shwe Soe, and Rossitza Setchi	
<b>Blockchain-Enabled ESG Reporting Framework for Sustainable Supply Chain</b> . . . . .	403
Xinlai Liu, Haoye Wu, Wei Wu, Yelin Fu, and George Q. Huang	
<b>Low-Sulphur Marine Fuels—Panacea or a New Threat?</b> . . . . .	415
Agnieszka Ubowska and Renata Dobrzyńska	
<b>Effect of Build Bed Location on Density and Corrosion Properties of Additively Manufactured 17-4PH Stainless Steel</b> . . . . .	425
Rachel Johnson, I. S. Grech, N. Wint, and N. P. Lavery	
<b>Control Systems Architecture with a Predictive Identification Model in Digital Ecosystems</b> . . . . .	439
Alexander Suleykin and Natalya Bakhtadze	
<b>Research on the Green Evaluation System of Manufacturing Process</b> . . . . .	451
Pengcheng Yan, Gang Zhao, Na Zhang, Xin Huang, Xiaolong Luo, and Shujun Yu	

**A Life Cycle Comprehensive Cost-Based Method for Active Remanufacturing Time Prediction** . . . . . 463  
 Xin Yao, Hua Zhang, Wei Yan, and Zhigang Jiang

**Analysis of Coal Gas Resource Utilization and Energy Flow View Model in Iron and Steel Enterprises** . . . . . 475  
 Xiao Li, Gang Zhao, Qi Zhou, Pengcheng Yan, Xiong Liu, and Shujun Yu

**Lightweight Design of Valve Body Structure Based on Numerical Simulation** . . . . . 485  
 Qi Zhou, Gang Zhao, Xin Huang, Na Zhang, and Xiaolong Luo

**Research on Quantitative Evaluation of Green Property of Iron and Steel Enterprises Based on BP Neural Network** . . . . . 497  
 Junsong Xiao, Gang Zhao, and Pengcheng Yan

**Research on Green Design of Valve Products Based on Response Surface Method** . . . . . 509  
 Xiong Liu, Gang Zhao, Xiao-long Luo, Na Zhang, and Xin Huang

**Integrated Electronic Systems for Acquisition of Customers for Transport and Logistics Services** . . . . . 521  
 A. Wiktorowska-Jasik, L. Filina-Dawidowicz, A. Cernova-Bickova, D. Możdrzeń, and D. Bickovs

**Mechanical Performance of Polylactic Acid from Sustainable Screw-Based 3D Printing** . . . . . 531  
 Paolo Minetola, Luca Fontana, Rossella Arrigo, Giulio Malucelli, and Luca Iuliano

**Organization and Implementation of Intermodal Transport of Perishable Goods: Contemporary Problems of Forwarders** . . . . . 543  
 L. Filina-Dawidowicz and S. Stankiewicz

**Analysis of Electric Power Consumption by the Heat Pump Used in the Spray Booth** . . . . . 555  
 Piotr Nikończuk and Wojciech Tuchowski

**Correction to: Using FFF and Topology Optimisation to Increase Crushing Strength in Equestrian Helmets** . . . . . C1  
 Shwe Soe, Michael Robinson, Khaled Giasin, Rhosslyn Adams, Tony Palkowski, and Peter Theobald

**Author Index** . . . . . 563

## About the Editors

**Dr. Steffen G. Scholz** is Head of the research team ‘Process optimization, Information management and Applications,’ part of the Institute for Automation and Applied Informatics (IAI), Karlsruhe Institute of Technology. Prof. Scholz is a Honorary Professor at Swansea University, UK and an Adjunct Professor at the Vellore Institute of Technology, India. He is also the Principal Investigator in the Helmholtz funded long-term programs ‘Digital System Integration’ and ‘Printed Materials and Systems.’ He has more than 20 years of experience in the field of system integration and automation, sustainable flexible production, polymer micro- & nano-replication, process optimization and control, with a recent emphasis on additive manufacturing and Industry 4.0 applications. In addition to pursuing and leading research, he has been very active with knowledge transfer to industry. He has been involved in over 30 national and international projects, and he won in excess of 20M EUR research grants, in which he has acted as Coordinator and/or Principal Investigator. Dr. Scholz’s academic output includes more than 150 technical papers and 5 books.

**Robert J. Howlett** is the Executive Chair of KES International, a non-profit organization that facilitates knowledge transfer and the dissemination of research results in areas including intelligent systems, sustainability and knowledge transfer. He is a Visiting Professor at Bournemouth University in the UK. His technical expertise is in the use of intelligent systems to solve industrial problems. He has been successful in applying artificial intelligence, machine learning and related technologies to sustainability and renewable energy systems; condition monitoring, diagnostic tools and systems; and automotive electronics and engine management systems. His current research work is focussed on the use of smart microgrids to achieve reduced energy costs and lower carbon emissions in areas such as housing and protected horticulture.

**Rossi Setchi** is a Professor in High-Value Manufacturing, Deputy Head of School and a Director of Research at the School of Engineering of Cardiff University. She has a distinguished track record of research in a range of areas including AI,

robotics, systems engineering, manufacturing, industrial sustainability, cyber-physical systems and Industry 4.0 and, in particular, has built an international reputation for excellence in knowledge-based systems, computational semantics and human-machine systems. She has published over 220 peer-reviewed papers. She is a Fellow of the Institution of Mechanical Engineers, Fellow of the Institution of Engineering and Technology, Fellow of the British Computer Society and a senior member of IEEE. She is an Associate Editor of the International Journal of Systems Science and IEEE Access and a member of the Editorial Board of a number of international journals.



# Bringing Success and Value in Sustainable Product Development: The Eco-design Guidelines



Lorenzo Maccioni  and Yuri Borgianni 

**Abstract** The relationships between the creation of value for both the environment and consumers have been insightfully investigated by the authors in previous studies. The results achieved in these studies have allowed the authors to deduce some design recommendations and represent the basis for further analyses of the perception of eco-designed products through quantitative data. In this paper, a sample of indications intended to support designers in developing sustainable and successful products was fine-tuned. These indications, embodied in eco-design guidelines, have been partially deducted from the evidence that emerged in previous works and partially inferred through a specific elaboration of data regarding the value perception of eco-design strategies. The guidelines have been evaluated by (eco-)design practitioners, whose evaluation shows the high perceived relevance of the guidelines.

## 1 Introduction

In order to support sustainable development, the implementation of eco-design cannot overlook its effect on products' value perception, appreciation and therefore market success and diffusion [1]. Indeed, a product that is not successful, even if it has a low environmental impact, does not contribute to solving the sociotechnical challenges required for sustainable development [2].

Actually, eco-design methods focus on reducing products' environmental impact only and tend to overlook the products' value perception [3]. This applies although it is acknowledged that fulfilling design requirements that differ from environmental ones is essential for developing good green products [4]. The focus of the authors' research is how to join the green and the success perspectives and to develop design

---

L. Maccioni (✉) · Y. Borgianni  
Free University of Bozen-Bolzano, 39100 Bolzano, Italy  
e-mail: [lorenzo.maccioni@unibz.it](mailto:lorenzo.maccioni@unibz.it)

Y. Borgianni  
e-mail: [yuri.borgianni@unibz.it](mailto:yuri.borgianni@unibz.it)

support tools. In the present paper, the authors capitalize on previous work, describe additional analyses and illustrate a first tentative design tool.

In particular, in previous studies, the authors investigated how the implementation of eco-design affects the consumer value perception (CVP) and consequently the products' success. The present paper gathers results and evidence emerged from these studies in order to transform the knowledge created through these explorative studies into a series of Eco-Design Guidelines (EDGs) (Sect. 3) that support eco-design in developing valuable and successful products. To do this, many insights and results can be directly translated into practical suggestions exploiting the results of the studies on success [5, 6] and on value perception [7]. However, while in many cases these contributions give rise directly to findings that are useful to address eco-design, in other cases, further data elaboration and discussion to achieve more applicable outcomes is needed (Sect. 2). Moreover, in order to get feedback from experts in (eco-)design, these EDGs have been evaluated through a Google form (Sect. 4). Results are presented and discussed in Sect. 5, which includes final remarks.

## 2 Combination of Prior Results to Extract Additional Evidence

The study carried out in [8] includes a database of products evaluated in terms of different dimensions of CVP. In that work, data were analyzed to investigate differences between green products and less environmentally friendly ones, and various insights into the competitive advantages (and disadvantages) can be found. However, no specific design suggestions emerged due to the level of specification used for characterizing sustainability endeavors (yes/no).

On the other hand, a study aimed at investigating the perceived implementation of eco-design strategies (EDSs) was carried out and presented in [9]. In that work, the same products leveraged in [8] were evaluated also in terms of perceived implementation of EDSs as defined in [4], i.e., Minimizing Material Consumption (MMC), Minimizing Energy Consumption (MEC), Minimizing Resources Toxicity and Harmfulness (MRTH), Optimizing Resources Renewability and Biocompatibility (ORRB), Product Lifespan Optimization (PLO), Extending the Lifespan of Materials (ELM) and Facilitating Disassembly (FD). Results show that the perceived implementation of EDSs (for each product) cannot be considered as a dummy variable (implemented or absent), but it should be considered differently.

In this way, it was possible to obtain (for the same products) the perceived level of implementation of the EDSs and their CVP. Subsequently, in order to investigate the relationship between the perceived implementation of EDSs (independent variable) and CVP (dependent variable), regressions were performed through the software R. More precisely, linear regressions were applied when the CVP was described by the 10 principal components (PCs) (see [8]) and logistic regressions were performed when the CVP was described by the questionnaire variables (QVs), i.e., the variables

captured through the questionnaire in [8]. Results, in terms of regressions coefficients, are shown in Table 1. The influence of the EDSs on PCs is shown in the upper part of the table, while the influence of the EDSs on the QVs is shown in its bottom part. For every relationship, the regression coefficient is reported if it has  $p$ -value  $< 0.05$  or it is reported with (.) if  $0.1 > p$ -value  $> 0.05$ ; it is omitted otherwise. The regression coefficient can be read as a metric of the specific EDS' power to positively (negatively) affect the dependent variable. The meaning of PCs and QVs is thoroughly explained in [8], but its general sense can be inferred through the name of the variables that characterize people's evaluations of and reactions to products, which have been shown to experiment participants by means of pictures.

**Considerations on the value perception of MMC** The positive relationship with IV (due to a positive perception of Novelty, Creativity and Advantages) means that products implementing MMC are usually perceived innovative and they stimulate the consumers' curiosity and information foraging. However, even if these products are considered inventive, they are not perceived interesting and a clear relationship with Preference and Quality has not emerged. Indeed, the negative relationship with

**Table 1** Regressions coefficients describing the effect of EDSs on PCs and QVs

Principal components	MMC	MEC	MRTH	ORRB	PLO	ELM	FD
Innovative value (IV)	0.45	-0.48	1.66	-0.42	0.38	-0.91	0.40
Consciously approaching the task (CAT)	0.31	-0.21.					
Voluntary wide exploration (VWE)		0.28					
Implicit task effort (ITE)							-0.17
Information foraging (IF)	0.75	-0.39			-0.44	-0.28	-0.16.
Curiosity and exploration (CE)	0.70	-0.29	-0.36	0.63	-0.36	-0.35	
Pupil dilation (PD)			0.34				
Ordinary value (OV)	-1.06	0.57	-0.49	-0.38	0.97	0.41	-0.72
Price overestimation (PO)		-0.24	0.43	-0.25	-0.52		
Level of arousal (LA)					0.20		
Questionnaire variables	MMC	MEC	MRTH	ORRB	PLO	ELM	FD
Absence_of_disadvantages					1.03		-0.57
Advantages	0.65	-0.71	2.85	-0.98	0.65	-1.47	0.42
Interest	-0.52				0.75		-0.66
Knowledge	-1.97	1.23		-0.91	1.84	0.76	-0.60
Novelty_Creativity	2.75	-1.97	3.09	0.44	-1.21	-2.00	1.96
Preference			1.84	-0.74	0.88	-0.66	0.32.
Quality		-0.75	2.51	-1.11	1.08	-1.13	
Willingness_to_Pay	0.39.	-0.51	2.02	-0.66	0.59	-1.30	0.46

OV (due to a negative interest and knowledge) means that consumers favor other kinds of products. Moreover, the positive relationship with CAT, IF and CE means that these products are perceived complex to understand and to evaluate.

**Considerations on the value perception of MEC** Products implementing MEC show positive relationships with OV (due to a positive relationship with Knowledge). This indicates that products implementing MEC are commonly used and experienced by consumers (even if they tend to underestimate costs). This explains the negative relationships with IF and CE (they already know the products, then long and accurate explorations are not necessary for evaluation purposes) and the negative relationship with IV (low perception of novelty and creativity). However, the positive relationship with Knowledge combined with the negative ones concerning Advantages and Quality lead to the conclusions that the products implementing MEC are usually inadequate for the consumers' expectations. This means that implementing MEC is necessary for everyday products, but the current products are overall deemed unsatisfactory.

**Considerations on the value perception of MRTH** In this case, it stands out that the ordinal regressions (carried out on the QVs) show only positive coefficients (when statistically significant). This means that products implementing MRTH are perceived highly innovative (positive relationship with IV, Novelty and Creativity, Advantages and Preferences). In addition, it is possible to assume that consumers are willing to buy products implementing MRTH since both Willingness to Pay and PO show positive relationships. Therefore, even if a negative relationship emerges when it comes to OV, it is possible to state that implementing MRTH overall leads to attractive (highlighted also by the positive relationship with PD) and acceptable solutions.

**Considerations on the value perception of ORRB** The only positive relationships emerged are with CE and Novelty, Creativity (even if with  $0.1 > p\_value > 0.05$ ). This means that products implementing ORRB are perceived original and stimulate curiosity. On the other hand, no IV nor OV is perceived. Therefore, consumers are unwilling to buy (negative relationship with Willingness to Pay and with PO) and unwilling to accept (negative relationship with Advantages, Preferences and Quality). Eventually, implementing ORRB leads to the worst value perception (compared with the other EDSs), limiting the chances of success of the product (compared with the less environmentally friendly ones).

**Considerations on the value perception of PLO** This is the only EDS that presents a positive relationship with both IV and OV. In addition, it is the only EDS showing a significant (and positive) relationship with LA. Therefore, implementing PLO leads to increased value perception in terms of Preferences, Quality, Interest, functional value (Advantages and Absence of disadvantages), economic value (Willingness to Pay) and emotional value (LA). This is also supported by the fact that there is a positive relationship with Knowledge. Eventually, even if implementing PLO leads to a bad perception of Novelty, Creativity, PO, CE and IF (the products do not

surprise consumers and do not stimulate their curiosity), it is possible to state that implementing PLO deserves a priority among the others EDSs since it could lead to satisfying products.

**Considerations on the value perception of ELM** It emerges that consumers declare the Knowledge of the products implementing this EDS (and it affects the positive relationship with OV). However, all the other relationships (if statistically significant) are negative. In particular, it can be noticed that products implementing ELM are not perceived Creative or new and they do not display Advantages or Quality characteristics. Therefore, implementing ELM often leads to inadequate solutions consumers are not willing to pay for.

**Considerations on the value perception of FD** In this case, implementing FD leads to perceive IV through creative solutions. These solutions are perceived as good compromises since there is a balance between Advantages (positive relationship) and Absence of disadvantages (negative relationship) with a positive Willingness to Pay. However, the negative Interest and Knowledge lead to a negative perception of OV.

### 3 Inferring the Eco-design Guidelines

In the present section, the EDGs have been elaborated based on both the interpretation of the outcomes of previous section and the results of the previous studies. As a deductive process took place, the emerged EDGs are preceded by and presented together with a brief motivation.

**Lifespan optimization, transition to Product Service System and circular economy are opportunities for value creation** The regressions performed in [5] underline that principles underpinning Product Service System (PSS) favor success. In addition, the results described in Sect. 2 highlight that implementing the EDS of PLO leads to innovative and acceptable solutions and that this strategy requires priority over others. Indeed, the product lifecycle scenario should be clear to designers in order to implement other strategies. Therefore, based on these observations (and other knowledge supporting the objectives), the following EDG have been formulated.

*In eco-design, prioritize the optimization of the product lifecycle. Indeed, the understanding of the product scenario clarifies the design process that follows and drives toward acceptable solutions. Before implementing any strategy, you should:*

- *Consider every possible scenario that contextualizes the solution in a Circular Economy or Product Service System context.*
- *Include functionalities in the same solution delivering additional value. To the scope, it is worth considering the functions of similar systems (TV broadcasts and*

*the Internet), surrounding systems (the computer and the monitor) and systems performing opposite functions (the pencil and the eraser).*

- *Evaluate different Fields and Behaviors (mechanical, electric, magnetic, etc.) through which the function(s) can be performed.*

**Product Reliability; it goes beyond product architecture** In [5], product reliability emerged as a success driver. By observing the most successful cases of the products implementing eco-design principles aimed at increasing the products' reliability, it is possible to notice that the increase in product reliability and/or the reduction of auxiliary components is not achieved with integral or modular architectures, but through a change of the physical functioning principle, e.g., iPod, Wi-Fi, touchscreen, electrical thermometer. Therefore, the EDG has been formulated as follows.

*Before trying to make a product more reliable through modular architectures (providing the possibility to replace components that will be damaged) or through integral architectures (reducing the number of components that can be damaged), explore different physical functioning principles.*

**Be radical inside and conservative outside** In [7], it is pointed out that implementing a "change of field" is perceived as a new and creative endeavor, but the advantages can be counterbalanced by disadvantages noticed in the solutions. In addition, a positive willingness to pay has emerged in contrast to preference, interest and perception of quality. It can be inferred that solutions changing field are perceived innovative but not sufficiently mature. Therefore, further efforts have to be made to reduce their real or perceived disadvantages. This can be done by keeping the fundamental (perceivable and valuable) characteristics of "old" products in the "new" ones.

*Solutions exploiting new behaviors, fields or working principles are always perceived innovative but not sufficiently mature to be adopted. Understand what (structural, aesthetic, perceptual) features characterize traditional products and reproduce/copy them in the new solutions in order to increase the perception of familiarity.*

**Consumer Empowerment; be repairable is not a competitive factor in a purchase situation** The effect of maintenance on success is discussed in [5]. Repairable products admit being damaged (it is a success moderator) while modifying products for maintenance comprises self-repairing products or products that do not require maintenance at all (it is a success catalyst). In addition, while during maintenance there is no change of ownership before and after the operation, this is not always ascribable to "repair." What can be inferred by these considerations is the following EDG.

*Develop self-repairing products or products that do not require maintenance at all. If the solution has to foresee repairing and/or maintaining during its life, introduce services that minimize the customer's involvement.*

**Packaging performs many functions that should not be underestimated** In [7], it is discussed that implementing “change of substance” leads to a negative perception of quality, a low level of interest and a negative preference. In addition, this is followed by a negative willingness to pay, by a perception of disadvantages and an unclear perception of advantages. Moreover, the low level of affordances was highlighted by the significant positive effect on ITE and the negative one on PD. This result suggests that products implementing change of substance may not be competitive with the baseline ones. However, these solutions could be successful in specific market sectors targeted to peculiar consumers [5]. Therefore, the following EDG has been developed.

*When you change the product’s substance (solid, liquid, gas) to reduce the environmental impact of its packaging or transportation, stress the reason beyond this kind of solution and try to promote new benefits from this radical change in order to capture specific market sectors.*

**Focal area packaging + transport; it is an essential part of the value chain** In [5], it emerged that the speed of delivery and the safety during transport/distribution are critical to success. Therefore, these competing factors cannot be compromised. The EDG is formulated as follows.

*Avoid solutions that jeopardize the speed of delivery of the product to the customer and the safety during transport/distribution. When possible, use and distribute local products or components.*

**Learn from competition; be disruptive in creating eco-value and/or boost other competing factors** According to Sect. 2, implementing MMC and MEC hardly leads to satisfactory and appreciable results. Therefore, marginal improvements in terms of material content or energy consumption cannot guarantee a competitive advantage (unless it is disruptive). This means that considering additional competing factors is essential to penetrate the market. To this respect, the following EDG has been formulated.

*Do not limit your product’s competitive advantage to a marginal improvement in terms of energy efficiency or material consumption.*

**Focal area chemical content; suppliers are enablers** Section 2 shows how implementing MRTH could lead to the perception of high innovativeness and appreciation. Therefore, implementing MRTH can be considered a powerful value driver and an opportunity to succeed.

*Evaluate the chance of reducing resources toxicity and harmfulness, especially if consumers consider the product’s material and behavior as such. In any case, avoid increasing toxicity and harmfulness, although these are counterbalanced by different lifecycle advantages.*

**Do not turn your eco-orientation into a threat for the consumer** As it is possible to notice in Sect. 2, implementing ORRB is highly risky in terms of value perception. In the eco-design thinking, there is a sort of implicit rule that associates the renewability and the biocompatibility to the value creation for the consumer. However, this does not apply regularly; indeed, very often, consumers tend to associate the increase of renewability or biocompatibility performances as an increase of cost they are not willing to pay for. The economic value is not expendable for the majority of consumers and eco-designers have to be aware of that, especially when renewability and biocompatibility are in play. Therefore, the following EDG was formulated.

*Do not neglect the quality–price ratio when you aim to resources’ renewability and biocompatibility.*

**The use phase is the main success driver** In [6], it is discussed that eco-design efforts involving the use phase of products, differently than all the other lifecycle stages, affects success chances positively. Sustainability-oriented changes in this stage might result straightforward to consumers; as opposed to lifecycle phases, they have more limited sensitivity toward and control over. Consequently, the easily recognized advantages can be seen as a source of value with positive repercussions on market success. Therefore, the following EDG has been formulated.

*Implement actions that improve (the perception of) environmental sustainability during the use phase irrespective of the most critical product lifecycle stage.*

## 4 Preliminary Verification of the Eco-design Guidelines

A preliminary verification of the EDGs was performed analyzing feedback gathered through a specific online questionnaire created through Google forms and shared on appropriate web platforms. The goal of the questionnaire was to get feedback (on the EDGs) by members of Design Society through its Web site, especially involving the Sustainable Design Special Interest Group through its LinkedIn page.

More specifically, the following introduction was added to the questionnaire, in order to explain the rationale behind the survey.

“A product re-designed following the classic eco-design EDGs will most likely present a lower environmental impact. However, if this will not replace less environmental friendly products, it will not contribute to sustainable development. Therefore, eco-design should not be applied without considering product’s perception, appreciation, adoption and ultimately success. Therefore, what is the relationship between sustainability-oriented endeavors and designs’ success, appreciation and perceived value?

An ongoing research by the authors has investigated this question and resulted in the deduction and formulation ten EDGs. Please read them and provide your expert evaluation through this link”.



The text was followed by the list of EDGs as described in the Sect. 3 (text in italics). Through the link, the respondents were invited to evaluate the following dimensions of the ten EDGs through 6-point Likert scale (0–5).

- Usefulness: to investigate the utility of the EDGs in supporting the (eco-)design process in achieving success and sustainability;
- Reasonability: to understand if the EDGs conflict with the current practice of (eco-)designer;
- Applicability in design practice: with the aim of understanding if the EDGs results too abstract or inappropriate;
- Originality: to figure out how different the EDGs are from the existing ones;
- Clarity: to verify the correct formulation;
- General-purpose: to check that the EDGs are not too specific or valid for certain industrial domains only;
- Relevant: to understand if the knowledge of these EDGs can provide benefits by bridging gaps that were not filled before.

Eventually, 14 questionnaires were filled in approximately two months.

Moreover, the EDGs were tested in an eco-ideation session by 28 master students attending the course “Development and operation of product/service-systems” (M.Sc. Engineering Design and Innovation) at Denmark Technical University. The EDGs were introduced to the students, and a case study was provided to apply them. After the eco-design session, they were asked to evaluate the EDGs through the same Google form and a fraction of them filled in the questionnaire. More precisely, it was possible to gather also the answers of 17 participants who had the opportunity to test the guidelines before evaluating them. Therefore, 31 evaluations were overall gathered, 14 from (eco-)design practitioners who based their evaluation on the perceptions of the EDGs and 17 (eco-)design practitioners who tested the EDGs concretely.

## 5 Results, Discussions and Outlook

Figure 1 shows the distribution of the answers among the seven dimensions investigated. Participants who tested the EDGs before evaluating them are shown in black. Participants that did not tested the EDGs before evaluating them are shown in gray.

The histograms overall shows positive results for all dimensions. In particular, all participants considered the EDGs relevant for the purpose explained in the introductory part of the survey and sufficiently general in scope. The originality of the EDGs results the most argued evaluation metric. This could mean that these EDGs were implicitly known (although sometimes not considered), but they had never been made explicit.

In order to highlight the differences in evaluations between the two groups of participants, ordered logistic regressions with the statistical software Stata were performed. Here, the questionnaire dimensions were used as dependent variables,

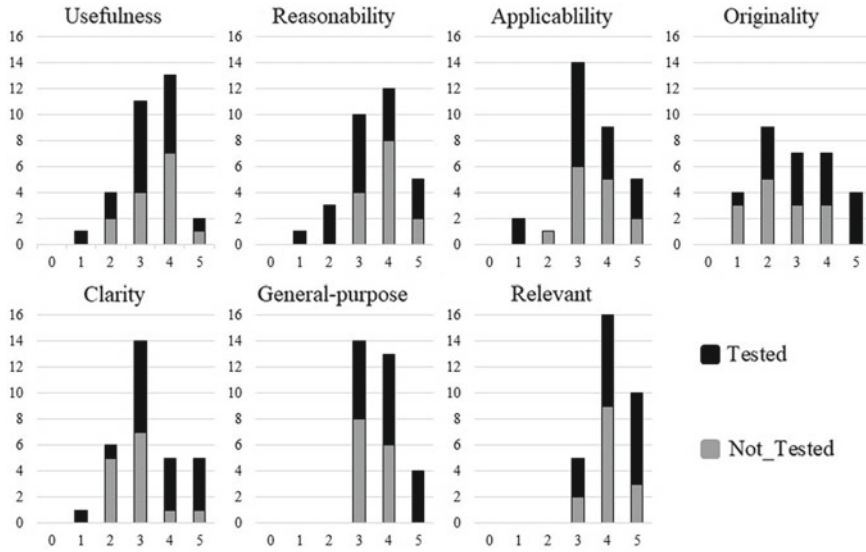


**Fig. 1** Distribution of the answers among dimensions investigated considering if the evaluation was made by a participant that tested the EDGs (black) or a participant did not test the EDGs (gray)

while the independent variable was the effective use of the EDGs by evaluators (dummy variable). Results shows that the participants who tested EDGs before evaluating them had a significant better perception of the EDGs in terms of their being more:

- Original (coefficient 1.31,  $p\_value$  0.047);
- Clear (coefficient 1.45,  $p\_value$  0.047);
- and General (coefficient 1.18,  $p\_value$  0.098).

Actually, to the best of the authors' knowledge, no similar indications for eco-designers are publicly available whose scope is to combine environmental safeguard and customer value. This aspect, beyond representing the original contribution of the paper, remarks the potential relevance of the EDGs. Their preliminary testing provided encouraging outcomes, which allow for a full validation of the EDGs without any need for revision. Future work includes the articulation of the EDGs in design processes, as they are attributed of different priority and they affect different design phases. Means to present them and organize them in a real-case eco-design process are currently under authors' investigation. To the scope, useful indications can be found in [10, 11].

Moreover, it is in author's expectations to present and propose the EDGs as a complement of and not as substitute for consolidated eco-design practices, as the latter would require changing designers' mindsets and a likely rejection of the new tool. This is also consistent with the rationale behind presenting the EDGs as indications and warnings and not as a part of a newly developed design methodology.

**Acknowledgements** The study is supported by the projects EYE-TRACK and few sECONds funded by the Free University of Bozen-Bolzano with the calls CRC2017 and RTD2019, respectively.

## References

1. Skerlos, S.J.: Promoting effectiveness in sustainable design. *Proc. CIRP* **29**, 13–18 (2015)
2. She, J.: Designing Features that Influence Decisions about Sustainable Products. Ph.D. Thesis, Iowa State University, Ames, Iowa, (2013)
3. Maccioni, L., Borgianni, Y., Rotini, F.: Sustainability as a value-adding concept in the early design phases? insights from stimulated ideation sessions. In: Campana, G., Howlett, R., Setchi, R., Cimatti, B. (eds.) *Sustainable Design and Manufacturing 2017, SDM 2017, Smart Innovation, Systems and Technologies*, vol. 68, pp. 888–897. Springer, Cham (2017)
4. Vezzoli, C., Manzini, E.: *Design for Environmental Sustainability*. Springer, London (2008)
5. Maccioni, L., Borgianni, Y., Pigosso, D.: Can the choice of eco-design principles affect products' success? *Design Science* **5**, E25 (2019)
6. Borgianni, Y., Maccioni, L., Pigosso, D.: Environmental lifecycle hotspots and the implementation of eco-design principles: does consistency pay off? In: Ball, P., Huaccho, Huatuco L., Howlett, R., Setchi, R. (eds.) *Sustainable Design and Manufacturing 2019, KES-SDM 2019, Smart Innovation, Systems and Technologies*, vol. 155, pp. 165–176. Springer, Singapore (2019)
7. Maccioni, L., Borgianni, Y.: Investigating the Value Perception of Specific TRIZ Solutions Aimed to Reduce Product's Environmental Impact. In: *International TRIZ Future Conference*, pp. 282–294. Springer, Cham (2019)
8. Maccioni, L., Borgianni, Y., Basso, D.: Value perception of green products: an exploratory study combining conscious answers and unconscious behavioral aspects. *Sustainability* **11**(5), 1226 (2019)
9. Maccioni, L., Borgianni, Y., Pigosso, D.C., McAloone, T.: Are eco-design strategies implemented in products? A study on the agreement level of independent observers. In: *International Design Conference (DESIGN2020)* (2020)
10. Pigosso, D.C., Rozenfeld, H., McAloone, T.C.: Ecodesign maturity model: a management framework to support ecodesign implementation into manufacturing companies. *J. Clean. Prod.* **59**, 160–173 (2013)
11. Bacciotti, D., Borgianni, Y., Cascini, G., Rotini, F.: Product Planning techniques: investigating the differences between research trajectories and industry expectations. *Res. Eng. Design* **27**(4), 367–389 (2016)

# The Identification and Selection of Good Quality Data Using Pedigree Matrix



Xiaobo Chen and Jacquetta Lee

**Abstract** Most data-based studies require significant amounts of data to support their decision-making process. Apart from increasing data quantity, scientists tend to be aware of the quality of data that influences the robustness of the results. A Pedigree matrix method is presented to characterize the data quality aspects and quantify the quality rating. Five quality aspects (reliability, completeness, temporal, geographical and technological representativeness) are defined as the characteristics to describe how well the reference data is fit for the underlying study. Reference rules are made subjectively for allocating the quality rating, which enable the computer to select appropriate data effectively from among different data sources. The overall data quality rating is calculated reflecting the quality level and converted to the four-parameter Beta probability distribution for uncertainty quantification. This is complemented by the Monte Carlo simulation that identifies uncertainty hotspots, to further improve the quality of identified data. This study provides an effective way to identify the data of good quality through the definition of reference rules. Making such rules can help the users to effectively capture the descriptive information regarding the data quality, further assess the quality levels consistently. The four-parameter Beta distribution is used for quantitative transformation, since it is appropriate to represent expert judgement. Therefore, the definition of distribution parameters is flexible depending on the expert understanding of uncertainty. This strength extends the application of the method to different data systems. Further research can focus on the development of reference rules for different quality aspects, as well the integration of the Pedigree matrix in various data systems.

## 1 Introduction

Frequently, decisions are made based on the relevant scientific information, which suffers from complex and uncertain circumstances. Thus, the new task for scientists is not only to gather data to support the decision-making process, but also to

---

X. Chen (✉) · J. Lee

Centre for Environment and Sustainability, University of Surrey, Guildford, UK

e-mail: [xi.chen@surrey.ac.uk](mailto:xi.chen@surrey.ac.uk)

© The Editor(s) (if applicable) and The Author(s), under exclusive license to Springer Nature Singapore Pte Ltd. 2021

S. G. Scholz et al. (eds.), *Sustainable Design and Manufacturing 2020*, Smart Innovation, Systems and Technologies 200, [https://doi.org/10.1007/978-981-15-8131-1\\_2](https://doi.org/10.1007/978-981-15-8131-1_2)

provide quality assurance of that data such that it guarantees the robustness of the decision. The data quality assurance can thus influence the understanding of the accuracy and precision of scientific results. A notational scheme for expressing and communicating uncertainty and quality, so-called NUSAP (Numeral, Unit, Spread, Assessment and Pedigree), has been proposed by Funtowicz and Ravetz [1], in which Pedigree is a method to capture the descriptive information necessary for evaluating data quality. Represented in a matrix form, Pedigree enables the users to analyse the qualitative aspects of data, through an expert elicitation procedure, which eliminates the use of poor quality data. The conceptual idea of Pedigree has been widely used in life cycle assessment (LCA) as an approach to evaluate input data quality in the life cycle inventory phase. For example, Weidema and Wesnaes [2] provided a matrix-based method to establish data quality indicators (DQIs) that relate to specific aspects of data quality. Later, the method was commonly accepted in LCA fields [3–6] and implemented in the LCA database—*Ecoinvent* [7, 8]. The method converts the qualitative DQIs to numerical values as uncertainty factors according to expert judgement, which represent the uncertainty of the input data by its probability distribution.

Despite its wide application in LCA during the last decade, the main research on the Pedigree matrix focuses on the determination of the numerical uncertainty factors [9–11]. Few works of literature give attention to the determination of the quality aspects and their associated quality levels. Although most Pedigree matrices have an explicit definition concerning the quality aspects, different individuals may have different intuitive judgements; these thereby influence the consistency of quality evaluation. An additional concern is that data quality is a relative term with respect to the specific case under study. Hence, the feature of data quality may not remain constant under different circumstances. For example, data from the European statistics database may not be geographically representative for research in any Asian countries. Thus, the users of the Pedigree matrix must evaluate each data point on a case by case basis, which is time-consuming and ineffective if a great amount of data is required. Attention has been raised recently by Edelen and Ingwersen [12], who addressed that the common Pedigree matrix should be improved to reproduce the “best fit” data. Therefore, this study explores a modified Pedigree matrix that can optimize the data quality evaluation process, aiming to establish a consistent and cost-effective way to identify and select appropriate data.

## 2 Method

### 2.1 Pedigree Matrix

The role of the Pedigree matrix is to convert the descriptive expert opinions regarding a set of DQIs to the scaling scores that reflect the quality levels. Table 1 shows the Pedigree matrix modified from *Ecoinvent 3.0* [7]. The first column includes the five

Table 1 Pedigree matrix based on Ecoinvent 3.0

DQI/Rating	1	2	3	4	5
Reliability	Verified data based on measurements (experimental data)	Non-verified data based on measurements or verified data based on calculation (historical/calculation data)	Non-verified data based on calculation or partly based on qualified estimates	Qualified estimates (e.g. expert judgements) or educated guesses	Non-qualified estimates or uneducated guesses
Completeness	Data from all sites relevant to the market considered (>80%)	Data from sites relevant to market considered (60–80%)	Data from sites relevant to market considered (50–60%)	Data from only one site relevant to market considered (<40%)	Unknown
Temporal representativeness	Less than 3 years of difference	Less than 6 years of difference	Less than 10 years of difference	Less than 15 years of difference	More than 15 years
Geographical representativeness	Data from area of study	Data from larger area in which area of study is included	Data from outside area with similar conditions	Data from outside area with slight similar conditions	Data from unknown or distinctly different area
Technological representativeness	In-house data (known process and materials)	Data of the same technology from other enterprises	Data from processes and materials under study but from different technology	Data on related processes or materials (proxy)	Data on laboratory scale or from different technology

DQIs (reliability, completeness, temporal, geographical and technological representativeness), and the first row includes the five numerical scores (1–5) indicating the quality levels from very good to very poor, respectively. The quality definition is described in each cell of the table. The users should select both quality indicator and its corresponding quality level for evaluating the targeted data, and the data quality is recorded in the Pedigree form as *data (R, C, TiR, GR, TeR)*, in which the abbreviated letters within the parentheses indicate the quality ratings of the DQIs. According to their definitions, the DQIs are separated into two groups: (1) absolute aspect reflects the quality of data itself, which contains reliability and completeness. It is a measure of the goodness associated with the production of data. For example, data of good quality should come from the experimental measurement with an appropriate sample size. Lack of scientific verification leads to lower quality; (2) relative aspect measures the suitability of data associated with the underlying study, which includes temporal, geographical and technological representativeness. For example, data from the area of the underlying study is more suitable than any data outside the study area in terms of geographical representativeness.

**Reliability** is the term to describe the goodness to which the data itself is generated from a source of strong scientific robustness. The general term of reliable data includes data based on acceptable theorem or from verified observations. When there is no verification on data sources or data is qualitatively estimated, its reliability lacks such strength and is ranked with a higher rating. According to Table 1, the data point should be presented with its source description, which can be used directly to assess the overall quality level.

**Completeness** is the term to describe whether the reference data covers all the sites relevant to the market considered. The measure of completeness is to check whether the sample can accurately represent the characteristics of the whole population in the relevant sites. It starts with the data that covers all the relevant sites, and then the data with degressive coverage is ranked with the higher rating. According to Table 1, the data point should be presented with its completeness description, which can be used directly to assess the overall quality.

**Temporal representativeness** is the term to describe whether the reference data is within the same period as well as the underlying study. It measures the time difference between the reference data and the underlying study. The “*if...then*” term is used to determine the temporal quality rating. For example, if the time difference is equal or less than three years, then the quality rating is ranked as one. Hence, given the age of reference data and the date of the underlying study, the time difference can be calculated and then allocated to the corresponding quality rating.

**Geographical representativeness** is the term to describe whether the reference data is within the same geographical region as well as the underlying study. Given the locations of both reference data and the underlying study, a matrix table is established to allocate the degree of geographical representativeness. The cross-check table is created to divide the locations into three levels: world, continents and countries and the degrees are determined following subjective rules based on the expert’s opinions referring to the definition in Table 1.

**Table 2** Example of the cross-check table for allocating geographical representativeness

		Reference data						
		World	Africa	Algeria	Egypt	Kenya	South Africa	Tunisia
Assessment	World	1	3	4	4	4	4	4
	Africa	3	1	2	2	2	2	2
	Algeria	4	2	1	3	3	3	3
	Egypt	4	2	3	1	3	3	3
	Kenya	4	2	3	3	1	3	3
	South Africa	4	2	3	3	3	1	3
	Tunisia	4	2	3	3	3	3	1

Due to the page limitation, Table 2 only shows a part of the matrix table. For example, if the underlying study needs data of interest from Kenya (see the assessment column), but only global data (see the reference data row) is available, the quality rating regarding geographical representativeness is denoted as 4.

**Technological representativeness** is the term to describe whether the reference data relates the same technology applied in the underlying study. Similar to the method to assess the geographical representativeness, a cross-check table is established to allocate the quality rating, given the information about the industrial sector for both reference data generated and the underlying study. The reference rules are made based on the expert opinions. Table 3 shows an example of the matrix table for allocating technological representativeness. For example, technology (process or materials) applied in the aerospace industry is assumed to be similar to the automobile and transport industries, so the quality rating regarding technological representativeness is denoted as 2.

Following the rules above, an Excel-based tool is developed to assess the quality of the targeted data from different sources and then rank them by calculating the overall quality rating.

**Table 3** Example of a cross-check table for allocating technological representativeness

		Reference data					
		Aerospace	Space	Consumer vehicles	Goods vehicles	Rail transport	Infrastructure
Assessment	Aerospace	1	2	2	2	2	3
	Space	2	1	3	3	3	4
	Consumer vehicles	2	3	1	1	1	3
	Goods vehicles	2	3	1	1	1	3
	Rail transport	2	3	1	1	1	3
	Infrastructure	3	4	3	3	3	1



## 2.2 Approach for Quantitative Transformation

For calculating the overall quality rating, the weighting average is applied to aggregate all the five DQIs into a single quality rating, proposed by the International Reference Life Cycle Data System (ILCD) handbook [13]:

$$DQR = \frac{R + C + TiR + GR + TeR + X_w + 4}{i + 4}$$

where

DQR	Overall data quality rating
<i>R</i>	Reliability
<i>C</i>	Completeness
<i>TiR</i>	Temporal representativeness
<i>GR</i>	Geographical representativeness
<i>TeR</i>	Technological representativeness
<i>X<sub>w</sub></i>	The weakest quality level among the DQIs
<i>i</i>	Number of applicable DQI.

There are two reasons for the application of this weighting approach. Firstly, the consideration of the weakest quality level among the DQIs highlights the influence of the lowest quality aspects on the DQR. Secondly, although only five DQIs are considered in this study, instead of six DQIs proposed by the ILCD handbook, the application of the equation is flexible without regarding the DQI numbers. Given the DQR, the four-parameter Beta distribution is to transfer the quality rating to the probability distribution [11]. The traditional Beta distribution with two shape parameters  $\alpha$  and  $\beta$  can randomize the value on the range [0, 1], and it is possible to introduce two scale parameters representing the minimum  $a$  and maximum  $b$  that scale the range on  $[a, b]$  [14]. Therefore, four-parameter Beta distribution enables the distribution scale to any real number. Additionally, Beta distribution is commonly accepted when no prior knowledge of the data's probability distribution is available and thus is suitable in this case to represent the expert judgement for data quality evaluation [15]. Table 4 shows the reference rule for assigning the four-parameter Beta distribution according to the DQR. As in a standard Beta distribution, the parameters  $\alpha$  and  $\beta$  define the shape of distribution, while the range parameter is used to define the ranging values  $a$  and  $b$ , which are the minimum and maximum values of any real number denoted as  $X$  between the range  $X * (1 \pm \text{Range}\%)$ . For a calculated DQR laid with any range, a corresponding Beta distribution is assigned to represent the uncertainty quantitatively.

**Table 4** Four-parameter Beta distribution parameters for DQR

Data quality rating range (DQR)	Beta distribution parameters		
	$\alpha$	$\beta$	Range (+-%)
$DQR \leq 1$	5	5	10
$1 < DQR \leq 1.5$	4	4	15
$1.5 < DQR \leq 2$	3	3	20
$2 < DQR \leq 2.5$	2	2	25
$2.5 < DQR \leq 3$	1	1	30
$3 < DQR \leq 3.5$	1	1	35
$3.5 < DQR \leq 4$	1	1	40
$4 < DQR \leq 4.5$	1	1	45
$4.5 < DQR \leq 5$	1	1	50

### 2.3 Monte Carlo Simulation

When the DQR as a source of uncertainty is represented in terms of probability distribution, the Monte Carlo simulation generates a random number for the input variable based on the given probability distribution. Then the random number can be used to estimate the output through the complex model. Thus, after a large number of iterations, a range of all possible values for the output can be obtained that represent the shape of the output distribution. In general, the Monte Carlo simulation generates two sorts of result: (1) uncertainty range in the input and the output, which identify the biggest data gaps among the uncertain variables. In this case, it refers to the data of the poorest quality; (2) sensitivity index referring to the uncertain variables that influence mostly the uncertainty in the output. Both results are used to identify the uncertainty hotspots, for which the data collection will effectively reduce the overall uncertainty in the output.

### 2.4 Case Study for Selecting Data of Good Quality

In this section, a hypothetical case study is created in an Excel-based spreadsheet to demonstrate our proposed method. The case study needs to estimate the energy consumption for manufacturing a product, containing three raw materials: copper, aluminium and titanium alloy. Since there is no primary data available, reference data should be used to fill the data gaps. Taking copper as an example, assuming that the date of the case study is the current year by default, the mining location is in Chile, and the technology will be applied in the aerospace industry. Then two reference sources are found, as shown in Table 5. Based on the reference rules defined in Sect. 2.1, an Excel-based tool can automatically allocate the quality ratings for both reference sources (Table 6). The two absolute DQIs (reliability and completeness)

**Table 5** Descriptive information on copper

	Reliability	Completeness	Date	Location	Industrial sector
Case study	<i>n.a.</i>	<i>n.a.</i>	2020	Chile	Aerospace
<i>Ref. [1]</i>	Verified data partly based on assumption	Data coverage [85%, 95%]	2007	South America	Goods vehicles
<i>Ref. [2]</i>	Qualified estimates by industrial experts	Data coverage [50%, 75%]	2010	Europe	Rail transport

*n.a.* not applicable

**Table 6** Quality ratings and associated Beta distribution parameters for *Refs. [1, 2]*

Case study	Data quality indicators						Beta distribution parameters from Table 4		
	R	C	TiR	GR	TeR	DQR	$\alpha$	$\beta$	Range (%)
<i>Ref. [1]</i>	2	2	4	2	2	3.11	1	1	35
<i>Ref. [2]</i>	4	4	3	4	2	3.67	1	1	40

are determined directly from the descriptive information in Table 5. The three relative DQIs (temporal, geographical and technological representativeness) are determined following the reference rules. The DQR for both reference data is derived by the equation in the above section. For example, the DQR for *Ref [1]* is calculated as follows:

$$Ref. [1] \text{ DQR} = \frac{2 + 2 + 4 + 2 + 2 + 4 * \max(2, 2, 4, 2, 2)}{5 + 4} = 3.11$$

Likewise, *Ref. [2]* DQR is 3.67. Since the DQR measures the data quality level, a smaller rating refers to the higher-quality level. Therefore, *Ref. [1]* is more appropriate for the underlying study than *Ref. [2]*. Likewise, the same method is applied to choose the appropriate data sources for the other materials and processes in the case study under consideration. Given the different DQRs for all the input data points, different Beta distribution parameters should be selected according to Table 4. For example, Table 6 shows the selection of four-parameter Beta distribution for copper with the shape parameters ( $\alpha = 1, \beta = 1$ ) and the scale parameters (uncertainty range = 35%). Given these four parameters, the distribution of CO<sub>2</sub> emissions for copper extraction can be generated in Fig. 1.

To keep it simple, this study has not modelled the manufacturing processes as the real industry does, but summed the energy consumption of all the processes. To analyse uncertainty and sensitivity, the four-parameter Beta distributions are selected according to the DQR of each data point, then the Monte Carlo simulation (1000 iterations) is applied to estimate uncertainty range and sensitivity index. Finally, a four-quadrant matrix is established for identifying uncertainty hotspots (Fig. 2), with uncertainty on the x-axis and sensitivity on the y-axis. The red-dotted lines divide

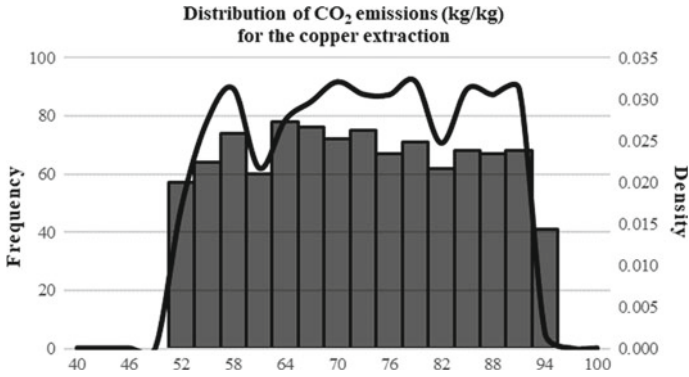


**Fig. 1** Distribution of CO<sub>2</sub> emissions for the copper extraction process according to the four-parameter Beta distribution

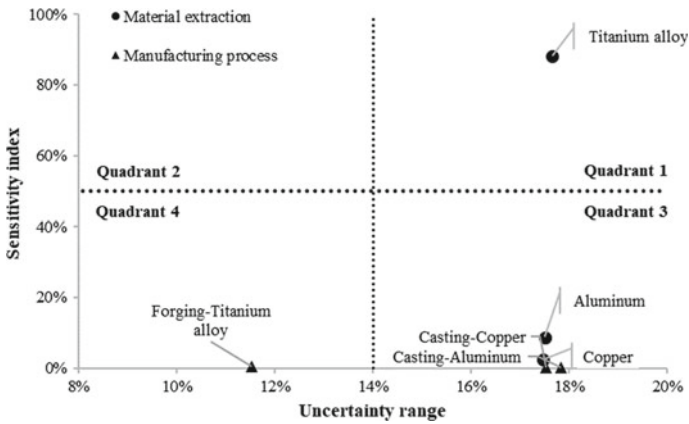


**Fig. 2** Four-quadrant matrix for identifying uncertainty hotspots

the matrix into four parts, in which the data points located on the quadrant 1 (i.e. high uncertainty and the system are highly sensitive to those data points) are considered as uncertainty hotspots.

The result indicates that data regarding the titanium alloy at the material extraction stage has higher uncertainty and sensitivity, so that improving the quality of such data will be most effective at reducing the overall uncertainty. Regarding the other data points (e.g. data on the quadrant 3), although they have almost the same uncertainty range, they have few influences on the overall uncertainty due to the low sensitivity. Therefore, any efforts for data quality improvement may not deliver for reduced uncertainty.

### 3 Discussion

This study introduces an effective method to facilitate the identification of the appropriate data. Although the referred Pedigree matrix is frequently used in LCA studies, the proposed method can be applied in different areas for data quality evaluation, since it mainly focuses on how to describe the intrinsic characteristics of data quality and how to assess it effectively.

The separation of the quality aspects into two groups is in accord with the standard definition of data quality [16], in which data quality is defined as the degree to which a set of aspects of data fulfils requirements. The requirements do not only concern the quality of data itself (e.g. reliable data sources and complete sampling), but also the expectations of the users, like how well the data fits for intended uses. It means that the degree of data quality partially relies on the using circumstance, rather than a “perfect” and “absolute” rating that never change irrespective of whenever or wherever it is used. Hence, a better understanding of data quality aspects provides a more rigorous statement of quality evaluation for supporting the decision-making process.

Capturing expert knowledge is always a time-consuming and costly process, since there is no standard format to record the expert judgements. Various statements may lead to inconsistent opinions, even significant disagreements among the experts. This study proposes the reference rules for allocating the quality ratings regarding the relative quality aspects. On the one hand, it is efficient for the users to optimize the data selection process. Once the underlying study is defined, the reference rules can retrieve the data sources and identify the most appropriate data via a simple computational program. Hence, it does not require many manual efforts for quality evaluation and data selection, especially in a complex model with hundreds of input variables. Additionally, it maintains consistency when determining the quality rating by setting up the standard rules. Although the rules for the quality aspects are assumed subjectively, once fixed, the quality rating will not be influenced by different expert opinions.

Regarding the three relative quality aspects, reference rules are made differently. Temporal representativeness can be assessed mathematically by setting the data age threshold, which defines how old the reference data is regarding the underlying study. Thus, a well-defined threshold enhances the consensus between the experts. Geographical representativeness can be assessed by setting the regional levels. Computationally, the three geographical levels are readily modelled given a standard rule. However, the city-based data or site-specific data is not included in the matrix table, because their quality varies under circumstance. Some site-specific data may be representative on the country level, others may not. Therefore, the users should be aware of the use of such data and assess its quality on a case by case basis. The assessment of technological representativeness heavily depends on expert knowledge that varies among people, as well as the type of technology that may have no difference among the industrial sectors, or be quite different within the same sector. This study only proposes an example of some industrial sectors, which may have

an approximate level of technology, but its application is still limited. Further study is needed to refine the reference rules for determining the quality rating regarding technological representativeness.

Instead of log-normal distribution used in the Pedigree matrix of the *Ecoinvent* version, this study applies the four-parameter Beta distribution for quantitative transformation. The uncertainty factors used in *Ecoinvent* were initially determined by expert judgement, afterwards refined using empirical data [9], which strengthened the use of the Pedigree matrix with an accurate estimation of uncertainty. However, the determination of such empirically based uncertainty factors requires large human efforts that should be repeated when new data is updated. Additionally, its application is limited as the uncertainty factors are derived based on the fixed data sources. In contrast, Beta distribution applied in this study attributes subjective uncertainty ranges, which can be varied depending on the data sources and changed according to the expert's knowledge about uncertainty. In our point of view, the Pedigree matrix, as a subjective evaluation method, does not require very high accuracy of uncertainty estimation, but a ranking order is good enough for identifying the uncertainty hotspots. Uncertainty parameters determined in both log-normal and Beta distributions reflect the quality levels (i.e. the higher the quality level is, the smaller the uncertainty factor is), so the selection of distributions does not affect the order of uncertainty. Therefore, the flexibility of its application is enhanced for the small price of some accuracy.

The results of the sensitivity analysis indicate the levels of uncertainty of input variables and their impacts to the overall uncertainty. This provides the decision-makers a better understanding of the impactful uncertainty and leads them to fill the data gaps effectively by improving the quality of identified data.

## 4 Conclusion

This study proposes a method to effectively optimize the data quality evaluation in the form of Pedigree matrix. The classification of quality aspects and the reference rules for quality rating allocation ensure the users select the appropriate data effectively when they start seeking data from different sources. The quantitative assessment of the data quality enables them to better understand the goodness of data and which data should be improved.

The reference rules keep the assessment of quality rating consistent, reducing the deviations or human errors when recording the descriptive information from the expert judgements. However, the application of reference rules may be limited, firstly because knowledge of data quality is described variously, thus the assumptions for making the rules still need to be justified depending on the databases. Secondly, this study does not consider the integration of Pedigree matrix in an existing database that does not contain any information regarding data quality, thus the capture of data quality knowledge is still a challenge for building the database with quality assurance.

The quantitative transformation was designed to convert a quality rating to an uncertainty factor. Through the Monte Carlo simulation, data collection will be focused towards the uncertainty hotspots, and on improving those data that have poor quality. Although the use of Beta distribution introduces the subjective factor that may influence the estimation of uncertainty, its flexibility can extend the application of the Pedigree matrix in LCA to other fields that require significant amount of data.

**Acknowledgements** This work has been conducted as part of the PLEIADES project that has received funding from the European Union's Seventh Programmes for research, technological development and demonstration under grant agreement No. 603843.

## References

1. Funtowicz, S.O., Ravetz, J.R.: Science for policy: Uncertainty and quality. In: Uncertainty and quality in science for policy. Springer, Berlin (1990)
2. Weidema, B., Wesnaes, M.S.: Data quality management for life cycle inventories—an example of using data quality indicators. *J. Clean. Prod.* **4**(3–4), 167–174 (1996)
3. van der Sluijs, J., Kloprogge, P., Risbey, J., Ravetz, J.: Towards a synthesis of qualitative and quantitative uncertainty assessment: applications of the numeral, unit, spread, assessment, pedigree (NUSAP) system. In: International Workshop on Uncertainty, Sensitivity and Parameter Estimation 2003, Rockville, USA (2003)
4. May, J.R., Brennan, D.J.: Application of data quality assessment methods to an LCA of electricity generation. *Int. J. Life Cycle Assess.* **8**(4), 215–225 (2003)
5. Ewertowska, A., Pozo, C., Gavalda, J., Jimenez, L., Guillen-Gosalbez, G.: Combined use of life cycle assessment, data envelopment analysis and Monte Carlo simulation for quantifying environmental efficiencies under uncertainty. *J. Clean. Prod.* **166**, 771–783 (2017)
6. Miah, J.H., Griffiths, A., McNeill, R., Halvorsen, S., Schenker, U., Espinoza-Orias, N., Morse, S., Yang, A.D., Sadhukhan, J.: A framework for increasing the availability of life cycle inventory data based on the role of multinational companies. *Int. J. Life Cycle Assess.* **23**(9), 1744–1760 (2018)
7. Weidema, B.P., Bauer, C., Hischer, R., Mutel, C., Nemecek, T., Reinhard, J., Vadenbo, C., Wernet, G.: Overview and Methodology: Data Quality Guideline for the Ecoinvent Database Version 3. Swiss Centre for Life Cycle Inventories (2013)
8. Muller, S., Lesage, P., Ciroth, A., Mutel, C., Weidema, B.P., Samson, R.: The application of the pedigree approach to the distributions foreseen in ecoinvent v3. *Int. J. Life Cycle Assess.* **21**(9), 1327–1337 (2016)
9. Ciroth, A., Muller, S., Weidema, B., Lesage, P.: Empirically based uncertainty factors for the pedigree matrix in ecoinvent. *Int. J. Life Cycle Assess.* **21**(9), 1338–1348 (2016)
10. Coulon, R., Camobreco, V., Teulon, H., Besnainou, J.: Data quality and uncertainty in LCI. *Int. J. Life Cycle Assess.* **2**(3), 178 (1997)
11. Kennedy, D.J., Montgomery, D.C., Rollier, D.A., Keats, J.B.: Data Quality. *Int. J. Life Cycle Assess.* **2**(4), 229–239 (1997)
12. Edelen, A., Ingwersen, W.W.: The creation, management, and use of data quality information for life cycle assessment. *Int. J. Life Cycle Assess.* **23**(4), 759–772 (2018)
13. JRC: ILCD handbook. General guide for life cycle assessment—Detailed guidance. European Commission, Joint Research Centre—Institute for Environment and Sustainability, Luxembourg (2010)

14. Johnson, N.L., Kotz, S., Balakrishnan, N.: Chapter 21: Beta Distributions. In: Continuous Univariate Distributions, 2nd edn. Houghton Mifflin Boston (1970)
15. Kennedy, D.J., Montgomery, D.C., Quay, B.H.: Data Quality. Stochastic environmental life cycle assessment modeling. *Int. J. Life Cycle Assess.* **1**(4), 199–207 (1996)
16. ISO: ISO 9000:2015 Quality management systems—Fundamentals and vocabulary. International Organization for Standardization, Geneva, Switzerland (2015)



# Understanding Customer Preference: Outline of a New Approach to Prioritise Sustainability Product Information



Sze Yin Kwok , Sophie I. Hallstedt , and Veselka Boeva 

**Abstract** The communication of sustainability values shared between product developers and customers is an important catalyst for effective collaboration that inspires sustainable consumption. Despite the many tools developed for assessing and communicating the product's sustainability performance, customers are facing difficulties in understanding product sustainability information. The knowledge gaps remain underexplored about how product sustainability information is perceived and how this impacts customer purchasing behaviour. This paper outlines a new approach, driven by both backcasting and forecasting thinking, for understanding and modelling customer preferences for product sustainability information. We report findings from a case study of a large workplace furniture manufacturer. The study explored the potential of (i) identifying prioritised sustainability attributes using sustainability design space (SDS) and (ii) applying machine learning to model customer preferences.

## 1 Introduction

Consumer purchasing behaviour has ethical, resource, waste and community impact implications, and their collective effects are significant [1]. Sustainable product development is one of the main enablers towards addressing the global sustainability challenge. The communication of sustainability values shared between product developers and customers is an important catalyst for effective collaboration that inspires sustainable consumption and helps to reach sustainability goals [2].

In order to be able to make well-informed decisions and purchases sustainably, customers need to have enough 'product sustainability information'—information of the attributes related to the sustainability performance of product and/or company and the knowledge to understand this information in order to relate their behaviour with the potential impact on the planet [3, 4].

---

S. Y. Kwok (✉) · S. I. Hallstedt · V. Boeva  
Blekinge Institute of Technology, Valhallavägen 1, Karlskrona 371 41, Sweden  
e-mail: [sze.yin.kwok@bth.se](mailto:sze.yin.kwok@bth.se)

© The Editor(s) (if applicable) and The Author(s), under exclusive license to Springer Nature Singapore Pte Ltd. 2021

S. G. Scholz et al. (eds.), *Sustainable Design and Manufacturing 2020*, Smart Innovation, Systems and Technologies 200, [https://doi.org/10.1007/978-981-15-8131-1\\_3](https://doi.org/10.1007/978-981-15-8131-1_3)

Sustainability challenges are complex and wicked problems that are linked to numerous aspects which require a wealth of knowledge to comprehend. For instance, a product's sustainability performance can be measured in terms of its greenhouse gas emission, use of resources, energy efficiency, material choice, possibility to repair/reuse/recycle, code of conduct for supplier, animal welfare, etc. Many tools have been developed in the attempt to measure these factors and translate the data into something comprehensible for customers. Over 400 ecolabels or certification schemes have been developed in 207 countries, covering 240 product groups [5]. Sustainability reporting, such as Global Reporting Initiative (GRI) and Corporate Social Responsibility (CSR), as well as ISO standards (e.g. ISO 14040, 14006, 14001) were used by many of the world's largest companies. Marketing tools such as public campaigns and advertisements are also employed to convey the message [2, 6].

Despite the many tools developed, consumers are still facing difficulties in understanding product sustainability information [5], and these existing tools are still inefficient in addressing the communication gap [2]. The knowledge gaps remain under-explored about how consumers perceive product sustainability information and how this impacts their purchasing behaviour [7]. There is a need for research to clarify why consumers adopt environmental labels [4] or even sustainability information in general.

This paper reports initial findings from an ongoing research work that aims at supporting sustainability communication through proposing a novel approach to model customer preference for product sustainability information. This paper presents the outline of the proposed approach and reports results from a case study.

## 2 Outline of the Proposed Approach

Perception of sustainability information varies between people. For example, Rahbar and Whid's [8] study shows that different ethnic groups differ in their awareness, recognition and perception of ecolabel. The degree of consumer motivation depends on how distinct types of information relate to the consumer's personal relevance and personal values [9]. The concept of eco information individualisation has been proposed to appeal to users with different interests in learning product sustainability information and shopping sustainably [5, 7].

Increasing number of companies considers to improve the transparency of their product sustainability information and helps their customers in their choice. They share an interest in the real competitive advantage brought by having a deep understanding of the customer preference for sustainability information, specific to their companies' products, to anticipate needs and offer differentiated products. We propose a new approach to guide product developers to understand and model customers preference for product sustainability information (Fig. 1). The approach consists of four stages:

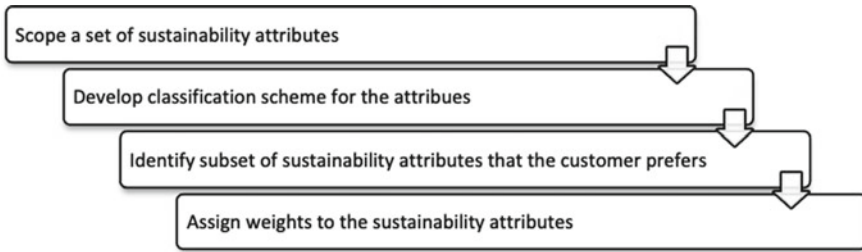


**Fig. 1** Stages of the proposed approach for constructing sustainability preference model

1. **Scope a set of sustainability attributes**—The first stage involves the identification of a set of sustainability attributes that are relevant to the product development company.
2. **Develop classification scheme for the attributes**—Due to the complexity of the sustainability challenges, the number of related information may be large. Classification scheme(s) can potentially support sense-making.
3. **Identify subset of customer personalised sustainability attributes**—Studies of customers can define criteria for downselection of the sustainability attributes based on individual customer’s interests. In this case, the ‘individual customer’ is not necessarily a person but can be an organisation or company.
4. **Assign weights to the sustainability attributes**—Patterns of purchasing behaviour can provide insights into weighting each sustainability attribute in relation to individual customer’s preference. A repeated process can result in different preferred information architecture for different customers.

This approach can potentially be used qualitatively and/or quantitatively. Qualitative methods (e.g. user-centred design methods, the sustainability design space method [10]) can be applied in all of the four stages to identify people’s needs and preferences. The proposed approach can also guide quantitative research, for example using data analytics to create preference model. To the authors’ best knowledge, it is the first approach that encompasses both backcasting thinking (through an adaptation of framework for strategic sustainable development (FSSD) [11]) and forecasting thinking (using data analytics) for modelling customer preference for sustainability information.

### 3 Case Study

In this section, we present a case study concerned with the potential methods to be included within the proposed approach, in particular for shaping the first stage of the proposed approach that focuses on scoping and identifying a set of relevant sustainability attributes.



**Fig. 2** Methods used in the case study

We have studied a major workplace furnishings manufacturer based in Sweden with customers from about 40 countries. This company offers furniture solutions for various types of workplace, such as offices, restaurants, hospitals and schools. The customers of this business-to-business company are often large organisations which procure in large quantities; therefore, their purchasing choices can have a significant sustainability impact. This company is selected because it is an influential case to study. This large product development company can be considered a corporate leader in sustainability in furniture industry. Not only they have taken a variety of measures in monitoring their sustainability performance and communicating their results to the external world, through the use of ecolabels, certificates, supplier code of conduct and sustainability reports, they also have recently developed a sustainability indexing tool called *The Better Effect Index (BEI)* [12]. It is believed that studying this case can provide insights into raising the standards of sustainability information visualisation for other companies. Studying this case company and their context-specific, industry-initiated, open-source information tool also offers a new direction in future research, as our research uses a bottom-up approach which distinguishes itself from other existing research on sustainability information tool that aims at developing universal sustainability indicator which can be applied to as many types of product as possible.

The case study (Fig. 2) can be divided into four stages: (i) a brief literature review was conducted to understand current situation about sustainability information provision tools used by companies; (ii) documents about the practice of sustainability communication of the case company (including sustainability report, sustainability declaration of their product series, detailed instructions about their web-based sustainability indexing tool, ecolabel requirements specification, etc.) were collected and analysed; (iii) the method *sustainability design space (SDS)* [10] was applied on the case company to test its suitability for identifying and prioritising sustainability criteria; (iv) a semi-structured in-depth interview was conducted to validate the outcomes from applying SDS and offers a more complete picture of other topics related to this research. The interview lasted for 4 h and was conducted with the sustainability manager who played a key role in developing the sustainability indexing tool as well as developing other sustainability communication strategies for the case company. Specifically, the results from this case study revolve around three themes as follows:

- The company's practices related to sustainability information provision for customers;
- The potential values of using SDS to identify a set of relevant sustainability attributes for products of the case company;

- The opportunities and challenges of applying machine learning techniques for modelling customer preference for sustainability information.

## 4 Practice of the Case Company: A Sustainability Index

In 2017, the case company launched a web-based sustainability information provision tool, *The Better Effect Index (BEI)* [12], that gives easy-to-understand results about how sustainable a product is. The index was developed with the intention to balance comprehensiveness and simplicity. It covers both ecological and social aspects of sustainability performance of the company’s products, assessed through qualitative and quantitative methods. The result is a simple score between 1 and 3. Table 1 shows the sustainability information covered in the index, 20 sustainability attributes are grouped under six categories, namely raw materials and resources, climate, pure materials, social responsibility, reuse and ergonomics. When assessing a product series, a score between 1 and 3 is given to each sustainability attribute. The final score is a total average of the scores of all categories, which average the attributes’ scores within the category.

**Table 1** Information structure of the case company’s sustainability indexing tool [12, 13]

Raw materials and resources	Climate	Pure materials	Social responsibility	Reuse	Ergonomics
Knowledge of the origin of the raw materials	Inward transport	Fulfilled levels of chemical content	Code of conduct for suppliers	Possible to repair/renovate	Enables customisation
Knowledge of conditions in the production chain	Outward transport	Fulfilled levels of emissions	Suppliers which have been risk-assessed	Possible to recycle materials	Enables movement
Resource optimisation	Suppliers (fossil-free energy in manufacturing)	Good material choice	Inspected suppliers from risk countries	Made of recycled material	Improves the acoustic environment
	Producers (fossil-free energy in manufacturing)				
	Proportion of material with low climate impact				

## 5 Potential Values of the Sustainability Design Space

To support effective consideration of sustainability perspective early in product development, Hallstedt [10] has developed a method called the *sustainability design space* (SDS). This method provides an approach for identifying sustainability criteria in any manufacturing company, and the sustainability criteria can be used for decision support in product innovation process. The SDS method incorporates a backcasting perspective from a definition of success [10, 11]. Backcasting begins by imagining success in the future, then assessing current situation through the lens of this success definition, before considering and choosing actions to be taken in order to achieve the vision defined [11, 14]. One of the outcomes of SDS is a strategic sustainability criteria matrix sorted according to product life cycle phases and socio-ecological sustainability principles. There are three steps within the SDS process and an optional fourth step that guides the development of a qualitative measurement scale for the criteria, called the *sustainability compliance index* (SCI).

- Step 1. Collect existing sustainability-related requirements and tactical design guidelines;
- Step 2. Review all product life cycle phases through sustainability principles;
- Step 3. Reduce and select the criteria and guidelines using meta-criteria;
- Step 4 (Optional). Develop *sustainability compliance index* (SCI) scale.

The first stage of the approach proposed by this paper focuses on the identification of a set of relevant sustainability attributes for company, so the research question was: Can we apply SDS for identifying prioritised sustainability criteria for the case company?

Following the first three steps of the SDS method, we analysed the documents collected from the company. A range of sustainability criteria was identified and mapped against the two dimensions related to product life cycle phases and sustainability aspects guided by sustainability principles [11, 15], as presented in Table 2. This outcome was created with reference to previous experiences, from other research projects, in applying SDS on other manufacturers from very different industries. We did not go through the optional steps of devising tactical design guidelines nor creating the *sustainability compliance index* (SCI), since these two steps were originally designed to support decision-making in sustainable product innovation process which is not the focus of this research.

In the in-depth interview, the researcher talked the interviewee through the theoretical background of SDS and presented the detailed steps about how it was applied. Then the interviewee was given time to go through all the detailed contents in the SDS created for the case company. The interviewee was asked to give feedback to the following questions during the interactive discussion with the researcher:

- What are the differences between the ways to identify sustainability criteria used by BEI and that can be achieved through applying SDS?

- Are the outcomes presented in Table 2 valid and applicable for the case company? Is it possible to prioritise or downselect the list of criteria? If yes, what would be the judging criteria?
- What would be the challenges if SDS is used for scoping the set of relevant sustainability attributes for the purpose of communicating with their customers? Should we apply SDS when scoping the set of relevant sustainability attributes?

The responses are summarised as follows.

**Table 2** Sustainability design space (SDS) of the case company

Decision aspects concerning product life cycle phases	Sustainability aspects guided by sustainability principles [12, 14]			
Raw materials: materials and chemicals that are used for the product components and/or its production	No use of critical materials regarding availability and sustainability; see material criticality list	No materials for products and/or production used that contain or result in emissions of substances included in the Substitute It Now (SIN) candidate list	No use of raw materials/chemicals and its production that cause physical degradation	No organisational practices at the suppliers of raw materials that create structural obstacles for people’s health, influence, competence, impartiality and meaning-making
Production: production by suppliers of sub-components and materials, as well as production of products at the own company	Only recycled materials are used, with no metal emissions, and all scrap metals are recycled into pure fractions	No emissions and waste products from production sites (even at the suppliers) contain substances in the SIN list	No production of product or product components used that cause degradation of nature by physical means	No organisational practices during production and post processes that create structural obstacles for people’s health, influence, competence, impartiality and meaning-making
	Only renewable energy sources are used in the production processes while optimising energy efficiency	Reuse and recycle all leftover materials and substances from the production processes		

(continued)

**Table 2** (continued)

Decision aspects concerning product life cycle phases	Sustainability aspects guided by sustainability principles [12, 14]			
Distribution: transportation of materials, substances and products connected to the company products and its production	Only renewable fuels are used for distribution of materials, substances and products	Use the most efficient transportation to minimise critical emissions, such as greenhouse gases, NOx and particles.	No new land areas, otherwise used for renewable resources and recreation, are used for transportation of materials, substances and/or products	No risk today or in the future for inefficient and unsafe transports of materials, substances and products related to the company’s products. No organisational practices during distribution that create structural obstacles for people’s health, influence, competence, impartiality and meaning-making
Use and Maintenance: activities and design that affect the sustainability impact during the usage and maintenance	Optimised design of the product from a material and energy perspective	The design of the product contains no restricted substances or materials	The design of the product does not contribute to degradation of nature due to noise, odour, ground pressure or emissions during use and/or maintenance of products	Product use does not create structural obstacles for people’s health, influence, competence, impartiality and meaning-making
	Optimised maintenance solutions			No organisational practices during maintenance that create structural obstacles for people’s health, influence, competence, impartiality and meaning-making

(continued)



**Table 2** (continued)

Decision aspects concerning product life cycle phases	Sustainability aspects guided by sustainability principles [12, 14]			
End of Life: activities and design that affect the sustainability impact during the end of life phase	All valuable materials/component are returned to the value chain for remanufacturing and recycling	Prevent emissions and waste and make sure that emissions and waste from end of life phase do not contribute to an accumulation in nature	No physical degradation of nature caused by waste from end of life phase	No organisational practices during end of life activities that create structural obstacles for people’s health, influence, competence, impartiality and meaning-making

**5.1 What Are the Differences Between the Ways to Identify Sustainability Criteria Used by BEI and that Can Be Achieved Through Applying SDS?**

When developing BEI, the decisions about what attributes to be included were made based on what they knew about the situation at the time that included product requirements and their customers’ knowledge or interests at the time. The selection of the sustainability attributes was largely limited by the company’s vision, the company’s or the customers’ knowledge or simply practicality. This risks missing certain aspects of sustainability or missing some sustainability attributes which would become increasingly important over time. On the other hand, the SDS created in this case study incorporated backcasting thinking and included long-term targets that could guide the company to make strategic plan [10]. In relation to sustainability communication, the inclusion of long-term targets could help company to show their vision to their customers.

When identifying sustainability criteria with SDS, the scoping process does not predominantly depend on knowledge of current situation or limited by existing conditions. One can draw a more complete and comprehensive picture about how to reach for sustainable solution. Therefore, SDS would be useful to companies for deriving a thorough list of sustainability indicators and ensuring all sustainability aspects are covered. The long-term perspective can be used to guide the company to search for information that is important but missing. An example of information missing from BEI, which was reminded by SDS during the interview, was waste handling in production. The systems perspective, life cycle perspective and the sustainability principles lens incorporated within SDS can also provide insights into how to structure the vast variety of sustainability information. Besides, SDS can help company

to evaluate if the right indicator was chosen, for example, in BEI under the category 'raw materials and resources', one of the attributes is 'knowledge of the origin of the raw materials'. A possible scenario is that using BEI, a product may get a good score for the material choice because the company has a lot of the knowledge about the origin of the material, however may be critical material or conflict material was used which should not be considered as a sustainable choice. This consideration is covered in the SDS (in the top left cell), but not in BEI.

### ***5.2 Are the Outcomes Presented in Table 2 Valid and Applicable for the Case Company? Is It Possible to Prioritise or Downselect the List of Criteria? if Yes, What Would Be the Judging Criteria?***

The interviewee went through all the criteria in the SDS (Table 2) and thought all of them were valid and applicable for the case company, although these criteria were not equally important. Some are more relevant for furniture industry than the other.

SDS was first developed for and applied in product development context [10], and the downselection process was guided by specific criteria written for usage in early product development phase. Since the research reported in this paper focused on sustainability communication with customers which happened in the downstream of the value chain, we examined with the interviewee to explore the possibility of downselection of prioritised sustainability criteria. The interviewee was able to select a number of sustainability criteria from the SDS in a short time that shows prioritisation was possible. When asked about the judging criteria used when selecting prioritised sustainability criteria, the interviewee said the decisions were based on the requirements or interests from their customers. Other stakeholders' interests, for example legal requirements, may be important for product development, but played a less important role in this research project on sustainability communication. The interviewee also said because she had a clear understanding about customers' interests related to procurement and ecolabels, with this meta-criterion in mind, the prioritisation process was easy.

### ***5.3 What Would Be the Challenges if SDS Is Used for Scoping the Set of Relevant Sustainability Attributes for the Purpose of Communicating with Their Customers? Should We Apply SDS When Scoping the Set of Relevant Sustainability Attributes?***

The initial motivation of developing an information provision tool is to provide easy-to-understand and engaging information for customers. The long-term criteria identified are the backbone for SDS, but these are not detailed or simple enough to be effectively communicated to customers as they are. There is a need for extra step(s) of adaptation, backed by further research, to translate these identified sustainability criteria into easily comprehensible sustainability attributes, for example through linking them to relevant sustainability indicators.

In summary, the potential benefits brought by SDS make it a valuable choice for further research on its application.

## **6 Opportunities and Challenges of Applying Machine Learning Techniques**

Advances in technology allow the capturing of an ever-increasing amount of contextual data from our everyday life. Big data and marketing analytics are two of the increasingly popular computational tools that can analyse and reveal patterns related to customer behaviour and interactions. In particular, Bayesian analysis' ability to capture individual-level customer heterogeneity provides lots of opportunities in solving marketing science problems [16].

In this section, we explore the potential of data mining and machine learning techniques for modelling customer preferences for sustainability information. This quantitative approach can be carried out in parallel with qualitative research that uses methods such as interview or SDS. The results from both approaches can potentially complement each other and facilitate triangulation to validate the preference model creation.

We believe this exploration of methods using data mining and machine learning techniques can be conducted in two stages, first utilising the power of data mining and knowledge discovery techniques in analysing existing situation, the lessons learnt can then provide a basis for the second stage that aims at creating predictive model.

**Stage 1. Building preference model of existing customers** The goal of this stage is to develop a data-driven approach that learns characteristic patterns of the purchase decisions made by the customers based on historical data about their purchase and derives weights of their preference through data analysis and aggregation.

Two types of data are useful for driving this data analytics process: product data and customer information. For this initial exploration, we suggest to kick off the

exploration with this list of product characteristics: ratings for a list of sustainability attributes, price, qualified certifications/ecolabels, materials and basic product information such as weight and colours. Data about customer purchase history can include information about product series bought by the customer, quantity of products bought, amount of money spent, size of company/organisation, location, nature of business, time of purchase, geographical distribution of the customer company/organisation, etc. The underlying assumption is that the product sustainability information is displayed at the time of purchase, and the customer makes consistent purchasing decisions in consideration of this information.

Alternatively, a hybrid approach can be used which combines the above data-driven approach with knowledge-based approach—the knowledge gained from the case study about *The Better Effect Index (BEI)* or from applying SDS can be used for data labelling. In this way, we will be able to build customer profiles presenting weighted preferences for different sustainability attributes.

Customer profiles consisting of weighted preference can provide insights into the cognitive processes that underlie the customers' purchasing behaviour. This information can help the customers to evaluate whether their purchasing behaviours are aligned with their goals and additionally facilitate them in expressing their requirements to product suppliers. The preference model can be used by product developers to support sustainability communication through informing the design of individualised sustainability information display [5, 7].

## **Stage 2. Creating predictive model to predict the interests of future customers**

Customer preference model can provide a base for forecasting the customer demand of product sustainability features. A predictive model can potentially help answering the question of: What will be the demand for certain sustainable product attributes? How to identify the most profitable customers for sustainable solutions? What is the right price for a product with certain sustainable attributes? For example, we can group the customers by using clustering techniques which provide clusters of customers with (i) similar profiles (e.g. size of company, location) or (ii) similar purchasing behaviours (e.g. types of sustainable products bought). By comparing customer profiles, when there is a new customer, the predictive model can suggest sustainability features that the new customer may be interested in. By comparing purchasing behaviour, when a new sustainable product is launched, the company can target potential buyers and design marketing strategies.

In theory, the discussed approach can be applied to model individual customer or organisational customer sustainability preferences, as long as the necessary data is available.

## 7 Conclusion and Future Works

Effective communication of companies' sustainability performance can increase the chance of a shift towards more sustainable consumption pattern. Despite the proliferation of tool development in the area, consumers are still facing difficulties in understanding sustainability information related to products.

This paper has presented an ongoing research study that aims to help companies improve communication of product sustainability performance. Outline of a new approach to model customer preference for sustainability information is discussed. This paper also reports findings from a case study that explored the potential of scoping a set of relevant sustainability attributes using the sustainability design space (SDS). The potential values of SDS are discussed, and a future research direction will be to investigate how to translate the prioritised sustainability criteria into sustainability attributes that are relevant for companies and understandable for their customers, through connecting the criteria to pertinent sustainability indicators. We also consider the opportunities and challenges of using data mining and machine learning to model customer preferences. These results provide ideas for future research to approach the problem of understanding customer perception towards product sustainability information.

**Acknowledgements** Financial support from the Knowledge Foundation in Sweden is gratefully acknowledged. Sincere thanks to the industrial research partners.

## References

1. Young, W., Hwang, K., McDonald, S., Oates, C.J.: Sustainable consumption: green consumer behaviour when purchasing products. *Sustain. Dev.* **31**, 20–31 (2010)
2. S.Y. Kwok, S.I. Hallstedt: Towards strategic sustainable product development: challenges and opportunities for communicating sustainability in a value chain. In: *Norddesign 2018 Conference*, 2018, pp. 1–14
3. Kaiser, F., Wolfing, S., Fuhrer, A.: Environmental attitude and ecological behavior. *J. Environ. Psychol.* **19**(1), 1–19 (1999)
4. Thøgersen, J., Haugaard, P., Olesen, A.: Consumer responses to ecolabels. *Eur. J. Mark.* **44**(11/12), 1787–1810 (2010)
5. Kwok, S.Y., Harrison, D., Malizia, A.: Designing individualisation of eco information: a conceptual framework and design toolkit. *Int. J. Sustain. Eng.* **7038**(July), 1–11 (2017)
6. K. Töpfer, L. Shea: *Communicating sustainability: How to produce effective public campaigns* (2005)
7. S.Y. Kwok, D. Harrison, S. Qin: Designing an individualised eco information system: a conceptual framework. In: *19th DMI: Academic Design Management Conference: Design Management in an Era of Disruption* (2014)
8. Rahbar, E., Wahid, N.A.: Ethno-cultural differences and consumer understanding of eco-labels: an empirical study in Malaysia. *J. Sustain. Dev.* **3**, 255–262 (2010)
9. H. Noel, *Basics Marketing 01: Consumer Behaviour*. Fairchild Books, New York (2008)
10. Hallstedt, S.I.: Sustainability criteria and sustainability compliance index for decision support in product development. *J. Clean. Prod.* **140**, 251–266 (2017)

11. Broman, G.I., Robèrt, K.H.: A framework for strategic sustainable development. *J. Clean. Prod.* **140**, 17–31 (2017)
12. Kinnarps: The Better Effect Index—About Kinnarps (2018). Available: <https://www.kinnarps.com/about-kinnarps/the-better-effect-index/>. Accessed: 06 May 2019
13. Kinnarps: Instructions for assessment. Kinnarps AB, Kinnarp (2017), pp. 1–7
14. Dreborg, K.H.: Essence of backcasting. *Futures* **28**(9), 813–828 (1996)
15. Missimer, M., Robèrt, K.H., Broman, G.: A strategic approach to social sustainability—Part 2: a principle-based definition. *J. Clean. Prod.* **140**, 42–52 (2017)
16. Allenby, G.M., Bradlow, E.T., George, E.I., Liechty, J., McCulloch, R.E.: Perspectives on bayesian methods and big data. *Cust. Needs Solut.* **1**(3), 169–175 (2014)

# Sustainable Supply Chain Management in Fast-Moving Consumer Goods Organizations



Yang Chen and Luisa Huaccho Huatuco 

**Abstract** This research focuses on sustainable supply chains in the fast-moving consumer goods (FMCG) sector in China. The literature review covers sustainability, sustainable development, corporate social responsibility as well as the trends in the sustainable supply chain management. The methodology consists on qualitative semi-structure interviews with managers, employees and consumers knowledgeable in sustainable supply chain management in Chinese FMCG organizations. The findings show that large FMCG organizations have set sustainability goals to adopt a series of actions on managing their supply chain, while some small FMCG organizations do not have enough capability to implement them. Furthermore, the developing trend for the sustainable supply chain is toward the use of the advanced technologies for increasing competitive advantage. A discussion of results is provided in the light of recent literature findings as well as some future research avenues are proposed.

## 1 Introduction

As all industries move towards a more sustainable future, it is becoming more and more common to understand the environment of suppliers and customers, social and economic impacts and feasibility [1]. Fast-moving consumer goods (FMCG) have a short shelf life, so they need to be sold rapidly at low cost, e.g., food and toiletries, whereas consumer goods are more durable and have a longer shelf life, e.g., furniture and electronic devices. So, the main difference between the two types is the speed at which they are sourced, produced, distributed, consumed and disposed or recycled. This paper focuses on FMCG because of their higher impact on sustainability due to the rapid rate at which planet resources are getting used, depleted and restored.

---

Y. Chen

Leeds University Business School, University of Leeds, Leeds LS2 9JT, UK

L. Huaccho Huatuco (✉)

The York Management School, University of York, York YO10 5GD, UK

e-mail: [luisa.huatuco@york.ac.uk](mailto:luisa.huatuco@york.ac.uk)

In addition, due to the rapid development of the fast-moving consumer goods (FMCG) sector in China in recent years, and that sustainability has become a major trend in supply chain research and practice, the research question in this paper is: *how are sustainable supply chain practices being implemented by Chinese FMCG organizations?*

This paper is structured as follows. Section 2 covers a literature review on sustainable supply chains, then move on specifically to FMCG sustainable supply chains. In Sect. 3, the qualitative methodology used to analyze the interviews is presented. Section 4 focuses on the findings on FMCG supply chains and trends in sustainable supply chains. Section 5 presents a discussion of the key findings in relation to relevant literature and wider industry. Finally, Sect. 6 draws some conclusions and recommendations including some limitations and avenues for future research.

## 2 Literature Review

### 2.1 Sustainable Supply Chains

The goal of sustainable supply chains is to create, protect and grow long-term environmental, social and economic values for all stakeholders involved in bringing products and services to market [2]. There is no denying that going green and becoming environmentally friendly is the future road for many organizations. Moreover, in order to cater to the future development, many organizations begin to provide products or services in a way that does not negatively affect the environment. This way will not deplete natural resources, exacerbate climate change, nor lead to social inequality or injustice [3]. One of the ways organizations achieve this sustainability agenda is to check the entire manufacturing process, from the place where raw materials are obtained to the entire process in the factory, to the use of their products or services [4].

There are three ways to help organizations make their supply chains more sustainable. Firstly, identifying key issues in the entire supply chain. Secondly, linking the organization's supply chain sustainable development goals to the global sustainable development agenda. Thirdly, helping suppliers manage their supply chain sustainability impact [5].

### 2.2 FMCG Sustainable Supply Chains

Consumers are increasingly expecting their products to be manufactured and distributed in an ethical manner without adversely affecting the environment or consuming natural resources. FMCG have the power needed for this vision to materialize, for example, [6] found that FMCG organizations that focus not only on



economic goals, but also on societal and ecological (environmental) goals, achieve more effective implementation of sustainable supply chain practices and compete more easily in the market.

Consumers are also worried about food waste and plastic packaging [7]. They want to see consumer-oriented organizations demonstrate sustainable practices in their businesses, such as focusing on human rights, limiting carbon emissions [8] and reducing the use of non-renewable energy and water. People are concerned about the seasonal supply of food and its sources. They want to limit their carbon footprint by buying local products and focusing on distributed rather than centralized supply chains [9]. In the UK, the British government indicates that it will maintain the current food safety, food labeling and food quality standards [10].

Nielsen, a market research organization, reported that 66% of the global customers surveyed were willing to pay more for sustainable commodities. Customers are looking for sustainable food that is environmentally sustainable and comes from ethical sources. While increasing the number of health and safety issues, efforts should be made to achieve zero waste and minimize the impact on the environment. Optimizing the load in the logistics process can reduce mileage, emissions and carbon footprint [11, 12]. Consumers are increasingly aware of unnecessary packaging, especially disposal of single-use plastic [13]. They are concerned about recycling to avoid polluting our oceans [14]. The FMCG industry is highly competitive, so sustainable packaging is a major driving force to reduce costs while considering environmental and social impacts [15]. Some global FMCG organizations are regarded as leaders in sustainable supply chain management, for example: Coca-Cola, Nestle, Procter & Gamble, Unilever and Nike. Table 1 presents the comparison of sustainable supply chain management between two FMCG organizations: P&G and Unilever.

**Table 1** Sustainable supply chain management in P&G [16] and Unilever [17]

Sustainable SCM	P&G	Unilever
Sustainable goal	Realize and stimulate a positive impact on the strategy	Achieve sustainable and profitable growth
Packaging	Double the amount of recycled materials used in packaging products	Providing in-package services to reduce carbon footprint
Transportation	Designing a more sustainable and cost-effective way of transporting goods	Return vehicle project reduced the carbon dioxide emission
Innovation	Its famous brands will be packaged in fully post-consumer recycled (PCR) plastic	One-year pilot project involving the use of high-knowledge technology
Cooperation with other organizations	Domtar and P&G are working together to increase the supply of FSC-certified wood fiber	JD in China and Unilever make cooperation to upgrade return vehicle project

### 3 Methodology

This study uses a qualitative methodology to analyze the data from semi-structured interviews, which included: a purchasing department manager, a warehouse staff member, a staff member in a small FMCG organization and two consumers who often purchase FMCG. Although the sample is small, it covers a wide range of roles within the supply chain from purchasing, warehousing, production, distribution as well as consumers. The interview questions are included in the Appendix.

The interviews were conducted in Summer 2019 via Skype. Table 2 summarizes the profiles of the interviewees, the purchasing manager worked in an large FMCG organization X, and the warehouse staff member worked in a large logistics organization Y in China and have business cooperation with a large FMCG organization W, while the third interviewee worked in a small FMCG organization Z in China, but this participant knows a lot about the organization's supply chain. The other two interviewees did not work at FMCG organizations, but as FMCGs consumers, they provided comments about their consumer experience.

For the analysis, 'axial coding' was followed [18: 108]. So, the reasoning moved from coding to data, as opposed to open coding when the reasoning moves from data to coding. The relationships between salient categories (axes) and sub-categories can be generated, modified, refined, elaborated or rejected through axial coding. The following steps were followed: list of codes, data collection, data needed to fill categories, axial coding (describing categories) and list of categories. For the reassembling phase of the analysis, the 'constructing arguments' principles were used [19: 157].

**Table 2** Profiles of interviewees

Interviewee	Industry sector	Organization code	Job	Years of experience	Length of interview
Manager	Purchasing department	X (large FMCG organization)	Purchasing manager	3 years	1 h
Staff A	Warehouse	Y (large logistics organization)	Warehouse staff	4 years	50 min
Staff B	Organization's operation department	Z (small FMCG organization)	Office worker	8 years	45 min
Consumer A			Student		30 min
Consumer B			Student		30 min

## 4 Findings

### 4.1 FMCG Sustainable Supply Chains

For sustainable supply chain management, different roles with different organizations have different views. The first question was about the sustainable goal of an organization. The purchasing manager said their sustainability goal was to reduce environmental pollution in supply chain. The purchasing manager said:

Sometimes, people often think that small organizations always produce fake and inferior products, and the environmental pollution is relatively high, but in fact, large organizations, even the world's top 500 organizations, really cause the greatest harm to the environment. [Purchasing Manager, organization X]

Because the total production of large organization is very large, the additive effect of environmental damage is also very large. Many organizations purchase or produce raw materials which contain types and quantities of chemicals which may cause great pollution. For example, in China, the raw materials for plastic recycling used by many large organizations are waste plastics from various industries and families. Their sources and varieties are very complex, and various pollutants may include in these raw materials. When producing these plastics, emissions in the production process destroy the balance of the surrounding natural environment. The purchasing manager talked about a series of measures taken by organization X to reduce environmental pollution:

Organization X's washing products in China do not contain phosphorus. The organization has developed a series of phosphorus-free technologies, and the use of various detergents will be described in detail in the product description. The pigment and essence in detergent have a limited impact on the environment. At the same time, as part of the material research, the essence and pigment consumers use can be safely degraded through environmental bio-degradation assessment tests and will not cause adverse effects on the environment. [Purchasing Manager, organization X]

The purchasing manager said organization X's vision is to completely change the way of dealing with the waste. At present, organization X has already achieved the goal of zero landfill of production waste in nine factories. Although waste generation is inevitable, it can be recycled for reproduction or sold to a third party to produce other materials to achieve zero landfill. When asked how difficult is it for the organization to implement sustainable supply chain management, the manager said that for organization X, to implement these measures, it needs to continuously bring in high-tech talents and technologies, and this problem is the biggest difficulty for them.

Since 2010, organization X has implemented the supplier scorecard for environmental sustainability, which aims to track and encourage suppliers to take the initiative to improve and innovate on environmental issues. In the first year, organization X does not require suppliers to complete scorecards, but in 2011, scorecards were included in the supplier rating assessment, which affected them to conduct

more businesses with organization X. The selection of suppliers needs comprehensive consideration. Under the same circumstances, organization X could prefer to choose those environmentally friendly organizations.

Staff A worked in a large logistics organization Y in China, and this organization has business cooperation with FMCG organization W. Staff A did not know the sustainability goals of organization W. But according to the information provided by their Web site of organization W, their sustainability supply chain goal is to save energy. As said by staff A:

Organizations Y and W make cooperation to upgrade return vehicle project to build green supply chain. Organization Y's logistics timeliness is mainly realized by the national warehouse distribution network. Business stores choose the appropriate warehouse layout according to their own needs. Large businesses have a wide range of sales coverage. In order to enable consumers across the country to receive goods in short time, they can choose to place the goods in organization Y's eight Regional Logistics Centers, thus covering the whole country and achieving the best timeliness. Upgrading return vehicle project greatly improves the efficiency of logistics operation and reducing carbon dioxide emissions. [Staff B, organization Y]

According to the news, the return vehicle project completed 150 times of transportation in seven months, which not only saved the end-to-end logistics cost, but also reduced the carbon dioxide emission by 215 tons. In addition, the implementation of the return car project can also improve the efficiency of logistics operation, increase the stock of organization Y warehouse, and further drive the overall sales volume. Organizations Y and W's return car project is a big innovation for organization W in the field of sustainable supply chain. In the future, the whole chain from commodity production packaging, warehousing to delivery, transportation and distribution will improve the utilization rate of resources, reduce end-to-end costs and reduce waste of resources, thus achieving the goals of energy conservation, consumption reduction, low carbon and environmental protection and maximizing the green effect.

In terms of the difficulty, Staff A talked about some of his views, he thought that need to cooperate with local large logistics organizations to develop green logistics in China. Otherwise, it is difficult to make a big breakthrough in logistics field by itself.

The third interviewee is staff B who worked in a small FMCG organization Z, and she has worked in this field for nearly ten years. When talking about the sustainability supply chain goal of the organization, she said the organization did not have specific targets for a sustainable supply chain and the only goal for her organization is to make profit. But surprisingly, the organization has adopted some measures in the sustainable supply chain. This organization chose to cooperate with other small organizations when transporting goods to the same place to save costs, and this action reduces carbon dioxide emissions from the perspective of a sustainable supply chain. This action is similar to organization W's green logistics approach, but their goal is not similar. To organization W, corporate social responsibility is what they must fulfill, but to a small organization, making profit is what they only focus on. About the difficulty, staff B said that the manager in this organization is not aware of developing a sustainable supply chain. Although everyone knows this concept, how

**Table 3** Summary of interviewees’ comments

Axial codes	Manager	Staff A	Staff B	Consumers A and B
	Organization X	Organization Y	Organization Z	
Sustainability goal of the organization	Reduce environmental pollution	Save energy	Organization Z do not have sustainability goals	Unknown
Specific actions taken by an organization	Washing products do not contain phosphorus.	Upgrade return vehicle project	Cooperate with other organizations during transporting	Consumer A: the packaging had become environmentally friendly
				Consumer B: the products are delivered from the nearby warehouse to save energy
The difficulty of take actions	Bring in high-tech talents and technologies	Seek for other organizations to cooperate in China	Not aware of developing sustainability	Unknown

to survive in the market is the most important thing for small organizations. Table 3 presents the summary of interviews.

### 4.2 Trends in Sustainable Supply Chains

For the warehouse staff in local logistics organization, the trends in sustainable supply chain are in line with the development of China. Traditional logistics only pays attention to the forward logistics from resource exploitation to production and consumption and ignores the reverse logistics formed by the recycling of waste materials and renewable resources. Recycling logistics includes recycling of raw materials by-products, recycling of packaging waste, recycling of waste materials, collection and recycling of resource waste, etc.

There is still a big gap between China’s green logistics and that of developed countries. However, as currently, some of the world’s major logistics organizations have entered China, and multinational logistics organizations are rushing into the Chinese market. As China’s economy has become a part of the global economy, it is necessary to speed up the green logistics, and logistics organizations must speed up the adjustment and integration. Otherwise, they will lose their competitiveness. It can be said that the development of green logistics is an important basis for participating in global logistics competition. Staff A gave the following suggestion:

Organizations in China should strengthen the establishment of green logistics concept and the implementation of sustainable supply chain management to realize the promotion of organization's interests, personal interests and national interests. [Staff B, organization Y]

Staff B does not have any views about the trends in global supply chain, but she hopes that small organizations will have the ability to develop sustainable supply chain practices.

## 5 Discussion

The research question in this study was: *how are sustainable supply chain practices being implemented by Chinese FMCG organizations?* From the findings, FMCG organizations have implemented sustainable supply chain management in various aspects. As mentioned in the interview results, many large FMCG organizations set their sustainability goals and have taken many actions. Many of these organizations focus on reducing waste, because with the development of the economy, waste has always been a high concern in society. Large organizations usually create economic effects and environmental effects simultaneously. They have the ability to save costs and protect the environment at the same time in the process of achieving sustainability goals. Therefore, for large FMCG organizations, the implementation of sustainable supply chain needs to set goals first, and then take corresponding measures according to the goals. However, for small FMCG organizations, there is no additional capacity to achieve sustainable development at this stage. In order to implement sustainable supply chain strategy, FMCG organizations should continuously improve their supply chain management capability. Because FMCG organizations have their own unique historical background and their own supply chain strategies are not easy to be imitated, they can have certain competitive advantages in the market [20].

In the process of implementing the sustainable supply chain, FMCG organizations will generate economic, social and environmental impacts. One of the most obvious impacts is the environmental one. As mentioned before, many organizations have aimed to reduce waste, zero discharge water waste, and these actions are effective in protecting the environment.

For FMCG organizations, the implementation of sustainable supply chain practices requires a large amount of investment [21]. This will correspondingly reduce the expenses of the organization in other aspects and will have negative impact on the sales and operation of its products. Especially for small FMCG organizations, the implementation of sustainable supply chain could bring a negative influence on the organization's operation. Therefore, considering these shortcomings, the organization should have enough capabilities to effectively develop a sustainable supply chain.

In terms of the similarity between this study and past research, many large organizations have set sustainability goals, which is consistent with the responses given by the interviewees. In the explanation of the trend of the supply chain, both this study and previous research have mentioned that the customer–supplier relationship plays an important role in the improvement of the supply chain. In order to establish a truly sustainable partnership, FMCG organizations need to establish a stronger customer–supplier relationship.

Concerning the differences between this study and previous research, we know that more consumers are concerned about plastic waste and have taken many measures about recycling. However, during the interviews, organizations X and Y focused more on the use of raw materials and gas emissions reduction in transportation. Regarding the trend of sustainable supply chain, interviewees not only noticed the improvement of customer–supplier relationship which also is included in the literature, but also turned their attention to the role of science and technology.

## 6 Conclusions

For FMCG organizations, developing sustainable supply chain practices is a challenge. Based on the pros and cons in this study, the following conclusions are made:

1. Large FMCG organizations need to disseminate the concept of sustainable supply chains so that employees can have a deeper understanding of what it entails.
2. FMCG organizations need to strengthen their information systems to ensure correct information exchange in the supply chain process. Because in many sections of the supply chain, cooperation with other organizations is involved, and accurate and timely information exchange is required under these circumstances.
3. Although small FMCG organizations do not have enough capacity to develop sustainable supply chains, they can study it through cooperation with large organizations.
4. Future trends show that consumers will be more and more inclined to buy environmentally friendly products, so small organizations need to continuously improve themselves in order to survive in the market.

The limitations of this study include the small sample size and the topic may appear too broad. So, in the future research, the sample size would need to be increased and an aspect of sustainability in supply chains could be chosen. Additionally, other methodologies could be used, such as survey questionnaire. Another future research avenue could investigate how the sustainable supply chain practices of large FMCG organizations can be better diffused to the small FMCG organizations' context.

## Appendix

### Interview topics and questions

Topics	Questions
Sustainable supply chain management (SCM)	What is the sustainable goal of an organization, and how to link the goal with its actions?
	How to help organizations to achieve effective sustainable supply chain management? and give some examples.
	How difficult do you think it is for the organization to implement sustainable supply chain management?
Trends in sustainable SCM	Could you tell us the development trend of sustainable supply chain management in the future?

## References

- Castillo, V.E.: Supply chain integrity: a key to sustainable supply chain management. *J. Bus. Logist.* **39**(1), 38–56 (2018)
- Rogers, D.S.: Sustainability is free: the case for doing the right thing. *Suppl. Chain Manage. Rev.* **15**(6), 10–17 (2011)
- Carter, C.R., Rogers, D.R.: A framework of sustainable supply chain management: moving toward new theory. *Int. J. Phys. Distrib. Logist. Manage.* **38**(5), 360–387 (2008)
- Golicic, S.L., Smith, C.D.: A meta-analysis of environmentally sustainable supply chain management practices and firm performance. *J. Suppl. Chain Manage.* **49**(2), 78–95 (2013)
- Klassen, R.D., Vereecke, A.: Social issues in supply chains: capabilities link responsibility, risk (opportunity), and performance. *Int. J. Prod. Econ.* **140**(1), 103–115 (2012)
- Liczmańska-Kopcewicz, K., Mizera, K., Pyplacz, P.: Corporate social responsibility and sustainable development for creating value for FMCG sector enterprises. *Sustainability* **11**(5808), 1–14 (2019)
- Lan, Z., Daiwei, H.: Sustainable logistics network modeling for enterprise supply chain. *Math. Probl. Eng.* **47**, 1–11 (2017)
- Theißen, S., Spinler, S., Huchzermeier, A.: Reducing the carbon footprint within Fast-moving consumer goods supply chains through collaboration: The manufacturer's perspective. *J. Suppl. Chain Manage.* **50**(4), 44–61 (2014)
- Angeles-Martinez, L., Theodoropoulos, C., Lopez-Quiroga, E., Fryer, P.J., Bakalis, S.: The honeycomb model: A platform for systematic analysis of different manufacturing scenarios for fast-moving consumer goods. *J. Clean. Prod.* **193**, 315–326 (2018)
- Brindley, C., Oxborrow, L.: Aligning the sustainable supply chain to green marketing needs: a case study. *Ind. Mark. Manage.* **43**(1), 45–55 (2014)
- Colicchia, C., Melacini, M., Perotti, S.: Benchmarking supply chain sustainability: insights from a field study. *Benchmarking* **18**(5), 705–732 (2011)
- Colicchia, C., Creazza, A., Dallari, F.: Lean and green supply chain management through intermodal transport: insights from the fast-moving consumer goods industry. *Prod. Plann. Control* **28**(4), 321–334 (2017)



13. Ma, X., Park, C., Moultrie, J.: Factors for eliminating plastic in packaging: The European FMCG expert's view. *J. Clean. Prod.* **256**, 1–20 (2020)
14. Magnier, L., Mugge, R., Schoormans, J.: Turning ocean garbage into products—consumer's evaluations of products made of recycled ocean plastic. *J. Clean. Prod.* **215**, 84–98 (2019)
15. Delai, I., Takahashi, S.: Corporate sustainability in emerging markets: insights from the practices reported by the Brazilian retailers. *J. Clean. Prod.* **47**, 211–221 (2013)
16. P&G. P&G environmental sustainability. Available from: <https://us.pg.com/environmental-sustainability/>. Accessed 26 May 2020
17. Unilever. Sustainable Living. Available from: <https://www.unilever.com/>. Accessed 26 May 2020
18. Boeije, H.: Analysis in qualitative research. SAGE Publications Ltd., London (2010)
19. Charmaz, K.: Constructing grounded theory. A guide through qualitative analysis. SAGE Publications Ltd, London (2006)
20. Lu, C.: Walmart's successful supply chain management. <https://www.tradegercko.com/blog/supply-chain-management/incredibly-successful-supply-chain-management-walmart> (2018). Accessed on 26 May 2020
21. Davis-Peccoud, J., Duchnowski, S.: Working with suppliers for sustainable food supply chains. Bain Company. Brief available at: <https://www.bain.com/insights/working-with-suppliers-for-sustainable-food-supply-chains/> (2018). Accessed on 26 May 2020

# Test Stand for Metamaterials Dynamic Properties Examination



Knitter Remigiusz , Blazejewski Andrzej , Krolikowski Tomasz ,  
Zmuda Trzebiatowski Piotr , and Zuchniewicz Jerzy 

**Abstract** Experiments and computer studies on metamaterial issues allow to improve designing of entire devices using 3D CAD technology and finite element methods. Research and their effects are aimed at replacing the mechanisms by the elements made with additive technology. The technology enables using the same metamaterial producing the device or part with various internal structures. While maintaining identical dimensions, the internal structure of the device affects the properties, particularly dynamic properties. For this purpose, apart an appropriate computer model, the particular test is required for rapid and effective prototyping. Therefore, in the paper, the test stand consisted on: The signal generator, the vibration generator and laser vibrometer are proposed. The following is the post for preliminary experimental research.

## 1 Introduction

The fused deposition modeling (FDM) technology is part of a family of incremental manufacturing technologies. Its development began with the invention by Statasys Ltd. and the 1989 the patented [1]. STL file system and the first 3D printer [2]. FDM technology uses polymer thermoplastics, i.e., plastics of the production class. It is the most widely distributed and available on the market in many varieties and colors. The most common is acrylonitrile-co-butadiene-co-styrene (ABS). The rapid development of this method allowed to introduce many more new materials such as: PET-G, PLA, PVA, TPU, PEEK or HIPS, for complex models' production and manufacturing. Currently, FDM technology is very popular, because of cheap 3D printers' availability on the market [3]. The low price does not reduce its usability in industrial applications. The pursuit of production usable objects together with

---

K. Remigiusz · B. Andrzej · K. Tomasz (✉) · Z. T. Piotr  
FM, Koszalin University of Technology, Sniadeckich str. 2, Koszalin 75-453, Poland  
e-mail: [tomasz.krolikowski@tu.koszalin.pl](mailto:tomasz.krolikowski@tu.koszalin.pl)

Z. Jerzy  
Alplast sp. z.o.o, Niekanin Sliwkowa 1, Niekanin 78-100, Poland

the development of FDM methods and computational tools allow us to anticipate and design desirable properties and characteristics of the products. In recent years, many articles have been published regarding the testing of mechanical properties of structures manufactured using FDM technology and polymeric materials. Dawoud et al. compared the mechanical properties of standard samples produced applying injection molding and incremental technology. The authors broadly discussed the effects of the gap between fibers of the material and their angle, which occurs at the production. It depends on the material application density and the direction of material application. In this way, the whole product is built up in distinguishing particular layers. Similar research has been published by Sood et al. [4, 5]. In their work, they also took into account the height of the layer and the orientation of the generated sample in the working space of the machine. They omitted and did not take into account the negative aspects of the gap between adjacent fibers. Authors applied the surface response method using the results of the planned experiment. They also presented other approach to mechanical properties prediction, based on neural networks. It demonstrated the greater ability to model the nonlinear features of the product. By contrast, Casavola et al. used the classical theory of laminates to prepare and apply the model of produced in FDM technology structure. In the studies, they confirmed the orthotropic character of the strength properties of the products [6–10].

Proposed test stand brings possibility of mechanical test but authors are considering testing other properties of 3D printed parts and articles. For example, discussed by Dobrzyńska a fire safety [11] and toxic hazards [12, 13]. The other issue is thermal conductivity presented by Nikończuk et al. [14, 15]. Thermal conductivity is helpful in heat recovery units presented by Królikowski et al. [16].

Taking into consideration the above-mentioned aspects, the aim of this work is to initiate discussions on metamaterials' specific prosperities, introduced using the additive method [17, 18]. On one hand, there are developed parametric numerical models, designed thanks to advanced CAD and FEM methods [19–21]. They support prediction of the mechanical properties of metamaterial structures already. On the other hand, in order to create the adequate metamaterial structure model, additional effort has to be made, in comparison with isotropic materials. Therefore, often enough, it is demanded to modify the model parameters with the information supplied by an experimental data.

Process of additive production releases a lot of low temperature waste heat. Similar problem applies to painting technologies. Heat recovery in spray booth was discussed by Nikończuk [22, 23], and he also considered reliability of heat recovery unit [15, 24]. Particle emission in 3D printing was discussed by Królikowski [5]. Low temperature heat recovery was proposed by Adamkiewicz et al. [25].

Sustainable technologies also include waste management and it applies to solids and liquids. Waste fluids management was discussed by Ubowska et al. [19, 26].

## 2 The Test Stand Design and Conception

The stand has been designed and made based on experience after the modeling of elements with a metamaterial structure. The tests have carried out using the stand, which verifies the structure properties such as: vibration damping abilities, critical deformation or modal identification. The stand's concept is relatively simple and introduces an input-output procedure. The input, which assumes a proper excitation (load) of the examined, particular structure and eventually the measurements and analyses of the deformation velocity are shown as the output. Therefore, the owned Frederiksen vibration generator and the self-made test supporting frame (Fig. 4) were used as the main parts of the test stand (Figs. 1 and 2).



Fig. 1 Vibration generator Frederiksen 2185.00—main view

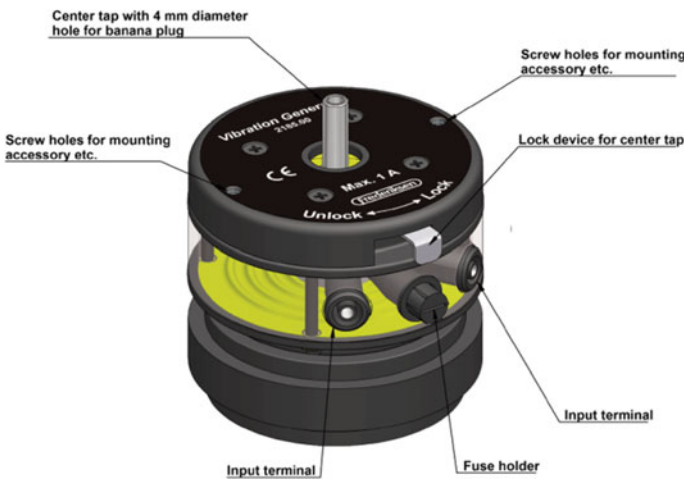


Fig. 2 Vibration generator Frederiksen 2185.00—inputs and vibration output

The proper excitation periodic signal (harmonic, square, triangular) can be induced by using signal generator Frederiksen 2502.50 (Fig. 3) and finally transferred to the vibration generator. The vibrator is used to convert electrical impulses from the signal generator to mechanical vibrations. The signal from the generator supplies the coil, placed in the magnetic field produced by the cylindrical magnet (Fig. 4).

In the end, vibratory tests were performed by measuring the tested samples deformation velocity, i.e., output. The deformations were generated as the result of input load. Next, this impact taken over and absorbed with the examined element and was measured on the base of the laboratory instrument without the use of a vibrating

**Fig. 3** Laboratory stand-signal generator [30]



**Fig. 4** Test stand with the tested element



**Fig. 5** VH 300+ , laser vibrometer for vibration velocity measurements



element (accelerometers), thanks to the Ometron VH 300+ laser vibrometer. Preliminary tests were used to compare the effect of different metamaterial application and, in this way, different structures of designed vibro-isolator (Fig. 5).

### 3 Test Sample Geometry and Material Characteristics

In the first phase of the research, it was necessary to examine the material and confirm the hypothesis about the influence of internal structures on mechanical properties. The test samples were made using TPU rubber-like material with the following properties (Fig. 6; Table 1).

The metamaterial test sample has a deformable structure and active elements that can be controlled and simulated using the finite element method. In some aspects, the examined sample resembles a composite, in which the reaction between the constituent materials, the shape and arrangement of the component materials are controlled dynamically, so that it affects the mechanical properties of the metamaterial. The presented research is a preliminary stage of work on the durability and vibro-isolation examination of elements printed on spatial printers in various technologies. At this stage, the fused deposition model method (FDM) was considered. PET material admixed with metal powders was obtained for the production of initial prototypes. All these solutions were made for scientific purposes to select the most advantageous sample in terms of the price of production and obtaining material from recycling sources. After testing the samples printed and subjected to destruction in static tearing, the construction of this stand started. Hereby, the dynamic (vibration) feature of the test stand was developed.

**Fig. 6** Tested element (vibro-isolator)

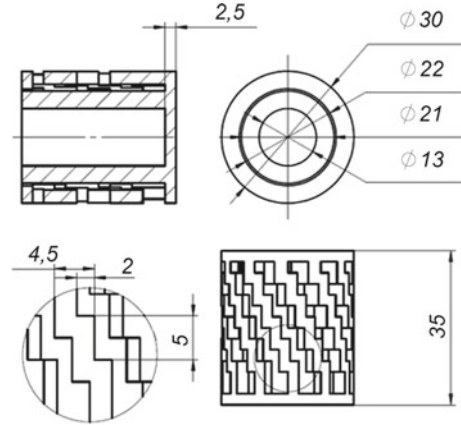


**Table 1** Specification of material used for testing

Properties	ASTM No	Units	Material
Hardness	D2240	Shore D	40
Density	–	g/cm <sup>3</sup>	1.16
Water absorption	D570	%	0.6
Mold shrinkage	D955	%	0.8
Tensile stress at 10% strain	D638	kg/cm <sup>2</sup>	44
Tensile stress at break	D638	kg/cm <sup>2</sup>	270
Elongation at break	D638	%	680
Flexural modulus	D790	kg/cm <sup>2</sup>	680
Tear strength	D1004	kN/m	115
Izod impact strength/notcher	D256	kg * cm/cm	N.B.
Resilience	D2632	%	57
Melting point	D3418	OC	157
HDT	D648	OC	70
Resistance to surface abrasion	D1044 (wheel H-19)	Mg	95

## 4 Conclusions

Computer modeling [15, 27–29] using the FEM method and the experimental test shows that metamaterials can be introduced relatively easily in the design process, even if these material properties are described as orthotropic. Linear elastic, isotropic

properties with plasticity give acceptable results. The test stand was used to determine the tensile strength diagrams of chosen samples. Taking into account, the values and shapes, both diagrams obtained from experiments and modeling converge. The measuring stand has been self-built and is at the stage of testing and comparing the results. Thanks to the possibility of experimental research on metamaterial mechanisms, we will be able to learn and model the internal structure to achieve the desired effects. The development of these designing and modeling methods definitely contributes to the growth of the number of elements, made using 3D printing, in order to replace classic mechanical units.

## References

1. Patent US 5 121 329 (1989)
2. Dziejewit, P., Janiszewski, J.: Ocena jakościowa procesu deformacji regularnych struktur komórkowych wykonanych techniką druku 3D. *Mechanik* 3/2018s. 250–252 (2018)
3. Kinsler, P., McCall, W. The Futures of Transformations and Metamaterials. Blackett Laboratory, Imperial College London, London
4. Knitter, R., Królikowski, T.: Mechanical metamaterial manufactured by increasing technology. *Mechanik* 7 502–504 (2018). <https://doi.org/10.17814/mechanik.2018.7.65>
5. Krolikowski, T., Knitter, R., Blazejewski, A., Glowinski, S., Kaminski: Emission of particles and VOCs at 3D printing in automotive. In: Ball, P., Huaccho Huatuco, L., Howlett, R., Setchi, R. (eds.) *Sustainable Design and Manufacturing 2019. KES-SDM 2019. Smart Innovation, Systems and Technologies*, vol. 155 (2019). Springer, Singapore
6. Krolikowski, T., Knitter, R., Blazejewski, A.: Computer modeling and testing of structural metamaterials. 4–5 September 2019 “23rd International Conference on Knowledge-Based and Intelligent Information & Engineering Systems” *Procedia Computer Science* (2019). ISSN: 1877-0509 <https://doi.org/10.1016/j.procs.2019.09.429> (poz. 841 konf. punkt. 70)
7. Qi, H.J., Joyce, K., Boyce, M.C.: Durometer hardness and the stress-strain behavior of elastomeric materials. *Rubber Chem. Technol.* **76**(2), 419–435 (2003)
8. Schumacher, C., Bickel, B., Rys, J., Marschner, S., Daraio, C., Gross, M.: Microstructures to control elasticity in 3D printing. *ACM Trans. Graph.* **34**, 4 (2015)
9. Yu, X., Zhou, J., Liang, H., Jiang, Z., Wu, L.: Mechanical metamaterials associated with stiffness, rigidity and compressibility: a brief review. *JMPS* **486**, 12/2017 (2017). *Progress in Material Science*
10. Zhao, Y., Lei, C., Patterson, J.C.: PIV measurements of the K-type transition in natural convection boundary Layers. *Exp. Thermal Fluid Sci.* **101**, 62–75 (2019). <https://doi.org/10.1016/j.expthermflusci.2018.09.007>
11. Dobrzyńska, R.: The impact of equipment materials on the fire safety of coaches. In: Ball, P., Huaccho Huatuco, L., Howlett, R., Setchi, R. (eds.) *Sustainable Design and Manufacturing 2019. KES-SDM 2019. Smart Innovation, Systems and Technologies*, vol. 155. Springer, Singapore (2019)
12. Afshar-Mohajer, N., Wu, C.-Y., Ladun, T., Rajon, D.A., Huang, Y.: Characterization of particulate matters and total VOC emissions from a binder jetting 3D printer. *Build. Environ.* **93**, 293–301 (2015)
13. Dobrzyńska, R.: Selection of outfitting and decorative materials for ship living accommodations from the point of view of toxic hazard in the initial phase of fire progress. *Polish Maritime Res* **16**(2), 72–74 (2009). <https://doi.org/10.2478/v10012-008-0025-5>
14. Nikończuk, P., Dobrzyńska, R.: Preliminary measurements of overspray sediment’s thermal conductivity. *Ochrona przed korozją*, **61**(2), 40–42 (2018). <https://doi.org/10.15199/40.2018.2.3>



15. Nikończuk, P.: Preliminary modeling of overspray particles sedimentation at heat recovery unit in spray booth. *Eksploatacja i Niezawodność—Maintenance and Reliability* **20**(3), 387–393 (2018). <http://dx.doi.org/10.17531/ein.2018.3.6>
16. Królikowski, T., Nikończuk, P.: Finding temperature distribution at heat recovery unit using genetic algorithms. *Proc. Comput. Sci.* **112**(2017), 2382–2390 (2017). <https://doi.org/10.1016/j.procs.2017.08.100>
17. Krolkowski, T., Knitter, R., Stachnik, M.: Thermo-mechanic tests using 3d printed elements. 4–5 September 2019 “23rd International Conference on Knowledge-Based and Intelligent Information & Engineering Systems” *Procedia Computer Science* (2019). ISSN: 1877-0509 <https://doi.org/10.1016/j.procs.2019.09.430> (poz. 841 konf. punkt. 70)
18. Novakova-Marcincinova, L., Novak-Marcincin, J.: Testing of materials for rapid prototyping fused deposition modelling technology. *World Acad Sci Eng Technol* **70**, 2012 (2012)
19. Jakubowski, M., Stachnik, M., Sterczyńska, M., Matysko, R., Piepiórka-Stepuk, J., Dowgiałło, A., Ageev, V., Knitter, R.: CFD analysis of primary and secondary flows and PIV measurements in whirlpool and whirlpool kettle with pulsatile filling: Analysis of the flow in a swirl separator. *J. Food Eng.* **258**, 27–33 (2019)
20. Kaminski, K., Krolkowski, T., Blazejewski, A., Knitter, R.: Significant parameters identification for optimal modelling of the harp type flat-plate solar collector. In: Ball P., Huaccho Huatuco L., Howlett R., Setchi R. (eds.) *Sustainable Design and Manufacturing 2019. KES-SDM 2019. Smart Innovation, Systems and Technologies*, vol. 155. Springer, Singapore (2019)
21. Kaminski, K., Znaczko, P., Lyczko, M., Krolkowski, T., Knitter, R.: Operational properties investigation of the flat-plate solar collector with poliuretane foam insulation. 4–5 September 2019 “23rd International Conference on Knowledge-Based and Intelligent Information & Engineering Systems” *Procedia Computer Science* (2019). ISSN: 1877-0509 <https://doi.org/10.1016/j.procs.2019.09>
22. Nikończuk, P.: Study of heat recovery in spray booths. *Metal Finish* **111**(6), 37–39
23. Nikończuk, P.: Preliminary analysis of heat recovery efficiency decrease in paint spray booths. *Trans. IMF* **92**(5), 235–237 (2014). <https://doi.org/10.1179/0020296714Z.000000000200>
24. Nikończuk, P., Rosochacki, W.: The concept of reliability measure of recuperator in spray booth. *Eksploatacja i Niezawodność—Maintenance and Reliability* **22**(2), 265–271 (2020). <http://dx.doi.org/10.17531/ein.2020.2.9>
25. Adamkiewicz, A., Nikończuk, P.: Waste heat recovery from the air preparation room in a paint shop. *Archiv Thermodyn* **40**(3), 229–241 (2019). <https://doi.org/10.24425/ather.2019.130003>
26. Ubowska, A., Olawa, M.: Selection of sorbents for removing operating fluids at the vehicle dismantling station. In: Ball, P., Huaccho Huatuco, L., Howlett, R., Setchi, R. (eds) *Sustainable Design and Manufacturing 2019. KES-SDM 2019. Smart Innovation, Systems and Technologies*, vol 155. Springer, Singapore (2019)
27. Krolkowski, T., Suslow, W.: Analityczny projekt informatyzacji przedsięwzięcia szkoleniowego. *ZNWEiI: 5–23 PK Koszalin 2019* (2019)
28. Krolkowski, T., Suslow, W.: A concept of a training project IT management system. 4–5 September 2019 “23rd International Conference on Knowledge-Based and Intelligent Information & Engineering Systems” *Procedia Computer Science* (2019). <https://doi.org/10.1016/j.procs.2019.09.317>. ISSN: 1877-0509 (poz. 841 konf. punkt. 70)
29. Zając, W., Andrzejewski, G., Krzywicki, K., Królikowski, T.: Finite state machine based modelling of discrete control algorithm in LAD diagram language with use of new generation engineering software. In: *23rd International Conference on Knowledge-Based and Intelligent Information & Engineering Systems*, 4–5 September 2019. *Procedia Computer Science* (2019). ISSN: 1877-0509. <https://doi.org/10.1016/j.procs.2019.09.431>
30. Glowinski, S., Andrzej, B., Krolkowski, T., Knitter, R.: Gait recognition: a challenging task for MEMS signals identification. *Sustainable*. In: Ball, P., Huaccho Huatuco, L., Howlett, R., Setchi, R. (eds.) *Sustainable Design and Manufacturing 2019. KES-SDM 2019. Smart Innovation, Systems and Technologies*, vol. 155. Springer, Singapore (2019)

# An Association Rule-Based Approach for Storing Items in an AS/RS



Sara Antomarioni , Maurizio Bevilacqua ,  
and Filippo Emanuele Ciarapica 

**Abstract** Warehouse management activities are critical from an organizational point of view since they can cause a sensitive loss of efficiency. When dealing with automated storage and retrieval systems, the allocation of items to a specific storage cell is a challenging issue since it is the unique modifiable variable due to the constructive characteristics of the warehouse. The vast amount of data available in this field allows the development of policies for an efficient allocation of the items through the development of data mining-based approaches. In this perspective, the current work proposes a roadmap for the allocation of items to the storage cells of an automated storage and retrieval system through the association rule mining. The procedure is, at first, generally described, and, then, applied to the case study of a shoe manufacturer.

## 1 Introduction

In the current operating scenario, the information sources used by organizations are required to deal with a large amount of data related to the operations field [1]. Understanding such data is the key to successful development in terms of organizational performance, but the traditional statistical techniques are no more sufficient to pursue this aim. For this reason, there is a growing focus on the application of data mining (DM)-based techniques to manage them.

Warehouse management represents one of the key activities from an organizational point of view: Indeed, any kind of inefficiency at this level may compromise the downstream processes [2]. As noted by several researchers (e.g., [3–5]), the picking activity is one of the more wasteful activities in the management of a warehouse.

---

S. Antomarioni (✉) · M. Bevilacqua · F. E. Ciarapica  
Università Politecnica delle Marche, Ancona, Italy  
e-mail: [s.antomarioni@pm.univpm.it](mailto:s.antomarioni@pm.univpm.it)

M. Bevilacqua  
e-mail: [m.bevilacqua@staff.univpm.it](mailto:m.bevilacqua@staff.univpm.it)

F. E. Ciarapica  
e-mail: [f.e.ciarapica@staff.univpm.it](mailto:f.e.ciarapica@staff.univpm.it)

Hence, a challenging research goal is to apply strategies for reducing such wastes. In this perspective, the aim of the current work is proposing a procedure for items' allocation in an automated storage and retrieval system (AS/RS). Indeed, in the case of a traditional picker-to-part approach, there are several variables to act on to improve the performance of the picking process, e.g., changing the picking routes or re-engineering the layout of the warehouse. In the case of an AS/RS, instead, the layout is constrained by the construction features of the machine; an interesting solution is characterized by the possibility of aggregating items frequently picked together in close areas in order to reduce the picking time.

Hence, considering the benefits of both extracting useful information from a large amount of data and improving the efficiency of the picking process, the objective of this work is defining a procedure for storing items in an AS/RS using a well-known DM technique—the association rule mining (ARM). This technique, indeed, allows the identification of the relationships among items frequently picked together by analyzing a historical dataset. Specifically, the picking frequency of each item is determined by calculating the support metric, while the confidence metric defines the matching of the items in the stock keeping unit. The use of both the metrics and the application to an AS/RS differentiates the current work from the existing literature; indeed, in [6], a similar procedure aiming at batching the order picking is applied to a manual warehouse, taking into consideration only the support metric.

In the following sections, a brief theoretical background on warehouse management policies is provided, then the methodology is described (Sect. 3) and applied to a case study (Sect. 4) to improve the understandability of the proposed approach. Discussion and final remarks are provided in Sect. 5.

## 2 Background

AS/RSs are widely used for storing and retrieving raw, semi-finished or finished items since the 1950s because of the benefits driven by the full automation [7]. In the existing literature, the principal objectives proposed by researchers can be classified into three categories: improving the operating efficiency, minimizing costs and minimizing picking distances [8]. Researchers provided different approaches to pursue these aims: for example, [7] found that the dedicated storage assignment policy increases retrievals' efficiency, at the expense of the utilization rate, while random storage assignment policies are characterized by high space utilization rates [9]. Other approaches regard class-based [10, 11] or full-turnover-based policies [12].

A wide range of techniques can be applied to optimize warehouse operations. For example, simulated annealing is used in [13, 14], while a genetic algorithm is proposed in [15]. Swarm intelligence-based approaches also have space in this field of research, such as ant colony optimization [16] and particle swarm optimization [17]. Other data-driven techniques are also applied to address this issue. In [18], the allocation of the stock keeping units is based on a correlation and cluster analysis of frequently picked items; in [8], the clustering is performed considering the support

(i.e., probability of picking) of the items frequently picked together and its application is performed on a traditional manual warehouse. In [6], the association rule mining is used for aggregating order metrics, basing on the support metric. In [19], instead, multidimensional scaling and ARs are used for locating items in the same aisle, also considering the vehicle routing problem.

Existing literature contributions highlight the interest of the research community toward the application of DM-based policies for warehouse improvement and management. In this sense, the current work represents a promising application of the association rule mining to define the position of the items in an AS/RS characterized by trays that can store different items.

### 3 Research Approach

The research approach proposed in this study aims at creating a guideline for capitalizing on the benefits brought by a data mining technique, i.e., the association rule mining [20], and applying it to solve a real problem. Indeed, the storage of a large number of components under the hypothesis of constrained space can be critical for the correct warehouse management. In the following sub-sections, the basics definitions of the association rule mining are described and, then, the implementation of the research approach is detailed.

#### 3.1 Association Rule Mining

The association rule mining (ARM) is a methodology aiming at the extraction of interesting, previously unknown, hidden relations from large amounts of data [21]. The ARM can provide valid support in the data understanding process and, thus, in the decision making, through the identification of attribute-value conditions frequently occurring together [22, 23].

Let  $B = \{b_1, b_2, \dots, b_n\}$  be a set of Boolean items and  $T = \{t_1, t_2, \dots, t_D\}$  be the set of all transactions. Each transaction  $t_i$  contains a set of items  $(i_1, i_2, \dots)$ , hereafter *item-set*, taken from  $B$ . In order to contextualize the definitions provided, and  $b_k$  represents the picking of an item  $i_k$ ; a transaction, instead, is defined as the set of items picked during a unique picking process.

An implication in the form  $\alpha \rightarrow \beta$  is an association rule (AR) if both  $\alpha$  and  $\beta$  are item-sets belonging to  $B$ , and their intersection set is null (i.e., they have no items in common).  $\alpha$  and  $\beta$  are, respectively, named body and head of the rule. Several metrics can be determined to define the goodness of an AR. For the aim of this study, the following ones are introduced:

$$S(\alpha\beta) = \frac{\#\{\alpha \cup \beta\}}{T} \quad (1)$$

$$C(\alpha\beta) = \frac{S(\alpha, \beta)}{S(\alpha)} \quad (2)$$

Equation (1) is the expression of the support ( $S(\alpha, \beta)$ ) of the rule  $\alpha \rightarrow \beta$ : it is calculated as the probability of finding both  $\alpha$  and  $\beta$  in a transaction  $T$  of the dataset. Noteworthy, the support is defined both for a rule and for a single item-set. Equation (2), instead, is the confidence  $C(\alpha\beta)$  of the AR. It represents the conditional probability of finding  $\beta$  in a transaction containing  $\alpha$ . The confidence measures the strength of the rule, while the support gives information on the statistical significance.

Mining the ARs requires a two-step procedure:

1. The frequent item-sets have to be identified; an item-set is considered “frequent” if it appears in the dataset more frequently than a support threshold specified by the user, i.e., minimum support. In this work, the algorithm chosen for the item-set extraction is the FP-growth [24].
2. Given the frequent item-sets (*f.i.*) identified in step 1, all the ARs  $\alpha \rightarrow \beta$  such that  $\alpha \cup \beta = f.i.$  and whose confidence  $C(\alpha\beta)$  is higher than a confidence threshold specified by the user, i.e., minimum confidence.

### 3.2 Items Allocation Procedure

The procedure to allocate the items for the first time to the AS/RS can be summarized into five steps:

1. Historical data analysis: The whole procedure relies on a thorough data analysis process. Indeed, being a data-driven approach, there is a need for a reliable dataset to base the study. Specifically, the necessary data are the picking lists related to a relevant time interval. Indeed, the aim of the work is defining the allocation of the items according to the associations among them. In this sense, the items frequently picked together should be placed close to each other. Moreover, information on the dimensions of the items and some characteristics like volume occupied by each item or if they can be superimposed have to be taken into account.
2. Items’ support calculation and sorting: In order to define the sequence, in which the items should be allocated, there is a need for estimating its picking frequency. This value can be calculated by defining the support of each item. Indeed, the definition provided in (1), can be arranged as:

$$S(\alpha) = \frac{\#\{\alpha\}}{T} \quad (3)$$

The list is ordered by descending  $S(\alpha)$ .

3. Storage allocation selection: The first item to be allocated is the one having the highest  $S(\alpha_1)$ . Item  $\alpha_1$  is allocated to the most convenient storage. In particular, the closer the storage to the picking point, the more efficient the picking procedure will be. According to the proposed research approach, the whole quantity of the item has to be allocated in this phase, possibly using multiple storages.
4. AR mining: The ARs are mined, as explained in Sect. 3.1. Those having  $\alpha_1$  as head are taken into account in order to define which items should be placed in the same storage as  $\alpha_1$ . The list of the rules is ordered by decreasing  $C$ .
5. Items' allocation: The first item allocated to the same storage of  $\alpha_1$  (e.g.,  $\alpha_2$ ) is such that the rule  $\alpha_1 \rightarrow \alpha_2$  has the highest confidence among all the possible ARs  $\alpha_1 \rightarrow \alpha_k$ . If the quantity of  $\alpha_2$  cannot be completely allocated to the storage, then it is partially allocated; the procedure restarts by selecting the following item of the list created in 2. Otherwise, the second item per confidence is stored, i.e., the procedure restarts from 4.

The procedure ends when all the items are allocated or when the available space is saturated.

## 4 Application of the Proposed Approach

The research approach presented in Sect. 3 is applied to the case study of a shoe manufacturing company. Specifically, the company is switching from a picker-to-part policy toward the implementation of an AS/RS (part-to-picker policy). The AS/RS implemented is a vertical warehouse equipped with a vertical handling unit of the machine responsible for moving the trays, which are the storage units. Each tray is equipped with sliding bearings allowing them to slide on the storage shelves. Since each tray should contain more than one item, vertical and longitudinal separators can be installed. In the current application, separators divide each tray into 12 storage cells (SC). The aim of the company is improving warehouse management through the AS/RS so that the picking process is more efficient. The first decision in this perspective regards the inclusion in the allocation process only of relevant items: Indeed, being the company a shoe manufacturer, the impact of the fast-changing characteristics typical of the fashion products has to be taken into account. In particular, items which do not appear in the bill of material of shoes for the current year shall be excluded from the analysis. In this application, the dataset considered included the picking orders of the previous year; 9943 items are not included in the analysis since they are not in the bill of materials, resulting in 14,377 items and 11,283 picking orders. In Table 1, an excerpt from the dataset analyzed is reported: Each row represents a picking order whose identifier is reported in the first column, while the columns contain the items; each of the following columns contains the quantity of a specific item picked during the corresponding picking order.

**Table 1** Excerpt from the analyzed historical dataset

Picking orders	$\alpha_1$	$\alpha_2$	$\alpha_3$	$\alpha_4$	$\alpha_5$	$\alpha_6$	$\alpha_7$	...	$\alpha_{14377}$
P.O. 1	1	0	1	3	0	5	5	...	0
P.O. 2	1	3	0	3	1	0	0	...	0
P.O. 3	0	0	0	0	0	0	0	...	1
P.O. 4	0	0	1	0	2	0	0	...	1
P.O. 5	0	0	0	0	4	4	0	...	6
P.O. 6	3	3	0	0	0	0	0	...	0
P.O. 7	0	0	5	0	0	0	1	...	0
P.O. 8	0	0	0	1	0	0	3	...	0

Then, from such a dataset, the procedure is applied: The support of the *f.i.* is determined by setting the minimum support threshold to 0; the software chosen for this purpose is RapidMiner (<https://rapidminer.com/>), a data analytics platform.

Figure 1 displays the process implemented in RapidMiner for carrying out the procedure. Each tool represents a specific action executed by the software: The first tool enables the reading of the dataset, while the second one allows the filtering only of relevant items; this module can be useful in case of sensitivity analysis or a narrowing of the study. The data conversion tool aims at modifying the data types so that the FP-growth algorithm for *f.i.* identification can be applied; in this application, the number of items composing the *f.i.* is set to 2. Lastly, the ARM module enables the generation of the ARs, by filtering the ones having confidence lower than the minimum confidence threshold; in this case, even such threshold is set to 0, in order to have the widest range of information possible. At the end of the process, the output is the complete list of the *f.i.* and ARs among the items. According to the proposed procedure, the *f.i.* have to be ordered by descending support. An example of items' support, the quantity to be allocated, and the maximum quantity allocable to an SC are reported in Table 2.

Hence,  $\alpha_1$  is the first item that has to be allocated to the first tray of the AS/RS: to stock the 194 units, 2.425 SC are necessary. This means that two SC will be saturated, while the third one contains only 34 units of  $\alpha_1$ . The ARs having  $\alpha_1$  as the body of the rule are extracted, in order to determine the further items to be stored in the same tray (Table 3).

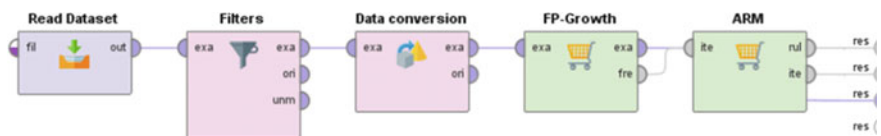


**Fig. 1** Process implemented in RapidMiner for frequent item-sets definition and association rule mining

**Table 2** List of items ( $\alpha$ ) ordered by descending support

$\alpha$	$S(\alpha)$	$Q(\alpha)$	$Q_{\max}(\alpha)^{SC}$
$\alpha_1$	0.107	194	80
$\alpha_2$	0.101	86	110
$\alpha_3$	0.096	103	30
$\alpha_4$	0.095	155	80
$\alpha_5$	0.093	54	80
$\alpha_6$	0.090	280	80
$\alpha_7$	0.081	127	110
$\alpha_8$	0.078	106	40
$\alpha_9$	0.074	131	30
$\alpha_{10}$	0.056	56	35

**Table 3** ARs having  $\alpha_1$  as body

$\alpha$	$B$	$C(\alpha \rightarrow \beta)$
$\alpha_1$	$\alpha_3$	0.331
$\alpha_1$	$\alpha_4$	0.331
$\alpha_1$	$\alpha_2$	0.297
$\alpha_1$	$\alpha_6$	0.266
$\alpha_1$	$\alpha_{11}$	0.238
$\alpha_1$	$\alpha_{12}$	0.238
$\alpha_1$	$\alpha_7$	0.232
$\alpha_1$	$\alpha_{13}$	0.230
$\alpha_1$	$\alpha_{14}$	0.225
$\alpha_1$	$\alpha_9$	0.197
$\alpha_1$	$\alpha_{15}$	0.177
$\alpha_1$	$\alpha_{16}$	0.162
$\alpha_1$	$\alpha_{17}$	0.125
$\alpha_1$	...	...

The first item considered is  $\alpha_3$  since the rule  $\alpha_1 \rightarrow \alpha_3$  has the highest confidence: From the data reported in Table 2, each SC can contain a maximum of 30 units, so 3 SC are required to store the 103 items currently on stock. Then,  $\alpha_4$  is allocated to the tray, occupying two further SC, followed by  $\alpha_2$  that requires another storage cell. The last three SC are dedicated to  $\alpha_5$ : The quantity to allocate would require 3.5 SC; hence, the amount in excess (40 units) will be allocated to another tray, according to the procedure. Figure 2 illustrates the composition of the current tray.

The first tray is now full, so the procedure restarts by selecting the second non-assigned item from Table 2: Since  $\alpha_1, \alpha_2, \alpha_3, \alpha_4$  are already stored, the first item assigned to the second tray is  $\alpha_5$ . When all the items are assigned to a tray, the procedure ends. Starting from the total allocation performed according to the proposed



**Fig. 2** Composition of the first tray

$\alpha_1$	$\alpha_1$	$\alpha_1$	$\alpha_3$
$\alpha_3$	$\alpha_3$	$\alpha_4$	$\alpha_4$
$\alpha_2$	$\alpha_6$	$\alpha_6$	$\alpha_6$

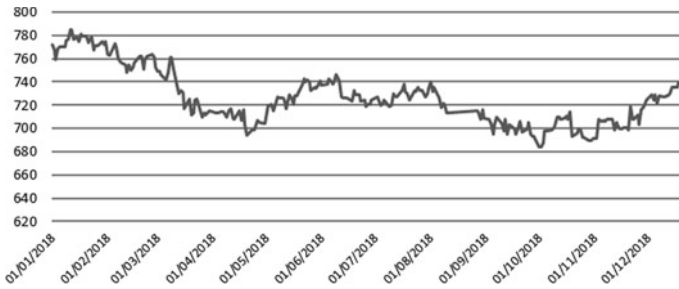


**Fig. 3** Trend of the number of trays daily required during the simulated year

roadmap, a simulation is carried out to verify the trend of the number of trays needed during the year: Picking orders and refilling list of a whole year are taken into account (Fig. 3). In this way, the saturation level is taken into account, in order to verify whether the ASRS is suitable for a possible increase of demand. On average, the 19% of the SC is saturated—ranging between 6.37 and 46.23%. In this sense, an increase in stock level can be supported by the current infrastructure, making it flexible enough even for storing different product categories (e.g., work in progress or finished goods). In order to identify whether the preparation of the picking lists can be carried out during a working shift, it is necessary to evaluate the duration of the picking processes: The average picking time is calculated for different scenarios. On average, a picking list can be prepared in 135 s, guaranteeing the achievement of the required daily number of lists—on average, 780—in less than one shift (5 h and 46 min). In the worst case, that is, during the peak production days, the required number of preparations is performed in 8 h and 15 min, making it necessary to work a little overtime.

## 5 Discussion and Conclusions

The methodology proposed in this work is aimed at supporting company managers during the improvement of warehouse operations. A promising approach for the management of items in an AS/RS is provided, showing how the application of a data mining-based methodology can help in improving a traditional process. Indeed, the reason for the selection of the ARM is related to intuitive thinking: If two items were picked together in the past, they would likely be in the same picking order

even in the future. This aspect is related to the fact that the basic components of a shoe are limited and fixed, even though several different models exist and their combination in a picking order is not fixed. In this case, having the chance of analyzing a vast amount of data guarantees that a wide range of cases is taken into account. Anyway, data quality plays a vital role in this process: If they are not collected and recorded accurately, the risk is to create erroneous relationships that worsen the overall performance of the picking process. In order to ensure the accuracy of the picking execution, each SC can contain only a single item; the downside could be a penalization in terms of saturation level of the SC: Indeed, in the worst-case scenario, an entire SC could contain one unit of an item. If space availability represents the scarce resource of a specific application, such a constraint could be removed, by assigning more than one item to an SC through the ARs. Alternatively, the dimension of the SC could be reduced if there are not strict geometrical constraints of the items. The definition of the minimum confidence threshold also has an impact on the number of rules defined. For instance, considering the example reported in Sect. 4, if the minimum confidence threshold was 0.3, only items  $\alpha_3$  and  $\alpha_4$  would have been assigned to the tray as “successors” of item  $\alpha_1$ . To saturate the tray, the rules having  $\alpha_3$  as rule’s body would have to be considered since it is the one having the second highest support (Table 2). Having careful warehouse management harbors benefits even for other organizational areas, lowering the risk of raw materials shortages and lesser delays. The majority of the works rely on applications to traditional manual warehouses; thus, it is essential to extend the applications to the AS/RS field. Further developments of this study regard the introduction of a multi-criteria decision-making tool to support the decision-makers in the assignment, possibly comparing different scenarios including unconsidered constraints.

## References

1. Antomarioni, S., Pisacane, O., Potena, D., Bevilacqua, M., Ciarapica, F.E., Diamantini, C.: A predictive association rule-based maintenance policy to minimize the probability of breakages: application to an oil refinery. *Int. J. Adv. Manuf. Technol.* (2019). <https://doi.org/10.1007/s00170-019-03822-y>
2. Ciarapica, F.E., Giacchetta, G., Paciarotti, C.: Facility management in the healthcare sector: Analysis of the Italian situation. *Prod. Plan Control* **19**, 327–341 (2008). <https://doi.org/10.1080/09537280802034083>
3. Tompkins, J.A., White, J.A., Bozer, Y.A., Tanchoco, J.M.A.: *Facilities Planning*. Wiley, Hoboken (2010)
4. Richards, G.: *Warehouse Management: A Complete Guide to Improving Efficiency and Minimizing Costs in the Modern Warehouse*. Kogan Page Publishers (2014)
5. Bevilacqua, M., Ciarapica, F.E., Antomarioni, S.: Lean principles for organizing items in an automated storage and retrieval system: An association rule mining—Based approach. *Manag Prod Eng Rev* **10** (2019). <https://doi.org/10.24425/mper.2019.128241>
6. Chen, M.C., Wu, H.P.: An association-based clustering approach to order batching considering customer demand patterns. *Omega* **33**, 333–343 (2005). <https://doi.org/10.1016/j.omega.2004.05.003>

7. Roodbergen, K.J., Vis, I.F.A.: A survey of literature on automated storage and retrieval systems. *Eur. J. Oper. Res.* **194**, 343–362 (2009). <https://doi.org/10.1016/j.ejor.2008.01.038>
8. Chuang, Y.F., Lee, H.T., Lai, Y.C.: Item-associated cluster assignment model on storage allocation problems. *Comput. Ind. Eng.* **63**, 1171–1177 (2012). <https://doi.org/10.1016/j.cie.2012.06.021>
9. Graves, S.C., Hausman, W.H., Schwarz, L.B.: Storage-retrieval interleaving in automatic warehousing systems. *Manage. Sci.* **23**, 935–945 (1977). <https://doi.org/10.1287/mnsc.23.9.935>
10. Bortolini, M., Faccio, M., Ferrari, E., Gamberi, M., Pilati, F.: Design of diagonal cross-aisle warehouses with class-based storage assignment strategy. *Int. J. Adv. Manuf. Technol.* **100**, 2521–2536 (2019). <https://doi.org/10.1007/s00170-018-2833-9>
11. Bortolini, M., Accorsi, R., Gamberi, M., Manzini, R., Regattieri, A.: Optimal design of AS/RS storage systems with three-class-based assignment strategy under single and dual command operations. *Int. J. Adv. Manuf. Technol.* **79**, 1747–1759 (2015). <https://doi.org/10.1007/s00170-015-6872-1>
12. Hausman, W.H., Schwarz, L.B., Graves, S.C.: Optimal storage assignment in automatic warehousing systems. *Manage. Sci.* **22**, 629–638 (1976). <https://doi.org/10.1287/mnsc.22.6.629>
13. Dharmapriya, U.S.S., Kulatunga, A.K.: New Strategy for Warehouse Optimization-Lean warehousing. In: *International Conference on Industrial Engineering and Operations Management*. Kuala Lumpur, pp. 513–519 (2011)
14. Grosse, E.H., Glock, C.H., Ballester-Ripoll, R.: A simulated annealing approach for the joint order batching and order picker routing problem with weight restrictions. *Publ Darmstadt Tech Univ Inst Bus Stud* (2014)
15. Tsai, C.Y., Liou, J.J.H., Huang, T.M.: Using a multiple-GA method to solve the batch picking problem: considering travel distance and order due time. *Int. J. Prod. Res.* **46**, 6533–6555 (2008). <https://doi.org/10.1080/00207540701441947>
16. Saidi-Mehrabad, M., Dehnavi-Arani, S., Evazabadian, F., Mahmoodian, V.: An Ant Colony Algorithm (ACA) for solving the new integrated model of job shop scheduling and conflict-free routing of AGVs. *Comput. Ind. Eng.* **86**, 2–13 (2015). <https://doi.org/10.1016/j.cie.2015.01.003>
17. Lin, C.C., Kang, J.R., Hou, C.C., Cheng, C.Y.: Joint order batching and picker Manhattan routing problem. *Comput. Ind. Eng.* **95**, 164–174 (2016). <https://doi.org/10.1016/j.cie.2016.03.009>
18. Accorsi, R., Manzini, R., Maranesi, F.: A decision-support system for the design and management of warehousing systems. *Comput. Ind.* **65**, 175–186 (2014). <https://doi.org/10.1016/j.com.pind.2013.08.007>
19. Yener, F., Yazgan, H.R.: Optimal warehouse design: literature review and case study application. *Comput. Ind. Eng.* **129**, 1–13 (2019). <https://doi.org/10.1016/j.cie.2019.01.006>
20. Agrawal, R., Imieliński, T., Swami, A.: Mining association rules between sets of items in large databases. *ACM SIGMOD Rec* **10**(1145/170036), 170072 (1993)
21. Fayyad, U.M., Irani, K.B.: Multi-interval discretization of continuous-valued attributes for classification learning. *Proc 13th Int Jt Conf Artif Intell* (1993) <https://doi.org/10.1109/TKDE.2011.181>
22. Chen, W.C., Tseng, S.S., Wang, C.Y.: A novel manufacturing defect detection method using association rule mining techniques. *Expert Syst. Appl.* (2005). <https://doi.org/10.1016/j.eswa.2005.06.004>
23. Buddhakulsomsiri, J., Siradeghyan, Y., Zakarian, A., Li, X.: Association rule-generation algorithm for mining automotive warranty data. *Int. J. Prod. Res.* (2006). <https://doi.org/10.1080/00207540600564633>
24. Han, J., Cheng, H., Xin, D., Yan, X.: Frequent pattern mining: Current status and future directions. *Data Min Knowl Discov* (2007). <https://doi.org/10.1007/s10618-006-0059-1>

# Infrastructure Sharing Model as a Support for Sustainable Manufacturing



Joanna Helman , Maria Rosienkiewicz , Mateusz Molasy ,  
and Mariusz Cholewa 

**Abstract** Sharing Economy allows using cheaper and simpler methods of alternative resource usage for sustainable manufacturing. One of elements of Sharing Economy is Infrastructure Sharing. Its idea is based on the fact that there is a lot of production and research infrastructure, but due to the changes in terms of manufacturing companies' and in research institutions' needs these resources are used only in specific situations and vast number of infrastructure is not fully exploited. A review of the literature and trends observed on the European market shows that the phenomenon of Infrastructure Sharing requires a deeper reflection on this topic. The aim of the paper is to present a new model of Infrastructure Sharing dedicated to support sustainability of advanced manufacturing. The Infrastructure Sharing model formulated within International Synergic Crowd Innovation Platform has been developed to hinder the gap with identified problems with low infrastructure's utilization. The paper presents the functionality of sharing unused capacities of production and research machines and equipment. Also, the implementation of the Infrastructure Sharing model within a dedicated pilot action is discussed. Stakeholders can use the new business model to increase infrastructure utilization rate and to help make the right investment decision in technology. Infrastructure Sharing offers the possibility to test infrastructure/technologies and gives the possibility to better utilize and commercialize technologies.

## 1 Introduction

According to Chesbrough the “innovation process is currently facing a paradigm shift”—there is a fundamental change in the approach how companies deal with innovation in developing new ideas and then capitalizing them [1]. Research on innovation development trends shows that number of companies implementing elements of Open Innovation into their activities is rapidly growing [2]. Firms are capturing

---

J. Helman (✉) · M. Rosienkiewicz · M. Molasy · M. Cholewa  
Department of Laser Technologies, Automation and Production Organization, Wrocław  
University of Science and Technology, Wyb. Wyspiańskiego 27, 50-370 Wrocław, Poland  
e-mail: [joanna.helman@pwr.edu.pl](mailto:joanna.helman@pwr.edu.pl)

value from Sharing Economy approaches such as crowdsourcing, crowdfunding, and microworking. It is necessary for keeping up with global competition to apply those new phenomena, tools, and methods. Even though that the Open Innovation foundations were defined over a decade ago, its business models are still in the process of development, and therefore, it is necessary to continue research to develop a dedicated environment that will enable stakeholders the full use of the new approaches [3].

One of the elements of Open Innovation is Sharing Economy. The idea of sharing resources (understood as infrastructure, competences, and skills) is based on the fact that on the European market there is a lot of infrastructure, but due to the fact that needs of manufacturing companies are changing, and in research institutions, these resources are used only in specific situations, and a vast number of i.a. infrastructure is not exploited. Number of machines is rarely utilized or their production capacity is not fully used. It can be noticed, especially in research organizations that infrastructure bought for the purposes of European co-funded projects, after their finalization is often barely utilized. Therefore, there are considerations on European level how to increase the usage of existing industrial research infrastructures.

## 2 Sharing Economy Concept Towards Infrastructure Sharing

The act of “sharing” is nothing new due to the fact that barter exchange existed long time ago, so it can be stated that it is as old as humans [4–7]. However, “Sharing Economy” is foreseen as something innovative (keeping in mind the ancient perspective of existence of countertrade) and is described as a new phenomenon born in the Internet age [8]. Recently, the term Sharing Economy is gaining more and more popularity understood as the form of “a new culture of sharing based on fee payment through online platforms” [9]. Belk defines Sharing Economy as the “acquisition or distribution of a source coordinated by people for compensation or a certain fee” [8]. The Sharing Economy changes the approach on how goods and services are consumed—from the traditional model of single ownership to shared use with economic benefits [10]. The Sharing Economy allows using cheaper and simpler methods of alternative resource usage [11].

Although sharing of economy has been taking place for several years and is constantly growing, it can be seen that this phenomenon is still in its early stages of development. Researchers are trying to find the quintessence of the Sharing Economy, focusing on such research problems like describing how to define contemporary sharing and how to label it, developing classification of sharing phenomena, defining how to meet evolving challenges in the context of sharing regulation [10]. In recent years, researchers have also conducted studies on the determining the factors that are motivating consumers to participate in sharing physical goods, like economic gain [12] and cost saving [13], familiarity, utility, and trust [14] and enjoyment of sharing

[15]. Sharing is also perceived as a “non-ownership alternative to obtaining product benefits” [16]. Bearing in mind the previous definition, sharing is often seen through the prism of more sustainable, ecological, and ultimately more cost effective than ownership [17].

## **2.1 Infrastructure Sharing**

Sharing has been explored in various contexts considering various goods including car sharing, apartment sharing, and commercial physical product sharing systems [9]. However, there is not much research done on sharing industrial infrastructure. Most of papers are devoted to transportation Infrastructure Sharing (logistic fleet, cars, bikes, etc.) [18–22] or mobile infrastructure [23–25].

The idea of “sharing infrastructure” is based on the fact that there are many research and industrial infrastructure scattered across various organizations on the market, however, due to the fact that the needs of manufacturing companies are changing (combined together with the increasing competition), and these resources are used only in specific situations, a huge number of equipment is not used properly (number of machines are rarely utilized or their production capacity is not fully used). What is more, manufacturing companies often do not have the knowledge about existing infrastructure in their—or neighbouring—regions. By the new phenomenon of sharing infrastructure, developing countries, and growing economies could take full advantage of technological and industrial development that is enabled by simplified access to technology.

Due to the lack of classification of “sharing infrastructure” concept within advanced manufacturing authors of this paper propose the definition stating that “sharing infrastructure is sharing free capacity of machines and equipment in order to increase their use and strengthen the economy towards sustainable development of industry” as an explanation of this phenomenon.

Taking into account literature review and trends observed on the European market, the aim of the paper is to present a new model of Infrastructure Sharing dedicated to advanced manufacturing to support concept of sustainable manufacturing.

## **3 Infrastructure Sharing Within SYNERGY Project**

Due to the fact that Sharing Economy was identified as a very beneficial approach, and one of its components—Infrastructure Sharing is not so widely used, authors of this paper have developed and implemented a new model of Infrastructure Sharing within the SYNERGY project. Project “SYnergic Networking for innovativeness Enhancement of central european actoRs focused on hiGh-tech industrY” (acronym SYNERGY) is co-financed within Interreg Central Europe programme. One of the programme’s priorities is cooperating on innovation to make Central Europe more

competitive with its specific objective to improve sustainable linkages among actors of the innovation systems for strengthening regional innovation capacity in Central Europe. The project is oriented on the most promising modern industrial technologies (KPA: Key Project's Areas): additive manufacturing; micro- and nanotechnology-related processes and materials; and Industry 4.0.

The main aim of the SYNERGY project is to develop a Synergic Crowd Innovation Platform (SCIP) that will allow applying approaches of Open Innovation and Sharing Economy. The idea is to set up a platform ensuring crowdfunding and crowdsourcing for innovative solutions for the Central European society. As a part of functionality of the SCIP, an Infrastructure Sharing mechanism has been developed.

Within the research performed by SYNERGY Project Partners under catalogue on best practices and success stories of crowd innovation approaches, 33 Internet platforms at international and regional level in Central European countries were evaluated towards a possibility of implementing Open Innovation approaches like crowdfunding, crowdsourcing, micro-working and Infrastructure Sharing. The results of this transregional research showed that there is a lack of both international and regional solutions that would fully implement the assumed functionality for sharing infrastructure. There are few platforms that offer some basic functionalities of Infrastructure Sharing, however, they cannot be examples on how to fully implement Infrastructure Sharing model.

The aim of those platforms is to rent/hire robots to manufacturers. The cost of robotic workers depends on the equipment needed, the task the robot will need to perform, and the hours worked. It is not possible to upload an offer related to sharing research infrastructure.

This is why the SYNERGY project is focusing on development of a model for sharing resources. Within the Synergic Crowd Innovation Platform it is foreseen to enhance innovation using shared resources thanks to two services:

- Industrial research infrastructures sharing,
- Competences and skills sharing.

### ***3.1 Infrastructure Sharing Methodology***

Many organizations are facing difficulties with the decision on investing in an infrastructure. They are not sure how it can be ensured that the infrastructure is fully used or it should be used properly. Also, the question which use cases exist in a company or a research organization for this technology should be considered before the purchase.

This is where the SYNERGY project can help—the tool has been developed to make infrastructure available to companies, research institutions, and universities. Stakeholder can use the new business model to help make the right investment decision in technology and increase infrastructure utilization rate. Infrastructure Sharing offers the possibility to test infrastructure/technologies and gives the possibility to

better utilize and commercialize technologies. The main benefits for research institutions, technology parks, and companies which will utilize the developed solution of sharing infrastructure within SCIP are i.a.:

- Promoting technology and competence in an international environment,
- Increasing the use of own infrastructure,
- Lowering the costs by sharing infrastructure,
- Increasing turnover thanks to easier investment decision for companies,
- Acquiring new partners and customers,
- Testing a new business model based on Sharing Economy.

The dedicated tool developed within Synergic Crowd Innovation Platform (SCIP)—Infrastructure Sharing functionality (<https://synergyplatform.pwr.edu.pl>) is a living database of infrastructure located mainly in Central Europe. The infrastructure in majority can be assigned to one (or more than one) of the three previously mentioned KPAs. The functionality of the platform assumes two main actors and their “lines”. It is represented in Fig. 1.

One of the actors is the *Infrastructure Provider*—it is a person/organization that is having an infrastructure that is not fully occupied and can be shared with others. In the first step, the *Infrastructure Provider* is logging in and setting an account on the platform and in the next step describing the owned infrastructure. The information such as name of the infrastructure, short information about it, possible application and activities that can be done on it, the place where it is located and what are the boundaries of utilizing it (price and possibilities of use—rental, research performed by owner, workshop for possible usage, and/or usage according to agreement) should

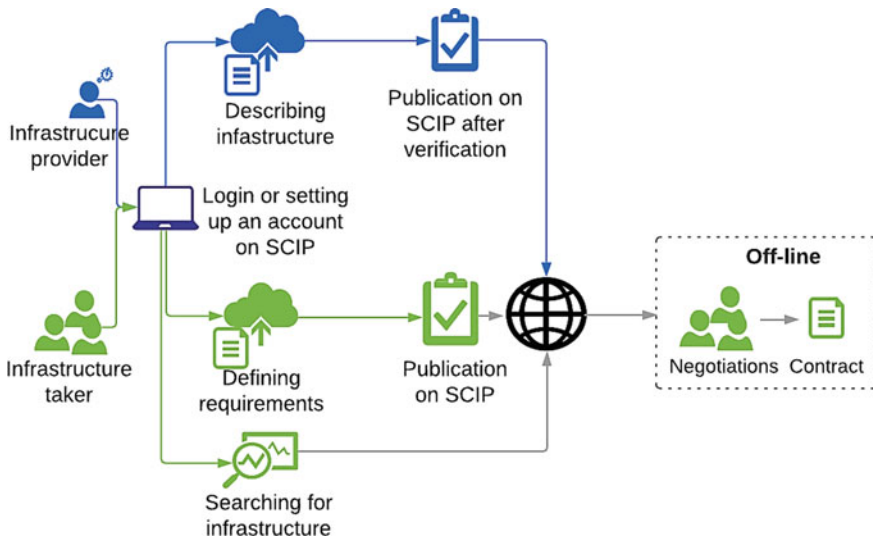


**Fig. 1** General scheme of Infrastructure Sharing on SYNERGY platform



be provided. After the registration the submission is being verified by the moderator and published on the platform.

The other actor is *Infrastructure Taker*—this user can have two options for using the platform—*search existing database of infrastructure* or *defining requirements*. *Search option* can be according to name, description, organization, possibilities of use factors or free search based on keywords. To see the details, one has to click the name of the infrastructure. To search for already submitted infrastructure, the user does not have to be registered nor logged in at the platform.

When the *Infrastructure Taker* finds the appropriate infrastructure that would like to use, they have to contact the *Infrastructure Provider* by a dedicated form. Then, negotiations between users can be done and the contract on *Infrastructure Sharing* shall be signed.

The *defining requirements option* is similar to describing the owned infrastructure. The *Infrastructure Taker* describes all requirements that needs to be met or specifies what kind of actions will be performed so others might see if they have such infrastructure (that is not yet registered on the platform) and are willing to share it, so then they can contact the *Infrastructure Taker* with more details.

Project consortium has prepared general conditions of *Infrastructure Sharing* that should be considered:

- *Infrastructure Provider* must define a timetable according to which the beneficiaries can have access to his premises, specifying accessibility rules, and allowed working hours.
- *Infrastructure Provider* must set the economic conditions according to which the beneficiaries are entitled to use their facilities, specifying the allowed amount of time and the technical equipment which can be used by the beneficiaries, as well as define technical personnel relevant for handling the equipment/carrying out the work on the infrastructure.
- Beneficiaries engage to respect the technical and financial specifications provided by the *Infrastructure Provider*.
- Beneficiaries present to involved parties their project's requirements and needs in terms of facilities' usage and to update them on a regular base about the implementation process, needed corrective/integrative actions included.
- Beneficiaries and *Infrastructure Provider* subscribe a specific agreement which defines the conditions applicable to each single case. The specific agreement represents the terms of reference for the usage of the given infrastructure within the network.

### 3.2 Implementation of the Infrastructure Sharing Model: Pilot Action

To test the proposed model, the international *Rent-a-robot* pilot action within SYNERGY project has been foreseen. It is based on the whole planned functionality of the platform, however, to obtain more results of matchmaking *Infrastructure Providers* with *Infrastructure Takers*, the *defining requirements option* has been withdrawn from the testing phase. During pilot action users would be able to use the following paths:

- To search existing database of infrastructure,
- To register their own infrastructure,
- To use already registered infrastructure—which in fact means contacting a person who is offering the particular infrastructure.

The general scheme of the international pilot action *rent-a-robot* is presented in Fig. 2. The pilot action will be done as an online campaign where different Central European organizations will participate as *Infrastructure Providers* and *Infrastructure Takers*. The steps of testing the Infrastructure Sharing approach are as follows:

1. *Infrastructure Provider* uploads to the SCIP offers related to infrastructure.
2. *Infrastructure Taker* is searching for the machines they could use.
3. *Infrastructure Taker* declares the way of using the infrastructure.
4. Sides are merged, partners get in contact.
5. The voucher is received by *Infrastructure Taker*.
6. Sides are sharing infrastructure.
7. *Infrastructure Taker* is preparing a short success story about the *Infrastructure Sharing* campaign.

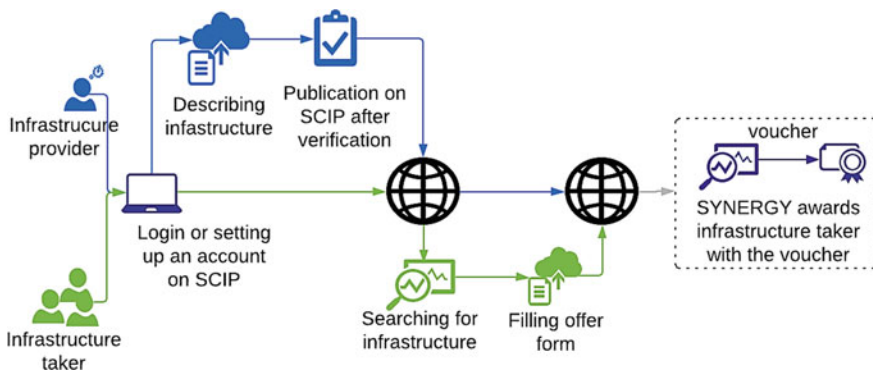


Fig. 2 Infrastructure sharing rent-a-robot pilot action scheme

The first step is exactly the same as described in the model presented in the previous chapter—the *Infrastructure Provider* is describing the owned infrastructure with all necessary information. In the database accumulating, all entries on infrastructure that can be shared the *Infrastructure Taker* is searching for the machines or services that they are willing to use. Based on that, the *Infrastructure Taker* is selecting the appropriate infrastructure and submits the short description of their company and describes interest in the infrastructure and how and when use the infrastructure will be used. Then, the potential partners are merged and partners get in contact.

In the next step, the jury consisting of two SYNERGY team member's awards with the voucher the *Infrastructure Taker* who drafted a successful plan of usage of shared infrastructure. In this case, the voucher is received by the winning *Infrastructure Taker* that could use it for investing in rental fees and consulting by the infrastructure giver on how to use and configure the robot.

## 4 Conclusions

As stated in the paper, one of the elements of Open Innovation is Sharing Economy. Sharing resources allows using cheaper and simpler methods of alternative resource usage for sustainable manufacturing such as i.a. infrastructure, competences, and skills sharing. One of elements of Sharing Economy is Infrastructure Sharing. Its idea is based on the fact that on the European market there is a lot of infrastructure, but due to the changes in terms of manufacturing companies' and in research institutions' needs these resources are used only in specific situations, a vast number of infrastructure is not exploited. Number of machines is rarely utilized or their production capacity is not fully used. It can be noticed, especially in research organizations that infrastructure bought for the purposes of European co-funded projects, after their finalization is often barely utilized. Therefore, there are considerations on European level how to increase the usage factor of existing Industrial Research Infrastructures. A review of the literature and trends observed on the European market shows that the phenomenon of Infrastructure Sharing requires a deeper reflection on this topic.

Based on abovementioned issues, authors of this paper decided to present a new approach and new model of Infrastructure Sharing dedicated to advanced manufacturing. Due to the lack of classification of sharing infrastructure concept, authors of this paper proposed the definition stating that "sharing infrastructure is sharing free capacity of machines and equipment in order to increase their use and strengthen the economy towards sustainable development of industry" as an explanation of this phenomenon. The Infrastructure Sharing model established within International Synergic Crowd Innovation Platform has been developed to make infrastructure available to companies, research institutions, and universities. Infrastructure Sharing offers the possibility to test infrastructure/technologies and gives the possibility to better utilize and commercialize technologies. Stakeholders can use the new business model to increase infrastructure utilization rate and to help make the right investment decision in technology.

The aim of the paper has been achieved by presenting a new model of Infrastructure Sharing dedicated to advanced manufacturing that is ready-to-use. The new model proposed by authors answers the identified problems with low infrastructure's utilization by introducing the functionality of sharing unused capacities of production and research machines and equipment. It can be stated that the Infrastructure Sharing model supports the development of Open Innovation environment and sustainable manufacturing. Additionally, to the benefits of the developed solution i.a. promoting technology and competence in an international environment, increasing the use of own infrastructure, lowering the costs by sharing infrastructure, increasing turnover thanks to easier investment decision for companies, acquiring new partners and customers, as well as testing a new business model based on Sharing Economy can be considered.

**Acknowledgements** The research leading to these results has received funding from Interreg Central Europe programme priority Innovation and knowledge development under grant agreement No CE1171, project SYNERGY (SYnergic Networking for innovativeness Enhancement of central european actoRs focused on hiGh-tech industrY) as well as from funds of Polish Ministry of Science and Higher Education for science in 2018–2020 for the implementation of an international project.


## References

1. Chesbrough, H.: *Open Innovation: The New Imperative for Creating and Profiting from Technology*. Harvard Business Press, Brighton (2006)
2. *Open innovation 2.0 yearbook 2016*, European Commission, Directorate-General for Communications Networks, Content and Technology
3. Rosienkiewicz, M. et al.: SYNERGY Project: open innovation platform for advanced manufacturing in Central Europe, intelligent systems in production engineering and maintenance. *Adv Intell Syst Comput* **835**, 306–315
4. Botsman, R., Rogers, R.: *What's Mine is Yours*. Harper Business (2010)
5. Cheng, X., Fu, S., Vreede, G.-J.: A mixed method investigation of Sharing Economy driven car-hailing services: online and offline perspectives. *Int. J. Inf. Manag.* **41**(August), 57–64 (2018)
6. Ertz, M., Durif, F., Arcand, M.: Collaborative consumption: conceptual snapshot at a buzzword. *J. Entrepreneurship Educ.* **19**(2), (2016)
7. Sundararajan, A.: *The Sharing Economy: The End of Employment and the Rise of Crowd-Based Capitalism*. MIT Press (2016)
8. Belk, R.: You are what you can access: sharing and collaborative consumption online. *J. Bus. Res.* **67**(8), 1595 (2014)
9. Bucher, E., Fieseler, C., Lutz, C.: What's mine is yours (for a nominal fee)—Exploring the spectrum of utilitarian to altruistic motives for internet-mediated sharing. *Comput. Hum. Behav.* **62**(September), 316–326 (2016)
10. Milanova, V., Maas, P.: Sharing intangibles: Uncovering individual motives for engagement in a sharing service setting. *J. Bus. Res.* **75**, 159–171 (2017)
11. Eckhardt, G.M., Bardhi, F.: The relationship between access practices and economic systems. *J. Assoc. Consum. Res.* **1**(2), 210–225 (2016)
12. Eckhardt, G.M., Bardhi, F.: The sharing economy isn't about sharing at all. *Harvard Business Review*, January 28 (2015)

13. Neoh, J.G., Chipulu, M., Marshall, A.: What encourages people to carpool? An evaluation of factors with meta-analysis. *Transportation* (2015)
14. Möhlmann, M.: Collaborative consumption: determinants of satisfaction and the likelihood of using a Sharing Economy option again. *J. Consum. Behav.* **14**, 193–207 (2015)
15. Hamari, J., Sjöklint, M., Ukkonen, A.: The sharing economy: why people participate in collaborative consumption. *J. Assoc. Inf. Sci. Technol.* **67**, 2047–2059 (2016)
16. John, N.A.: The social logics of sharing. *Commun. Rev.* **16**(3), 113–131 (2013a)
17. Lambertson, C.P., Rose, R.L.: When is ours better than mine? a framework for understanding and altering participation in commercial sharing systems. *J. Market.* **76**(4), 2012
18. Hua, Y., Zhao, D., Wang, X., Li, X.: Joint infrastructure planning and fleet management for one-way electric car sharing under time-varying uncertain demand. *Transp. Res. Part B: Methodol.* **128**, 185–206 (2019)
19. Roni, M., Yi, Z., Smart, J.: Optimal charging management and infrastructure planning for free-floating shared electric vehicles. *Transp. Res. Part D: Transp. Environ.* **76**, 155–175 (2019)
20. Zhang, H., Sheppard, C., Lipman, T., Zeng, T., Moura, S.: Charging infrastructure demands of shared-use autonomous electric vehicles in urban areas. *Transp. Res. Part D: Transp. Environ.* **78** (2020)
21. Faghih-Imani, A., Eluru, N.: Determining the role of bicycle sharing system infrastructure installation decision on usage: case study of montreal BIXI system. *Transp. Res. Part A: Policy Pract.* **94**, 685–698 (2016)
22. Latham, A., Michael Natrass, M.: Autonomous vehicles, car-dominated environments, and cycling: Using an ethnography of infrastructure to reflect on the prospects of a new transportation technology. *J. Transp. Geogr.* **81** (2019)
23. Meddour, D.-E., Rasheed, T., Gourhant, Y.: On the role of Infrastructure Sharing for mobile network operators in emerging markets. *Comput. Netw.* **55**(7), 1576–1591 (2011)
24. Simo-Reigadas, J., Municio, E., Morgado, E., Castro, E., Prieto-Egido, I.: Sharing low-cost wireless infrastructures with telecommunications operators to bring 3G services to rural communities. *Comput. Netw.* **93**(Part 2), 245–259 (2015)
25. Oughton, E., Frias, Z.: The cost, coverage and rollout implications of 5G infrastructure in Britain. *Telecommun. Policy* **42**(8), 636–652 (2018)

# A Correlation Study Between Weather Conditions and the Control Strategy of a Solar Water Heating System



Znaczo Paweł , Kamiński Kazimierz , and Zuchniewicz Jerzy 

**Abstract** The paper presents the results of experimental research on the correlation between atmospheric conditions and control strategy in solar water heating systems. Methods for assessing sunlight conditions have been presented. The results in the form of harvested solar energy depending on weather conditions have been presented and the best control strategy for individual sunshine condition have been proposed.

## 1 Introduction

Currently, we are able to observe a high level of development associated with solar thermal technology. However, it mainly occurs in the field of efficiency and reliability of solar collectors and storage units design [1]. Manufacturers of solar systems usually offer new absorbers, different insulation materials, improved glass covers or completely new solar collectors design. Rarely can we hear something new about improvements or new methods in the field of solar water heating control strategy [2]. When the topic of control in solar heating systems is discussed, the subject of research is usually reduced only to the solar collector, excluding other components of the system.

Several useful numerical models and experimental works have been carried out and presented in literature [3–10]. These works enabled us to achieve a very high technical advancement in this research area. However, the use of such advanced tools and methods in order to create high-efficiency control algorithms, still remains incomplete [11–19].

In the typical commercial kits, with closed solar collector loop, the flow rate is the only control parameter operated by a control unit [20, 21]. The speed of the pump is dependent on the temperature difference between the collector array outlet

---

Z. Paweł (✉) · K. Kazimierz  
FM, Koszalin University of Technology, Sniadeckich str. 2, Koszalin 75-453, Poland  
e-mail: [pawel.znaczo@tu.koszalin.pl](mailto:pawel.znaczo@tu.koszalin.pl)

Z. Jerzy  
Alplast sp. z.o.o, Niekanin Sliwkowa 1, Niekanin 78-100, Poland

and storage tank bottom section, hereinafter referred to as  $\Delta T$ . Two types of strategies are commonly used. One is the “bang-bang” strategy, where the mass flow rate is set to maximum or zero, based on the threshold value. On the other hand the proportional strategy can be used, where the mass flow rate increases with the increase of  $\Delta T$  value [6]. All currently used control methods have several significant disadvantages. Basically, creation of the universal pump operation characteristics is not possible due to the number of parameters and variables in the Hot Water Solar System. The collector’s fastening elements with the frame have been designed in the form of metamaterial structures [22–24]. This contributed to the possibility of dynamic change of elements through 3D prints using the FDM method with an admixture of rubber and PET.

## 2 Experimental Set-up

The experimental setup consists of two mutually cooperating hydraulic loops. The main loop, with two flat-plate solar collectors of a total area  $4 \text{ m}^2$  and the auxiliary loop for working fluid stabilisation (URT). A water tank with a capacity of  $440 \text{ [l]}$  was used to store heat energy. The water tank at the test stand was equipped with mixing circuits to prevent heat stratification (PR2) (Fig. 1).

To control the working medium flow rate, the solar controller TECH ST-402 N PWM was used (FC). The controller cooperates with PT1000 temperature sensors. One of them measures the working medium temperature on the collector outlet ( $T_{\text{out}}$ ) and the other one is the working fluid temperature sensor on the water tank (WT). The flow through solar collectors loop was driven by rotational pump, with PWM input port. The mass flow rate was measured with ENKO-MPP600 electromagnetic flow meter. The measured data were recorded by NI-DAQ data acquisition system (Fig. 2).

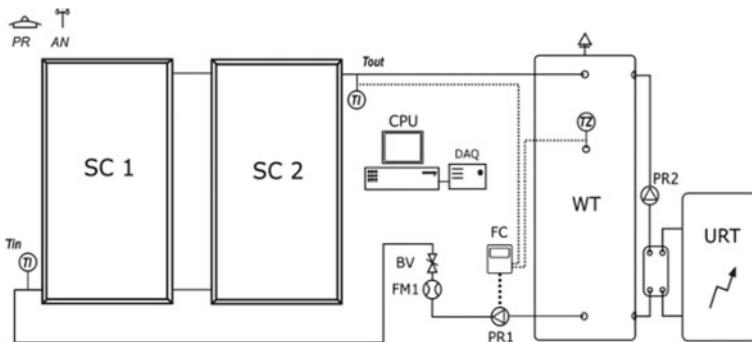


**Fig. 1** Diagram of the test stand for solar systems

**Fig. 2** Outdoor platform with solar flat-plate collectors



Experimental tests were carried out at a solar system testing laboratory located in the building of the Koszalin University of Technology. Research works were carried out in the period of May 2016–July 2019. Their main purpose was to provide data related to the impact of changes in mass flow rate of the working medium on the thermal efficiency of a solar hot water system. The measurements were carried out during sunny days, when the value of global solar radiation ( $G\beta$ ) exceeded the critical value set at 500 [W/m<sup>2</sup>].

### 3 Experimental Results and Evaluation Criteria

A series of tests was carried out to assess the impact of mass flow settings on the system's thermal efficiency. In each measurement day the correlation between the  $\Delta T$  and mass flow rate was modified. Because the results of thermal efficiency test are strongly correlated to weather conditions thus directly comparing them seems inappropriate.

To eliminate the difference in weather conditions during each test day, three factors have been proposed to facilitate the evaluation of collected measurement data.

The first of the proposed factors  $X_{\text{Sol}}$  is the ratio of heat energy accumulated in the water storage to the total energy of solar radiation at the collectors surface, according to the equation:

$$X_{\text{Sol}} = \frac{E_z}{E_{\text{rad}}} \quad (1)$$

where:  $E_z$  is the amount of heat energy stored in the water tank during the measurement day:

$$E_z = (T_k - T_p) \cdot c_f \cdot M_z \quad (2)$$



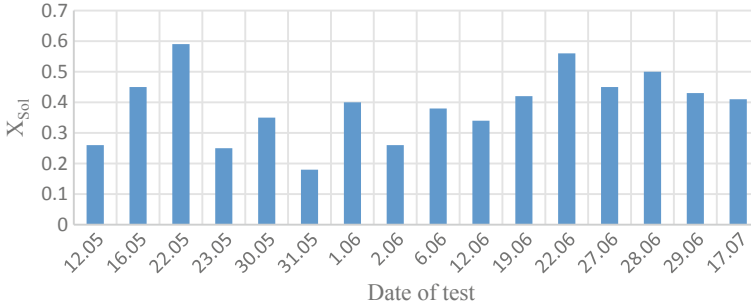


**Fig. 3** The  $X_{Sol}$  factor values for selected test days

where:  $T_k$ ,  $T_p$  are initial and final temperatures respectively,  $c_f$  is a specific heat of working fluid and  $M_z$  is the mass of the working fluid.

The value  $E_{rad}$  in the Eq. (3) describes the amount of total solar energy at the collector surface during test period, according to the equation:

$$E_{rad} = \int_{t_0}^{t_f} G_{\beta} A_c dt \quad (3)$$

where:  $G_{\beta}$  is the total solar radiation at collectors surface,  $A_c$  is the collectors aperture surface and  $t_0$ ,  $t_f$  are the initial and final test time.

The  $X_{Sol}$  is a factor, which describes how efficiently the solar system converts the energy from the surface of solar collectors into the thermal energy stored in water tank. The range of changes of this factor is:  $0 \leq X_{Sol} \leq 1$ . The higher this factor is, the less heat loss occurs in the system. The most desirable value of the  $X_{Sol}$  factor will be equal to one. Such a case would mean that the solar system used all of the solar energy it received at the input and converted it into thermal energy without any heat loss. In fact, this is obviously impossible.

Figure 3 presents the values of the factor  $X_{Sol}$  for selected measurement days.

Another evaluation factor developed to assess the thermal efficiency of the solar system was  $X_{\dot{Q}_u}$ . Similarly to the previous factor, the nominator has the value of heat energy accumulated in water tank, but the denominator of this factor is the value of the useful power extracted from the solar collectors, according to the equation:

$$X_{\dot{Q}_u} = \frac{E_z}{E_c} \quad (4)$$

where:  $E_z$  is the amount of heat energy stored in the water tank and  $E_c$  describes the amount of useful energy extracted from the collectors during test period:

$$E_c = \int_{t_0}^{t_f} \dot{Q}_u dt \quad (5)$$

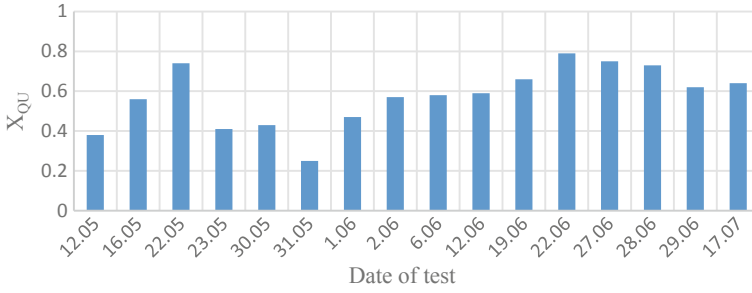


**Fig. 4** The  $X_{\dot{Q}_u}$  factor values for selected test days

Figure 4 presents the values of the factor  $X_{\dot{Q}_u}$  for selected measurement days.

The relation between the presented coefficients requires additional discussion. For both factors, it should be remembered that the inequality  $X_{\dot{Q}_u} > X_{Sol}$  will always be true due to the thermal losses and optical efficiency of solar collectors.

The coefficients  $X_{Sol}$  and  $X_{\dot{Q}_u}$  can be used to characterize the quantity of incoming solar radiation and amount of useful power extracted from solar collectors, during test day. However, the rate of changes in solar energy flux density, which is very important in control strategy, needs also to be taken into account.

In order to describe the fluctuations of the power supply for solar collectors during the test period, the  $E_{var}$  indicator has been developed.

$$E_{var} = \frac{k_{var}}{k_t} \tag{6}$$

where:  $k_t$  is the total number of measurement time samples taken during the test day and  $k_{var}$  is the sum of the time samples, during which the solar energy changes of intensity appears, according to the conditional statement:

$$t_{var} = \begin{cases} t_{var} \Rightarrow |G_{\beta_i} - G_{\beta_{i-1}}| < \Delta G_{cr} \\ t_{var} + 1 \Rightarrow |G_{\beta_i} - G_{\beta_{i-1}}| \geq \Delta G_{cr} \end{cases} \tag{7}$$

where: the  $G_{\beta_i}$  is the global radiation intensity recorded during each time sample (10s) and the  $\Delta G_{cr}$  is the threshold value of radiation intensity changes, which value was specified as  $\Delta G_{cr} = 5[\text{W/m}^2]$ .

The value of  $E_{var}$  is in the range of:  $0 \leq E_{var} \leq 1$ . It determines the variability of the incoming solar radiation by comparing subsequent readings. The high value of this factor indicates a very large variation of the solar radiation throughout the day, to which it relates.

Figure 5 presents the values of the factor  $E_{var}$  for selected test days.

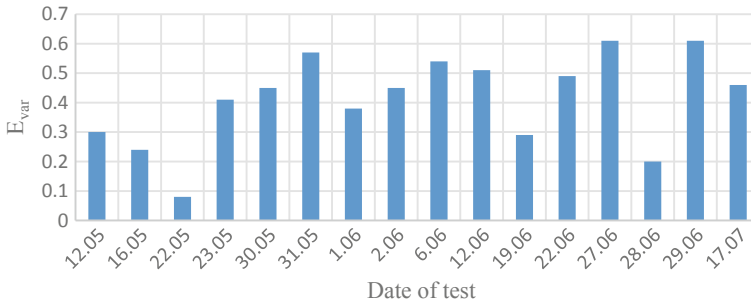


Fig. 5 The  $E_{var}$  factor values for selected test days

### 4 Results and Discussion

The energy efficiency study of the solar system were carried out using a proportional control strategy. The controller has been programmed to operate in three different modes, i.e. rapid, mid and slack. The specific dependency between the  $\Delta T$  and mass flow rate  $\dot{m}_f$  for each mode is presented in the Fig. 6.

Each time, before starting the measurement day, the hydraulic system parameters were set to initial values and one of the three controller settings was selected. After completing the measurement work, data from days with similar atmospheric conditions were grouped together, based on the indicators  $E_{rad}$  and  $E_{var}$ . Hereby, four types of days were distinguished. In each day type, with similar weather conditions, different control modes were used (Fig. 7).

The first group (I) included days with a high ratio of  $E_{rad}$  and low  $E_{var}$ . This means that they were characterized by high intensity of solar radiation, rarely interrupted during measurements. The example of the first type (I) sunlight conditions is May 22, 2018, presented in Fig. 8.

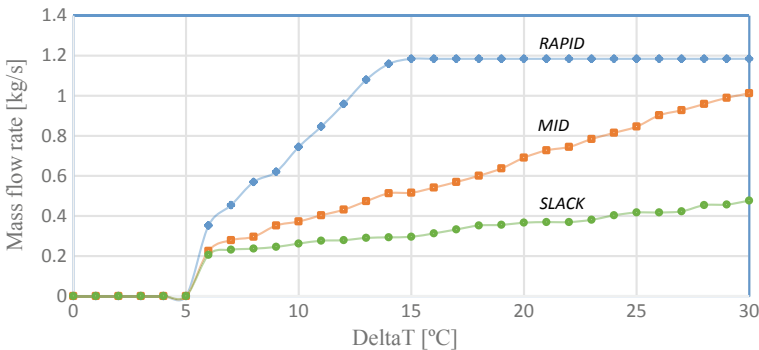


Fig. 6 The controller operating modes

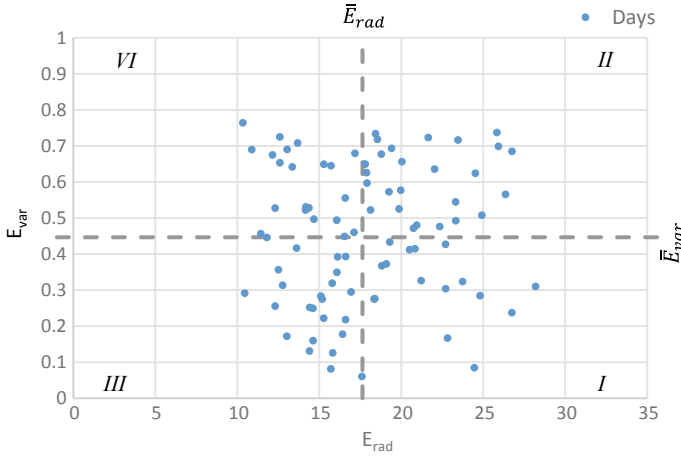


Fig. 7 Division of test days based on the indicators  $E_{var}$  and  $E_{rad}$  values

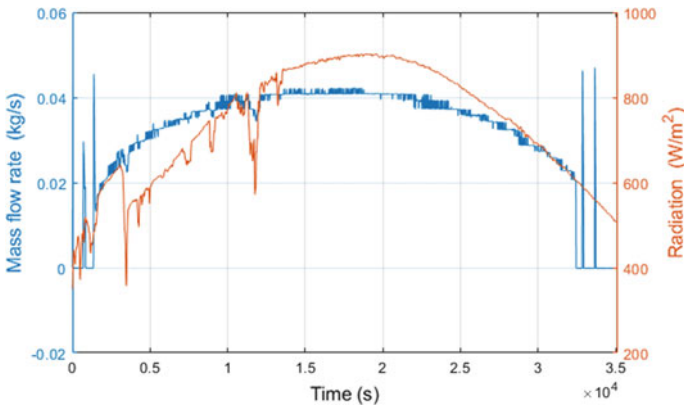
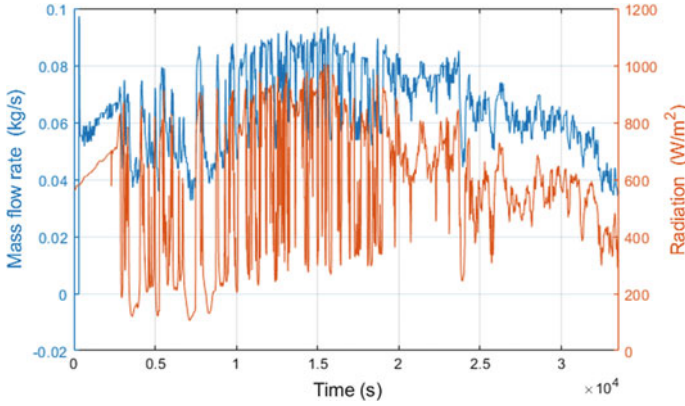


Fig. 8 The first type (I) of sunlight conditions and flow rate response, May 22, 2018

The conducted experimental research indicates that during days with continuous and uninterrupted solar operation, the highest values of  $X_{Sol}$  and  $X_{\dot{Q}_u}$  coefficients were achieved for MID and RAPID control modes. Therefore, due to the higher electric energy consumption for RAPID control mode, of electrical energy, the MID mode is recommended.

In the second group (II) there were days with high sunlight intensity conditions, but also with high rate of changes in radiation during the test. The representative of such a day is June 22, 2018 (Fig. 9).

It turns out that the highest values of  $X_{Sol}$  and  $X_{\dot{Q}_u}$  coefficients were achieved using the RAPID mode. This is due to the higher efficiency of energy transfer from



**Fig. 9** The second type (II) of sunlight conditions and flow rate response, June 22, 2018

short-term pulses of solar energy to the storage tank than in the case of lower mass flow rate control modes.

Days from the third group (III) of sunlight conditions are characterized by low values of  $E_{rad}$  and  $E_{var}$  coefficients. This means that the low density of solar radiation was recorded, while maintaining its stability. A selected example of such a day is May 16, 2017 (Fig. 10).

An increase in the value of  $X_{Sol}$  and  $X_{\dot{Q}_u}$  coefficients was observed for smaller mass flow rate modes in collector loops, using the *SLACK* mode. This avoided the critically low  $\Delta T$  values and the pump turn-offs that occurred when using the *MID* and *RAPID* modes.

The last fourth group (IV) of sunlight conditions is represented by days with low sunshine and frequent interruptions in solar energy supply. Days of high cloudiness and low visibility dominated here. One of these days was June 22, 2019 (Fig. 11).

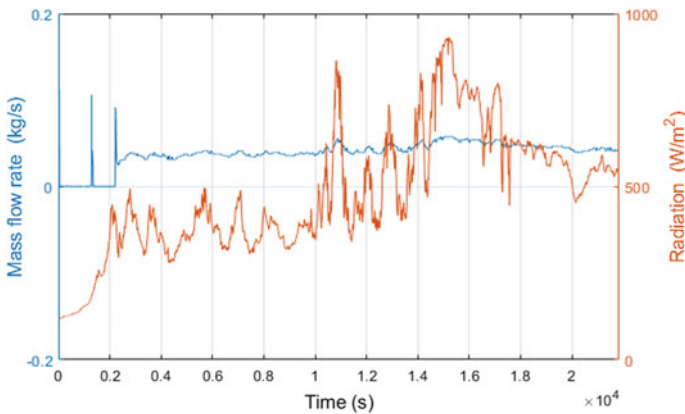


**Fig. 10** The third type (III) of sunlight conditions and flow rate response, May 16, 2017

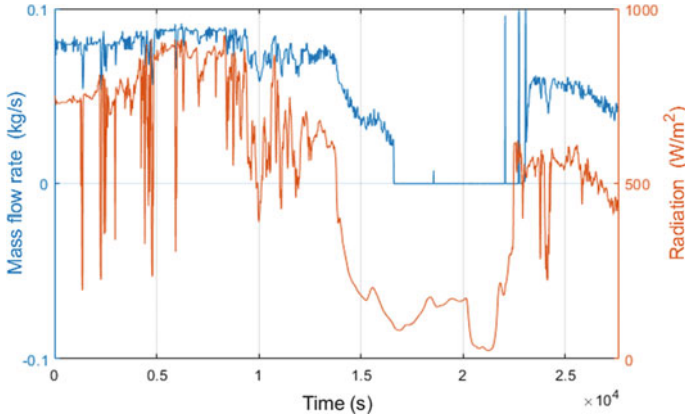


**Fig. 11** The fourth type (IV) of sunlight conditions and flow rate response, May 16, 2017

The analysis of the values of the  $X_{Sol}$  and  $X_{\dot{Q}_u}$  coefficients for these days related that the best solar harvest processing results were achieved for the *SLACK* control mode. Compared with other modes, *Slack* allowed to obtain higher thermal energy in the tanks. The *MID* and *RAPID* modes, on the other hand, tend to an unprofitable movement of the heat energy from the storage tank into the collectors loop.

The list of average values of the  $X_{Sol}$  and  $X_{\dot{Q}_u}$  coefficients for individual types of sunlight conditions is presented in Table 1.

In each group of the sunlight conditions types, noticeable differences of the values of the  $X_{Sol}$  and  $X_{\dot{Q}_u}$  were observed, depending on the controller mode. This confirms the need to create control algorithms that have the ability to self-adapt to weather conditions. This also means that it is possible to increase the efficiency of the Solar Water Heating System by adapting the control strategy to the prevailing weather conditions. The effects of this work will be used to develop a modern self-adaptive proportional controller and to study adaptive algorithms used in Solar Systems control strategies.

**Table 1** Average values of  $X_{Sol}$  and  $X_{\dot{Q}_u}$  for different types of sunlight conditions and control modes

Type of sunlight condition	Average for day type		Most efficient control mode	Average for most efficient control mode	
	$\bar{X}_{Sol}$	$\bar{X}_{\dot{Q}_u}$		$\bar{X}_{Sol}$	$\bar{X}_{\dot{Q}_u}$
I	0.54	0.66	MID	0.61	0.74
II	0.39	0.61	RAPID	0.45	0.7
III	0.57	0.63	SLACK	0.59	0.76
IV	0.36	0.55	SLACK	0.41	0.64

## References

1. Sontake, V.C.H., Kalamkar, V.R.: Solar photovoltaic water pumping system—a comprehensive review. *Renew. Sustain. Energy Rev.* **59**, 1038–1067 (2017)
2. Budea, S., Bădescu, V.: Improving the Performance of systems with solar water collectors used in domestic hot water production. *Energy Procedia* **112**, 398–403 (2017)
3. Jakubowski, M., Stachnik, M., Sterczyńska, M., Matysko, R., Piepiórka-Stepuk, J., Dow-giałło, A., Ageev, O., Knitter, R.: CFD analysis of primary and secondary flows and PIV measurements in whirlpool and whirlpool kettle with pulsatile filling: analysis of the flow in a swirl separator. *J. Food Eng.* **258**, 27–33 (2019)
4. Kaminski, K., Krolikowski, T., Blazejewski, A., Knitter, R.: Significant parameters identification for optimal modelling of the harp type flat-plate solar collector. *Sustainable Design and Manufacturing (SDM19)*, 4–5 July 2019. Springer (2019), pp. 495–507. <https://doi.org/10.1007/978-981-13-9271-9>
5. Kaminski, K., Znaczko, P., Lyczko, M., Krolikowski, T., Knitter, R.: Operational properties investigation of the flat-plate solar collector with Poliuretane Foam Insulation. 23rd International Conference on Knowledge-Based and Intelligent Information & Engineering Systems, *Procedia Computer Science*, 4–5 September 2019. ISSN: 1877-0509. <https://doi.org/10.1016/j.procs.2019.09.344>
6. Kicsiny, R., Farkas, I.: Improved differential control for solar heating systems. *Sol. Energy* **86**, 3489–3498 (2012)
7. Królikowski, T., Nikończuk, P.: Finding temperature distribution at heat recovery unit using genetic algorithms. *Proc. Comput. Sci.* **112**(2), 382–2390 (2017)
8. Nikończuk, P.: Study of heat recovery in spray booths. *Met. Finish.* **111**(6), 37–39 (2013)
9. Nikończuk, P., Dobrzyńska, R.: Preliminary measurements of overspray sediment’s thermal conductivity. *Ochrona Przed Korozją* **61**(2), 40–42 (2018)
10. Nikończuk, P.: Preliminary modeling of overspray particles sedimentation at heat recovery unit in spray booth. *Eksploatacja i Niezawodność—Maintenance and Reliability* **20**(3), 387–393 (2018). <http://dx.doi.org/10.17531/ein.2018.3.6>
11. Glowinski, S., Blazejewski, A., Krolikowski, T., Knitter, R.: 4–5 July 2019 “Gait recognition: a challenging task for MEMS signals identification” *Sustainable Design and Manufacturing (SDM19)*, pp. 473–485. Springer 2019 <https://doi.org/10.1007/978-981-13-9271-9>
12. Głowiński, S., Błażejowski, A., Krzyżyński, T.: Human gait feature detection using inertial sensors and wavelets analysis. *Biosys. Biorob. Wearable Robot Challenges Trends* **16**, 397–401 (2016)
13. Głowiński, S., Błażejowski, A., Krzyżyński, T.: Inertial sensors and wavelets analysis as a tool for pathological gait identification. *Innovations in Biomedical Engineering, Advances in Intelligent Systems and Computing*. Springer, Berlin (2016), pp. 106–114. [https://doi.org/10.1007/978-3-319-47154-9\\_13](https://doi.org/10.1007/978-3-319-47154-9_13)
14. Hamed, M., Fellah, A., Brahim, A.B.: Parametric sensitivity studies on the performance of a flat plate solar collector in transient behavior. *Energy Convers. Manag.* **78**, 938–947 (2014)
15. Jaszczak, S., Nikończuk, P.: Identification of the plant dynamic using genetic algorithms. 2016 21st International Conference on Methods and Models in Automation and Robotics (MMAR), *Miedzyzdroje* (2016), pp. 516–519. <https://doi.org/10.1109/mmar.2016.7575189>
16. Jaszczak, S., Nikończuk, P.: Synthesis of spray booth control software in programmable controller. *Przegląd Elektrotechniczny* **91**(11), 182–185. <https://doi.org/10.15199/48.2015.11.44>
17. Kalogirou, S.A.: Solar thermal collectors and applications. *Prog. Energy Combust. Sci.* **30**, 231–295 (2004)
18. Nikończuk, P., Rosochacki, W.: The concept of reliability measure of recuperator in spray booth. *Eksploatacja i Niezawodność—Maintenance and Reliability* **22**(2), 265–271 (2020). <http://dx.doi.org/10.17531/ein.2020.2.9>

19. Zajac, W., Andrzejewski, G., Krzywicki, K., Krolikowski, T.: Finite state machine based modelling of discrete control algorithm in LAD diagram language with use of new generation engineering software. 23rd International Conference on Knowledge-Based and Intelligent Information & Engineering Systems. *Procedia Computer Science*, 4–5 September 2019. ISSN: 1877-0509. <https://doi.org/10.1016/j.procs.2019.09.431>
20. Ghorab, M., Entchev, E., Yang, L.: Inclusive analysis and performance evaluation of solar domestic hot water system (a case study). *Alexandria Eng. J.* **56**(2), 201–212 (2017)
21. Yao, Ch., Hao, B., Liu, S., Chen, X.: Analysis for common problems in solar domestic hot water system field-testing in China. *Energy Procedia* **70**, 402–408 (2015)
22. Krolikowski, T., Knitter, R., Blazejewski, A., Glowinski, S., Kaminski, K.: Emission of particles and VOCs at 3D printing in automotive. *Sustainable Design and Manufacturing (SDM19)*, 4–5 July 2019. Springer (2019), pp. 485–495. <https://doi.org/10.1007/978-981-13-9271-9>
23. Krolikowski, T., Knitter, R., Blazejewski, A.: Computer modeling and testing of structural metamaterials. 23rd International Conference on Knowledge-Based and Intelligent Information & Engineering Systems. *Procedia Computer Science*, 4–5 September 2019. ISSN: 1877-0509 <https://doi.org/10.1016/j.procs.2019.09.429>
24. Krolikowski, T., Knitter, R., Stachnik, M.: Thermo-mechanic tests using 3d printed elements. 23rd International Conference on Knowledge-Based and Intelligent Information & Engineering Systems. *Procedia Computer Science*, 4–5 September 2019. ISSN: 1877-0509. <https://doi.org/10.1016/j.procs.2019.09.430>



# Industry 4.0—Supporting Industry in Design Solutions—All-in-One Computer Cover



Krolikowski Tomasz , Knitter Remigiusz , Blazjewski Andrzej ,  
Zmuda Trzebiatowski Piotr , Zuchniewicz Jerzy , and Bak Aleksander 

**Abstract** The paper presents an invention in the form of an all-in-one computer case designed in cooperation with a technical university under the Industry 4.0 program. All-in-one computer cases are widely used primarily in all areas that use personal computers. This kind of unit can also be used to operate the vehicle charging stations, parking lots, urban bike rental, etc. Compared to desktop units, all-in-one computers take up significantly less space on the computer stand. As a result of using components installed in laptops, they are characterized by higher energy efficiency and lower heat emission. The compact design of the equipment means that it can be moved to another place or taken on a trip at any time. All-in-one machines are currently widely used, offering equipment for both basic office work and advanced programs requiring considerable hardware resources.

## 1 Introduction

The current known concept of the computer housing allows almost any expansion depending on the needs of modifying or expanding the computer equipment.

The classic computer case is built around the motherboard based on existing standards (e.g., ATX, BTX, ITX), which define the position of expansion card slots in the housing (usually the back wall) and the mounting points of the motherboard to the tray. Similarly, the size and arrangement of the mounting holes for remaining computer components (HDD, fans, power supplies, optical drives) are standardized. However, the position of them in the housing, the methods used for their installation (sleds, hooks, latches, screws), or the amount of mounting bays provided depend on the designer and allow wide freedom of design. This concept, consisting of standardized components, allows to easily create enclosures tailored to user needs (e.g.,

---

K. Tomasz (✉) · K. Remigiusz · B. Andrzej · Z. T. Piotr  
FM, Koszalin University of Technology, Koszalin 75-453, Poland  
e-mail: [tomasz.krolikowski@tu.koszalin.pl](mailto:tomasz.krolikowski@tu.koszalin.pl)

Z. Jerzy · B. Aleksander  
Alplast sp. z.o.o, Niekanin Sliwkowa 1, Niekanin 78-100, Poland

a housing with space for 10 optical drives for the construction of a DVD copier, or with a separate space for water cooling radiators).

These enclosures apply to desktop computers in a traditional form consisting of a chassis, monitor, and other devices, but not in all-in one type.

All-in-one (AIO) computers are typically based on components used in laptops. This type of housing design restricts or even prevents access to the computer for unauthorized persons and provides reduced levels of revealing emissions.

This study raises the theme of the new AIO computer housing concept for self-assembly of base components. It is characterized by a rear panel connected to a movable motherboard tray suspended on the bracket, with a power circuit filter, a ventilation panel and supports for fixing the computer power supply. The front panel is a supporting structure for a ventilation module with fan and a HDD gasket. The body of the housing is complemented by a door with a multi-ratchet lock, mounted on hinges, and preventing access to functional blocks.

## 2 Object Characteristics

The purpose of the invention was to develop an all-in-one computer case design that would allow the user to independently and tool-free mounting any components such as screen matrix, motherboard, graphics card, and hard disk.

The presented construction is characterized by:

- detachable frame,
- removable rear wall,
- front wall with mounting holes for computer components.

The side surfaces of the frame have hooking elements. Preferably one of the side surfaces of the frame has at least one tab element in the form of a tab. And computer casing has an offset element on which there is at least one inlet opening.

The subject of the invention is presented in the drawings. The diagram in Fig. 1 shows the computer case without the rear wall and with the screen matrix frame removed in Fig. 2. The retainer in enlarged view presents details of the latch, and Fig. 3 shows the computer in a rear view.

From the descriptions of other inventions, e.g., from the description of the invention US2019064877 published on 28.02.2019, a diagram of the upper case assembly for a portable computer is known. The assembly may have an integral, uniform (e.g., homogeneous) upper housing formed from one part. The integrated upper shell acts as the housing and frame of the laptop. The integrated top case also serves as the basic structure of a laptop. The assembly may contain various components, such as keyboards, touch panels, printed circuit boards, and drives, which are carried through the lower part of the integral upper housing. The integrated upper housing can be made of an aluminum plate that has been machined to form walls, holes, attachment areas, and cosmetic areas of the upper housing.

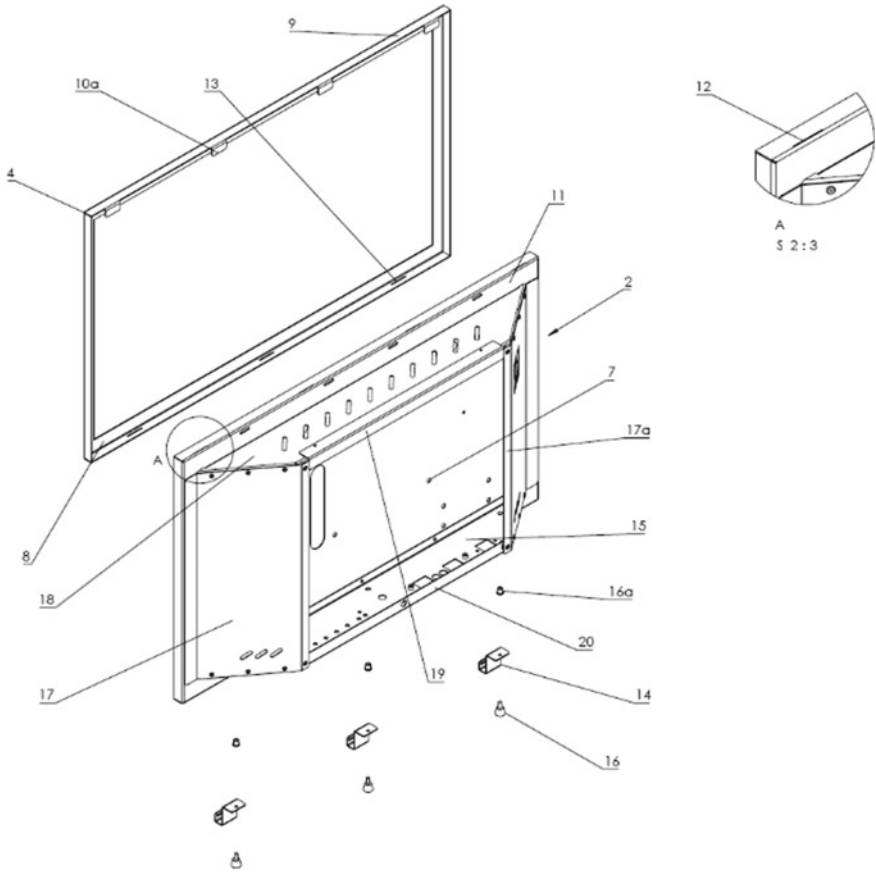


**Fig. 1** Subject of the study without back wall and screen matrix frame

In addition, from another solution available in the patent database (invention P.369394 published 2006-02-06, BUP 3/2006), a computer case is known having a rectangular body in which the front plate has a pocket in which the removable disk drive box is placed. The upper plate of the housing body is equipped with a socket with a handle. A closing mechanism is located on the side housing plate. In addition, the side plates and bottom plate have holes for attaching the feet. Depending on the needs, the housing can be placed vertically or laid horizontally.

Both types of enclosures do not apply to AIO computers. In the described construction, it was decided to combine the advantages of solutions known from portable and desktop computers:

- Compact design with a high level of component integration—known from laptops.
- Easy to modify and expand computer components—known from desktop computers.

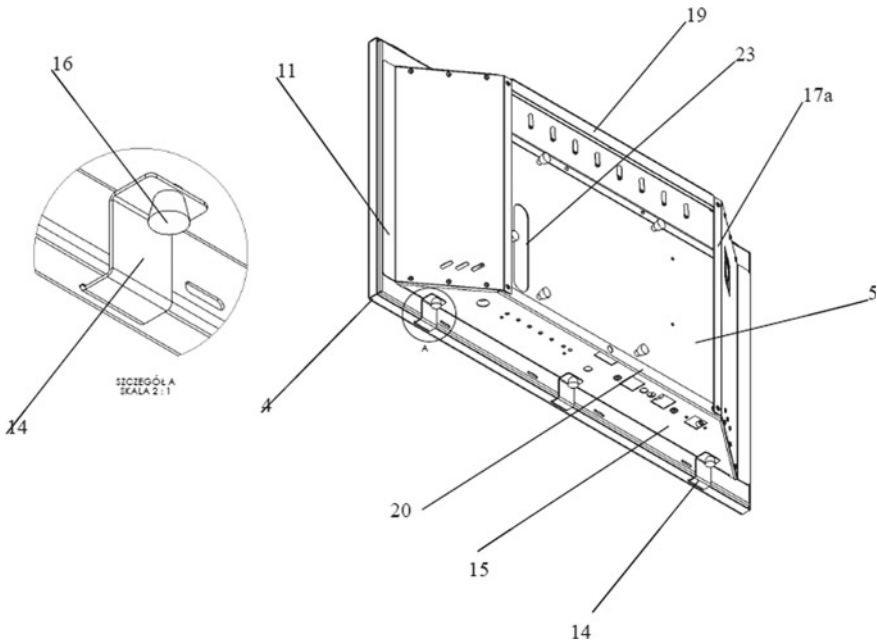


**Fig. 2** Applied fixing elements

Combination of presented functions was not found in the AIO solutions available on the market, which are much closer in terms of design solutions for laptops.

### 3 Applications Implemented in Production

The authors of the project have also prepared solutions, based on the all-in-one housing, of new generations of multimedia reception kiosks based on the Cloud Integrator platform. The kiosk working system should be composed of basic modules created using the so-called builder (understood as a tool for quickly creating and updating basic kiosk functionalities, mainly requiring device drivers, e.g., card feeder, receipt printer, microphone, and speakers). However, all processes will take place in the cloud with which the kiosk is connected remotely. Thanks to this, it will be possible to commercially use ready-made programming solutions, which are provided by e.g., Google (Speech API, TensorFlow) or movement identification [1–3]. A platform for creating additional functionality in the form of online services related to the functioning of the reception kiosk without restrictions related to the technical layer of the kiosk or in the design and selection of functions. The Cloud platform should allow the manager to directly manage the functioning of the kiosk directly at the target customer while offering additional services that allow the sale

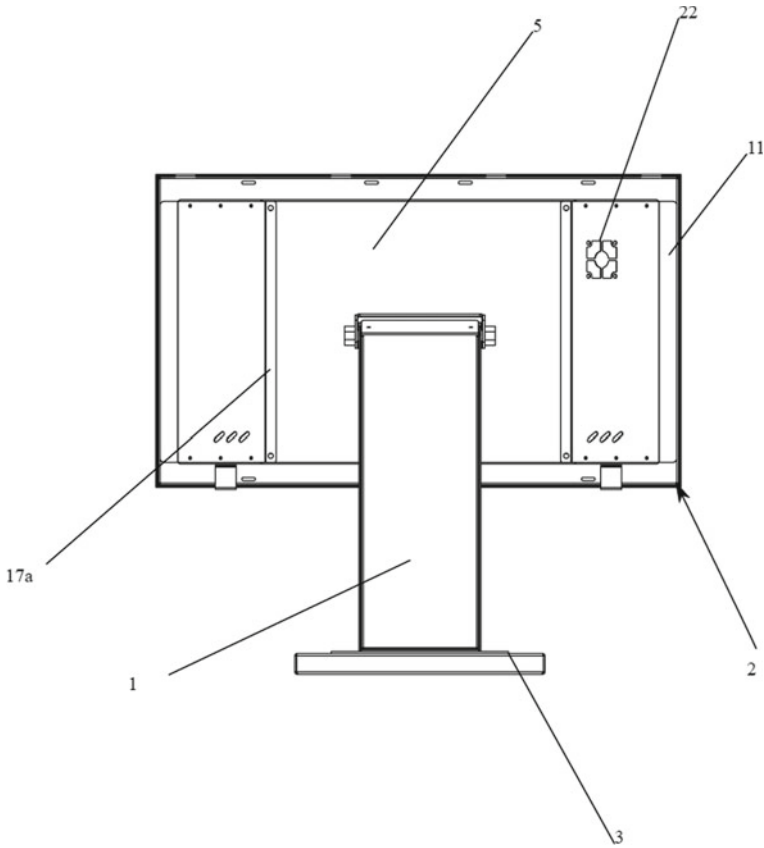


**Fig. 3** Rear view of the computer case

of additional services to the end-user or become a layer of additional functionalities of the kiosk system itself.

The technical implementation of the offered services should operate similarly: The kiosk software connects to the Cloud Integrator platform (via the Internet), which performs the device request, returning specific data required by the kiosk and complete the order. For example, a kiosk requires speech or message translation into Chinese. The appropriate message is sent to the online platform, which contains the necessary connections and executive software, which translates the phrase and sends back in the form of translated text or speech.

The Cloud Integrator platform should allow the construction of additional service models for the reception kiosk, any size, and enable scaling of the infrastructure necessary for their implementation by dynamic allocation of resources and prioritization. Created models, answers, and initiated functionalities should be immediately ready for use and made available through a predictive platform that allows to handle thousands of parallel queries and terabytes of data. The platform should be integrated

with the functionality supporting data preprocessing as well as with the mechanism of management and archiving of client systems of reception kiosks responsible for reliable access to the recovery of stored information.

The element that aims to distinguish the Cloud Integrator platform from among the available environments is the ability to use neural network algorithms to detect and decipher patterns and correlations (similar to learning and reasoning) between individual models of user activities, both based on statistical distributions and neural network algorithms in conjunction with the TensorFlow framework, which allows to use pre-built neural networks in the services offered by the platform to build more advanced functions and interact with target users. This kind of functionality allows the use of a kiosk both as a training unit and control unit with fast dynamic identification [4] and control algorithms reconfiguration [5–7].

## 4 Components Cooling Assumptions

Based on the thermal power emitted by the electronics, the minimum air volume required to cool the components can be determined. Convective heat exchange between a solid and the surrounding air depends on the heat transfer coefficient and the difference in air and solid temperature. The convective heat flux  $dQ_k/dt$  is described by the equation [8, 9]:

$$\frac{dQ_k}{dt} = F\alpha_k(T_{cs} - T_p) \quad (1)$$

For air, the value of the heat transfer coefficient  $\alpha_k$  is approximately equal 7 [W/m<sup>2</sup>K] for free convection and 50 [W/m<sup>2</sup>K] for forced convection.

After the transformation of Eq. (1), the relationship describing the relation of heat exchange to surface size was obtained:

$$F = \frac{dQ_k}{dt} \frac{1}{\alpha_k(T_{cs} - T_p)} \quad (2)$$

Changes in the temperature of the solid body and the air flowing around are depended on the heat exchange stream and their mass and specific heat value:

$$\Delta T = \frac{Q_k}{cm} \quad (3)$$

where

- $c$  specific heat [J/(kgK)],
- $m$  object mass [kg].

Mass of solid is constant while the mass of exchanged air depends on its physical properties:

$$m_p = \int_0^{\tau} \rho_p \frac{dV_p}{dt} dt, \quad (4)$$

where

$\rho_p$  air density [kg/m<sup>3</sup>],  
 $dV_p/dt$  airflow volume [m<sup>3</sup>/s],  
 $\tau$  the period of time in which the air absorbs heat from the object [s].

Using Eqs. (3) and (4), the required volume of air needed to achieve the expected rate of change of air temperature  $d\Delta T/dt$  can be calculated:

$$\frac{dV_p}{dt} = \frac{\frac{dQ_k}{dt}}{\rho_p c_p \frac{d\Delta T}{dt}} \quad (5)$$

Further work included determining the internal cubature of the enclosure, the location of the components that are the main heat sources and ventilation openings in the enclosure. It was also required to carry out a heat balance of all kiosk construction elements. Therefore, simulation tests of temperature distribution [10] and heat dissipation from the surroundings of heat emission sources [11, 12] in a closed space with forced airflow were conducted with CFD models [13]. Study took into consideration the efficiency of heat exchange similar to spray booth [14] with particle sedimentation [15, 16] and reliability estimating [17]. The following figures show research results for the selected electronic system component—power supply with fan (Fig. 4a) and ventilation holes (Fig. 4b). Figure 4a shows the position of the fan and the direction of airflow (arrow), while Fig. 4b shows the position of the ventilation holes and the forced airflow into the device interior. Location of heat sources in the interior is shown in Fig. 4c. Figure 4d shows the temperature distribution [K] in the interior and velocity vectors [m/s] of air movement (Fig. 5).

When designing the final product, the authors also conducted a simulation strength analysis before starting production. The research included a simulation of stresses generated when the user rests on the casing during operation of the computer.

After applying 500 N (50 kg) to the surface, maximum displacements of 1.124e + 01 mm were obtained (Fig. 6).

After strength analysis, the type of material for production was selected. The enclosures will be made of a sheet of black cold-rolled low-carbon steel, electrolytically galvanized (EN 10152) grade DC01A (Table 1).

The enclosures will be protected against corrosion by applying a primer and powder coating. The color of the housing will be chosen by the customer. Further, personalization options will also be available, e.g., LED backlight or illuminated logo on the front cover.

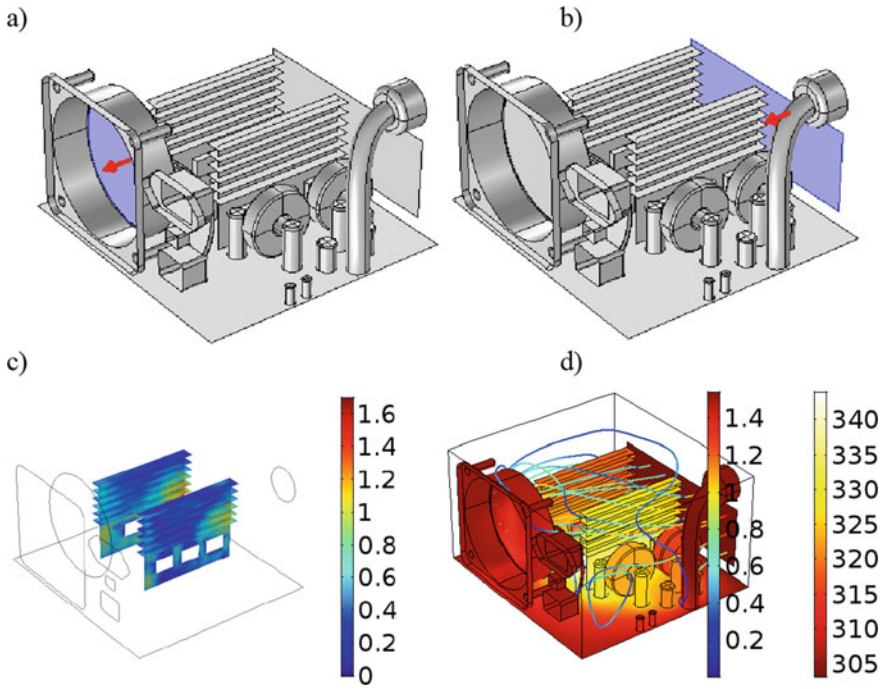


**Fig. 4** Tested computer power supply element placed in a closed space with the airflow forced by the fan (a) and throwing it out through the ventilation holes (b) located behind heat sources (c). Together with the visualization of temperature distribution and air velocity (d)



**Fig. 5** One of the concepts of the all-in-one housing. Visualization of the control panel



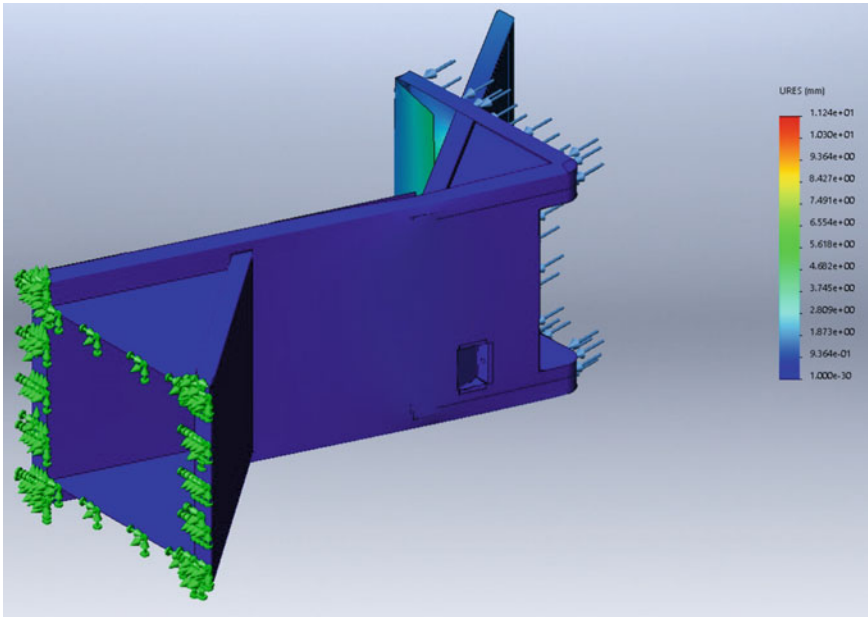


**Fig. 6** Static analysis 1-Displacement–Displacement 1

The stationary version of the kiosk prototype based on the All-in-one casing is made of cold-rolled low-carbon steel sheet DC01A grade 1 mm thick. The part preparations were made by laser cutting, and the bending of the edges was done on a press brake. Connections of the housing’s structural elements were made using the MIG/MAG method—electric arc welding between metal and fusible electrode with an inert gas shield. Other connections were made using traditional Sariv screws and rivets typically used for assembling personal computers. The prototype version was not equipped with a keyboard due to the use of the touch screen.

Screwed elements allow easy access by a service technician to replace damaged electronic components of the reception kiosk. The sides of the kiosk are made of polycarbonate, which, depending on the customer’s needs, gives the possibility to adjust color and transparency (Fig. 7).

An individual GUI has been developed for the proposed kiosk. Implemented functionality was developed on the basis of tests conducted in hotels on end-users (guests and hotel employees). Based on the results of surveys in the first stage, the dominants of the resulting structure were determined. Thanks to the responses of the participants, it was found what elements of the product are most important for the potential user. The main focus was on adjusting the height of the countertop, where components for controlling the device were to be located. The average female phantom 50 cm and the largest male 95 cm were used in the study. Necessary elements were placed in a radius convenient for users from this range. Designing the other parts followed the same rule. This also applies to the control panel and components

**Table 1** DC01A sheet properties

Steel grade	Number	Surface	Re [Mpa]	Rm [Mpa]	A <sub>80</sub>	r <sub>90</sub> min	n <sub>90</sub> min.	Steel composition			
								C max. %	P max. %	S max. %	Mn max. %
DC01	1.0330	A	140 do 280	270 do 410	28	–	–	0.12	0.045	0.045	0.60

**Fig. 7** Reception kiosk prototype—phase after assembly of kiosk controls



that facilitate use. The age and social groups selected during the survey have an impact on the selection and use of specific functions

The idea was to create neutral interface. Due to the wide range of recipients and their identification, it was decided to create a minimalistic layout neutral for the environment. Most of the responders preferred specific styles, which had to be avoided when designing a neutral interface for the device, not for a specific recipient. Choosing a font was guided by the lack of ornaments such as serifs or scaling of individual letter elements. Due to the technical limitations, the decision was made to not personalize the user interface and neutral colors with added cool shade of blue were chosen. For this stage, the technical possibilities of introducing the software on devices with different resolutions had a great impact. By solving the problem of combining expectations and possibilities, a horizontal layout with a fixed taskbar was created, maintaining its readability and functionality in every case (Fig. 8).

To perform vibro-isolators for the prototype, elements containing metamaterials were used. Structural elements containing metamaterials are made of PET material with metal powders.

## 5 Summary

According to the authors, the advantage of the presented invention is a simple all-in-one computer case, that allows user to mount components such as matrix, motherboard, graphics card, hard drive alone and without use of any tools. Thanks to this construction, the user can independently compose a computer with his preferred



**Fig. 8** Production of the finished product with the all-in-one casing used

parameters and assemble it in a practical all-in-one housing. Further research will aim to optimize shape and heat dissipation without the use of fans (passive cooling), as well as the use of recycled materials in production. Research is currently underway on the use of PET waste for 3D printing [8, 9, 18] of computer cases.

## References

1. Glowinski, S., Błazejewski, A., Krolikowski, T., Knitter, R.: Gait recognition: a challenging task for MEMS signals identification. In: Sustainable Design and Manufacturing (SDM19), 4–5 July 2019. Springer (2019), pp. 473–485. <https://doi.org/10.1007/978-981-13-9271-9>
2. Głowiński, S., Błazejewski, A., Krzyżyński, T.: Human gait feature detection using inertial sensors and wavelets analysis. *Biosyst. Biorob. Wearab. Robot. Challenges Trends* **16**, 397–401 (2016)
3. Głowiński, S., Błazejewski, A., Krzyżyński, T.: Inertial sensors and wavelets analysis as a tool for pathological gait identification. In: *Innovations in Biomedical Engineering, Advances in Intelligent Systems and Computing*, Springer (2016), pp. 106–114. [https://doi.org/10.1007/978-3-319-47154-9\\_13](https://doi.org/10.1007/978-3-319-47154-9_13)
4. Jaszczak, S., Nikończuk, P.: Identification of the plant dynamic using genetic algorithms. In: 2016 21st International Conference on Methods and Models in Automation and Robotics (MMAR), Miedzyzdroje (2016), pp. 516–519. <https://doi.org/10.1109/mmar.2016.7575189>
5. Jaszczak, S., Nikończuk, P.: Synthesis of spray booth control software in programmable controller. *Przełąd Elektrotechniczny* **91**(11), 182–185. <https://doi.org/10.15199/48.2015.11.44>
6. Lokietek, T., Jaszczak, S., Nikończuk, P.: Optimization of control system for modified configuration of a refrigeration unit. *Proce. Comput. Sci.* **159**, 2522–2532 (2019). <https://doi.org/10.1016/j.procs.2019.09.427>

7. Zajac, W., Andrzejewski, G., Krzywicki, K., Krolikowski, T.: Finite state machine based modelling of discrete control algorithm in LAD diagram language with use of new generation engineering software. 23rd International Conference on Knowledge-Based and Intelligent Information & Engineering Systems. *Procedia Computer Science*, 4–5 September 2019. ISSN: 1877-0509. <https://doi.org/10.1016/j.procs.2019.09.431>
8. Krolikowski, T., Knitter, R., Blazejewski, A., Glowinski, S., Kaminski, K.: Emission of Particles and VOCs at 3D Printing in Automotive. In: *Sustainable Design and Manufacturing (SDM19)*, 4–5 July 2019. Springer (2019), pp. 485–495 <https://doi.org/10.1007/978-981-13-9271-9>
9. Krolikowski, T., Knitter, R., Blazejewski, A.: Computer modeling and testing of structural metamaterials. In: 23rd International Conference on Knowledge-Based and Intelligent Information & Engineering Systems. *Procedia Computer Science*, 4–5 September 2019. ISSN: 1877-0509. <https://doi.org/10.1016/j.procs.2019.09.429>
10. Królikowski, T., Nikończuk, P.: Finding temperature distribution at heat recovery unit using genetic algorithms. *Proc. Comput. Sci.* **112**(2), 382–2390 (2017)
11. Kaminski, K., Krolikowski, T., Blazejewski, A., Knitter, R.: Significant parameters identification for optimal modelling of the harp type flat-plate solar collector. In: *Sustainable Design and Manufacturing (SDM19)*, 4–5 July 2019. Springer (2019), pp. 495–507. <https://doi.org/10.1007/978-981-13-9271-9>
12. Kaminski, K., Znaczo, P., Lyczko, M., Krolikowski, T., Knitter, R.: Operational properties investigation of the flat-plate solar collector with Poliuretane foam insulation. In: 23rd International Conference on Knowledge-Based and Intelligent Information & Engineering Systems. *Procedia Computer Science*, 4–5 September 2019. ISSN: 1877-0509. <https://doi.org/10.1016/j.procs.2019.09.344>
13. Jakubowski, M., Stachnik, M., Sterczyńska, M., Matysko, R., Piepiórka-Stepuk, J., Dow-giałło, A., Ageev, O., Knitter, R.: CFD analysis of primary and secondary flows and PIV measurements in whirlpool and whirlpool kettle with pulsatile filling: analysis of the flow in a swirl separator. *J. Food Eng.* **258**, 27–33 (2019)
14. Nikończuk, P.: Study of heat recovery in spray booths. *Met. Finish.* **111**(6), 37–39 (2013)
15. Nikończuk, P., Dobrzyńska, R.: Preliminary measurements of overspray sediment's thermal conductivity. *Ochrona Przed Korozją* **61**(2), 40–42 (2018)
16. Nikończuk, P.: Preliminary modeling of overspray particles sedimentation at heat recovery unit in spray booth. *Eksploracja i Niezawodność – Maintenance and Reliability* **20**(3), 387–393 (2018). <http://dx.doi.org/10.17531/ein.2018.3.6>
17. Nikończuk, P., Rosochacki, W.: The concept of reliability measure of recuperator in spray booth. *Eksploracja i Niezawodność—Maintenance and Reliability 2020* **22**(2), 265–271. <http://dx.doi.org/10.17531/ein.2020.2.9>
18. Krolikowski, T., Knitter, R., Stachnik, M.: Thermo-mechanic tests using 3d printed elements. In: 23rd International Conference on Knowledge-Based and Intelligent Information & Engineering Systems. *Procedia Computer Science*, 4–5 September 2019. ISSN: 1877-0509. <https://doi.org/10.1016/j.procs.2019.09.430>
19. Krolikowski, T., Suslow, W.: A concept of a training project IT Management System. In: 23rd International Conference on Knowledge-Based and Intelligent Information & Engineering Systems. *Procedia Computer Science*, 4–5 September 2019. ISSN: 1877-0509. <https://doi.org/10.1016/j.procs.2019.09.317>

# Development of a Robotic System with Stand-Alone Monocular Vision System for Eco-friendly Defect Detection in Oil Transportation Pipelines



Amith Mudugamuwa , Chathura Jayasundara , Han Baokun, and Ranjith Amarasinghe 

**Abstract** This paper presents development of a pipeline defect detection (PDD) system and designing main components of the system to reduce the risk of environmental pollution due to pipeline accidents. Main feature presented is a robotic system including a pipe navigation mechanism and a vision system. ExPIRo robot platform developed at the previous stage of the research is used as the moving mechanism for the robotic system with minor modifications. Vision system is developed by the integration of a camera module, a single board computer and a remote workstation. PDD system presented provides remote monitoring and analyzing features by utilizing the remote workstation for data storage. MATLAB-based image acquisition algorithm is performed on LATTEPANDA single board computer, whereas the defect identification algorithm is performed on HP Envy 6-1012TX Ultra-Book laptop. GUI developed for the system visualizes the stages of image analysis and displays result while updating the result of each image for defect identification purpose. External surface defects having significant appearance abnormalities are tested using the presented PDD system, images of pipe segments are captured, and defects are successfully identified.

## 1 Introduction

Among various transportation methods, pipelines are the most common fluid transportation method. Crude oil, natural gas and steam are highly utilized as energy sources utilized in both domestic and industrial applications, and for transportation and distribution of fluidic energy sources. Also, water and sewer transportation is

---

A. Mudugamuwa (✉) · C. Jayasundara · H. Baokun  
College of Mechanical and Electronics Engineering, Shandong University of Science and Technology, Qingdao, China  
e-mail: [amith.mudugamuwa@gmail.com](mailto:amith.mudugamuwa@gmail.com)

R. Amarasinghe  
Department of Mechanical Engineering, University of Moratuwa, Katubedda, Sri Lanka  
Center for Advanced Mechatronics Systems, University of Moratuwa, Katubedda, Sri Lanka

done using pipes because of the ability to customize and extendibility [1]. Generally, pipeline networks are located in populated areas, whereas long-distance mass fluid transportation pipelines are located in deserted areas. Critical applications such as nuclear power plants utilize different types of pipes with suitable parameters according to the application, and these applications require a higher level of safety [2]. Due to these facts, pipe inspection and defect detection has become an interest of researchers at present. Pipeline accidents lead to monetary losses, environmental pollution and health hazards affecting human activities and in the worst case bring life risks to living beings. In the year 2010, two petroleum pipelines exploded in Dalian city in Liaoning province, China releasing about 11,000 barrels of oil to the sea causing a massive ecological disaster. In the year 2013, an oil pipeline of Sinopec Corp Oil Company exploded in Huangdao city in Shandong province, China resulting in 55 deaths. Likewise, massive oil pipeline disasters have taken place worldwide, negatively affecting the ecological system [3].

Commonly, indoor and outdoor pipe inspection task is carried out using human resource, and disadvantages such as lack of human resource, time consumption for training, quality of inspection results, safety-related problems and high cost for inspection have become a challenge in maintaining the growing pipe network resulting studies toward automation, robotics and mechatronics-based systems [4]. D. Misiunas studied on failure monitoring in water supply systems and presented different types of pipe defects, which are fundamentally categorized as geometrical defects, defects resulting in metal loss, planar discontinuities and changes in the pipe material [5]. Several pipe defects are shown in Fig. 1.

The literature is available on PDD systems with suitable sensing systems required for various testing methods and remote workstations. With time, nondestructive



**Fig. 1** Pipe defects

testing (NDT) became popular due to the nature of minimum alteration to the system, ability to iterate the test at the same location, reduce material wastage, comparative low cost for testing and reduce time consumption due to on-site testing capability [6, 7]. NDT methods are widely used to detect, localize and observe defects in both metallic and non-metallic pipes. Visual inspection, imaging techniques, penetrant testing, magnetic particle testing, ultrasonic testing, eddy-current testing, acoustic testing, vibration testing, microwave testing and radiographic testing are few common methods discussed in the literature under PDD [8–12]. At present, eco-friendly inspection techniques and testing methods are at interest of researchers rather than using testing methods that utilize chemicals, radioactive material to minimize imbalance of the present ecological system of the world.

Imaging techniques utilized in vision systems are rapidly advancing due to applicability, simple arrangement of sensor and higher feature extraction ability such as color, area and shape. D. Kragic et al. categorized vision systems in robotics into monocular and binocular, depending on the camera configuration [13]. W. Ting et al. proposed an in-pipe system using an active stereo omnidirectional vision sensor to detect and classify internal cracks and corrosions [14]. N.A.B.H. Yahya et al. developed a vision-based in-pipe inspection robot and successfully demonstrated identification of pipe geometry [15]. Therefore, studies on in-pipe vision-based defect detection systems have advanced, yet external surface defect detection based on vision systems lacks progress due to complexity of navigation and defects identification. The presented research is a study on external pipe inspection and external surface geometrical defects identification using a robotic system based on vision sensing.

## **2 Proposed System**

The proposed system consists of a robotic system, communication system and a remote workstation.

### ***2.1 Robotic System***

Main components of the robotic system are the moving mechanism, sensor system, control hardware, control algorithm and the power source. The main objective in the development of the robot system is to navigate on the external surface of the pipeline and collect data to identify defected segments of the pipeline using a suitable sensor sub-system.



## **2.2 *Communication System***

Three communication requirements are identified in designing the proposed PDD system. The first is to control the navigation, the second is to activate and deactivate image acquisition algorithm (IAA), and the third is to transmit data acquired from the camera module to the remote workstation. These requirements are preferably satisfied by wireless communication methods, because wired methods dramatically reduce mobility and the range of the PDD system. Compared to wired communication methods, wireless methods have disadvantages in network safety and data loss.

## **2.3 *Remote Workstation***

The remote workstation of the proposed PDD system provides monitoring and analyzing features. Data acquisition system stores data in the remote workstation, and because of this arrangement, data manipulation is done according to the requirements remotely without interfering with robot control or image acquisition system control.

# **3 Design and Development of the System**

## **3.1 *Navigation on Pipelines***

Pipeline robots are classified into two categories which are Internal Pipeline Robots (IPRs) [16] and External Pipeline Robots (EPRs) [17], depending on moving surface of the pipe. IPRs are only able to maneuver when the pipeline is at maintenance status, and because EPRs do not contact with the fluid conveyed inside the pipeline, EPRs have the capability to maneuver at operational status of the pipeline. Remotely controlled EPR, ExPIRo is the moving mechanism developed for the proposed robotic system. ExPIRo is developed with an ability to move on pipes with varying diameter and capable of vertical climbing. Figure 2 shows the design and the fabricated robot platform.

## **3.2 *Vision System Hardware***

Figure 3 shows the main hardware components of the vision system. A CMOS sensor module disassembled from a web camera is used as the camera module for the vision sensing system. Selected web camera is a with  $480 \times 640$  pixel resolution. LATTEPANDA single board computer is selected as the onboard main controller for

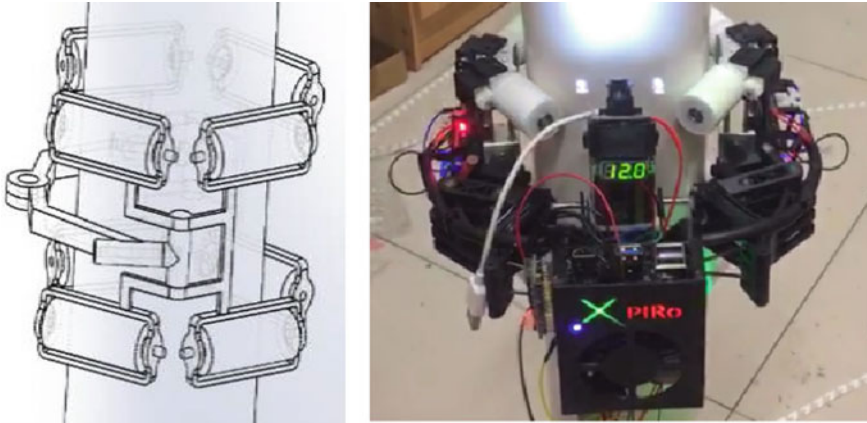


Fig. 2 ExPIRo robot platform

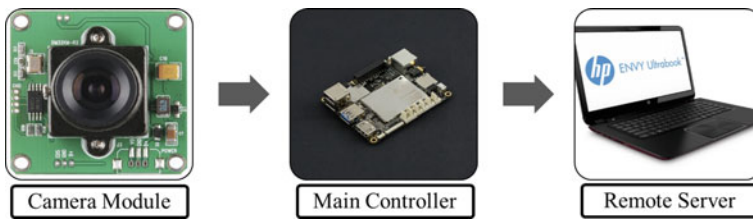


Fig. 3 Main components of the vision system

image acquisition setup of the PDD system and data transmission from the robotic system to the remote server. LATTEPANDA supports Windows 10 and performs with an Intel Quad Core 1.8 GHz processor. 4 GB RAM and 64 GB flash memory assist high performance for vision sensing. HP Envy 6-1012TX Ultra-Book laptop is used as the remote workstation to store acquired images and to perform image analysis to identify defected pipe segments. The selected remote server performs with an Intel Core i5 processor, 8 GB RAM and 2 GB VGA and runs on Windows 8.1 operating system.

**Mounting the Camera Module and Onboard Controller Board** Camera module is mounted at the front end of the moving mechanism to restrain the robot system from running into defected areas of the pipe, and the LATTEPANDA is mounted on top of the battery for symmetric weight distribution and is shown in Fig. 4.

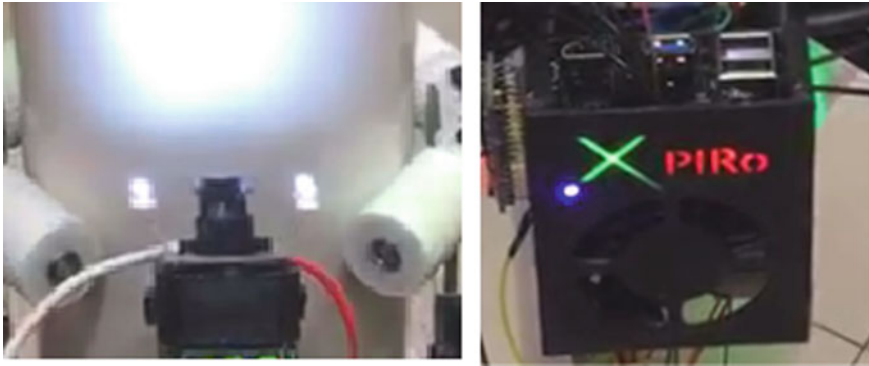


Fig. 4 Camera mount and LATTEPANDA mount

### 3.3 Image Acquisition Algorithm (IAA), Defect Identification Algorithm (DIA) and Graphical User Interface (GUI)

MATLAB software is used to develop the IAA and DIA. Acquire Images and Video from UVC Compliant Webcams (AIVUCW), hardware support package for MATLAB is utilized in IAA to initiate the connection between LATTEPANDA and camera module. IAA is deployed on LATTEPANDA, and DIA is deployed on the remote server. IAA captures images and stores the image in '.jpg' format on the remote server. DIA reads the stored images and performs image analysis. Then, it displays the analysis result of the previous image until the next image is processed. Synchronically, DIA stores the result of each image analysis on the remote server for monitoring. GUI is developed using MATLAB GUI GUIDE, and Fig. 5 shows

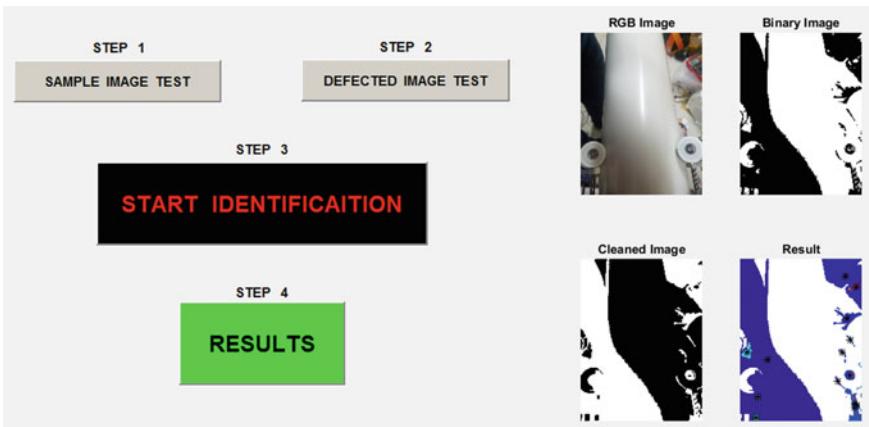


Fig. 5 GUI for pipe inspection

the GUI with additionally developed in-built options to test a pipe image without a defect and an image with a defect.

Moore-Neighbor tracing algorithm modified by Jacob's stopping criterion is the image preprocessing algorithm used in DIA. Moore-Neighbor tracing algorithm identifies the contour of the pixel pattern, and the Jacob's stopping criterion is used in order to avoid inability of the fundamental Moore-Neighbor stopping criterion to trace a large family of patterns in an image.

### ***3.4 Communication and Data Transmission***

Three communication requirements are present in the developed PDD system. The first is to control the ExPIRo robot navigation. The second is to activate and deactivate IAA. The third is to transmit data acquired from the camera module to the remote workstation. These requirements are preferably satisfied by wireless communication methods, because wired methods dramatically reduce mobility and the range of the PDD system. Radio frequency-based wireless communication module is used to send control commands from the remote controller to ExPIRo because the robot is navigated in the field. Bluetooth is used to send commands separately to the LATTEPANDA to initiate and terminate IAA. Wi-Fi is used to initiate communication link between the LATTEPANDA and the remote workstation. In-built Wi-Fi receiving module of LATTEPANDA and the in-built Wi-Fi receiving module in HP Envy 6-1012TX laptop are configured to a transmitting-receiving setup for image storing.

### ***3.5 Power Source***

Power requirement of the LATTEPANDA is 5 V and 2 A. The lithium-polymer battery used to drive motors for navigating ExPIRo robot platform satisfies the power requirement of LATTEPANDA, and the camera module is powered through the USB 2.0 port in LATTEPANDA. With this setup, the battery has the ability to supply power to the robotic system.

### ***3.6 Control System Architecture***

Figure 6 shows the control flow chart of the PDD system including robotic system, communication system and remote workstation.

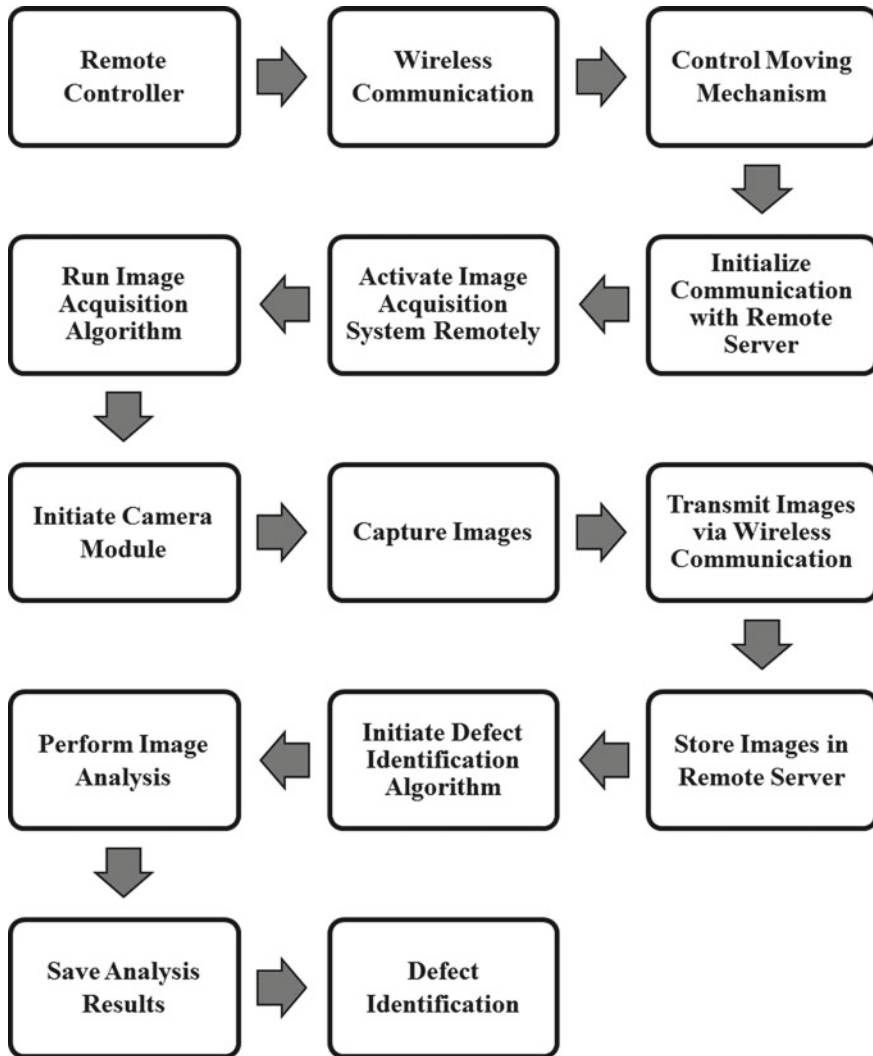


Fig. 6 Control system architecture

### 3.7 Testing Platform

For the testing platform, a white PVC pipe is used having 110 mm outer diameter and 150 cm length. To represent defects, pieces of black tape with different shapes are pasted on the pipe for clear color difference between the pipe and defects. Thereby, the defect identification is simplified. In real applications, the color difference is not black and white, yet a noticeable color difference is present. Figure 7 shows the robot on the testing platform and Fig. 8 shows the images used to test the PDD system.

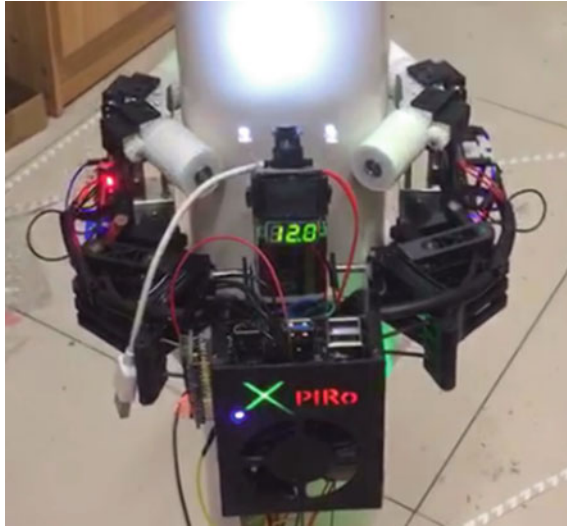


Fig. 7 Testing platform of the PDD system (robot on the pipe)



Fig. 8 Test images (Image 1 top left corner, Image 9 bottom left corner)

## 4 Results

Figure 9 a–c shows image analysis results of a horizontal pipe without a defect, with a circular shape defect on the outer surface and with a triangular shape defect on the outer surface, respectively.

Image analysis result of each image is saved in one single file to identify defected images. Figure 10 shows the report generated with the analysis results of 16 images.

As shown in Fig. 10 among the 16 images captured, Image 6, Image 7, Image 8, Image 14, Image 15 and Image 16 are successfully identified as images with defected pipe segments.

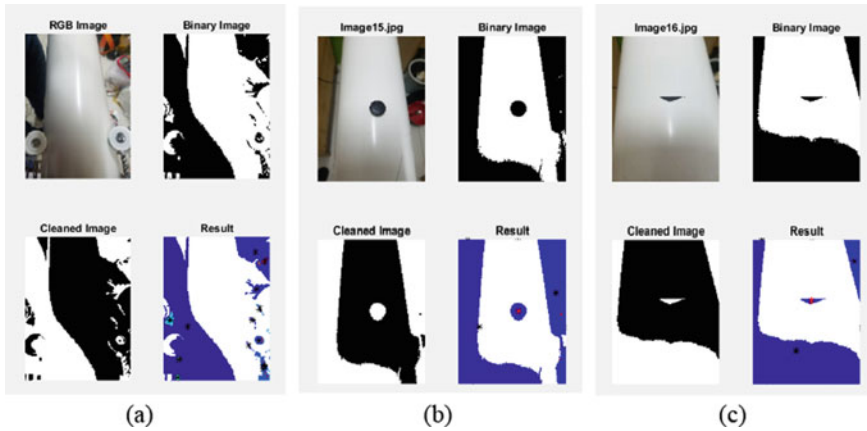


Fig. 9 Visualization of pipe inspection

Image1.jpg	Good	Image10.jpg	Good
Image2.jpg	Good	Image11.jpg	Good
Image3.jpg	Good	Image12.jpg	Good
Image4.jpg	Good	Image13.jpg	Good
Image5.jpg	Good		
-----		Image14.jpg	Defect Detected
Image6.jpg	Defect Detected		
-----		Image15.jpg	Defect Detected
Image7.jpg	Defect Detected		
-----		Image16.jpg	Defect Detected
Image8.jpg	Defect Detected		
-----		Image17.jpg	NO Image Found
Image9.jpg	Good	Image17.jpg	NO Image Found

Fig. 10 Image analysis results

## 5 Conclusion

Developed PDD system demonstrates successful integration of hardware including an EPR, camera module, single board computer and remote workstation using wireless communication and is capable of successfully detecting external surface defects having significant appearance abnormalities on the testing pipe. Using ExPIRo as the moving mechanism, the robot system demonstrates additional features such as moving on vertically fixed pipes and moving on pipes with varying diameter at a range from 110 mm to 120 mm. Furthermore, the developed PDD system operates outside of the pipeline it is suitable for pipe networks having long pipelines more than other alternative testing methods because this system operates while the pipe network is operational for fluid transportation where most of the other techniques require maintenance status for inspection. The vision system is adaptable to alternative navigation mechanisms with minor changes in the mounting mechanism and is developed as a stand-alone control system to increase adaptability and to reduce

interferences from other systems. The vision system requires the defected area and the pipe to have a significant color difference for accurate defect identification; therefore, the presented prototype of the system is not suitable to operate under low light conditions.

Ongoing work under this research is implementing an expandable communication network, developing an artificial neural network (ANN) and implementing machine learning techniques to increase adaptability of the PDD system to real applications. Additionally, multiple camera configuration and infrared thermal imaging technique are identified as suitable advancements for pipe imaging in future developments to increase suitability of the vision system for pipelines having large diameters, higher thicknesses and longer in length.

## References

1. Baokun, H., Xiyang, L., Bing, L., Huaqian, B., Xiangguang, J.: Study on acoustic source characteristics of gas pipeline leakage. *Noise & Vibration Worldwide* **50**(3), 67–77 (2019)
2. Remote visual inspection in the nuclear, pipeline and underwater industries. *NDT E Int.* **31**(5), 383 (1998)
3. Bonvicini, S., Antonioni, G., Cozzani, V.: Assessment of the risk related to environmental damage following major accidents in onshore pipelines. *J. Loss Prev. Process Ind.* **56**, 505–516 (2018)
4. Shukla, A., Karki, H.: Application of robotics in onshore oil and gas industry—A review Part I. *Robot. Autonom. Syst.* **75**, 490–507 (2016)
5. Misiunas, D.: Failure Monitoring and Asset Condition Assessment in Water Supply Systems, p. 349
6. Gao, B., Zhang, H., Woo, W.L., Tian, G.Y., Bai, L., Yin, A.: Smooth nonnegative matrix factorization for defect detection using microwave nondestructive testing and evaluation. *IEEE Trans. Instrum. Meas.* **63**(4), 923–934 (2014)
7. Cataldo, A., Cannazza, G., De Benedetto, E., Giaquinto, N.: A new method for detecting leaks in underground water pipelines. *IEEE Sens. J.* **12**(6), 1660–1667 (2012)
8. Nguyen, L.T., Kocur, G.K., Saenger, E.H.: Defect mapping in pipes by ultrasonic wavefield cross-correlation: a synthetic verification. *Ultrasonics* **90**, 153–165 (2018)
9. Kim, H.M., Yoo, H.R., Rho, Y.W., Park, G.S.: Detection method of cracks by using magnetic fields in underground pipeline. In: 2013 10th International Conference on Ubiquitous Robots and Ambient Intelligence (URAI), Jeju, Korea (South) (2013), pp. 734–737
10. Norli, P.: Ultrasonic Detection of Spark Eroded Notches in Steel Plates, p. 5
11. Li, Y., Yang, J., Qiu, C., Yang, J., Song, S., Wang, F.: Shear circumferential guided waves in coated gas pipeline. In: 2017 Symposium on Piezoelectricity, Acoustic Waves, and Device Applications (SPAWDA), Chengdu, China, 2017, pp. 481–485
12. Ebrahimi-Zadeh, J., Dehmollaian, M., Mohammadpour-Aghdam, K.: Electromagnetic time-reversal imaging of pinholes in pipes. *IEEE Trans. Antennas Propagat.* **64**(4), 1356–1363 (2016)
13. Kragic, D., Christensen, H.I.: A framework for visual serving. In: Crowley, J.L., Piater, J.H., Vincze, M., Paletta, L. (eds.) *Computer Vision Systems*, vol. 2626. Springer, Berlin (2003), pp. 345–354
14. Wu, T., Lu, S., Tang, Y.: An in-pipe internal defects inspection system based on the active stereo omnidirectional vision sensor. In: 2015 12th International Conference on Fuzzy Systems and Knowledge Discovery (FSKD), Zhangjiajie, China (2015), pp. 2637–2641



15. Department of Mechanical and Manufacturing Engineering, Faculty of Engineering, University Putra Malaysia, Malaysia, Binti Haji Yahya, N.A., Ashrafi, N., Humod, A.H.: Development and Adaptability of In-Pipe Inspection Robots. *IOSRJMCE* **11**(4), 1–8 (2014)
16. Dai, J., Xu, Y., Zhang, W.: SPC ROBOT: A Novel Pipe-Climbing Robot with Spiral Extending of Coupled Differential (2017), pp. 1088–1093
17. Chatzacos, P., Markopoulos, Y.P., Hrissagis, K., Khalid, A.: On the development of a modular external-pipe crawling omni-directional mobile robot. *Industrial Robot* **33**(4), 9 (2006)

# Analysis and Assessment of Bottom-Up Models Developed in Central Europe for Enhancing Open Innovation and Technology Transfer in Advanced Manufacturing



Maria Rosienkiewicz , Joanna Helman , Mariusz Cholewa ,  
Mateusz Molasy , and Grit Krause-Juettler 

**Abstract** In this paper, new phenomena and models supporting innovativeness of manufacturing companies are discussed. Quadruple helix innovation model and a sharing economy concept are presented. A role of innovation as a crucial factor of sustainable manufacturing is addressed. The main aim of the paper is to analyse and assess selected bottom-up models and approaches developed for enhancing open innovation and technology transfer in industrial companies in Central Europe. Research methodology is composed of an analysis of the models which have been developed within three international projects co-funded from the Interreg Central Europe programme, namely SYNERGY, TRANS<sup>3</sup>Net and NUCLEI. Five IT tools are presented and investigated. Moreover, activities supporting their implementation process are indicated to underline the new, innovative and holistic approach of creating an effective cooperation environment, with particular emphasis on the area of advanced manufacturing.

## 1 Introduction

According to the latest European innovation scoreboard, the EU's average innovation performance has improved [1]. Although for the first time the EU's performance has surpassed the USA, yet still China, Canada, Australia and Japan maintain a performance lead over the EU. In order to improve the innovation performance, the European countries should pay special attention to open innovation (OI)—one of the most important components of the European innovation system, “where all stakeholders need to be involved and create seamless interaction and mash-up for

---

M. Rosienkiewicz (✉) · J. Helman · M. Cholewa · M. Molasy  
Department of Laser Technologies, Automation and Production Organization, Wrocław  
University of Science and Technology, Wyspiańskiego 27, 50-370 Wrocław, Poland  
e-mail: [maria.rosienkiewicz@pwr.edu.pl](mailto:maria.rosienkiewicz@pwr.edu.pl)

G. Krause-Juettler  
CIMTT Centre for Production Engineering and Management, Faculty of Mechanical Engineering,  
Technische Universität Dresden, 01062 Dresden, Germany

ideas in innovation ecosystems” [2]. A good example of companies strongly relying on external innovation is Google, Apple or Amazon— “according to BCG’s, Most Innovative Companies 2019 Report, 75% of the top 50 most innovative companies use incubators, 81 per cent leverage academic partnerships, while 83 per cent partner with other companies” [3].

Experiences gained from a number of research and industrial projects carried out in Central Europe (CE) lead to a conclusion that support for innovation is still rather limited in the scope, transnational cooperation is relatively poor, and there are still many barriers hindering industrial companies (especially SMEs) from cooperating with universities and research organizations [4–6]. The traditional, “local-based”, approach to innovation development and technology transfer does not support efficiently companies operating in advanced manufacturing (AM) sector. Therefore, to overcome the innovation barriers in CE regions, where AM is a strong branch of economy, it is particularly important to support industrial companies with providing the “innovation-friendly ecosystem” based on OI paradigm [7]. Development and implementation of models, tools and methods enhancing OI in advanced manufacturing is especially crucial, due to the reason that such solutions are—so far—rather limited and only fledging in Central European industrial companies. The flagship industrial examples of products developed on the OI basis include Zortrax M200—professional desktop 3D printer [8], Olli—the smart, safe and sustainable vehicle [9] or LM3D—the first highway-ready, 3D-printed car [10].

## **2 Literature Review on Open Innovation Phenomena in Terms of Advanced Manufacturing**

One of the major challenges in modern manufacturing is the implementation of sustainable and at the same time innovative manufacturing systems [11]. According to Dassisti et al., one of the crucial goals of sustainable manufacturing (SM) is the development of innovative manufacturing processes and systems [12]. Zindani et al. indicate “three pillars that define the term sustainability: social directions, economic factors and environmental concerns” [8]. As Rauter et al. underline “innovation plays a crucial role by fostering a greater level of sustainability in company activities” [13]. “Many studies highlight the importance of innovation for sustainability as well as the goals of sustainable development” [14]. Hence, as social directions and innovation are of great importance for SM, it can be stated that, although in the literature countless ways and models for innovation development can be found, currently, in the era of Industry 4.0, it seems that the most adequate solutions supporting innovativeness of manufacturing companies are those based on OI and Open Innovation 2.0 (OI 2.0). OI can be defined as “the use of purposive inflows and outflows of knowledge to accelerate internal innovation and expand the markets for external use of innovation, respectively” [15], whereas according to publications of European Commission, OI2.0 is “a new paradigm based on a quadruple helix model where government,

industry, academia and civil participants work together to co-create the future and drive structural changes far beyond the scope of what any one organization or person could do alone. This model encompasses also user-oriented innovation models to take full advantage of ideas' cross-fertilization leading to experimentation and prototyping in real-world setting" [2].

Business models which are based on open innovation paradigm are still shaping, and hence, there is a requirement to perform research towards building a dedicated environment, where companies could fully benefit from the new phenomena, tools and methods based on i.a. sharing economy, crowdsourcing, crowdfunding and micro-working. This approach is also consistent with the concept of the regional innovation system, in which the innovation process is considered as a social phenomenon involving various regional actors [4]. It is based on the assumption that there is a subsystem generating the knowledge (science) as well as a subsystem exploiting the knowledge economically (economy) in order to contribute to the competitiveness of a whole region [16–19]. Important factor from the innovativeness point of view is also internationalization, due to the reason that combining different national competencies leads to release of innovation capabilities [20]. What is more, as Ahuja et al. underline, a very important element of sustainable and innovative manufacturing is human factor [21], which directly corresponds to the quadruple helix innovation model [22]. Therefore, it is expected that involving representatives of society in the manufacturing processes and facilitating them bottom-up activities will lead to enhancement of innovativeness of industrial companies. These activities may be for instance social product development [23, 24] or micro-working, which is a new form of working beyond organizational boundaries, created mostly by social media technologies, in which engagement in work is posted by organizations or individuals on a web-based and third-party platform in exchange for monetary remuneration [9, 25].

Last but not least, aspect related to open innovation environment creation is a concept of sharing economy [26], which has become widespread globally as an innovative service business model [27]. It can be defined as the "acquisition or distribution of a source coordinated by people for compensation or a certain fee" [28] or as "an umbrella term that describes an emerging consumption trend: online peer-to-peer economic activities for sharing among consumers through intermediary service firms" [27]. From an advanced manufacturing point of view, this business model is interesting not only in terms of competences and skills sharing, but especially in terms of industrial research infrastructure sharing because it may result i.a. in lowering the costs of infrastructure usage, increasing turnover, thanks to easier investment decision and testing advanced technologies without necessity to buy them first. The literature analysis and research performed within a number of European projects lead to a conclusion that creating a real living open innovation environment and supporting technology transfer in advanced manufacturing need bottom-up initiatives and activities.

### 3 Research Methodology

The main aim of this paper is to present, analyse and assess selected bottom-up models and approaches developed for enhancing open innovation and technology transfer in advanced manufacturing in Central Europe. In order to reach the defined goal, a research methodology has been developed and schematically presented in Fig. 1. Following the presented methodology, the research discussed in this paper is focused on analysis of three Central European projects dealing with technology transfer enhancement and support of OI environment development. According to Fig. 1, the three investigated projects will be introduced—namely SYNERGY, TRANS<sup>3</sup>Net and NUCLEI (all co-funded from Interreg Central European programme).

Next, the models developed within each project and their implementation in the form of tools will be presented. Afterwards, an analysis of the tools will be performed, followed by the analysis of the event formats developed in each project. Finally, the conclusion will be formulated on the basis of the executed comparison. Each of the abovementioned projects was established as a bottom-up initiative of Central European consortium partners. In total, the analysis covers 12 regions from 8 countries. A list of countries and regions involved in each analysed project is presented in Table 1.

The first investigated project will be SYNERGY (08.2017–10.2020), which stands for “synergic networking for innovativeness enhancement of Central European actors focused on high-tech industry”. SYNERGY’s main goal is to enhance innovativeness in European regions through strengthening linkages and beyond border cooperation to create synergy between SMEs, industry, research, intermediaries and policy-makers. The project scope is mainly oriented on advanced manufacturing with a special focus on the most promising modern industrial technologies. SYNERGY follows the quadruple helix innovation model [22], due to the fact that project partners represent not only entities based on triple helix innovation model—4 higher education and research institutions, 1 SME, 2 business support organizations and government as an associated partner, but also the project aims at direct involvement of the society through implementation of crowdsourcing, crowd funding and micro-working tools and pilot actions [7].

**Fig. 1** Scheme presenting research methodology

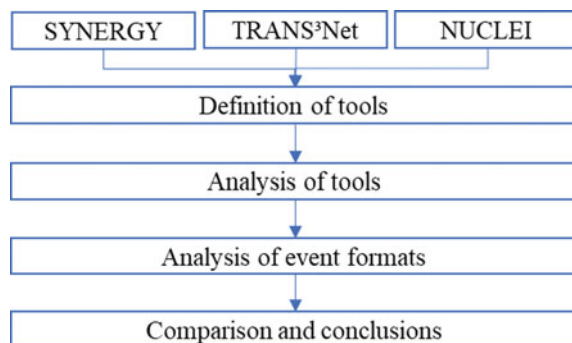


**Table 1** Countries and regions involved in each analysed project

No.	Country	Region	SYNERGY	TRANS <sup>3</sup> Net	NUCLEI
1	Austria	Upper Austria	X		X
2	Croatia	Adriatic Croatia	X		
3	Czech Republic	Prague			X
4		Usti Region		X	
5	Germany	Baden Württemberg	X		X
6		Bavaria			X
7		Saxony	X	X	
8	Italy	Emilia Romagna	X		X
9		Veneto			X
10	Poland	Lower Silesia	X	X	X
11	Slovakia	Košice Region			X
12	Slovenia	Western Slovenia	X		

The second analysed project will be TRANS<sup>3</sup>Net (07.2016–09.2019)—“Increased effectiveness of transnational knowledge and technology transfer through a trilateral cooperation network of transfer promoters”. Its main objective was to shape conditions for building up a well-working innovation system in tri-national regions of border area between Germany, Czech Republic and Poland which is characterized by a low level of transnational cooperation between science and industry. TRANS<sup>3</sup>Net aimed at establishing strong ties and a self-sustaining cooperation between all key players relevant for knowledge and technology transfer and development of solutions overcoming the multifaceted obstacles concerning transnational cooperation [29].

NUCLEI (07.2016–06.2019) stands for “network of technology transfer nodes for enhanced open innovation in the Central European advanced manufacturing and processing industry”. The main aim of the NUCLEI project was to establish a transnational innovation management model in Central European regions and to create a transnational pool of knowledge that supports advanced manufacturing innovation beyond regional borders. Moreover, NUCLEI’s purpose was to assess the “distance-to-target” between the actual needs and technological interests of advanced manufacturing industrial companies and the technology transfer services currently provided by the selected excellence nodes concerned in the project [5, 30].

## 4 Analysis of Models

As presented in the research methodology scheme, after short introduction of SYNERGY, TRANS<sup>3</sup>Net and NUCLEI, the models developed within each project and their implementation in the form of tools will be discussed. Each model has been

**Table 2** Table captions should be placed above the tables

Project	Tool	Technological area
SYNERGY	SCIP—synergic crowd innovation platform	Additive manufacturing, micro- and nanotechnology, Industry 4.0
TRANS <sup>3</sup> Net	Map of transfer promotors innovation web portal	Not defined
NUCLEI	Transnational web-ATLAS technology digital periscope	Automotive, automation and robotics electronics, mechatronics, ICT

developed to support technology transfer and open innovation in advanced manufacturing in a little bit different way. Within SYNERGY project, the main tool that has been developed is synergic crowd innovation platform (SCIP). It is combined with the matchmaking tool, which enables the user to search, profile, cluster and reach innovation-oriented organizations based on their activities and experience gained from successful project realizations in order to enhance networking and linking regional actors from research, industry and intermediaries. SYNERGY's approach is based on open innovation rules and especially, the quadruple helix innovation model. TRANS<sup>3</sup>Net is focusing mainly on enhancing knowledge and technology transfer in cross-border regions through direct linking “transfer promotors”. The implementation of this approach was done i.a. through development of two IT tools, namely (1) map of transfer promotors and (2) innovation web portal. NUCLEI on the other hand, aiming at changing the traditional innovation management services for Central Europe advanced manufacturing industries from a “local-based” support approach to a transnational pool of knowledge supporting innovation in businesses beyond own regional borders [5], developed two supporting tools—(1) transnational web-ATLAS and (2) technology digital periscope. Table 2 presents technological areas assigned to each project.

Developed within SYNERGY project SCIP (<http://synergyplatform.pwr.edu.pl>) is a platform ensuring crowdfunding and crowdsourcing for innovative solutions for the Central European society. The platform is also implementing micro-working, which is an approach where community solves smaller tasks which are then reassembled into an overall result at the end. The SCIP enables its users to take part in a number of pilot actions including: “Simulated crowd funding”, “Vouchers for research and innovation projects”, “Rent-a-robot”, “Crowd innovation for companies”, “Design and prototype a model”—presenting a social product development approach. What is more, the tool contains the database of the high-tech infrastructure located in Central European regions and offers a possibility of infrastructure sharing through matchmaking the owners with those looking for the easy access to the advanced technologies.

Developed within TRANS<sup>3</sup>Net project, the map of transfer promotors (<http://map.trans3net.eu>) is an online tool including descriptions of transfer-promoting institutions that support science and industry in the implementation of collaborative research projects and in transferring knowledge and technology. It provides an overview about which of these actors are available in a geographical area and what they can contribute

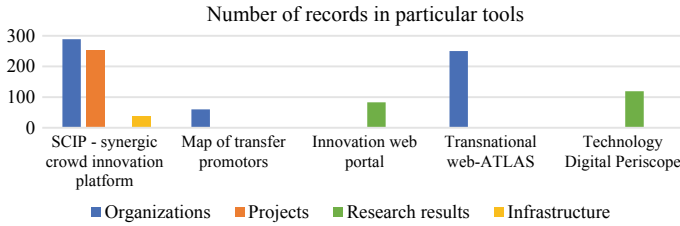


**Fig. 2** Number of records in particular tools

to such collaboration processes [31]. The second tool, the innovation web platform, includes the so-called technology profiles that describe available research results in a short, understandable and application-oriented way targeting mainly SMEs. Technology profiles serve as starting points for collaboration between science and industry [32].

Transnational web-ATLAS developed within NUCLEI project is a map that consists of the selected research institutions, small, medium, large enterprises and intermediaries. All entities are displayed with a pin on the map of Europe. The project has decided to colour code the pins according to the business field and to the technology field, respectively. The first map shows an overview of the entities, and the different colours mark the five technologies field addressed by NUCLEI. The tool has been created on the basis of pool of excellence. The second NUCLEI solution is technology digital periscope, being a “tool to support and speed-up the access to the existing state-of-the-art R&D results and products by their systematization and exportability. Results included in the periscope are from the field of advanced manufacturing and processing industry. Results cover highly important key enable technologies (KET) such as robots, production processes, ICT, electronics, modelling and visualization” [33]. If analyse all types of information which have been collected and then introduced to the abovementioned tools, they can be grouped into four main categories: organizations, projects, research results and infrastructure. Current records registered in the discussed tools are presented in Fig. 2.

Analysis of Fig. 2 shows that the biggest number of records can be found in the SYNERGY’s tool—579 (289 organizations, 253 projects and 37 infrastructures). Second score refers to organizations which can be found in NUCLEI’s web-ATLAS (250). TRANS<sup>3</sup>Net project has identified 83, while NUCLEI 119 ready to commercialize research results. It needs to be clearly underlined however that all the abovementioned tools need users (critical mass) to be successful. As number of different platforms in Central Europe and worldwide is increasing rapidly, meta platforms creation should be considered. It would be much easier for a company if the knowledge and information which is so far dispersed in many sources could be approached from one meta platform. Nevertheless, bottom-up approach represented in all three projects shows that different types of organization see a common problem of hidden information locally and define a need of sharing this knowledge transnationally through online channels. Thus, particular networks of partners and their stakeholders



**Table 3** Number of participants in particular events

Event type	Number of events	Number of participants	Average
Design thinking idea meeting	7	132	19
Simulated sharing networking workshop	7	123	18
Open seminar	21	727	35
Transnational working table	10	342	34
TRANS <sup>3</sup> Net.visit	6	168	28
TRANS <sup>3</sup> Net.show	2	119	60
TRANS <sup>3</sup> Net.training	2	53	27
TRANS <sup>3</sup> Net.dialogue	2	49	25

start to become more open to international collaboration. It is especially important in advanced manufacturing sector which is quite specific and by definition rather reluctant to openness. All three discussed projects followed a holistic approach of creating an effective and innovative cooperation environment, therefore not only tools have been developed, but also dedicated event formats. Hence, another bottom-up approach investigated in this research is different event prototypes which were designed, developed and tested within the presented projects. Their role was i.a. to support efficient implementation of the abovementioned tools. Apart from other types of events, SYNERGY project developed and tested design thinking idea meetings and simulated sharing networking workshops, TRANS<sup>3</sup>Net project designed and implemented—TRANS<sup>3</sup>Net.visit, TRANS<sup>3</sup>Net.show, TRANS<sup>3</sup>Net.training and TRANS<sup>3</sup>Net.dialogue, whereas NUCLEI project proposed and validated—Open Seminars and Transnational Working Tables. Table 3 presents statistics of the particular events.

In total, within these events, the presented projects reached 1713 participants representing different target groups—i.a. SMEs, large companies, regional and national authorities, business support organizations (BSO) and higher education and research institutions. It can be stated that such initiatives are required to create living and working linkages of actors operating in advanced manufacturing in Central Europe. Especially, BSO and research organizations should be the responsible for creating trustworthy environment where together with companies' innovations can be developed and technology efficiently transferred.

## 5 Conclusions

The main conclusion from the presented research is that different types of organizations see the common need to share the information about their resources, competences and experience transnationally. To answer this requirement, a number of tools and events have been created and validated within Central European projects. Next

step should be an integration of this knowledge to make it easily available from one source for all potentially interested actors. What also needs to be underlined is that “cross-cultural understanding is the key to open innovation in an increasingly international setting” [3]. Participation of Central European entities in international or transnational networks can significantly enhance their level of innovativeness. It is expected that the tools and events presented in this paper will contribute to development of OI environment, technology transfer and support of sustainable manufacturing in Europe by:

- closing the knowledge gap: due to a lack of both financial and human resources, the target groups (mainly SMEs) are struggling to track developments in advanced manufacturing,
- promoting of new technologies and integration in new value chain,
- supporting companies in becoming factories of the future by providing the necessary tools for responding to changing conditions and business model levels,
- sharing knowledge, resources and exchanging experiences as an important basis for mutual learning, networking and efficient cooperation.

**Acknowledgement** The research leading to these results has received funding from Interreg Central Europe programme priority innovation and knowledge development under grant agreement No. CE258 for TRANS<sup>3</sup>Net and No. CE1171, project SYNERGY as well as from funds for science of Polish Ministry of Science and Higher Education for the implementation of an international co-financed project.

## References

1. Hollanders, H., Es-Sadki, N., Merkelbach, I.: European Commission, Directorate-General for Internal Market, Industry, Entrepreneurship and SMEs: European Innovation Scoreboard 2019. <https://ec.europa.eu/docsroom/documents/38781/attachments/1/translations/en/renditions/native> (2019)
2. <http://ec.europa.eu/digital-single-market/en/open-innovation-20> Last Accessed 26 Feb 2020
3. [www.asianscientist.com/2020/01/features/ipi-techinnovation-secrecy-synergy-open-innovation/](http://www.asianscientist.com/2020/01/features/ipi-techinnovation-secrecy-synergy-open-innovation/). Last Accessed 26 Feb 2020
4. Krause-Juettler, G.: Promoting cross-border cooperation between science and small businesses as a source of innovation. In: *Intelligent Systems in Production Engineering and Maintenance*. pp. 118–127. Springer International Publishing, Cham (2019)
5. [www.interreg-central.eu/Content.Node/NUCLEI-Handbook-2.pdf](http://www.interreg-central.eu/Content.Node/NUCLEI-Handbook-2.pdf). Last Accessed 27 Feb 2020
6. Cholewa, M., Helman, J., Molasy, M., Rosienkiewicz, M.: Identification of Challenges to be Overcome in the Process of Enhancing Innovativeness Based on Implementation of Central European Projects Funded from Interreg Programme. In: *Intelligent Systems in Production Engineering and Maintenance*. pp. 185–194. Springer International Publishing, Cham (2019)
7. Rosienkiewicz, M., Helman, J., Cholewa, M., Molasy, M.: SYNERGY Project: Open Innovation Platform for Advanced Manufacturing in Central Europe. In: *Intelligent Systems in Production Engineering and Maintenance*. pp. 306–315. Springer International Publishing, Cham (2019)

8. [www.kickstarter.com/projects/zortrax/zortrax-m200-professional-desktop-3d-printer](http://www.kickstarter.com/projects/zortrax/zortrax-m200-professional-desktop-3d-printer). Last Accessed 04 Mar 2020
9. [www.localmotors.com/meet-olli/](http://www.localmotors.com/meet-olli/). Last Accessed 04 Mar 2020
10. [www.forbes.com/sites/tjmccue/2015/11/13/worlds-first-3d-printed-road-ready-car-lm3d-by-local-motors/#21a5333b2aa0](http://www.forbes.com/sites/tjmccue/2015/11/13/worlds-first-3d-printed-road-ready-car-lm3d-by-local-motors/#21a5333b2aa0). Last Accessed 04 Mar 2020
11. Zindani, D., Kumar, K., Davim, J.P.: Sustainability Manufacturing Systems Design. In: Encyclopedia of Renewable and Sustainable Materials. pp. 512–518. Elsevier (2020)
12. Dassisti, M., Chiarello, F., Fantoni, G., Priarone, P.C., Ingarao, G., Campana, G., Matta, A., Cimatti, B., Colledani, M., Frigerio, N., Forcellese, A., Simoncini, M.: Benchmarking the sustainable manufacturing paradigm via automatic analysis and clustering of scientific literature: A perspective from Italian technologists. *Procedia Manuf.* **33**, 153–159 (2019)
13. Rauter, R., Perl-Vörsbach, E., Baumgartner, R.J.: Sustainable Open Innovation and its influence on economic and sustainability innovation performance. Presented at the The XXVI ISPIM Conference —Shaping the Frontiers of Innovation. Budapest (2015)
14. Kuzma, E., Padilha, L.S., Sehnem, S., Julkovski, D.J., Roman, D.J.: The relationship between innovation and sustainability: A meta-analytic study. *J. Cleaner Prod* (2020)
15. Chesbrough, H.W.: Open innovation: the new imperative for creating and profiting from technology. Harvard Business School Press, Boston, Mass (2003)
16. Krause-Juettler, Grit: Cross-border Collaborations between Science and SMEs: Empirical Findings and Strategic Considerations Illustrated by the Example of the Saxon-Czech Border Region, in: UIIN (ed.), University-Industry Interaction: Challenges and solutions for fostering entrepreneurial universities and collaborative innovation, 6–15, (2017)
17. Cooke, P.: Regional innovation systems—an evolutionary approach. In: Regional innovation systems, pp. 1–18. Routledge, London (2004)
18. Cooke, P.: Regional innovation systems: competitive regulation in the new Europe. *Geoforum* **23**, 365–382 (1992)
19. Doloreux, D., Parto, S.: Regional innovation systems: current discourse and unresolved issues. *Technol. Soc.* **27**, 133–153 (2005)
20. Lundquist, K.-J., Tripll, M.: Towards cross-border innovation spaces. A theoretical analysis and empirical comparison of the Öresund region and the Centropae area. SRE Discussion Papers, 2009/05, WU Vienna University of Economics and Business, Vienna (2009)
21. Ahuja, J., Panda, T.K., Luthra, S., Kumar, A., Choudhary, S., Garza-Reyes, J.A.: Do human critical success factors matter in adoption of sustainable manufacturing practices? An influential mapping analysis of multi-company perspective. *J. Cleaner Prod* (2019)
22. McAdam, M., Debackere, K.: Beyond ‘triple helix’ toward ‘quadruple helix’ models in regional innovation systems: implications for theory and practice: Beyond ‘triple helix’ toward ‘quadruple helix’ models. *R&D Manage.* **48**, 3–6 (2018)
23. Forbes, H., Schaefer, D.: Social product development: the democratization of design. *Manuf. Innov. Procedia CIRP.* **60**, 404–409 (2017)
24. Bertoni, M., Larsson, A., Ericson, Å., Chirumalla, K., Larsson, T., Isaksson, O., Randall, D.: The rise of social product development. *Int. J. Netw. Virtual Organisat.* **11**, 188 (2012)
25. Cherry M.A.: Beyond Misclassification: The Digital Transformation of Work (February 18, 2016), Legal Studies Research Paper No. 2016–2, Comparative Labor Law & Policy Journal, Forthcoming; Saint Louis (2016)
26. Sari, R., et al.: Sharing economy in people, process and technology perspective: a systematic literature review (September 12, 2019). *Int. J. Mech. Eng. Technol.* **10**(3), 1008–1024 (2019)
27. Hwang, J.: Managing the innovation legitimacy of the sharing economy. *Int. J. Q. Inn.* **5** (2019)
28. Belk, R.: You are what you can access: Sharing and collaborative consumption online. *J. Bus. Res.* **67**, 1595–1600 (2014)
29. <http://interreg-central.eu/Content.Node/TRANS3Net.html>. Last Accessed 26 Feb 2020
30. <http://interreg-central.eu/Content.Node/NUCLEI.html>. Last Accessed 26 Feb 2020
31. TRANS<sup>3</sup>Net report Development and implementation map of transfer promotors
32. TRANS<sup>3</sup>Net report Development and implementation of innovation web platform (IWP)
33. <http://transfertech.eu>. Last Accessed 27 Feb 2020

# A Simplified TRIZ Approach Involving Technology Transfer for Reducing Product Energy Consumption



Davide Russo , Christian Spreafico , and Matteo Spreafico 

**Abstract** The literature is full of attempts to integrate eco-improvement and problem solving methods. Practically, no generalist problem solving method is born with a specific green purpose; also, for this reason, every time we apply a method to improve a product, the solution found could not be more sustainable than the previous one. Among the most effective methods for problem solving, there is TRIZ, which, differently from others, has in its fundamentals, several concepts in line with environmental sustainability: It pushes to find solutions that optimize the use of existing resources without adding new ones and suggests to simplify the systems towards their “essential” structure (TRIZnicks would say “ideal”). This article is a further testimony of TRIZ’s potential also in the world of eco-design. It proposes a simplified TRIZ approach, to produce sustainable solutions, based on a few key points of the TRIZ methodology that are easy to implement even for a non-expert in the field. These fundamentals are integrated with a documental research module designed for the transfer of knowledge between different technological areas. The goal of the tech transfer module is to find in the early stages of the problem those who have already solved similar problems in different sectors and from here start building their own solution model. In our case, it has been applied to reduce the energy consumption in the use phase of an industrial dishwashing machine developed by Elframo company. The solution, which is currently under patent pending, has saved more than 90% of the energy.

## 1 Introduction

The great part of the environmental impacts of many products derives from the energy consumption during the use phase [1].

In order to mitigate them, many eco-design activities have focused on reducing them and have become almost mandated for the most energy-intensive products, as established by various reference standards (e.g. [2]).

---

D. Russo (✉) · C. Spreafico · M. Spreafico  
University of Bergamo, Via Marconi 5, 24044 Dalmine (Bg), Italy  
e-mail: [davide.russo@unibg.it](mailto:davide.russo@unibg.it)

© The Editor(s) (if applicable) and The Author(s), under exclusive license to Springer Nature Singapore Pte Ltd. 2021  
S. G. Scholz et al. (eds.), *Sustainable Design and Manufacturing 2020*, Smart Innovation, Systems and Technologies 200, [https://doi.org/10.1007/978-981-15-8131-1\\_12](https://doi.org/10.1007/978-981-15-8131-1_12)

129

In addition, the increase in the degree of severity of EU directives (e.g. EU Energy labels) is influencing product design practices also through a substantial rethinking of the requirements for the next generation products [3].

However, both the main eco-design approaches (e.g. [4, 5]) and the most recent ones (e.g. [6, 7]) are focused on reducing consumption through optimization activities rather than radical innovation. This because eco-innovation tips do not guarantee better results for what concerns sustainability [8].

Methods to support systematic innovation, such as TRIZ (e.g. [9, 10]) or one of its many variants related to eco-design (e.g. [11, 12]) can be more suitable for the second one.

However, despite many attempts, many approaches are still considered too general and difficult to apply, especially for non-expert users.

In addition, although some of them can easily lead to more innovative solutions, these are not necessarily greener.

This because, according to [13], at the same time, general-purpose idea generation tools do not usually show any specific preference to sustainable aspects, since their overall purpose is product success and the identification of unexplored market opportunities. Therefore, the attention to sustainability is random, not taken for granted and presumably dependent on designers' sensibility towards environmental and human problems. This thesis is also supported by different studies that quantitatively assessed the solutions resulting from TRIZ tools. According to [14], solutions deriving from the same TRIZ tools (i.e. the trends of evolution) and concerning different aspects (e.g. materials and aesthetics) can both be better than pejorative compared to traditional solutions.

With this paper, we want to fill this gap, by proposing a step-divided methodology for guiding the designer through a rigid and guided path of radical innovation for the device and specifically aimed at reducing the impact of consumption during the use phase.

## 2 Methodology

Different approaches (theories, methods and tools) can be used for supporting redesign of a technical system (e.g. a device). The great part of them (e.g. finite elements, computational fluid dynamic, quality function deployment, function-behaviour-structure) suggests to optimize the system or to substitute one technology with another one more efficient.

TRIZ, instead, exclusively starts from a very restricted area of the problem. It focuses on the object-product OP transformation and on the main function to be provided for this transformation. The "object" (O) is the entity that undergoes the action (main function), by transforming it into the "product" (P). A popcorn machine, for example, uses hot oil to transform corn into popcorn. TRIZ starts from analysing corns parameters instead of analysing how the popcorn machine is actually made. The goal is to identify alternatives to create the same effect, (alternatives for heating

transfer, for preparing corn to be heated and for controlling popcorn transformation). From here, we start to create the ideal behaviour for our solution (heating only what is really necessary, without any energy waste) and implementing it into a real structure (without adding unnecessary parts).

This approach is winning also from an eco-design point of view, because it allows to save resources (both material and energy).

In the traditional TRIZ, the behaviour identification is demanded to the pointer to effects [15]. It suggests how to link a function or a parameter change to a list of suitable physical effects. In recent years, many efforts have been provided to overcome limits of this tool, for example, taking advantage of what the new information retrieval technologies offer. The authors have developed their own search engine capable of identifying not only physical effects but also technologies using the information contained in the patent database [16].

This tool is integrated into a step by step methodology based on TRIZ.

It consists of the following steps.

### **STEP 1—Definition of the main function (object-product transformation)**

The objective of the first step is to identify the main function of the system. This action works on one or more “objects” that are transformed into “products”. All our activity starts from here, the object-product OP transformation, the enabling function and the context in which it occurs.

### **STEP 2—Functional decomposition and technology transfer**

The purpose of the second step is to collect and organize all the possible ways for making the OP transformation, focusing on the minimal energy consumption required to achieve this goal. This step consists in

- Decomposing the current system by listing all the parameters dealing with the object, the product and their transformation;
- Exploiting the parameters as triggers for identifying all the alternative behaviours and the physical effects. It is made by hypothesizing how each parameter should change in order to obtain the desired effect and linking this transformation to a suitable enabling physical effect (i.e. heating corns by radiation, conduction, convection, microwave, laser, etc.). To systematize this activity, it is important to recover knowledge both to establish the right way we want to modify the parameters and to establish the most suitable effect to generate this change. A dedicated technology transfer tool was used by authors.
- the alternatives are graphed in a special tree map and enriched with other information about enabling technologies and/or exemplary cases or patents.

### **STEP 3—Identification of the new behaviour**

In this phase, we select the most suitable behaviour from the technology transfer tree. All promising behaviours are tested through an experimental campaign for checking feasibility and optimizing their working parameters. Finally, the best behaviour is selected to be implemented in the step 4.

### STEP 4—Design a new structure

Sketch a new structure for realizing the chosen behaviour, paying a particular attention in identifying the available resources (as prescribed by TRIZ theory) from the working environment.

## 3 Case Study

In order to show how the proposed methodology can be applied for eco-improving a real product, it has been strictly applied to the redesign of a drying system for an industrial ribbon dishwasher.

In this chapter, all the steps of the methodology are described in detail, by dedicating a subsection for each of them, by describing how their indications are practically applied and by showing the provided results.

The part illustrated in Fig. 1 is currently located downstream of the washing and rinsing chambers in relation to the direction of flow of the dishes or utensils that are placed inside a basket on a conveyor belt.

Automatic dishwashers are designed to satisfy a throughput rate of 75–280 baskets/h or up to 7200 plates/h. At the end of the process, there is a drying chamber. Before our intervention, it contained a centrifugal fan drawing the dry air from outside the chamber and an electric coil, placed under the fan, heating the air, which finally invested the plates or tools. The dishes must come out of the process completely dry in order to be immediately reused.

The main criticality of the drying chamber was given by energy consumption (9 kW).

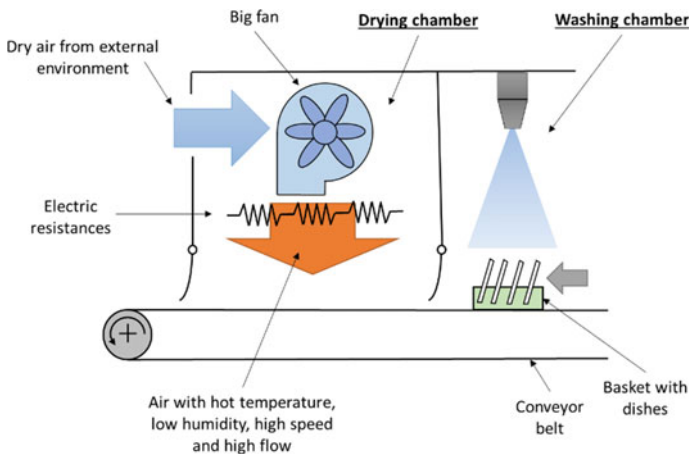


**Fig. 1** Current drying chamber for conveyor dishwasher

In this configuration, the dishes were dried by investing them with a flow of dry hot air. The global energy consumption of the drying chamber was 9 Kwh distributed between fans (1 kW) and electric heaters (8 kW). The layout of the coils represented a barrier for the air that had to pass through them; as a result, even the fans designed to push the air, positioned upstream of the barrier, were oversized to recover this pressure drops.

The collaboration between the University of Bergamo and Elframo concerned the redesign of the top of the range drying unit. In the following, only the main steps of the methodology applied to this project are described. A complete explanation of the functioning of the solution can be found in the Italian patent application n.102019000020448.

**STEP 1—Definition of the main function (object-product transformation)**

Our goal is to remove the water from all surfaces of the dishes that pass through the dryer. Figure 2 shows the OP transformation, where the object can be represented by a portion of water attached to the surface of the plate, while the product can be constituted by different portion of water (small drops detached from the surface and a portion of water already attached).

**STEP 2—Technology transfer**

In the initial configuration, the dishes were dried by investing them with a flow of dry hot air. The global energy consumption of the drying chamber was 9 kWh distributed between fans (1 kW) and electric heaters (8 kW). The layout of the coils represented a barrier for the air that had to pass through them; as a result, even the fans designed to push the air, positioned upstream of the barrier, were oversized to recover this pressure drops.

Step 2 consists in decomposing the OP transformation into parameters and links them to physical effects. As far as the plate is concerned, its temperature, stiffness, roughness and the inclination have been identified. As far as water is concerned, we worked on the residual quantity on the plate, the shape, the footprint on the ground, the temperature, the surface tension and its adhesion strength.

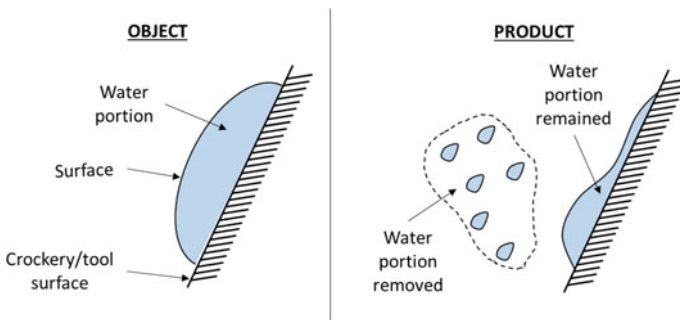


Fig. 2 Object-product transformation



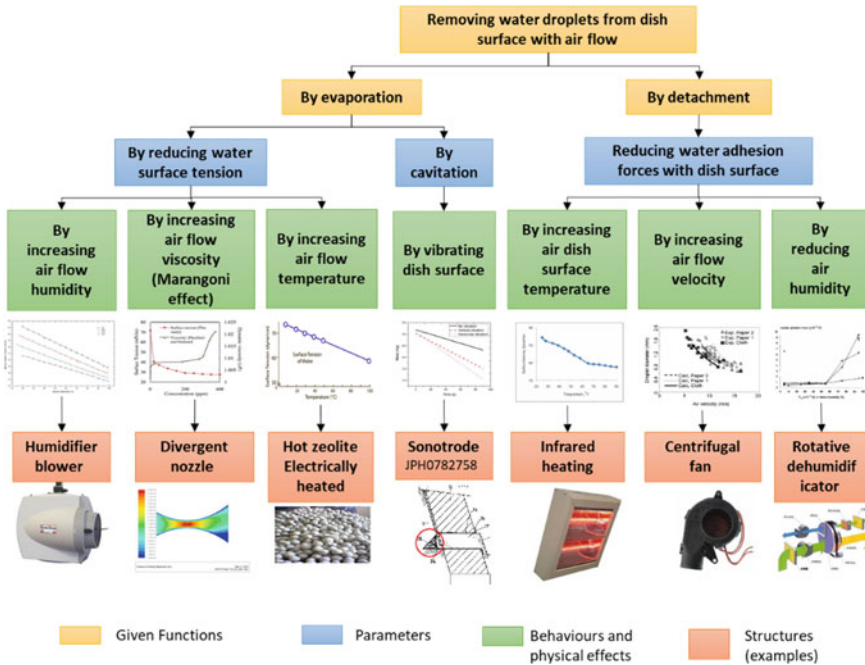


Fig. 3 Technology transfer tree

Finally, for air, the temperature, speed, vorticity and relative humidity were considered. For each of these parameters, we wondered how they could be modified to obtain the elimination of water, linking the variation of the parameters to a list of functions that the system must provide.

The tree map resulting from technology transfer is reported in Fig. 3.

In order to be able to choose one branch rather than another from the many options available, it was necessary to carry out test campaigns, which we performed with the company. Among them, those providing the most interesting results for reducing the energy consumption were the use of humid warm air and the reduction of the flow speed.

To evaluate the optimal value of the required air temperature and humidity, an experimental campaign was carried out, during which several drying tests were carried out with flows at different temperatures, and their effectiveness was evaluated in relation to the amount of water mass still present on the tableware, measured by means of a precision weight scale. The results of the test have shown that, as with the heating of the run-off water, an increase in the performance of the elimination of the water is expected, up to a specific value, beyond which the system no longer shows significant improvements. Figure 4a shows the graph of the temperature tests. On the orders, the residual mass of water on the plate (in grams) after drying is shown. Two tests were performed, one on a bottom plate and one on a flat plate, while each

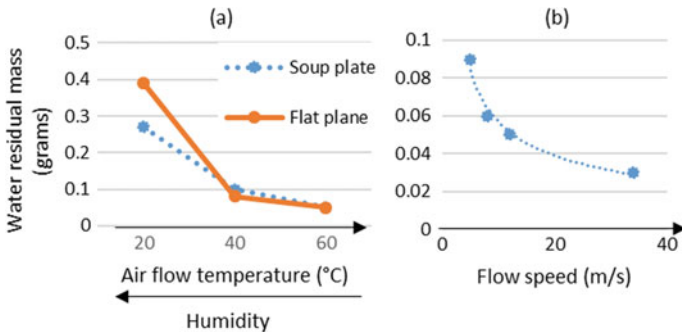


**Fig. 4** **a** Effects of the temperature on drying process in terms of water residual mass. **b** Effects of flow speed on drying process in terms of water residual mass

of the six points on the graph indicates the average measurement of the results of 20 tests.

Through other tests, we analysed the effect of the reduction of the air flow velocity on the evaporation (Fig. 4b). Also, in this case, the limited reduction of the flow does not lead to a substantial worsening of the drying performances: this data can therefore be exploited to reduce consumption.

**STEP 3—Identification of the new behaviour**

The hypothesized new behaviour (Fig. 5) aims to remove the great part (up to 70%) of water from the dish surface through a pure mechanical action and to evaporate the remaining part by evaporating it through heating.

For carrying out the first step, we exploited a high flow of warm humid air, by collecting it from the environment of the washing chamber and by simply accelerating it without heating or dehumidifying it. We spray the air coming out of the washing phase, 100% humid and hot, and it is fired without any barrier. In the second

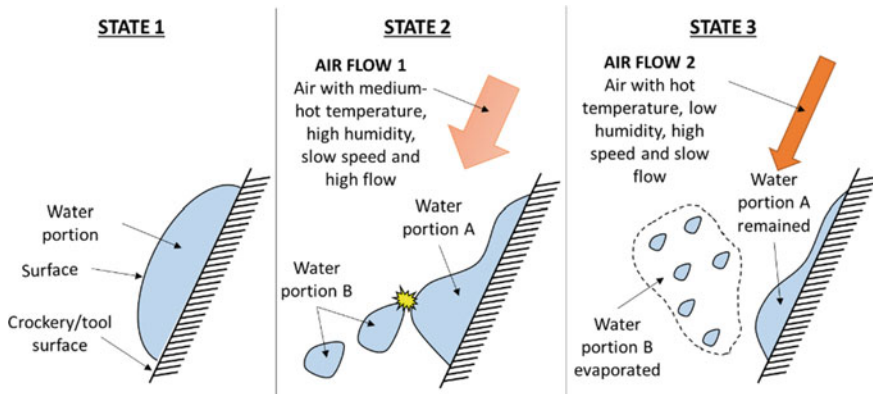


**Fig. 5** New hypothesized behaviour

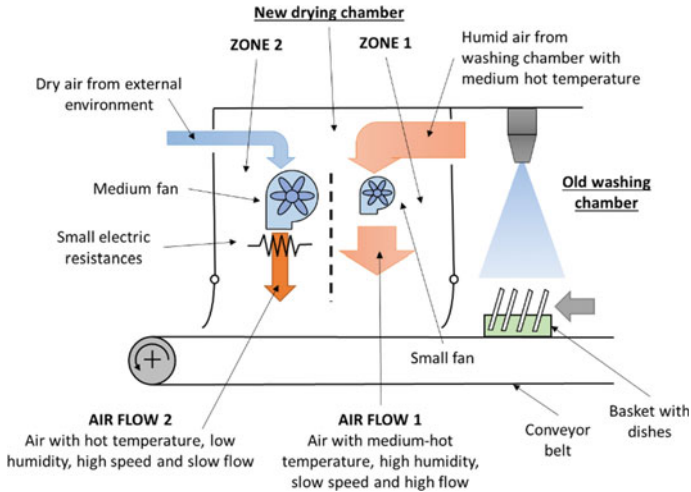


**Fig. 6** New structure for the drying chamber

step, for evaporating the remaining part of the water, we used a limited flow of hot dry air with high speed. This hypothesis could theoretically reduce the overall energy consumption of the chamber up to 90%, allowing us to eliminate the electric resistances and reduce the fan speed rate in the first part of the chamber, where the first flow is generated, and to introduce smaller resistances and high speed fan only in the final part for providing the second flow.

#### **STEP 4—Identification of the new structure**

The last step concerns the design of a new structure able to realize the new hypothesized behaviour by exploiting the available resources.

The new designed structure for the air chamber (Fig. 6) is made by two separate zones: the zone 1 is demanded to realize the state 2 of the behaviour, while the zone 2 is demanded for the state 3. The zone 1 includes one small fan, and it exploits (as resource) the humid air from the washing chamber. The zone 2 includes 1 medium fan and 1 small electric resistance.

In comparison with the old drying chamber, it drastically reduces the consumption of the electrical resistances and the fan. A first prototype has been realized and is still under testing.

## **4 Conclusions**

In this paper, a methodology for product eco-innovation aiming at reducing the energy consumptions, and so the related environmental impacts, has been proposed.

This methodology involves some typical TRIZ steps and technology transfer module. The starting point is the focusing on the object-product transformation rather than on the entire current devices. Then, its parametrical quantification is provided, and for each modified parameter, one or more possible way of functioning is investigated. Through technology transfer, we identify new physical effects and structure, to be exploited for hypothesizing a new expected behaviour and so a new structure for the device, exploiting the available resources within the working environment.

The methodology has been successfully applied for redesigning the drying chambers of Elframo rack conveyor dishwashers. The results allow a reduction of the consumption up to 90%, they have been developed in a prototype, currently under testing and described in patent application.

## References

1. Helu, M., Vijayaraghavan, A., Dornfeld, D.: Evaluating the relationship between use phase environmental impacts and manufacturing process precision. *CIRP Ann.* **60**(1), 49–52 (2011)
2. European Commission. Communication from the Commission to the European Parliament, the Council, the European Economic and Social Committee and the Committee of the Regions Closing the Loop—an EU Action Plan for the Circular Economy (2015)
3. De Almeida, A., Santos, B., Martins, F.: Energy-efficient distribution transformers in Europe: impact of Ecodesign regulation. *Energ. Effi.* **9**(2), 401–424 (2016)
4. Luttrupp, C., Lagerstedt, J.: EcoDesign and The Ten Golden Rules: generic advice for merging environmental aspects into product development. *J. Clean. Prod.* **14**(15–16), 1396–1408 (2006)
5. Wimmer, W. The ECODESIGN checklist method: a redesign tool for environmental product improvements. In: Proceedings First International Symposium on Environmentally Conscious Design and Inverse Manufacturing, pp. 685–688. IEEE (1999)
6. Lee, C.K., Lee, J.Y., Choi, Y.H., Lee, K.M.: Application of the integrated ecodesign method using the GHG emission as a single indicator and its GHG recyclability. *J. Clean. Prod.* **112**, 1692–1699 (2016)
7. Andriankaja, H., Vallet, F., Le Duigou, J., Eynard, B.: A method to ecodesign structural parts in the transport sector based on product life cycle management. *J. Clean. Prod.* **94**, 165–176 (2015)
8. Borgianni, Y., Maccioni, L., Pigosso, D.: Environmental lifecycle hotspots and the implementation of eco-design principles: does consistency pay off? In: International Conference on Sustainable Design and Manufacturing, pp. 165–176. Springer, Singapore (2019)
9. Altshuller, G.S.: Creativity as an exact science: the theory of the solution of inventive problems. Gordon and Breach (1984)
10. Russo, D., Serafini, M., Rizzi, C.: Is TRIZ an ecodesign method? In: International Conference on Sustainable Design and Manufacturing, pp. 525–535. Springer, Cham (2016)
11. Russo, D., Rizzi, C., Spreafico, C.: How to build guidelines for eco-improvement. In: International Conference on Sustainable Design and Manufacturing, pp. 879–887. Springer, Cham (2017)
12. Bersano, G., Fayemi, P.E., Schoefer, M., Spreafico, C.: An eco-design methodology based on a-LCA and TRIZ. In: International Conference on Sustainable Design and Manufacturing, pp. 919–928. Springer, Cham (2017)
13. Bovea, M., Pérez-Belis, V.: A taxonomy of ecodesign tools for integrating environmental requirements into the product design process. *J. Clean. Prod.* **20**(1), 61–71 (2012)
14. Vidal, R., Salmeron, J.L., Mena, A., Chulvi, V.: Fuzzy cognitive map-based selection of TRIZ (theory of inventive problem solving) trends for eco-innovation of ceramic industry products. *J. Clean. Prod.* **107**, 202–214 (2015)

15. Salamatov, Y.: *The Right Solution at the Right Time*. Insytec BV (1999)
16. Russo, D., Montecchi, T., Caputi, A.: Tech-finder: a dynamic pointer to effects. In: 16th International TRIZ Future Conference vol. 1, No. 3, pp. 79–87 (2018)

# Calculating Domestic Environmental Impacts: Challenging and Solutions for an Interactive Configurator



Christian Spreafico  and Davide Russo 

**Abstract** The domestic consumptions are commonly claimed to be more than 60% of global GHG emissions and between 50 and 80% of total land, material and water use. In the last few years, a lot of methods and tools to estimate those impacts have been proposed in the literature and diffused on public administration portals (e.g. European Commissioner for the Environment) and on private Websites. However, an overall analysis of all the factors that contribute to the consumption of an entire home and the development of a support tool is still lacking. This paper discusses the main parameters to be considered for the analysis and the methods for calculating the environmental impacts, and it proposed a supported tool, in the form of an interactive configurator. It allows the user to enter the main data about her/his own home, the constituting components (e.g. appliances) and her/his habits and behaviours (i.e. ways of use), and then, after the processing, it provides the results, in terms of environmental impacts (kg of equivalent CO<sub>2</sub>) of the entire home and the constituting components, by also showing possible more sustainable alternatives.

## 1 Introduction

Several methods and tools for assessing domestic environmental impacts are available in the literature and on WWW.

European Commission allows through its numerous portals to access to a lot of supporting reports for domestic LCA and interactive tools. Energy-efficient products portal contains information about the average annual impacts of some domestic appliances (e.g. TV, washing machines, heaters, refrigerators). Photovoltaic Geographical Information System (PGIS), hosted by EU Science Hub, can be used for calculating the efficiency of PV modules, installed in a determined area, in order to determine the saved electricity.

---

C. Spreafico (✉) · D. Russo  
University of Bergamo, Via Marconi 5, 24044 Dalmine (Bg), Italy  
e-mail: [christian.spreafico@unibg.it](mailto:christian.spreafico@unibg.it)

Within scientific literature, many more contributions report theoretical or empirical data about energy consumptions and environmental impacts of several appliances: ovens (e.g. [1]), hobs (e.g. [2]), refrigerators (e.g. [3]), vacuum cleaners (e.g. [4]), etc.

However, the results (i.e. environmental impacts and consumptions) deriving from these studies, methods and tools cannot be adopted, or at least immediately, for assessing the impact of an entire home for some reasons.

According to some authors (e.g. [5]), the data about the impacts of appliances are not consistent due to subjective choices during the evaluations and different system boundaries and considered lifetime.

In addition, they are criticized by many authors (e.g. [6]) to be too limited, by not considering all the possible environmental variables and the users' ways of interactions and settings.

One of the causes of these shortcomings also concerns the lack of works of collection and review of the many pertinent sources, and consequently of a shared standard for summarizing the many parameters quantifying the common domestic activities. Consequently, to date, these data are disseminated in a very large and too heterogeneous literature, often difficult to access and comprehend, since they have been developed by experts from different thematic areas (economy, energy, geography, etc.) characterized by their own specific jargon and methodological procedure.

The objectives of this paper are (i) Discussing and collecting the main parameters and the models to be considered for calculating the environmental impacts of the appliances, from scientific literature and normative. (ii) Proposing an interactive tool including a data entry module and a graphical overview of the domestic impacts, focusing on proposing possible more sustainable alternative appliances and components.

## **2 Assessing the Impacts for Production/Distribution/Disposal**

In addition to the impacts deriving from the use phase, those related to other phases of the lifecycle (i.e. production, distribution and end-of-life) can be useful for enlarging the spectrum of the overall analysis or from allowing a more complete comparison of alternative appliances, not only limited to the use phase: e.g. a condensing boiler is less impactful than a conventional one during the use, but not during production [7]. So, in order to justify its choice, the environmental impacts arising from the lower consumptions must compensate the increments from the production. Such considerations must also consider the expected product lifetime.

Data about the environmental impacts of the production/disposal of several appliances can be easily found in the literature: washing machine (e.g. [8]), coffee machine (e.g. [9]) microwave oven (e.g. [10]), etc.

However, the sources must be accurately selected in relation to the boundaries of the analysis and, in particular, the geographical provenience, which can substantially influence the provided results, e.g. in relation to the impacts deriving from the considered transportation distances of the raw materials and the final product.

### 3 Calculating the Environmental Impacts of Domestic Components During the Use Phase

In order to estimate the environmental parameters (Fig. 1) related to the use phase of an entire home, several parameters and related models about the home structure, the occupants and the appliances have to be taken into account.

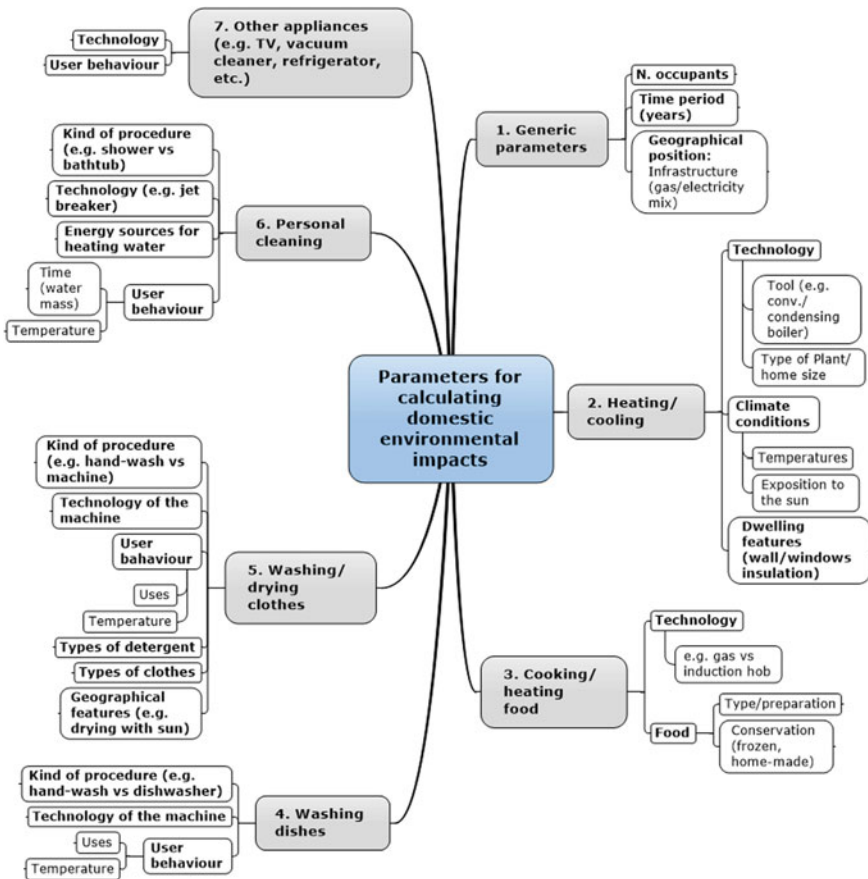


Fig. 1 Overview of the main parameters affecting the domestic impacts



In the following, the parameters and the related models are discussed in detail along with their sources.

### ***3.1 Generic Parameters***

Among them, the number of occupants and the time period (years) of the analysis contribute to proportionally increase the consumption and the impacts of the appliances during the use phase. The features of the infrastructure for the production and the distribution of energy, both gas and electricity mix contribute instead to the impacts through their specific conversion index (kg CO<sub>2</sub> eq/kWh). Those indexes strictly depend by the reference country and by the geographical region/province, and they generally change every year due to the infrastructure upgrades. European Environment Agency collects the averages historical electrical indexes for all the state members, while open-source project ElectricityMap ([www.electricitymap.org](http://www.electricitymap.org)) contains indexes even for parts of some world countries, which are updated in real time for considering every modification in networks configurations.

### ***3.2 Environmental Heating/Cooling***

The technology of the heating tool affects the impact in a substantial manner, generally of different percentage points (e.g. conventional vs. condensing boilers—[7]), due to the different efficiency values. The heating plant and the home size (i.e. floor area and volume, height, number of floors, etc.) are proportional to the consumptions. In addition, the type of energy source (e.g. natural gas, oil, wood, pellet) for domestic heating is strictly related to the emissions of human-toxic compounds, such as NO<sub>x</sub> (e.g. [11]) in addition to the kg CO<sub>2</sub> eq. (e.g. [12]).

The climate conditions firstly affect the consumptions through the differences between the external and internal temperatures. The Heating Degree Days and the Cooling Degree Days are widely used indicators for estimating the required load. They change in different geographical areas and during the years. Eurostat (EU commission) portal contains all the averages HDD/CDD historical series for the state members, while in literature, some studies (e.g. [13]) report the HDD/CDD values for different cities. The main limitations of HDD/CDD arise from the operating time and the internal temperature that are to be assumed as constant and fixed. The degree of exposure of the home to the sun influences the consumptions through the solar heating from the outside passing through walls and windows (e.g. [14]).

The dwelling features (i.e. types of walls, windows, roof and basement) influence the environmental impacts in terms of loss energy from heating. [7], by comparing the impacts of the same boiler in two different dwellings from the same city and characterized from different insulation systems (i.e. state of the art vs. one from the 1990s) identified differences included between 40% and 55%. Some studies from

literature provide the models for calculating the loss of energy through walls and windows in relation to the kind of constituting materials, their density and thickness (e.g. [15]). In particular, these data can be gathered from different sources. Just to provide some of examples, the normative UNI 6946 ([16]) provides the parameters relative to the internal and external thermal resistance of the materials, while [17] and [18] provide useful data about wall insulation materials and single/double-glazed windows.

For what concern the environmental cooling function, the same considerations of the heating can be maintained. Also, in this case, the type of the plant, the dwelling features and the geographical factors (Cooling Degree Days) play a crucial role (e.g. [19]). The parameters considered for heating and its calculation models can be used also for cooling.

### ***3.3 Cooking/Heating Food***

The types of hobs and ovens are related to the impacts due to the types of used sources (e.g. gas vs. electricity) and the energy efficiency depending on the technology. Some studies from the literature compare the impacts of different hobs (e.g. gas vs. induction—[1]) or ovens (e.g. gas vs. electric—[2, 20]). The type of cooked food affects the impacts because of the differences in terms of required time of preparation and temperature for cooking/heating. Several studies in the literature (e.g. [1, 20]) report the impacts deriving from the preparations of one portion of different foods (e.g. pasta, sauce, vegetables, omelette, chicken, etc.). The modalities of food conservations (i.e. frozen, chilled and home-made meals) influence the impacts too in terms of the different energies required for their preparation during the heating phases (e.g. [20, 21]).

### ***3.4 Washing Dishes***

The kind of procedure (i.e. hand washing, drying machine) affects the impacts in relation to the different quantity of used water and its temperature. Some authors (e.g. [22]) compare the impacts of the two procedures. The technology of the drying machine influences the consumptions through its power and efficiency. Different authors (e.g. [23, 24]) provide estimations for the specific consumption (i.e. kWh/setting or kWh per use). The influence of the user behaviour is related to the frequency of use and the choice of the programs of the drying machine (e.g. [25]).

### **3.5 *Washing/Drying Clothes***

The kind of procedure (i.e. hand washing, washing machine/drying machine) affects the impacts, principally in terms of the quantity of used water. The technology of the washing/drying machine is related to energy efficiency and water temperature. Some authors provide the specific standard consumptions for washing machine in terms of energy per use (e.g. [8, 23]), in accordance with machine models and different programs. The user behaviour determines instead the frequency of use and the choice of the programs of the machines. Some authors (e.g. [25]) identified different kinds of standard users in relation to their habits and their ecological sentiment, by showing how they influence the impacts. The type of detergent has different impacts on the environment. UK Department for Environment, Food and Rural Affairs estimated them for conventional powder, compact powder, powder tablet, compact liquid, liquid tab. The kinds of clothes influence the programs to be used in the machines in terms of quantity of water and temperature. The geographical features in terms of averages temperature and solar insulation influence both the washing and the drying process. [26] estimated the difference in some European countries.

### **3.6 *Personal Cleaning***

The choice between bathtub and shower influences the impacts in terms of water consumption that is statistically lower for the shower. The types of technologies such as jet breaker allow to same water and so to reduce the impacts. The energy sources and technologies for water heating influence the impacts in a substantial manner. Several studies report the consumptions and the impacts of different technologies such as gas/electric water heating (e.g. [27]) and solar water heating (e.g. [28]). Finally, the user behaviour plays a fundamental role on the use of water and its temperature.

### **3.7 *Other Appliances***

The main aspects to be considered for calculating the impacts of other appliances (e.g. TV, computers, smartphones, refrigerator, vacuum cleaner, etc.) are the technology related to energy efficiency (e.g. energy class) and the time of use (e.g. efficient products portal).

## 4 “My House”—Environmental Configurator

An interactive configurator for estimating the domestic environmental, including all the useful data, described so far, for estimating the domestic impacts of a home and its main components during the lifecycle has been developed, currently through excel worksheets. The configurator consists of four parts (Fig. 2): (1) the data entry module, through which the user enters the home features, the data about the operative context, the appliances features and her/his habits/behaviours; (2) the database containing the information about the environmental impacts coefficient for each component, collected from the literature; (3) the calculation module, combining the data entered by the user with the impacts coefficient from database for determining the environmental impacts and the (4) visualization of the results (environmental impacts).

“My house” is a database of environmental impacts implemented in a domestic products configurator. It is a very versatile tool suitable for many implementations.

Figure 3 shows the module in which the user enters the data of his home and the system automatically creates a ranking of the components that have the greatest impact on climate change.

In this way, we can identify the critical issues within the own home environment. In addition to this, if the house is in one of the three geographical areas covered by the data collection (Italy, France or Germany), we can compare results with the national averages, recalculated taking into account the general conditions imposed at the beginning of the data entry. This more detailed evaluation increases the number of criteria for identifying criticalities and planning improvement strategies.

For each function, data from alternative components (i.e. gas vs. electric oven) were collected. This tool can be used both for comparing them by identifying the most ecologic alternatives and also for comparing different ways of use, by switching between the various options within the data entry module. In this way, the user

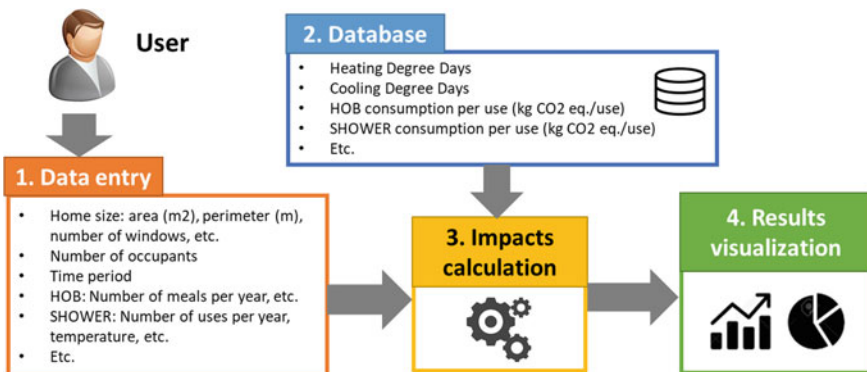


Fig. 2 Functioning scheme of the interactive configurator for domestic environmental impacts

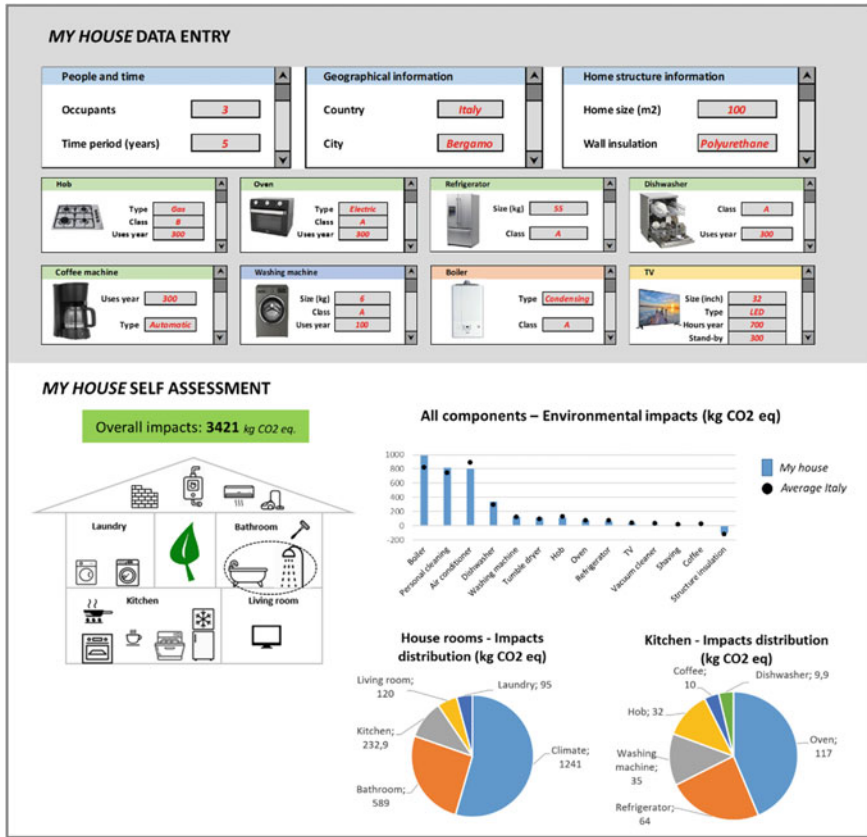


Fig. 3 Interactive configurator for domestic environmental impacts—Data entry module and Visualization of the results

can trace them and investigating the most ecologic behaviours for using a certain appliance.

In addition, by crossing these data with the impact of each national energy sources, it is also possible to determinate the most sustainable options and build the optimal home configuration from one’s own situation. In the future developments, the construction of an eco-improvement tool based on this database is being studied.

## 5 Conclusions

In this paper, the main parameters to be considering for assessing the environmental impacts of an entire home and its components (e.g. appliances), during the entire

lifecycle, have been widely discussed, and some sources from literature and administration portals (e.g. EU commission for environment) have been presented for each of them.

The considered parameters have been divided according to the related components and the related aspects: technology (e.g. typologies, powers, sizes, efficiency/energetic classes), geography (e.g. Degree Days, degree of insulation), infrastructure for energy generation and distribution (e.g. electricity mix), user behaviour and habits.

Some criteria for the selection of the sources for each parameter have been provided too (e.g. geographical provenience).

Finally, an interactive configurator for assessing the environmental impacts of an entire home in terms of kg CO<sub>2</sub> eq. has been presented, which consists of three modules: (1) data entry, for collecting the main information about the context of application (i.e. home structure and geographical position), the types of appliances (i.e. models and size) and the data related to user's behaviours and habits (e.g. number of meals per year cooked with hob, number of uses of the washer machine/tumble dryer, internal temperature during winter and summer). (2) Intelligence containing all the discussed parameters for calculating the impacts starting from the data collected by the user. (3) Visualization of the results proposing the overall environmental impacts for the home and its components.

Future developments of this work deal with the definition of an extended set of documents from the literature and comprehensive analyses summarizing the main results achievable through the proposed configurator. In this way, we want to propose a comparison of the domestic impacts in different EU countries, based on the national average data, and we want to quantify the weights of the different usage habits through a rigorous sensitivity analysis.

## References

1. Landi, D., Consolini, A., Germani, M., Favi, C.: Comparative life cycle assessment of electric and gas ovens in the Italian context: an environmental and technical evaluation. *J. Clean. Prod.* **221**, 189–201 (2019)
2. Favi, C., Germani, M., Landi, D., Mengarelli, M., Rossi, M.: Comparative life cycle assessment of cooking appliances in Italian kitchens. *J. Clean. Prod.* **186**, 430–449 (2018)
3. Monfared, B., Furberg, R., Palm, B.: Magnetic versus vapor-compression household refrigerators: a preliminary comparative life cycle assessment. *Int. J. Refrigerat* **42**, 69–76 (2014)
4. Gallego-Schmid, A., Mendoza, J.M.F., Jeswani, H.K., Azapagic, A.: Life cycle environmental impacts of vacuum cleaners and the effects of European regulation. *Sci. Total Environ.* **559**, 192–203 (2016)
5. Andrae, A.S., Andersen, O.: Life cycle assessments of consumer electronics—are they consistent? *Int. J. Life Cycle Assess.* **15**(8), 827–836 (2010)
6. Ross, S.A., Cheah, L.: Uncertainty quantification in life cycle assessments: Interindividual variability and sensitivity analysis in LCA of air-conditioning systems. *J. Ind. Ecol.* **21**(5), 1103–1114 (2017)

7. Vignali, G.: Environmental assessment of domestic boilers: A comparison of condensing and traditional technology using life cycle assessment methodology. *J. Clean. Prod.* **142**, 2493–2508 (2017)
8. Yuan, Z., Zhang, Y., Liu, X.: Life cycle assessment of horizontal-axis washing machines in China. *Int. J. Life Cycle Assess.* **21**(1), 15–28 (2016)
9. Brommer, E., Stratmann, B., Quack, D.: Environmental impacts of different methods of coffee preparation. *Int. J. Consum. Stud.* **35**(2), 212–220 (2011)
10. Gallego-Schmid, A., Mendoza, J.M.F., Azapagic, A.: Environmental assessment of microwaves and the effect of European energy efficiency and waste management legislation. *Sci. Total Environ.* **618**, 487–499 (2018)
11. Gustafson, P., Barregard, L., Strandberg, B., Sällsten, G.: The impact of domestic wood burning on personal, indoor and outdoor levels of 1, 3-butadiene, benzene, formaldehyde and acetaldehyde. *J. Environ. Monit.* **9**(1), 23–32 (2007)
12. Monteleone, B., Chiesa, M., Marzuoli, R., Verma, V.K., Schwarz, M., Carlon, E., et al.: Life cycle analysis of small scale pellet boilers characterized by high efficiency and low emissions. *Applied Energy* **155**, 160–170 (2015)
13. De Rosa, M., Bianco, V., Scarpa, F., Tagliafico, L.A.: Historical trends and current state of heating and cooling degree days in Italy. *Energy Convers. Manag.* **90**, 323–335 (2015)
14. Stazi, F., Marinelli, S., Di Perna, C., Munafò, P.: Comparison on solar shadings: Monitoring of the thermo-physical behaviour, assessment of the energy saving, thermal comfort, natural lighting and environmental impact. *Sol. Energy* **105**, 512–528 (2014)
15. Dombaycı, Ö.A., Gölcü, M., Pancar, Y.: Optimization of insulation thickness for external walls using different energy-sources. *Appl. Energy* **83**(9), 921–928 (2006)
16. UNI 6946: Building components and building elements—Thermal resistance and thermal transmittance—Calculation method (2008)
17. Su, X., Luo, Z., Li, Y., Huang, C.: Life cycle inventory comparison of different building insulation materials and uncertainty analysis. *J. Clean. Prod.* **112**, 275–281 (2016)
18. Switala-Elmhurst, K., Udo-Inyang, P.: Life cycle assessment of residential windows: saving energy with window restoration. In: *ASC Proceedings of the 50th Annual Conference* (2014)
19. Jakubcisonis, M., Carlsson, J.: Estimation of European Union residential sector space cooling potential. *Energy Policy* **101**, 225–235 (2017)
20. Rivera, X.C.S., Azapagic, A.: Life cycle costs and environmental impacts of production and consumption of ready and home-made meals. *J. Clean. Prod.* **112**, 214–228 (2016)
21. Rivera, X.C.S., Orias, N.E., Azapagic, A.: Life cycle environmental impacts of convenience food: Comparison of ready and home-made meals. *J. Clean. Prod.* **73**, 294–309 (2014)
22. Porras, G.: *Life Cycle Comparison of Manual and Machine Dishwashing in Households* (Doctoral dissertation) (2019)
23. Laicane, I., Blumberga, D., Blumberga, A., Rosa, M.: Reducing household electricity consumption through demand side management: The role of home appliance scheduling and peak load reduction. *Energy procedia* **72**, 222–229 (2015)
24. Santori, G., Frazzica, A., Freni, A., Galieni, M., Bonaccorsi, L., Polonara, F., Restuccia, G.: Optimization and testing on an adsorption dishwasher. *Energy* **50**, 170–176 (2013)
25. Stamminger, R.: Modelling resource consumption for laundry and dish treatment in individual households for various consumer segments. *Energ. Eff.* **4**(4), 559–569 (2011)
26. Schmitz, A., Stamminger, R.: Usage behaviour and related energy consumption of European consumers for washing and drying. *Energ. Eff.* **7**(6), 937–954 (2014)
27. Piroozfar, P., Pomponi, F., Farr, E.R.: Life cycle assessment of domestic hot water systems: A comparative analysis. *Int. J. Constr. Manage.* **16**(2), 109–125 (2016)
28. Greening, B., Azapagic, A.: Domestic solar thermal water heating: A sustainable option for the UK? *Renewable Energy* **63**, 23–36 (2014)

# Additive Manufacturing of Continuous Carbon Fiber-Reinforced Plastic Components



Stefan Junk, Manuel Dorner, and Claus Fleig

**Abstract** Additive manufacturing is a rapidly growing manufacturing process for which many new processes and materials are currently being developed. The biggest advantage is that almost any shape can be produced, while conventional manufacturing methods reach their limits. Furthermore, a lot of material is saved because the part is created in layers and only as much material is used as necessary. In contrast, in the case of machining processes, it is not uncommon for more than half of the material to be removed and disposed of. Recently, new additive manufacturing processes have been on the market that enables the manufacturing of components using the FDM process with fiber reinforcement. This opens up new possibilities for optimizing components in terms of their strength and at the same time increasing sustainability by reducing materials consumption and waste. Within the scope of this work, different types of test specimens are to be designed, manufactured and examined. The test specimens are tensile specimens, which are used both for standardized tensile tests and for examining a practical component from automotive engineering used in student project. This project is a vehicle designed to compete in the Shell Eco-marathon, one of the world's largest energy efficiency competitions. The aim is to design a vehicle that covers a certain distance with as little fuel as possible. Accordingly, it is desirable to manufacture the components with the lowest possible weight, while still ensuring the required rigidity. To achieve this, the use of fiber-reinforced 3D-printed parts is particularly suitable due to the high rigidity. In particular, the joining technology for connecting conventionally and additively manufactured components is developed. As a result, the economic efficiency was assessed, and guidelines for the design of components and joining elements were created. In addition, it could be shown that the additive manufacturing of the component could be implemented faster and more sustainably than the previous conventional manufacturing.

---

S. Junk (✉)

Department of Business and Engineering, Laboratory of Rapid Prototyping, Offenburg University, Klosterstr. 14, 77723 Gengenbach, Germany  
e-mail: [stefan.junk@hs-offenburg.de](mailto:stefan.junk@hs-offenburg.de)

M. Dorner · C. Fleig

Department of Mechanical and Process Engineering, Offenburg University, Badstr. 24, 77652 Offenburg, Germany



## 1 Introduction

Additive manufacturing has developed rapidly in recent years. As a result, new processes and new materials keep coming onto the market. This means that the limited choice of materials that still exists and the low strength values are being overcome more and more [1]. An example of this new development is the combination of material extrusion (MEX) using fused layer modeling (FLM) of plastic filaments with the reinforcement by short and long fibers. The advantage of the FLM is the simple and inexpensive system technology. The material costs for plastic filament are also significantly lower compared to the costs of metal powder [2]. However, the components manufactured using FDM have the disadvantage that they can only provide low strength values.

Therefore, this contribution aims to investigate the extent to which reinforcing the components using fibers can lead to an improvement in material properties. Different types and orientations of fibers are examined. A practical example from the automotive sector is chosen to implement these findings. Particular attention is paid to the design of the component and the connection to other components. As another aim, improvements for the sustainability of such components are also analyzed.

## 2 Literature Review

In a very comprehensive study, it was already shown in 2016 that short fiber reinforcement made it possible to significantly increase the Young's modulus. The results in the FDM process can be more than tripled by using short fibers. Through the directed use of long fibers, the strength values can be doubled [3]. The short fibers can be used in various forms, e.g., as powder for selective laser sintering or as filament for FDM [4].

When using long fibers, the selection of the fiber material plays an essential role in achieving the increase in strength that can be achieved. It has been shown that glass fibers enable better values than Kevlar fibers. The highest increase in strength could be achieved with the help of carbon fibers [5, 6] When using long fibers, various parameters must also be considered that have a significant influence on the material properties. These parameters include the filling pattern, the insertion angle and the number of layers with reinforcement [6]. Further extensive studies have shown that the properties of the components can be significantly influenced, in particular by varying the filling pattern and the insertion angle. Generally, to determine the characteristic values, tensile tests were carried out [7].

In order to determine the failure of the components in the event of breakage, scanning electron microscopes are also used [7]. With regard to the prediction of the mechanical properties of composite materials, a consistent and robust mathematical method, namely asymptotic homogenization, has already been used to predict the

longitudinal, transverse and in-plane shear modules of carbon-reinforced lamellas [8]. This new method is used in practice in many applications, when components with low weight are advantageous. There are currently interesting applications in robotics and aircraft design [9, 10]. But challenges were also found, such as a low fiber volume fraction (vf) of the products and the printing restrictions of the systems [10].

### 3 Fused Layer Modeling (FLM)

In the FDM printing process, a filament represents the starting material to be processed. The filament is transported to the nozzle by transport rollers which are driven by a stepper motor. The extrusion die (nozzle) is continuously kept at the melting temperature to liquefy the filament and apply it to the build platform. As the filament is pushed through the nozzle, various stepper motors control the axes, which are responsible for the movement of the print head or the build platform.

#### 3.1 FLM with Fiber Reinforcement

The processing of continuous fibers within the FLM process is a new approach in additive manufacturing, which is why there are not yet many printers that can process fibers. Currently, the most common way to process short fibers using the FLM process is to bind the fibers into the filament and otherwise process them as usual. The 3D printer “Mark two” from Markforged uses this process and is shown in Fig. 1a). If a fiber is processed in addition to the plastic filament, a second stepper motor comes into action, which conveys the fiber. In this process, a layer is first extruded with plastic, and then, the fiber is laid over it in the desired orientation. The filament is stored in a “dry box” and transported to the printing nozzle via a tube

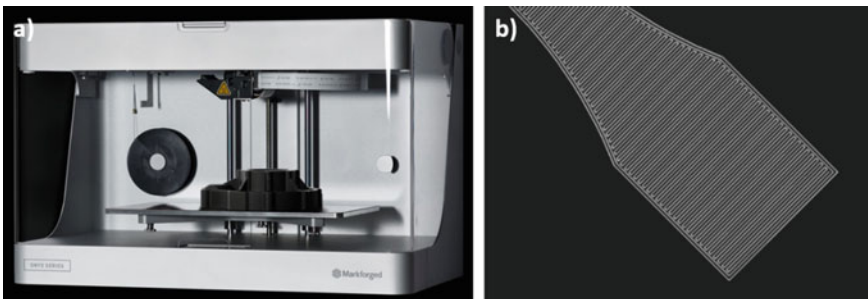


**Fig. 1** a) 3D printer for fiber reinforcement Markforged “Mark two” and b) Screenshot of the software for data preparation with CAD data of a tensile test and arrangement of the fibers

made of Teflon. The filament is thus protected from the moisture and thereby retains its original material properties.

### ***3.2 Software for Data Preprocessing***

The software for data preprocessing used in this contribution is also provided by Markforged and is specially tailored to the printer and the printing process. This software called “Eiger” can be operated very easily and intuitively thanks to the clear graphical user interface. The CAD data are uploaded in STL format, and the print settings are made using “Eiger” software. In the software, the arrangement and the number of fibers for the reinforcement can be determined. The geometry and arrangement of the fibers are shown graphically and can therefore be easily checked (see Fig. 1b).

An important point for the additive manufacturing process is the orientation of the component on the build platform. This choice of orientation is supported by the software. The adhesion of the part to the build platform can be improved by very useful setting options. Furthermore, the printing process can be paused to embed components in the print. So, it is possible to print RFID chips, nuts or magnets directly into the component. This function is used in the context of this work for the embedding of connecting parts.

### ***3.3 Filament and Carbon Fibers***

The basis for each print is the thermoplastic filament used, which is pressed through the heated nozzle. “Onyx” is a product name of Markforged, which, according to Markforged, is made up of nylon (PA6) and micro-carbon fibers. According to the manufacturer, the filament should be much easier to process than ABS and still achieve up to 1.4 times the stiffness. This composite material is also said to have better dimensional stability and a higher surface quality than conventional filaments.

Microfibers are generally referred to as mineral fibers with a diameter of less than 3  $\mu\text{m}$ . The heat tolerance or the shape tolerance when exposed to temperature is also at a maximum of 145 °C far above that of PLA. Markforged specifies 36 MPa for the “Onyx” filament as tensile strength. The Mark two also supports the printing of various types of long fibers. The carbon fiber was chosen in this work as it is known as a high-performance, high-strength and extremely light material.

## 4 Determination of Material Characteristics

To determine the material characteristics, standardized test methods such as tensile tests are suitable, which are statistically representative due to the standard and, above all, comparable to other materials that were tested under the same conditions.

### 4.1 Preparation of Tensile Tests

Although the preparation of the specimen and the execution of the tensile test have a very large influence on the results, there are still no standardized test methods for 3D-printed samples. For the tensile tests, the test procedure according to DIN EN ISO 527 is a sensible standard [11]. Thus, all tensile tests have been carried out according to this standard, and so, the comparability with other material properties is given.

A tensile testing machine with an optical recording of the change in length was used (see Fig. 2a). In advance, a very high tensile stress is assumed for the type 1B sample, which could lead to an overload of the test facility. A proportionally reduced sample is therefore selected for the specimen with orientation of the fibers in the direction of the force. Figure 2b shows a printed batch of the unreinforced tensile specimens of type 1B. The build platform was always equipped with two samples for each orientation so that eight tensile samples could always be produced per batch.

In this case, all settings for the tensile tests are made in accordance with DIN EN ISO 527. Specimen of the three different arrangements and orientations A to C are printed. Both unreinforced samples, which only contain short fibers (indication O), and reinforced samples, which also contain long fibers (indication F), are used. All samples with short fibers (AO, BO and CO) show expected values that are comparable with the manufacturer's specifications.

For sample AO, the filament lines were arranged parallel to the direction of force. As expected, orientation A has good tensile strength and high elongation at break. If

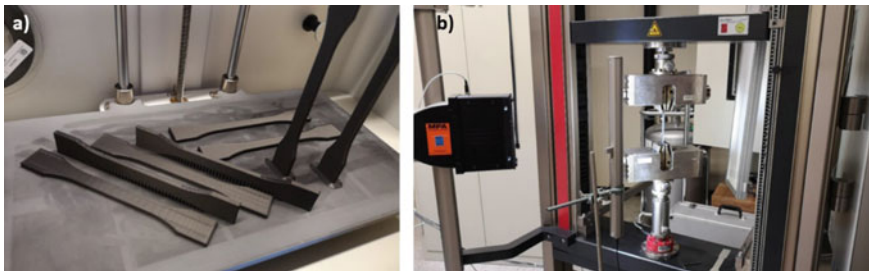


**Fig. 2** a 3D-printed specimen with different orientations in the installation space and b specimen in the tensile testing machine with optical measuring device

**Table 1** Results from tensile tests

Specimen orientation	Young's modulus (Mpa)	Strength (MPa)	Elongation (%)
AO	1310	33.9	14.7
AF	62,500	333.0	0.5
BO	990	35.7	25.5
BF	4772	36.8	1.1
CO	1440	25.4	2.9
CF	4717	40.0	1.6

Reinforcement *O*: short fibers only, *F*: long fibers

it was possible to arrange each individual layer so that the filament lines point in the direction of the force, even higher tensions could be achieved. Unfortunately, this option is not possible with the current data preparation software.

In orientation BO, the filament lines were arranged at 45°. Even if this is not the optimal orientation of the layers, samples B have better tensile strengths with a higher elongation at break than sample A. This is again due to the orientation. With orientation A, every second layer is rotated by 90°, which means a considerable loss in tensile strength for this layer. Even if the arrangement below 45° is not optimal, the layers that are rotated can withstand higher tensions when combined. Orientations CO were printed in upright position. The tensile force therefore acts vertically on the additively produced layers. This orientation already suggests a lower tensile strength because the connection between the layers has a lower bond.

The analysis of the strengths and orientations in Table 1 shows large differences. The elongation at break is very low compared to the other orientations. There is no way for the filament to lengthen so that the break occurs as soon as the binding force of the layers is exceeded. Nevertheless, the connection between the layers seems to be better than with the flat printed samples. Due to the small cross section that has to be printed, the previously printed layer is still at a sufficiently high temperature to bond very well. This also leads to the slightly higher tensile strengths.

As expected, the sample AF had exceptionally good results with the fibers oriented in the direction of the force. They are characterized also by excellent reproducibility. In addition, the low elongation is extremely pronounced in this sample, since the fibers have no possibility of being elongated in any form by alignment. The two samples BF and CF show significantly lower strength values. With this orientation, however, the strains are higher than with specimen AF because the fibers can align themselves when force is applied, and thus, a little more stretch is achieved. Even though higher tensile strengths could be achieved compared to the unreinforced samples, the fiber did not seem to be able to absorb the force after alignment, which is why the results lag far behind those of sample AF.

For the additive manufacturing process with plastic, the material characteristics turned out to be exceptionally good. The orientation AF has outstanding properties. Compared to the orientation AF, pure aluminum with a tensile strength of 60–90 MPa,

an elastic modulus of 70,000 MPa and an elongation at break of 20% even show a much poorer tensile strength.

## 5 Test Component from Automotive Engineering

The next goal is to design and to implement a component from a realistic application. A component of a student project was selected for this. The experimental vehicle “Schluckspecht” is a vehicle developed by a team of students, which was designed to compete in the “Prototype class” at the Shell Eco-marathon (see Fig. 3a). The aim of the marathon is to cover the longest possible distances with as little energy as possible [12]. In order to achieve efficient driving behavior, good aerodynamics and low weight are aimed for. As a result, fiber-reinforced 3D printing is an optimal alternative to conventionally manufactured components. For this work, the so-called wings or the tension strut between the wheel carrier connections was selected (see Fig. 3b).

There are now a large number of processing methods with carbon fibers on the market, but only the processing of prepregs is dealt with here, since this method is also to be used for the construction of the body of the experimental vehicle. For the conventional manufacturing of the tension strut from CFRP prepregs, first of all the model of the part and, depending on the procedure, also the negative of the part must be produced. Since the prepregs are stored at approximately minus 18 °C, a certain thawing time must be planned, which varies depending on the requirements of the finished component. The thawed layers must be laid on top of each other without wrinkles, considering the direction of the fibers, whereby laminating is not directly on the model surface but on a so-called tear-off fabric. At the end, the surface must be covered with a fleece, and the part must remain in a sealing film sealed with sealing tape under vacuum. The fleece serves to absorb the excess resin. Application of vacuum is necessary to work out the excess resin and to press the individual prepreg layers together. The part must now be placed in an oven under vacuum and cured and cured at temperatures.

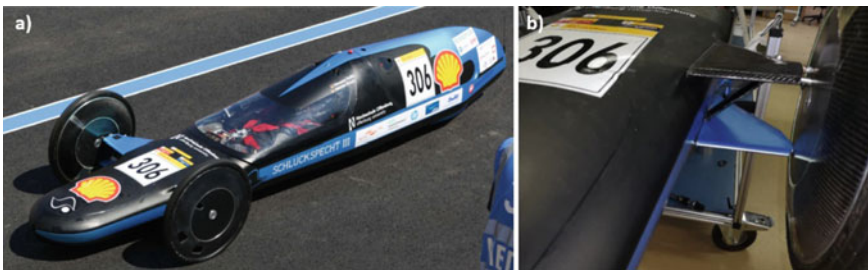


**Fig. 3** a Experimental vehicle and b Chassis with test component: tension strut

## 5.1 Requirements for the Design of the Test Component

There are some points for the design of the new tension strut which must be observed in order to obtain a meaningful improvement. An important requirement is, for example, to reduce the total weight of approximately 90 g of the existing tension strut by at least 5%. Despite the weight saving, the rigidity should be maintained so that the tension strut can withstand all loads.

Due to the high time pressure during the competitions, the connections should be very easy to install. Disassembly should also be as straightforward as possible. Since a wheel carrier already exists in the current design and this should not be changed, the connection points of the wheel carrier must be precisely recorded and transferred to the new design. In view of the goal of driving as fuel-efficiently as possible, the shape of the connection with regard to its aerodynamics must not deteriorate. Besides of lightweight design, the aim is to maintain the shape and not to enlarge the projected area.

## 5.2 Design of the Tension Strut

The force of the tension strut lies on a straight line, which is why it can also be clamped and tested in the tensile testing machine. The advantages of this test are evident, since the exact force can be applied via the clearly measured change in length. Furthermore, a statement can be made about the force from which the tension strut fails.

To carry out the experiment, it is now necessary to test the tension strut (see Fig. 4a and b) under realistic conditions. To do this, appropriate aluminum inlays must be designed and manufactured. With the help of these inlays, the tension strut can be optimally clamped and tested. An additional function of the 3D printer can be used for the inlays. It is possible to stop printing at a certain layer to insert the inlays and continue printing afterward. In order to improve the connection, some glue is placed on the surface of the inlay before it is inserted. This form fit and the additional gluing provide an optimal transmission of power. As can be seen in Fig. 4c, there is a threaded hole in the middle of the inlay, into which the ball joints can be screwed during assembly. For the form fit in additively manufactured components,

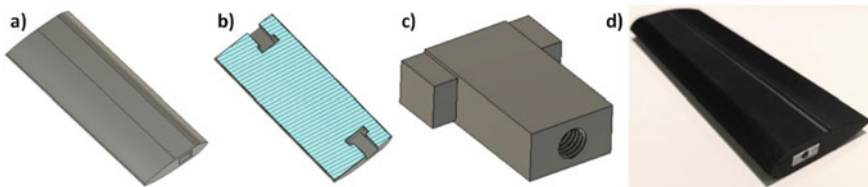


**Fig. 4** **a** CAD model of the tension strut with fiber reinforcement, **b** section of the tension strut with recess for inlays, **c** aluminum inlay and **d** 3D-printed strut with inlay

it makes sense to create a continuous transition of the form so that the force is also transmitted evenly. The small shoulders that can be seen on the top in Fig. 4c are required to center the inlays and are intended to ensure that the threaded holes are aligned vertically.

With the result of the tensile tests, the number and also the position of the fibers can be determined. The proportionally reduced sample (Type 1BA) has a tensile strength of 333 MPa with a cross section of 20 mm<sup>2</sup> or with 48 fiber lines in cross section (see Table 1). Theoretically, the resulting force is 6660 N. For the tension strut, a tensile force of 1000 N should be aimed for, which should be achieved with only a few fibers. In the cross section of the component, 75 fibers can be placed in a central layer. For the tension strut, fibers are therefore placed in the direction of force in the middle and in the upper as well as the lower edge layers in order to stiffen the tension strut against bending stresses. The upper and lower fiber layers are placed exactly one layer above or below the inlays in order to establish a good connection to them.

### 5.3 Additive Manufacturing and Testing of the Tension Strut

The finished tension strut with the embedded inlays is shown in Fig. 4d. For the tensile test, an installation-friendly clamping construction must now be considered. With this clamping construction, the tension strut is clamped between the clamping jaws and tested under real conditions. This test set-up is illustrated in Fig. 5a. For the tensile test, a test speed of 20 mm/min was selected.

Since the tension strut was printed with infill, there would be no point in specifying a tension in this case, since the exact cross section in the fracture surface cannot be determined. Here, it makes sense to apply the force via the traverse path, which is shown in Fig. 5b. It can be seen here that the first breaks of some fibers occurred at 2500 N. Further breaks in fiber strands occurred at 3750 N before the tension strut

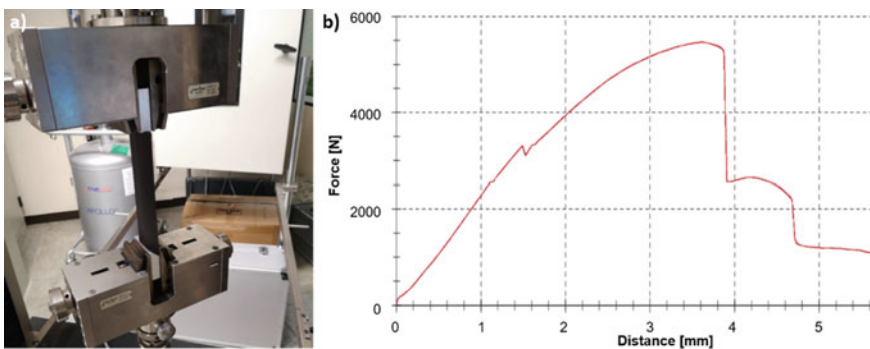


**Fig. 5** a) Clamping of the tension strut during tensile tests and b) result of the tensile tests



finally failed at 5459 N. A little stretching was to be expected from the tensile tests. This expectation was also confirmed, as illustrated in the diagram.

It is interesting that the strut itself has hardly deformed, only the inlay is torn out. It is therefore clear that the structure of the tension strut can withstand the applied force without great deformation. The weak point is the connection between the inlays and the fiber. A redesign of this connection is recommended. The strut would already withstand the specified load of 1000 N.

#### ***5.4 Consideration of Weight, Manufacturing Time and Sustainability***

The additive manufacturing of the tension strut initially leads to a significant reduction in the manufacturing time. For the conventional manufacturing process, a time expenditure of approximately 3–4 days is estimated. In contrast, 3D printing only takes about 15 h. The workload also differs significantly. While in conventional manufacturing, a lot of process steps has to be done by hand (e.g., insertion of prepregs), the 3D printing can run almost completely automatically. 3D printing also offers cost advantages, since only the machine hours for the printer and the material have to be paid. Conventional manufacturing, on the other hand, requires expensive tools and devices.

With regard to sustainability, additive manufacturing also offers advantages. The tension strut presented here is approximately 4.5% lighter than the conventionally manufactured component. This can reduce fuel consumption and thus CO<sub>2</sub> emissions. Resource consumption is also significantly reduced in additive manufacturing. This eliminates many work steps and the associated energy consumption (e.g., cooling of prepregs, application of vacuum). Many raw materials savings are made, e.g., blanks for the manufacturing of tools, fleeces for the packing and sealings for the application of vacuum.

## **6 Conclusion**

In this contribution, additively manufactured components made of plastic filament with fiber reinforcement were examined. It was confirmed that the alignment of the fibers has a significant influence on the strength of tensile specimens. The highest tensile strength values of over 330 MPa could be achieved within the FDM process if the fibers were inserted parallel to the direction of force.

On the basis of these results, a tensile strut for the chassis of a test vehicle was developed. The connection of the component to the other chassis components was also considered. With the help of an inserted component made of aluminum, the forces between the components could be transferred. The examination of the

fiber-reinforced, additively manufactured component with the inlay showed that the required forces of 1000 N are more than sufficiently endured.

In terms of sustainability, the newly developed component has shown that additive manufacturing through lightweight design offers a slight reduction in weight and thus in fuel consumption. Even more significant advantages can be achieved in the additive manufacturing process due to the extensively reduced production times and resource consumption.

For further work, it is recommended to further improve the connection between the inlay and the component. By reducing the cross section or using less material, the tensile strut can be made even lighter with sufficient rigidity. Thus, the printed tension strut is a clear improvement in terms of manufacturability, weight and freedom of design. The manufacturability of the components is also considerably simplified compared to conventional manufacturing and thus offers new possibilities for many applications.

## References

1. Gibson, I., Rosen, D., Stucker, B.: Additive Manufacturing Technologies. Springer, New York (2015)
2. Devine, D.M.: Polymer-Based Additive Manufacturing. Springer International Publishing, Cham (2019)
3. Matsuzaki, R., Ueda, M., Namiki, M., Jeong, T.-K., Asahara, H., Horiguchi, K., Nakamura, T., Todoroki, A., Hirano, Y.: Three-dimensional printing of continuous-fiber composites by in-nozzle impregnation. *Scientific Reports* (2016)
4. Zhou, W.D., Chen, J.S.: 3D Printing of Carbon Fiber Reinforced Plastics and their Applications. MSF (2018)
5. Dickson, A.N., Barry, J.N., McDonnell, K.A., Dowling, D.P.: Fabrication of continuous carbon, glass and Kevlar fibre reinforced polymer composites using additive manufacturing. *Additive Manufacturing* (2017)
6. Argüello-Bastos, J.D., González-Estrada, O.A., Ruiz-Florián, C.A., Pertuz-Comas, A.D., V-Niño, E.D.: Study of mechanical properties under compression failure in reinforced composite materials produced by additive manufacturing. *J. Phys. Conf. Ser.* (2018)
7. Argüello-Bastos, J.D., Ruiz-Florián, C.A., González-Estrada, O.A., Pertuz-Comas, A.D., Martínez-Amariz, A.: Compression tests performed in reinforced rigid matrix composite varying the reinforcement material. *J. Phys. Conf. Ser.* (2018)
8. Dutra, T.A., Ferreira, R.T.L., Resende, H.B., Guimarães, A.: Mechanical characterization and asymptotic homogenization of 3D-printed continuous carbon fiber-reinforced thermoplastic. *J. Braz. Soc. Mech. Sci. Eng* (2019)
9. Yao, X., Luan, C., Zhang, D., Lan, L., Fu, J.: Evaluation of CF-embedded 3D printed structures for strengthening and structural-health monitoring. *Mater Design* (2017)
10. Koga, Y., van der Klift, F., Todoroki, A., Ueda, M., Hirano, Y., Matsuzaki, R.: The printing process of 3D printer for continuous CFRTP. *International SAMPE Symposium and Exhibition*, 1–9 (2016)
11. DIN EN ISO 527-1:2012-06, *Kunststoffe\_- Bestimmung der Zugeigenschaften\_- Teil\_1: Allgemeine Grundsätze (ISO\_527-1:2012)*. Beuth Verlag GmbH, Berlin (2012)
12. Junk, S., Fleig, C., Fink, B.: Improvement of sustainability through the application of topology optimization in the additive manufacturing of a Brake Mount. In: Campana, G., Howlett, R.J., Setchi, R., Cimatti, B. (eds.) *Sustainable Design and Manufacturing 2017*, vol. 68, pp. 151–161. Springer International Publishing, Cham (2017)

# Scalability Analysis in Industry 4.0 Manufacturing



Riccardo Accorsi, Marco Bortolini, Francesco Gabriele Galizia,  
Francesco Gualano, and Marcella Oliani

**Abstract** In the recent years, reconfigurable manufacturing systems (RMS) emerged as a new class of manufacturing systems aiming to adapt the production capacity in a quick, efficient and cost-effective way, through a set of six core features, i.e. modularity, integrability, scalability, convertibility, customisation and diagnosibility. This paper focuses on the scalability attribute, i.e. the ability of the manufacturing system to rapidly adapt to fluctuations of the market demand, providing metrics to evaluate the scalability of machines, in both discrete manufacturing and process manufacturing industries, which produce different types of goods. The proposed metrics are applied to an industrial case study from the discrete and the process manufacturing industries to highlight the different trend of the scalability attribute.

## 1 Introduction and Literature Review

Within the current industrial context, manufacturing companies are facing radical changes forcing to improve their standard in product and process design and management [1]. Dynamic market demand, flexible batches and short product life cycles are just some of the key factors driving the transition from the traditional manufacturing systems to the so-called next generation manufacturing systems (NGMSs) [2, 3]. In this new scenario, reconfigurable manufacturing systems (RMS) emerge as an effective manufacturing solution able to provide a response to the dynamic market requests and to overcome the main limitations of traditional manufacturing systems, e.g. dedicated, flexible and cellular manufacturing systems [1, 4]. Such results are reached thanks to their six core features, which are modularity, integrability, diagnosibility, convertibility, customisation and scalability [5–8]. These features make RMSs dynamic systems with the capacity and functionality to follow the market changes and to produce a higher variety of customised products. According to Koren et al. [9], among the above-mentioned six features, scalability represents the most

---

R. Accorsi · M. Bortolini · F. G. Galizia (✉) · F. Gualano · M. Oliani  
Department of Industrial Engineering, Alma Mater Studiorum (University of Bologna, Viale Del Risorgimento 2, 40136 Bologna, Italy  
e-mail: [francesco.galizia3@unibo.it](mailto:francesco.galizia3@unibo.it)

important one because of the crucial need to best manage the uncertainty of the market demand. Such feature can be defined as the ability to easily modify production capacity by adding or removing manufacturing resources, e.g. working machines and changing components of the system to manage the changing demand. Such reconfiguration should be performed quickly, rapidly reacting to market changes, incrementally, providing the exact capacity required by the market, and in a cost-effective way, to remain competitive [10]. The literature on the topic shows that the first study proposed in this field is by Son et al. [11], defining a mathematical procedure for upgrading the capacity of serial lines composed of CNC machines. Deif and ElMaraghy [12] face the problem of how to supply the exact capacity in response to market changes defining a capacity scalability dynamic model based on a control approach to indicate the best design for the scalability controller. Wang and Koren [13] propose a methodology for scalability planning considering, as objective function, the minimisation of the number of machines needed to meet the new market demand. Gumasta et al. [14] introduce a mathematical formulation of the scalability measure considering scalability as the ability to maintain cost effectiveness when workload grows. Furthermore, the scalability metric is included in the development of a general reconfigurability index [14, 15]. Wang et al. [15] propose quantitative models for RMS scalability introducing the concept of gradient adjustment, which indicates that the amount of RMS scaling is not random and, instead, production capacity should be adjusted according to an adjustment gradient based on the actual condition of the RMS. Moreover, the RMS is able to generate many configurations during the entire life cycle by reconfiguring the system, with each configuration having a certain production capacity. Koren et al. [9] introduce a mathematical model, which maximise the system throughput after reconfiguration and present an industrial case study to validate the method. Such study offers a set of guidelines for system design for scalability to guide industrial companies and designers of modern manufacturing systems. Cerques et al. [10] define new metrics to assess the scalability of RMSs by considering all configurations that can be obtained. Such metrics focus on two relevant aspects of the systems, i.e. the takt time and the number of resources of the system, and show how it is possible to adapt multi-objective metrics to this context, considering the two characteristics as multi-objective criteria. The literature review on the topic shows that the existing methods and models proposed for scalability focus just on the discrete manufacturing industry. This paper enlarges the perspective proposing metrics to assess the scalability in both discrete manufacturing and process manufacturing industries, which produce different types of goods. According to this background, the remainder of the paper is organised as follows. Next, Sect. 2 introduces the new metrics to model scalability in discrete and process manufacturing industries, while in Sect. 3, a numerical case study applies the proposed metrics. Finally, Sect. 4 concludes the paper with final remarks and future research opportunities.

## 2 Scalability of Manufacturing Systems

The scalability refers to the capability of a manufacturing system to adjust easily the system production capacity by adding/removing manufacturing machines, i.e. reconfigurable machine tools (RMT), in response to a change of the market demand. According to this definition, the scalability function at the production volume  $q$  can be modelled as in Eq. (1).

$$s(q) = \frac{\partial C(q)}{\partial q} \quad (1)$$

$s(q)$  in Eq. (1) describes the relation between the variation of the production capacity  $C$  as function of the market demand  $q$ . In particular, with the increase of the market demand, it is required to equip the manufacturing system with new machines, e.g. RMTs, to provide a greater production capacity. In this paper, the scalability analysis is performed for discrete manufacturing and process manufacturing industries, which produce different types of goods. In particular, discrete manufacturing deals with assembling goods and making goods that are exact. The products are typically manufactured in individually defined batches. Thus, in discrete manufacturing, the product is made by sequential steps made in one or more processes. On the other side, process manufacturing uses formulations or recipes producing goods that cannot be disassembled.

### 2.1 Scalability in Discrete Manufacturing Industry

To model scalability in discrete manufacturing industry, a manufacturing system organised into several production lines is considered. Each production line includes the same number of working machines, e.g. RMTs, having the same productivity rate. Next, Fig. 1 shows the step function, in red, modelling the trend of the system production capacity  $C$  as function of the market demand  $q$ , neglecting any production losses.

The manufacturing system is subject to a number of reconfigurations to progressively satisfy the increasing market demand. Moreover, the  $y$ -axis shows the quantities of installed production capacity ( $C_i$ ) at each reconfiguration, while the  $x$ -axis shows the market demand values. In particular,  $Q_i$  represents the market demand values corresponding to the maximum capacity of the manufacturing system at the  $i$ -th reconfiguration. Since the production capacity trend as function of the market demand in the discrete manufacturing industry is modelled as a step function, the scalability function at the production volume  $q$  is equal to 0, for all the values assumed by  $q$  different from the maximum production capacity  $Q_i$ , as in Eq. (2).

$$s(q) = 0, \forall q \neq Q_i \quad (2)$$

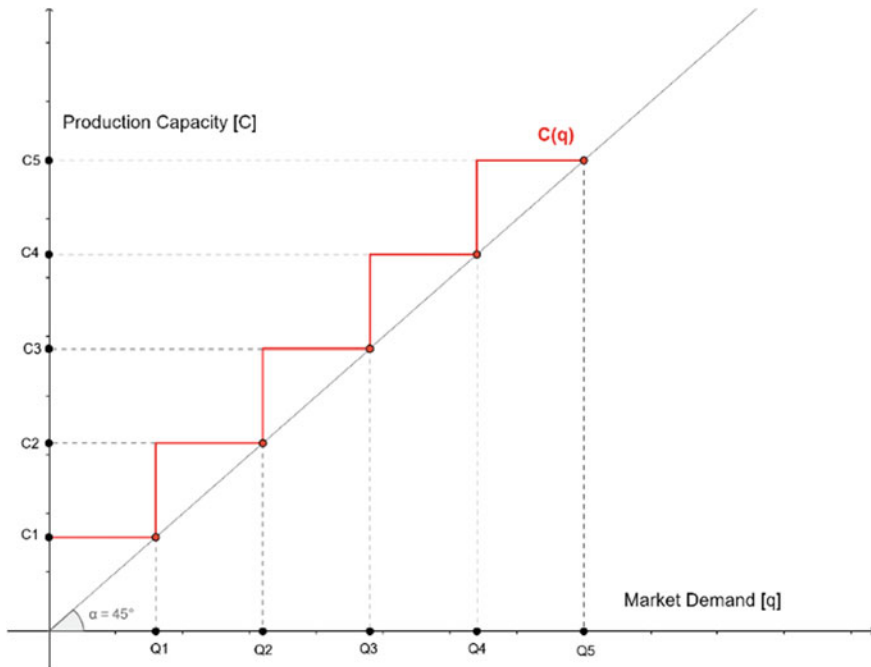


**Fig. 1** Production capacity trend as function of the market demand in the discrete manufacturing industry

This means that when the market demand value is lower than the maximum production system capacity at the *i*-th reconfiguration, the addition of new machines into the manufacturing system is not required. Otherwise, new machines need to be included. The following Eq. (3) represents the variation of the installed production capacity as effect of an increasing market demand:

$$s(q \geq Q_i) = \frac{C_{i+1} - C_i}{1} \tag{3}$$

Therefore,  $s(q)$  in discrete manufacturing can be modelled as a Dirac  $\delta$  function, i.e. a set of impulses that arise when the market demand  $q$  is greater than the maximum system production capacity having a value equal to  $C_{i+1} - C_i$ , as in Fig. 2.

Since scalability is the ability of a manufacturing system to easily modify its production capacity in response to a changing market demand, the maximum scalability value is when  $\Delta C = C_{i+1} - C_i$  is minimised and the number of reconfigurations  $N$  needed to face the market demand is maximised. Furthermore, from the scalability analysis proposed in this study, it appears that when the market demand is less than  $Q_i$ , the installed production capacity not needed to meet the demand value  $q$  is considered as waste capacity. The average wasted capacity (AWC) is modelled as in Eq. (4), by applying the *Integral Mean Value Theorem*:

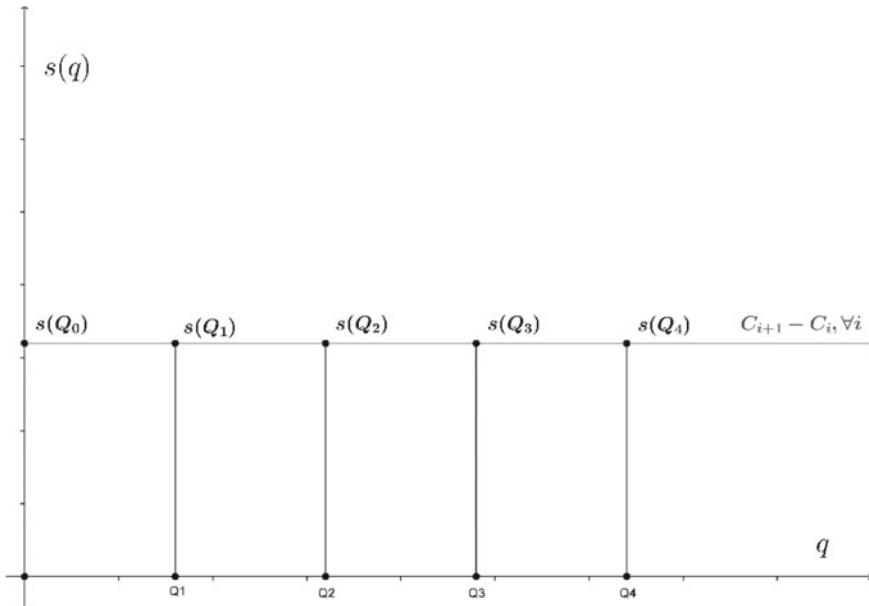


Fig. 2  $s(q)$  graph, Dirac  $\delta$  function

$$AWC = \frac{1}{Q_{max}} \int_0^{Q_{max}} (C(q) - q) dq \tag{4}$$

According to this definition, the scalability value is maximised when the AWC is close to 0.

The analysis performed so far is based on the assumption that no production losses occur during the manufacturing process, i.e. ideal case. To include such relevant issue within the boundaries of this study, a coefficient  $\eta$  representing the overall efficiency of the manufacturing system (in  $[0,1]$ ) is introduced, getting  $C^* = \frac{q}{\eta}$  (blue line in Fig. 3).

The new line, representing the real case, is out of phase with the ideal line, i.e. case of no production losses, by an angle  $\varphi$ . Such angle can be analytically determined as follows:

$$\varphi(\eta) = \arctan\left(\frac{1}{\eta}\right) - \frac{\pi}{4} \tag{5}$$

Considering production losses in the analysis, a greater production capacity is needed to meet the market demand  $Q_i$ , compared to the previous case. Furthermore, the steps of the  $C(q)$  curve (see Fig. 1) will have a smaller area value compared to the previous ideal case. In this case, the AWC is modelled as in Eq. (6):

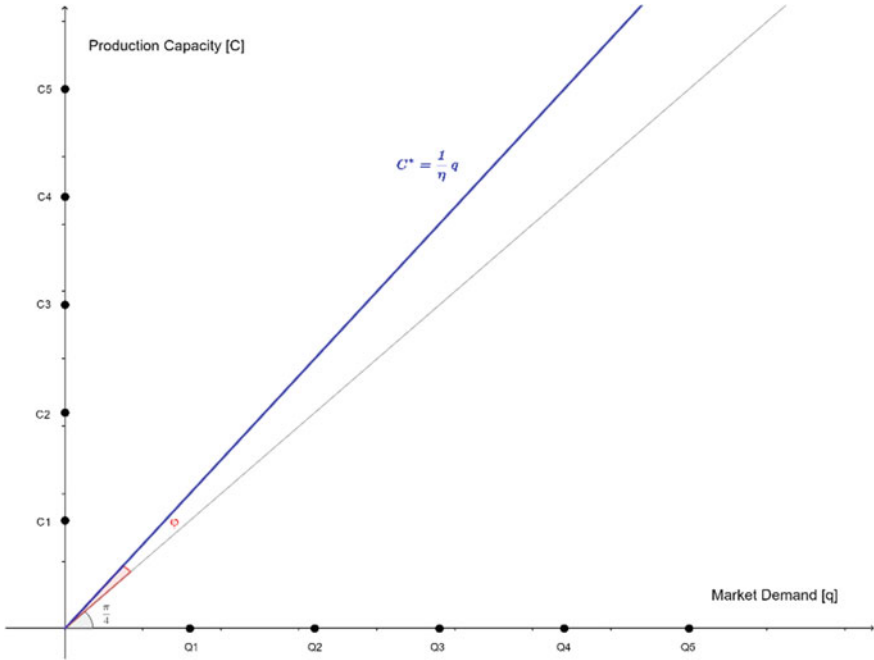


Fig. 3 Relation between production capacity and market demand considering production losses

$$AWC = \frac{1}{Q_{\max}} \int_0^{Q_{\max}} \left( C(q) - \frac{q}{\eta} \right) dq \tag{6}$$

The area of a single step is

$$A = \frac{(\Delta C \cdot \Delta q)}{2} = \frac{\Delta C \cdot C \eta}{2} = \frac{(\Delta C^2 \cdot \eta)}{2} \tag{7}$$

While the number of machines required to meet the market demand from 0 to  $Q_{\max}$  is

$$N_{\text{mac}} = \frac{Q_{\max}}{\Delta q} \tag{8}$$

The formulation of AWC follows

$$AWC = \frac{(\Delta C^2 \cdot \eta)}{2} \cdot \frac{Q_{\max}}{\Delta q} \cdot \frac{1}{Q_{\max}} = \frac{(\Delta C^2 \eta)}{2} \cdot \frac{1}{\Delta C \cdot \eta} = \frac{\Delta C}{2} \tag{9}$$



Equation (9) shows that the scalability does not depend by the efficiency  $\eta$  of the manufacturing system but by its capability to adapt to the market changes in a rapid and cost-effective way.

## 2.2 Scalability in Process Manufacturing Industry

In process manufacturing industry, the production capacity curve as function of the market demand can be modelled as

$$C(q) = \alpha q^\beta \tag{10}$$

where  $\alpha$  and  $\beta$ , i.e., respectively, the coefficient and the exponent, represent the key mathematical parameters to model the production capacity curve, with  $\alpha \eta q^\beta - q \geq 0 \forall q \in [0, Q_{\max}]$ ,  $\alpha \geq 0$ ,  $\beta \geq 0$ , while the scalability function is

$$s(q) = \alpha \beta q^{\beta-1} \tag{11}$$

In the case of process manufacturing industry, Eqs. (4) and (6) remain the same, while Eq. (9) is as in the following:

$$AWC = \frac{\alpha}{\beta+1} Q_{\max}^\beta - \frac{Q_{\max}}{2} \tag{12}$$

## 3 Numerical Application

### 3.1 Case Study of Discrete Manufacturing Industry

For the case of discrete manufacturing industry, in this study, a manufacturing system characterised by one production line is considered. The main data and parameters are summarised in the following Table 1:

**Table 1** Numerical data for the discrete manufacturing case study

Parameters	Data
$\Delta C$	320 pcs/day
$Q_{\max}$	3520 pcs/day
$\eta$	0.9
$\varphi(\eta)$	3.01°

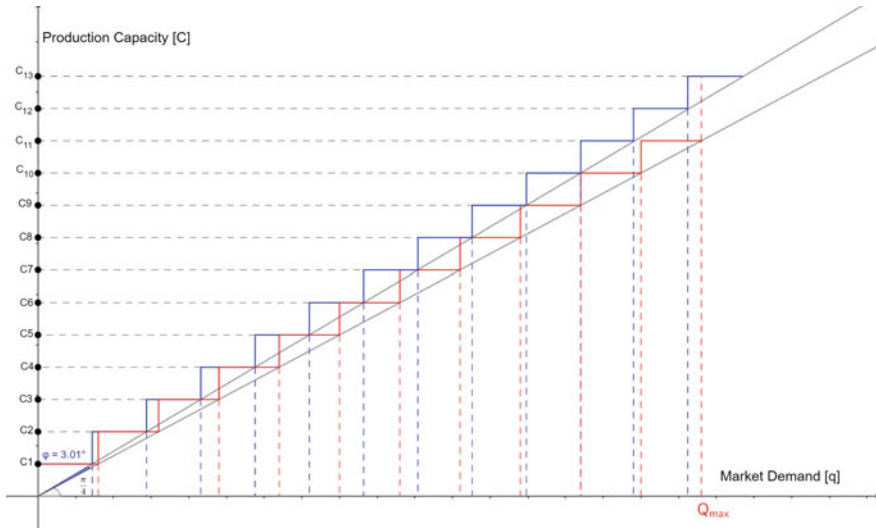


**Fig. 4** Trend of the production capacity as function of the market demand in the ideal and real case

**Table 2** Results for the discrete manufacturing case study

	$\Delta q = \Delta C * \eta$ [pcs/day]	Number of production lines	A (pcs)	AWC (pcs/day)
Ideal case	320	11	51,200	160
Real case	288	13	46,080	160

Next, Fig. 4 shows the trend of the system production capacity as function of the market demand in the ideal case ( $\eta = 1$ , blue curve) and in the real case ( $\eta = 0.9$ , red curve). Main results are in Table 2.

Results show that the AWC has the same value for both the ideal and real case. Furthermore, to produce the same maximum production value, a greater number of production lines is needed in the real case.

### 3.2 Case Study of Process Manufacturing Industry

For the case study of process manufacturing industry, in this analysis,  $\eta = 0.9$  and  $\beta = 1$  are considered, getting  $\alpha \sim 1.5$ . The production capacity curve  $C(q)$  is in the next Fig. 5.

The scalability function is

$$s(q) = \alpha = 1.5$$

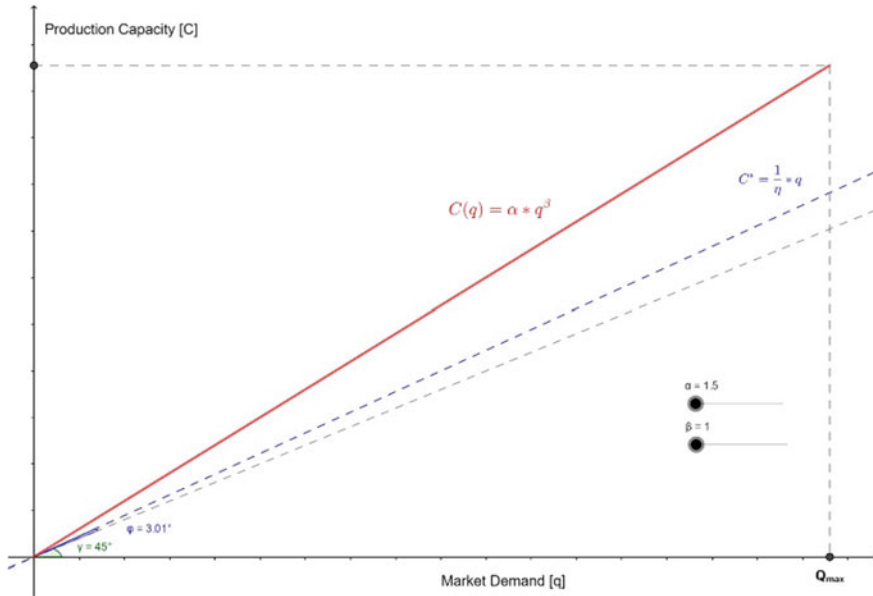


**Fig. 5** Trend of the production capacity as function of the market demand in the process manufacturing industry

Conversely to the case of discrete manufacturing industry, the scalability function is not a Dirac  $\delta$  function, i.e. set of impulses, but a step corresponding to a value on the y-axis, i.e.  $s(q)$  axis, equal to  $\alpha$ , as in Fig. 6.

Finally, the AWC is as in the following, by applying (12):

$$AWC = 684 \frac{\text{units of account}}{\text{day}}$$

If no production losses occur ( $\eta = 1$ ),  $AWC = 880 \frac{\text{units of account}}{\text{day}}$ .

## 4 Conclusions

Scalability is a crucial characteristic of modern reconfigurable manufacturing systems (RMSs), representing the ability to adapt the production capacity to the changing demand in a quick, efficient and cost-effective way. However, such feature has not received a lot of attention in current literature. This paper provides metrics to assess the scalability of machines in discrete manufacturing and process manufacturing industries, which produce different types of goods. The proposed metrics are applied to a numerical case study from the discrete and process manufacturing industries to highlight the different trend of the scalability attribute.

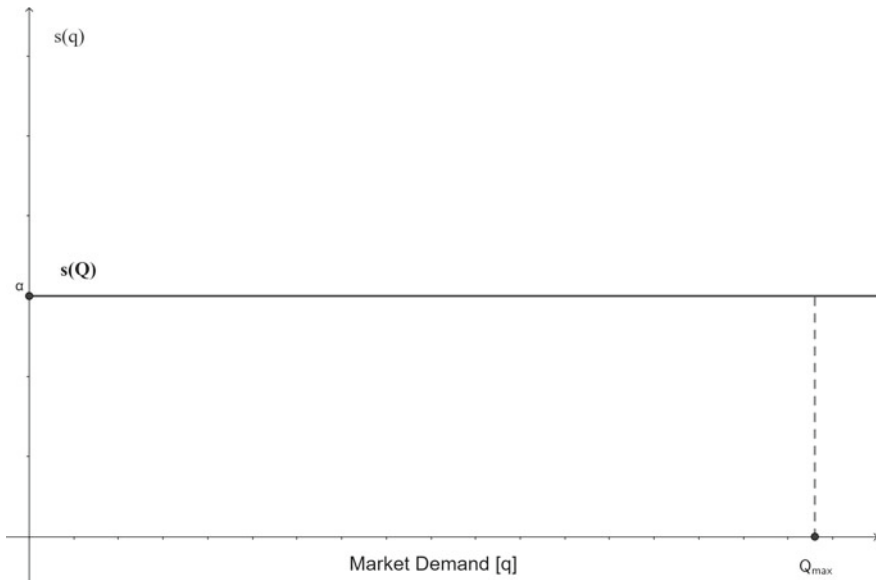


**Fig. 6**  $s(q)$  graph in the process manufacturing industry

Future research includes the application of the proposed metrics to larger instances and the modelling of the remaining key characteristics of RMSs, i.e. modularity, convertibility, integrability, diagnosibility and customisation.

## References

1. Bortolini, M., Galizia, F.G., Mora, C.: Reconfigurable manufacturing systems: literature review and research trend. *J. Manuf. Syst.* **49**, 93–106 (2018)
2. Mehrabi, M.G., Ulsoy, A.G., Koren, Y.: Reconfigurable manufacturing systems: key to future manufacturing. *J. Intell. Manuf.* **11**(4), 403–419 (2000)
3. Molina, A., Rodriguez, C.A., Ahuett, H., Cortes, J.A., Ramirez, M., Jimenez, G., Martinez, S.: Next-generation manufacturing systems: key research issues in developing and integrating reconfigurable and intelligent machines. *Int. J. Comput. Int. Manuf.* **18**(7), 525–536 (2005)
4. Koren, Y., Heisel, U., Jovane, F., Moriwaki, T., Pritschow, G., Ulsoy, G., Van Brussel, H.: Reconfigurable manufacturing systems. *CIRP Ann. Manuf. Technol.* **48**(2), 527–540 (1999)
5. Setchi, R.M., Lagos, N.: Reconfigurability and reconfigurable manufacturing systems: state-of-the-art review. *IEEE Int. Conf. Ind. Inf.* 529–535 (2004)
6. Bi, Z.M., Lang, S.Y., Shen, W., Wang, L.: Reconfigurable manufacturing systems: the state of the art. *Int. J. Prod. Res.* **46**(4), 967–992 (2008)
7. Koren, Y., Shpitalni, M.: Design of reconfigurable manufacturing systems. *J. Manuf. Syst.* **29**(4), 130–141 (2010)
8. Bortolini, M., Galizia, F.G., Mora, C., Pilati, F.: Reconfigurability in cellular manufacturing systems: a design model and multi-scenario analysis. *Int. J. Adv. Manuf. Technol.* **104**(9–12), 4387–4397 (2019)

9. Koren, Y., Wang, W., Gu, X.: Value creation through design for scalability of reconfigurable manufacturing systems. *Int. J. Prod. Res.* **55**(5), 1227–1242 (2017)
10. Cerqueus, A., Delorme, X., Dolgui, A.: Analysis of the scalability for different configurations of lines. In: *Reconfigurable Manufacturing Systems: From Design to Implementation*, pp. 139–160. Springer, Cham (2020)
11. Son, S.Y., Lennon Olsen, T., Yip-Hoi, D.: An approach to scalability and line balancing for reconfigurable manufacturing systems. *Int. Manuf. Syst.* **12**(7), 500–511 (2001)
12. Deif, A.M., ElMaraghy, W.H.: A control approach to explore the dynamics of capacity scalability in reconfigurable manufacturing systems. *J. Manuf. Syst.* **25**(1), 12–24 (2006)
13. Wang, W., Koren, Y.: Scalability planning for reconfigurable manufacturing systems. *J. Manuf. Syst.* **31**(2), 83–91 (2012)
14. Gumasta, K., Kumar Gupta, S., Benyoucef, L., Tiwari, M.K.: Developing a reconfigurability index using multi-attribute utility theory. *Int. J. Prod. Res.* **49**(6), 1669–1683 (2011)
15. Wang, G.X., Huang, S.H., Yan, Y., Du, J.J.: Reconfiguration schemes evaluation based on preference ranking of key characteristics of reconfigurable manufacturing systems. *Int. J. Adv. Manuf. Technol.* **89**(5–8), 2231–2249 (2016)

# An Investigation of the Porosity Effects on the Mechanical Properties and the Failure Modes of Ti–6Al–4V Schwarz Primitive Structures



Shuai Ma, Qian Tang, Qixiang Feng, Jun Song, Ying Liu, and Rossitza Setchi

**Abstract** Porous structures fabricated using additive manufacturing demonstrate significant advantages due to their mechanical properties and light weight. However, their manufacture using selective laser melting still requires considerable research. This study investigated the mechanical properties and the failure modes of Ti–6Al–4V-built Schwarz primitive structures. Samples with five different porosities, ranging from 60 to 85%, were designed and fabricated; all samples had a length of 20 mm and consisted of 2.5-mm porous units. Compression tests were conducted to study their mechanical properties. The results show that their elastic modulus ranged from  $1239.63 \pm 23.69$  to  $3453.20 \pm 105.95$  MPa, and their ultimate strength ranged between  $44.82 \pm 0.22$  and  $266.31 \pm 0.73$  MPa. A camera used to record the failure processes revealed that Ti–6Al–4V Schwarz primitive structures exhibit brittle behaviour. Two failure modes were observed; diagonal shear was found in the 60–80% porosity samples, while unit brittle fracturing was observed in the 85% samples. This study contributes new knowledge about the design of Schwarz primitive structures and provides guidelines for choosing the appropriate porosity to meet different application requirements.

## 1 Introduction

Ti–6Al–4V is widely used in tissue engineering and in the automobile and aerospace industries due to its good mechanical properties, biocompatibility, anti-corrosion properties and light weight [1, 2]. It has a density of  $4.43 \text{ g/cm}^3$ , its ultimate strength is 900 MPa, and its Young's modulus is 113 GPa [3]. However, traditional processing methods limit its applications because they cannot fabricate complex structures,

---

S. Ma · Q. Tang (✉) · Q. Feng · J. Song  
State Key Laboratory of Mechanical Transmissions, Chongqing University, Chongqing 400044, China  
e-mail: [tqqu@cqu.edu.cn](mailto:tqqu@cqu.edu.cn)

Y. Liu · R. Setchi  
Cardiff School of Engineering, Cardiff University, Cardiff CF243AA, UK

such as lattice structures. Although topology optimization can design optimal structures according to requirements, lattice structures play an important role in various processes, such as cell growth, cooling and energy absorption, which the optimal structures cannot satisfy.

Additive manufacturing is a promising method of processing complex lattice structures. For example, selective laser melting (SLM) is suitable for processing metallic powders, such as 316L, Ti-6Al-4V and 18Ni300 [4-7].

Array lattice structures are widely used because they can be designed using the control function; their shape and properties can be adjusted by choosing different core parameters. Generally, lattice structures can be divided into strut and surface structures. Strut structures, such as body-centred cubic (BCC) systems, can easily reach high porosity and light weight. However, successful processing is usually limited by the strut's limited angle. Surface structures, such as triply periodic minimal surfaces (TPMS), are designed by the complex control functions. Their advantages are that they are self-supporting, lightweight, have low stress concentrations and large surface areas. Due to these properties, TPMS structures have promising application prospects.

Ti-6Al-4V lattice structures generally exhibit brittle behaviour. Their failure modes and mechanical properties such as the elastic modulus and yield strength can be affected by their shape, unit size and porosity. Therefore, these parameters should be taken into consideration when designing products.

In Schwarz primitive (Schwarz-P or SP) structures, a type of TPMS structure, the effect of porosity on failure modes has hardly been studied. This study addresses this research gap by investigating the mechanical properties of SP structures with five different porosities and observing their failure modes. In this experiment, the porosities varied from 60 to 85%, and the SP structures consisted of 2.5-mm long units. Compression tests were conducted to study the structures' mechanical behaviour and failure characteristics.

This paper is organized as follows. Section 2 reviews the literature on lattice structures. Section 3 presents the design and experimental methods of this study. Section 4 reports the results of the compression tests. Section 5 presents the conclusions.

## 2 Related Work

Selective laser melting allows for designing and fabricating complex lattice structures using metallic materials. Lattice structures have been researched extensively. Du Plessis et al. built four strut and four TPMS structures and compared their various properties. Their results revealed that TPMS structures are more advantageous for tissue engineering [8]. Their smooth and curved surfaces allow graded design [6]. Scholars have also researched the graded design of Schwarz primitive structures in order to change their failure mode. Shixiang et al. designed uniform and graded gyroid and Schwarz-P structures. Their compression tests showed that the graded SP structure can prevent shear slippage [9]. Zeyao et al. combined Schwarz primitive

with three other structures to create a new design and found that the new design method was better than the individual structure [10].

The porosity, pore and unit size and other design parameters can affect the structure's mechanical behaviour [11, 12]. Maskery et al. studied the effects of unit size on failure modes and energy absorption by designing five gyroid structures of different unit sizes with a 22% volume fraction. Their results revealed that the samples with larger cell sizes exhibited localized fracture, while the smaller cell sizes led to diagonal shear failure [13]. Maszybrocka et al. designed Schwarz's diamond structures of 60 and 80% porosities consisting of 1.25, 2.5 and 3.75 mm long units. Their compression results revealed that there was no difference in the failure mode of any specimen; however, this may have been because they compared samples of only two porosities [14].

Despite the aforementioned research, the effects of porosity on the failure modes have rarely been reported in detail. In cases where there are specific unit size requirements, such as in scaffold designing [15], it is important to investigate and choose the appropriate porosity to ensure that it does not affect the failure mode.

### 3 Design and Experimental Methods

This section presents the design and manufacturing method of SP structures and the experimental methods for compression. Samples with five different porosities were designed and fabricated using SLM. The lattice structures were then tested by compression experiments. A camera was used to record the destruction processes.

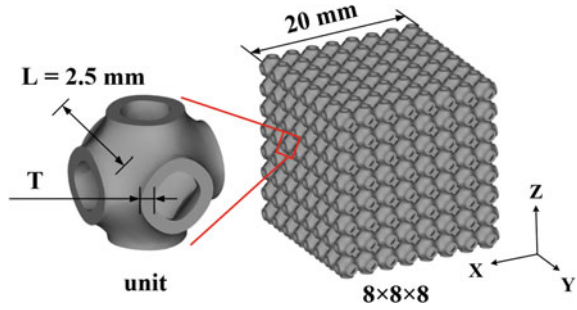
#### 3.1 Design of Schwarz Primitive Structures

Lattice structures are lightweight, and their mechanical properties can be adjusted to suitable levels according to requirements. With the development of additive manufacturing, selective laser melting allows for the design and fabrication of lattice structures relatively accurately. Schwarz-P structures are TPMS structures that have smooth and curved surfaces. The Schwarz structures were built using the following function:

Where  $t$  controls the shape of the structure. For our Schwarz-P structures,  $t$  is equal to 0. In Fig. 1,  $L$  is the unit's length and  $T$  is its thickness. The Schwarz-P unit was built with the Creo software and exported to a.stl file. The unit was arrayed with the Magics software to obtain a computer-aided design (CAD) model file. To investigate the effects of porosity to the failure modes, the unit length in this study was kept at 2.5 mm, the unit number of the CAD model was  $8 \times 8 \times 8$ , and the length was 20 mm. The five porosities, 60%, 70%, 75%, 80% and 85%, were achieved by setting the thickness  $T$  at 0.44, 0.32, 0.27, 0.22 and 0.16 mm, respectively.



**Fig. 1** Schwarz-P structure unit and the CAD model of compression



### 3.2 Manufacturing and Compression Test of Schwarz-P Structures

The.stl CAD model files were inputted to the SLM 500 machine (Solutions, Germany). The samples were fabricated using Ti-6Al-4V powder (Ti Bal., Al ~ 5.50–6.75%, V ~ 3.50–4.50%, C max. 0.08%, et al., TLS Technik Ltd.). The process parameters are shown in Table 1. Three specimens of each structure were fabricated for the compression tests. The building direction was the z-axis.

The samples were cut off from the platform by wire electrode cutting. An ultrasonic cleaner was used to remove the residual powder inside the samples. None of the parts was post-processed. The samples were named SP60, SP70, SP75, SP80 and SP85 according to their respective porosities (Fig. 2).

To examine the mechanical properties and observe the destruction processes of compression, the universal testing machines (MTS 100 KN and Avery Denison

**Table 1** Process parameters of the SLM machine

Power	Scan speed	Scan interval	Layer thickness	Spot diameter
240 W	1100 mm/s	0.12 mm	0.03 mm	0.075 mm

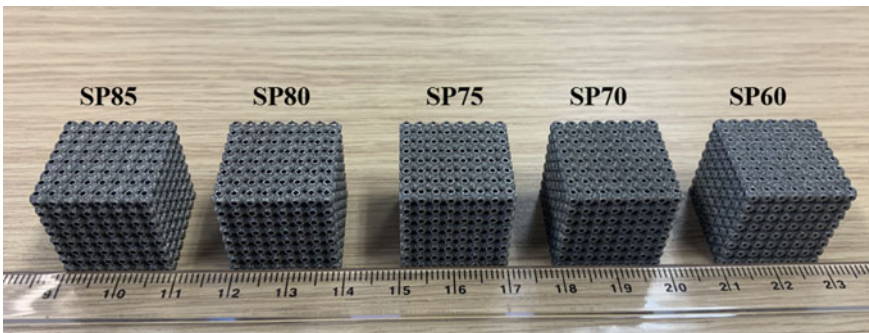


**Fig. 2** Ti-6Al-4V Schwarz-P structures manufactured by SLM

600 kN) were used to test each sample. The upper crosshead was loaded on the  $z$ -axis with a speed of 2 mm/min. The samples were not restricted on the  $x$ - and  $y$ -axes. The force and displacement were recorded by a computer to calculate the strain and stress.  $E$ ,  $\sigma_{UTS}$  and  $\epsilon_{UTS}$  represent the elastic modulus, the ultimate strength (UTS) and the strain of  $\sigma_{UTS}$ , respectively. The camera (iPhone XR, Apple Ltd.) recorded the destruction process of each sample at 60 frames per second (FPS). It was loaded to the samples with about 0.45 strain unless the part was shattered.

## 4 Results and Discussion

This section reports the mechanical properties of the Schwarz-P structures and describes the failure modes found by analysing the failure processes of the compression tests.

### 4.1 Mechanical Properties of the Schwarz-P Structures

The force–displacement curves were obtained from the compression tests in order to create the stress–strain diagrams. In Fig. 3, curve AB represents the elastic stage. The blue dashed line is the linear fitting of the AB curve; its slope represents the structure’s elastic modulus. Spot B represents the structure’s peak stress, represented by  $\sigma_{UTS}$ . The strain of  $\sigma_{UTS}$  is  $\epsilon_{UTS}$ .

The properties of each structure specimen were calculated as mean  $\pm$  standard deviation. The results are shown in Table 2. Specimen SP60 exhibited the highest  $E$  and  $\sigma_{UTS}$  values. As can be seen in the table, lower porosity was correlated with

**Fig. 3** Schematic of the elastic modulus  $E$ , the ultimate strength  $\sigma_{UTS}$  and the strain of ultimate strength  $\epsilon_{UTS}$

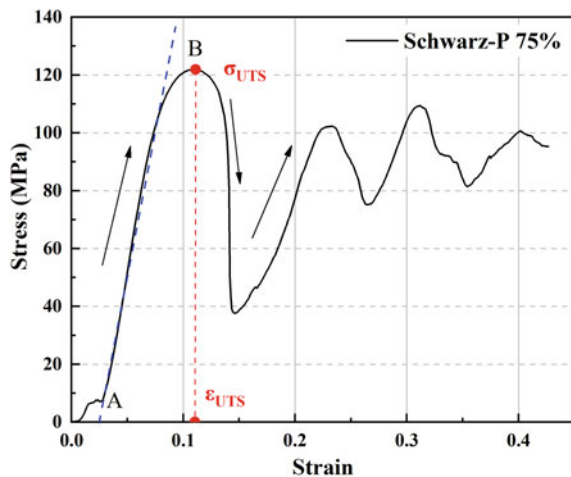


**Table 2** Mechanical properties and strain of the ultimate strength of the Schwarz-P structures

Sample	E (MPa)	$\sigma_{UTS}$ (MPa)	$\epsilon_{UTS}$
SP60	3453.20 $\pm$ 105.95	266.31 $\pm$ 0.73	0.1346 $\pm$ 0.0106
SP70	2398.60 $\pm$ 77.29	163.49 $\pm$ 0.46	0.1130 $\pm$ 0.0017
SP75	1984.10 $\pm$ 22.82	121.70 $\pm$ 0.44	0.10.70 $\pm$ 0.0021
SP80	1567.23 $\pm$ 27.25	81.87 $\pm$ 0.38	0.0849 $\pm$ 0.0037
SP85	12.39.63 $\pm$ 23.69	44.82 $\pm$ 0.22	0.732 $\pm$ 0.0053

higher  $E$  and  $\sigma_{UTS}$  values. The standard deviations show that the stability of the mechanical properties is good. It is interesting to note that the  $\epsilon_{UTS}$  also higher with the lower porosities, which means that low-porosity structures can withstand greater deformation before the stress peak spot.

## 4.2 Failure Modes of the Schwarz-P Structures

The distortion processes of each specimen were recorded and used to analyse the failure characteristics combined with the stress–strain curves. Two main failure modes were observed: diagonal shear and unit brittle fracturing.

Diagonal shear was observed in SP60, SP70, SP75 and SP80. Figure 4 shows this kind of failure process in SP70. Figure 4a shows the failure process of Specimen 1 (S1) of SP70. Figure 4b) shows the deformation images of Specimen 2 (S2) of SP70 at each main point. The main points are shown in Fig. 4c. The failure mode of S1 is similar to that of S2 but is shown in another side view, where the 45° diagonal shear band is visible. The stress–strain curve rose and fell several times. Combined with the failure process shown in Fig. 4b, it can be observed that the stress reached the peak value  $\sigma_{UTS}$  at the end of the elastic stage (0.113 strain). Then, the bottom layer collapsed, and the stress–strain curve declined. Next, the upper layer was compressed and densified, and the curve rose; the structure's strength recovered by a maximum of 0.95  $\sigma_{UTS}$ . In the other side view of the failure process, a diagonal shear band appeared in S2, as shown in Fig. 4b, at an angle of 45° to the compression direction. It is interesting that at the 0.131 strain, the crack appeared in the middle of the unit (on the diagonal shear band) along the compression direction. Moreover, at the 0.225 strain of S1, the bottom layer collapsed because the structure slipped along the diagonal shear band. The other side of this can be observed in the failure process of S2 at the 0.228 strain.

Unit brittle fracturing was only observed in SP85, the weakest and highest-porosity structure. The failure process is shown in Fig. 5. The image of 0.35  $\sigma_{UTS}$  shows the first collapse of the structure, which then recovered to 0.48  $\sigma_{UTS}$ . Analysis of the specimen's image at Spot A, where the initial cracks occurred, revealed that the structure first cracked at the junction of each unit and along the compression direction.

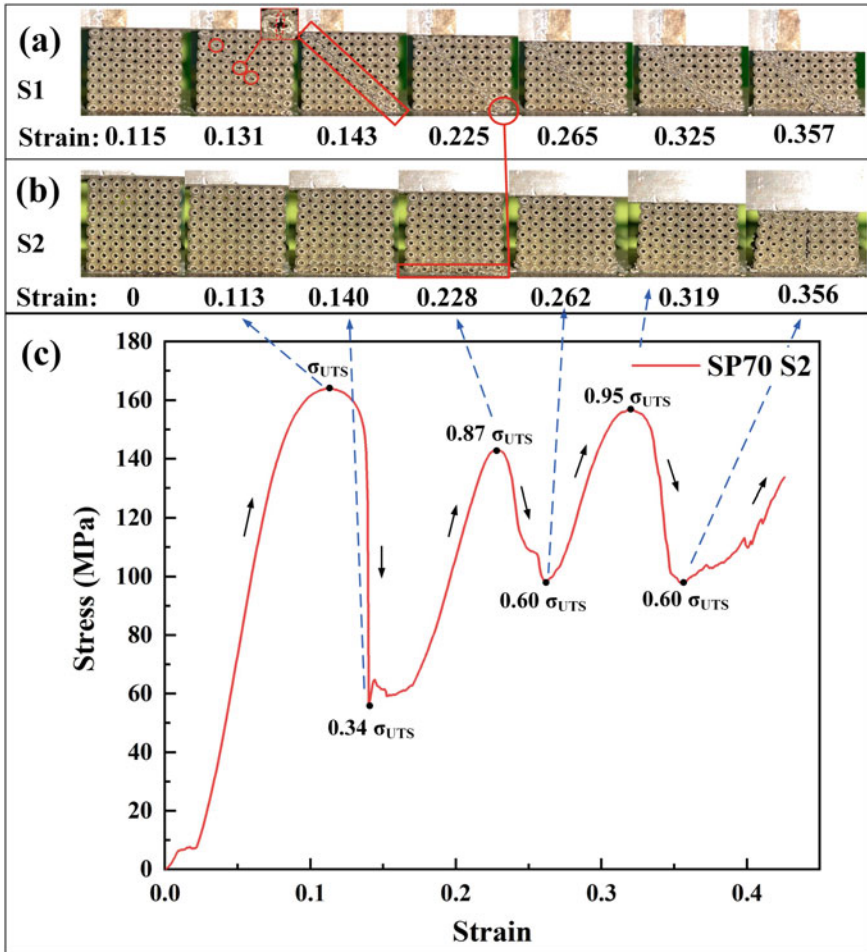


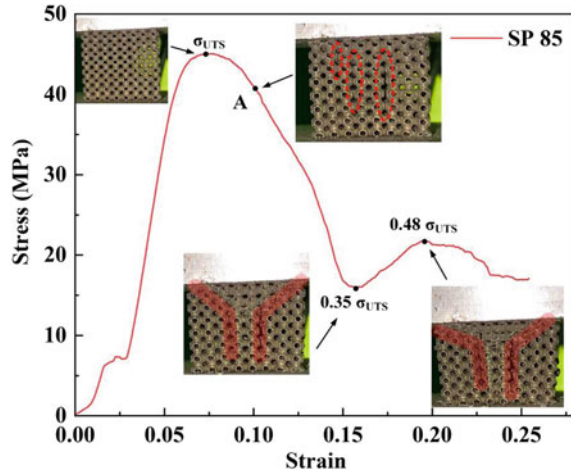
Fig. 4 a b Failure process of Specimens 1 (S1) and 2 (S2) of SP70, c stress–strain diagram of S2

Then the cracks expanded, causing the entire structure to collapse. Compared with the diagonal shear, this kind of failure mode led to structure failure at a 0.25 strain.

## 5 Conclusion

This study investigated the mechanical properties of SLM-built Ti–6Al–4 Schwarz-P structures with five porosities, ranging from 60 to 85%. The analysis of the failure processes of the specimens demonstrated that the failure mode is affected by porosity. The results can be summarized as follows:

**Fig. 5** Stress–strain diagram and the failure process of SP85



- (1) The mechanical properties of the Schwarz-P structures are high stability and repeatability. The elastic modulus and ultimate strength of the structures ranged from  $1239.63 \pm 23.69$  to  $3453.20 \pm 105.95$  MPa and from  $44.82 \pm 0.22$  to  $266.31 \pm 0.73$  MPa, respectively. The 60% porosity structure had the highest  $\epsilon_{UTS}$ , which means that it can withstand greater elastic deformation.
- (2) Regarding the failure modes related to the different porosities, diagonal shear was found in the 60–80% porosity structures, while unit brittle fracturing was observed in the 85% porosity samples. The strength of the former structures recovered several times before failure. When specific unit sizes are required, a porosity lower than 80% should be chosen to prevent structures failure due to cracks at the junction of each unit.

**Acknowledgements** This paper was supported by the Natural Science Foundation of China (Grant No: 51975073, No. 51805052), Chongqing Science and Technology Bureau (No. cstc2018 jszx-cyzdX0102) and the China Scholarship Council (CSC). The authors wish to thank ASTUTE 2020 (Advanced Sustainable Manufacturing Technologies). This operation, supporting manufacturing companies across Wales, has been part-funded by the European Regional Development Fund through the Welsh Government and the participating Higher Education Institutions. The authors also like to thank workshop in Cardiff University for the compression tests.

## References

1. Brandt, M., Sun, S.J., Leary, M., et al.: High-value SLM aerospace components: from design to manufacture. *Adv. Mater. Res.* **633**, 135–147 (2013)
2. Lim, C.W.J., Le, K.Q., Lu, Q., Wong, C.H.: An overview of 3-D printing in manufacturing, aerospace, and automotive industries. *IEEE Potentials* **35**, 18–22 (2016)

3. Feng, Q., Tang, Q., Soe, S., Liu, Y., Setchi, R.: An investigation into the quasi-static response of Ti6Al4V lattice structures manufactured using selective laser melting. In: Setchi R., Howlett R.J., Liu Y., Theobald P. (eds.) pp. 399–409.: Springer International Publishing, Cham
4. Feng, Q., Tang, Q., Liu, Y., et al.: Quasi-static analysis of mechanical properties of Ti6Al4V lattice structures manufactured using selective laser melting. *Int. J. Adv. Manuf. Technol.* **94**, 2301–2313 (2018)
5. Ma, S., Tang, Q., Feng, Q., et al.: Mechanical behaviours and mass transport properties of bone-mimicking scaffolds consisted of gyroid structures manufactured using selective laser melting. *J. Mech. Behav. Biomed.* **93**, 158–169 (2019)
6. Song, J., Tang, Q., Feng, Q., et al.: Effect of heat treatment on microstructure and mechanical behaviours of 18Ni-300 maraging steel manufactured by selective laser melting. *Opt. Laser Technol.* **120**, 105725 (2019)
7. Ma, C., Gu, D., Dai, D., et al.: Microstructure evolution and high-temperature oxidation behaviour of selective laser melted TiC/TiAl composites. *Surf. Coat. Technol.* **375**, 534–543 (2019)
8. du Plessis, A., Yadroitsava, I., Yadroitsev, I., le Roux, S.G., Blaine, D.C.: Numerical comparison of lattice unit cell designs for medical implants by additive manufacturing. *Virtual Phys. Prototyp.* **13**, 266–281 (2018)
9. Yu, S., Sun, J., Bai, J.: Investigation of functionally graded TPMS structures fabricated by additive manufacturing. *Mater Design* **182**, 108021 (2019)
10. Chen, Z., Xie, Y.M., Wu, X., et al.: On hybrid cellular materials based on triply periodic minimal surfaces with extreme mechanical properties. *Mater Design* **183**, 108109 (2019)
11. Gümruk, R., Mines, R.: Compressive behaviour of stainless steel micro-lattice structures
12. Yan, C., Hao, L., Hussein, A., Young, P., Raymont, D.: Advanced lightweight 316L stainless steel cellular lattice structures fabricated via selective laser melting. *Mater Design* **55**, 533–541 (2014)
13. Maskery, I., Aboulkhair, N.T., Aremu, A.O., Tuck, C.J., Ashcroft, I.A.: Compressive failure modes and energy absorption in additively manufactured double gyroid lattices. *Add. Manuf.* **16**, 24–29 (2017)
14. Maszybrocka, J., Gapiński, B., Dworak, M., Skrabalak, G., Stwora, A.: The manufacturability and compression properties of the Schwarz Diamond type Ti6Al4V cellular lattice fabricated by selective laser melting. *Int. J. Adv. Manuf. Technol.* **105**, 3411–3425 (2019)
15. Van Bael, S., Chai, Y.C., Truscetto, S., et al.: The effect of pore geometry on the in vitro biological behavior of human periosteum-derived cells seeded on selective laser-melted Ti6Al4V bone scaffolds. *Acta Biomater.* **8**, 2824–2834 (2012)

# Including Ergonomic Principles in the Design and Management of Reconfigurable Manufacturing Systems



Marco Bortolini, Lucia Botti, Emilio Ferrari, Francesco Gabriele Galizia, and Cristina Mora

**Abstract** In recent years, the adoption of reconfigurable systems represents a primary strategy to improving flexibility, elasticity and efficiency in both manufacturing and assembly. Despite their automation level, such systems still require actions by human operators, e.g. assembly/disassembly auxiliary custom modules. These operations rise safety and ergonomic issues because of the human–machine interaction and cooperation. This paper follows this stream introducing a mathematical model for the design of reconfigurable manufacturing systems (RMSs) requiring manual workers to perform repetitive tasks. The aim is to support the design of efficient and sustainable RMSs aiming at reducing the overall time required for parts, and auxiliary modules travel among the available machines and the time needed for the assembly and disassembly auxiliary module operations, improving the workers' occupational health and safety. Given the characteristics of the reconfigurable machines, the assembly/disassembly auxiliary modules and the required manufacturing process, the model defines the best assignment of the auxiliary modules to the reconfigurable machines and the part flows. Each solution ensures an acceptable risk level for repetitive movements, as required by regulations on occupational health and safety.

## 1 Introduction and Literature Review

The global competition characterizing the twenty-first century is forcing industrial and manufacturing companies to introduce radical changes to their traditional manufacturing systems, moving towards the next-generation manufacturing systems, i.e. the reconfigurable manufacturing systems (RMSs) [1–3]. RMSs appeared in the

---

M. Bortolini · E. Ferrari · F. G. Galizia (✉) · C. Mora  
Alma Mater Studiorum—University of Bologna, Viale Del Risorgimento 2, 40136 Bologna, Italy  
e-mail: [francesco.galizia3@unibo.it](mailto:francesco.galizia3@unibo.it)

L. Botti  
Interdepartmental Research Center on Security and Safety (CRIS), University of Modena and Reggio Emilia, 41125 Modena, Italy

mid-1990s to gather the advantages of both dedicated serial lines and flexible manufacturing systems, addressing the challenges and the changes introduced in the manufacturing industry by globalization [1]. These changes mainly include the need to increase the introduction of new product variants and the responsiveness to large fluctuations in product demand and production mix.

Manufacturing organizations are contrasting the limitations and features of traditional and flexible manufacturing systems by adopting the RMSs. RMSs are characterized by reconfigurable machine tools with an adjustable and modular structure consisting of auxiliary modules that allow machine scalability and convertibility [4, 5]. Such tools are able to realize a specific range of operations [6]. In a RMS, the manufacturing process for the production of parts and products drives the selection of suitable auxiliary modules to perform the required task. The recent literature shows different approaches supporting RMS designers for the evaluation and the selection of RMS configurations among the sets of available alternatives between module-machine combinations [3]. In 2016, Kouki [7] proposed a multi-criteria decision support approach for the facility layout reconfiguration in RMSs. Such method includes both strategic and operational indicators to evaluate the layout reconfiguration decisions during RMS operation. More recently, Eguia et al. proposed a two-phase approach supporting the design of a cellular RMS with alternative routing and multiple time periods [6]. Bortolini et al. propose an optimization model for the design of cellular RMSs. The model determines the part routing mix and the auxiliary module allocation best-balancing the part flows among the machines and the effort to install the modules on the machines [8]. In the existing studies, the indicators adopted for the choice of the RMSs configurations are mainly related to performances of the technical components of the manufacturing system, assuming safe and healthy working conditions. This assumption requires further investigations; i.e. the presence of unsafe or unhealthy working conditions may lead to high absenteeism, reduced productivity and lower quality of products [9]. Manual operations in manufacturing usually involve physical efforts and significant stress on upper limbs, shoulder and low back. These conditions produce a negative impact on the productivity, causing a critical reduction of the process performances and high costs for the manufacturing companies. Epidemiological studies show that manual material handling (MMH) of loads, awkward postures and high repetitive movements are the cause of several diseases, such as cumulative trauma and work-related musculoskeletal disorders (WMSDs) [10]. Working activities involving frequent manual handling operations and repetitive movements of the upper limb increase the weariness of workers and their fatigue, with the consequence of reducing their satisfaction, their performance and their safety [11]. Moreover, WMSDs lead to an increase in absenteeism so, as a consequence, they are considered the cause of more than 40% of annual lost time [12].

Despite their automation level, RMSs require actions to be performed directly by human operators, e.g. material handling, WIP load/unload, tool set-up, etc., rising relevant safety-, human factor- and ergonomics-related issues [13]. Hence, human factors and ergonomics-related indicators should be investigated, together with performance indicators, when designing a RMS. Recently, Bortolini et al. proposed



a methodological and operative framework, aiming to support the identification of manual activities that will be required in a RMS. The identified manual activities are combined with specific health- and safety-critical areas aiming to improve workers' safety and health, and to prevent the presence of high-risk working conditions.

In this context, this paper introduces a mathematical model supporting the design of RMSs that require manual workers to perform repetitive tasks. The aim is to support the design of efficient and sustainable RMSs in terms of reducing the time required for assembly and disassembly operations, and improving the workers' occupational health and safety. Each solution ensures an acceptable risk level for repetitive movements, as required by the International Standards on occupational health and safety.

## 2 Problem Statement and Analytic Modelling

This section introduces the model for the ergonomic design and management of cellular RMSs. The manufacturing environment consists of multiple reconfigurable machine cells (RMCs) characterized by a set of machines, i.e. reconfigurable machine tools (RMTs). Each RMT has a library of basic and auxiliary modules. The basic modules are structural elements fixed to the RMT, while auxiliary modules are kinematical elements that can be assembled or disassembled when needed to provide different operational capabilities to the machine. Since these operations represent repetitive movements continuously performed by the human operators, the model includes the risk assessment methodology for the evaluation of repetitive movements requiring low loads and high frequency, i.e. OCRA method. Specifically, this method evaluates the exposure of the workers to ergonomic risk factors, comparing the daily number of actions performed by the upper limbs of the workers during repetitive tasks, to the corresponding number of recommended actions that the worker may perform in safety conditions [14, 15]. Next, Fig. 1 shows a schematic of the considered cellular RMS structure, derived from [8].

### 2.1 Problem Description, Assumptions and Notations

The defined cellular RMS design model starts from a fixed RMT-RMC assignment and, by using the information about the operation sequence and the compatibility among auxiliary modules, operations and RMTs, explores how to best-balance the part flows among RMCs and the effort to install the auxiliary modules on the RMT on which the part is located. To reach this goal, the proposed design model minimizes the sum of the inter-cell part travel time, the set-up time to assemble and disassemble the auxiliary modules and the auxiliary module travel time determining the product batch flows, the best allocation of the modules to the RMTs and the module flows among the RMTs.

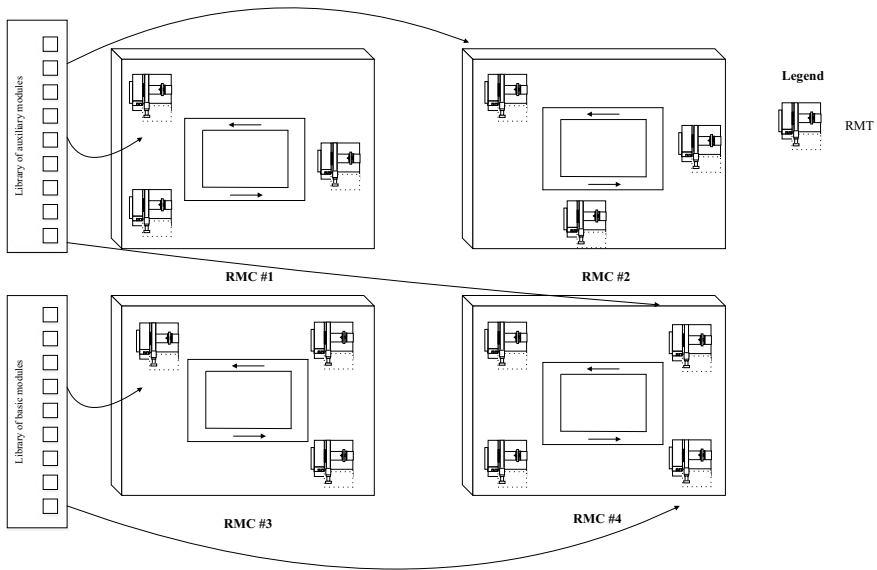


Fig. 1 Schematic of a cellular RMS structure, derived from [8]

The following notations are used.

- Indices

$i$	parts $i = 1, \dots, M$
$o$	operations in part work cycle $o = 1, \dots, O_i$
$m$	RMTs $m = 1, \dots, Z$
$h$	auxiliary modules $h = 1, \dots, H$
$j$	RMCs $j = 1, \dots, N$
$t$	time periods $t = 1, \dots, T$
$k$	modules type $k = 1, \dots, K$

- Parameters (standard and OCRA)

$G_{omk}$	1 if operation $o$ can be performed on RMT $m$ using an auxiliary module of type $k$ ; 0 otherwise [binary]
$r_{it}$	definition of the operation in which the batch of part $i$ is in period $t$
$t_{ijj_1}$	travel time for batch of part $i$ from cell $j$ to cell $j_1$ [min/batch]
$\lambda_{mk}$	assembly time of module type $k$ on RMT $m$ [min/module]
$\mu_{mk}$	disassembly time of module type $k$ from RMT $m$ [min/module]

(continued)

(continued)

$\tau_{om}$	time to perform operation $o$ on RMT $m$ [min/op]
$MAC_{mj}$	1 if RMT $m$ is assigned to RMC $j$ ; 0 otherwise [binary]
$\xi$	available time per RMT [min/machine]
$R$	maximum number of modules per RMT and period [#]
$\delta_i$	planned production volume during a predefined period of time for part $i$ [parts]
$T_{kjj_1}$	travel time for auxiliary module type $k$ from RMC $j$ to RMC $j_1$ [min/module]
$A_{hk}$	1 if auxiliary module $h$ belongs to type $k$ ; 0 otherwise [binary]
$\eta_{TCA,mk}$	number of technical actions for the assembly of module type $k$ on RMT $m$ [#]
$k_f$	constant of frequency of technical actions per minute
$FMA_{mk}$	force multiplier for the assembly of module type $k$ on RMT $m$
$P_{MA,mk}$	posture multiplier for the assembly of module type $k$ on RMT $m$
$Re_{MA,mk}$	repetitiveness period multiplier for the assembly of module type $k$ on RMT $m$
$AMA_{mk}$	additional multiplier for the assembly of module type $k$ on RMT $m$
$RC_M$	recovery period multiplier
$t_M$	duration multiplier
$\eta_{TCD,mk}$	number of technical actions for the disassembly of module type $k$ on RMT $m$ [#]
$FMD_{mk}$	force multiplier for the disassembly of module type $k$ on RMT $m$
$P_{MD,mk}$	posture multiplier for the disassembly of module type $k$ on RMT $m$
$Re_{MD,mk}$	repetitiveness period multiplier for the disassembly of module type $k$ on RMT $m$
$AMD_{mk}$	additional multiplier for the disassembly of module type $k$ on RMT $m$
$\xi_{mk}^{MA}$	$k_f \cdot FMA_{mk} \cdot P_{MA,mk} \cdot Re_{MA,mk} \cdot AMA_{mk} \cdot t_M$
$\xi_{mk}^{MD}$	$k_f \cdot FMD_{mk} \cdot P_{MD,mk} \cdot Re_{MD,mk} \cdot AMD_{mk} \cdot t_M$

- Decisional variables

$F_{ijj_1t}$	1 if batch of part $i$ moves from RMC $j$ to RMC $j_1$ in period $t$ ; 0 otherwise [binary]
$D_{hjj_1t}$	1 if auxiliary module $h$ moves from RMC $j$ to RMC $j_1$ in period $t$ ; 0 otherwise [binary]
$W_{mit}$	1 if batch of part $i$ is processed by RMT $m$ in period $t$ ; 0 otherwise [binary]
$V_{mht}$	1 module $h$ is on RMT $m$ in period $t$ ; 0 otherwise [binary]
$\sigma_{miht}$	1 if RMT $m$ works part $i$ using module $h$ in period $t$ ; 0 otherwise [binary]
$X_{mht}$	1 if module $h$ is assembled on RMT $m$ in period $t$ ; 0 otherwise [binary]
$Y_{mht}$	1 if module $h$ is disassembled from RMC $m$ in period $t$ ; 0 otherwise [binary]

- Objective function

$\min \psi$	Total part and auxiliary module travel time and module assembly/disassembly time [min]
-------------	--

## 2.2 Model Formulation

The analytic formulation of the proposed cellular RMS ergonomic design model is in the following.

$$\begin{aligned} \psi = & \sum_{t=1}^T \sum_{m=1}^Z \sum_{h=1}^H X_{mht} \cdot \left( \sum_{k=1}^K \lambda_{mk} \cdot A_{hk} \right) + \sum_{t=1}^T \sum_{m=1}^Z \sum_{h=1}^H Y_{mht} \cdot \left( \sum_{k=1}^K \mu_{mk} \cdot A_{hk} \right) \\ & + \sum_{i=1}^M \sum_{j=1}^N \sum_{j_1=1}^N \sum_{t=1}^{T-1} F_{ijj_1t} \cdot t_{ijj_1} + \sum_{h=1}^H \sum_{j=1}^N \sum_{j_1=1}^N \sum_{t=1}^{T-1} D_{hjj_1t} \cdot \left( \sum_{k=1}^K T_{kj_1} \cdot A_{hk} \right) \quad (1) \end{aligned}$$

The model is subject to the following feasibility constraints:

$$\begin{aligned} \sum_{m=1}^Z W_{mit} &= 1 \\ \forall t, i \end{aligned} \quad (2)$$

$$\sum_{h:A_{hk}=1} \sigma_{miht} = W_{mit} \cdot \sum_{o:r_{it}=o} G_{omk} \quad \forall i, t, m, k \quad (3)$$

$$\begin{aligned} V_{mht} &\leq \sum_{i=1}^M \sigma_{miht} \\ \forall m, h, t \end{aligned} \quad (4)$$

$$\sigma_{miht} \leq V_{mht} \quad \forall i, m, h, t \quad (5)$$

$$\begin{aligned} \sum_{m=1}^Z V_{mht} &\leq 1 \\ \forall h, t \end{aligned} \quad (6)$$

$$\begin{aligned} W_{mit} &\leq \sum_{k=1}^K \sum_{o:r_{it}=o} G_{omk} \\ \forall m, i, t \end{aligned} \quad (7)$$

$$\begin{aligned} \sum_{h=1}^H V_{mht} &\leq R \\ \forall m, t \end{aligned} \quad (8)$$

$$\sum_{m=1}^Z \sum_{h=1}^H A_{hk} \cdot V_{mht} \leq \sum_{h=1}^H A_{hk} \quad \forall k, t \quad (9)$$

$$V_{mhl} \leq X_{mhl} \quad \forall m, h \quad (10)$$

$$V_{mhT} \leq Y_{mhT} \quad \forall m, h \quad (11)$$

$$X_{mht+1} \geq V_{mht+1} - V_{mht} \quad \forall m, h, t = 1, \dots, T - 1 \quad (12)$$

$$Y_{mht} \geq V_{mht} - V_{mht+1} \quad \forall m, h, t = 1, \dots, T - 1 \quad (13)$$

$$F_{ijj_1t} \leq \sum_{m=1}^Z \sum_{k=1}^K \sum_{o:r_{it}=o} G_{omk} \cdot \text{MAC}_{mj} \quad \forall i, j, j_1, t = 1, \dots, T - 1 \quad (14)$$

$$F_{ijj_1t} \leq \sum_{m=1}^Z \sum_{k=1}^K \sum_{o:r_{it+1}=o} G_{omk} \cdot \text{MAC}_{mj_1} \quad \forall i, j, j_1, t = 1, \dots, T - 2 \quad (15)$$

$$W_{mit} \leq \sum_{j=1}^N \sum_{j_1=1}^N F_{ijj_1t} \cdot \text{MAC}_{mj} \quad \forall i, m, t = 1, \dots, T - 1 \quad (16)$$

$$W_{miT} \leq \sum_{j=1}^N \sum_{j_1=1}^N F_{ijj_1T-1} \cdot \text{MAC}_{mj_1} \quad \forall i, m \quad (17)$$

$$\sum_{j=1}^N \sum_{j_1=1}^N F_{ijj_1t} = 1 \quad \forall i, t = 1, \dots, T - 1 \quad (18)$$

$$\sum_{j_1=1}^N F_{ij_1jt} = \sum_{j_1=1}^N F_{ijj_1t+1}$$

$$\forall i, j, t = 1, \dots, T - 2 \quad (19)$$

$$\sum_{h=1}^H \sum_{k=1}^K (X_{mht} \cdot \lambda_{mk} \cdot A_{hk} + Y_{mht} \cdot \mu_{mk} \cdot A_{hk}) + \sum_{i=1}^M \sum_{o:r_{it}=o} (W_{mit} \cdot \tau_{om} \cdot \delta_i) \leq \xi$$

$$\forall m, t \quad (20)$$

$$V_{mht} \leq \sum_{j=1}^N \sum_{j_1=1}^N D_{hj_1t} \cdot \text{MAC}_{mj}$$

$$\forall h, m, t = 1, \dots, T - 1 \quad (21)$$

$$V_{mht} \leq \sum_{j=1}^N \sum_{j_1=1}^N D_{hj_1T-1} \cdot \text{MAC}_{mj_1}$$

$$\forall h, m \quad (22)$$

$$\sum_{j=1}^N \sum_{j_1=1}^N D_{hj_1t} = 1$$

$$\forall h, t = 1, \dots, T - 1 \quad (23)$$

$$\sum_{j_1=1}^N D_{hj_1t} = \sum_{j_1=1}^N D_{hj_1t+1}$$

$$\forall h, j, t = 1, \dots, T - 2 \quad (24)$$

$$\sum_{m=1}^Z \sum_{k=1}^K (X_{mht} \cdot \lambda_{mk} \cdot A_{hk} + Y_{mht} \cdot \mu_{mk} \cdot A_{hk})$$

$$+ \sum_{j=1}^N \sum_{j_1=1}^N \sum_{k=1}^K D_{hj_1t} \cdot T_{kj_1} \cdot A_{hk}$$

$$+ \sum_{m=1}^Z \sum_{i=1}^M \sum_{o:r_{it}=o} \sigma_{mit} \cdot \delta_i \cdot \tau_{om} \leq \xi \quad \forall h, t \quad (25)$$

$$\begin{aligned}
& \sum_{m=1}^Z \sum_{k=1}^K \sum_{h=1}^H A_{hk} \cdot (X_{mht} \cdot \eta_{TCA,mk} + Y_{mht} \cdot \eta_{TCA,mk}) \\
& \leq 2.2 \cdot \sum_{m=1}^Z \sum_{k=1}^K \sum_{h=1}^H A_{hk} \cdot (X_{mht} \cdot \xi_{mk}^{MA} \cdot \lambda_{mk} + Y_{mht} \cdot \xi_{mk}^{MD} \cdot \mu_{mk}) \\
\forall t
\end{aligned} \tag{26}$$

$$F_{ijjt} \text{ binary } \forall i, j, j_1, t \tag{27}$$

$$D_{hjjt} \text{ binary } \forall h, j, j_1, t \tag{28}$$

$$W_{mit} \text{ binary } \forall i, m, t \tag{29}$$

$$V_{mht}, X_{mht}, Y_{mht} \text{ binary } \forall m, h, t \tag{30}$$

$$m_{iht} \text{ binary } \forall m, i, h, t \tag{31}$$

Equations from (1) to (25) ensure the correct working of the cellular RMS. Equation (26) represents the crucial part of the proposed procedure. Such formulation is derived from the International Standard ISO 11228-3 [16] and restricts the OCRA index value to a threshold limit value for each task [15], i.e. assembly and disassembly auxiliary modules. In this way, an acceptable risk level for repetitive movements is ensured, as required by regulations on occupational health and safety.

### 3 Conclusions and Further Research

In the last years, several studies have been published proposing innovative methods and tools for the design and management of RMSs. However, many open questions remain and several practical challenges represent fertile areas of research. Among these, the impact on safety, ergonomics and human factors coming from the switch to such emerging systems is not yet widely studied. Indeed, despite their high level of automation, RMSs still require the performance of repetitive actions to be performed by human operators as assembly/disassembly auxiliary modules, making necessary the design of industrial settings, which are healthy and safe for human workers. This paper fills this gap defining an optimization model for the ergonomic design of cellular RMS including the OCRA risk assessment, as required by the Italian regulations, restricting its value to a threshold limit value for each task according to the ISO 11228-3. Future developments deal with the application of the proposed model to an industrial case study to better verify and validate the proposed procedure.

## References

1. Koren, Y., Gu, X., Guo, W.: Reconfigurable manufacturing systems: Principles, design, and future trends. *Front. Mech. Eng.* **13**(2), 121–136 (2018)
2. Bi, Z.M., Lang, S.Y.T., Shen, W., Wang, L.: Reconfigurable manufacturing systems: The state of the art. *Int. J. Prod. Res.* **46**(4), 967–992 (2008)
3. Bortolini, M., Galizia, F.G., Mora, C.: Reconfigurable manufacturing systems: literature review and research trend. *J. Manuf. Syst.* **49**, 93–106 (2018)
4. Bortolini, M., Galizia, F.G., Mora, C.: Dynamic design and management of reconfigurable manufacturing systems. *Procedia Manuf.* **33**, 67–74 (2019)
5. Landers, R.G., Min, B.K., Koren, Y.: Reconfigurable machine tools. *CIRP Ann. Manuf. Technol.* **50**(1), 269–274 (2001)
6. Eguia, I., Molina, J.C., Lozano, S., Racero, J.: Cell design and multi-period machine loading in cellular reconfigurable manufacturing systems with alternative routing. *Int. J. Prod. Res.* **55**(10), 2775–2790 (2017)
7. Kouki, S.: A TOPSIS based multi-criteria decision support approach for facility layout reconfiguration. *Int. Res. J. Emerg. Trends Multidiscip.* ISSN (2016)
8. Bortolini, M., Galizia, F.G., Mora, C., Pilati, F.: Reconfigurability in cellular manufacturing systems: a design model and multi-scenario analysis. *Int. J. Adv. Manuf. Technol.* **104**(9–12), 4387–4397
9. Botti, L., Mora, C., Regattieri, A.: Application of a mathematical model for ergonomics in lean manufacturing. *Data in Brief* **14**, 360–365 (2017)
10. Deros, B.M., Daruis, D.D.I., Basir, I.M.: A study on ergonomic awareness among workers performing manual material handling activities. *Procedia Soc. Beh. Sci.* **195**, 1666–1673 (2015)
11. Azizi, N., Zolfaghari, S., Liang, M.: Modeling job rotation in manufacturing systems: the study of employee's boredom and skill variations. *Int. J. Prod. Econ.* **123**(1), 69–85 (2010)
12. Xu, Z., Ko, J., Cochran, D., Jung, M.-C.: Design of assembly lines with the concurrent consideration of productivity and upper extremity musculoskeletal disorders using linear models. *Comput. Ind. Eng.* **62**, 431–441 (2012)
13. Bortolini, M., Botti, L., Galizia, F.G., Mora, C.: Safety, ergonomics and human factors in reconfigurable manufacturing systems. In: Benyoucef, L. (ed.) *Reconfigurable Manufacturing Systems: From Design to Implementation*. Springer International Publishing (2020)
14. Occhipinti, E.: OCRA: a concise index for the assessment of exposure to repetitive movements of the upper limbs. *Ergonomics* **41**, 1290–1311 (1998)
15. Botti, L., Mora, C., Regattieri, A.: Integrating ergonomics and lean manufacturing principles in a hybrid assembly line. *Comput. Ind. Eng.* **111**, 481–491 (2017)
16. International Standard Organization: ISO 11228-3:2007. *Ergonomics. Manual handling. Part 3: Handling of low loads at high frequency* (2007)



# Non-conventional Warehouses: Comparison of the Handling Performances



Marco Bortolini, Francesco Gabriele Galizia, Mauro Gamberi,  
Francesco Gualano, and Ludovica Diletta Naldi

**Abstract** This paper proposes a comparison of the handling performances of three non-conventional warehouses, i.e., Chevron, Diagonal Cross Aisle, and Fishbone, toward the traditional layout. A multi-scenario analysis is provided by using a tool developed in Visual Basic for Application environment. The goal is to compare the most relevant layouts, by using the same set of hypotheses, to assess their technical sustainability and convenience. The inputs are the storage area, the width of the aisles, and the dimension of the unit loads. The travelled distances are computed in the optimal configuration and by adopting a central pickup and delivery point. Key outcomes highlight that Chevron and Fishbone layouts present effective configurations for the majority of the shape factors (savings up to 23%), while the Diagonal Cross Aisle layout presents the highest saving for a depth ratio of 4:1 (26%).

## 1 Introduction and Literature Review

Unit load (UL) warehouses are effective solutions to receive and store products moved using pallets [1]. A warehouse has several purposes, e.g., to supply the dynamic customer demand, to reduce the time-to-market, to stabilize prices, etc. [2]. Because of the most time-consuming activities, not adding value to the products, are the UL Storage and Retrieval (S&R) actions, the design of a warehouse plays a relevant role in getting handling efficiency, technical, and economic sustainability [3]. The reduction of the travelled distances within the warehouse leads to lower costs and to a higher productivity, further reducing the vehicle energy consumption [4]. In addition, the increase of the warehouse dimensions makes the travel distance a key factor to be managed [5].

For these reasons, in the last decades, the literature on the design of UL warehouses increases and researches support the adoption of non-conventional warehouses (NCWs). These emerging layouts have several benefits and advantages

---

M. Bortolini · F. G. Galizia · M. Gamberi · F. Gualano (✉) · L. D. Naldi

Department of Industrial Engineering, Lma Mater Studiorum—University of Bologna, Viale Del Risorgimento 2, 40136 Bologna, Italy  
e-mail: [francesco.gualano2@unibo.it](mailto:francesco.gualano2@unibo.it)

© The Editor(s) (if applicable) and The Author(s), under exclusive license to Springer  
Nature Singapore Pte Ltd. 2021

S. G. Scholz et al. (eds.), *Sustainable Design and Manufacturing 2020*, Smart Innovation,  
Systems and Technologies 200, [https://doi.org/10.1007/978-981-15-8131-1\\_18](https://doi.org/10.1007/978-981-15-8131-1_18)

toward traditional layouts, i.e., they allow shortening the travelled distances meeting economic and sustainable goals.

Generally, a NCW is obtained by relaxing typical constraints of traditional warehouses, e.g., adding oriented cross-aisles or adopting a different rack orientation [6]. In this field, two frequently studied layouts are the Fishbone and the Flying-V, proposed by [1]. These configurations implement a previous idea proposed by [7]. In particular, the Fishbone has a middle diagonal and straight aisle with vertical picking aisles above and horizontal picking aisles below, while Flying-V has parallel picking aisles and orthogonal cross-aisles at the top and bottom of the warehouse. These layouts, under random storage assignment and for single command operations, allow to reduce the expected travelled distances by more than 20% [8]. Additionally, the literature proposes the so-called Diagonal Cross Aisle, as a variation of the aforementioned designs characterized by no changes in the rack positioning, leading to savings ranging from 7 to 17%. Current literature contributions explore these configurations by considering different metrics to enhance the handling performances, e.g., adopting different assignment policies [9–11] and varying the S&R operating mode [9, 12, 13]. Some authors extend the previous analysis on Fishbone by changing some of the boundary conditions [14]. Furthermore, [3] proposes three feasible alternatives to traditional layouts called Chevron, Butterfly, and Leaf. Such layouts have optimized oriented picking aisles presenting distance savings from 10 to 20%. [15–18] evaluate the performances considering multiple pickup and delivery points (P&D).

The existing literature models NCWs allocating the ULs continuously within the available space. In addition, lacks exist in comparing the performances of the existing layouts under comparable design hypotheses and assignment policies. The goal of this paper is to fill these gaps investigating which layout has the best performances, in terms of travelled distances (techno-economic sustainability), considering a common set of assumptions, e.g., position and number of the P&D points, storage area, etc., in order to achieve comparable results.

According to the introduced background and goals, the remainder of this paper is organized as follows. Section 2 states the problem, lists the hypotheses, and outlines the reference layouts. Section 3 shows the analytical functions computing the expected travelling distances. Section 4 applies the approach and discusses the key results, while the last Sect. 5 concludes the paper with final remarks and future research opportunities.

## 2 NCW Layouts and Hypotheses

This section highlights the reference layouts analyzed in this study (Fig. 1) and introduces the variables and the parameters to size each of them.

The Chevron layout [3] in Fig. 1a is a NCW characterized by 45° racks and a central crossing aisle. Figure 1b shows the Diagonal Cross Aisle layout [8] characterized by the inclusion of couple of symmetric diagonal straight aisles crossing the racks. In this

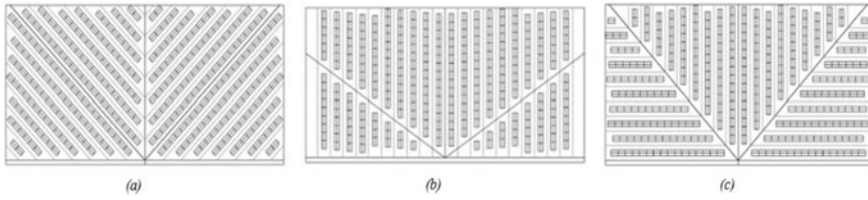


**Fig. 1** NCWs: Chevron (a), Diagonal Cross Aisle (b), Fishbone (c)

layout, the rack orientation is as in traditional layouts. Finally, Fig. 1c illustrates the Fishbone layout [1] presenting two 45° oriented cross-aisles and orthogonal couples of racks at its two sides.

All these layouts share a common set of hypotheses even if each of them is characterized by specific features [1, 3, 8]. The common assumptions are in the following:

1. One central P&D point on the front aisle (origin of axes);
2. The problem is symmetric respect to the P&D point;
3. UL warehouse adopting single command (SC) cycles;
4. The storage assignment policy is random, the items have equal probability of being S&R;
5. Two ISO1 Eur-Epal ULs per bay.

The following parameters and notations are defined:

- $P, Q$  represent the length and the width of the warehouse, respectively [mm];
- $A = P \cdot Q$  is the available storage area [m<sup>2</sup>];
- $\alpha$  is the angle between the diagonal aisles/racks and the  $x$ -axis [°];
- $B$  is the shape factor;
- $M_1, M_2$  are the length and the width of the base module, respectively [mm];
- $K$  is the width of the aisle [mm];
- $p_x, p_y$  are the length and the width of the pallet, respectively [mm];
- $g$  is the lateral gap between the ULs and the rack [mm];
- $\gamma^S, \beta_j^S, \lambda_j^S$  are the number of the aisles, the number of the bays and the length of the aisles, with  $S = \{\text{Chevron} - \text{CH}; \text{Diagonal} - \text{DG}; \text{Fishbone} - \text{FB}\}$  and  $j$  for aisles.

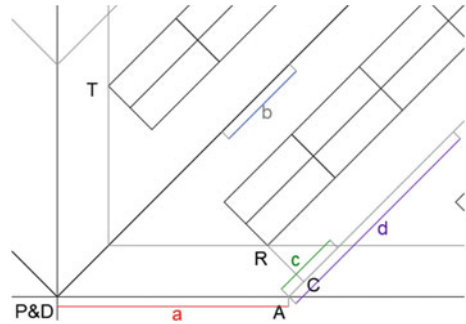
### 2.1 Chevron Design

Figure 2 shows the parameters to univocally refer to the position of each bay within the Chevron NCW.

Analytically, Eq. (1) follows:

$$a = \frac{M_1}{\sin \alpha} \quad b = M_2 \quad c = \frac{M_2}{2} + \overline{AC} \tag{1}$$

**Fig. 2** Parameters of Chevron layout



where:

- $a$  is the distance between the first aisle and the P&D point and the distance between the intersection of the  $x$ -axis (or  $y$ -axis) and the central lines of two consecutive aisles;
- $b$  is the distance between two consecutive access points to the bays within an aisle;
- $c$  is the distance to travel along the central line of the aisle if the bay is on the left side of the aisle (or on the right side if we consider the aisles over the main diagonal aisle);
- $d$  is the distance to travel along the central line of the aisle if the bay is on the right side of the aisle or on the left side if we consider the aisles over the main diagonal aisle.

These parameters are the same for the other layouts in the following.

Given these parameters, it is possible to get the number of the aisles, the spans, and the bays. The number of the aisles is in Eq. (2):

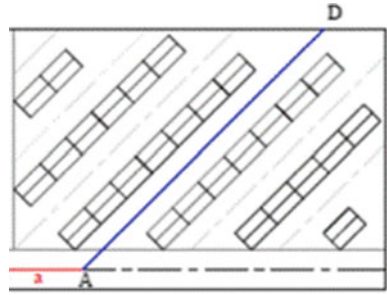
$$\gamma^{\text{CH}} = \text{floor}\left(\frac{P}{2 \cdot a}\right) + \text{floor}\left(\frac{Q - \frac{K}{2}}{a}\right) \quad (2)$$

Due to the specific configuration of the warehouse, the length of each aisle is variable. Consequently, the number of the bays is different for each aisle. In addition, the number of the bays that are on the right side of the aisle is not equal to those on the left side. Considering the aisles under the middle diagonal, two cases occur:

- if the picking aisle ends on the right limit of the warehouse, the length of the aisle is in the following:

$$\lambda_j^{\text{CH}} = \frac{\frac{P}{2} - [(4 \cdot px + 4 \cdot g + K) \cdot \cos \alpha + \frac{K}{2}]}{\cos \alpha} - \frac{a \cdot (j^{\text{CH}} - 1)}{\cos \alpha} \quad (3)$$

**Fig. 3** Detail to get the aisle length



- if the picking aisle ends on the top of the warehouse,  $\lambda_j^{CH}$  is obtained as the distance between points A and D of Fig. 3.

A similar result is reached for the aisles above the main diagonal aisle. Consequently, the number of the bays for each aisle is in Eq. (4):

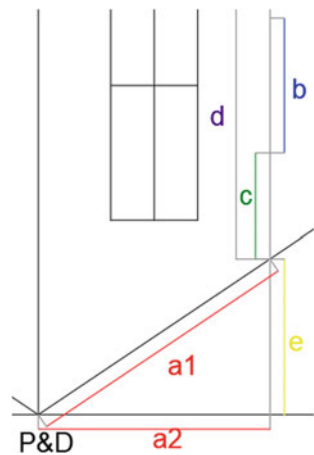
$$\beta_j^{CH} = \text{floor}\left(\frac{\lambda_j^{CH} - c}{b}\right) \tag{4}$$

### 2.2 Diagonal Cross Aisle Design

The Diagonal Cross Aisle NCW is characterized by the parameters in Fig. 4.

The number of the aisles comes from Eq. (5):

**Fig. 4** Parameters of Diagonal Cross Aisle layout



$$\gamma^{\text{DG}} = \text{floor}\left(\frac{\frac{P}{2} - \frac{K}{2}}{a_2}\right) \quad (5)$$

The length of each aisle follows two cases:

- if the aisle is above the diagonal cross aisle (Eq. 6):

$$\lambda_j^{\text{DG}} = \left(Q - \frac{K}{2}\right) - \left(c - \frac{b}{2} + e\right) - (j^{\text{DG}} - 1) \cdot e \quad (6)$$

- if the aisle is under the diagonal cross aisle (Eq. 7):

$$\begin{aligned} \lambda_j^{\text{DG}} = Q - & \left[ \left(Q - \frac{K}{2}\right) - \left(c - \frac{b}{2} + e\right) - (j^{\text{DG}} - 1) \cdot e \right] \\ & - \left(\frac{K}{\cos \alpha}\right) - [2 \cdot (p_x + g) \cdot \tan \alpha] - K \end{aligned} \quad (7)$$

Finally, the number of the bays for each aisle is in Eq. (8):

$$\beta_j^{\text{DG}} = \text{floor}\left(\frac{\lambda_j^{\text{DG}}}{b}\right) \quad (8)$$

### 2.3 Fishbone Design

The parameters that define the Fishbone NCW are in Fig. 5.

Adopting the same approach, the number of the aisles is in Eq. (9):

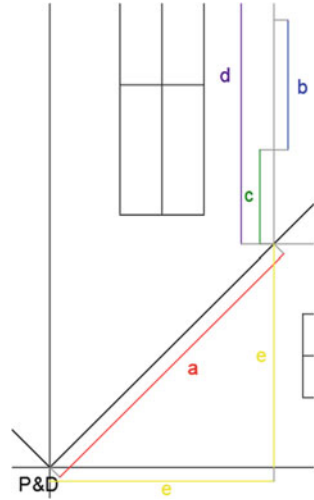
$$\gamma^{\text{FB}} = \text{floor}\left(\frac{Z - \frac{(\frac{K}{2} + g + p_x)}{\cos \alpha}}{a}\right) \quad (9)$$

To compute the length of the aisle,  $\lambda_j^{\text{FB}}$ :

- if the aisle is above the diagonal aisle (Eq. 10):

$$\lambda_j^{\text{FB}} = \left(Q - \frac{K}{2}\right) - \left(c - \frac{b}{2} + e\right) - (j^{\text{FB}} - 1) \cdot e \quad (10)$$

**Fig. 5** Parameters of Fishbone layout



- if the aisle is under the diagonal aisle (Eq. 11):

$$\lambda_j^{FB} = \left(\frac{P}{2}\right) - \left(c - \frac{b}{2} + e\right) - (j^{FB} - 1) \cdot e \tag{11}$$

Finally, the number of the bays comes from Eq. (12):

$$\beta_j^{FB} = \text{floor}\left(\frac{\lambda_j^{FB}}{b}\right) \tag{12}$$

### 3 Single Command Travel Distances

This section outlines the functions getting the single command cycle distances to reach a generic bay within the warehouse.

#### 3.1 Chevron Layout

For this layout, two equations rise depending on the position of the bay within the aisle. Considering the region of the warehouse under the central diagonal aisle,

Eq. (13) is used if the bay is on the left side of the aisle, while Eq. (14) is used if the bay is on the right side of the aisle.

For the region above the main diagonal aisle, Eqs. (13)–(14) are inverted.

$$d_1^{\text{CH}} = 2 \cdot (a \cdot j^{\text{CH}} + b \cdot \beta_j^{\text{CH}} + c) \quad (13)$$

$$d_2^{\text{CH}} = 2 \cdot (a \cdot j^{\text{CH}} + b \cdot \beta_j^{\text{CH}} + d) \quad (14)$$

### 3.2 Diagonal Cross Aisle Layout

The inclusion of the diagonal cross aisle increases the number of possible paths to reach the same location. Eight cases arise, Eqs. (15)–(22):

$$d_1^{\text{DG}} = 2 \cdot (a_1 \cdot j^{\text{DG}} + b \cdot \beta_j^{\text{DG}} + d) \quad (15)$$

$$d_2^{\text{DG}} = 2 \cdot (a_2 \cdot j^{\text{DG}} + e \cdot j^{\text{DG}} + b \cdot \beta_j^{\text{DG}} + d) \quad (16)$$

$$d_3^{\text{DG}} = 2 \cdot (a_1 \cdot j^{\text{DG}} + b \cdot \beta_j^{\text{DG}} + c) \quad (17)$$

$$d_4^{\text{DG}} = 2 \cdot (a_2 \cdot j^{\text{DG}} + e \cdot j^{\text{DG}} + b \cdot \beta_j^{\text{DG}} + c) \quad (18)$$

$$d_5^{\text{DG}} = 2 \cdot (a_1 \cdot j^{\text{DG}} + b \cdot \beta_j^{\text{DG}} + c) \quad (19)$$

$$d_6^{\text{DG}} = 2 \cdot (a_1 \cdot j^{\text{DG}} + b \cdot \beta_j^{\text{DG}} + d) \quad (20)$$

$$d_7^{\text{DG}} = 2 \cdot (a_2 \cdot j^{\text{DG}} + e \cdot j^{\text{DG}} - c - b \cdot \beta_j^{\text{DG}}) \quad (21)$$

$$d_8^{\text{DG}} = 2 \cdot (a_2 \cdot j^{\text{DG}} + e \cdot j^{\text{DG}} - d - b \cdot \beta_j^{\text{DG}}) \quad (22)$$

Equations (15) and (16) are used if the bays are located on the right side of the aisle in the region above the diagonal cross aisle. In detail, Eq. (15) describes the path passing through the diagonal cross aisle, while Eq. (16) describes the path by moving on the front of the warehouse. Equations (17) and (18) are used if the bay is on the left side of the aisle and they refer, respectively, to diagonal path and to orthogonal rectangular path. Equations (19) and (20) refer to the path described by using the diagonal cross aisle to reach the bay located, respectively, on the left side and on the



right side of the aisle. Finally, Eqs. (21) and (22) illustrate the travelled distance by moving on the front of the warehouse to reach the bays located, respectively, on the left side and on the right side of the aisle.

### 3.3 Fishbone Layout

Considering the region above the diagonal aisle, two equations rise (Eqs. 23–24):

$$d_1^{\text{FB}} = 2 \cdot (a \cdot j^{\text{FB}} + b \cdot \beta_j^{\text{FB}} + d) \quad (23)$$

$$d_2^{\text{FB}} = 2 \cdot (a \cdot j^{\text{FB}} + b \cdot \beta_j^{\text{FB}} + c) \quad (24)$$

where Eq. (23) is used for the bays that are on the right side of the aisle, while Eq. (24) is for the bays located on the left side. Finally, considering the horizontal racks under the diagonal cross aisle, Eq. (23) is for the bays on the left side and Eq. (24) is for the bays on the right side.

## 4 Results and Discussion

This section evaluates the travelled distances of the presented layouts by using a customized tool developed in Visual Basic for Application environment. A multi-scenario analysis is presented by changing the shape factor,  $B$ , in the range from 1 to 4 with a step of 0.5 and considering a reference warehouse area of 5500 m<sup>2</sup>. The other adopted parameters come from the standard practice. Particularly:  $M_1 = 4800$  mm,  $M_2 = 2800$  mm,  $g = 100$  mm,  $px = 800$  mm,  $py = 1200$  mm and  $K = 3000$  mm. For the Chevron and Fishbone NCWs,  $\alpha^{\text{CH}} = \alpha^{\text{FB}} = 45^\circ$  while for the Diagonal Cross Aisle NCW, the optimal value of  $\alpha^{\text{DG}}$  for each shape factor comes from the optimization of the layout, according to [8]. The simulation outcomes are presented in Fig. 6.

Figure 6 shows that Chevron and Fishbone layouts are comparable for the most of the shape factors, ranging from 17 to 23%. The Diagonal Cross Aisle layout rises as potential effective solution for high shape factors, characterized by 26% of saving distances.

Globally, the three NCW layouts, in the operative condition of the simulation, allow shortening the travelled distances, confirming their advantages as shown in [8, 11, 12, 14–16]. These results outline the relevance of NCWs in reducing the travelling distances, paving the way toward sustainable inbound logistic systems.

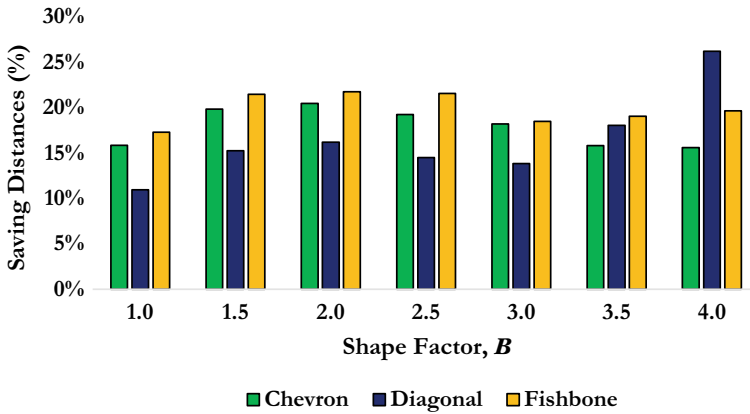


**Fig. 6** Multi-scenario analysis, outcomes

## 5 Conclusions and Further Research

In the last decades, the literature proposes innovative and non-conventional warehouse (NCW) layouts with the aim of speeding up the warehouse activities, making them sustainable from the techno-economic point of view. In this scenario, this paper proposes a comparison of the handling performances, in terms of distance savings, of three main NCW solutions, i.e., Chevron, Diagonal Cross Aisle, and Fishbone, toward the traditional layout with parallel racks and aisles. Results show that Chevron and Fishbone layouts are the most effective configurations for the majority of the shape factors, highlighting the highest savings up to 23% for a warehouse with a shape factor of 2:1, while the Diagonal Cross Aisle layout presents the highest value for a shape factor of 4 (savings of about 26%). Future research includes the comparison of further NCWs under different boundary conditions, e.g., class-based storage assignment strategy, vertical distances, multiple pickup and delivery (P&D) points, etc., considering relevant industrial contexts to spread the adoption of NCWs in industry.

## References

1. Gue, K.R., Meller, R.D.: Aisle configurations for unit-load warehouses. *IIE Trans.* **41**, 171–182 (2009)
2. Pohl, L.M., Meller, R.D., Gue, K.R.: *Turnover-Based Storage In Non-Traditional Unit-Load Warehouse Designs* (2011)
3. Öztürkoğlu, O., Gue, K.R., Meller, R.D.: Optimal unit-load warehouse designs for single-command operations. *IIE Trans.* **44**, 459–475 (2012)
4. Bassan, Y., Roll, Y., Rosenblatt, M.J.: Internal layout design of a warehouse. *AIIE Trans.* **12**(4), 317–322 (1980)

5. Pohl, L., Meller, R., Gue, K.: Optimizing fishbone aisles for dual command operations in a warehouse. *Naval Res. Logist. (NRL)* **56**(5), 389–409 (2009)
6. Gu, J., Goetschalckx, M., McGinnis, L.: Research on warehouse design and performance evaluation: a comprehensive review. *Eur. J. Oper. Res.* **203**(3), 539–549 (2010)
7. White, J.: Optimum design of warehouses having radial aisles. *AIIE Trans.* **4**(4), 333–336 (1972)
8. Bortolini M., Faccio M., Gamberi M., Manzini R.: Diagonal cross-aisles in unit load warehouses to increase handling performance. *Int. J. Prod. Econ.* **170**(Part C), 838–849 (2015)
9. Pohl, L.M., Meller, R.D., Gue, K R.: Turnover-based storage in non-traditional unit-load warehouse designs. *IIE Trans.* **43**(10), 703–720 (2011). <https://doi.org/10.1080/0740817x.20.https://doi.org/10.549098>
10. Accorsi, R., Bortolini, M., Ferrari, E., Gamberi, M., Pilati, F.: Class-based storage warehouse design with diagonal cross-aisle. *Logforum* **14**(1), 9 (2018)
11. Bortolini, M., Faccio, M., Ferrari, E., et al.: Design of diagonal cross-aisle warehouses with class-based storage assignment strategy. *Int. J. Adv. Manuf. Technol.* **100**, 2521–2536 (2019). <https://doi.org/10.1007/s00170-018-2833-9>
12. Pohl, L.M., Meller, R.D., Gue, K.R.: An analysis of dual-command operations in common warehouse designs. *Transp. Res. Part E Logist. Transp. Rev.* **45**(3), 367–379 (2009a)
13. Galvez, O.D., Ting, C.J.: Analysis of unit-load warehouses with non-traditional aisles and multiple P&D points. In: *The 13th Asia-Pacific Conference on Industrial Engineering and Management Systems*, pp 2011–2021 (2012)
14. Jiang, M.X., Feng, D.Z., Zhao, Y.L., Yu, M.F.: Optimization of logistics warehouse layout based on the improved Fishbone layout. *Syst Eng. Theory Pract.* (11), 24 (2013)
15. Öztürkoğlu Ö.: Investigating the robustness of aisles in a non-traditional unit-load warehouse design: leverage. In: *2015 IEEE congress on evolutionary computation (CEC)*, pp 2230–2236 (2015)
16. Öztürkoğlu Ö. Effects of varying input and output points on new aisle designs in warehouses. In: *2016 IEEE congress on evolutionary computation (CEC)*, pp 3925–3932 (2016)
17. Öztürkoğlu, Ö., Kocaman, Y., Gümüšoğlu, s: Evaluating Chevron aisle design in unit load warehouses with multiple pickup and deposit points. *J. Fac. Eng. Archit. Gazi. Univ.* **33**(3), 793–807 (2018)
18. Kocaman, Y., Öztürkoğlu, Ö., Gümüšoğlu, Ş. *Cent Eur J Oper Res. Aisle designs in unit-load warehouses with different flow policies of multiple pickup and deposit points* (2019)

# Saving Lives and Saving the Planet: The Readiness of Ireland's Healthcare Manufacturing Sector for the Circular Economy



Carla Gaberšček , Sinéad Mitchell , and Audrey Fayne 

**Abstract** Healthcare manufacturing is one of the leading creators of single-use products in Ireland and accounts for 11% of waste generated. Industry and businesses can play a significant role in tackling unsustainable production and consumption levels. Circular Economy (CE) practices could play a major role in the sustainability of health care and medical device manufacturing. This study aimed to develop an understanding of the current state of these company's readiness for the Circular Economy. An online survey was carried out with key employees in this industry to understand their perception of CE and what might drive more circular models. This study found that there was very little knowledge of CE within this industry. Despite this, some aspects of CE had been implemented, driven by cost saving initiatives. The barriers to implementation identified included a lack of prioritization and funding to develop more sustainable models of production. It was also found that financial assistance (e.g. grants) together with policy and legislation could unlock opportunities to develop a more circular model. This study adds to the limited empirical literature on CE barriers and opportunities to manufacturing organisations operating in Ireland.

## 1 Introduction

### 1.1 Background

Worldwide, natural resources are being used beyond planetary supply, primarily due to unsustainable production and consumption patterns including products being discarded after one use [1]. Ireland is contributing to this problem. In 2018, around 426,500 tons of municipal waste were accepted into Irish landfills [2]. Over 300 million tons of plastic are produced in Ireland every year, half of which comprises

---

C. Gaberšček · S. Mitchell (✉) · A. Fayne  
National University of Ireland Galway, Galway H91HX31, Ireland  
e-mail: [sinead.mitchell@nuigalway.ie](mailto:sinead.mitchell@nuigalway.ie)

S. Mitchell  
Ryan Institute for Environmental, Marine and Energy Research, Galway, Ireland

single-use items. 11% of Ireland's waste [3] comes from healthcare manufacturing, an industry very important to the Irish economy [4] but which is one of the leading creators of single-use products such as gloves, gowns, catheters or surgical instruments.

Single-use products were not always seen as a negative. Disposable/single-use business models emerged in the 1980s and 1990s, and were initially developed in health care for infection control, convenience and cost savings [5]. However, given the amount of waste produced by single-use products and the subsequent impacts, it is imperative that industry works towards reversing environmental damage and reducing levels of production and consumption [6, 7]. As an unintended but advantageous consequence, such a move may also lead to companies realizing greater economic revenues [8].

One way for industry to approach this problem is to embrace a Circular Economy model (CE) which aims to eliminate the inefficiencies inherent in a traditional linear model of take, make and waste [1]. It is based on the three principles of: designing out waste and pollution; keeping products and materials in use for as long as possible and regenerating natural systems [9]. Business needs to be part of the solution to reverse damaging environmental practices [10]. CE offers many opportunities to manage and reduce waste in health care and has been successfully used to implement sustainable procurement [11–14], effective waste minimization, safe reuse, reprocessing and recycling [11] and new business models [9]. Studies have shown that CE adoption could also reduce cycle time in production and improve customer lead times, in turn increasing incomes and attracting new customers related to more sustainable processes and products [15]. Finally, it could also lead to developing closer relationships with customers and suppliers, opening new markets and generating higher profits. This is despite the reported challenges in recovering value from reusable devices caused by a lack of communication between various stakeholders such as employees, waste management staff, procurement and the end markets.

The current literature indicates that there are various eco-innovations already developed such as Design for the Environment (DfE), Waste to Energy (WtE) and Product Service Systems (PSS) that could be implemented by the medical manufacturing industry to incorporate circular elements. However, their implementation is mixed. Design for the Environment in the medical industry lags in its performance, despite this being the best place to address the issues, as most of the environmental impact is decided at this stage [3, 16]. Optimizing the traditional waste cycle by adopting Waste to Energy is used as one way of diverting waste from landfills and reduce environmental impacts somewhat [17]. Product Service Systems is an instrument that could support CE models and manage resources effectively [18] if the systems are well designed to reduce environmental impacts [1]. However, the opportunities would need to change the business model significantly, and it may only be suitable for larger medical equipment rather than other products [1, 15].

Industrial symbiosis could play a significant role in adopting many of the eco-innovations mentioned above. Industrial Symbiosis is the process by which waste or by-products of an industry or industrial process become the raw materials for another [19]. Cross-sector collaborations and innovation are needed to operationalize

a symbiotic system, but limitations are reported, in particular among small and medium enterprises [20]. There are also particular challenges in the Medical industry compared with other sectors due to it being a high-risk field (which could endanger health or lives) and there are strict regulations in place [21]. Nonetheless, there has been a recent emergence of a small number of companies managing the reprocessing of single-use devices (such as Siemens, Philips, GE and Stryker Sustainability Solutions) [21].

Despite the small pockets of reported activity, overall, there is a lack of research in the area of the Circular Economy and the healthcare manufacturing sector [15]. Hence this paper aims to assess Ireland's healthcare manufacturing companies' readiness for the Circular Economy. It looks at their current environmental management practices and attitudes to the Circular Economy. It examines the main drivers, motivators and barriers, while also looking into future opportunities for the industry. This research contributes to the unique perspective of this highly regulated sector and helps to develop an understanding of how these companies could prepare for the opportunities of circular manufacturing models.

## **2 Methodology**

This paper presents the views of people working in the healthcare manufacturing industry on the Circular Economy in Ireland. It asks specific questions on the environmental management practices within their organizations, their views on aspects related to the circular economy, and what would motivate them and their companies to become more circular.

### ***2.1 The Approach***

This study seeks insights into practices and readiness of companies for the Circular Economy in Ireland, while taking into account the realities of their highly regulated manufacturing environment. It considers differing views across various levels of employees, from CEO and senior management to production operatives. The theoretical perspective is post-positivist because it involves investigating the perspectives of employees as well as measuring, for example, the environmental management practices related to the Circular Economy readiness.

The methods of analysis used were a literature review followed by a quantitative questionnaire, which was adapted from earlier studies conducted in Denmark and the UK. [15, 20].

## ***2.2 The Survey Instrument***

The survey instrument posed questions in the following key areas:

1. The profile of the respondent and the company
2. Familiarity with the Circular Economy (CE), eco-innovation and industrial symbiosis and current activities and opportunities
3. Personal and perceived company attitudes to CE opportunities
4. Drivers, motivators and barriers of CE

The questionnaire was carried out online. It employed a non-probability convenience sampling method as it was distributed through regional business support organizations.

The questionnaire comprised 26 questions, a mixture of multiple choice and a scale rating to ensure the reliability and validity. Likert scales were mainly used to quantify opinions, interest or perceived efficacy [22]. A Likert-scale rating was used to allow for qualitative data on a nominal scale and allowed for comparison between companies and respondents. The scales consist of one 7-point scale with the rest being a 5-point scale. As the Circular Economy is a relatively new concept to most people much of the questions are subjective. As the survey seeks opinions, it may lead to some qualitative data or inconsistencies in the data.

## ***2.3 Limitations***

The main limitation of this study was the relatively low sample size of twenty-nine, despite it being distributed to hundreds of company contacts. Response bias is also a factor, in that only persons with an interest in the area may have responded to the questionnaire.

# **3 Results and Discussion**

## ***3.1 Respondent Profile***

A total of 29 respondents completed the survey, almost half (48%) were OEMs, 38% were contract manufacturers and the remainder comprised pharmaceutical, consultancy, diagnostic and R&D companies. Most of the respondents (79%) represented large companies employing over 500 people. The professional profile included some senior management perspectives (14%), but the majority of respondents were middle-tier occupations such as Engineers and Specialists (72%). The majority of respondents worked in manufacturing/operations and quality/regulatory departments.

### 3.2 *Familiarity with the Circular Economy*

Thirty-four per cent of respondents had never heard of the concept of CE when initially asked. Thirty-eight per cent who had heard of CE were not sure what it was. Only two of respondents claimed to be very familiar with the concept and indicated that their companies were working towards it. Only one person in a senior management position knew what CE was. Most of the 'Do not know' answers came from lower-tier employees, such as product builders and technicians. After the initial question about familiarity of the concept, a simple definition was provided. This was to ensure that they understood the concept sufficiently to be able to provide meaningful answers to the survey.

### 3.3 *Opportunities and Current Activities in the Circular Economy*

While there was an initial lack of familiarity of the Circular Economy, after reading the definition, 63% of respondents claimed that their understanding of the Circular Economy had improved by a significant amount. Most of respondents (76%) believed there could be opportunities in their companies and over half (55%) of respondents recognized that their company was actively exploring CE opportunities. Almost half (45%) of respondents were personally interested in getting involved in CE activities, but only 31% perceived that their companies were interested.

When asked what the company is currently doing, 90% reported recycling 'Waste reduction through procurement' featured highly with 62% of companies active in this area which indicates a deeper commitment to sustainability. Despite so few respondents having knowledge of the CE concept at the outset of the questionnaire, 52% reported activities related to 'design or redesign of products to reduce waste' and 'refurbishment'. This was higher than expected, but many manufacturing companies implement lean manufacturing and continuously strive to eliminate waste in its products and processes. Engineers/Specialist selected the highest number of answers claiming their companies currently practice 8 out of 9 possible processes. Senior Management/Director had the next highest with product builders only selecting 1 possible process.

Almost half (48%) of respondents believed CE opportunities could be realized through 'recycling', whereas 'using different raw materials' (e.g. recyclable) in their packaging and manufacturing of products came in second highest (45%). 'Product or service design' and 'reuse' of materials or products was seen as an opportunity by many (41%) and 'refurbishment of fixtures and machinery' was selected by almost a third (31%). When it came to higher level strategies, 38% of respondents saw 'Business Strategy change' and 'Procurement & Supply chain' as a viable opportunity. Better use or implementation of ERP systems was suggested as a support towards CE. No current or future opportunity could be seen by 10% of respondents (all of



which were OEMs). When presented with the range of opportunities, those in senior roles could envisage all of them as potential opportunities within their company. This is to be expected as respondents at this level would be used to looking for high-level opportunities for saving money and improving process efficiency.

### **3.4 Drivers, Motivators and Barriers of CE in Healthcare Manufacturing**

Responses related to main drivers to company CE adoption highlight a significant link to *cost savings* (72%), which was expected. *New business opportunities* and *supply chain* ranked the second and fourth drivers of adoption, which are both linked to cost savings and/or increased revenues. However, *government legislation* ranked third, which was not surprising in such a highly regulated industry. A quarter of respondents believed CE was *always part of our business model*. However only one respondent (in senior management) connected CE to *part of future vision for growth and competitive advantage*.

When asked what would motivate them to change their business to a CE approach in future, *reducing waste*, *driving increased future profits* and *having a sustainable business strategy* ranked top motivators with 69% of respondents in agreement. Although *Supply chain* was cited by 41% as a main driver for current actions, a *constrained resource supply* or *resource price fluctuation* was not seen as a significant future motivator (only 14% selected this option).

*Customers actively seeking our products*, *social conscience* and *seen as part of future vision for growth and competitive advantage* were additional responses entered by the senior management. This cohort also recognized all options to adopt the Circular Economy approach, and did not see the supply chain as a barrier. It is unclear if this was because future education is needed on the importance of this aspect or whether they consider their supply chains to be mature enough and ready for CE.

Internal factors are the main barriers hindering these companies' approach to CE. Over half (52%) of respondents selected *Internal prioritization* and 41% choose *internal funding and resources*. Employees at technician level report external barriers, feeling *customer perception* and *policy and legislation* acting as a hindrance. This is possibly because they are aware of the process-level restrictions and rules constraining their daily tasks and assume they are insurmountable barriers at a higher level. It is interesting they think customer perception would be a hindrance given that reducing waste and supporting the environment are seen by many customers as positive company behaviours. It is possible that this view will change over time as sustainability and CE become an order qualifier or an order winner in this sector.

### **3.5 Unlocking CE Opportunities, Eco-innovation and CE Readiness**

#### **Unlocking CE opportunities**

This survey indicates that '*Enabling policy & legislation*' is the biggest contributing factor to help unlock Circular Economy opportunities for the respondents, followed by '*financial assistance*'. Senior employees recognized all options presented to them as helpful to unlock CE opportunity, whereas production staff have a limited perspective that relate only to the products they are building. Better '*design for disassembly*' and '*collaborations within industry*' was recognized by many (37%). To a lesser degree '*viable take back mechanisms*' and '*greater collaboration with other industries*'. These both feed into the 24% of respondents that thought R&D knowhow with a more knowledgeable technical team and a higher value for remanufactured goods and materials would be of assistance. '*Senior management buy in*' was chosen by 34% of respondents but interestingly not by many senior managers, perhaps showing they do not consider their opinion will influence measures. Once again both senior management, directors, engineers and specialist have selected all options. Product builders and lower-tier employees have selected options to do with products themselves, as opposed to any external factors.

#### **Eco-innovation**

Respondents rated their readiness to change towards eco-innovation as medium-highly ready to change their business model towards eco-innovation. This was a uniform response over all tiers of employees within companies. However, they are unsure of their potential to minimize resource consumption or to change raw materials for recycled ones or to use by-products as raw materials. There is a clear trend in a higher rating of lower-tier occupations and a significant decrease in rating as you move up the tiers of employment to top-tier employees.

#### **Industrial Symbiosis**

The opportunity for investment in eco-innovation and/or industrial symbiosis was in the middle at a rating of 2.5 overall. However, senior management, directors, managers and supervisors all rated the opportunity at a lower than average rating. The ratings for a company's readiness to change its business model towards industrial symbiosis showed very mixed opinion. However, results show a willingness to cooperate and communicate, particularly among senior management.

## **4 Conclusion**

The concept of the Circular Economy is not well known in the healthcare manufacturing industry in Ireland. However, when it is explained to them, the majority of respondents could see its potential. Many respondents are personally driven to

move towards CE, but not all believed their companies were. It is interesting to note that the difference between the companies' attitude and personal attitudes when it came to the Circular economy. All senior management respondents claimed to already be exploring opportunities or interested in exploration of these opportunities both personally and professionally. Middle-tier respondents were the only ones to be negative towards their company's attitude. This may represent a top management idealistic view of what is happening as opposed to ordinary workers for whom it not a priority. The opportunities identified align with Witjes and Lozano's [12] belief that '*Collaboration between procurers and suppliers throughout the procurement process can lead to reductions in raw material utilization and waste generation, whilst promoting the development of new, more sustainable, business model.*' Results also correlate to Moultrie *et al*'s [5] ideas when they say, despite this the medical device industry faces sustainability concerns common to the design process in many commercial areas, such as waste and consumption of scarce materials. It is a concern that OEMs were less likely to envisage opportunities, perhaps due to the likelihood that they have a longer history of being rigidly regulated which the company culture may struggle to see beyond. As with any business, managing costs is the biggest driver and motivator (rather than as environmentally conscious decisions) which is in agreement with many previous studies [5].

The main barriers to CE were seen as internal, which was surprising and a cause for concern, especially because these were chosen by senior management. It was encouraging to see that all respondents in senior positions could see potential for eco-innovations, including industrial symbiosis. It was surprising however, to see senior management rate so highly their ability to exchange information with other companies. This may just be due to the locality of healthcare manufacturing companies to each other, as Ireland is a very small country and this industry is clustered together in industrial parks or they can see the benefits that this could bring to the business as well as the environment around it.

Education on the benefits of the Circular Economy needs to be given to show that in the long term, it is good for the environment, whilst also leading to business benefits. Respondents are aware that there are Circular Economy opportunities in all companies, but being able to see these opportunities and exploiting them are very different things. There are no disputes that single-use items need to be replaced but without any incentives to implement change, such as packaging to recyclable materials, the associated costs involved will make this prohibitive. Better design for disassembly or even higher value put on remanufactured goods would all be simple steps to unlocking Circular Economy opportunities within the Irish healthcare manufacturing industry. More research into suitable materials for reuse and reprocessing needs to be undertaken to show companies the benefits and cost saving that can be had from these processes. Responsibility for implementing change lies with government and companies alike. Attitudes need to change away from purely cost-based incentives and look towards sustainability.

Government and companies need more communication to develop realistic plans to meet Circular Economy goals.

It is clear from this study that more communication is needed within companies themselves to develop a consensus between all tiers within the company. All employees no matter their status need to be working towards a common goal. Internal barriers need to be broken and offering incentives to employees regardless of their role to come up with innovative ideas to help the business, gives them a sense of pride and appreciation. Readiness and potential towards eco-innovation and industrial symbiosis ideas can be subjective. They do not directly correlate to willingness or even want for companies to implement these ideas. Industrial symbiosis can help companies work together to spread costs of research into innovative ways to reduce waste and make the most out of the resources they have. Working together can benefit smaller as well as larger companies due to the shared investment and intellectual benefits of working with other likeminded companies.

In summary, Irelands healthcare manufacturing companies are far from being ready for the Circular Economy. The opportunities are there, but more work is needed to find the best ways to exploit these opportunities within this industry. Until education is given as to the major benefits of implementing these concepts, they will not be done from an environmentally conscious decision standpoint. Legislation and incentives need to be introduced to motivate companies into adopting more Circular Economy concepts, to safeguard our planets resources for future generations to come.

This study adds to the limited empirical literature on CE barriers and opportunities to manufacturing organisations operating in Ireland. Further research into this field needs to be done to explore in depth how to make the most out of the opportunities presented. Research also needs to be undertaken to discover the best materials to be used to make it safer for reprocessing devices and instruments, along with biodegradable or recyclable packaging of such devices as well as design for ease of disassembly.

**Acknowledgements** The authors of this study would like to acknowledge the participants in healthcare manufacturing in Ireland for engaging with the study.

## References

1. Michelini, G., Moraes, R.N., Cunha, R.N., Costa, J.M., Ometto, A.: From linear to circular economy: pss conducting the transition. In: 9th CIRP IPSS Conference: Circular Perspectives on PSS. São Paulo (2017)
2. EPA.: EPA Waste Data Release. EPA, Wexford (2019)
3. Fuery, J., de Eyto, A., Maher, C.: Sustainable design strategies for medical devices—Investigations of the Irish multinational business context in product development and sustainable design. In: First International Conference on Sustainable Intelligent Manufacturing (SIM). Leira (2011)
4. Irish Medtech Association.: About the Medtech Sector. IBEC, 20 December 2019. [Online]. Available: [https://www.irishmedtechassoc.ie/Sectors/IMDA/IMDA.nsf/vPages/Medtech\\_sect-or-about-the-medtech-sector!OpenDocument](https://www.irishmedtechassoc.ie/Sectors/IMDA/IMDA.nsf/vPages/Medtech_sect-or-about-the-medtech-sector!OpenDocument). Accessed 20 Dec 2019
5. Moultrie, J., Sutcliffe, L., Maier, A.: Exploratory study of the state of environmentally conscious design in the medical device industry. *J. Cleaner Prod.* **108**, 363–376 (2015)

6. Heltberg, R., Siegel, P.B., Jorgensen, S.L.: Addressing human vulnerability to climate change: toward a 'no-regrets' approach. *Global Environ. Change (J.)* **19**(1), 89–99 (2009)
7. Sullivan, R., Gouldson, A.: The governance of corporate responses to climate change: an international comparison. *Business Strat. Environ.* **26**(4), 413–425 (2017)
8. T. Murray, "IPCC Report Reveals Urgent Need For CEOs To Act On Climate," Washington, 2018
9. Ellen MacArthur Foundation: Towards the Circular Economy: Economic and Business Rationale for an Accelerated Transition. Ellen MacArthur Foundation, Cowes (2015)
10. Mitchell, S., O'Dowd, P., Dimache, A.: Manufacturing SMEs doing it for themselves: developing, testing and piloting an online sustainability and eco-innovation toolkit for SMEs. *J. Sustain. Eng* (2019)
11. Voudrias, E.A.: Healthcare waste management from the point of view of circular economy. *Waste Manage.* **75**(1), 1–2 (2018)
12. Witjes, S., Lozano, R.: Towards a more circular economy: proposing a framework linking sustainable public procurement and sustainable business models. *Res. Conserv. Recycling* **112**(1), 37–44 (2016)
13. Sustainable procurement practice. *Bus. Strate. Environ.* **20**(2), 94–106 (2011)
14. Viani, C., Vaccari, M., Tudor, T.: Recovering value from used medical instruments: a case study of laryngoscopes in England and Italy. *Res. Conserv. Recycling* **111**(1), 1–9 (2016)
15. Gaberščik, C.: The Readiness of Ireland's Healthcare Manufacturing Companies to the Circular Economy. National University of Ireland Galway, Galway (2019)
16. Karlsson, M., Öhman, P.D.: Material consumption in the healthcare sector: Strategies to reduce its impact on climate change—The case of Region Scania in South Sweden. *J. Cleaner Prod.* **13**(10–11), 1071–1081 (2005)
17. Malinauskaite, J., Jouhara, H., Czajczyńska, D., Stanchev, P., Katsou, E., Rostkowski, P., Thorne, R.J., Colón, J., Ponsá, S., Al-Mansour, F., Anguilano, L., Krzyżyńska, R., López, I., Vlasopoulos, A., Spencer, N.: Municipal solid waste management and waste-to-energy in the context of a circular economy and energy recycling in Europe. *Energy* **141**(1) 2013–2044
18. Tukker, A.: Product services for a resource-efficient and circular economy—a review. *J. Cleaner Prod.* **97**(1), 76–91 (2015)
19. European Commission: Industrial Symbiosis: Realising the Circular Economy. European Commission, 27 January 2014. [Online]. Available: [https://ec.europa.eu/environment/ecoap/about-eco-innovation/experts-interviews/20140127\\_industrial-symbiosis-realising-the-circular-economy\\_en](https://ec.europa.eu/environment/ecoap/about-eco-innovation/experts-interviews/20140127_industrial-symbiosis-realising-the-circular-economy_en). Accessed 20 Jan 2020
20. Pigosso, D.C.A., Schmiegelow, A., Andersen, M.M.: Measuring the readiness of SMEs for eco-innovation and industrial symbiosis: development of a screening tool. *Sustainability* **10**(8) (2018)
21. Kane, G., Bakker, C., Balkenende, A.: Towards design strategies for circular medical products. *Res. Conserv. Recycling* **135**(1), 38–47 (2018)
22. Bishop, P., Herron, R.L.: Use and misuse of the Likert item responses and other ordinal measures. *Int. J. Exercise Sci.* **8**(3), 297–302 (2015)

# Effect of Milling Speed and Time on Graphene-Reinforced AA2024 Powder



Mulla Pekok, Rossitza Setchi, Michael Ryan, and Quanquan Han

**Abstract** Aluminium is the third most abundant material in the Earth's crust and, along with its alloys, is essential in many engineering sectors, including aerospace, automotive, defence, marine, construction, and medicine, owing to its high damage tolerance, fatigue resistance, conductivity, corrosion resistance, and low density. Despite this, some mechanical properties of Aluminium do not yet satisfy increasing industrial demands. Reinforcing aluminium alloys with other elements is considered as a means of providing additional strength. This study aims to investigate the effect of milling speed and time on graphene-reinforced aluminium alloy powder, intended for use in selective laser melting (SLM), prepared using high-energy ball milling (HEBM). The experimental study indicates that using a slow milling speed (100 rpm) for up to 2 h does not affect the shape of the powder substantially, and the graphene nanoparticles (GNPs) do not adhere to the powder surface in a metal matrix composite (MMC). However, a faster milling speed (250 rpm) flattens and crumbles the powder, and adheres the graphene sheets to the alloying powder, due to the higher impact energy produced by centrifugal and Coriolis forces.

---

M. Pekok (✉) · R. Setchi · M. Ryan · Q. Han  
Cardiff School of Engineering, Cardiff University, Cardiff CF24 3AA, UK  
e-mail: [pekokma@cardiff.ac.uk](mailto:pekokma@cardiff.ac.uk)

R. Setchi  
e-mail: [setchi@cardiff.ac.uk](mailto:setchi@cardiff.ac.uk)

M. Ryan  
e-mail: [ryanm6@cardiff.ac.uk](mailto:ryanm6@cardiff.ac.uk)

Q. Han  
e-mail: [Hanjunguan@sdu.edu.cn](mailto:Hanjunguan@sdu.edu.cn)

Q. Han  
Shandong University, Jinan, China

# 1 Introduction

Aluminium is one of the most abundant and extensively used non-ferrous metals, and is outstandingly important for many engineering sectors, including aerospace, automotive, and marine, owing to its strength, corrosion resistance, conductivity, density, malleability, cost, and recyclability [1]. According to the International Aluminium Institute (IAI) [2], 63,690 thousand metric tonnes of aluminium were globally produced in 2019. The global production of primary aluminium is growing by approximately 6% every year. The global market price of high strength aluminium alloys was almost \$38 Billion in 2018, and could reach \$55 Billion by 2023, demonstrating the enormous importance of the aluminium and its alloys [3].

Aluminium alloys such as AA2024, with copper as the principle alloying element and magnesium as a secondary element are prevalently preferred in many industrial applications (i.e. aircraft, automotive parts, structural applications, truck frames, fasteners, fittings, and numerous other applications) due to their strength-to-weight ratio, fatigue resistance, and damage tolerance [4, 5]. Nevertheless, technological improvements and significant developments in material science have accelerated the need for new materials, alloys, or MMCs which have higher mechanical properties [6, 7].

selective laser melting (SLM) is a significant additive manufacturing (AM) technology which draws substantial attention among engineering sectors, due to its short fabrication lead time and fast production of components with complex geometries [8]. SLM manufactures components by applying a laser beam to selected part of a thin layer of metal powder, melting the powder particles together. Another layer is deposited on top of the solidified powder and is again melted with the laser [9]. This process repeats until the desired object is constructed. The optimised ball milling parameters, determined from the results of the present work, will be used in the preparation of MMC powder for future studies using SLM.

Ball milling can be used for various purposes, such as particle size reduction, comminution and intermixing of multiple materials. There are numerous milling techniques available (e.g. attrition, Spex shaker, vibrator mixer); however, the most common technique for high-speed grinding of solid particles is planetary ball milling [10]. The working principle of ball milling (see Fig. 1) is that the supporting disk ( $rot_d$ , clockwise) and bowls ( $rot_b$ , anticlockwise) turn in opposite directions around their own centre points. Due to the different rotational axes of the main disc and the milling bowls, reversed rotation creates a 'D shape' movement of balls inside the bowl under the influence of Coriolis and centrifugal forces of disk and bowl rotations. These forces help to increase the kinetic energy inside the bowls. Consequently, high-energy ball-to-ball and ball-to-wall impacts effectively grind and blend material which is placed in the grinding bowls.

The choice of optimum mechanical milling process parameters is essential in order to have homogeneously dispersed advanced composite powders. Numerous internal and external factors (i.e. milling time, pause time, speed, weight ratio, process control

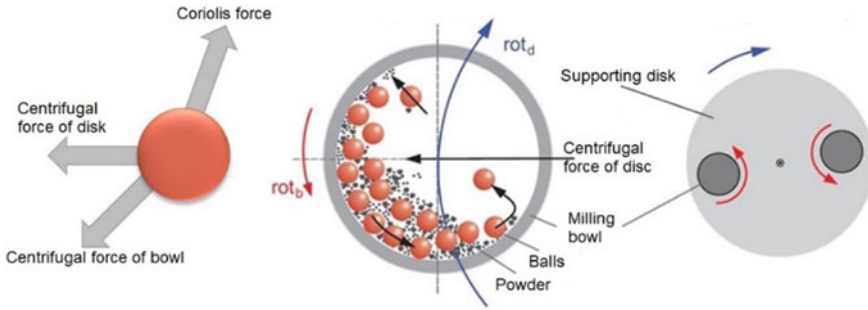


**Fig. 1** Working principle of HEBM [11]

agent (PCA), milling type, material type and size, the atmosphere of the bowl and the temperature of the bowl during milling) can affect the quality of the milled composite.

GNPs have the capability to increase the mechanical properties (e.g. strength and hardness) of some as fabricated alloy samples when prepared using the ball milling technique. For instance, the strength of pure copper is increased approximately 25% by adding GNPs with high-energy ball milling [12]. Similarly, the hardness of pure aluminium is increased about 75% by adding graphene sheets with ball milling techniques [13]. Additionally, the HEBM technique was used to mix GNPs and AlSi10Mg alloy, and successfully increased the ultimate tensile strength and yield strength of the alloy 3 and 5% respectively [8]. The alloying elements of AA2024 (Al, Cu, Mg, Si) demonstrate significant positive effects on strength when reinforced with graphene independently, or as an alloy.

However, there are some challenges in using graphene as a reinforcement material. Firstly, graphene reacts with aluminium above 500 °C and can form  $Al_4C_3$  during manufacture. Additionally, a certain amount of  $Al_4C_3$  can enhance the wettability; thus, mechanical strengthening of the fabricated sample can be positively affected [13]. Another significant challenge is that agglomeration and defects in the reinforcement material can be observed during HEBM of graphene, due to the strong Van der Waals attraction, huge surface area,  $\pi$  to  $\pi$  interaction and high impact energy, unless an appropriate milling time and rotation speed is applied [14].

This study aims to investigate the effect of milling speed and time on GNP-reinforced aluminium 2024 alloy, examining the particle size distribution, the particle Diameters of the Volume ( $D_v$ ) of 10, 50 and 90%, and scanning electron microscope (SEM) images of the milled powder. Fast (250 rpm) and slow (100 rpm) milling speeds were examined after three milling times (0.5, 1 and 2 h). Additionally, the effect of adding a PCA to the powder and milling balls is investigated.



## 2 Materials and Methods

### 2.1 Powder Characteristics

Gas-atomised AA2024 powder with a particle range size of 2–86  $\mu\text{m}$  was obtained from LPW Technology Limited (Philadelphia, USA) for the present study. The particle  $D_v$  10, 50, and 90% are 20  $\mu\text{m}$ , 37.6, and 63.1  $\mu\text{m}$ , respectively, obtained using a Malvern Mastersizer 3000 (Malvern, UK). The chemical composition of the nano-powder is 4Cu–1.4Mg–0.4Mn–0.1Si–0.1Fe–bal.Al (wt%).

GNPs were obtained from Sigma-Aldric (Dorset, UK). The surface area of the graphene is between 50 and 80  $\text{m}^2/\text{g}$ , and the 10, 50, and 90% particle  $D_v$  (again analysed using the Malvern Mastersizer 3000) are 11.2, 35.1, and 93.1  $\mu\text{m}$ , respectively.

### 2.2 HEBM Parameters and Process

Aluminium 2024 alloy (80 g), 0.2 wt% graphene (0.16 g) and 2 wt% stearic acid (1.6 g, used as a PCA) were added to the milling bowl with a ball-to-powder weight ratio of 10:1, using a mixture of large and small milling balls (800 g). A milling time of 10 min, followed by a pause time of 10 min, was repeated 12 times. The cycle was paused at 0.5, 1 and 2 h in order to take a sample of the MMC. Atmospheric air was used inside the bowls during milling in order to prevent an exothermic reaction between the fresh aluminium surfaces and air, when taking samples at 0.5, 1, and 2 h. However, the powder was stored in a glove box under argon gas to prevent further oxidation after milling process is completed.

## 3 Results and Discussion

### 3.1 Effect of PCA to Milled Powder

The PCA was added into milling bowl in order to prevent cold welding and accumulation of the milled powder. A wide range of control agents have been examined in practice; however, different percentage of stearic acid in milling bowl was extensively preferred due to the sufficiency of the acid to the welding and powder contamination [12, 15]. In the present study, raw aluminium alloy powder was tested with and without stearic acid (2 wt%) for 15 min to examine the effect of the agent on the milled powder (Fig. 2). During the milling process, the temperature inside the bowl increased to 70 °C and the stearic acid, (which has a low melting point), melted, and covered the surface of the bowls and the milling balls. Thus, the aluminium powder

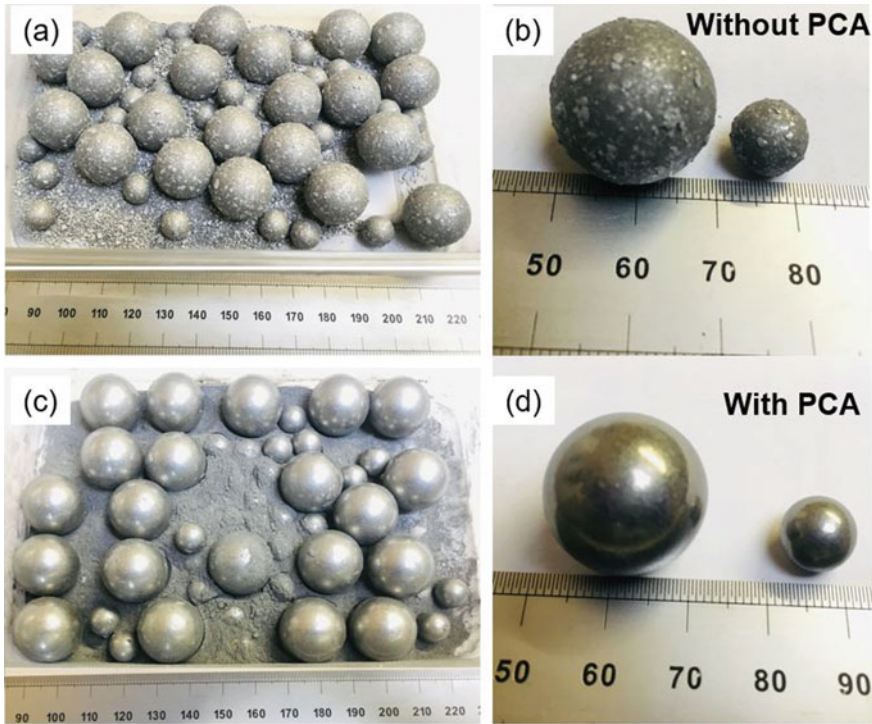


**Fig. 2** Milling balls and powder after 15 min of milling time without (a–b) and with 2% of PCA (c–d)

was prevented from accumulating and sticking onto the milling ball surface during grinding (Fig. 2b–d). Without PCA, the powder agglomerated and stuck onto both the milling balls and bowl surfaces (Fig. 2a–c).

### 3.2 *The Particle Size Distribution and $D_v$ of the MMC After Slow Milling Speed*

The particle size distributions and powder shapes for raw AA2024, graphene, and milled powders are shown in Fig. 3. The aluminium alloy powders are not spherical, and the median particle  $D_v(50)$  of the alloy and graphene are  $37.6 \mu\text{m}$  and  $35.1 \mu\text{m}$ ; however,  $D_v(10)$  and  $D_v(90)$  of the elements show big differences. The particle size distributions after milling at a slow speed (100 rpm) for short milling times (0.5, 1 and 2 h) are also represented in Fig. 3. The powder distribution is approximately between 10 and  $70 \mu\text{m}$  for raw aluminium and between 5 and  $150 \mu\text{m}$  for graphene before the milling process. However, the powder particle size for the milled MMC after 0.5-h ranges between 5 and  $110 \mu\text{m}$ , and bigger particles become more distinct.

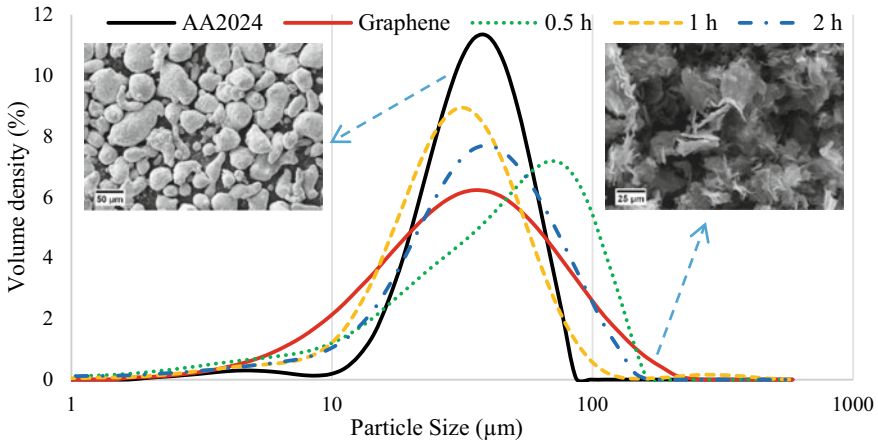


**Fig. 3** Powder shape and particle size distribution of raw materials (AA2024 and Graphene) and the milled powders after milling times of 0.5, 1, 2 h at 100 rpm

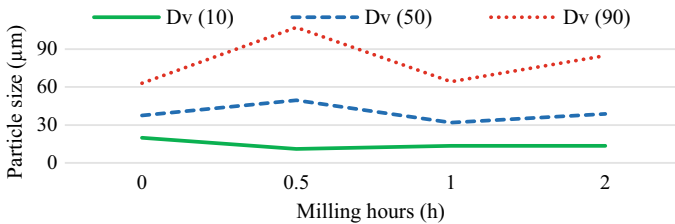


**Fig. 4** Particle Dv of 10, 50, and 90% of the powder after milling times of 0, 0.5, 1, 2 h, at 100 rpm

The reason for this is because a short milling time (0.5-h) at 100 rpm agglomerates the powders. Moreover, the accumulated large graphene sheets are not sufficiently separated because of the low impact energy inside the milling bowl at the beginning of the process.

The particle Dv of 10, 50, and 90% are shown in Fig. 4. At the beginning from 0 to 0.5-h milling time, Dv(10) decreases, but Dv(90) increases, due to the lower Dv(10) and higher Dv(90) of the graphene compared to the aluminium alloy. However, further milling causes a fluctuation in Dv(50) and Dv(90). This may indicate the disintegration of graphene sheets first (1-hour milling time), and then agglomeration of alloying powder and graphene (2-hours milling time).

### 3.3 Graphene Distribution in MMC After Slow Milling Speed

Figure 5 shows the SEM images of the milled MMC after different milling times

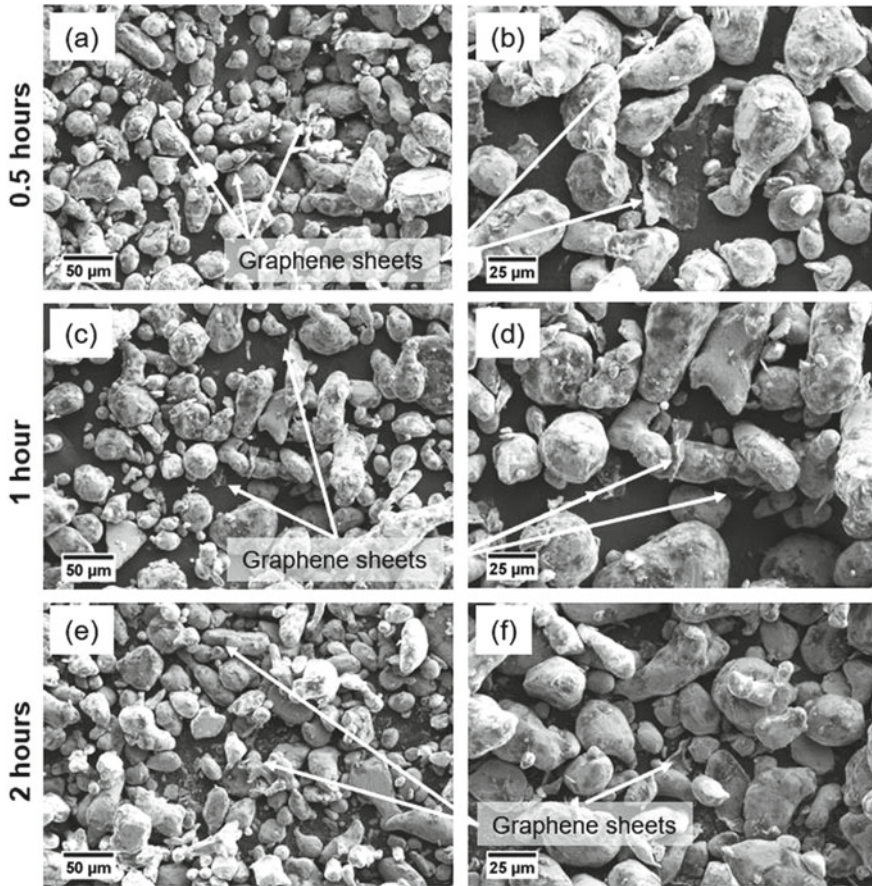


**Fig. 5** SEM images showing the distribution of the graphene sheets in MMC after the milling times of 0.5, 1, 2 h at 100 rpm

(0.5, 1 and 2 h) at 100 rpm. The shape of the alloy powder is not extensively changed and the graphene sheets, which are indicated in Fig. 5 are not embedded inside the alloy powders due to the low impact energy. Moreover, agglomerated graphene sheets could not be dispersed in a short milling time (0.5–hours); nevertheless, further milling up to 2 h has separated the sheets and distributed the graphene in the MMC more homogeneously than after a short milling time. Furthermore, even after two hours milling the powder shape is not dramatically changed; however, the graphene sheets are still not adhered to the aluminium alloy surface, owing to the low impact energy. On the other hand, some parts of the surface of the alloy powder have been coloured black by the graphene, which is made up of a honeycomb shape of black carbon molecules.

### 3.4 The Particle Size Distribution and Dv of the MMC After Fast Milling Speed

The particle size distribution of raw aluminium alloy, graphene, and milled MMC after different milling times are shown in Fig. 6. The volume of small particles less than 10  $\mu\text{m}$  is dramatically increased using a faster milling speed (250 rpm) in comparison to the slow milling speed, because high-energy impacts crumble both the aluminium alloy and graphene particles. Additionally, the volume density of bigger particles greater than 100  $\mu\text{m}$  is also enhanced using a faster milling speed, due to both the accumulation of the aluminium powder, and large agglomerations of graphene sheets.

Figure 7 depicts the Dv(10, 50 and 90) of the MMC. Reinforcing graphene (which has a low Dv(10) and high Dv(90)) into aluminium alloy for 0.5 h shows an identical effect as when using a slow milling speed. However, further milling time increases the particle size, owing to both accumulations of the elements and enlargement of the surface area of the powder with high impact energy. In order to achieve a constant deposited layer for the additive manufacturing (AM) process, the volume of particles

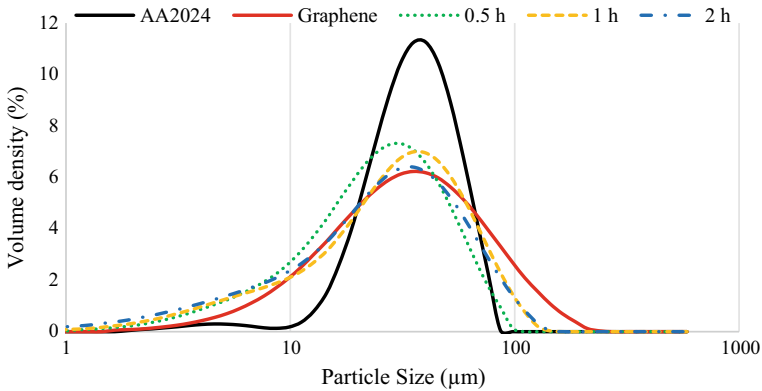


**Fig. 6** Particle size distribution of raw materials (AA2024 and Graphene) and the milled powders after the milling times of 0.5, 1, 2 h at 250 rpm

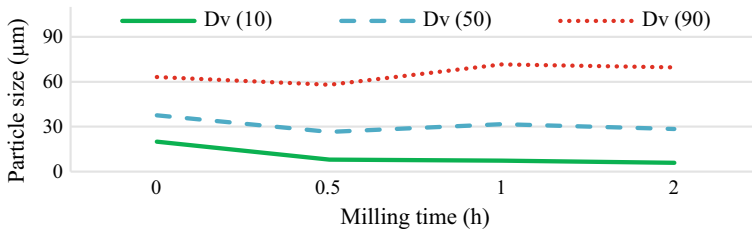


**Fig. 7** Particle Dv of 10, 50, and 90% of the MMC after the milling times of 0, 0.5, 1, 2 h at 250 rpm

with a size above 90% should not be high, otherwise, larger particles may negatively affect the layer deposition process.

### 3.5 Graphene Distribution in MMC After Fast Milling Speed

SEM images after different milling times at 250 rpm milling speed are shown in Fig. 8. The aluminium alloy powder shape has clearly been flattened by the high impact energy of milling balls. The graphene platelets have been crumbled into small pieces and stuck on the surface of the powder. Even though most of the graphene sheets has been dispersed, some accumulated graphene sheets remain visible inside the MMC. Hence, visual identification of graphene among the flattened powders is

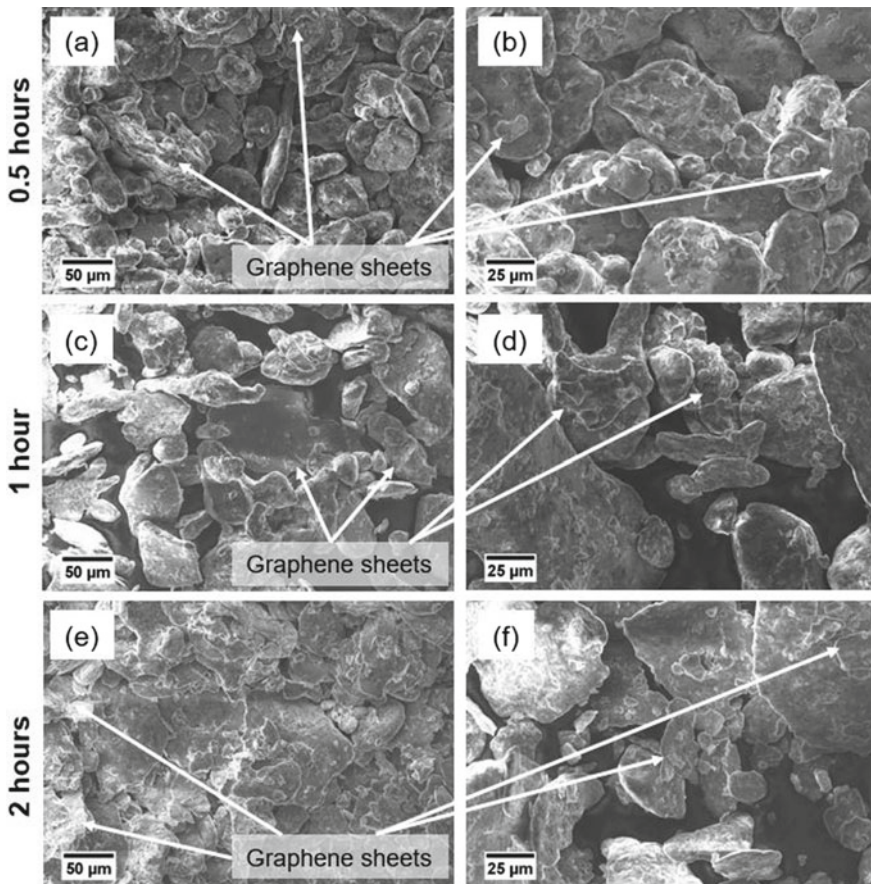


**Fig. 8** SEM images showing the distribution of the graphene sheets in MMC after the milling times of 0.5, 1, 2 h at 250 rpm

difficult. Additionally, flattened particles inside MMC become more distinct when the milling time is increased up to 2 h (see Fig. 8). On the other hand, the non-spherical form of the powder may negatively affect the deposition quality of the AM process.

## 4 Conclusion

This research investigates the effect of milling time and speed on graphene-reinforced AA2024 by HEBM. The particle size distribution, the  $D_v$  of 10, 50 and 90%, and SEM images of the MMC were analysed. The following conclusions are drawn from the experimental study:

1. The volume density of powder under 10  $\mu\text{m}$  decreases when increasing the milling speed from 100 to 250 rpm, owing to the fact that high impact energy accumulates the particles and small graphene sheets are stuck onto the surface of the powder.
2. The powder shape at slow milling speed remains nearly identical to the shape of the raw alloy powder, due to the low collision energy of the milling balls; however, the powders forms flakes at high milling speeds due to the higher impact energy. Additionally, slow milling speeds create insufficient impact energy to stick the graphene sheets onto the powder. Increasing the milling speed to 250 rpm creates flattened powder particles, which are not convenient for AM processing, as non-spherical powders may lead to uneven layer thicknesses.
3. The  $D_v$  of 10, 50, and 90% for slow speed milling show fluctuations with time, owing to the separation of graphene sheets and accumulation of the particles as a result of further milling. However, the particle diameters at the fast milling speed show a more gradual trend, due to the immediate flattening of the powder shape. Further milling increases the surface area of the powders as a consequence of the high-energy impacts on the particles.

This study shows that the milling times and speeds of HEBM have a significant impact on MMC. It is concluded that a high milling speed has some positive effects (for instance the graphene sheets are stuck onto the aluminium powder particles); however, flattened powders are not convenient for AM processing. On the other hand, slow milling speed allows does not affect the form of the powder shape, but the graphene platelets are not homogeneously dispersed inside the MMC. Further study, examining longer milling hours and a range of milling speed between 100 and 250 rpm are required in order to develop a more comprehensive understanding of the effect of the processing parameters.

**Acknowledgements** The authors wish to thank ASTUTE 2020 (Advanced Sustainable Manufacturing Technologies). This operation, supporting manufacturing companies across Wales, has been part-funded by the European Regional Development Fund through the Welsh Government and the participating Higher Education Institutions. This study is also supported by the ministry of national education of Turkey.

## References

1. Chen, F., Gupta, N., Behera, R., Rohatgi, P.: Graphene-reinforced aluminum matrix composites: a review of synthesis methods and properties. *JOM* 837–845 (2018)
2. Knapp, R.: Primary Aluminium Production. World Aluminium, 2020. [Online]. Available: <http://www.world-aluminium.org/>
3. Wood, L.: High Strength Aluminum Alloys Market by End-use Industry Type (Automotive & Transportation, Aerospace & Defense, Marine), Alloy Type (Cast, and Wrought), Strength Type (High, and Ultra-high Strength), and Region—Global Forecast to 2023. Market Research Report (2018)
4. Davis, J.: Aluminum and Aluminum Alloys. In: *Alloying: Understanding the Basics*. ASM International, Ohio (2011)
5. Patil, D.C., Venkateswarlu, K., Kori, S.A., Das, G., Das, M., Alhajeri, S.N., Langdon, T.G.: Mechanical Property Evaluation of an Al-2024 Alloy Subjected to HPT Processing. *Mater. Sci. Eng.* 1–9 (2014)
6. Brock, H.: Sustainable Solution. Aluminum Industry Vision, Washington, D.C. (2001)
7. Prasad, N., Wanhill, R.: *Aerospace Materials and Material Technologies*. Springer, Singapore (2016)
8. Wang, Y., Shi, J., Lu, S., Wang, Y.: Selective laser melting of graphene-reinforced inconel 718 superalloy: evaluation of microstructure and tensile performance. *J. Manuf. Sci. Eng.* **139**(4), 1–6 (2016)
9. Zhang, H., Zhu, H., Qi, T., Hu, Z., Zeng, X.: Selective laser melting of high strength Al–Cu–Mg alloys: processing, microstructure and mechanical properties. *Mater. Sci. Eng., A* **656**, 47–54 (2016)
10. Gupta, R.K., Murty, B.S., Birbilis, N.: *An Overview of High-energy Ball Milled Nanocrystalline Aluminum Alloys*. Springer, Cham (2017)
11. Wilkening, M., Düvel, A., Pflügl, F.P., Silva, K., Breuer, S., Šepelák, V., Heitjans, P.: Structure and ion dynamics of mechanothesized oxides and fluorides. *Technische Informationsbibliothek Hannover* **232**, 107–127 (2017)
12. Yue, H., Yao, L., Gao, X., Zhang, S., Guo, E., Zhang, H., Lin, X., Wang, B.: Effect of Ball-milling and graphene contents on the mechanical properties and fracture mechanisms of graphene nanosheets reinforced copper matrix composites. *J. Alloys Comp.* **691**, 755–762 (2017)
13. Hu, Z., Chen, H., Xu, J., Nian, Q., Lin, D., Chen, C., Zhu, X., Chen, Y., Zhang, M.: 3D printing graphene-aluminum nanocomposites. *J. Alloys Comp.* **746**, 269–276 (2018)
14. Nieto, A., Bisht, A., Lahiri, D., Agarwal, A.: Graphene reinforced metal and ceramic matrix composites: a review. *Int. Mater. Rev.* **62**(5), 241–302 (2016)
15. Han, Q., Setchi, R., Evans, S.L.: Characterisation and milling time optimisation of nanocrystalline aluminium powder for selective laser melting. *Adv. Manuf. Technol.* **88**, 1429–1438 (2017)



# Mechanical Behavior of NiTi-Based Circular Tube Chiral Structure Manufactured by Selective Laser Melting



Chenglong Ma, Dongdong Gu, Jie Gao, Wei Chen, Yingjie Song,  
and Rossitza Setchi

**Abstract** In this work, a new NiTi-based circular tube chiral (CTC) structure with compression-induced-twisting effect was proposed, inspired by the *spiranthes cernua*'s tendril, which was then manufactured by selective laser melting (SLM). The compressive deformation behavior and coupled twisting feature of NiTi-based CTC structure were disclosed in detail based on the experimental method and simulation approach. It was found that the twisting angle per axial strain  $\lambda$  achieved by the experiment and the simulation was roughly consistent with the result (1.5068°/%) based on the theoretical calculation within a small deformation. As the strain increased, the  $\lambda$  rapidly declined and finally stabilized at round 0.6°/%. Furthermore, the recoverable behaviors of the axial strain and the twisting angle after the unloading were also evaluated in views of the reversible martensitic transformation of NiTi alloys. After six cycles, the recoverable strain or twisting angle ratio could reach approach to 1. This work could be expected to provide a guiding significance to some degree for the development of functional components (such as smart actuators) with a stable and reversible twisting behavior applied in the aerospace field.

## 1 Introduction

Chirality was first introduced by Sir William Thomson to describe the property of handedness [1]. In natural systems, there exist a variety of chiral structures, such as helical goat horns, right-handed and left-handed sea shell, twisting flower petals and stems, DNA, etc. [1, 2]. These chiral structures in biological materials can exhibit strong out-of-plane bearing capacity and low in-plane stiffness, from mechanical aspects of view. Inspired by them, various types of 2D chiral mechanical metamaterials have been proposed. Specially, due to the non-centrosymmetric

---

C. Ma · D. Gu (✉) · J. Gao · W. Chen · Y. Song  
College of Materials Science and Technology, Nanjing University of Aeronautics and  
Astronautics (NUAA), Nanjing 210016, People's Republic of China  
e-mail: [dongdonggu@nuaa.edu.cn](mailto:dongdonggu@nuaa.edu.cn)

C. Ma · R. Setchi  
School of Engineering, Cardiff University, CF24 3AA Cardiff, UK

© The Editor(s) (if applicable) and The Author(s), under exclusive license to Springer  
Nature Singapore Pte Ltd. 2021

S. G. Scholz et al. (eds.), *Sustainable Design and Manufacturing 2020*, Smart Innovation,  
Systems and Technologies 200, [https://doi.org/10.1007/978-981-15-8131-1\\_21](https://doi.org/10.1007/978-981-15-8131-1_21)

geometrical relation, the in-plane compressive and shear deformation of 2D chiral mechanical structures can be partially coupled, thus resulting in a series of multifunctional mechanical properties such as the negative Poisson's ratio effect, the vibration attenuation capacity, impact energy absorption ability, etc [3]. As for the vibration attenuation capacity, it can be attributed to formation of wave mitigation features and adjustable bandgap structures of 2D chiral mechanical structures during the loading. Local resonances bring about an elastic energy storage, therefore showing the vibration attenuation capacity [1]. For an enhanced impact energy absorption ability, it results from the localized deformation of the whole structure within the contact region induced by the compression-shear coupling effect [1]. In a word, benefit from the unique structural topology and multifunctional mechanical properties of these 2D chiral mechanical structures, more and more industrial applications have emerged, including morphing airfoils [4], auxetic stents [5], flexible electronics [6], etc., exhibiting a huge potential.

In comparison with 2D auxetic structures, 3D chiral mechanical structures normally possess more complex geometrical configurations, which resultantly leads to a great challenge in the preparation aspect and a slow research progress [7]. Nevertheless, in the past few years, 3D printing or additive manufacturing technology has been prevailing around all the world, as a revolutionary new approach based on a novel materials incremental manufacturing philosophy [8]. This technology can endow structure design with a high degree of freedom, thus facilitating the development of a plenty of novel structures with any complex shapes, such as bionic porous scaffolds [9], large cross-scale porous structures [10]. In this condition, relevant researches on 3D chiral mechanical structures have started to spring up recently. However, most of 3D chiral mechanical structures existing in reported studies are made of polymer materials and limited investigations on metal-based 3D chiral mechanical structures have been conducted. Additionally, relevant discussions on the mechanical properties of 3D chiral mechanical structures are also confined to a condition where only small deformation occurs, which is not enough for engineering applications.

In this work, a new 3D chiral mechanical structure was proposed and fabricated by selective laser melting (SLM) using the shape memory material NiTi pre-alloyed powder. Reversible martensitic phase transformation within NiTi alloys was expected to be able to induce a unique mechanical behavior. Axial compressive tests including the cyclic compressive test were performed in order to assess the twisting behavior and recoverable rate of SLM-fabricated NiTi-based 3D chiral structure. Besides, to give more insight into the deformation mechanism of this 3D chiral structure, the corresponding numerical simulation was also conducted.

## 2 Geometrical Configuration and Theoretical Analysis

### 2.1 Circular Tube Chiral Structure (CTC)

The design inspiration of the CTC structure came from the climbing plant tendrils with chiral growth feature, such as *Spiranthes cernua* shown in Fig. 1a [11]. *Spiranthes cernua*, belonging to a kind of orchid, has tall erect densely flowered spiraling clusters of creamy white vanilla-scented flowers, widely distributed especially in low damp places of eastern and central North America. The tendrils with a spatial construction similar as that of a spiral spring can be endowed an excellent deformability. The three-dimensional model of a tendril was here simplified as a wire helicoid along the central axis of a circular tube (Fig. 1b). The periodicity or structural feature of the wire helicoid was conspicuous by demonstrating the characterized circular planes. On the basis of the single wire helicoid (the green one), more spiral wires with the same periodicity could be further introduced to create multiple wire helicoids (Fig. 1b). Subsequently, inspired by the multiple wire helicoids, a representative element (Fig. 1c) with simplified inclined struts different from the helical curves was extracted, which further constructed a novel circular tube chiral structure (Fig. 1d). The geometrical parameters for describing the CTC structure were defined as the angle  $\theta$  between the inclined strut and the axial direction (Fig. 1c), the length  $L$  of inclined struts, the height  $H$  between top circular plane and bottom circular plane, the diameter  $d$  of inclined struts and the diameter  $D$  of circular planes (Fig. 1d). The number of inclined struts is denoted as  $N$ . By adjusting the geometrical parameters ( $\theta$ ,  $D$ ,  $d$ , and  $L$ ) and the  $N$  of the CTC structure, different degrees of compression-shear coupling effect combining with various other mechanical properties could be obtained. Note that,  $L$  here could be denoted as the relation between  $H$  and  $\theta$ , namely  $H/\cos\theta$ .

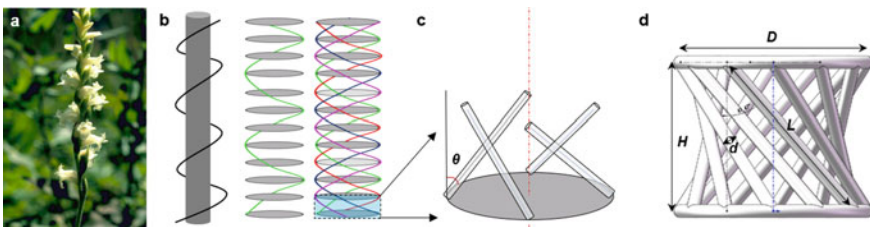


**Fig. 1** a Macro image of *spiranthes cernua* [11]; b The simplified model of the tendril and the evolved multi-helix structure; c The simplified representative element extracted from the multi-helix structure; d The proposed CTC structure in this work

## 2.2 Theoretical Analysis of Compression-Shear Coupling

Mechanical behavior of chiral materials could be described on the basis of the micropolar theory. According to the micropolar theory, each material point is endowed with six degrees of freedom consisting of three rotational degrees of freedom  $\phi_i$  and three translational degrees of freedom  $u_i$ . For a general linear elastic micropolar medium with no residual stress, the relationship between the stress tensor and the strain tensor can be described as follows [7]:

$$\sigma_{ij} = A_{ijkl}\varepsilon_{kl} + B_{ijkl}\varphi_{kl}, \quad m_{ij} = C_{ijkl}\varepsilon_{kl} + D_{ijkl}\varphi_{kl} \quad (1)$$

where  $A_{ijkl}$  and  $D_{ijkl}$  represent the elastic modulus matrix and shear modulus matrix, respectively,  $B_{ijkl}$  and  $C_{lkij}$  are reciprocal each other and describe the coupling of translational to rotational degrees of freedom and vice versa,  $i, j, k$ , and  $l = 1, 2$  and  $3$ . The tensor components  $\sigma_{ij}$  and  $\varepsilon_{ij}$  connect to the generalized stress field and strain field, while the tensor components  $m_{ij}$  and  $\varphi_{ij}$  connect to the torque field and the rotational field. To achieve a coupling between translational and rotational degrees of freedom,  $B_{ijkl} = C_{lkij} \neq 0$  should be met, which means the centrosymmetry needs to be broken [7].

As for the proposed chiral structure in this study, it was obvious that the tensor components  $B_{ijkl}$  and  $C_{ijkl}$  were no longer 0. X. Li et al. deduced the twist angle per axial strain of a square tube consisting of 2D Z-shaped shear-compression coupling materials [12]. The simplified model and the corresponding boundary conditions of the 3D square tube structure subjected to axial compressive loading were shown in Fig. 2a. The top square edge could move freely while the bottom square edge was constrained ( $u_x = u_y = 0$ ). During the compression, the top square edge rotated about the center axis and consequently the moving track of its vertex followed an arc with a radius of  $\sqrt{2} \cdot a/2$ . Hence, it was inferred that the 3D square tube structure (Fig. 2a) was equivalent to 3D circular tube structure (Fig. 2b). Hence, the twist angle per axial strain of the CTC structure for small deformation could be also expressed as:

$$\lambda = \frac{1}{100} \frac{\varphi}{\varepsilon} \approx \frac{3.6}{\pi} \frac{\delta_h H}{\delta_v a} = \frac{3.6}{\pi} \frac{16H^2(a^2 + H^2) - 12H^2d^2}{16a^2(a^2 + H^2) + 12a^2d^2} \quad (2)$$

where  $\delta_h$  and  $\delta_v$  were the displacements of the 2D structure in horizontal direction and vertical direction after compression (Fig. 2a), respectively. Therefore, it could be found that a linear relation between the twist angle and the axial strain existed. However, for a large deformation, the above linear relation might not be met.

With regarding to the effective elastic moduli and compression-shear coupling of the 3D CTC structure, the corresponding 2D Z-shaped structure (Fig. 2d) was focused on, in consideration of the complexity of the 3D CTC structure. Then, the Z-shaped structure could be further expanded into a network. In this condition, the mechanical properties of the network could be equivalent to those of the square lattice

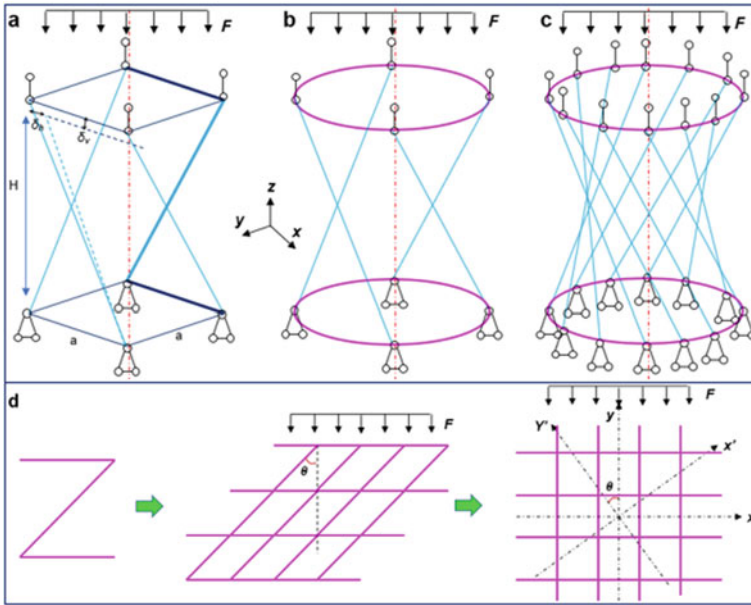


**Fig. 2** **a** The simplified 3D square tube structure; **b** The simplified 3D circular tube structure; **c** The simplified CTC structure proposed in this work; **d** 2D Z-shaped structure and the corresponding expanded network and the square lattice

under an off-axial loading. Therefore, for the effective elastic moduli of the square lattice on the principal directions, it could be expressed as [12]:

$$E_x = E_y = \frac{\pi d}{4L} E_s, \quad G_{xy} = \frac{3\pi d^3}{32L^3} E_s \tag{3}$$

where  $E_s$  was the Young's modulus of the material used in this structure. Based on the Eq. (3), the components  $Q_{ij}$  ( $i, j = 1, 2, 3$ ) of modulus tensor  $[Q_{ij}]$  could be written as:  $Q_{11} = kE_x$ ,  $Q_{22} = kE_y$ ,  $Q_{33} = G_{xy}$ ,  $Q_{12} = kv_y E_x$ ,  $Q_{21} = kv_x E_y$ , where  $k$  was  $(1 - \nu_x \nu_y)^{-1}$ . Due to the less contribution of the Poisson's ratio, the  $Q_{ij}$  was further expressed as:  $Q_{11} = E_x$ ,  $Q_{22} = E_y$ ,  $Q_{33} = G_{xy}$ ,  $Q_{12} = Q_{21} = 0$ . On the other hand, the relation between the principal modulus and off-axial modulus for 2D material or structure could be established in the following matrix form:

$$\begin{bmatrix} Q'_{11} \\ Q'_{22} \\ Q'_{12} \\ Q'_{33} \\ Q'_{13} \\ Q'_{23} \end{bmatrix} = \begin{bmatrix} m^4 & n^4 & 2m^2n^2 & 4m^2n^2 \\ n^4 & m^4 & 2m^2n^2 & 4m^2n^2 \\ m^2n^2 & m^2n^2 & m^4 + n^4 & -4m^2n^2 \\ m^2n^2 & m^2n^2 & -2m^2n^2 & (m^2 - n^2)^2 \\ m^3n & -mn^3 & mn^3 - m^3n & 2(mn^3 - m^3n) \\ mn^3 & -m^3n & m^3n - mn^3 & 2(m^3n - mn^3) \end{bmatrix} \begin{bmatrix} Q_{11} \\ Q_{22} \\ Q_{12} \\ Q_{33} \end{bmatrix} \tag{4}$$

where  $m$  and  $n$  respectively denoted  $\sin \theta$  and  $\cos \theta$ ,  $Q'_{ij}$  ( $i, j = 1, 2, 3$ ) was the component of off-axial modulus tensor. Hence, the modulus component of the network based on the 2D Z-shaped structure on the principal directions could be estimated according to the above equation.

### 3 Experimental Procedures and Numerical Simulation

#### 3.1 SLM Preparation and Mechanical Characterization

The regular spherical NiTi pre-alloyed powder with a size of 15–53  $\mu\text{m}$  and a nominal composition of Ni<sub>50.6</sub>Ti<sub>49.4</sub> was used. The SLM process was performed in the SLM-150 machine developed by NUAA. The detailed laser processing parameters included laser power of 250 W, scanning speed of 1200 mm/s, layer thickness of 30  $\mu\text{m}$ , hatch spacing of 60  $\mu\text{m}$ . Besides, the laser beam followed a zigzag pattern and then rotated by 90° for the next layer. The characterized parameters for CTC structure included  $\theta$  of 41°,  $D$  of 10.70 mm,  $d$  of 0.7 mm, and  $H$  of 8.7 mm.

The compressions were performed on a CMT5205 testing machine using a cross head velocity of 2 mm/min. For the fracture test, the test was conducted at the room temperature. For the cyclic test, the test temperature was 10°C higher than the martensite-to-austenite transformation finish temperature. All compressive tests were controlled by the displacement mode. The samples for the compressive tests kept the SLM-built condition but the lubricating oil was added. Besides, a Tungsten filament scanning electron microscope was used to observe the fracture surface.

#### 3.2 Numerical Simulation

Deformation behavior of the CTC structure was simulated based on the ANSYS LS-DYNA commercial software. Two parallel structural steel plates were added as rigid bodies, attaching to the top and the bottom surface of the CTC structure, respectively. Both the upper plate and the lower plate were meshed by the hex dominant with a size of 0.5 mm, while the CTC structure was meshed by tetrahedrons with a size of 0.2 mm. The coefficient of friction in the contact region of the plate and the CTC structure was set as 0.1. The material of the CTC structure model was set as NiTi alloy and the corresponding material properties included mass density of 6500 kg/m<sup>3</sup>, Young's modulus of 69 GPa, and Poisson's ratio of 0.40. Subsequently, the loading process was controlled by the displacement mode with a moving velocity of 2 mm/min.

## 4 Results and Discussion

### 4.1 Compressive Fracture Process and Twisting Behavior

Figure 3 shows the compressive fracture process and the corresponding force-displacement curve as well as the fracture morphology of SLM-fabricated NiTi-based CTC structure. It was found that as the axial load increased gradually, the top circular side occurred to rotate around the center axis (Fig. 3a). Apparent twisting deformation of the inclined struts could be observed. Relationship between the load and the displacement was plotted in Fig. 3b, from which the measured force values could be identified corresponding to Fig. 3a. According to the Fig. 4b, the whole deformation process could be divided into six stages, including the linear elastic stage (0–0.3 mm), the first plateau stage (0.3–0.9 mm), the hardening stage (0.9–1.2 mm), the second plateau stage (1.2–3.3 mm), the densification stage (3.3–4.2 mm) and the collapse stage (> 4.2 mm). As the accumulated displacement reached ~4.2 mm, the inclined strut occurred to break and the failure position emerged at the connected points between the struts and the top or bottom circular side (Fig. 3a). The corresponding fractured surface morphology of the broken strut is displayed in Fig. 3c and d. The fibrous morphology with gray and rough surface indicated that an apparent shear tough fracture was obtained.

To better understand the deformation mechanism of the CTC structure, the predicted stress contour images of the CTC structure at different strains are given in Fig. 4. It showed that the maximum stress emerging in the structure reached 604.5 MPa when the strain was 3.448% (0.3 mm). But the stress level in the most part of the inclined struts was in a range of 186.9–365.9 MPa. As the strain increased to 6.896% (0.6 mm), the average stress level in the inclined struts increased to 490.5 MPa. According to our previous investigations [13], the critical stress  $\sigma_{cm}$

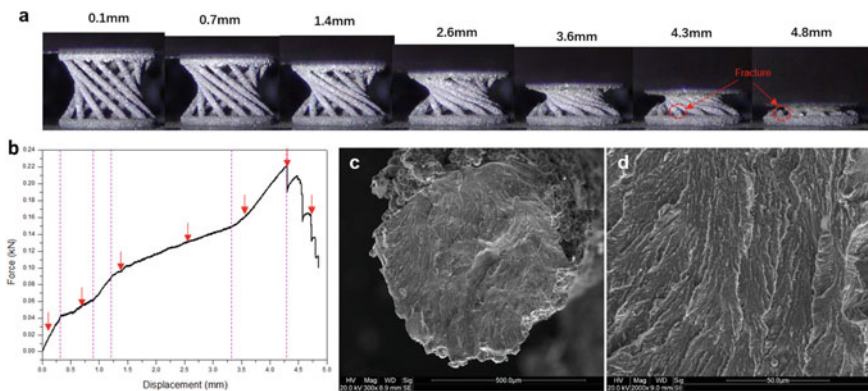


**Fig. 3** a The CTC structure at various displacements; b The force-displacement curve; c and d The fracture surface morphology of the inclined strut at low and high magnification

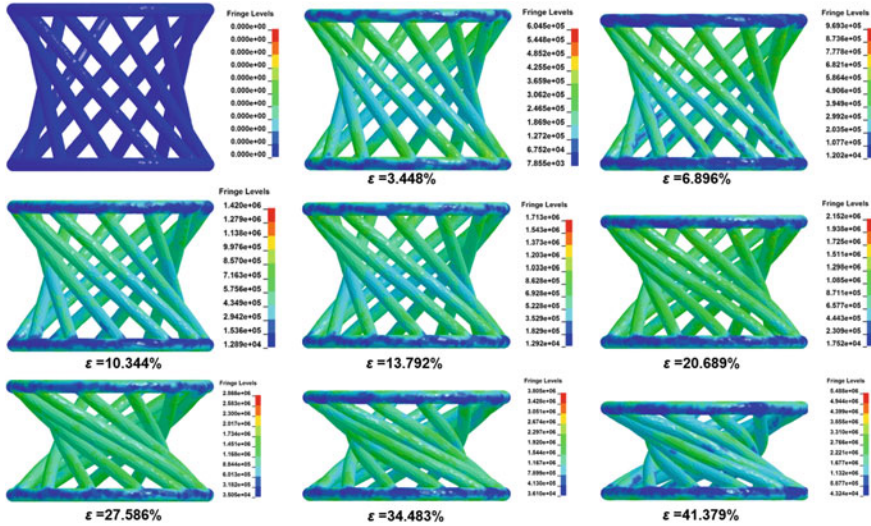
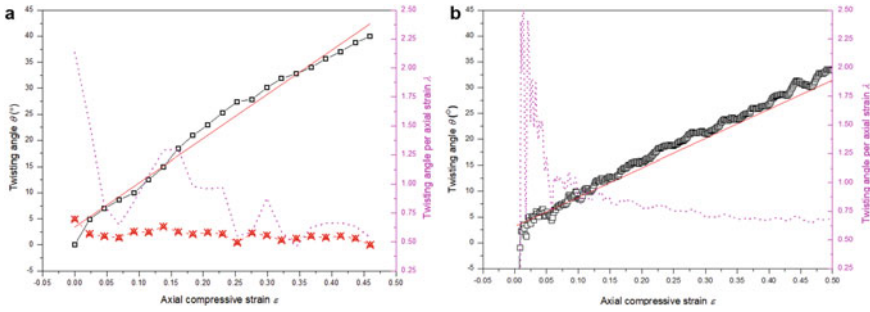


Fig. 4 Stress evolution at different accumulated axial strain (The unit was kPa)

for martensite transformation fluctuated at around 400 MPa. That meant the formation of the first plateau stage (0.3–0.9 mm) could be mainly attributed to stress-induced martensitic transformation. Besides, localized bending could be observed at the regions close to two ends of the struts, further leading to inhomogeneous stress distribution which was believed to account for the plateau stage with a gentle slope. With the strain further increasing to 10.344% (0.9 mm), almost all region of these inclined struts exhibited a high stress level more than the  $\sigma_{cm}$ . In this condition, a strain hardening occurred when the detwinning or twinning to more favorable orientations started to dominate during the deformation of these struts. At an accumulated strain of 13.793% (1.2 mm), localized bending in the regions close to two ends of the struts became more apparent, inducing a higher stress level of 1203–1713 MPa and more inhomogeneous stress distribution. In this condition, the strain hardening saturated and slip started to play a main role. The yield effect in some stress concentration regions occurred and meanwhile the yield area gradually increased with the strain increasing, thus contributing to the second plateau stage with a gentle slope. As the strain was more than 34.483% (3 mm), it was found that the predicted maximum stress within the structure went up rapidly with the strain. All inclined struts with a large twisting deformation were squeezed together, thus leading to a remarkable increase of the structure’s modulus and resultant large slope of the force-displacement curve in Fig. 3b. Hence, this stage was characterized as the densification stage.

Furthermore, twisting deformation of the CTC structure during the loading was analyzed in details (Fig. 5). The twisting angle change was plotted as a function of axial compressive strain, according to the experimental results (Fig. 5a) and simulated results (Fig. 5b). The relationships between the twisting angle and the axial compressive strain could be roughly considered as a linear one. Although there existed a little





**Fig. 5** The relationship between the axial compressive strain and the twisting angle. **a** Experimental results; **b** Simulated results

difference in the slopes of their fitted lines, it was found that the change trend of the twisting angle with the axial strain was highly consistent in these two cases. Within a small deformation ( $< 4.6\%$ ), the twist angle per axial strain  $\lambda$  decreased continuously from  $2.13^\circ/\%$  to  $0.81^\circ/\%$  with the strain increased, based on the experimental data. It also showed that the  $\lambda$  was  $1.52^\circ/\%$  when the strain reached  $2.3\%$ . For the simulation result, the predicted  $\lambda$  fluctuated in a range of  $1.1\text{--}2.5^\circ/\%$  within a strain zone of  $0\text{--}4.6\%$  and stabilized at around  $1.6^\circ/\%$  within a strain zone of  $2.3\text{--}4.4\%$ . On the other hand, according to the Eq. (2) in Sect. 2.2, the  $\lambda$  could be estimated as  $1.5068^\circ/\%$ . Hence, it was found that the  $\lambda$  obtained by three different methods was roughly consistent, which also suggested that the simulation results were convinced. Besides, from the Eq. (2), it further predicted that the  $\lambda$  would decline continuously with the strain. The corresponding experimental and simulated results also showed the similar change trend. For the large deformation case, the Eq. (2) was limited. From the experimental and simulated results, it was observed that the overall trend of the  $\lambda$  with the strain declined rapidly and finally stabilized at around  $0.6^\circ/\%$ . According to the relation (4), when the angle  $\theta$  was in a range of  $(0, \pi/4)$ , the compressive modulus component decreased monotonically with the  $\theta$ , while the shear modulus component increased monotonically with the  $\theta$ ; when the angle  $\theta$  was in a range of  $(\pi/4, \pi/2)$ , the opposite condition emerged. Considering that the initial angle  $\theta$  was  $41^\circ$ , an axial strain increment of  $\sim 13\%$  was required before the  $\theta$  increased to  $45^\circ$ . Hence, in the initial  $\sim 13\%$  strain, the axial deformation became relatively easy but the shear deformation became difficult, which also well accounted for the reason of a rapid decline for the  $\lambda$  in the small deformation period. Note that, for the experiment result, it showed that the  $\lambda$  experienced an apparently increasing period within  $7\text{--}15\%$  strain, which could be attributed to the occurrence of distortion in the struts.

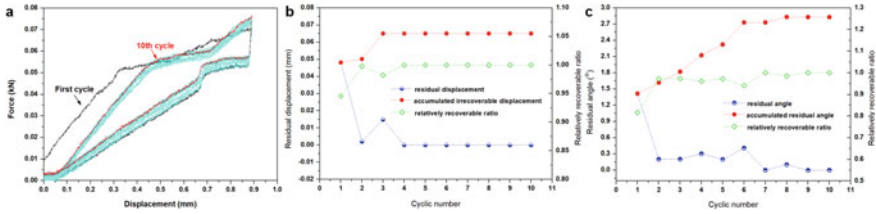


**Fig. 6** **a** Cyclic compressive force-displacement curves; **b** and **c** The residual displacement or twisting angle (blue color), accumulated irrecoverable displacement or twisting angle (red color) and their relatively recoverable ratio (green color) as a function of cyclic number

## 4.2 Cyclic Compressive Loading-Unloading and Twisting Recoverability

In view of the reversible martensitic transformation in NiTi alloys, the cyclic compressive behavior of SLM-fabricated NiTi-based CTC structure was further assessed. Ten loading-unloading cycles were recorded at the same displacement of 0.89 mm (10.2% strain), as shown in Fig. 6a. The corresponding recoverable behavior was mainly focused on (Fig. 6b and c). For the first cycle, a relatively larger residual displacement was obtained, thus leading to a relatively low recoverable ratio of 0.94. In this condition, grain orientations within the structure were relatively random, prone to trigger the slip and irreversible twinning. As the cyclic number increased, the orientation texture along the loading direction got gradually enhanced, consequently contributing to an increased recoverable ratio. When the cyclic number came to four, the relatively recoverable rate for each cycle started to stabilize at around 1 and the corresponding accumulated irrecoverable displacement was kept at 0.065 mm. The recoverable behavior of the twisting angle after unloading was mainly controlled by the reversible axial displacement. But some differences could be also observed. From Fig. 6c, the accumulated residual twisting angle continuously rose from the first cycle to the sixth cycle, although the residual displacement had decreased to zero since the fourth cycle. The above difference might be attributed to inevitable fictional effect between the circular side and the compression plate when the twisting deformation occurred. After the sixth cycle, multiply repeated frictions efficiently reduced the coefficient of friction, thus contributing to a small residual twisting angle.

## 5 Conclusion

In this work, a new compression-induced-twisting structure, namely NiTi-based circular tube chiral (CTC) structure was proposed and manufactured by SLM. The compression fracture test and cyclic compression test were performed, respectively, showing an excellent large deformation capacity and a high recoverable rate. The

compressive deformation mechanism and the corresponding compression-induced-twisting behavior of NiTi-based CTC structure got disclosed in detail, based on the experimental method, simulation approach, and theoretical calculation.

**Acknowledgements** This work was supported by the financial support from the National Natural Science Foundation of China (No. 51735005 and U1930207). The authors also wish to thank ASTUTE 2020 (Advanced Sustainable Manufacturing Technologies). This operation, supporting manufacturing companies across Wales, has been part-funded by the European Regional Development Fund through the Welsh Government and the participating Higher Education Institutions. Besides, Chenglong Ma specially thanks for the financial support from the UK-China Joint Research and Innovation Partnership Fund PhD Placement Programme and the Funding for Outstanding Doctoral Dissertation in NUAU (No. BCXJ17-05).

## References

1. Wu, W., Hu, W., Qian, G., Liao, H., Xu, X., Berto, F.: Mechanical design and multifunctional applications of chiral mechanical metamaterials: a review. *Mater. Des.* **180**, 107950 (2019)
2. Avnir, D., Huylebrouck, D.: On left and right: chirality in architecture. *Nexus Netw. J.* **15**(1), 171–182 (2013)
3. Lorato, A., Innocenti, P., Scarpa, F., Alderson, A., Alderson, K.L., Zied, K.M.: The transverse elastic properties of chiral honeycombs. *Compos. Sci. Technol.* **70**, 1057–1063 (2010)
4. Li, D.C., Zhao, S.W.: A review of modelling and analysis of morphing wings. *Prog. Aerosp. Sci.* **100**, 46–62 (2018)
5. Wu, W.W., Song, X.K., Liang, J.: Mechanical properties of anti-tetrachiral auxetic stents. *Compos. Struct.* **185**, 381–392 (2018)
6. Fu, H.R., Nan, K.W., Bai, W.B.: Morphable 3D mesostructures and microelectronic devices by multistable buckling mechanics. *Nat. Mat.* **17**, 268–276 (2018)
7. Fernandez-Corbaton, I., Rocks Corbatontuhl, C., Ziemke, P., Gumbsch, P., Albiez, A., Schwaiger, R., Frenzel, T., Kadic, M., Wegener, M.: New twists of 3D chiral metamaterials. *Adv. Mater.* **31**, 1807742 (2019)
8. Han, Q., Gu, Y., Setchi, R., Lacan, F., Johnston, R., Evans, S.L., Yang, S.: Additive manufacturing of high-strength crack-free Ni-based Hastelloy X superalloy. *Addit. Manuf.* **30**, 100919 (2019)
9. Gómez, S., Vlad, M.D., López, J., Fernández, E.: Design and properties of 3D scaffolds for bone tissue engineering. *Acta Biomater.* **42**, 341–350 (2016)
10. Zheng, X., Smith, W., Jackson, J., Moran, B., Cui, H., Chen, D., Ye, J., Fang, N., Rodriguez, N., Weisgraber, T., Spadaccini, C.M.: Multiscale metallic metamaterials. *Nat. Mater.* **15**, 1100 (2016)
11. <https://commons.wikimedia.org/wiki/File:Spiranthes-cernual.web.jpg>
12. Li, X., Yang, Z., Lu, Z.: Design 3D metamaterials with compression-induced-twisting characteristics using shear–compression coupling effects. *Extreme Mech. Lett.* **29**, 100471 (2019)
13. Ma, C., Gu, D., Lin, K., Dai, D., Xia, M., Yang, J., Wang, H.: Selective laser melting additive manufacturing of cancer pagurus’s claw inspired bionic structures with high strength and toughness. *Appl. Surf. Sci.* **469**, 647–656 (2019)

# Energy Utilization Analysis and Optimization of Corrective Insoles Manufactured by 3D Printing



M. J. Kirby, Rachel Johnson, A. Rees, and C. A. Griffiths

**Abstract** The foot orthotic insole market is forecast to surpass a value of 3.6 billion USD by 2021. This vast industry continues to rely on foam milling and other subtractive methods of manufacturing, which have proven to be wasteful and inefficient. Leaps in digital manufacturing have enabled the technology to enter a plethora of industries, with the promise of increased customization accompanied with reduced waste generation. Despite boasting these valuable traits, the explosive proliferation of 3D printing in conjunction with mounting pressure to incorporate sustainable practices, means that research must be focused on maximizing the material and energy efficiency of the technology. This paper employs a Design of Experiments (DoE) approach for the optimization of two prefabricated insoles, adjusting percentage infill and layer height to obtain data regarding the effects of these parameters on print time, filament usage volume, and energy consumption. Key conclusions formed from the study were that infill density is the dominant factor effecting material consumption and power usage, whereas layer height has the greatest influence on production time. The data presented in this study has the potential to aid not only in the development of mass producible additive manufactured (AM) insoles, but also to advance the understanding of the environmental impact of AM technologies.

## 1 Introduction

### 1.1 Anatomical Insoles

Anatomical insoles are functional additions to any shoe, used primarily to apply a force on the body to counteract the effects of a biomechanical disorder; for example flat feet, which can be hereditary, or simply caused by a foot or ankle injury [1]. Deformities such as this often have a transitive effect on the rest of the supporting

---

M. J. Kirby · R. Johnson · A. Rees (✉) · C. A. Griffiths  
College of Engineering, Swansea University, Swansea, UK  
e-mail: [andrew.rees@swansea.ac.uk](mailto:andrew.rees@swansea.ac.uk)

joints above the foot/ankle, also known as the kinetic chain, manifesting as symptomatic conditions such as shin splints, Achilles tendonitis, and plantar fasciitis. Insoles secondary beneficial aspect is that they provide improved cushioning when compared to the original factory shoe insole, alleviating some of the pain associated with the impact caused by walking [2].

Traditional methods of manufacturing insoles, like Computer Numerical Control (CNC) foam milling, continue to be the industry standard, despite the rapid proliferation of three-dimensional (3D) printing; a substantially more customizable, less wasteful and in many ways, cheaper alternative [3, 4]. One of the reasons for the delayed uptake of 3D printing is that suitable materials with comparable mechanical properties to the Ethylene-vinyl acetate (EVA) foam employed in traditional milling processes are not yet readily available to the extent that would be required for the mass production of insoles. A pertinent study conducted by Salles and Gyi in 2013 compared the functionality of traditionally manufactured insoles with additive manufacturing (AM) insoles [5]. One of their conclusions was that of the limited array of materials available for AM, none displayed the cushioning properties required to rival their machined counterparts.

The relevance of reducing the underpinning manufacturing energy and material usage in the orthotic insole industry can be evidenced in the expansion of the global foot orthotic insole market value increased from approximately 2.7 billion USD in 2015 to over 3.1 billion USD in 2018 [6]. This figure is forecast to grow to almost 3.7 billion USD by 2021 [6].

The aim of this study, through the employment of a Design of Experiments (DoE) approach, is to quantify the energy and material usage for the manufacture of anatomical insoles through 3D printing.

## **2 State of the Art**

### ***2.1 Orthotic Insole Manufacturing Techniques and Comparison***

While a diverse range of natural and synthetic materials are used in the manufacture of foot orthoses, they are often categorized into three main types; soft, semi-rigid, and rigid. The recent development of advanced materials, such as carbon graphite fibre and silicon, have allowed the fabrication of orthosis devices to progress at a rapid rate, as well as the corresponding manufacturing techniques.

## 2.2 3D Printing Insoles

With use of customization and control as the experimental conditions, Salles et al., produced AM manufactured insoles to be tested on study participants for 3 months. In particular, participants were blindly assigned either a personalized ‘glove fit’ insole mimicking the geometry of their feet, while the remaining participants were given control insoles that copied the geometry of the test shoe’s factory insole. The research found that the ‘glove fit’ insoles considerably improved the comfort in the heel area and general fit of the participants during running, when compared to the control article. This was done by minimizing ankle dorsiflexion, thus reducing the peak pressure at the point of impact with the ground. However, the study observed that discomfort under the arch persisted throughout the test period. The research concluded that with the advancement of 3D printing technology, AM manufactured personalized insoles can be used as an affordable and beneficial addition to footwear [5].

In contrast, Davia-Aracil et al., conducted research into a developing an innovative programme focused entirely on simplifying the design and production of AM manufactured personalized insoles, where users could specify desired support dimensions. Through this, the researchers concluded that although the footwear industry could benefit hugely from additive manufacturing, it currently lacks the CAD tools and experience to exploit the technological advancements of 3D printing [7].

## 2.3 Sustainable AM Techniques

The quality and functionality of components have been the predominant focus of research into the optimization of manufacturing processes over recent decades, while the energy efficiency and subsequent environmental impact of said processes have been somewhat overlooked. However, as the emphasis on sustainable production grows, with the creation of laws and standards such as ISO 14000, Researchers and Engineers are being put under increasing pressure to drastically improve environmental management [8]. By incorporating an additional design stage into the Life Cycle Assessment (LCA) of a product with the sole purpose of reducing AM processes’ environment impact, Tang et al., were able to compare the CO<sub>2</sub> produced by CNC and AM processes. The research showed that, for the same product, AM techniques produce considerably less CO<sub>2</sub> and have lower energy consumption than CNC milling [9].

In a study by Peng it was concluded that 3D printing can be optimized through multi-objective process optimization with an emphasis on ‘green’ performance. In particular, the research found that through the use of model-based energy evaluation built on initial CAD models, optimal energy utilization can only be achieved during all stages of manufacture [10].

Griffiths et al., establishing a Design of Experiments (DoE) approach to optimizing additive manufacturing techniques. In particular, the investigation studied the efficacy of inputting environmentally conscious build parameters into a FDM process to analyze the response. The research concludes that layer height is the most significant parameter with regards to energy consumption and production time [11]. Additional research supporting this concept was introduced by Mognol et al., who focused on determining a set of constraints with the purpose of reducing the electrical energy consumption of three AM processes [12].

The aim of this study, through the employment of a Design of Experiments (DoE) approach, is to quantify the energy and material usage for the manufacture of anatomical insoles through 3D printing.

### 3 Methodology

#### 3.1 Materials and Equipment

To establish the optimal build parameter settings, percentage infill and layer height will be varied to minimize the energy and material consumption of the FDM manufacturing process. To ensure an informed assessment of the build parameter influence is achieved, two distinct prefabricated insoles geometries have been selected for testing. In particular, a 7 mm Heel Lift and a  $\frac{3}{4}$  length Heel Cup Arch Support (Fig. 1).

The chosen material for the tests, Polylactic acid (PLA), is a biodegradable polymer manufactured from plants including sugarcane and corn, and is one of the most frequently used materials in printing technologies.

The AM equipment used was an Ultimaker 2 + (Fig. 2); a printer that uses Fused Filament Fabrication (FFF) technology. The printer used 2.85 mm diameter PLA filament. The remaining key technical characteristics of the Ultimaker 2 + are displayed in Table 1.



**Fig. 1** Heel lift (Left) and arch support (Right)

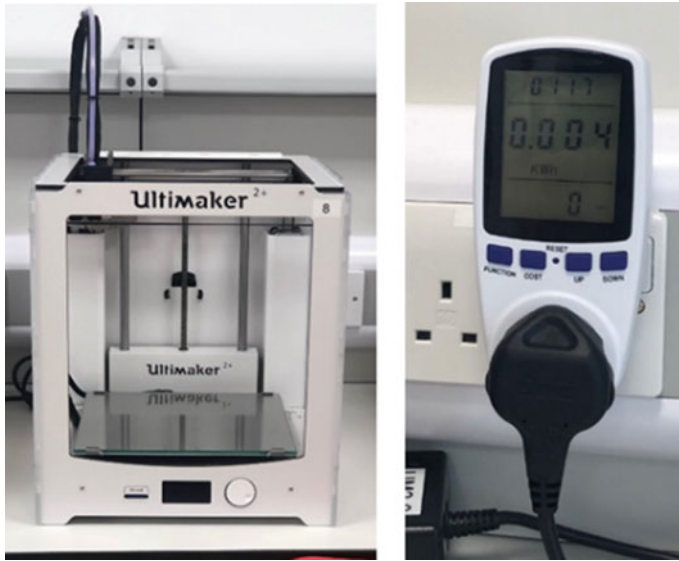


**Fig. 2** Ultimaker 2 + (left) and power usage meter (Right)

**Table 1** Ultimaker 2 + specification [13]

Characteristic	Value
Build volume (mm <sup>3</sup> )	223 × 223 × 205
Build speed (mm <sup>3</sup> /s)	< 16
Nozzle diameter (mm)	0.4
XYZ resolution (μm)	12.5(x), 12.5(y), 5(z)

To facilitate the measurement of power consumption throughout each of the tests, a power usage meter with the ability to measure cumulative power intake was required. The power usage meter chosen, pictured in Fig. 3, measured the total energy usage

### 3.2 Design of Experiments

Through a Design of Experiments (DoE) the processing variables percentage infill and layer height were adjusted. In addition, a control experiment (A0 and H0) was conducted whereby an infill of 100%, 0.15 mm layer height, 0.7 mm shell thickness, a shell number of 2, and a print speed of 50 mm/s were used. Table 2 displays the DoE array of combinations used within the experiments. Also, a triangular infill pattern was used throughout all tests due to its high ratio of perpendicular compressive strength to print time, when compared to other infill patterns [14, 15].



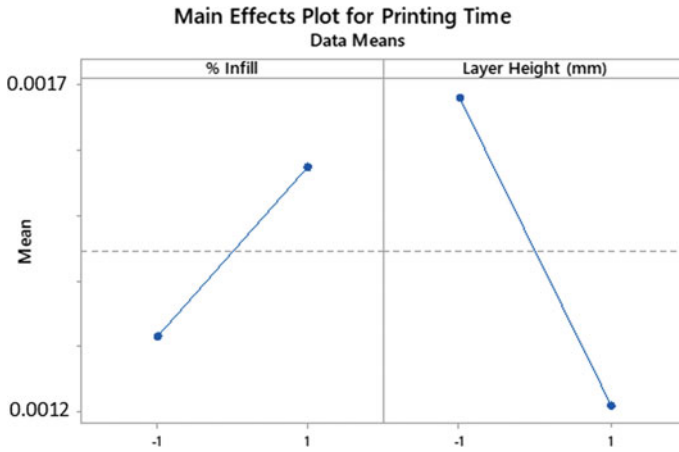


Fig. 3 Heel lift

Table 2 Design of experiments for each insole

Case ID	% Infill	% Infill Plot Key	Layer Height (mm)	Layer Height Plot Key
A0	100	N/A	0.15	N/A
A1	40	1	0.15	-1
A2	40	1	0.2	1
A3	20	-1	0.15	-1
A4	20	-1	0.2	1
H0	100	N/A	0.15	N/A
H1	60	1	0.15	1
H2	60	1	0.1	-1
H3	10	-1	0.15	1
H4	10	-1	0.1	-1

## 4 Results and Discussion

### 4.1 Printing Time

For the Heel Lift component, the experimental results suggest that percentage infill and layer height have a significant effect on the overall print time. The Main Effects plots displayed in Figs. 3 and 4 highlight that, for both specimens, a greater layer height corresponds to a decrease in print time. This is supported by a 27.83% average reduction in production time for the Heel Lift between the two tested levels. This can be attributed to a reduction in the quantity of layers required to produce an equivalent structure.

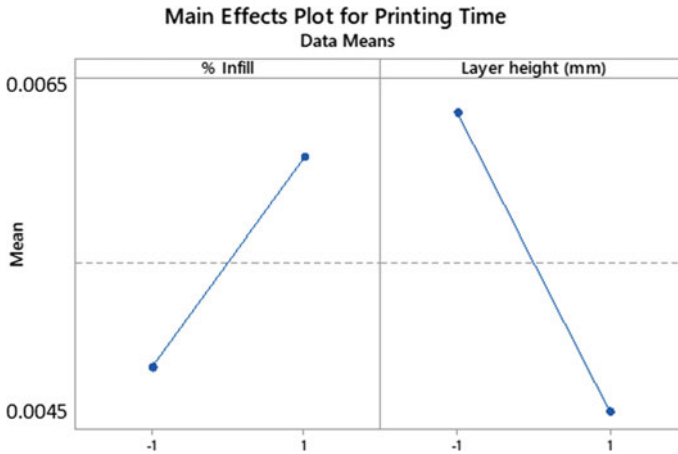


**Fig. 4** Arch support

A very similar outcome can be observed from the Arch Support data involving print time. This is referring to layer height being the critical factor, exhibiting a 29.49% drop in print time between 0.15 mm layer thickness and 0.2 mm. Varying the percentage infill had a sizeable yet reduced influence of 21.23% and 16.33% for the Arch Support and Heel Lift respectively. Since nozzle diameter and print speed were kept constant throughout the experiment, it can be deduced that the overall increase in density of the printed structure caused by increased infill resulted in a greater amount of PLA required, and consequently lengthened the production time (Fig. 4).

## 4.2 Filament Usage

The specific factor causing the most significant change in filament usage volume in both specimens is percentage infill, by a substantial margin. This is displayed clearly in Figs. 5 and 6, and has been calculated to have caused a 27.08% and 30.88% reduction in the Heel Lift and Arch Support respectively. Hence a decrease in the percentage infill will result in a decrease in material consumption, but will also have damaging effects on the mechanical properties of the printed part.

However, modifying the layer height evidently has a negligible effect on material usage, with the variation from 0.1 mm to 0.15 mm resulting in a 2.77% increase for the Heel Lift, whereas the change from 0.15 mm to 0.2 mm produced a 3.64% decrease in filament consumption for the Arch Support. This can be attributed to the fact that increasing layer height causes filament extrusion rate to increase, up to the nozzle diameter.

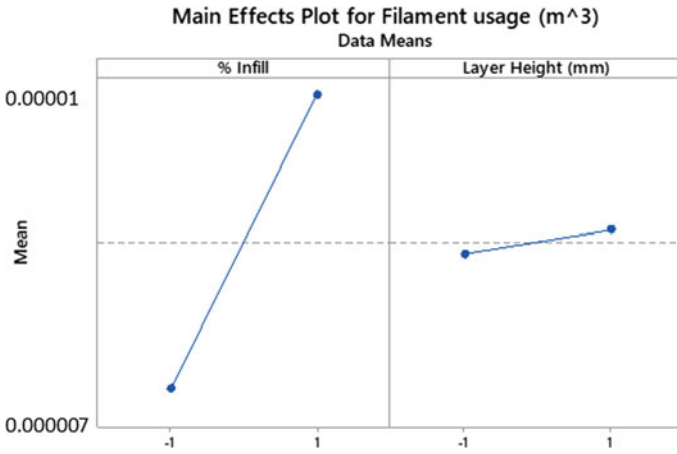


Fig. 5 Heel lift

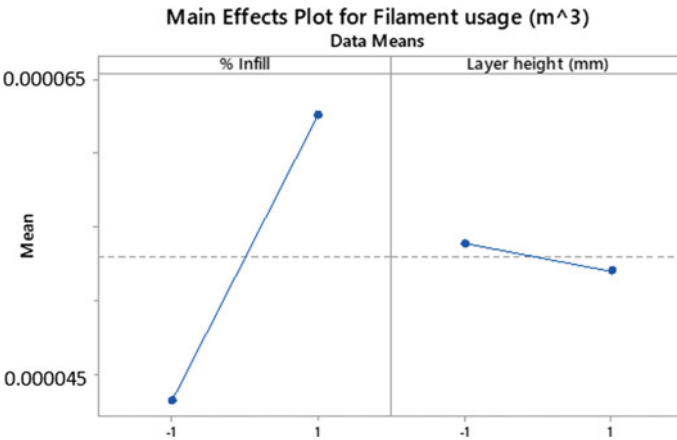


Fig. 6 Arch support

Although it has a minor influence, and would require testing in isolation to provide a clearer outcome, one aspect of the data regarding layer height warrants mentioning. Figures 9 and 10 show that for both insoles, a layer thickness of 0.15 mm increased the filament usage volume. As a result of this, the critical settings for reducing filament usage are 10% infill and 0.1 mm layer height for the Heel Lift, while 20% infill along with a 0.2 mm layer thickness are recommended for the Arch Support.

### 4.3 Power Usage

With respect to energy consumption, inconsistencies are present in the effects of both build parameters. The key factor for the Heel Lift is layer height (Fig. 7) with a reduction of 27.16%. This is compared to a 31.01% drop due to percentage infill having a greater impact on the Arch Support (Fig. 8). As stated in Sect. 4.1, increasing the layer height cuts the print time due to a reduction in the number of layers required to reach a specified part height. A lower print time causes a subsequent decline in energy consumption, and supports the conclusion presented by Griffiths et al. [11]. The impact of percentage infill on the Arch Support indicates that the increased

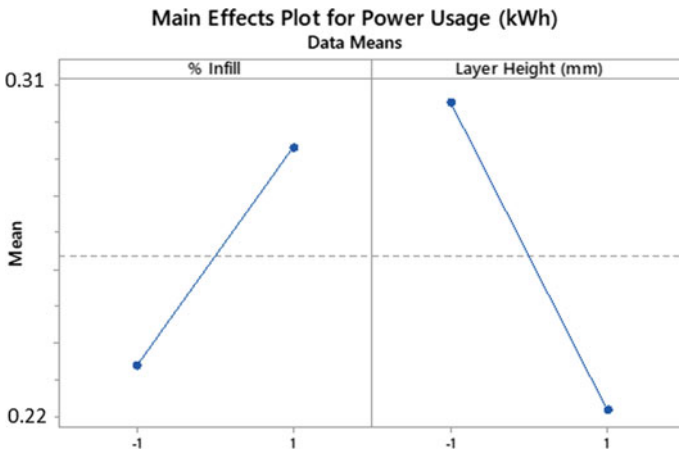


Fig. 7 Heel lift

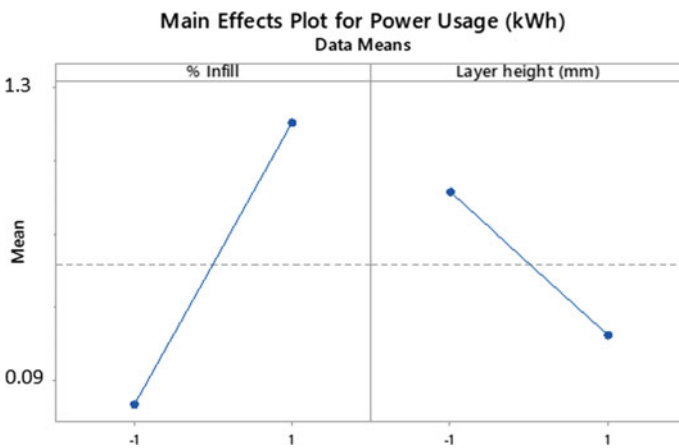


Fig. 8 Arch support

**Table 3** Experimental Data for All Cases

Case ID	% Infill	Layer height (mm)	Printing time (d:h:m)	Filament usage (m <sup>3</sup> )	Power usage (kWh)
A0	<b>100</b>	<b>0.15</b>	<b>01:06:55</b>	<b>0.000119805</b>	<b>3.765</b>
A1	40	0.15	00:10:10	0.000063411	1.285
A2	40	0.2	00:07:15	0.000061816	1.216
A3	20	0.15	00:08:03	0.000044337	1.027
A4	20	0.2	00:05:37	0.000042232	0.706
<b>H0</b>	<b>100</b>	<b>0.15</b>	<b>00:02:54</b>	<b>0.000011164</b>	<b>0.394</b>
H1	60	0.15	00:01:53	0.000010079	0.246
H2	60	0.1	00:02:39	0.000009952	0.340
H3	10	0.15	00:01:36	0.000007464	0.198
H4	10	0.1	00:02:11	0.000007145	0.270

number of direction changes as a result of a higher infill density causes a simultaneous increase in energy consumption.

Focusing on the Arch Support, considerable disparities were observed in the effect of layer height. At 40% infill, it experienced only a 5.37% reduction in energy consumption between a 0.15 mm and 0.2 mm layer height (Table 3). However, for the same change in layer height but at 20% infill, this difference was 31.26%. Corresponding values of 27.65% and 26.67% were obtained for the Heel Lift; a difference of only 0.98%. This is compared to the 25.89% difference for the Arch Support, displaying the impact of interacting parameters on power consumption, irrespective of the singular build parameters used.

For both samples, percentage infill is optimized with the lower value, and works in conjunction with a higher layer height to minimize energy usage. The optimal settings for each part, of those tested, are as follows; 10% infill and 0.15 mm layer height for the Heel Lift, while the Arch Support would benefit from a 20% infill and 0.2 mm layer height.

## 5 Conclusion

The key objectives of this paper is to investigate the optimal settings of build parameters in the manufacture of anatomical insoles by 3D printing in a bid to improve energy and material efficiency. Through conducting a DoE approach the following conclusions can be drawn:

- When printing the Arch Support a considerable resultant difference was observed in energy usage when utilizing identical layer heights when modifying the level of infill density. This leads to a conclusion that interactions are present between the build parameters.

- Layer height proved to be the most influential factor with respect to print time. A higher layer thickness results in less layers, or greater z-axis increments required to achieve an equivalent part thickness, thus reducing the production time.
- When optimizing for material consumption the Heel Lift must be manufactured with a 0.1 mm layer height at 10% infill, while the Arch Support should use 20% infill with a 0.2 mm layer thickness.
- For optimal energy consumption the Heel Lift requires a 10% infill with a 0.15 mm layer height. The Arch Support requires a 20% infill and a layer height of 0.2 mm.

## 6 Future Consideration

Performing tensile tests on the printed specimens could be used to further expand the corrective aspect of the insoles whereby additional functionality could be gained by varying the resultant mechanical properties to align with the varying biomechanical requirements of the end user.

**Acknowledgements** The author would like to acknowledge the financial support of the College of Engineering, Swansea University to facilitate conference funding.

## References

1. Crabtree, P., Dhokia, V., Newman, S., Ansell, M.: Manufacturing methodology for personalised symptom-specific sports insoles. *Robot. Comput.-Integr. Manuf.* **25**(6), 972–979 (2009)
2. Tuff, S.: Do you really need an \$800 custom insole? [Internet]. *Nytimes.com*. (2019) [cited 10 Dec 2018]. Available from <https://www.nytimes.com/2006/06/22/fashion/thursdaystyles/22Fitness.html>
3. Lipson, H., Kurman, M.: In: *Fabricated: The New World of 3D Printing*. Indianapolis, Ind. J. (2013)
4. Gebler, M., Schoot Uiterkamp, A., Visser, C.: A global sustainability perspective on 3D printing technologies. *Energ. Policy* **74**, 158–167 (2014)
5. Salles, A., Gyi, D.: An evaluation of personalised insoles developed using additive manufacturing. *J. Sports Sci.* **31**(4), 442–450 (2013)
6. Foot orthotic insoles market size globally 2015–2021| Statistic [Internet]. *Statista*. (2019) [cited 13 Feb 2019]. Available from <https://www.statista.com/statistics/888548/foot-orthotic-insoles-market-size-global/>
7. Davia-Aracil, M., Hinojo-Pérez, J., Jimeno-Morenilla, A., Mora-Mora, H.: 3D printing of functional anatomical insoles. *Comput. Ind.* **95**, 38–53 (2018)
8. International Standards Organization (ISO). *ISO 14000: Environmental Management*. Geneva, ISO (2015)
9. Tang, Y., Mak, K., Zhao, Y.: A framework to reduce product environmental impact through design optimization for additive manufacturing. *J. Clean. Prod.* **137**, 1560–1572 (2016)
10. Peng, T.: Analysis of energy utilization in 3D printing processes. *Procedia CIRP.* **40**, 62–67 (2016)
11. Griffiths, C., Howarth, J., De Almeida-Rowbotham, G., Rees, A., Kerton, R.: A design of experiments approach for the optimisation of energy and waste during the production of parts manufactured by 3D printing. *J. Clean. Prod.* **139**, 74–85 (2016)

12. Mognol, P., Lopicart, D., Perry, N.: Rapid prototyping: energy and environment in the spotlight. *Rapid Prototyping J.* **12**(1), 26–34 (2006)
13. Ultimaker 2 + Specification sheet [Internet]: Ultimaker (2013) [cited 13 Feb 2019]. Available from <https://ultimaker.com/file/download/productgroup/Ultimaker%20+%20and%20Ultimaker%20%20Extended+%20specification%20sheet.pdf/5b924f26322d6.pdf>
14. Dudescu, C., Racz, L.: Effects of raster orientation, infill rate and infill pattern on the mechanical properties of 3d printed materials. *ACTA Univ. Cibiniensis.* **69**(1), 23–30 (2017)
15. TESTING 3D printed Infill patterns for their strength [Internet]: YouTube. (2018) [cited 20 Mar 2019]. Available from <https://www.youtube.com/watch?v=upELI0HmzHc>
16. Kuznetsov, V., Solonin, A., Tavitov, A., Urzhumtsev, O., Vakulik, A.: Increasing of strength of FDM (FFF) 3D printed parts by influencing on temperature-related parameters < strong > </strong > of the Process (2018)
17. Gunaydin, K.: The effect of layer thickness to the tensile stress: experimental studies. In: *International Congress on 3d Printing (Additive Manufacturing) Technologies and Digital Industry.* Istanbul (2018)

# Effect of Remelting Process on Surface Quality and Tensile Behaviour of a Maraging Steel Manufactured by Selective Laser Melting



Jun Song, Qian Tang, Qixiang Feng, Shuai Ma, Quanquan Han, and Rossitza Setchi

**Abstract** Selective laser melting (SLM) of 18Ni-300 maraging steel is of substantial interest due to its wide application as a mould material in automotive sectors. Selective laser remelting (SLRM) is often employed during SLM, which offers the potential to improve quality of the metallic parts fabricated by SLM. This study investigated the effect of the remelting process on the surface quality and tensile strength of 18Ni-300 maraging steel manufactured by SLM. The experimental results demonstrated that the remelting process was found to contribute to a smoother surface morphology on the top surface and no obvious observed difference in the side surface morphology. The SLM-built and SLRM-built samples exhibited the Ra roughness values of  $3.11 \pm 0.31 \mu\text{m}$  and  $3.44 \pm 0.48 \mu\text{m}$ , respectively, which showed no significant difference. The Ra values on the side surface increased from  $7.76 \pm 0.25 \mu\text{m}$  to  $11.57 \pm 3.44 \mu\text{m}$  after remelting. This was because more powder particles were exposed to molten pools during remelting. In addition, the yield strength increased from  $890 \pm 27 \text{ MPa}$  to  $938 \pm 36 \text{ MPa}$  after the remelting process, whereas the ultimate tensile strength remained at the same level. The SLM-built and SLRM-built samples achieved the ultimate tensile strength values of  $1068 \pm 12 \text{ MPa}$  and  $1070 \pm 19 \text{ MPa}$ , respectively. Moreover, both processing conditions showed a ductile fracture mode. These significant findings indicate the possibility of combining SLM and selective laser remelting to produce better performing 18Ni-300 maraging steel components.

## 1 Introduction

Selective laser melting (SLM), as a kind of laser powder bed fusion-additive manufacturing technique, offers the ability to manufacture metallic components directly

---

J. Song · Q. Tang (✉) · Q. Feng · S. Ma  
State Key Laboratory of Mechanical Transmissions, Chongqing University, Chongqing 400044, China  
e-mail: [tqcqu@cqu.edu.cn](mailto:tqcqu@cqu.edu.cn)

Q. Han · R. Setchi  
Cardiff School of Engineering, Cardiff University, Cardiff CF24 3AA, UK



from the metallic powder feedstock in a layer-by-layer manner, which has been widely employed in automotive, aerospace and biomedical domains [1]. The obvious advantages of the SLM process are that this advanced technique has no limitations on design freedom and can manufacture more complex structures compared with conventional techniques like casting, forging, or machining [2]. Many researchers have demonstrated that a large range of metallic components have been successfully manufactured using SLM, including steels [3, 4], titanium [5], superalloys [6, 7], aluminium [8] and metallic matrix composites [9, 10].

Due to the high strength and toughness, good weldability and machinability of 18Ni-300 maraging steel, it has been widely applied in manufacturing industries as a mould material [11]. Several studies have been carried out to investigate the manufacturability of this material using SLM, subsequently demonstrating that using SLM for 18Ni-300 maraging steel results in considerably good performance compared with those manufactured using conventional techniques [4, 12]. This favourable performance of the as-built 18Ni-300 maraging steel parts using SLM can be achieved by carefully selecting some significant processing parameters, such as laser power, scan speed, hatch spacing and scan strategies. However, the wrong choices of processing parameter combinations lead to some unacceptable results. For example, low energy density input can result in balling formation, whereas high energy density contributes to thermal cracks, gas pores and residual stress [13]. Moreover, due to the limitation of this process, manufacturing fully-dense parts manufactured using SLM is not possible and the surface characteristics are not acceptable. Therefore, studies on the improvement of densification and surface quality should be conducted based on SLM-manufactured 18Ni-300 maraging steel.

Accordingly, the aim of the present paper is to investigate the effect of the global remelting process on the surface quality and tensile strength of 18Ni-300 maraging steel manufactured using SLM. The rest of the paper is structured as follows: Sect. 2 will present the related works. In Sect. 3, materials and characterisation methods used in this paper will be illustrated. The results, analysis and discussions will be presented in Sect. 4. Finally, the concluding remarks and future work will be listed in Sect. 5.

## 2 Related Works

Due to the limitation of the SLM process, laser surface treatments are usually employed to modify the surface quality and improve the mechanical behaviours of metallic parts. Amongst the available techniques, the laser surface remelting (LSR) process is a typical method used to remelt selected areas of the final layers prior to finishing the whole manufacturing process. This process contributes to improving the top surface quality and refining the microstructure. Silva et al. [14] investigated the LSR of a Cu-11.85Al-3.2Ni-3Mn shape-memory alloy, and found that the grain refinement on the top surface resulted in lower transformation temperatures in the LSR sample compared with the as-cast one. Moreover, the LSR sample also showed

better fracture stress, ductility and micro-hardness. Han et al. [15] studied the effect of LSR on AlSi10Mg alloy fabricated using SLM. The authors found that the surface roughness Ra of the as-built sample decreased from 19.3 to 0.93  $\mu\text{m}$  after the LSR process. Furthermore, the LSR process contributed to a 19.5% improvement in micro-hardness. Because the LSR process can only be applied on the remelting of the top surface during the SLM process, the global remelting process, which is called selective laser remelting (SLRM), is applied throughout the SLM process. This means that the selected areas on the current layer are exposed to the laser beam two or more times during SLM. Several studies have been carried out to investigate the effect of this process on densification, surface quality and mechanical properties. For example, Yasa et al. [16] systematically studied the effect of the remelting process on the surface quality and density of 316L stainless steel and Ti6Al4V, and found that the improvement in surface quality after remelting contributed to obtaining almost full density. More recently, Yu et al. [17] investigated the effects of two remelting strategies on the top surface roughness of SLM-fabricated AlSi10Mg. The authors found that both strategies resulted in the same level of surface roughness. The Ra values decreased to 11.67  $\mu\text{m}$  (same direction) and 10.87  $\mu\text{m}$  (opposite direction), compared with the SLM sample, which had the Ra value of 20.67  $\mu\text{m}$ .

The aforementioned literature shows that SLRM has the potential to be a useful approach to promoting the densification and modifying the surface quality of samples fabricate using SLM. However, the effect of this additional process on the SLM of 18Ni-300 maraging steel is still unclear. To address this problem, this paper investigates the effect of remelting on the surface morphology and roughness, as well as tensile strength of 18Ni-300 maraging steel fabricated using SLM.

## 3 Materials and Methods

### 3.1 Powder Characteristics and SLM Processing

Figure 1a shows the particle size distribution of the 18Ni-300 maraging steel powder used in the present study. The average particle size of the powder was 29.11  $\mu\text{m}$ . Figure 1b shows the powder used in this study. As shown, a large proportion of powder particles were spherical, and a limited number of irregularly shaped powders and satellites were also observed.

The E-Plus M250 metal 3D machine equipped with a 500 W fibre laser source and a  $262 \times 262 \times 350 \text{ mm}^3$  build chamber was employed to fabricate the cubic samples ( $8 \times 8 \times 8 \text{ mm}^3$ ) and tensile samples. The fabrication was performed within a nitrogen atmosphere with an oxygen content less than 6000 ppm. Samples used for tensile tests were fabricated horizontally and then machined to the standard dimensions. A powder layer thickness of 40  $\mu\text{m}$  was maintained constantly for all fabrications. The SLM processing was carried out using a process parameter combination of a laser power, scan speed and hatch spacing of 285 W, 900 mm/s and 0.11 mm, respectively.

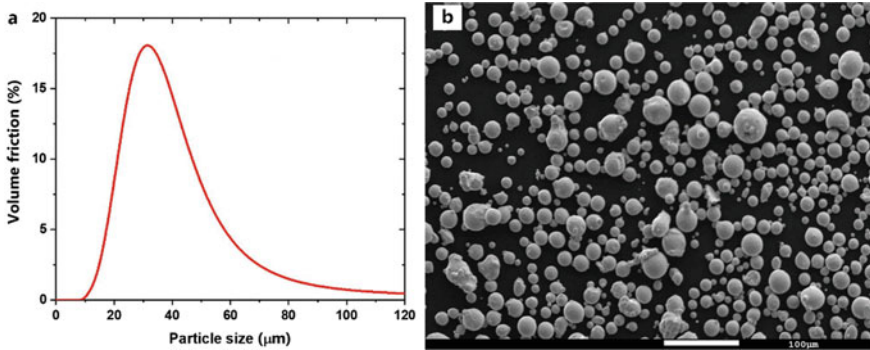


**Fig. 1** Particle size distribution and surface morphology of the 18Ni-300 maraging steel powder used in the present study

A short scanning strategy was employed with a rotational direction of  $16^\circ$  for adjacent layer.

The additional remelting process was conducted using the same machine. The previous experiment demonstrated that the process parameter combination of a laser power of 200 W, scan speed of 750 mm/s and hatch spacing of 0.13 mm, which was employed for the surface remelting treatment, contributed to the best surface finish for 18Ni-300 maraging steel. Therefore, the combination was adopted for the remelting process. In addition, the rotational direction between the SLM and SLRM processes on the same layer was constantly maintained at  $90^\circ$  with the same scanning strategy.

### 3.2 *Material Characterisation Techniques*

A Microtrac S3500 Mastersizer was employed to measure the particle size distribution of the 18Ni-300 maraging steel powder. After cutting the samples by wire-electrode from the base plate and removing their supports, cubic samples were subjected to ultrasonic cleaning for ten minutes prior to receiving material characterisation. The top and side surface morphologies of the samples were characterised using JEOL JSM-7800F scanning electron microscopy (SEM). Moreover, the surface roughness measurements were carried out using a non-contact 3D surface profiler (Sensofar Co., Barcelona, Spain). Finally, the tensile tests were performed on an MTC landmark servohydraulic test system at room temperature. The loading direction is perpendicular to the build direction of tensile samples. The same processing condition for tensile tests was repeated on three samples. The strain rate was maintained at a value of  $0.067 \text{ min}^{-1}$  and no extensometer was employed during the testing. Furthermore, the fracture morphology was observed using SEM.

## 4 Results and Discussion

### 4.1 Surface Morphology

The typical surface morphologies of the SLM-built (Fig. 2a and c) and SLRM-built (Fig. 2b and d) samples without any surface treatments are illustrated in Fig. 2. As shown in Fig. 2a, a number of balling and un-melted powder particles were observed, and limited open pores were also formed. Moreover, the solidification track in some areas was discontinuous. As shown in Fig. 2b, a smoother surface was obtained after the remelting process, compared with the top surface of the SLM-built sample. The balling and un-melted powder particles can be melted during remelting. Therefore, only a limited number of satellites have been observed. In addition, due to the high energy density input, some spatter was also observed. The smoother surface after remelting benefits the spreading quality of the subsequent powder layer, which can improve the densification and performance of the samples to some extent.

Figure 2c and d show the typical surface morphologies on the side surfaces of the samples fabricated using SLM. As shown, it seems that the remelting process had no significant impact on the side surface compared to SLM-built sample. No

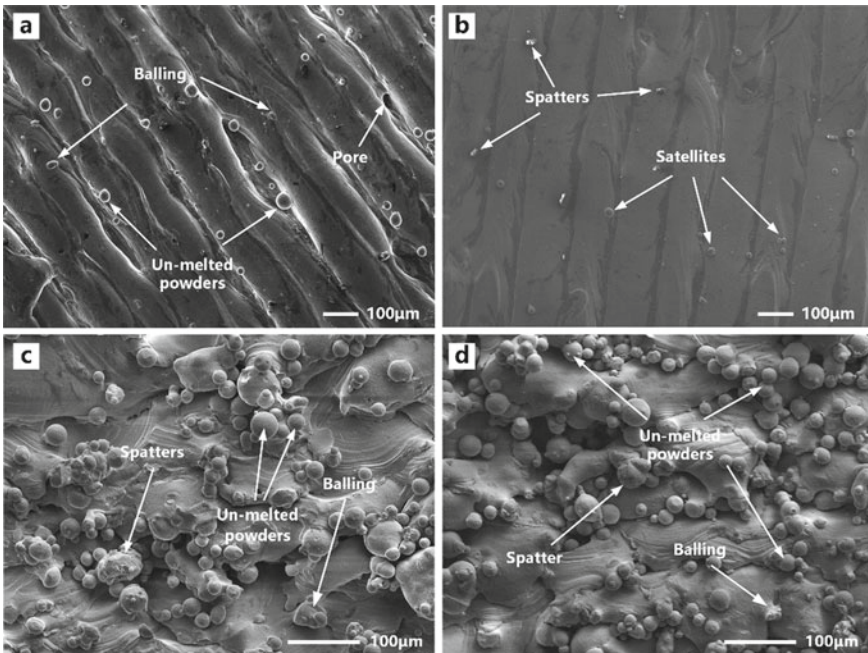


**Fig. 2** SEM micrographs showing the surface morphology of the samples: **a, b** top surfaces for SLM and SLRM, respectively; **c, d** side surfaces for SLM and SLRM, respectively

significant differences in terms of surface finish were observed between the SLM-built and SLRM-built samples. As Nasab et al. [18] discussed, defects on the side surface of the SLM-built and SLRM-built samples can be classified as un-melted powder particles, balling and large-sized spatters, which were formed on the side surface during the SLM process, as shown in Fig. 2c and d.

### 4.2 Roughness Analysis

Figure 3 shows the surface height maps and surface roughness on the top and side surfaces of the SLM-built and SLRM-built samples. As shown in Fig. 3a, the Ra value on the top surface of the SLM-built sample was  $3.11 \pm 0.31 \mu\text{m}$ . Although the remelting process resulted in a smoother surface finish, as discussed in Sect. 4.1, the Ra value on the top surface did not decrease, reaching up to  $3.44 \pm 0.48 \mu\text{m}$  (Fig. 3c). In addition, the top surface height maps showed difference between the

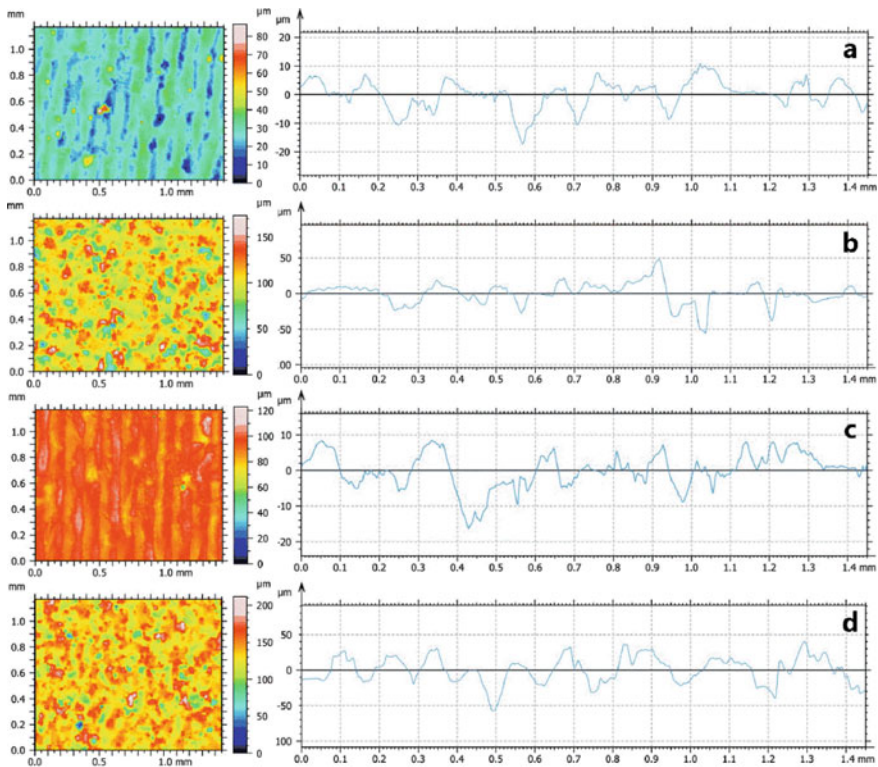


**Fig. 3** Surface height maps (left) and surface profiles (right) of the (a, c) top surfaces and (b, d) side surfaces of the SLM-built and SLRM-built samples, respectively

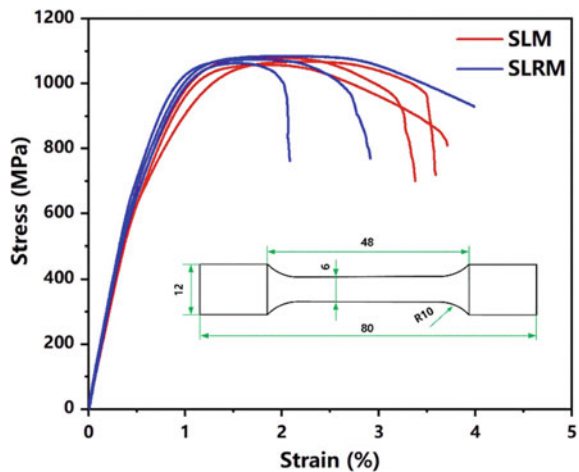
SLM-built and SLRM-built samples. The map on the top surface of the SLM-built sample had obvious peak and valley features. It can be seen that the valley feature was formed between two adjacent scanning tracks. The SLRM-built sample showed large areas having peaks, but no obvious valley features can be seen.

Figure 3b and d show the side surface height maps and surface roughness of the SLM-built and SLRM-built samples, respectively. The Ra value of the SLM-built sample was  $7.76 \pm 0.25 \mu\text{m}$ , which increased to  $11.57 \pm 3.44 \mu\text{m}$  after remelting. The slight increase in roughness on the side surface occurred because more powder particles were exposed to molten pools during the remelting process [17]. In addition, the surface maps between the two processing conditions showed no significant visible differences.

### 4.3 Tensile Strength

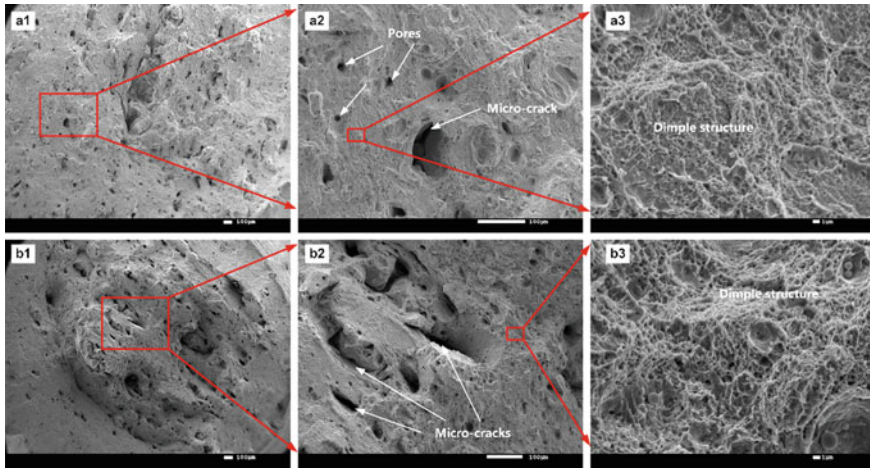
The stress-strain curves of the SLM-built and SLRM-built samples fabricated in horizontal direction without any post-treatment are shown in Fig. 4. The inserted image indicates the dimensions of the samples used for tensile testing. From the tensile stress-strain curves, the tensile properties of both the SLM-built and SLRM-built samples with three repetitions for each processing condition were shown to be consistent. In addition, Table 1 compares the yield strength (YS) and ultimate tensile strength (UTS) of the two processing conditions. As can be seen in Table 1, for the SLM-built samples, the YS and UTS values were  $890 \pm 27 \text{ MPa}$  and  $1068 \pm 12 \text{ MPa}$ , respectively. The YS values of the samples after the remelting process increased to  $938 \pm 36 \text{ MPa}$ , whereas the UTS showed no significant change in SLRM conditions compared to SLM conditions. The SLRM-built samples exhibited the UTS value of

Fig. 4 Stress-strain curve of the SLM-built and SLRM-built samples



**Table 1** Comparison of the tensile properties of the SLM-built and SLRM-built samples

Samples	YS (MPa)	UTS (MPa)
SLM-built	$890 \pm 27$	$1068 \pm 12$
SLRM-built	$938 \pm 36$	$1070 \pm 19$
Wrought [19]	760-895	1000-1170



**Fig. 5** SEM micrographs showing the fracture surfaces of the **a** SLM-built **b** SLRM-built samples

$1070 \pm 19$  MPa. In this testing, the tensile properties of both processing conditions satisfied the tensile strength of the wrought samples [19].

The typical fracture morphologies of both the SLM-built (Fig. 5a1-a3) and SLRM-built (Fig. 5b1-b3) samples following the tensile testing are shown in Fig. 5. It can be seen at high magnification, as shown in Fig. 5a3 and b3, that a large number of deep, dimple-like features were observed on the fracture surfaces of both the SLM-built and SLRM-built samples, suggesting that the fracture mode in both processing conditions was ductile fracture. In addition, different defects were also observed on the fracture surfaces for both processing conditions. As shown, massive pores were formed on the fracture surface of the SLM sample (Fig. 5a1 and a2). After remelting each layer, a large number of micro-cracks were observed (Fig. 5b1 and b2). Both defects can decrease the tensile strength of the final products.

## 5 Conclusions

In the present study, a comparison of using SLM and SLRM on 18Ni-300 maraging steel was conducted. The effect of remelting process on the surface morphology and roughness on the top and side surfaces was investigated. Moreover, the tensile

strength of the SLM-built and SLRM-built 18Ni-300 maraging steel samples fabricated in horizontal direction was also addressed. The significant findings are summarised as follows:

- (1) The remelting process contributed to a smoother top surface morphology. However, remelting showed no obvious influence on the side surface morphology. No significant side surface differences were observed between the two processing conditions.
- (2) The Ra values on the top and side surfaces of the SLM-built sample were  $3.11 \pm 0.31 \mu\text{m}$  and  $7.76 \pm 0.25 \mu\text{m}$ , respectively. Although the remelting process resulted in a smoother surface, the Ra value on the top surface of the SLRM-built sample was  $3.44 \pm 0.48 \mu\text{m}$ . The Ra value on the side surface increased to  $11.57 \pm 3.44 \mu\text{m}$  after remelting.
- (3) The tensile strength of the samples under SLM and SLRM conditions was tested. The SLM-built sample obtained the YS and UTS values of  $890 \pm 27 \text{ MPa}$  and  $1068 \pm 12 \text{ MPa}$ , respectively. The remelting process increased the YS and had no obvious impact on the UTS. The SLRM-built samples exhibited the YS and UTS values of  $938 \pm 36 \text{ MPa}$  and  $1070 \pm 19 \text{ MPa}$ , respectively.

**Acknowledgements** This paper was supported by the Natural Science Foundation of China (Grant No: 51975073, 51805052), and the Chongqing Science and Technology Bureau (No. cstc2018 jszx-cyzdX0102). The authors would like to show appreciation for the help from the Electron Microscopy Centre of Chongqing University (China) regarding the characterisation of surface and fracture morphology. The authors wish to thank ASTUTE 2020 (Advanced Sustainable Manufacturing Technologies). This operation, supporting manufacturing companies across Wales, has been part-funded by the European Regional Development Fund through the Welsh Government and the participating Higher Education Institutions.

## References

1. Kumar, P., Ramamurty, U.: Microstructural optimization through heat treatment for enhancing the fracture toughness and fatigue crack growth resistance of selective laser melted Ti 6Al 4 V alloy. *Acta Mater.* **169**, 45–59 (2019)
2. Ma, S., Tang, Q., Feng, Q., Song, J., Han, X., Guo, F.: Mechanical behaviours and mass transport properties of bone-mimicking scaffolds consisted of gyroid structures manufactured using selective laser melting. *J. Mech. Behav. Biomed. Mater.* **93**, 158–169 (2019)
3. Liverani, E., Toschi, S., Ceschini, L., Fortunato, A.: Effect of selective laser melting (SLM) process parameters on microstructure and mechanical properties of 316L austenitic stainless steel. *J. Mater. Process. Technol.* **249**, 255–263 (2017)
4. Song, J., Tang, Q., Feng, Q., Ma, S., Setchi, R., Liu, Y., Han, Q., Fan, X., Zhang, M.: Effect of heat treatment on microstructure and mechanical behaviours of 18Ni-300 maraging steel manufactured by selective laser melting. *Opt. Laser Technol.* **120**, 105725 (2019)
5. Feng, Q., Tang, Q., Liu, Y., Setchi, R., Soe, S., Ma, S., Bai, L.: Quasi-static analysis of mechanical properties of Ti6Al4V lattice structures manufactured using selective laser melting. *Int. J. Adv. Manuf. Technol.* **94**, 2301–2313 (2018)



6. Yi, J.H., Kang, J.W., Wang, T.J., Wang, X., Hu, Y.Y., Feng, T., Feng, Y.L., Wu, P.Y.: Effect of laser energy density on the microstructure, mechanical properties, and deformation of Inconel 718 samples fabricated by selective laser melting. *J. Alloys Compd.* **786**, 481–488 (2019)
7. Montero-Sistiaga, M.L., Pourbabak, S., Van Humbeeck, J., Schryvers, D., Vanmeensel, K.: Microstructure and mechanical properties of Hastelloy X produced by HP-SLM (high power selective laser melting). *Mater. Des.* **165**, 107598 (2019)
8. Ch, S.R., Raja, A., Nadig, P., Jayaganthan, R., Vasa, N.J.: Influence of working environment and built orientation on the tensile properties of selective laser melted AlSi10Mg alloy. *Mater. Sci. Eng., A* **750**, 141–151 (2019)
9. Han, Q., Setchi, R., Evans, S.L.: Synthesis and characterisation of advanced ball-milled Al-Al<sub>2</sub>O<sub>3</sub> nanocomposites for selective laser melting. *Powder Technol.* **297**, 183–192 (2016)
10. Kang, N., Ma, W., Heraud, L., El Mansori, M., Li, F., Liu, M., Liao, H.: Selective laser melting of tungsten carbide reinforced maraging steel composite. *Addit. Manuf.* **22**, 104–110 (2018)
11. Bai, Y., Yang, Y., Xiao, Z., Wang, D.: Selective laser melting of maraging steel: mechanical properties development and its application in mold. *Rapid Prototyp. J.* **24**, 623–629 (2018)
12. Mutua, J., Nakata, S., Onda, T., Chen, Z.: Optimization of selective laser melting parameters and influence of post heat treatment on microstructure and mechanical properties of maraging steel. *Mater. Des.* **139**, 486–497 (2018)
13. Gu, D., Hagedorn, Y., Meiners, W., Meng, G., Batista, R.J.S., Wissenbach, K., Poprawe, R.: Densification behavior, microstructure evolution, and wear performance of selective laser melting processed commercially pure titanium. *Acta Mater.* **60**, 3849–3860 (2012)
14. Da Silva, M.R., Gargarella, P., Gustmann, T., Botta Filho, W.J., Kiminami, C.S., Eckert, J., Pauly, S., Bolfarini, C.: Laser surface remelting of a Cu-Al-Ni-Mn shape memory alloy. *Mater. Sci. Eng. A.* **661**, 61–67 (2016)
15. Han, Q., Jiao, Y.: Effect of heat treatment and laser surface remelting on AlSi10Mg alloy fabricated by selective laser melting. *Int. J. Adv. Manuf. Technol.* **102**, 3315–3324 (2019)
16. Yasa, E., Deckers, J., Kruth, J.: The investigation of the influence of laser re-melting on density, surface quality and microstructure of selective laser melting parts. *Rapid Prototyp. J.* **17**, 312–327 (2011)
17. Yu, W., Sing, S.L., Chua, C.K., Tian, X.: Influence of re-melting on surface roughness and porosity of AlSi10Mg parts fabricated by selective laser melting. *J. Alloys Compd.* **792**, 574–581 (2019)
18. Nasab, M.H., Gastaldi, D., Lecis, N.F., Vedani, M.: On morphological surface features of the parts printed by selective laser melting (SLM). *Addit. Manuf.* **24**, 373–377 (2018)
19. Kempen, K., Yasa, E., Thijs, L., Kruth, J.P., Van Humbeeck, J.: Microstructure and mechanical properties of Selective Laser Melted 18Ni-300 steel. *Phys. Procedia.* **12**, 255–263 (2011)

# Event-Driven Knowledge Engineering as Enabling Technology Towards Configuration of Assistance Systems in Industrial Assembly



Matthias Plasch, Sharath Chandra Akkaladevi, Michael Hofmann, Christian Wögerer, and Andreas Pichler

**Abstract** Industrial assistance systems are increasingly used in modern production facilities to support employees, in order to cope with varying assembly processes, increased complexity and to reduce mental and physical stress. However, programming and configuring such systems, to provide assistance in a given assembly process context, is a challenging task and usually requires extensive programming knowledge. This paper presents an approach, combining human event recognition together with a semantic knowledge processing framework in order to enable intuitive programming and configuration. The presented method includes learning of assembly process knowledge, based on human demonstration. We demonstrate the applicability of this approach in two use cases: process learning and transfer, and user guidance for manual assembly.

## 1 Introduction and Motivation

Flexibilization of production systems is a widely discussed problem in industrial research to cope with the demands of high product variation and the demographic change. Recent initiatives [1, 2] generate valuable impulses towards the development and realization of smart production systems focusing on efficient but secure

---

M. Plasch (✉) · S. C. Akkaladevi · M. Hofmann · C. Wögerer · A. Pichler  
Profactor GmbH, Steyr-Gleink, Austria  
e-mail: [matthias.plasch@profactor.at](mailto:matthias.plasch@profactor.at)  
URL: <http://profactor.at>

S. C. Akkaladevi  
e-mail: [sharath.akkaladevi@profactor.at](mailto:sharath.akkaladevi@profactor.at)

M. Hofmann  
e-mail: [michael.hofmann@profactor.at](mailto:michael.hofmann@profactor.at)

C. Wögerer  
e-mail: [christian.woegerer@profactor.at](mailto:christian.woegerer@profactor.at)

A. Pichler  
e-mail: [andreas.pichler@profactor.at](mailto:andreas.pichler@profactor.at)

information transport between multiple actors and sensors within a manufacturing cell. The resulting complexity and information density also mean exposure of human workers to higher mental load and stress. Cognitive and physical assistance systems support human workers by reducing (a) mental and ergonomic stress, (b) the probability of mistakes, and (c) by increasing motivation and concentration. Moreover, the acceptance of advanced technologies in production facilities is potentially increased. Programming and adaptation of the behaviour of assistance systems is a tedious task and often requires a programmer. Moreover, process knowledge is often persisted/maintained centrally and therefore not accessible to workers on site.

This paper focuses on the application of *knowledge engineering* based on *Events*, which are detectable in an assembly cell, towards intuitive programming and configuration of assistance systems in an industrial assembly setting. As a long-term goal, these technologies could enable human workers to handle the complexity of smart production cells more easily, without having special programming skills, thus keeping them in the loop. In our recent work [3], we identified three main application areas in industrial assembly that potentially benefit of a combination of those technologies.

In this publication, we present first results considering use cases of *quality assurance*, an interactive system to ensure process quality in manual assembly, and *Process Teaching and Configuration* to learn assembly process knowledge to an assistance system. The key contributions are:

- (1) Description of an *event recognition system* to detect human events within an assembly work cell.
- (2) Introduction of a knowledge engineering approach to describe assembly process knowledge based on detectable events.
- (3) A Learning by Demonstration (LbD) approach to learn and transfer assembly process (AP) knowledge.

## 2 State of the Art

### 2.1 Event Recognition

Event recognition in relation to an AP can be defined as identifying the activities or interactions of agents in the environment. The terms gestures, actions, activities, and events have been used interchangeably [4]. An action, denoting a sequence of movements, that involves an agent interacting with an object is defined as an *event*. Events are high-level activities which are derived not directly from the sensor data, but from the interpreted information. In the literature, several hierarchical approaches are proposed and can be broadly divided into three categories. **Statistical approaches** use statistical state-based models to recognize activities (usually two layers), e.g. hidden Markov models (HMMs) and Bayesian networks (DBN) [5, 6]. **Syntactic approaches** model human activities as a string of symbols, where each symbol

corresponds to a low-level action. These approaches generally use a grammar syntax such as stochastic context free grammar (SCFG) to model activities [7]. **Description-based approaches** maintain the temporal, spatial, and logical relationships between low-level actions to describe complex activities [8].

Event recognition in industrial scenarios has not yet been widely researched. There are few approaches that show promise in this direction. An extensive review of event recognition approaches is given in [9]. Most approaches with task-driven goals only consider object localization for manipulation (often with simple structure). Thereby, they do not consider the problems associated with dynamic environments, such as tracking and manipulation of real-world objects (exceptions include [10, 11]).

## 2.2 *Semantic Knowledge Representation and Processing*

The domain of semantic knowledge representation and reasoning is an important area of artificial intelligence (AI) to represent domain relevant information on the one hand and to realize rules and approaches in order to solve complex problems based on, e.g. logical inference, similarly like humans do in a natural fashion. Databases like MongoDB [12] or CouchDB [13] make use of W3C standards, e.g. JSON or JSON-LD, to organize data document-based structure. A certain degree of reasoning functionality can be realized based on standard features, including free-text searching, distribution of data, and data analysis algorithms. Graph and ontology-based approaches [14] are further common approaches. AllegroGraph [15] combines document-based approaches with graph databases, is compliant with W3C/ISO standards including JSON, RDF(S), OWL [16] for expression of knowledge, and provides built-in OWL and RDFS reasoning engines.

Similarly, GraphScale [17] enhances the graph-database Neo4j [18] with OWL reasoning [14]. In the domain of robotics, Knowrob [11] builds on OWL/RDF knowledge representation, combined with enhanced reasoning and inference capabilities based on Prolog rules.

OWL and RDF graph-based knowledge management systems [14] require thorough understanding or modelling techniques. GraknAI [19] and OpenCog [20] use higher level schemes to express knowledge based on hyper-graphs. The developers explain [21] that this modelling schema is more intuitive and scalable for DB design. The built-in algorithms enable similar reasoning features comparable to OWL/RDF [22].

## 3 **General System Architecture**

An assistance system, providing cognitive or physical support to human workers in the domain of industrial assembly, needs to be able to perceive the environment and to understand the current situation of an AP. Figure 1 depicts a possible setting, where

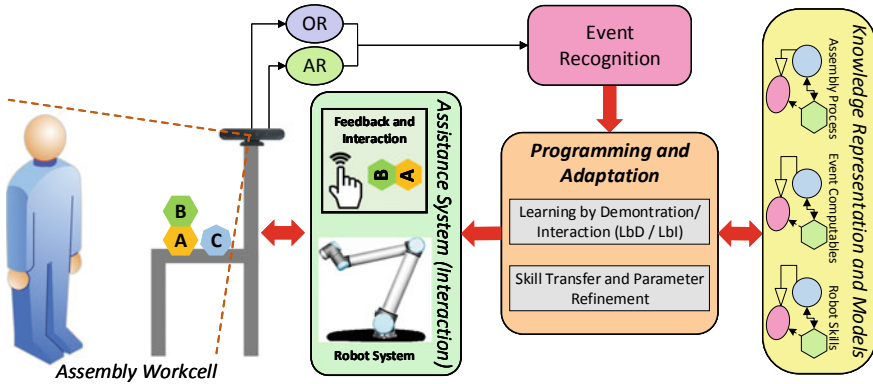


**Fig. 1** System architecture overview

the human is interacting with objects and parts on a work table, relevant to the AP. Further interfaces include an information screen, to provide instructions to the human, and a robotic system providing physical assistance. Such assistance could include support in lifting heavy parts, or acting as a “third hand”. In this work, we assume an existing execution layer, to realize a certain robotic behaviour. The assembly work cell is equipped with 2D and 3D vision sensor to observe the human worker as well as objects or parts (see objects A to C). Perception modules including *action recognition* (AR) and *object recognition* (OR) process and evaluate the acquired sensor data. All OR and AR classified data serve as input to the *event recognition* (ER) system. ER requires domain knowledge, i.e. definitions of rules to classify human events according to the relevant assembly process. A knowledge representation that covers (a) an AP model, (b) definitions of events, and (c) descriptions of skills of an assistance system (e.g. robot skills) is required. Covering these aspects in a sound description is of importance to reduce complexity reasoning processes. Moreover, each knowledge representation needs to include algorithms to store, retrieve, and reason about the abstracted domain knowledge. Finally, the architecture includes *programming and adaptation* software modules to (a) teach process knowledge to the assistance system applying methods of Learning by Demonstration (LbD) and (b) to transfer process knowledge recorded based on human events to an assistance system.

## 4 Methods and Approach

This section describes methods to implement a semantic framework that is described in Sect. 3, applicable to potential applications in industrial assembly.

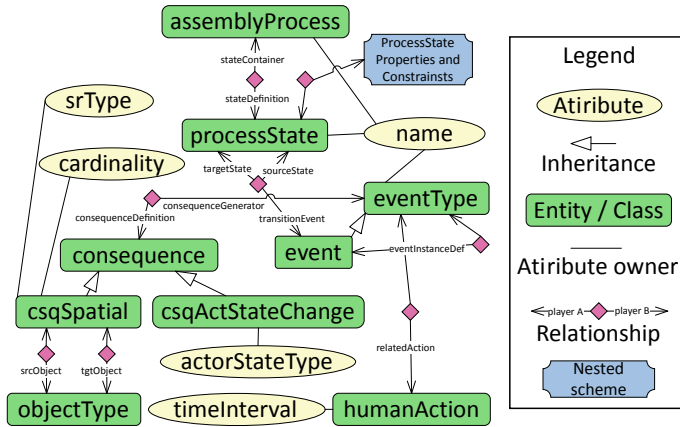


Fig. 2 Knowledge representation for event definitions, CSQs, and the AP (from [3])

### 4.1 Semantic Representation of Assembly Processes and Events

The definition of an event (see Sect. 2.1) was extended in our previous works [10] and [3] to cover interactions with other agents (e.g. robot) and to associate a temporal condition with the related action. This means that an event-related action needs to last for a given time frame. We define events to form a bridging entity between two (process) *states* of an AP according Fig. 2. Events affect the environment by generating causal effects, henceforth called *Consequences (CSQ)*, thus driving the AP from one state to the next. Based on the formal description of an AP in [23], a succeeding process state can be deduced by (a) extracting the parametrization of an event (action and objects/actors interacted with), (b) reasoning about the CSQs of an event, and (c) applying those CSQs to the origin process state that is defined based on its *state properties* [23]. For simplicity, state properties are referred only in Fig. 2 (“nested scheme” reference). Note that events differ from eventTypes (see scheme) in the sense that an event additionally includes a concrete parametrization of object instances and actor instances. Concerning CSQs, two types are currently supported. Entities of “csqSpatial” describe a change in the spatial-configurations of pairs of objects, also including the (dis)appearance of objects w.r.t the work table. CSQs of type “csqActStateChange” denote changes of the “internal” state of agents. The attribute “cardinality” tells that a CSQ applies to a defined number of entities, e.g. multiple pairs of object instances of similar types. The described definition of an eventType, including its generated CSQs, will be referred to as *EventComputables (EC)* in the further discussion of methods. To enable the transfer of human-demonstrated AP knowledge, to a robot-based assistance system we introduce *robot-SkillTypes (RST)* and *robotActions (RA)*. An RST describes a predefined behaviour, executable by a robot system. Similarly to eventTypes, an RST generates CSQs. A

concrete parametrized RST (i.e. object instances or process values) is defined as *RobotSkill (RS)*. Single or multiple RS executed in a sequence are denoted as an RA. By describing CSQs similarly for both, eventTypes and RSTs, the complexity of transferring AP knowledge to a robotic assistant is reduced.

## 4.2 Human Event Recognition

The ER system continuously observes the perception data streams of OR [24] and AR [3, 25] (see Fig. 1) to detect relevant events, characterized by ECs. The detailed functionality of the ER is elaborated in our previous work [3]. Summarized, the classification is based on comparing **reference** (perception) data (AR and OR), which is recorded upon start of a human action (AR), with **comparison** (perception) data (end of human action). A problem of the ER system is given by the requirement of domain knowledge, i.e. offline defined ECs for a given AP context. This domain knowledge also enabled filtering of potentially invalid event detections. Defining ECs manually requires detailed understanding of modelling concepts, at the level of a programmer. To overcome this limitation in flexibility, we extended the ER system to include a “recording” functionality to generate ECs online, based on a LbD approach. In this recording mode, we assume that any event recording, clearly starts with a detected human action (AR system), followed by a manipulation of objects (OR) or actors in the environment (e.g. robot system). The *programming and adaptation* software modules (see Sect. 3) trigger a reasoning process to evaluate logical conditions that determine the parametrization of the corresponding EC. This parametrization describes types of caused CSQs, related role-players (objects, actors), and temporal-conditions. These logical conditions are very much related to the definition of CSQs (Sect. 4.1) and summarized below.

The **Human Action Type** describes the human action that is performed on certain targets (objects or actors). An **Actor State-Change** describes changes of the “internal” states of an actor during an executed interaction (e.g. human, robot). **Spatial Configurations** express changes in the spatial configuration of instances of object types. Those can apply to multiple, equally typed object instance pairs (cardinality!), in different configurations: **Displacement**: An object instance is considered displaced, if the Euclidean distance of the POSES of reference image frame and current image frame exceeds a configurable threshold (given in mm). **Spatial Relation**: Two object instances are henceforth spatially related in a defined fashion. The detected POSES as well as the object type dimensions are used to determine spatial relations (e.g. *on-top-of*). **(Dis)Appearance**: An instance of an object type has appeared or disappeared.

**Temporal-Conditions** express that a certain human action has to follow a given temporal behaviour, e.g. lasting for a certain time-span. They are described using Allen’s Interval Algebra [26]. The **Sequence of Rules** describes combinations of the above rules that need to be fulfilled in a temporal sequence, for an event to be classified.

### 4.3 Learning AP Knowledge Based on Human Demonstrations

To learn the definition of an AP, extraction of knowledge from events, demonstrated by a human expert, is necessary. We assume an initial state  $S_I < P_{I1}, \dots, P_{InI} >$ , including state properties  $P_{xI}$  [10] describing (initial) constraints for actor states and spatial configurations objects. Given a current state  $S_X < P_{IX}, \dots, P_{nX} >$ , a subsequent state  $S_{YX} < P_{IYX}, \dots, P_{nYX} >$  is derived as a cause of an event  $E_Y < AT_Y, TO_Y, Csq_{iY}, \dots, Csq_{nY} >$ . The state properties of  $S_{XY}$  are derived by applying the CSQs  $Csq_{iY} >$ , to the origin state's properties  $P_{iX}$ . Hereby,  $AT_Y$  and  $TO_Y$  denote the event parametrization, i.e. the related actor and target object, respectively. Each type of CSQ requires rules, to describe how its effects are applied to process state properties. Those are offline defined within the knowledge representation. A full AP definition is recorded by learning state transitions in a sequence till reaching a final process state.

### 4.4 Transferring AP Knowledge to a Robotic Assistant

By transferring AP knowledge, described based on human events, a method towards intuitive programming of an assistance system can be realized. The main idea is to enable a robot system to replicate the taught AP execution. In Sect. 4.1, the definitions of RST, RS, and RA were introduced, where RTS is capable of generating CSQs similarly as eventTypes. Using these definitions, the transfer procedure is done by mapping generated CSQs of each human-demonstrated state transition, to relevant CSQs of a single or a sequence of RSTs. Given an AP state transition, the related event instance  $e$  functions as input of the algorithm. Firstly, the event parametrization as a map of key/value pairs, the eventType  $E$ , and the set of CSQs generated by this eventType  $C_E$  are retrieved. Afterwards, the knowledge base is queried for predefined RSTs and their generated CSQs:  $map < RST_i, C_{RSTi} >$ . Next, empty sets are initialized to hold CSQs mapped so far, and already identified, matching RSTs:  $RST_{\#} = \{\}, C_{\#} = \{\}$ . Then, the algorithm tries to find matching RSTs in order to generate an equivalent sequence of CSQs of a human event. This main loop is depicted in Fig. 3. The circled numbers are used in the explanation for reference. The main loop iterates over known RSTs and related CSQs (1). RSTs generating more CSQs than the compared event cannot be considered: next RST (2). Else a set to hold event CSQs is created, covered by the current RST  $RST_{ij}$ :  $C_{\#i}$  (3). The next loop iterates over  $RST_{ij}$  CSQs, to find matching event CSQs. The statement in (4) ensures that only event CSQs are considered only, which were not yet covered. Loop (5) checks for equivalence of the current RST CSQ  $C_{RSTij}$  with one of the uncovered event CSQs  $C_{Ek}$ . If equivalence is given, the set  $C_{\#i}$  is extended (5). For a RST to be considerable, all its CSQs need to match an event CSQ: see decision (6). If so,  $C_{\#}$  is extended with the event CSQs  $C_{\#i}$  covered by  $RST_{ij}$  and the given



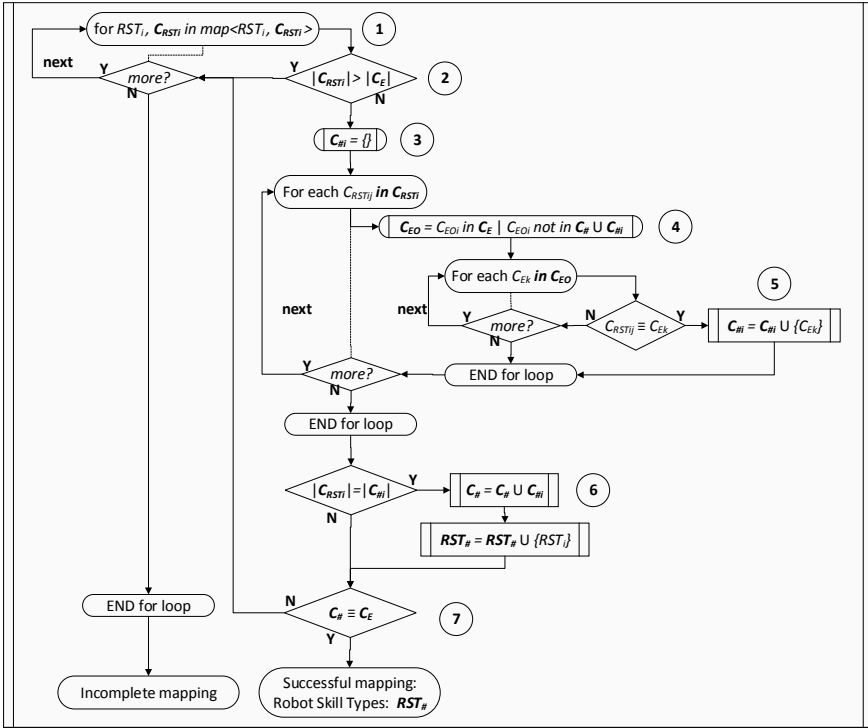


Fig. 3 Flowchart of the mapping algorithm from human events to robot skills

RST is required. Otherwise, the algorithm continues with the next RST: loop (1). If all event CSQs could be matched, the algorithm is finished, and the required RSTs for the considered event are known (7).

The remaining steps include the creation of RS instances for each identified RST and applying the parametrization of the origin event  $e$ . In this way, an equivalent RA can be generated. Repeating the process for all state transitions leads to a fully transferred AP knowledge.

### 5 Demonstration

In order to demonstrate the methods described in Sect. 4, a set-up related to Fig. 1 is established. The used perception systems for OR, AR, and ER are applied as explained in Sect. 4.2 and in referenced, the previous work. This demonstration assumes a predefined set of human actions and objects, but no predefined ECs. Knowledge representation and semantic reasoning is performed based on the GraknAI

knowledge processing framework (see Sect. 4.1). The assistance systems, are realized based on a GUI implementation (PySide [27]) and robot simulation (Gazebo [28]). To trigger the robot simulation accordingly, the XRob [29] runtime environment was integrated to generate and execute robot recipes. A glue-logic is required to coordinate the Programming and Adaptation modes described in Sect. 1.

### 5.1 Learning AP Knowledge by Demonstration and Transfer to a Robotic Assistant

As mentioned above, the system does not have knowledge about ECs. In the initial step, the user activates the recording mode for ECs using the interactive GUI. This is followed by the demonstration of single episodes of events of interest (Fig. 4a, c). The ECs are derived as explained in Sect. 4.2. To record an AP definition, EC recording is stopped and the AP recording functionality is triggered (Fig. 4c). This launches the ER system in detection mode, using the existing EC definitions. During demonstration of the AP, the system deduces process states and records state transitions. Once the AP demonstration is done, the AP definition can be stored in the knowledge base (see GUI). Figure 4d depicts a visualization of the recorded state transitions. Activating the bottom button of the GUI triggers the transfer of AP knowledge to the robot system. In case of the transfer being successful, a recipe, interpretable by

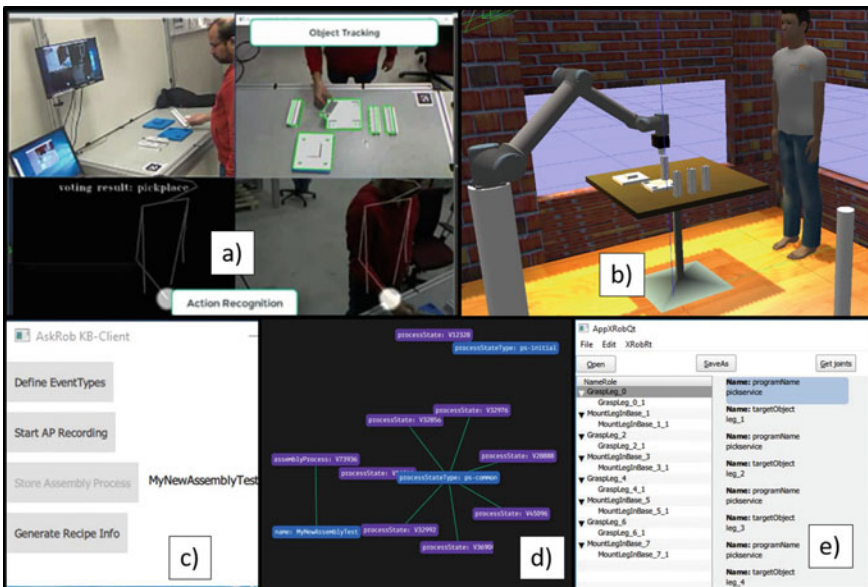
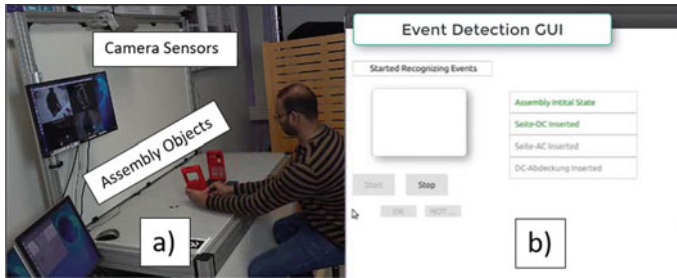


Fig. 4 Set-up to learn AP knowledge to the system: event recognition system (a), robot simulation (b), interactive GUIs (c and e), visualization of recorded knowledge (d)



**Fig. 5** Set-up for the quality assurance use case

the execution system XRob, is generated. The user may review/adapt recipe parameters using the recipe viewing GUI (Fig. 4e). Finally, the AP execution through the robot system can be triggered (Fig. 4b). In case of process variants, the existing AP definitions can be extended or changed by demonstrating new steps and storing the recorded AP under a new name. AP recording can also be paused to define further ECs and resumed afterwards.

## 5.2 User Guidance Towards Quality Assurance

Benefiting from the same framework, this demonstration involves the explained steps of deriving ECs and recording AP knowledge. This knowledge enables guidance of the human through the defined process, based on an interactive GUI. Two purposes are served: (a) explaining the sequence of process steps and (b) detecting whether specific events have already happened during the manual AP execution. A main requirement is to strictly avoid *false-positive* event detections. Such mistakes would suggest to the user that a process step has already happened. In case of non-detected events, the user is notified through the GUI to complete a process step or to manually confirm its execution (in case of a *true-negative* detection—event missed). Figure 5 shows the set-up for this application, with different types of objects/parts considered. The right-hand side of the figure depicts the interactive GUI, where events listed in green colour highlight detected events.

## 6 Conclusion and Future Work

This work combines human event recognition and knowledge engineering into a semantic framework. Moreover, we demonstrate its potential to make configuration and programming of assistance systems in industrial assembly more intuitively. The presented approach provides flexibility towards definition of novel events, which are relevant for configuring a process variant. Transferring process knowledge to a

robotic system is a promising approach to enable a simplified way of programming robotic assistance. The author's vision is to make the complexity of smart production cells including assistance systems manageable by human workers in the loop, without requiring extensive programming skills. Future work includes improving the usability of the prototypical implementation. Regarding process knowledge transfer, more flexibility towards tuning process parameters of the targeted assistance system is required. User studies are further planned to receive feedback from potential applicants and make the potential benefits of these technologies quantifiable.

**Acknowledgements** This research is funded by the projects MMAssist II (FFG, 858623), Teachbots (BMVIT) and Smart Factory Lab (funded by the state of Upper Austria).

## References

1. Zezulka, F., Marcon, P., Vesely, I., Sajdl, O.: Industry 4.0—an introduction in the phenomenon. *IFAC-PapersOnLine* **49**(25), 8–12 (2016)
2. Industrial Internet Consortium et al.: Industrial internet reference architecture (2015). Technical Article. Available online: <http://www.iiconsortium.org/IIRA.htm>. Accessed on 29 Aug 2018
3. Plasch, M., Akkaladevi, S.C., Hofmann, M., Pichler, A.: Human and workcell event recognition and its application areas in industrial assembly. In: Conference Proceedings of the Ninth International Precision Assembly Seminar (IPAS '2020) Kitzbühel, Austria, March 15–18, 2020
4. Poppe, R.: A survey on vision-based human action recognition. *Image Vis. Comput.* **28**(6), 976–990 (2010)
5. Jalal, A., Kim, Y.-H., Kim, Y.-J., Kamal, S., Kim, D.: Robust human activity recognition from depth video using spatiotemporal multi-fused features. *Pattern Recogn.* **61**, 295–308 (2017)
6. Raman, N., Maybank, S.J.: Activity recognition using a supervised non-parametric hierarchical hmm. *Neurocomputing* **199**, 163–177 (2016)
7. Pei, M., Jia, Y., Zhu, S.-C.: Parsing video events with goal inference and intent prediction. In: 2011 International Conference on Computer Vision, pp. 487–494. IEEE, New York (2011)
8. Zhu, Y., Nayak, N.M., Roy-Chowdhury, A.K.: Context-aware activity recognition and anomaly detection in video. *IEEE J. Sel. Topics Sign. Process.* **7**(1), 91–101 (2012)
9. Ramirez-Amaro, K., Yang, Y., Cheng, G.: A survey on semantic-based methods for the understanding of human movements. *Rob. Autonom. Syst.* (2019)
10. Akkaladevi, S.C., Plasch, M., Pichler, A., Rinner, B.: Human robot collaboration to reach a common goal in an assembly process. In: STAIRS, pp. 3–14 (2016)
11. Tenorth, M., Beetz, M.: Representations for robot knowledge in the knowrob framework. *Artif. Intell.* **247**, 151–169 (2017)
12. Chodorow, K.: *MongoDB: The Definitive Guide: Powerful and Scalable Data Storage*. O'Reilly Media, Inc. (2013)
13. CouchDB Team: *Couchdb 2.0 reference manual* (2015)
14. Ehrlinger, L., WöB, W.: Towards a definition of knowledge graphs. *SEMANTiCS (Posters, Demos, SuCCESS)* **48** (2016)
15. Inc Franz. Allegrograph: Semantic graph database. <https://allegrograph.com/products/allegrograph/> (2017)
16. OWL Working Group et al.: Owl 2 web ontology language document overview: W3c recommendation 27 October 2009
17. Liebig, T., Vialard, V., Opitz, M., Metzl, S.: Graphscale: Adding expressive reasoning to semantic data stores. In: International Semantic Web Conference (Posters & emos) (2015)

18. Neo4J Developers. Neo4j. Graph NoSQL Database [online] (2012)
19. Enterprise Grakn Labs. Grakn.ai: A knowledge graph. <https://grakn.ai/about> (2019)
20. Hart, D., Goertzel, B.: Opencog: A software framework for integrative artificial general intelligence. In: AGI, pp. 468–472 (2008)
21. Pribadi, H.: The grakn.ai ontology: Simplicity and maintainability. <https://blog.grakn.ai/the-grakn-ai-ontology-simplicity-and-maintainability-ab78340f5ff6> (2017)
22. Klarman, S.: A closer look at grakn.ai’s hypergraph datamodel. <https://blog.grakn.ai/modelling-data-with-hypergraphs-edff1e12edf0> (2017)
23. Akkaladevi, S.C., Plasch, M., Maddukuri, S., Eitzinger, C., Pichler, A., Rinner, B.: Toward an interactive reinforcement based learning framework for human robot collaborative assembly processes. *Front. Rob. AI* **5** (2018)
24. Akkaladevi, S., Ankerl, M., Heindl, C., Pichler, A.: Tracking multiple rigid symmetric and non-symmetric objects in real-time using depth data. In: 2016 IEEE International Conference on Robotics and Automation (ICRA), pp. 5644–5649. IEEE, New York (2016)
25. Akkaladevi, S.C., Plasch, M., Eitzinger, C., Pichler, A., Rinner, B.: Towards a context enhanced framework for multi object tracking in human robot collaboration. In: 2018 IEEE/RSJ International Conference on Intelligent Robots and Systems (IROS), pp. 168–173. IEEE, New York (2018)
26. Allen, J.F.: Maintaining knowledge about temporal intervals. In: *Readings in Qualitative Reasoning About Physical Systems*, pp. 361–372. Elsevier (1990)
27. Python Software Foundation. Project pyside2: Python bindings for the QT cross-platform application and UI framework. <https://pypi.org/project/PySide2> (2020)
28. OSRF. Gazebo: Robot simulation made easy. <http://gazebosim.org> (2014)
29. Akkaladevi, S.C., Pichler, A., Plasch, M., Ikeda, M., Hofmann, M.: Skill-based programming of complex robotic assembly tasks for industrial application. *e & i Elektrotechnik und Informationstechnik*, pp. 1–8 (2019)

# Computational Validation of Injection Molding Tooling by Additive Layer Manufacture to Produce EPDM Exterior Automotive Seals



I. Evans, A. Rees, C. A. Griffiths, and Rachel Johnson

**Abstract** During the design and development of ethylene propylene diene monomer (EPDM) exterior automotive seals, prototype components can only be manufactured through production tooling platforms by either injection molding or extrusion. Consequently, tooling is expensive and has long lead times. This paper investigates whether additive layer manufacture is a viable method for producing tooling used in injection molding of exterior automotive seals in EPDM. Specifically, a novel rapid tooling is a method that combines additive layer manufacture (ALM) with epoxy reinforcement. Computational validation is performed whereby the mechanical properties of the tool are evaluated. The research has concluded that the novel tooling configuration would be suitable for prototyping purposes which would drastically reduce both costly and environmentally detrimental pre-manufacturing processes. This work has laid the foundations to implement rapid tooling technology to the injection molding of prototype EPDM parts.

## 1 Introduction

### 1.1 EPDM Tooling Platforms

During product development, it is necessary to manufacture production parts for validation and testing. Vehicle exterior seals are made from EPDM, and currently, injection molding and extrusion is their only viable manufacturing method. Tooling for injection molding is traditionally machined from steel which has high costs and lead times, typically with lead times of 16–26 weeks for tooling for injection molding of EPDM exterior seals. EPDM is a very viscous material which requires high mold pressure during injection molding. Part design is often modified during product development which results in scraping or expensive modification cost of tooling.

---

I. Evans · A. Rees (✉) · C. A. Griffiths · R. Johnson  
College of Engineering, Swansea University, Swansea, UK  
e-mail: [andrew.rees@swansea.ac.uk](mailto:andrew.rees@swansea.ac.uk)

Currently, polyurethane (PU) prototype parts are producible; however, the resulting material properties do not fully align with EPDM which limits their application for prototyping purposes. Additive layer manufacture (ALM), also known as rapid prototyping (RP) or 3D printing, is capable of producing 3D geometries. However, for the application within this study, the process could be used to produce tooling opposed to the final component which is the traditional utilization of 3D printing.

There are seven main categories that ALM techniques fall under: stereolithography, digital light processing, selective laser sintering, fused deposition modeling, laminated object manufacture, material jetting, and binder jetting. Under each of these seven categories, there are numerous variations, each with their own advantages and disadvantages. Material properties, part size, accuracy, surface finish, and cost are some of the parameters that need to be considered when selecting the additive layer manufacturing technique to be used [1–3].

Rapid tooling is the term used to describe the process of producing tooling using ALM, either creating the tool directly or creating a master model from which the tool is created, categorizing rapid tooling into direct and indirect [4–6]. Utilizing rapid tooling can reduce the lead time and significantly reduce cost when compared to traditional machining. During product development stage when time is at a premium, rapid tooling offers a prominent alternative to traditional machining of injection molding tooling. Design changes are easier to accommodate when using rapid tooling allowing for quicker part improvements and consequentially reducing product lead time [4–6].

This paper investigates whether additive layer manufacture is a viable method for producing tooling used in injection molding of exterior automotive seals in EPDM. Specifically, a novel rapid tooling is a method that combines metal powder and epoxy, which uses ALM methods of selective laser sintering or binder jetting. Computational validation will be performed on ANSYS 19.1 software, where the mechanical and thermal properties of the tool will be evaluated. A topological tool design will be proposed that has adequate mechanical strength and thermal properties.

## 2 State of the Art

Utilizing rapid tooling can greatly reduce the manufacturing cost and lead time for tool production [5, 7–11]. Tool material, accuracy, surface finish, and mold life are some limitations of rapid tooling [7, 11–13]. Accuracy, thermal conductivity, and mechanical properties of the tool have a significant influence on injection molding cycle, part quality, and geometric complexity [14, 15].

Computer-aided evaluation for rapid tooling process selection and manufacturability for injection molding has been presented by Nagahanumaiah [7]. A methodology comprising of three major steps, rapid tooling process selection, manufacturability evaluation, and mold cost estimation, has been developed [7]. In addition, an integrated quality function deployment (QFD) and analytic hierarchy process

(AHP) methods were implemented in a visual C ++. The resulting computer-aided evaluation aids in the selection of the most appropriate rapid tooling in addition to providing costing models [7].

Au et al. have performed CAE and CFD validation on rapid tooling for injection molding of plastic [16]. Also, in an investigation by Rahmati et al. metal-filled stereolithography (SLA) rapid tooling cavity inserts were developed [17]. In particular, SLA is used to fabricate epoxy insert shells directly from CAD data which were then fitted into steel frames and reinforced with aluminum powder and epoxy resin mixture [17]. The research concluded that Moldflow Plastic Insight can be used to identify the optimal cooling system for the rapid tooling, and COMSOS/works can be used to evaluate the mechanical properties between solid and scaffolding assembly [17].

Structural analysis of a rapid prototype tooling made from photopolymer with stereolithography has been conducted by Huamin Zhou et al. [9]. The study predicted the deformation that occurs in the final part created in the rapid prototype tooling due to the thermal and mechanical loads of the filling process.

Stereolithography injection molding tooling experimental data were generated by Himasekhar et al. [15]. The data were used to evaluate the performance of the rapid prototype tool with regard to the distortion in each axis and the twist in the formed part. The validation results from the computational model were within 15% to the experimental data for each measurement. In addition, the research also highlighted the importance of the tooling material thermal conductivity to ensure a quality part is created [15].

Three-dimensional nonlinear coupled thermo-mechanical finite element method (FEM) model has been developed by Song et al. to analyze the dimensional accuracy for casting dies using rapid tooling molds [10]. The FEM analysis is nonlinear due to three main attributes: the material, geometry, and boundary conditions. In the study, it was found that convergence criterion and time steps directly influence the computational accuracy of the FEM model. Within the study, it was found that the simulated shrinkage ratio of the part casted in the rapid tooling mold was 1.108% which compares closely to the experimental shrinkage ratio of 1.158% [10].

This study will investigate whether a novel rapid tooling platform produced through additive layer manufacture is a viable method for the application of exterior automotive seals in EPDM. Specifically, computational validation is a rapid tool that combines metal powder and epoxy, which uses ALM methods of selective laser sintering. Computational validation will be performed where the mechanical properties of the tool will be evaluated.



### 3 Methodology

#### 3.1 Novel ALM Rapid Tooling

In this study, a novel rapid tooling concept is proposed whereby a shell produced through ALM is reinforced with an epoxy. Combining both ALM and epoxy rapid tooling will deliver a unique tooling platform that must initially be validated through computational simulation to inform the design constraints. In particular, the mechanical requirements.

Figure 1 illustrates the manufacturing route for the proposed rapid tooling techniques to manufacture tooling for the application of injection molding. In particular, initially, the shell will be produced via ALM to produce a near net insert (Table 1). Following this, a high-temperature RS-2243 epoxy is then poured into the tool to act as reinforcement. The geometry used within the investigation corresponds to the current tooling format used within the production of EPDM automotive door seals.

The injection molding parameters used within the investigation are summarized in Table 1.

**Computational Model**—Mechanical simulations will be performed by ANSYS static structural system. Static structural system is chosen over the transient structural system due to the steady-state nature of the application. A constant pressure of 140 MPa will be applied at the fluid interaction face to represent the injection pressure. Fixed geometry will be applied to faces which are in contact with other parts of the

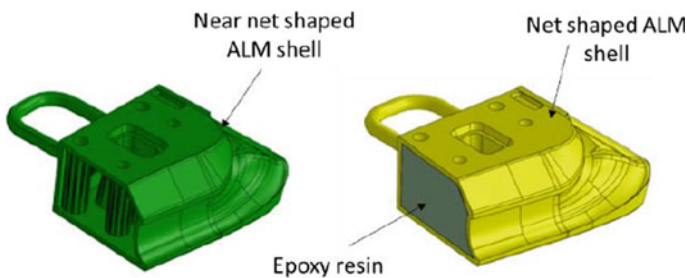
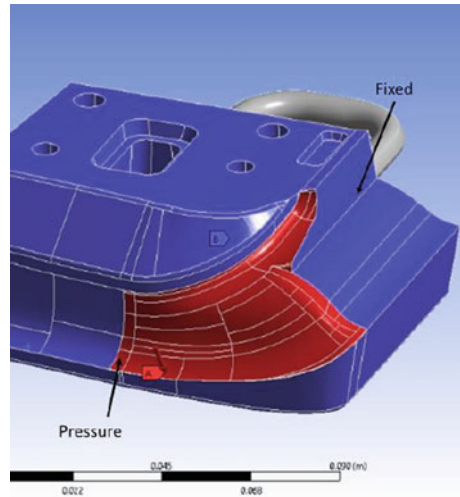


**Fig. 1** Process route to produce rapid tooling

**Table 1** Typical parameters for injection molding of EPDM exterior automotive seals

Parameter	Value
Injection pressure	1400 bar (140 MPa)
Clamping pressure	2000 bar (200 MPa)
Temperature of melt	125°C
Temperature of plate	200°C
Vulcanization time	85 s
Melt material	EPDM Dense 60 shore A

**Fig. 2** Mechanical model setup



tool. Figure 2 shows the physical set up of the mechanical simulation which includes a pressure and fixed geometries.

Contact setting between the two components of the part, the shell and reinforcement, in the computational model is set to be bonded. Analysis setting will be set to run for 1 s with ten time steps. Mesh sensitivity tests will be run to evaluate appropriateness of mesh characteristic to the application.

To investigate the effect of using different ALM materials, analysis was carried out on titanium, aluminum, and stainless steel. The properties are displayed in Table 2. In addition, all results from the ALM inserts were compared to a conventional P20 tool steel insert.

For the subsequent simulations, shell thickness, shell material, and reinforcement are independent parameters, while displacement and stress will be the dependent parameters. Shell thicknesses will vary between 2 and 12 mm.

## 4 Results and Discussion

### 4.1 Mesh Sensitivity Analysis

Mesh sensitivity analysis for the mechanical simulations were performed on the benchmark tool, which is a solid part made from P20 grade steel. In particular, the mesh sensitivity analysis compared maximum and average displacement and stress, and computational time against the number of elements for a linear- and quadratic-type mesh is displayed in Fig. 3.

**Table 2** Material and their properties to be used in computational simulations

Material name	P20 Grade steel	Ti6Al4V ELI-0406	Alsi10Mg	SS 316-0407	RS-2243 high-temperature epoxy
	Steel	Titanium	Aluminum	Stainless steel	Epoxy resin
Use	benchmark	shell	shell	shell	reinforcement
density (g/cm <sup>3</sup> )	7.85	4.42	2.68	7.99	1.8
Thermal conductivity (W/m°C)	46.5	8	190	16.2	0.85
Melting range (°C)	1460	1635	570	1371	170
Coefficient of thermal expansion ( $\mu/^\circ\text{C}$ )	11.8	9	21	16.0	32.4
Ultimate tensile strength (Mpa)	927	1085	366	624	34.3
Yield strength (Mpa)	716	985	220	494	27.5
Youngs modulus (Gpa)	204	126	64	190	9.61
Specific heat capacity (J/kg°C)	471	528	994	490	1200
Emissivity	0.4	0.25	0.15	0.15	0.9

The results conclude that a mesh which has 117,000 elements produces converged results for both the displacement and stress simulations, irrespective of the mesh type used. Computational time for the linear mesh is less; however, when analyzing at the converged maximum stress results, the linear mesh results is 35% smaller than for the quadratic mesh which is a significant deviation in results. Therefore, a quadratic mesh type is found to be more accurate.

## 4.2 Displacement

Figure 4 displays the maximum displacement of inserts manufactured with different shell thicknesses, materials, and with or without reinforcement. As can be seen in Fig. 4, there is a large difference in maximum displacement between parts with and without reinforcement material. With the 2 mm thick aluminum shell, the maximum displacement is 17.8 times larger in the part without reinforcement compared to the

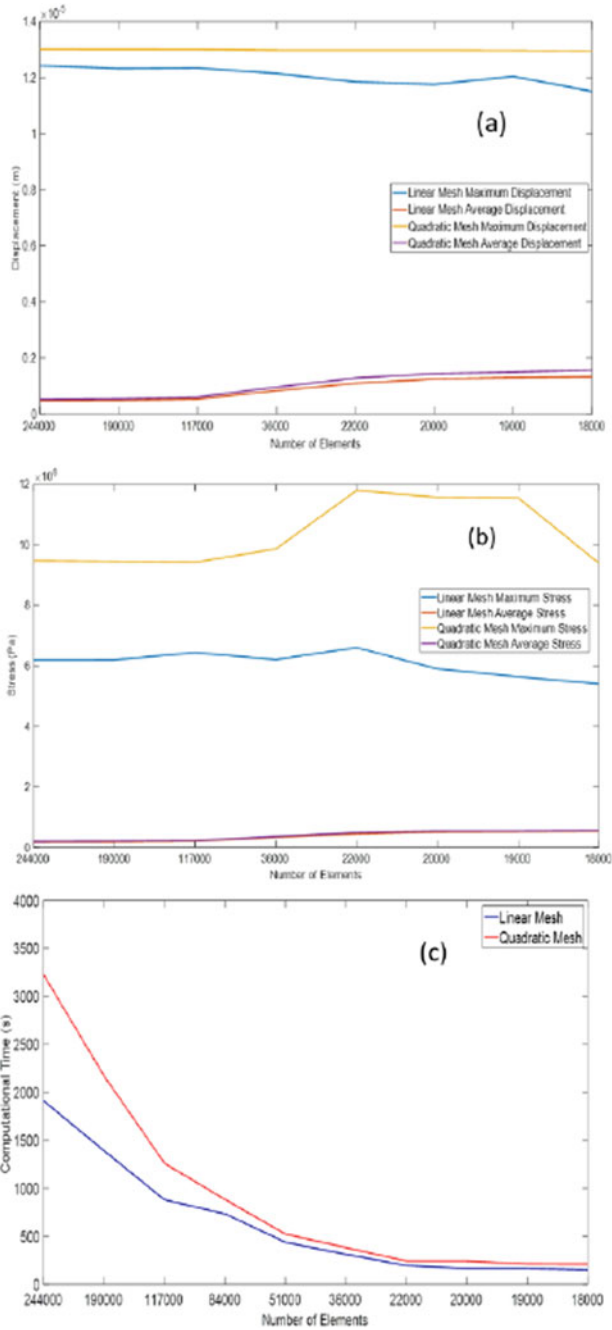


**Fig. 3** Mesh sensitivity analysis, comparing **a** maximum and average displacement, **b** maximum and average stress, and **c** computational time against number of elements for linear- and quadratic-type mesh

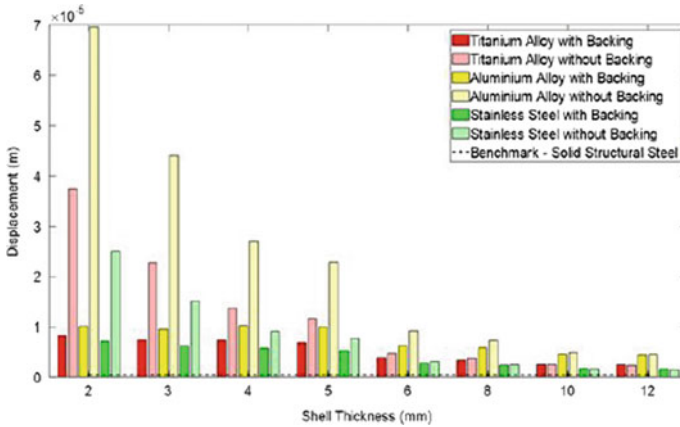


Fig. 4 Maximum displacement

part which had reinforcement. As the shell thickness increases, there is a reduction in the difference in maximum displacement between parts with and without reinforcement. However, the part with reinforcement always has the smaller maximum displacement compared to the same part without reinforcement. This is due to the mechanical strength that the reinforcement adds the part. The results conclude that maximum displacement levels only increases marginally after a shell thickness of 6 mm has been reached.

### 4.3 Stress

Figure 5 displays the maximum stress of parts with different thicknesses, materials, and with or without reinforcement. As seen in Fig. 5, the stress results follow the same trends as the displacement results in Fig. 4. ALM parts which have reinforcement have considerably lower maximum stress when compared to parts which have no reinforcement. It is also seen that the maximum stress in the parts decreases with an increase in shell thickness.

Comparing the ALM and benchmark parts, we see very similar maximum stress in parts with shell thickness of 10 mm or more regardless of material. To facilitate deeper analysis, the maximum stress has been compared with the material UTS, which is shown in Fig. 6.

As expected, the percentage of nodes with stress greater than its material UTS decreases with an increase in shell thickness and with the inclusion of reinforcement. Also as displayed in Fig. 6, the titanium shell rapid prototype tooling performs best, having significantly less nodes with stress over its material UTS compared to the aluminum and stainless-steel rapid prototype tooling. There was no exceeding of UTS stress witnessed in the titanium shell over 5 mm thick with reinforcement and

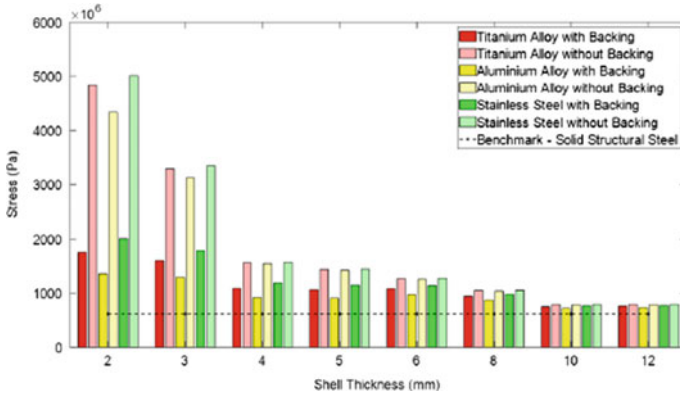


Fig. 5 Maximum stress

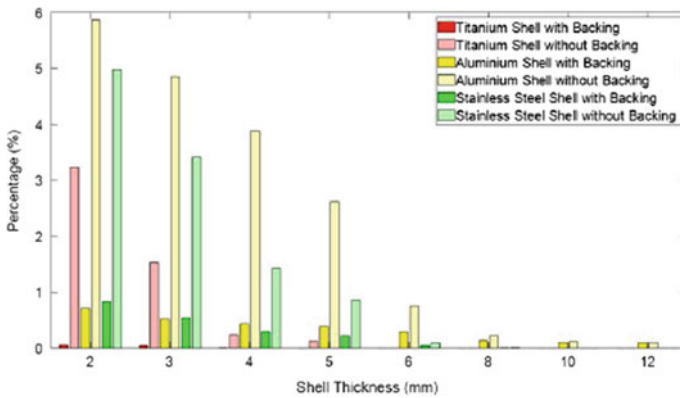


Fig. 6 Maximum stress compared to UTS

stainless-steel shell over 10 mm thick with reinforcement. Furthermore, the results conclude that maximum displacement levels only increase marginally after a shell thickness of 6 mm has been reached.

From the results, it can be concluded that ALM parts with shell thickness greater than 6 mm without reinforcement would also be suitable for prototype manufacture of EPDM parts using injection molding. When using a reinforced epoxy, an optimum wall thickness was found to be 6 mm.

## 5 Conclusion

A novel rapid tooling methodology has been proposed which combines metal powder and epoxy rapid tooling techniques. Computational validation has been performed on ANSYS 19.1 software to validate the suitability of the novel rapid tooling methodology to manufacture tooling for injection molding of EPDM exterior automotive seals. The main conclusions from the research are:

- Rapid prototype tooling produced by the proposed novel rapid tooling method is sufficient for prototype manufacture of EPDM parts by injection molding.
- Tooling inserts produced from titanium showed the best performance. In particular, the research concludes that when using reinforcement a 6 mm wall is optimal.
- Mechanical properties of rapid prototype tooling 2 mm thick shell with reinforcement and 8 mm thick shell without reinforcement are similar. Compared to the benchmark, both have similar stress results but much higher displacement results.

## 6 Future Work

The experimental testing is needed to validate the computational simulation findings. The characteristics of the bond between the shell and reinforcement need to be quantified. Evaluation of alternative material for the reinforcement is needed to optimize the rapid prototype tooling. Further research could evaluate the suitability of using a fluid as the reinforcement as it is incompressible.

## References

1. Yan, X., Gu, P.: A review of rapid prototyping technologies and systems. *CAD Comput. Aided Des.* (1996)
2. Pham, D.T., Dimov, S.S.: *Rapid Manufacturing: the Technologies and Applications of Rapid Prototyping and Rapid Tooling*. Springer, London (2001)
3. Gurr, M., Mülhaupt, R.: Rapid prototyping. *Ref. Modul. Mater. Sci. Mater. Eng.* (2016)
4. Rosochowski, A., Matuszak, A.: Rapid tooling: the state of the art. *J. Mater. Process. Technol.* **106**(1–3), 191–198 (2000)
5. Chua, C.K., Chou, S.M., Wong, T.S.: Rapid prototyping technologies and limitations. *Int. J. Adv. Manuf. Technol.* **14**, 146–152 (1998)
6. Kruth, J.-P.P., Leu, M.C.C., Nakagawa, T.: Progress in additive manufacturing and rapid prototyping. *CIRP Ann. Manuf. Technol.* **47**(2), 525–540 (1998)
7. Nagahanumaiah, Subburaj, K., Ravi, B.: Computer aided rapid tooling process selection and manufacturability evaluation for injection mold development. *Comput. Ind.* **59**(2–3), 262–276 (2008)
8. Levy, G.N., Schindel, R., Kruth, J.P.: Rapid manufacturing and rapid tooling with layer manufacturing (LM) technologies, state of the art and future perspectives. *CIRP Ann. Manuf. Technol.* **52**(2), 589–609 (2003)

9. Zhou, H., Li, D.: Integrated simulation of the injection molding process with stereolithography molds. *Int. J. Adv. Manuf. Technol.* **28**, 53–60 (2006)
10. Song, Y., Yan, Y., Zhang, R., Lu, Q., Xu, D.: Three dimensional non-linear coupled thermo-mechanical FEM analysis of the dimensional accuracy for casting dies in rapid tooling. *Finite Elem. Anal. Des.* **38**(1), 79–91 (2001)
11. Hague, R.J.M.: Unlocking the design potential of rapid manufacturing. In: *Rapid manufacturing: an industrial revolution of the digital age* (2006)
12. Sood, A.K., Ohdar, R.K., Mahapatra, S.S.: Improving dimensional accuracy of fused deposition modelling processed part using grey Taguchi method. *Mater. Des.* **30**(10), 4243–4252 (2009)
13. Saqib, S., Urbanic, J.: An experimental study to determine geometric and dimensional accuracy impact factors for fused deposition modelled parts: enabling manufacturing competitiveness and economic sustainability, pp. 293–298. Springer, Berlin, Heidelberg (2012)
14. Iyer, N., Ramani, K.: A study of localized shrinkage in injection molding with high thermal conductivity molds. *Inject Mould Technol.* **6**(2), 73–90 (2002)
15. Himasekhar, K., Lottey, J., Wang, K.K.: CAE of mold cooling in injection moulding using a three dimensional numerical simulation. *J Eng Ind.* **114**(2), 213–221 (1992)
16. Au, K.M., Yu, K.M.: A scaffolding architecture for conformal cooling design in rapid plastic injection moulding. *Int. J. Adv. Manuf. Technol.* **34**(5–6), 496–515 (2007)
17. Rahmati, S., Dickens, P.: Rapid tooling analysis of Stereolithography injection mould tooling. *Int. J. Mach. Tools Manuf.* **47**(5), 740–747 (2007)



# Impact of Nonplanar 3D Printing on Surface Roughness and Build Time in Fused Filament Fabrication



Ahmed Elkaseer , Tobias Müller , Dominik Rabsch, and Steffen G. Scholz 

**Abstract** Nonplanar 3D printing is a recently emerged approach to increase surface quality and part strength in additive manufacturing. In this paper, the impact of a nonplanar printing method utilized for the fused filament fabrication (FFF) technique on the resultant surface roughness of printed parts is presented. In particular, the influence of different inclination angles and part orientation on the obtainable surface quality was investigated by comparing a traditional planar printing strategy with a nonplanar finishing solution. A pyramidal geometry was utilized to assess the effect of inclination angle as well as part orientation and relative printhead movement on the surface characteristics. The results show a decrease in obtainable surface roughness for inclination angles up to 25°, while higher angles cause rougher surfaces when compared with results of planar 3D printing strategy. This can be explained by the way the nonplanar nozzle movements interact with previously deposited filament strands by deforming them due to the size of the nozzle and geometry of the 3D printed part. As a consequence, solutions for an improved nonplanar printing technique using Delta FFF printers are suggested that will be investigated in the future work.

## 1 Introduction

In contrast to subtractive manufacturing, where undesired material is removed away from a bulk workpiece, additive manufacturing (AM), also known as 3D printing,

---

A. Elkaseer (✉) · T. Müller · D. Rabsch · S. G. Scholz  
Institute for Automation and Applied Informatics, Karlsruhe Institute of Technology, 76344  
Eggenstein-Leopoldshafen, Germany  
e-mail: [ahmed.elkaseer@kit.edu](mailto:ahmed.elkaseer@kit.edu)

A. Elkaseer  
Faculty of Engineering, Port Said University, Port Fuad 42526, Egypt

S. G. Scholz  
Future Manufacturing Research Institute, College of Engineering, Swansea University, Bay  
Campus, Crymlyn Burrows, Swansea SA1 8EN, UK

Karlsruhe Nano Micro Facility (KNMF), Hermann-Von-Helmholtz-Platz 1, 76344  
Eggenstein-Leopoldshafen, Germany

adds material layer upon layer to form a desired object. Major advantages of this method are the relatively low amount of material waste as well as the ability to form complex geometries, therefore offering the freedom to redesign existing parts and create assembly like parts that can be produced in one print [1, 2]. AM processes exist for various materials and differ in the way the layers are fused to build an object. For example, metal objects are produced by melting or sintering of metal powders via a laser beam, among others [2]. These methods have shown potential to reduce weight and waste in fabrication of parts for aircrafts or improve the quality of personalized medical implants [3]. Other processes are binding a material powder via adhesives or cure polymers through ultraviolet irradiation [4], but the most prominent example for AM is fused filament fabrication (FFF) [5].

In FFF, a polymer filament is melted in a so-called hot-end and is then deposited on a bed by a nozzle to form a layer of the desired object following a computer-aided design (CAD). After finishing a layer, the nozzle or the bed moves vertically, and the next layer is deposited on top of the previous one. For FFF technology, various materials exist, also including particle-filled filaments as well as flexible elastomers like thermoplastic polyurethane (TPU). Nowadays, the most commonly used source material is polylactic acid (PLA), which is easy to print and biodegradable. With multi-extruder machines, it is even possible to build assemblies of different materials in a single printing process. However, FFF machines cannot directly print commonly used CAD models. Instead, they need instructions where to extrude which amount of molten filament. The interface between the CAD model and these instructions is a so-called slicer, which converts the model into a toolpath and adding further information for the printer such as print speed, nozzle temperature and is saving this information in a so-called g-code file.

The FFF approach is mainly used for rapid prototyping of polymer objects or production of customized parts, as lead time is low compared to other conventional techniques. In contrast, FFF is rarely found in mass production due to several disadvantages. One major drawback is the rough surface of 3D printed models, which is largely caused by the stair stepping effect. This effect is an approximation error of all layer-based manufacturing processes and can be reduced by decreasing layer thickness [2, 6]. However, decreased layer thickness goes along with increased building time, which is another drawback of FFF in mass production. This led to development of adaptive slicing techniques that adjust the layer height within a model dependent on surface angles, therefore finding a trade-off between speed and accuracy [7]. Nevertheless, thin layers and optimization of other process parameters only lower the error, but it is not possible to abolish it following these approaches. Especially when it comes to conventional FFF printing, with layer thickness between 0.05 and 0.3 mm, the deviation of the printed part from the CAD model increases dramatically at surface angles below 20° [8]. To overcome this issue, research focused on nonplanar layers via active Z-printing. This process was described by Chakraborty et al. as curved layer fused deposition modeling (CLFDM) and was stated to not only abolish the stair stepping effect, but also increase the strength of AM parts [9]. Therefore, they developed an algorithm that ensures lateral bonding of adjacent, deposited filament lines. However, there has been no detailed study to examine the effect of

the nonplanar printing approach on attributes of real printed objects. One application example of CLFDM, shown by Huang and Singamneni, is a combination of planar and nonplanar layers, where curved layers are placed on top of a planar scaffold. This shifts the stair stepping inside the part, improving its surface quality as long as several nonplanar layers are placed on top and strengthens the object by connecting planar layers in z-direction [7]. This statement was confirmed by them earlier, where it was shown that the fracture compressive load of CLFDM manufactured parts is clearly higher than for flat-layered parts [10], but also highly depends on the printed raster angle [11]. Further, Diegel et al. concluded that CLFDM offers the possibility to print electrical circuits in curved parts as the stair stepping no longer interrupts wires [12].

However, toolpath planning for nonplanar layers is a challenging topic, as the nozzle can collide with previously printed structures. Further, the printing angle relative to the inclination highly influences the surface quality, as it is possible that the nozzle of a 3-axis Cartesian 3D printer scratches previously extruded filament in the downward printing motion. In addition, the shape of an extruded line highly depends on the inclination angle and is not constant same as in planar printing. The best solution for these issues would be using a 5-axis printer, which could adjust the extruder axis to be perpendicular to the printed surface, therefore reducing scratching and exerting a constant pressure at the filament to provide a constant shape [13]. However, 5-axis 3D printing is much more complex regarding collision avoidance and negates some of the advantages of additive manufacturing. Further, it seems to be yet at early stage and machines as well as slicing software are scarce. Allen and Trask pointed out that using a Delta FFF printer is a good alternative to 5-axis printers. Such a system, where the extruder is moved by three triangular arranged arms, outperforms Cartesian printers in CLFDM when it comes to collision avoidance and printing speed [14].

To explore the possibility of CLFDM, a nonplanar slicing algorithm for 3-axis 3D printers that is based on an open source slicing software (Slic3r) was developed [8]. Slic3r is compatible with most FFF machines and so is the nonplanar slicing option. This approach combines a planar scaffold with nonplanar top surfaces, but is in contrast built on top of an existing slicing software, thus providing an easy to handle graphical user interface. However, the possibility to print a nonplanar surface is mainly restricted by the geometry of the extruder. Therefore, it is possible to set two parameters that are used for collision avoidance in the nonplanar Slic3r version. One is the maximum height of nonplanar surfaces, and the other is the maximum printable inclination, which depends on the nozzle angle. These values are used to calculate which surfaces could be printed in nonplanar mode and which cannot. Another important feature of the nozzle geometry is the flat area at their tip. This area might scratch neighboring filament lines as well as the currently laid line in a downward printing process, therefore decreasing surface quality. In this thesis [8], it is concluded that this mainly affects surfaces with a high inclination angle, where the stair stepping error is marginal. Further, an option preventing the scratching is missing on the software side. However, a fictional nozzle with a very small flat area

at the tip is shown which might also counteract the scratching issues whilst printing high angles.

Despite the fact that most articles about CLFDM state an improved surface quality, real measurements and comparison to flat layer printing are still omitted. Therefore, the aim of this study is to evaluate the maximum inclination angle at which the surface quality of nonplanar prints outperforms the roughness of planar printed models. Further, we investigated the reasons behind the angle-dependent varying surface quality of CLFDM manufactured parts. The answers to these questions might be helpful to increase the overall quality of 3D printed parts and especially reduce time-consuming post-processing steps which for some materials also include treatment with hazardous chemicals. Consequently, improving surface roughness directly at the printing step would increase sustainability by saving time, energy, and effort.

## 2 Materials and Methods

The material used in this study is PLA, which is the most common material in FFF. For testing of different inclination angles, seven pyramidal objects were designed. The lateral faces of these objects were showing inclination angles of  $5^\circ$  to  $35^\circ$  in steps of  $5^\circ$  relative to the building plate (Fig. 1). This offers the possibility to measure surface roughness at four different sides of each object. The structure was placed on a platform, as adhesion of the nonplanar layers to such should be better compared to nonplanar layers directly printed on a glass bed. Such a bad adhesion might result in errors on the test surface, which would in turn decrease the overall surface quality.

Each of the models in Fig. 1 was sliced with the nonplanar Slic3r version running with the constant settings mentioned in Table 1. For printing of the models, a Zmorph 2.0 SX printer was used. A relatively slow printing speed was chosen as the Z-axis of Cartesian FFF printers is not built for rapid movements that occur during printing with an active Z-axis. Therefore, the test objects were printed at 30 mm/s to avoid issues that could arise due to a vertical axis that is lagging behind. As

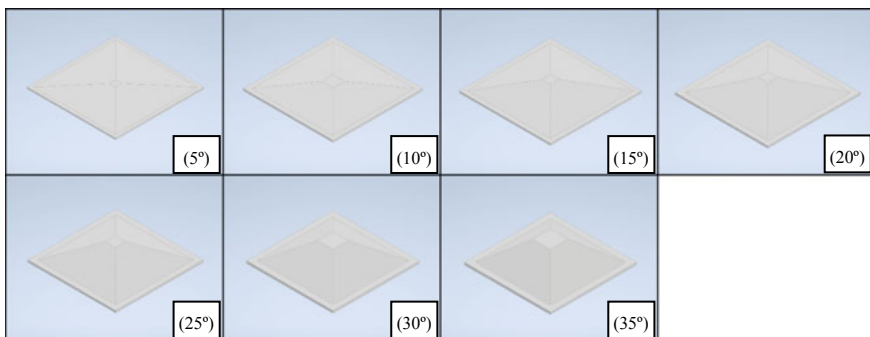


**Fig. 1** Models of printed objects with different inclination angles

**Table 1** Constant parameters

Constant parameter	Value	Unit
Bed temperature	60	°C
Top solid layers	5	No.
Bottom solid layers	3	No.
Outline shells	2	No.
Infill outline overlap	25	%
Printing speed	30	mm/s
Layer height	0.2	Mm
Infill pattern	rectilinear	–
Infill	20	%
Nozzle diameter	0.4	Mm
Infill angle	45	°

the geometry of the extruder offered the possibility to print all the models without collisions, the maximum nonplanar height was set to 15 mm, and for the maximum nonplanar angle, 60° was chosen. Due to some bugs in the g-code that were produced by the nonplanar Slic3r version, a post-processing script was written in python to remove corresponding printer movements. The script was designed to delete travel movements with identical start- and end-coordinates and remove unwanted extrusion in the air. Such an extrusion would cause collisions during later printing steps due to movements into the dripping position.

Further, each model with certain inclination angle was printed three times via the post-processed nonplanar g-code as well as three times in the planar mode, resulting in 42 test objects. Other printing parameters were kept constant and are shown in Table 1.

The build time of all objects was measured with the Zmorphs integrated timer. For each sample object, 12 roughness measurements were performed with a Keyence VHX 7000 microscope (Fig. 2a). Therefore, the surface roughness value ( $S_a$ ) of a 3 × 3 mm area was measured three times per side. Measurements were distributed (as shown in Fig. 2b); side-dependent average value was calculated. To place measured sides perpendicular to the microscope, fixtures of corresponding angles were used, and thus, no filters were used on the software side. Further, it was essential to use a less shiny, gray PLA filament as reflection might cause errors in an optical roughness measurement. For statistical comparison, the two-sample t test of the python “SciPy” library was used.

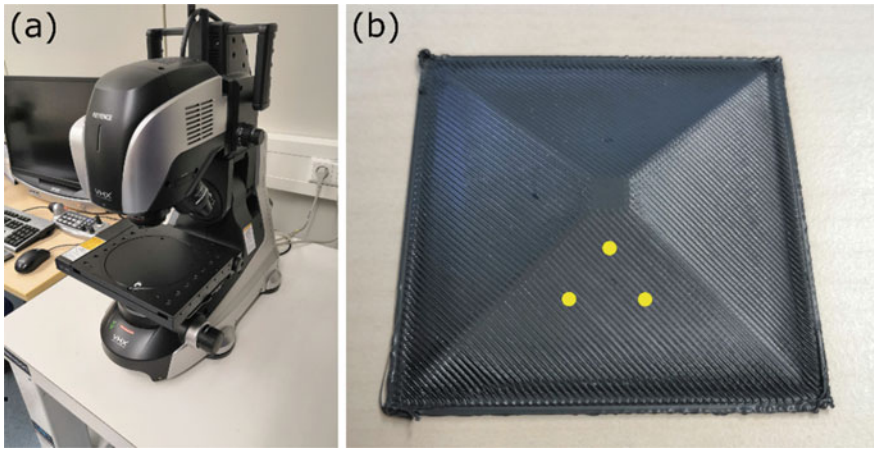


**Fig. 2** A Keyence VHX 7000 microscope B 15° test sample. Red dots indicate roughness measurements and were made at the specific side

### 3 Results and Discussion

#### 3.1 Surface Roughness

Figure 3 displays the results of the roughness measurements of the 42 test objects. The surface roughness of different angles is compared between the nonplanar and the

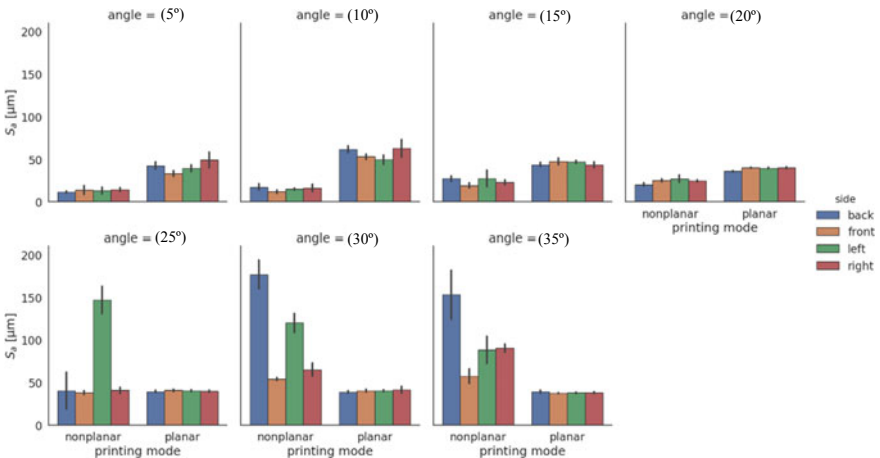


**Fig. 3** Surface roughness values ( $S_a$ ) of the different test parts. Each bar chart shows a different inclination angle, which is additionally split into nonplanar and planar printing mode. The color of bars depends on the side relative to where the printing process of the last layer started

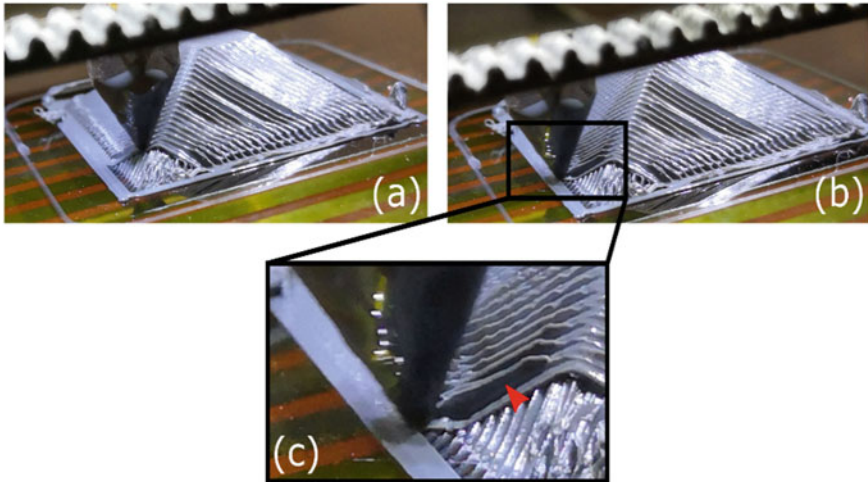


**Fig. 4** Printing process of the 35° test piece. **a** and **b** Zmorph nozzle movement scratches filament resulting in **c** protruding filament (red arrow) causing high surface roughness

planar printing mode. For each angle, the average roughness of all objects depending on the side relative to the printing process is shown. “Front” hereby indicates the side at which printing of the last layer starts in the right corner. Statistical analysis reveals that below an inclination angle of 25° in relation to the building plate, and the surface quality of nonplanar printed objects is clearly better than of planar printed parts. This confirms earlier statements that a combination of a planar scaffold and nonplanar layers is able to abolish the stair stepping effect [7]. However, at an angle of 25° the surface roughness of the left side is worse in nonplanar mode, while the front side is slightly better. The remaining two sides show no statistical significant difference between the printing modes. At inclination angles above 25°, the  $S_a$  value of nonplanar printed parts is clearly worse. This bad surface finish is the result of protruding filament that is scratched by the nozzle as shown in Fig. 4.

Interestingly, there is no big difference between the four sides of objects below an inclination angle of 25°, but at higher angles, different sides show distinct surface roughness when printed in nonplanar mode. In contrast, this diversity is not observable in any of the planar printed parts.

The explanation for these findings is related to the geometry of the nozzle. In 3-axis nonplanar printing, it is not possible to adjust the extruder axis to be perpendicular to the printed surface. Therefore, the flat area at the nozzle tip plays an important role in the resulting surface quality. Measurements of the Zmorph’s nozzle revealed that the diameter of the flat area is around 0.8 mm, which is twice the diameter of the filament extruding hole. This additional area is scratching the extruded filament in a downward printing motion. As the infill angle is 45° in the printed examples, two of the sides are always printed slightly upward (Fig. 5a), and the other two are printed slightly downward (Fig. 5b). Please note that upward and downward refer to

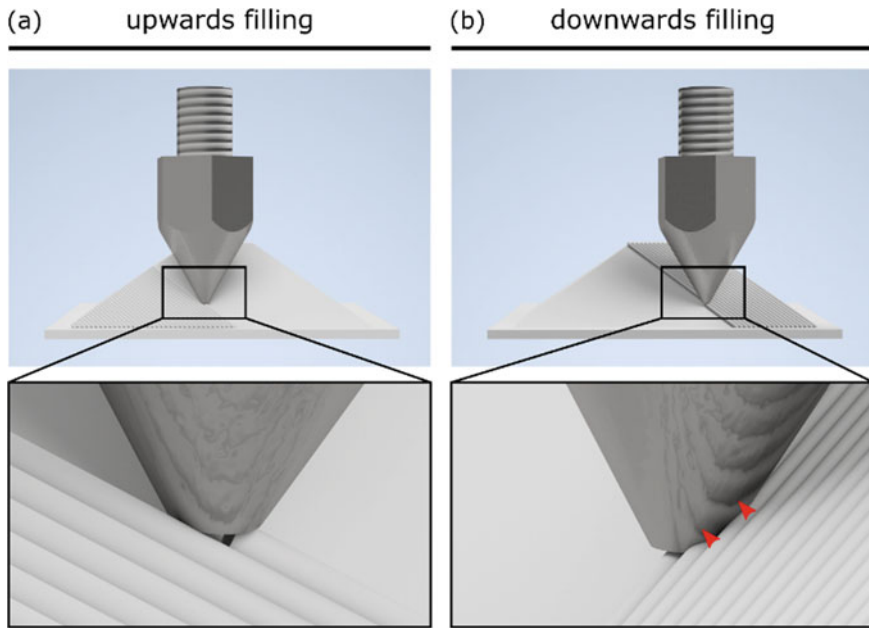


**Fig. 5** Printing of nonplanar surfaces of test pieces with an infill angle of  $45^\circ$ . The image shows a  $35^\circ$  part and the Zmorph nozzle depositing nonplanar filament lines on the inclination side upward vs. downward (red arrows). **a** During the upward filling, adjacent filament is slightly below currently deposited line, therefore resulting in minor scratching. **b** In a downward filling process, neighboring filament lines are slightly above the new line, which results in heavy scratching of them (red marks)

the direction in which the deposited layers are put next to each other. This leads to scratching of previously deposited filament when printing downward. Consequently, this results in a bad surface finish, which is clearly observable in the roughness of test pieces with an inclination of  $30^\circ$ . As the corner, where the printing of the last layer starts is defined as the front right, the left, and backside are the ones that are always printed downward. Hence, scratching of previously deposited filament at these sides increases the surface roughness value. In addition, if a line is printed downward, scratching occurs within the same line independent of neighboring filament. This scratching also messes up surface quality and gets even worse at high inclination angles like in the  $35^\circ$  parts.

Unfortunately, the here used slicing software has no option to counteract scratching by adding up some height when printing downward, like proposed in earlier studies [13]. However, the impact of such additional height on the shape of deposited filament lines, and hence the surface roughness, is an interesting starting point for further investigation.

Moreover, the shape of the nozzle tip was proposed to be an important factor in high-angle CLFFF [8]. Usage of customized nozzles nearly solely consisting of the



filament extruding hole and showing a very sharp opening angle might be another solution for filament scratching in 3-axis nonplanar printing.

### 3.2 Build Time

The build time of most models sliced via the nonplanar option was slightly higher than the building time of flat layer printed parts (Fig. 6). However, building time cannot be compared between objects with different inclination angles, as the models were not normalized, e.g., to an identical build volume.

Only the test part with an inclination angle of  $10^\circ$  was printed faster in nonplanar mode. Despite the fact that these differences might be neglectable, it is indispensable to mention that build time is solely comparable due to the similar printing speed of 30 mm/s. Like proposed by various authors, printing speed does not affect surface roughness the same way other factors, e.g., layer height do [15]. Accordingly, speed could be increased when printing with conventional planar settings, which is not the case for the nonplanar printing if a Cartesian system such as the Zmorph is used. Such printers were shown to have fast  $X$ - and  $Y$ -axis but have a  $Z$ -axis that is not built for rapid printing movements. Consequently, comparable building times are only reached by using robots with a faster reacting the  $Z$ -axis, e.g., Delta FFF machines [14].

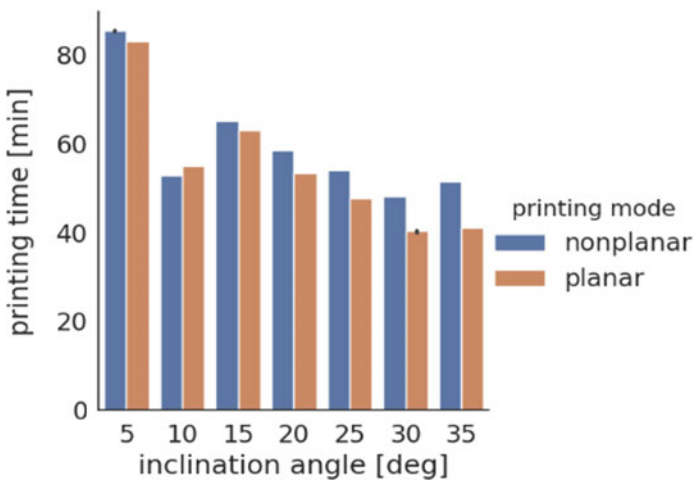


**Fig. 6** Printing time comparison of nonplanar and planar printed parts. Printing planar parts are always faster except for the part with the  $10^\circ$  inclination angle

## 4 Conclusion

The aim of this study is to reveal the impact of nonplanar printing on surface quality of FFF objects. It was clearly shown that at low inclination angles ( $< 25^\circ$ ), a common 3-axis 3D printer is able to improve the surface quality by adding nonplanar layers on top of a planar scaffold. In contrast, higher angles are printed better with the common layer-based technique. The main reason for this seems to be scratching of the nozzle tip. This happens, as the extruder axis is not perpendicular to the printing direction, when a 3-axis printer is used. However, the mentioned slicing tool is a good alternative to the rare 5-axis approaches as it counteracts the stair stepping effect, which causes the biggest error in parts with low inclination angles. This effect has minor impact on surface roughness at inclination angles above  $25^\circ$ . Consequently, it is possible to print higher quality surfaces with a nonplanar slicing tool, even with conventional Cartesian printers, and further investigation of the impact of nonplanar printing on other aspects like dimensional accuracy has to be done. There is also need for improving other printing parameters that are important in nonplanar printing. For example, it might be essential to examine the effect of printing speed on surface roughness. Despite the fact that speed was shown to not change surface roughness in planar printing, it can have a relation in nonplanar printed surfaces due to coordination of all three axes. Further, the tested nozzle does not have a perfect geometry, and it might be possible to improve the maximum angle at which nonplanar printed parts have a better surface finish, by creating customized nozzles. Also, the impact of varying nozzle height on surface quality is another topic that needs further research.

**Acknowledgements** This work was carried out with the support of the Karlsruhe Nano Micro Facility (KNMF, [www.knmf.kit.edu](http://www.knmf.kit.edu)), a Helmholtz Research Infrastructure at Karlsruhe Institute of Technology (KIT, [www.kit.edu](http://www.kit.edu)) and under the Helmholtz Research Programme STN (Science and Technology of Nanosystems) at KIT.

## References

1. Gebisa, A.W., Lemu, H.G.: Design for manufacturing to design for additive manufacturing: analysis of implications for design optimality and product sustainability. *Procedia Manuf.* **13**, 724–731 (2017)
2. Charles, A., Elkaseer, A., Thijs, L., Hagemeyer, V., Scholz, S.: Effect of process parameters on the generated surface roughness of down-facing surfaces in selective laser melting. *Appl. Sci.* **9**(6) (2019)
3. Murr, L.E.: Frontiers of 3D printing/additive manufacturing: from human organs to aircraft fabrication. *J. Mater. Sci. Technol.* **32**(10), 987–995 (2016)
4. Bikas, H., Stavropoulos, P., Chryssolouris, G.: Additive manufacturing methods and modeling approaches: a critical review. *Int. J. Adv. Manuf. Technol.* **83**, (2015)
5. Fauth, J., Elkaseer, A., Scholz, S.G.: Total cost of ownership for different state of the art FDM machines (3D printers). In: *Sustainable Design and Manufacturing 2019*, pp. 351–361. Springer, Singapore (2019)

6. Durgun, I., Ertan, R.: Experimental investigation of FDM process for improvement of mechanical properties and production cost. *Rapid Prototyping J.* **20**, (2014)
7. Huang, B., Singamneni, S.: A mixed-layer approach combining both flat and curved layer slicing for fused deposition modelling. *Proc. Inst. Mech. Eng. part B: J. Eng. Manuf.* **229**, (2014)
8. Ahlers, D., Wasserfall, F., Hendrich, N., Zhang, J.: 3D printing of nonplanar layers for smooth surface generation (2019)
9. Chakraborty, D., Reddy, B., Choudhury, A.: Extruder path generation for curved layer fused deposition modeling. *Comput. Aided Des.* **40**, 235–243 (2008)
10. Huang, B., Singamneni, S.: Alternate slicing and deposition strategies for fused deposition modelling of light curved parts. *J. Achievements Mater. Manuf. Eng.* **55**, 511–517 (2012)
11. Huang, B., Singamneni, S.: Curved layer fused deposition modeling with varying raster orientations. *Appl. Mech. Mater.* **446–447**, 263–269 (2013)
12. Diegel, O., Sarat, Huang, B., Gibson, I.: Getting rid of the wires: curved layer fused deposition modeling in conductive polymer additive manufacturing. *Key Eng. Mater.* **467–469**, (2011)
13. Jin, Y.-a., Du, J., Fu, G.: Modeling and process planning for curved layer fused deposition. *Int. J. Adv. Manuf. Technol.* **91**, (2017)
14. Allen, R.J.A., Trask, R.S.: An experimental demonstration of effective curved layer fused filament fabrication utilising a parallel deposition robot. *Additive Manuf.* **8**, 78–87, (2015)
15. Anitha, R., Arunachalam, S., Radhakrishnan, P.: Critical parameters influencing the quality of prototypes in fused deposition modelling. *J. Mater. Process. Technol.* **118**(1), 385–388 (2001)

# In-Process Digital Monitoring of Additive Manufacturing: Proposed Machine Learning Approach and Potential Implications on Sustainability



Amal Charles , Mahmoud Salem , Mandaná Moshiri ,  
Ahmed Elkaseer , and Steffen G. Scholz 

**Abstract** Additive Manufacturing (AM) technologies have recently gained significance amongst industries as well as everyday consumers. This is largely due to the benefits that they offer in terms of design freedom, lead-time reduction, mass-customization as well as potential sustainability improvements due to efficiency in resource usage. However, conventional manufacturing industries are reluctant to integrate AM within their established process chains due to the unpredictability of the process and the quality of the final parts that are printed. Conventional manufacturing process have the advantage of decades of research in developing process knowledge and optimization, which culminates in accurate process predictability. This gap in process understanding is one that AM will need to cover in a short time. AM does have the benefit of being a digital manufacturing process and with the adoption of advanced Artificial Intelligence (AI) and Machine Learning (ML) techniques in production lines, there may not have been a better industrial age for its implementation. This paper presents a case for actively developing AM processes using ML. Then a method for in-process monitoring of the printing process is presented and discussed. The main benefit from using the proposed system is an increase in the efficiency and final quality of the parts printed, as a result of which there is an increased efficiency in resource usage due to preventing material loss due to failed builds and defected parts.

---

A. Charles (✉) · A. Elkaseer · S. G. Scholz  
Institute for Automation and Applied Informatics (IAI), Karlsruhe Institute of Technology (KIT),  
76344 Eggenstein-Leopoldshafen, Germany  
e-mail: [amal.charles@kit.edu](mailto:amal.charles@kit.edu)

M. Salem  
Faculty of Engineering, Ain Shams University, Cairo, Egypt

M. Moshiri  
Department of Mechanical Engineering, Technical University of Denmark, Building 427,  
Produktionstorvet, 5, 2800 Kgs. Lyngby, Denmark

A. Elkaseer  
Faculty of Engineering, Port Said University, Port Said 42526, Egypt

S. G. Scholz  
Karlsruhe Nano Micro Facility, 76344 Eggenstein-Leopoldshafen, Germany

# 1 Introduction

Industry 4.0, also referred to as 'I4.0', is the term that is commonly used to describe the fourth industrial revolution. The term 'Industry 4.0' was coined by a German government project that dealt with advanced technologies that promoted the computerization/digitalization of the manufacturing industry. Therefore, one of the underlying aims of I4.0 is to create a network of digital manufacturing assets and highly skilled people along the entire value chain of a production process wherein each step can be controlled autonomously [3, 12, 24].

I4.0 is an umbrella term that is used to group together various automation, digital and social trends. Some of the contributing digital technologies include:

The Internet of Things (IoT), Augmented reality/Virtual reality, Autonomous robots, Additive Manufacturing (AM), Big data analytics, Machine learning and AI, Smart sensors and actuators, Cloud computing and Cyber security.

Additive Manufacturing is considered to be one of the key enabling technologies (KET) of I4.0 since it is first and foremost a digital manufacturing technology [7, 10, 16]. Since all pre-processing, designing, modelling, simulation, build process generation, monitoring as well as post-processing can all be accomplished using computer/digital systems [20]. Therefore, except for some tasks such as material loading or support removal, an AM machine can work completely autonomously [11]. Moshiri et al. have developed a framework to automate even the material loading and support removal processes for developing a first-time-right smart manufacturing system for tooling production [17].

Compared to conventional manufacturing techniques, AM technologies are considered to be more sustainable, this is due to the capacity of AM to only use the exact amount of material as is required by a part. Whereas in subtractive manufacturing a component usually starts as a block of solid bulk material which is then machined and finally reduced to its final shape. Resulting in large amount of scrap material that is produced and wasted. Niaki et al. have identified and presented the various determinants to clarify the role of sustainability and its benefits in the decision making process for the adoption of additive manufacturing my manufacturing companies. However, their investigations concluded that the biggest driver for the adoption of AM is the design freedom and its sustainability benefits are rarely a driver for adoption, even though literature claim immense benefits for sustainability [18]. While Böckin el al investigated the prevalence of AM in the automotive industry and conducted an assessment of environmental impact. Their findings showed that with the current levels of implementation of AM showed only moderate or negligible environmental improvements and concluded that future implementation of AM should seek to exploit the benefits of the technology as well as potential offered in remanufacturing and repairing [2]. This is in accordance with the view of the authors and this paper presents the case for the combination of AM with adjacent I4.0 technologies such as Machine learning (ML). This paper therefore presents an introduction on the various areas in AM where ML can be implemented followed by proposing an in-process monitoring and quality control system designed to implement ML in AM.

## 2 Current State of ML Implementation in AM

Most current approaches to implementing ML approaches to AM have been largely focused on developing process models for various AM processes and post-processes in order to enable printing parameters optimization and selection [4, 5, 21]. This is the most common application for ML. However, with the increased interest in digitalization thanks to the growth of the I4.0 philosophy, lots of work is currently focused on achieving ML assisted in-process monitoring and in-process control systems [17]. In fact, it is only recently that process monitoring systems are being introduced inside of AM systems, especially with regards to the laser based powder bed fusion (LPBF) and Fused filament fabrication (FFF) processes, the two most popular AM processes.

The implementation of monitoring system will be essential to learn more about the process and its quality and to correlate it to the product quality. The current industrial pull is driving in this direction, for having in situ monitoring of the process and closed-loop actions to compensate eventual issues that would generates defects in the product [19].

To monitor AM processes multiple solutions have been developed in the recent years, and they have been thoroughly presented in some review papers [9, 19, 23]. For the future application of AM technologies in specific industrial environment, the research and implementation of monitoring systems are the starting point for the correlation between process signatures and product quality, therefore to early understand the performance of a product before stepping into post-process quality control phases. The final objective of monitoring research will be a closed-loop feedback control of the process, that can self-optimize to guarantee the desired product's quality [8, 22].

## 3 In-Process Monitoring and Quality Control in FFF

Previous sections have depicted current levels of ML implementation in AM and the attempts to integrate in-process monitoring methods have been mentioned as well. The following section will present a methodology that consists of an in-process monitoring system for the FFF process and solution for using this monitoring data to deploy in-process quality control. The main benefit expected from the in-process monitoring system is an improvement in the print quality and as a result an improved level of sustainability due to preventing any wastage due to failed builds and defected parts.

Additive manufacturing processes generally consume a lot of time and material, so it is advantageous to detect and prevent fabrication defects during the process. Current monitoring approaches make the measurement and analysis after the process, which results in losses in time and raw material. As results, the proposed inline analysis methodology of the product will estimate the dimensional accuracy during the process and preforms correction/cancellation actions on the process. This is the

motivation to propose a convenient inline methodology to validation for 3D printing process. The proposed algorithm will measure the quality of the geometry and colours of 3D product during the process. The proposed quality control technique allows improvement of accuracy and reduction of machining time. The proposed solution is developed based on a computer vision technique and performed using an Embedded Linux platform with a high processing unit. This embedded kit interfaces with a camera system.

The proposed algorithm slices the STL file (the most common file format used in 3D printing which depicts the CAD geometry as raw, unstructured triangulated surfaces) of the desired shape into series of images in Z axis. The resolution of these images in pixel is mapped to the resolution of STL file in mm/ $\mu$ m/nm. The 3D printer fabricates the shape layer by layer via its G-code. The Embedded kit reads the layers of the G-code and after a preset group of layers (validation step) the camera will capture an image. The captured image is processed in order to detect the printed product. The proposed algorithm works to make a comparison between the captured image and the image from the slicing algorithm. The defects are then measured in pixels. Where every pixel refers to a physical measure amount in mm/ $\mu$ m/nm. After that, if there is error the s/w asks the operator to change the fabrication parameters (see the following section).

### ***3.1 Platform of the Proposed Solution***

The proposed camera is a 3.4 MP 2 lane MIPI CSI-2 with AR0330 CMOS image sensor from ON Semiconductor 2.2  $\mu$ m pixel. This camera is capable of streaming images high speed (38 fps with 3.4 MP and 60 fps with full HD 1080p) [13]. This speed enables the proposed solution to take action with low latency. This camera will interface with Jetson Nano Developer Kit [13]. The Jetson Nano Kit will deploy the software algorithm. It is an Embedded Linux platform with graphical processing unit (GPU) so it capable to run parallel applications. It is an effective approach for deploying deep neural networks (DNN) such as convolution neural networks (CNN) [14]. Also, it capable to run ML libraries such as tensorflow, pytorch, and keras library. The setup of hardware is shown in Fig. 1. The kit communicates with the kit/computer of the AM machine using IEEE 802.11. The kit reads the STL and G-code from the AM and applies the algorithms in order to apply the feedback (correction action) to the AM machine. The installing based on wireless enables the hardware to setup with mostly machine structure. The hardware is setup with five cameras in order to get the information of the 3D shape from all sides as shown in Fig. 2.

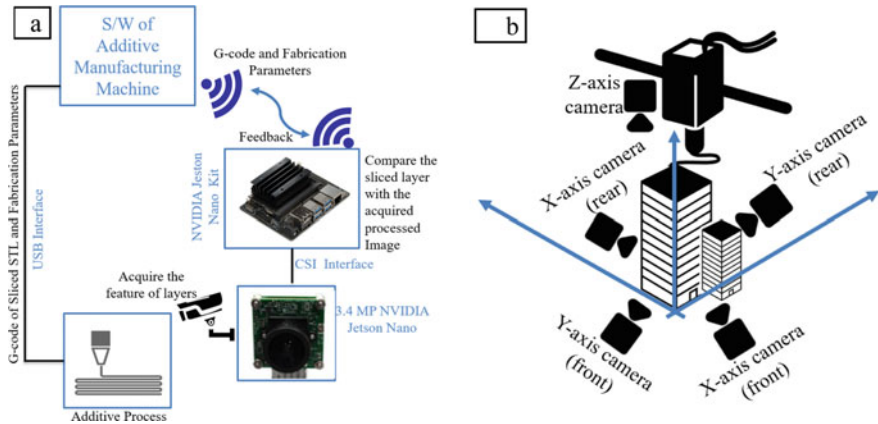


Fig. 1 a Hardware setup of the proposed solution and b camera setting to get all features

### 3.2 Quality Control Algorithm Methodology

The process will start after the setting of all fabrication parameters such as temperature of nozzle, material type, speed of head, speed of fan, etc. The operator will define these parameters. In addition, the number of tests (measurements) will be set, for which the computer vision algorithm will run during the printing process. The algorithm will calculate the heights at which the test will take place. The validation algorithm works to compare the captured images form five sides with the five reconstructed images form the sliced STL data structure. Then the error is calculated and the decision taking (continue printing or to edit the fabrication parameters). At any decision, the algorithm saves and exports a log file. The log file contains the fabrication parameters, the quality of the process, and all states of the process as shown in Fig. 2. This file feeds into the machine learning algorithm in order to make autonomous selection/editing of fabrication parameters without human interaction (see Sect. 6.3). A series of these files (log files) are used as the data set to make pre-learning phase for the reinforcement learning algorithm [6].

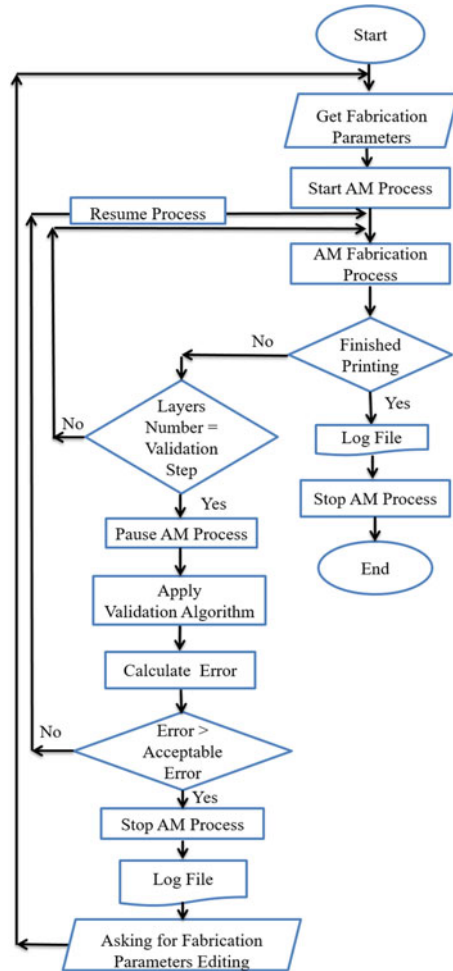
The image-comparing algorithm generated by compare every pixel based on bitmap is shown in Fig. 3.

### 3.3 Reinforcement Learning Algorithm for AM

This algorithm is devoted to selecting the suitable fabrication parameters for the AM process during run time. The algorithm is developed based on reinforcement learning. Reinforcement learning is the practice of machine learning models to achieve a decisions sequence. The agent practices to achieve an aim in a fuzzy and possibly irregular environment. The algorithm learns through a try and error approach to achieve the



**Fig. 2** AM quality control algorithm



problem solution. In order to lead the machine to carry out the desired achieve, the artificial intelligence use rewards and penalties approach for the performed actions.

In the stored data on the log files contains human actions for parameters changing in order to enhance the quality of the process. The training phase for the algorithm starts based on these files as simulator (offline) (Environments and Trainer) in order to minimize the cost of learning phase in reinforcement learning. After that, the algorithm is carried out to learn in lab environment during the manufacturing process.

In the proposed solution the algorithm learns from the true and false setting of the fabrication process parameters from the logging files. This step of learning produces a pre-trained model for the desired autonomous system.

As shown in Fig. 4, the agent learns from environment state and human feedback. The adding of human feedback in the reinforcement learning increase the efficacy

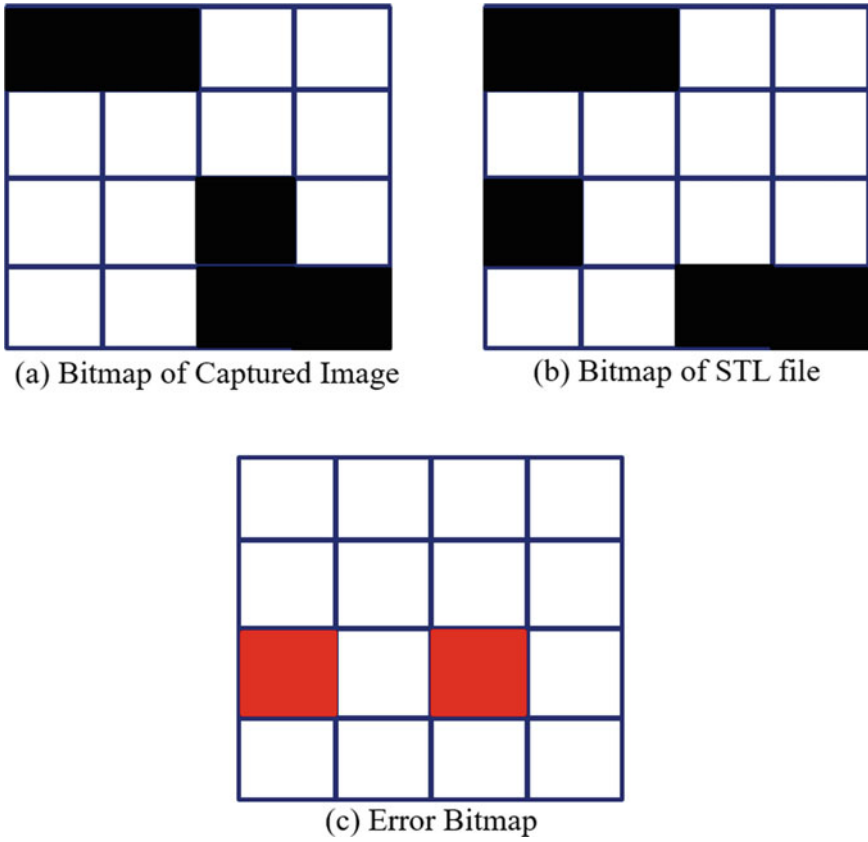


Fig. 3 Bitmap comparing algorithm for AM quality control

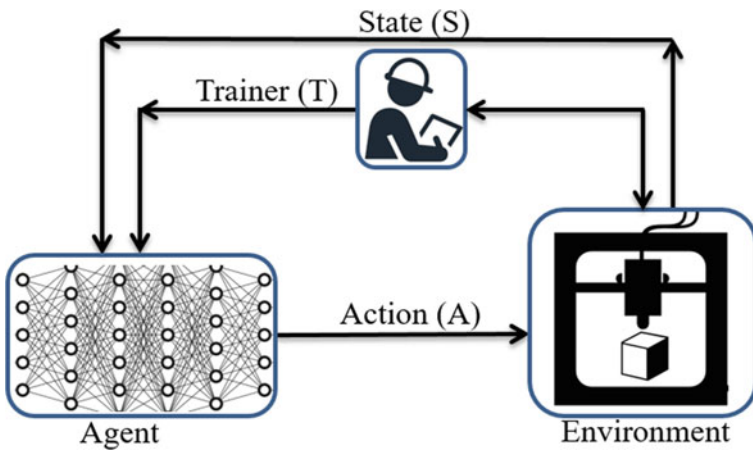


Fig. 4 Proposed reinforcement learning algorithm

of learning [1, 15]. In addition, learning from human feedback is more accurate rather than supervised decision. In our work, the algorithm has to learn from environment state after approve of human (AM inspector/operator) in order to take the true response. Furthermore, the human will evaluate the action of the learning effect of the algorithm.

The Reinforcement learning algorithm learns how to select the fabrication parameter for the AM machine in order to produce the high quality of product. This algorithm is used in the second learning phase of the agent. The agent works to drive the process without any human interaction and uses the pre-trained network as a start point for learning, then updates the weights based on the penalty and achieved algorithm by monitoring the output quality via computer vision as mentioned formerly. After that, the algorithm will be able to select and edit the fabrication process in order to produce a precise process. In addition, the algorithm will change/update the parameters of the process if there are any environmental changes such as humidity weather temperature, and vibration. Furthermore, by changing material type, the algorithm can estimate the suitable printing parameters for it due to its knowledge base.

It is worth emphasizing that the proposed approach is not limited to the FFF techniques, however, it has the possibility to be extended and applied to different AM techniques, e.g. LPBF.

## 4 Implications

This paper presents a case for the integration of ML techniques all along the AM process chain. AM processes are considered digital fabrication techniques due to the fact that every step in the process (design, simulation, pre-processing and production) can be initiated and completed from a central computer. This means that AM processes do have an advantage over conventional manufacturing processes that they possess inherent potential for integration with the digitalization techniques of I4.0.

However, as is evident from this paper, AM processes are currently plagued by a number of process instabilities, dimensional inaccuracies as well as a general lack of process knowledge. Conventional manufacturing techniques have the advantage that they are enriched by decades of process knowledge that had been established by research. This gap in knowledge between AM and conventional processes can only be filled by using ML and AI approaches at the current stage for the purposes of enabling learning, automation and self-optimization.

The implications of this are that AM processes can also reap all the benefits as promised by I4.0 approaches. It would mean that AM processes will then be able to be standardized and that parts produced by AM can be qualified for series production. Which are the two most important factors that would enable industrial implementation.

Through this implementation industries would be able to reap the benefits that AM has to offer in terms of increased design freedom, shorter supply chains as well as possibly improved lead times.

In terms of environmental implications, AM does already have the benefit of only using the exact amount of material that is needed to build a part. However, one of the problems that AM is starting to face is the wastage of material that piles up with each failed print job or post-processing operation. Employing a ML approaches to monitoring and controlling the process during printing could lead to the prevention of time, material and energy wastage. The further reduction of supply chain networks and de-centralized production plants also has the potential for reducing transportation requirements and thereby reducing the overall carbon footprint of the production process.

## 5 Conclusions

The proposed concept in this paper attempts to extend the capabilities of the AM process, utilizing the industry 4.0 technologies (i.e. Machine Learning) in order to improve the quality of the manufactured parts. In particular, the proposed approach to high quality AM products via computer vision and machine learning increases the profitability of the AM system. The reinforcement learning algorithm is developed to learn from both the human feedback as a trainer and the environment states. Such a hybrid algorithm helps minimize the cost (time and raw materials) of the training phase. It provides a reliable methodology for in-process quality control of AM process.

**Acknowledgements** This work was implemented under the STN programme, part of the Helmholtz association. In addition, the support of the Karlsruhe Nano Micro Facility (KNMF-LMP, <http://www.knmf.kit.edu/>) a Helmholtz research infrastructure at KIT, is gratefully acknowledged.

## References

1. Arumugam, D., Lee, J.K., Saskin, S., Littman, M.L.: %T Deep reinforcement learning from policy-dependent human feedback. (2019). ArXiv abs/1902.04257
2. Böckin, D., Tillman, A.-M.: Environmental assessment of additive manufacturing in the automotive industry. *J. Cleaner Prod.* **226**, 977–987 (2019). <https://doi.org/10.1016/j.jclepro.2019.04.086>
3. Carvalho, N., Chaim, O., Cazarini, E., Gerolamo, M.: Manufacturing in the fourth industrial revolution: A positive prospect in Sustainable Manufacturing. *Procedia Manuf.* **21**, 671–678 (2018). <https://doi.org/10.1016/j.promfg.2018.02.170>
4. Charles, A., Elkaseer, A., Thijs, L., Hagenmeyer, V., Scholz, S.: Effect of process parameters on the generated surface roughness of down-facing surfaces in selective laser melting. *Appl. Sci.* **9**(6), 1256 (2019). <https://doi.org/10.3390/app9061256>

5. Charles, A., Elkaseer, A., Thijs, L., Scholz, S.G.: Dimensional errors due to overhanging features in laser powder bed fusion parts made of Ti-6Al-4 V. *Appl. Sci.* **10**(7), 2416 (2020)
6. Christiano, P.F., Leike, J., Brown, T.B., Martic, M., Legg, S., Amodei, D.: Deep reinforcement learning from human preferences. In: NIPS (2017)
7. Dilberoglu, U.M., Gharehpapagh, B., Yaman, U., Dolen, M.: The role of additive manufacturing in the era of industry 4.0. *Procedia Manuf.* **11**, 545–554 (2017). <https://doi.org/10.1016/j.profmfg.2017.07.148>
8. Elkaseer, A., Mueller, T., Charles, A., Scholz, S.: Digital detection and correction of errors in as-built parts: a step towards automated quality control of additive manufacturing. In: Proceedings WCMNM, Portorož, Slovenia 2018, pp. 389–392. Research Publishing Services, Singapore (2018). [https://doi.org/10.3850/978-981-11-2728-1\\_58](https://doi.org/10.3850/978-981-11-2728-1_58)
9. Everton, S.K., Hirsch, M., Stravroulakis, P., Leach, R.K., Clare, A.T.: Review of in-situ process monitoring and in-situ metrology for metal additive manufacturing. *Mater. Des.* **95**, 431–445 (2016). <https://doi.org/10.1016/j.matdes.2016.01.099>
10. Fassi, I., Shipley, D.: In: *Micro-Manufacturing Technologies and their Applications*. Springer Tracts in Mechanical Engineering, 1st edn. Springer, Cham (2017)
11. Gibson, I., Rosen, D.W., Stucker, B.: Generalized additive manufacturing process chain. In: *Additive Manufacturing Technologies: Rapid Prototyping to Direct Digital Manufacturing*, pp. 59–77. Springer US, Boston, MA, (2010). [https://doi.org/10.1007/978-1-4419-1120-9\\_3](https://doi.org/10.1007/978-1-4419-1120-9_3)
12. Hermann, M., Pentek, T., Otto, B.: Design principles for industrie 4.0 scenarios. In: 2016 49th Hawaii International Conference on System Sciences (HICSS), 5–8 Jan. 2016, pp. 3928–3937. (2016). <https://doi.org/10.1109/hicss.2016.488>
13. Jetson, N.: Jetson nano developer kit (2019)
14. Jetsonhacks: (2019). <https://github.com/jetsonhacks> Last Access 17/6/2019
15. MacGlashan, J, Ho, M.K., Loftin, R., Peng, B., Wang, G., Roberts, D.L., Taylor, M.E., Littman, M.L.: Interactive learning from policy-dependent human feedback. In: Paper presented at the Proceedings of the 34th International Conference on Machine Learning, Proceedings of Machine Learning Research, (2017)
16. Mies, D., Marsden, W., Warde, S.: Overview of additive manufacturing informatics: a digital thread. *Integr. Mater. Manuf. Innov.* **5**, 114–142 (2016). <https://doi.org/10.1186/s40192-016-0050-7>
17. Moshiri, M., Charles, A., Elkaseer, A., Scholz, S., Mohanty, S., Tosello, G.: An industry 4.0 framework for tooling production using metal additive manufacturing-based first-time-right smart manufacturing system. *Procedia CIRP* **00**, 000–000 (2020)
18. Niaki, M.K., Torabi, S.A., Nonino, F.: Why manufacturers adopt additive manufacturing technologies: The role of sustainability. *J. Cleaner Prod.* **222**, 381–392 (2019). <https://doi.org/10.1016/j.jclepro.2019.03.019>
19. Özel, T., Altay, A.: Process monitoring of meltpool and spatter for temporal-spatial modeling of laser powder bed fusion process (2018). 10.1016/j.procir.2018.08.049
20. Paritala, P.K., Manchikatta, S., Yarlagadda, P.K.D.V.: Digital Manufacturing applications past current and future trends. *Procedia Eng.* **174**, 982–991 (2017). <https://doi.org/10.1016/j.proeng.2017.01.250>
21. Solheid, J., Elkaseer, A., Wunsch, T., Charles, A., Seifert, H., Pflöging, W.: Effect of process parameters on surface texture generated by laser polishing of additively manufactured Ti-6Al-4V, vol. 11268. SPIE LASE, SPIE (2020)
22. Spears, T.G., Gold, S.A.: In-process sensing in selective laser melting (SLM) additive manufacturing. *Integr. Mater. Manuf. Innov.* **5**(1), 16–40 (2016). <https://doi.org/10.1186/s40192-016-0045-4>
23. Tapia, G., Elwany, A.: A Review on process monitoring and control in metal-based additive manufacturing, **136**, (2014). <https://doi.org/10.1115/1.4028540>
24. Zezulka, F., Marcon, P., Vesely, I., Sajdl, O.: Industry 4.0—An Introduction in the phenomenon. *IFAC-PapersOnLine* **49**(25), 8–12 (2016). <https://doi.org/10.1016/j.ifacol.2016.12.002>

# Stakeholder-Driven Conceptualization of Open Innovation Approaches in the SYNERGY Project



Janin Fauth , Clarissa Marquardt , Giulia Di Bari , Nicola Raule , Johanna Lisa Ronco , and Steffen G. Scholz 

**Abstract** Since the late 90s, the way companies acquire novel ideas and bring resulting products to the market is in a paradigm shift moving towards open innovation concepts and making use of crowd-based approaches. This in particular affects the industrial technologies sector with its fast-moving advancements in the areas of Additive Manufacturing, Micro- and Nanotechnology and Industry4.0. Open innovation concepts together with stakeholder-driven engagement processes provide solutions for all parties involved in the innovation process—from research to intermediaries up to industrial realization. This paper reports an overview of the milestones of the open innovation evolution and describes the interactive engagement format established and carried out within the frame of the Interreg Central Europe (CE) project SYNERGY (CE1171) involving related stakeholder target groups in the conceptualization of an open innovation platform for state-of-the-art technologies. Creative formats like design thinking and crowdsourcing approaches were introduced to and applied by representatives from higher education and research, SMEs and industry and start-ups to create a catalogue of features required for the open innovation platform.

---

J. Fauth (✉) · C. Marquardt · S. G. Scholz  
Institute for Automation and Applied Informatics (IAI), Karlsruhe Institute of Technology (KIT),  
76344 Eggenstein-Leopoldshafen, Germany  
e-mail: [janin.fauth@kit.edu](mailto:janin.fauth@kit.edu)

G. Di Bari · N. Raule · J. L. Ronco  
Centro di Ricerca e Innovazione Tecnologica srl (CRIT), Vignola, MO, Italy

S. G. Scholz  
Karlsruhe Nano Micro Facility (KNMF), Karlsruhe Institute of Technology (KIT),  
Eggenstein-Leopoldshafen, Germany

# 1 Introduction

## 1.1 *Open Innovation Concepts for Industrial Technologies*

Open innovation (OI) is a multifaceted [1] and multi-level phenomenon [2], which embraces various innovation modes [3] evolving overtime. Several theories of open innovation have accompanied this evolution [4], resulting in a wide range of open innovation concepts and applications. Among these applications, crowdfunding and crowdsourcing are surely the most popular. Crowdfunding is described as “an Internet-based funding method for the realization of an initiative through online distributed contributions and micro-sponsorships in the form of pledges of small monetary amounts by a large pool of people within a limited timeframe” [5]; crowdsourcing is a practice where an ordering party, e.g. a company, turns to the crowd to solve a problem in exchange of a reward. Despite the roots of open innovation dating back to the “90s, with the first disquisition on companies’ absorption capacity [6], its definition as a novel concept [4] stems from Chesbrough’s idea that “open innovation is a paradigm that assumes that firms can and should use external ideas, as well as internal ideas, [...], as the firms look to advance their technology” [7]. In the early 2000s, open innovation appeared on the industrial scene as a new business knowledge methodology—opposite to close innovation—describing innovation processes characterized by an outward opening: a new paradigm to boost technology innovation, which does not stem from the intuition of few innovators, but by the involvement of communities [8].

This concept subsequently evolved into the new paradigm Open Innovation 2.0 (OI 2.0), introduced as part of the Digital Agenda for Europe [9] to tackle European key challenges. Open Innovation 2.0 aims at overturning the classical funnel-like linear open innovation model into an ecosystem-centred and cross-organizational view of innovation. The ecosystem characteristic represents the most important and distinguishing unit of success for an innovation exceeding by far the achievable outcomes and results by a single organization. OI 2.0 aims towards comprehensive networking and co-creative collaboration while involving all stakeholders from the Quadruple Helix Model namely government, academia, industry and—as a supplementary part to the triple helix model—the civil society [10].

This paper describes the design process of an open innovation engagement platform to facilitate stakeholder co-creation and collaboration towards a sustainable, ecosystem-centred approach of open innovation in Central Europe. The involvement of stakeholder groups from different professional backgrounds and regions will help to understand and map the communities’ needs and expectations for the envisioned open innovation environment supporting the stakeholder-centred transformation of innovation processes within advanced industrial technologies towards sustainable innovation.

## ***1.2 Stakeholder Engagement Concepts***

Along with the rise of OI 2.0, interactive stakeholder engagement formats have become increasingly important to provide appropriate exchange tools in collaboration networks and systems. Stakeholder engagement is described as the involvement of stakeholders that is people that are affected by or can affect the achievements of an organizations purpose, into organizational decision-making [11]. In particular, involving civil society as a representative for potential users and consumers, to better define the expected value of innovations, is considered an integral part of the innovation process as the fourth and novel component of the Quadruple Helix Model [10]. Thus, involving the civil society in open networks, where they can interact together with other stakeholders, guarantees on the one hand socially sustainable innovation approaches matching the physical innovations with social stakeholder expectations [12] and on the other hand, real opportunities for businesses, as it allows for market consensus testing for the launch of new products and services [13].

## ***1.3 Crowdsourcing***

Crowdsourcing is considered to be one possibility of stakeholder engagement in the frame of open innovation. Brabham defines crowdsourcing “as an online, distributed problem-solving and production model that leverages the collective intelligence of online communities to serve specific organizational goals” [14]. This implies the natural engagement of stakeholders into decision-making processes by inviting them to comment and share input on ideas and innovations that matter to them. In the context of this paper, crowdsourcing is considered to include all forms of sharing individual assets such as infrastructures, skills, competences and knowledge with experts from the crowd in creative and collaborative processes for the purpose of jointly solving specific research or innovation questions in the context of industrial technologies.

## ***1.4 Design Thinking***

Design thinking enables interactive stakeholder-driven product development whilst focusing on understanding the innovation process from a highly user-centred perspective. Brown [15] defines design thinking as “a discipline that uses the designer’s sensibility and methods to match people’s needs with what is technologically feasible and what a viable business strategy can convert into customer value and market opportunity”. This asks for constant feedback between the developed solutions and the target users within a six-step process.



The first step in the design thinking process is to fully “understand” a specific problem, the second is to “observe” and interact with the target groups with the outcomes of both steps allowing to “synthesize” all collected information towards the core problems. The next step “ideate” aims at generating new ideas to the established innovation spaces. The last two steps “prototype” and “test” aim at constructing the chosen ideas in a fully functioning prototype, testing it and providing user feedback in several feedback loops in order to acquire as much experience as possible from the target users [16].

## 2 The SYNERGY Project

The CE Interreg project SYNERGY (SYnergic Networking for innovativeness enhancement of central european actoRs focused on hiGh-tech industry) was designed to strengthen linkages, cooperation and synergies between industry and intermediaries, academia, policy makers and civil society (Quadruple Helix Approach) in Central Europe in the framework of OI 2.0. The aim of the project is to define new crowd innovation-based services made accessible via an online platform. In doing so, a new Synergic Crowd Innovation Platform (SCIP) has been developed as a space for co-creation and enhancement in open innovation offering a full set of tools and features on crowdfunding, crowdsourcing, micro-working and infrastructure sharing to effectively support independent, stakeholder-driven innovation processes. For this purpose, the project started with an analysis of relevant innovation projects and organizations covering the most promising industrial technologies, which were subsequently, clustered into “Synergic Networks” for the key technology areas of Additive Manufacturing and 3D-Printing, Micro- and Nanotechnology and Industry 4.0. Within the digital twin of these networks, the new developed SynPro IT-tool offers selective matchmaking options to facilitate co-creation and collaboration. Continuing the “Synergic Networking”, stakeholder engagement workshops on Design Thinking and Simulated Crowdsourcing were held to define the stakeholders’ needs and expectations on open innovation for the services on the SCIP, which will be tested in pilot actions and communicated in strategy trainings. This study focuses on the selected stakeholder engagement approaches for the definition and user-centred development of the platform. Figure 1 presents the scheme of the SYNERGY project and implementation flow.



**Fig. 1** Scheme of the SYNERGY project flow

### 3 Workshop Concept

Interactive workshop formats were selected as a proven means of stakeholder engagement to directly involve and interact with relevant stakeholder target groups to solve the main project research question, namely defining the stakeholders’ needs for trans-regional cooperation based on crowd innovation approaches for the development of the Synergic Crowd Innovation Platform. To encourage active participation, optimal engagement and effective co-creation processes among the stakeholders, the workshops were designed based on selected creative open innovation concepts such as Design Thinking and Simulated Crowdsourcing. The focus of the design thinking approach is to identify and fully understand the future main user groups of the platform and to ultimately define the key topics and needs related to the mandate of the identified individual user groups. Following up on these observations, the participants systematically ideate new solutions matching the identified key issues and needs followed by prototyping and testing of selected ideas with regard to the platform while providing user feedback during all steps of the development process. The Simulated Crowdsourcing workshop concentrated on involving the present crowd of stakeholders into the identification of information, skills, competences and infrastructures that could be shared on the platform. The two workshops are designed in a complementary and iterative manner both contributing to solve project-specific questions while allowing for systematic, logical and practical [11] stakeholder engagement.

The first stage of the workshop concept involves six regional workshops in Poland, Austria, Germany, Slovenia, Croatia and Italy followed by a joint international workshop held in Germany in the second stage while collecting input from all relevant trans-regional stakeholder groups. Figure 2 presents an overview of the synergistic workshop concept.

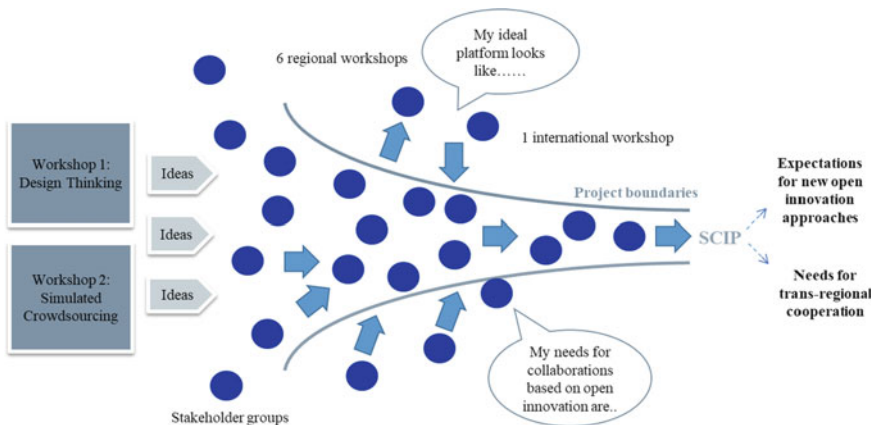


**Fig. 2** Overview of the synergistic workshop concept of stakeholder engagement in the frame of the development of an open innovation platform concept

The outcomes of the complementary workshops will be combined to jointly consolidate the main features for the conceptualization of the envisioned SCIP together with the stakeholders. A harmonized feedback form is used to collect stakeholder input and feedback for the different workshops and outcomes ultimately evaluated based on a five-step process aiming at the definition of stakeholder value propositions. This evaluation system presents the application of the concept for co-creating stakeholder value propositions as proposed by Frow and Payne [17] in a modified version. The resulting modified evaluation steps are (1) Identify stakeholders, (2) Define core values, (3) Evaluate stakeholder dialogue and knowledge sharing, (4) Identify stakeholder value co-creation opportunities and (5) Co-create stakeholders value propositions.

## **4 Workshop Results**

The following workshop results are based on input generated by 130 stakeholder representatives from R&D organizations, universities, large enterprises, SMEs, start-ups, business support organizations, industry clusters and NGOs that were recruited via the SYNERGY partner organizations. The outcomes from both workshops offer a comprehensive overview of the stakeholders' standpoints and needs for open innovation services resulting in the requirements for the SCIP. The following chapters present the detailed results according to the evaluation steps presented in the previous chapter.

### ***4.1 Identification of Stakeholders***

The stakeholder identification process focused on the pinpointing of the most important future user groups for the platform based on their existing needs, issues and professional backgrounds. As a result from the stakeholder engagement workshops, the three most important identified target user groups for the envisioned open innovation platform are start-ups, higher education and research organizations, industry and SMEs. Even if large industry and SMEs are usually considered two separate stakeholder groups, they did not show significant differences in their needs and issues related to the open innovation platform identified from both groups with the help of the harmonized feedback form. Industry and SMEs were therefore clustered together into one industrial target user group.

## 4.2 Definition of Core Values

One of the core values of the SYNERGY project is to increase and maximize the stakeholder value within advanced industrial technologies. As an essential and first step, the stakeholders’ core tasks and related needs and problems were defined to determine the activities needed to achieve these values. This allowed an overall picture and abstract representation of the different stakeholders’ points of view, whereby the consideration was limited to the three most important user groups namely start-ups, higher education and research, and industry and SMEs. Tables 1, 2 and 3 present the results for the respective target user groups.

### Start-Ups

See Table 1

### Higher Education and Research Organizations

See Table 2.

**Table 1** Profiling of the target group start-ups related to tasks, needs and problems

Tasks	Needs	Problems
Enhance innovation and growth	Cooperation partners (e.g. experts with experience)	Lack of experience
Develop and introduce new products and services	Possibilities for testing products and services	High competition and lack of customer base
Grow activities around established ideas	Financial assistance	Lack of financial sources
Increase the number of committed employees	New employees (e.g. offspring talents)	Lack of infrastructures

**Table 2** Profiling of the target group higher education and research related to tasks, needs and problems

Tasks	Needs	Problems
Research (and teaching)	Practical application and testing of research outputs	Confidentiality of new research outputs
Spread and generate new knowledge	Competent partners (e.g. for partial research results)	High administrative effort (e.g. large complexity of research proposals)
Networking and contacts to business and new research projects	Employment market (e.g. Ph.D. students) and (follow-up) financing	Problems to identify future users and competent partners
Publications	Possibilities for personal portfolio development	Publications required for personal and/or strategic development

**Table 3** Profiling of the target group industry and SMEs related to tasks, needs and problems

Tasks	Needs	Problems
Fulfil production targets and make profit	Knowledge database on: current research topics, market research results, etc.	Lack of knowledge on current research topics and technologies
Satisfy customer needs	Database for infrastructures to share (e.g. machines, etc.)	Lack of overview of potential partners
Strategic development and positioning	Cooperation partners (e.g. from research)	Lack of offspring and skilled workers
Provide competitive advantage	Employment market for offspring talents and skilled workers	Confidentiality of information

### Industry and SMEs

See Table 3.

## 4.3 Evaluation of Results from Stakeholder Dialogue and Knowledge Sharing

Following the overview of the various stakeholder points of view, the stakeholders' general needs and expectations for collaboration in an open innovation environment were evaluated based on the results from the extensive stakeholder communication and knowledge sharing processes in the workshops. This resulted in ideas for collaboration mechanisms in the form of sharing skills or competences and infrastructures in the advanced technologies sector and in the desired functionalities of the SCIP.

### Needs and Expectations for Sharing Skills and Competences

Stakeholders confirmed that the envisioned open innovation approach should provide collaboration mechanisms for sharing skills and competences in advanced industrial technologies. Stakeholders suggested different categories of skills and competences that could be shared via the open innovation platform. These categories are management services (e.g. innovation management services), experience and expertise (e.g. research expertise), knowledge from specialty areas (e.g. additive manufacturing) and design optimization (e.g. design optimization for additive manufacturing).

### Needs and Expectations for Sharing Infrastructures

The introduction of collaboration mechanisms facilitating sharing of infrastructures was also encouraged by the workshop participants. According to the workshops' results, ideas for infrastructures to be put at disposal and shared with interested parties in the form of renting, trainings or other applications are equipment (e.g. monitoring tools), facilities (e.g. innovation labs), infrastructure services (e.g. evaluation of data), materials and products (e.g. production lines) and computer applications (e.g. gamification applications).

### **Required Platform Functionalities**

Based on the key services that the platform should fulfil, the participants' ideas and expectations on future functionalities of the open innovation platform were evaluated, resulting in different categories of functionalities. In terms of technical functions, the potential users envisage, for example, matchmaking functionalities, a straightforward registration process, a user-friendly and intuitive user-interface, individual participants' profiles, intelligent searching and content mining mechanisms, rating systems for crowd-evaluation of project ideas and virtual reality features. Desired functionalities for communication and interaction comprise ideas like real-time communication possibilities, a discussion forum on general topics, a virtual co-working space and e-mail notification for successful matchmaking between platform users. Examples for content-related functionalities encompass thematic areas to cluster campaigns and challenges, an integrated business-science translator, links to external tools and contents and the demonstration of best practices and success stories.

To consolidate the workshops' outcomes and define the minimum requirements for the open innovation platform, the workshop participants voted on the nine most important features to be considered during the conceptualization and realization of the platform. This resulted in the following minimum requirements for the SCIP: user-friendly and intuitive interface, Web and mobile version, matchmaking option, sharing option for skills/infrastructures/services, communication tool, innovation challenges, automated notification system, training materials and crowdfunding feature.

## **5 Lessons Learnt and Outlook**

This study explored stakeholder-driven approaches towards the definition and initiation of successful trans-regional cooperation based on open innovation among relevant project stakeholders in Central Europe. To achieve this aim, iterative workshops on Design Thinking and Simulated Crowdsourcing were conducted to involve stakeholders from all project partner regions and varying professional backgrounds to understand their needs and issues related to open innovation within the context of advanced industrial technologies. This resulted in identifying the most relevant user groups, their key topics and issues for the planned open innovation platform contributing to consolidate a catalogue of required features as condition for the development of the final functionalities of the open innovation platform. The resulting initial stakeholder value propositions emphasized that matchmaking among innovation actors and a corresponding user-friendly, intuitive and mobile tool are the most important stakeholder topics. In addition, the importance of cooperation and communication between academics, research and industry was stressed, as these sectors are still considered as separate entities in some partner countries causing lack of awareness of the importance of such collaboration, while the Synergic Crowd Innovation Platform contributes towards filling this gap.

The SYNERGY project approach, which aims at satisfying the need of specific tools that support and provide a stable structure to connections among stakeholders, could become relevant in emergency situations such as the sudden spread of the Covid-19 worldwide pandemic. Indeed, two recent examples from the field of 3D-Printing [18, 19] have proven the existence and potential of the crowd innovation era. In these cases, different stakeholders merged their effort to provide innovative solutions to the lack of components for life saving ventilation devices. However, it can be noted that this kind of collaboration is mainly animated by the urgency of a social need and the nobility of the purpose and can happen only if the appropriate connections among stakeholders are already established. Furthermore, the link to the business world, with appropriate business models and success stories, is still missing. In this context, the SYNERGY approach aims at solving this issue by creating a stable collaboration framework among stakeholders.

Therefore, the analysis on the conceptualization of the SYNERGY open innovation approaches will be continued in future investigations while following up on the steps on co-creation of stakeholders' value propositions proposed by Frow and Payne [17]. Further opportunities for stakeholder value co-creation will be created within the SYNERGY project by the introduction of the open innovation platform and the involvement of all user groups into problem-solving processes within innovation campaigns and challenges. Consequently, the respective user experiences on the platform will be considered in the pilot actions to be held on the Synergic Crowd Innovation Platform (<https://synergyplatform.pwr.edu.pl/>) to adjust the co-creation of stakeholders' value propositions. All in all, the stakeholder-driven approach adopted under the SYNERGY project will result in shaping open innovation collaboration mechanisms according to the needs of stakeholders aiming at the creation of a socially sustainable innovation environment.

**Acknowledgements** This work was funded by the Interreg Central Europe program and carried out in the frame of the SYNERGY project (Grant Agreement CE 1171). The authors gratefully acknowledge the work and contribution of the project partners Wrocław University of Science and Technology, Profactor GmbH, TU Chemnitz Excellence Cluster MERGE, Josef Stefan Institute, STEP RI and CRIT s.r.l towards the realization and documentation of the regional and international workshops on Design Thinking and Simulated Crowdsourcing. Additionally, the authors acknowledge Jacqueline Didingier (KIT) for her contributions to the evaluation of the regional workshops as part of a student research paper. This work was also supported by the Karlsruhe Nano Micro Facility (KNMF, [www.knmf.kit.edu](http://www.knmf.kit.edu)), a Helmholtz Research Infrastructure at Karlsruhe Institute of Technology (KIT, [www.kit.edu](http://www.kit.edu)).

## References

1. Randhawa, K., Wilden, R., Hohberger, J.: A bibliometric review of open innovation: setting a research agenda. *J. Prod. Innov. Manag.* **33**, 750–772 (2016)
2. Bogers, M., Zobel, A.-K., Afuah, A., Almirall, E., Brunswicker, S., Dahlander, L., Frederiksen, L., Gawer, A., Gruber, M., Haefliger, S., Hagedoorn, J., Hilgers, D., Laursen, K., Magnusson, M.G., Majchrzak, A., McCarthy, I.P., Moeslein, K.M., Nambisan, S., Piller, F.T., Radziwon,

- A., Rossi-Lamastra, C., Sims, J., Ter Wal, A.L.J.: The open innovation research landscape: established perspectives and emerging themes across different levels of analysis. *Ind. Innov.* **24**, 8–40 (2017)
3. Spithoven, A., Clarysse, B., Knockaert, M.: Building absorptive capacity to organize inbound open innovation in traditional industries. *Technovation* **30**, 130–141 (2010)
  4. Lopes, A., Carvalho, M.: Evolution of the open innovation paradigm: towards a contingent conceptual model. *Technol. Forecast. Social Change* **132**(C), 284–298 (2018)
  5. Hossain, M., Oparaocha, G.O.: Crowdfunding: motives, definitions, typology and ethical challenges. *Entrepreneurship Res. J.* **7**(2) (2015)
  6. Cohen, W.M., Levinthal, D.A.: Absorptive-capacity—a new perspective on learning and innovation. *Adm. Sci. Q.* **35**, 128–152 (1990)
  7. Chesbrough, H.: *Open Innovation: The New Imperative for Creating and Profiting from Technology*. Harvard Business School Press, Cambridge (2003)
  8. Meige, A., Schmitt, J.: *Innovation Intelligence. Commoditization. Digitalization. Acceleration. Major Pressure on Innovation Drivers*. Lulu.com, United Kingdom (2015)
  9. European Commission: Communication from the Commission to the European Parliament, the Council, the European Economic and Social Committee and the Committee of the Regions - A Digital Agenda for Europe, COM(2010)245 (2010). <https://eur-lex.europa.eu/LexUriServ/LexUriServ.do?uri=COM:2010:0245:FIN:EN:PDF>
  10. Curley, M., Salmelin, B.: Open innovation 2.0: a new paradigm—White Paper. In: OI2 Conference Paper Open Innovation Strategy and Policy Group (OISPG) (2013). [http://ec.europa.eu/information\\_society/newsroom/cf/dae/document.cfm?doc\\_id=2182](http://ec.europa.eu/information_society/newsroom/cf/dae/document.cfm?doc_id=2182)
  11. Jeffery, N.: *Stakeholder Engagement: A Road Map to Meaningful Engagement*. The Doughty Centre for Corporate Responsibility, Cranfield School of Management (2009)
  12. Vallance, S., Perkins, H.C., Dixon, J.E.: What is social sustainability? A clarification of concepts. *Georum* **42**(3), 342–348 (2011)
  13. Ronco, J., Pelosi, L.: *Open innovation come modello di gestione della conoscenza per facilitare l'eco-innovazione, Energia, Ambiente e Innovazione* (2013)
  14. Brabham, D.C.: *Crowdsourcing*. MIT Press Essential Knowledge Series. MIT Press, London (2013)
  15. Brown, T.: Design thinking. *Harv. Bus. Rev.* **86**(6), 84–95 (2008)
  16. Grots, A., Pratschke, M.: Design Thinking—Kreativität als Methode. *Market. Rev. St. Gallen* **26**(2), 18–23 (2009)
  17. Frow, P., Payne, A.: A stakeholder perspective of the value proposition concept. *Eur. J. Mark.* **45**(1/2), 223–240 (2011)
  18. D Printing Media Network: <https://www.3dprintingmedia.network/covid-19-3d-printed-valve-for-reanimation-device/>. Last accessed 30 Mar 2020
  19. Inceptivemind: <https://www.inceptivemind.com/snorkeling-masks-turned-emergency-ventilators-fight-covid-19/12483/>. Last accessed 30 Mar 2020



# An Empirical Study of Visual Comfort in Office Buildings



Isilay Tekce , Deniz Artan , and Esin Ergen 

**Abstract** Visual comfort is an important indicator of both occupant satisfaction and work performance. The main goal of this study is to present the visual comfort-related factors that influence occupant satisfaction. To achieve this goal, a detailed literature analysis was conducted to determine the main factors that can be used to evaluate the effect of visual comfort on the satisfaction of office workers. Afterward, interviews were conducted with 12 facility managers, and related work orders created by the facility management teams were investigated to determine visual comfort-related complaint types. Based on the collected data, a hierarchical structure of visual comfort factors was created. Finally, 308 office workers were surveyed to determine (1) the number of respondents with complaints related to each visual comfort factor, (2) the level of importance of the visual comfort related factors, and (3) office worker's satisfaction levels for each factor. The findings reveal that the largest gap between the perceived importance and satisfaction appears in daylighting and visual privacy. The designers, facility managers, and renovators need to think of design strategies to provide more privacy and access to daylight to occupants in their working environments.

## 1 Introduction

Visual comfort is “a subjective condition of visual well-being induced by the visual environment” [1]. Lighting of the environment, visual privacy, connection to outdoor,

---

I. Tekce (✉)

Department of Architecture, Ozyegin University, 34794, Cekmekoy Istanbul, Turkey

e-mail: [isilay.tekce@ozyegin.edu.tr](mailto:isilay.tekce@ozyegin.edu.tr)

D. Artan · E. Ergen

Department of Civil Engineering, Istanbul Technical University, 34469 Maslak, Istanbul, Turkey

e-mail: [artande@itu.edu.tr](mailto:artande@itu.edu.tr)

E. Ergen

e-mail: [ergenesi@itu.edu.tr](mailto:ergenesi@itu.edu.tr)

and view are included in visual comfort. The architecture of the buildings and interior design of them affect the visual environment, therefore the visual comfort of the occupant directly. The aim of this paper is to provide insight to decision makers such as designers, facility managers, and renovators of office buildings on how office occupants perceive visual comfort. By determining visual comfort criteria and occupants' frequent complaints, the study unfolds common reasons behind visual discomfort and consequences of poor visual performance. A methodology involving the literature survey, expert interviews, and a survey that includes a large population of office building occupants was adopted in this paper in the quest to present empirical results on visual comfort, as previous literature is lacking survey-based empirical studies in this topic.

## 2 Methodology

In the first step, a detailed literature review was performed to determine the main factors that can be used to evaluate the effects of visual comfort on occupant satisfaction at the office buildings. The related articles, building performance evaluation systems, and post-occupancy evaluation (POE) surveys were reviewed to determine the factors. To analyze the findings of the literature review, frequency analysis and normative refinement methods were applied.

The second step included (1) performing interviews with 12 facility managers to verify the factors required to measure the effect of visual comfort on occupant satisfaction and (2) investigation of visual comfort-related work orders that were created by the facility management team in a computerized maintenance management software system. The findings included a list of occupant feedback, and complaint types related to visual comfort and a hierarchical structure were established using the factors determined by integrating the results of the interviews, document investigation, and the literature review. Once the factors and complaint types related to visual comfort were determined, 308 office employees were surveyed to determine: (1) the number of respondents with complaints related to each visual comfort factor (2) the level of importance of the visual comfort-related factors, and (3) office worker's satisfaction levels for each factor. Five-point Likert scale was used to rate the importance and satisfaction levels that ranged from (1) "not important at all" to (5) "very important" and (1) "not satisfied at all" to (5) "very satisfied," respectively. Occupants were selected on a voluntary basis, provided that the buildings (1) have operable windows and automation systems for HVAC control, (2) were new or recently retrofitted (preferably <10 years old), and (3) were being operated in their current form for a minimum of two years prior to the start of the study. The selected buildings are diverse in terms of the office design (i.e., cellular versus open-plan), purpose of use, facade, and floor covering types. Fifty-six percentage of the respondents are female, and 44% are male. Eight percentage of the respondent profile is senior managers, 25% is middle-level managers, and 67% is operational staff. The internal

consistency was checked by using Cronbach’s alpha coefficient to verify the reliability, and Anderson–Darling test was used to examine the normality distribution of the data.

### 3 Visual Comfort and Satisfaction

Many researchers investigated the effects of visual comfort to work performance and occupant satisfaction. [45] defined visual comfort as “a subjective condition of visual well-being induced by the visual environment.” Since light has a regulatory effect on biological clock of people, it plays an important role on performance and psychology of occupants. Since there is a direct relationship between human metabolism and exposed lighting amount during different times of the day, the duration of darkness and light explosion at the offices are affecting rhythms of occupants [2]. Right amount of lighting with correct angles has positive effects on physical and mental health. Therefore, the need for correct lighting underlines the importance of windows [3]. Besides providing advantages like timing, weather condition information to the occupants, windows also help to reduce claustrophobic feelings and to rest the eyes. Even though, windows help people to connect with outdoor or get sunlight, thermal discomfort of occupants sitting next to windows might be seen. According to [4], occupant who has the highest indoor environmental comfort is not the ones sitting next to windows, they are the ones relatively away from the windows but still be able to see the windows. Moreover, if the occupants are happy with the view, they show tolerance to the reflection [5]. Natural scenery is preferred over human-made environments since it helps to relieve mental fatigue [6]. Light stimulates the serotonin secretion in body and has an anti-depressive and stimulant effect; therefore, the brain is able to function in a faster way. The artificial lighting has an effect on how the occupant perceives the environment as nice, luminous, warm, cold, fresh, or gloomy. Illuminance distribution, luminous intensity, linearity of light, color of the light, warmth of the light, flashing, vibration are some of the important features of artificial lighting. Below is a list of visual comfort criteria and references obtained as a result of the literature analysis undertaken (Table 1).

**Table 1** Visual comfort criteria and references

	Criteria	References
Visual comfort	Daylighting	[7–23]
	Artificial lighting	[7, 8, 10, 12, 13, 14, 20–34]
	Glare	[7, 10–12, 15–18, 20, 21, 27, 28, 32, 35–40]
	Reflection	[37]
	Visual privacy	[12, 16, 20, 21, 33, 39, 41]
	View	[14–16, 18, 20, 21, 32, 38, 42–44]

As a result of frequency analysis and normative refinement processes, visual comfort criteria were identified as: (1) daylight, (2) artificial light, (3) glare, (4) reflection, (5) visual privacy, and (6) view. [46] defines visual comfort as the lighting conditions and the views from ones workspace. Appropriate lighting in office buildings is important to ensure the occupants' satisfaction and consequently improve their job performance [47]. It is evident that transmitting sufficient daylight to core zones while maintaining a visually comfortable work environment is critical for energy efficiency and enhanced indoor environmental quality [48]. In interior work places, discomfort glare may arise directly from bright luminaires, windows, or surface reflections. If discomfort glare limits are met, then disability glare is not usually a major problem [49]. Also, [3] showed that more attractive window views are beneficial to building occupants by reducing discomfort. Hence, in the context of this research, visual comfort is defined as a dimension involving criteria, namely daylighting, artificial lighting, glare and reflection, visual privacy, and view.

## 4 Findings

### 4.1 Feedback/Complaint Types for Visual Comfort

After determining the visual comfort factors from the literature, interviews were conducted with 12 facility managers to determine the occupant feedback/complaint types that are related to visual comfort. Also, work orders related to visual comfort were retrieved from the computerized maintenance management software systems. Table 2 shows the list of occupant feedback/complaints for visual comfort under the six factors, namely daylight, artificial light, glare, reflection, visual privacy, and view.

**Table 2** List of occupant feedback/complaints for visual comfort

	Visual comfort	List of feedback/complaints
1	Daylight	Not enough sunlight
2	Artificial light	Quality of the lighting in work environment, amount of lighting on my table, shadows created by lighting equipment, constant vibration of the lighting equipment
3	Glare	Glare caused by the lighting equipment, glare caused by the direct sunlight from the window
4	Reflection	Reflection on the screens
5	Visual privacy	No visual privacy in work environment, no visual privacy in meeting room, my computer screen can be seen
6	View	Not being able to see outside, view from my table

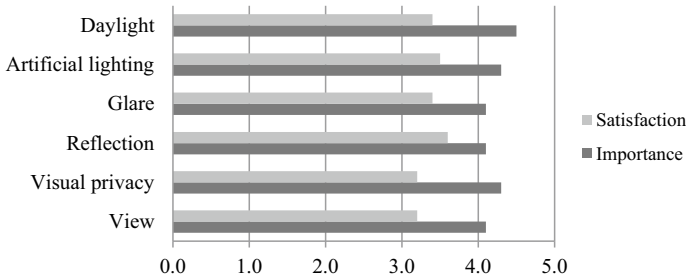


Fig. 1 Importance and satisfaction levels in visual comfort criteria

### 4.2 Importance and Satisfaction Levels for Visual Comfort

After determination of visual comfort criteria from the literature and visual comfort complaint types in the interviews undertaken with facility managers, a survey was undertaken with 308 office employees in the third step to determine: (1) the importance and satisfaction levels in visual comfort criteria and (2) number of respondents who have complaints in each complaint type. The importance and satisfaction levels were obtained using five-point Likert scale. The importance and satisfaction levels in visual comfort criteria are presented in Fig. 1. As for importance, office occupants find daylighting most important (4.5) followed by visual privacy (4.3) and artificial lighting (4.3). Glare, reflection, and view are perceived as less important criteria (4.1 each). On the other hand, occupants are most satisfied with reflection (3.6), followed by artificial lighting (3.5), glare (3.4), and daylighting (3.4). Occupants are least satisfied by view and visual privacy (3.3 each) in the offices.

### 4.3 Daylighting Satisfaction Levels and Complaints

In this section, office occupants were asked about their satisfaction levels regarding daylighting and their specific complaints about daylighting. Below is a distribution of daylighting satisfaction levels among the office building occupants. Results reveal that satisfaction levels of 36 occupants (12%) are 1 “not satisfied at all,” 48 occupants (16%) are 2 “not satisfied,” 51 occupants (16%) are 3 “neutral,” 100 occupants (32%) are 4 “satisfied,” and 73 occupants (25%) are 5 “very satisfied” (Fig. 2).

The number of respondents who have complaints in each complaint type that belongs to daylighting criteria is given in Fig. 3. Most frequent complaint related to daylighting is not enough sunlight in both summer and winter (reported by 102 respondents), followed by not enough sunlight in winter (reported by 24 respondents) and not enough sunlight in summer (reported by 4 respondents).

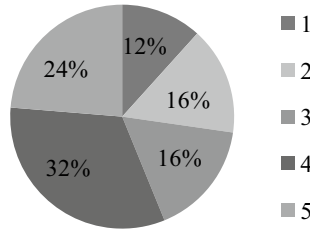


Fig. 2 Daylighting satisfaction levels



Fig. 3 Daylighting complaints

#### 4.4 Artificial Light Satisfaction Levels and Complaints

Office occupants were asked about their complaints about daylighting and their specific complaints about “quality of the lighting in work environment, amount of lighting on my table, shadows created by lighting equipment, constant vibration of the lighting equipment.” Distribution of satisfaction levels in artificial light criteria among the office building occupants is given in Fig. 4. Results reveal that satisfaction levels of 27 occupants (9%) are 1 “not satisfied at all,” 28 occupants (9%) are 2 “not satisfied,” 85 occupants (28%) are 3 “neutral,” 96 occupants (31%) are 4 “satisfied,” and 72 occupants (23%) are 5 “very satisfied.”

The number of respondents who have complaints in each complaint type that belongs to artificial light criteria is given in Fig. 5.

Most frequent complaint related to artificial light is “quality of the lighting in work environment” (reported by 62 respondents), followed by “amount of lighting on my table” (reported by 60 respondents).

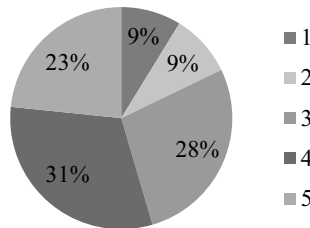


Fig. 4 Artificial light satisfaction levels

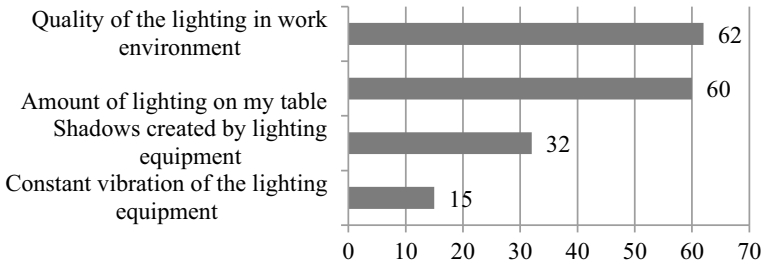


Fig. 5 Artificial lighting complaints

### 4.5 Glare Satisfaction Levels and Complaints

In this section, complaints regarding glare caused by the lighting equipment and direct sunlight from the window were questioned. Distribution of satisfaction levels in glare criteria among the office building occupants is given in Fig. 6. Results reveal that satisfaction levels of 27 occupants (9%) are 1 “not satisfied at all,” 33 occupants (11%) are 2 “not satisfied,” 106 occupants (34%) are 3 “neutral,” 79 occupants (26%) are 4 “satisfied,” and 63 occupants (20%) are 5 “very satisfied.”

Number of respondents in each complaint type that belongs to glare criteria is given in Fig. 7. Most frequent complaint related to glare is glare

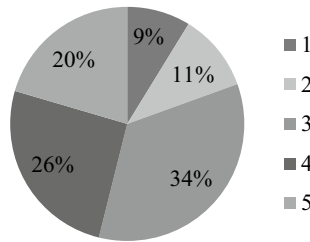


Fig. 6 Glare satisfaction levels

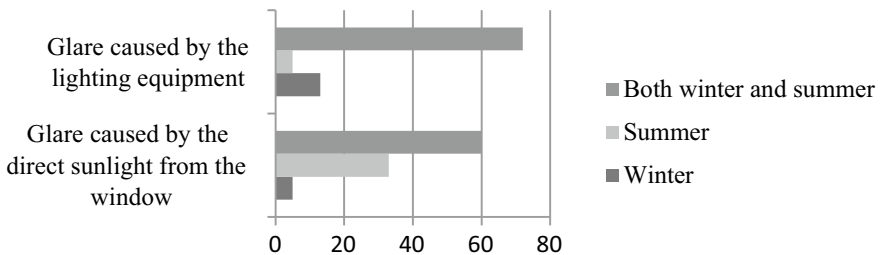
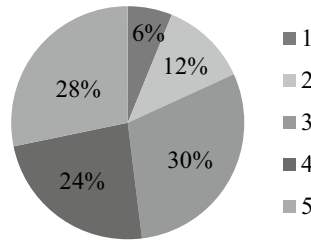
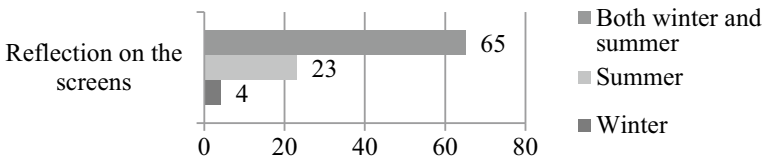


Fig. 7 Glare complaints



**Fig. 8** Reflection satisfaction levels



**Fig. 9** Reflection complaints

caused by the lighting equipment (reported by 90 respondents), followed by glare caused by the direct sunlight from the window (reported by 98 respondents).

#### 4.6 Reflection Satisfaction Levels and Complaints

Distribution of satisfaction levels in reflection criteria among the office building occupants is given in Fig. 8. Results reveal that satisfaction levels of 19 occupants (6%) are 1 “not satisfied at all,” 37 occupants (12%) are 2 “not satisfied,” 92 occupants (30%) are 3 “neutral,” 73 occupants (24%) are 4 “satisfied,” and 87 occupants (28%) are 5 “very satisfied.”

The number of respondents who have complaints in each complaint type that belongs to reflection criteria is given in Fig. 9. Most frequent complaint related to reflection is reflection on the screens in both summer and winter (reported by 65 respondents).

#### 4.7 Visual Privacy Satisfaction Levels and Complaints

Complaints about visual privacy in work environment and in meeting room were asked. Also, the level of complaint regarding the visibility of the personal computer screen was also asked. Distribution of satisfaction levels in visual privacy criteria among the office building occupants is given in Fig. 10. Results reveal that satisfaction levels of 35 occupants (11%) are 1 “not satisfied at all,” 60 occupants (20%) are 2 “not



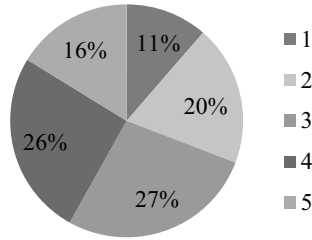


**Fig. 10** Visual privacy satisfaction levels

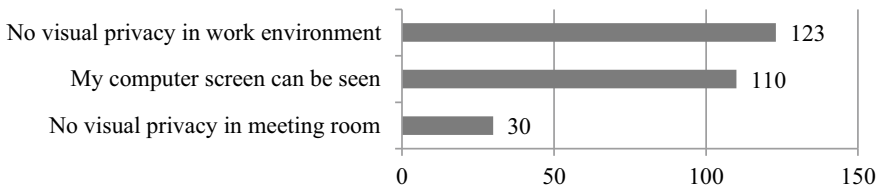


**Fig. 11** Visual privacy complaints

satisfied,” 84 occupants (27%) are 3 “neutral,” 79 occupants (26%) are 4 “satisfied,” and 50 occupants (16%) are 5 “very satisfied.”

The number of respondents who have complaints in each complaint type that belongs to visual privacy criteria is given in Fig. 11. Most frequent complaint related to visual privacy is “no visual privacy in work environment” (reported by 123 respondents), followed by “my computer screen can be seen” (reported by 110 respondents) and “no visual privacy in meeting room” (reported by 30 respondents).

### 4.8 View Satisfaction Levels and Complaints

Distribution of satisfaction levels in “view” criteria among the office building occupants is given in Fig. 12.

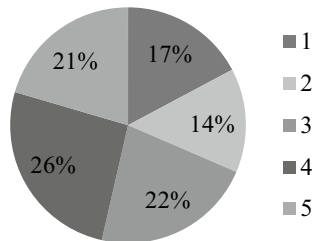


**Fig. 12** View satisfaction levels

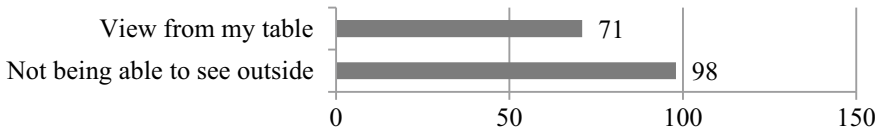


**Fig. 13** View privacy complaints

Results reveal that satisfaction levels of 53 occupants (17%) are 1 “not satisfied at all,” 44 occupants (14%) are 2 “not satisfied,” 68 occupants (22%) are 3 “neutral,” 80 occupants (26%) are 4 “satisfied,” and 63 occupants (121%) are 5 “very satisfied.” The number of respondents who have complaints in each complaint type that belongs to “view” criteria is given in Fig. 13. Most frequent complaint related to “view” “not being able to see outside” (reported by 98 respondents), followed by “view from my table” (reported by 71 respondents).

## 5 Conclusions

As for the importance of visual criteria, office occupants find daylighting most important (4.5) followed by visual privacy (4.3) and artificial lighting (4.3). On the other hand, occupants are most satisfied with reflection (3.6), followed by artificial lighting (3.5), glare (3.4), and daylighting (3.4). Occupants are least satisfied by view and visual privacy (3.3 each) in the offices. Findings show that average importance level in each visual comfort criteria is higher than the average satisfaction level. The largest gap between the perceived importance and satisfaction appears in daylighting and visual privacy.

In terms of daylighting, occupants are most dissatisfied by the insufficient sunlight in both summer and winter seasons in the offices. Lack of visual privacy in work environment as well as on the computer screens bothers a large portion of the occupants. While occupants are dissatisfied due to not being able to see outside or the view they see, they do not find this aspect very important. Quality of the artificial lighting in the work environment slightly dissatisfies the occupants. Reflection on the screens is not a frequent problem either. Glare is more frequently caused by the lighting equipment rather than direct sunlight from the windows, but is perceived as one of the least important criteria. It is not easy to compare the results obtained as there are only a few field studies undertaken investigating visual comfort in office buildings. Larger scale empirical studies are needed to understand the perceived visual comfort and complaints behind office occupants’ discomfort.

Since occupants are more dissatisfied with the lack of visual privacy and the insufficient sunlight in the offices, the designers, facility managers, and renovators need to think of design strategies to provide more privacy and access to daylight to occupants in their working environments. Also, in future studies, the visual comfort of office

workers has to be studied deeply by adding effects of visual tasks, eye pathologies, and disorders on the satisfaction that are often underestimated or neglected.

**Acknowledgements** This study was funded by the Scientific and Technological Research Council of Turkey (TUBITAK) (Grant no: 116M177). Authors would like to thank TUBITAK for their support. Authors also thank Murat Can Özkan and Nezih Yilmaz for data collection in building occupant surveys.

## References

1. Antoniadou, P., Papadopoulos, A.: Occupants' thermal comfort: State of the art and the prospects of personalized assessment in office buildings. *Energy Build.* **153**(2017), 136–149 (2017)
2. Brainard, G., Roberts, J., Veitch, J., and Van den Beld, G.: Ocular lighting effects on human physiology and behaviour. *CIE Publ.* **158** (2004)
3. Aries, M.B., Veitch, J.A., Newsham, G.R.: Windows, view, and office characteristics predict physical and psychological discomfort. *J. Environ. Psychol.* **30**(4), 533–541 (2010)
4. Charles, K., Veitch, J., Newsham, G., Marquardt, C., ve Geerts, J.: Satisfaction with Ventilation in Open-Plan Offices: COPE Field Findings. NRCC, Canada (2006)
5. Osterhaus, W.K.: Discomfort glare assessment and prevention for daylight applications in office environments. *Sol. Energy* **79**(2), 140–158 (2005)
6. Chen, P., Chang, C.: Human response to window views and indoor plants in the workplace. *HortScience* **40**(5), 1354–1359 (2005)
7. Afacan, Y., Demirkan, H.: The influence of sustainable design features on indoor environmental quality satisfaction in Turkish dwellings. *Architect. Sci. Rev.* **59**(3), 229–238 (2016)
8. Ahn, Y.H., Pearce, A.R.: Post occupancy study for green school facilities: case study of reedy fork elementary school. In: ICSDEC 2012: Developing the Frontier of Sustainable Design, Engineering, and Construction (pp. 585–592) (2013)
9. Alzoubi, H., Bataineh, R.F.: Pre-versus post-occupancy evaluation of daylight quality in hospitals. *Build. Environ.* **45**(12), 2652–2665 (2010)
10. Brown, C., Gorgolewski, M.: Assessing occupant satisfaction and energy behaviours in Toronto's LEED gold high-rise residential buildings. *Int. J. Energy Sect. Manage.* **8**(4), 492–505 (2014)
11. Galasiu, A.D., ve Veitch, J.A.: Occupant preferences and satisfaction with the luminous environment and control systems in daylit offices: a literature review. *Energy Build.* **38**(7), 728–742 (2006)
12. Gou, Z., Prasad, D., Lau, S.S.-Y.: Impacts of green certifications, ventilation and office types on occupant satisfaction with indoor environmental quality. *Architect. Sci. Rev.* **57**(3), 196–206 (2014)
13. Gultekin, P., Anumba, C.J., Leicht, R.M.: Case study of integrated decision-making for deep energy-efficient retrofits. *Int. J. Energy Sect. Manage.* **8**(4), 434–455 (2014)
14. Hauge, Å.L., Thomsen, J., Berker, T.: User evaluations of energy efficient buildings: Literature review and further research. *Adv. Build. Energy Res.* **5**(1), 109–127 (2011)
15. Healey, K., Webster-Mannison, M.: Exploring the influence of qualitative factors on the thermal comfort of office occupants. *Architect. Sci. Rev.* **55**(3), 169–175 (2012)
16. Heerwagen, J., Zagreus, L.: The human factors of sustainable building design: post occupancy evaluation of the Philip Merrill Environmental Center (2005)
17. Menadue, V., Soebarto, V., Williamson, T.: Perceived and actual thermal conditions: case studies of green-rated and conventional office buildings in the City of Adelaide. *Architect. Sci. Rev.* **57**(4), 303–319 (2014)

18. Paul, W.L., ve Taylor, P.A.: Comparison of occupant comfort and satisfaction between a green building and a conventional building. *Build. Environ.* **43**(11), 1858–1870 (2008)
19. Pheng Low, S., Gao, S., Lin Tay, W.: Comparative study of project management and critical success factors of greening new and existing buildings in Singapore. *Struct. Surv.* **32**(5), 413–433 (2014)
20. Preiser, W., Vischer, J.: *Assessing Building Performance*. Routledge, London (2006)
21. Singh, A., Syal, M., Korkmaz, S., Grady, S.: Costs and benefits of IEQ improvements in LEED office buildings. *J. Infrastruct. Syst.* **17**(2), 86–94 (2010)
22. Turpin-Brooks, S., Viccars, G.: The development of robust methods of post occupancy evaluation. *Facilities* **24**(5/6), 177–196 (2006)
23. Wagner, A., Gossauer, E., Moosmann, C., Gropp, T., Leonhart, R.: Thermal comfort and workplace occupant satisfaction—results of field studies in German low energy office buildings. *Energy Build.* **39**(7), 758–769 (2007)
24. Atkins, R., ve Emmanuel, R.: Could refurbishment of “traditional” buildings reduce carbon emissions? *Built Environ. Project Asset Manage.* **4**(3), 221–237(2014)
25. Cao, B., Ouyang, Q., Zhu, Y., Huang, L., Hu, H., Deng, G.: Development of a multivariate regression model for overall satisfaction in public buildings based on field studies in Beijing and Shanghai. *Build. Environ.* **47**, 394–399 (2012)
26. Jazizadeh, F., Ghahramani, A., Becerik-Gerber, B., Kichkaylo, T., Orosz, M.: Human-building interaction framework for personalized thermal comfort-driven systems in office buildings. *J. Comput. Civ. Eng* **28**(1), 2–16 (2014)
27. Kato, H., Too, L., Rask, A.: Occupier perceptions of green workplace environment: the Australian experience. *J. Corporate Real Estate* **11**(3), 183–195 (2009)
28. Laquatra, J., Pillai, G., Singh, A., Syal, M.M.: Green and healthy housing. *J. Architect. Eng.* **14**(4), 94–97 (2008)
29. Nahmens, I., Joukar, A., Cantrell, R.: Impact of low-income occupant behavior on energy consumption in hot-humid climates. *J. Architect. Eng.* **21**(2), B4014006 (2014)
30. Nicol, F., McCartney, K.: *Smart controls and thermal comfort project*. Final report (2000)
31. Rashid, M., Spreckelmeyer, K., Angrisano, N.J.: Green buildings, environmental awareness, and organizational image. *J. Corporate Real Estate* **14**(1), 21–49 (2012)
32. Seshadhri, G., Topkar, V.: Validation of a questionnaire for objective evaluation of performance of built facilities. *J. Perform. Constr. Facilities* **30**(1), 04014191 (2014)
33. Van Der Voordt, T.J.: Productivity and employee satisfaction in flexible workplaces. *J. Corporate Real Estate* **6**(2), 133–148 (2004)
34. Zalejska-Jonsson, A.: Parameters contributing to occupants’ satisfaction: green and conventional residential buildings. *Facilities* **32**(7/8), 411–437 (2014)
35. Bakker, L., Hoes-van Oeffelen, E., Loonen, R., Hensen, J.: User satisfaction and interaction with automated dynamic facades: a pilot study. *Build. Environ.* **78**, 44–52 (2014)
36. Brown, Z., Cole, R.J.: Influence of occupants’ knowledge on comfort expectations and behaviour. *Build. Res. Inform.* **37**(3), 227–245 (2009)
37. Garretón, J.Y., Rodriguez, R., Pattini, A.: Effects of perceived indoor temperature on daylight glare perception. *Build. Res. Inform.* **44**(8), 907–919 (2016)
38. Leder, S., Newsham, G.R., Veitch, J.A., Mancini, S., Charles, K.E.: Effects of office environment on employee satisfaction: a new analysis. *Build. Res. Inform.* **44**(1), 34–50 (2016)
39. Meir, I.A., Garb, Y., Jiao, D., Cicelsky, A.: Post-occupancy evaluation: an inevitable step toward sustainability. *Adv. Build. Energy Res.* **3**(1), 189–219 (2009)
40. Voelker, C., Beckmann, J., Koehlmann, S., Kornadt, O.: Occupant requirements in residential buildings: an empirical study and a theoretical model. *Adv. Build. Energy Res.* **7**(1), 35–50 (2013)
41. Parkin, J.K., Austin, S.A., Pinder, J.A., Baguley, T.S., Allenby, S.N.: Balancing collaboration and privacy in academic workspaces. *Facilities* **29**(1/2), 31–49 (2011)
42. Candido, C., Kim, J., de Dear, R., Thomas, L.: BOSSA: a multidimensional post-occupancy evaluation tool. *Build. Res. Inform.* **44**(2), 214–228 (2015). <https://doi.org/10.1080/09613218.2015.1072298>

43. Newsham, G., Birt, B.J., Arsenault, C., Thompson, A.J., Veitch, J.A., Mancini, S., Galasiu, A.D., Bradford, N.G., Macdonald, I.A., Burns, G.J.: Do 'green' buildings have better indoor environments? New evidence. *Build. Res. Inform.* **41**(4), 415–434 (2013)
44. Wilkinson, S.J., Reed, R., ve Jailani, J.: User satisfaction in sustainable office buildings: a preliminary study. Paper presented at the PRRES 2011: Proceedings of the 17th Pacific Rim Real Estate Society Annual Conference (2011)
45. BS EN 12665: Light and lighting—basic terms and criteria for specifying lighting requirements (2011)
46. Leech, J.A., Nelson, W.C., Burnett, R.T., Aaron, S., Raizenne, M.E.: It's about time: a comparison of canadian and american time-activity patterns. *J. Expo. Anal. Environ. Epidemiol.* **12**(6), 427–432 (2002)
47. Groth, A.: Climatic and non climatic aspect of indoor environment. In: *Energy Efficiency Building Design Guidelines for Botswana*, pp. 6–9 (2007)
48. Konis, K.: Predicting visual comfort in side-lit open-plan core zones: results of a field study pairing high dynamic range images with subjective responses. *Energy Build.* **77**, 67–79 (2014)
49. BS EN 12464-1: Light and lighting—lighting of work places Part 1: Indoor work places (2011)

# Heterogeneous Dual-Frequency IoT Network for Vital Data Acquisition



Mahmoud Salem , Islam El-Maddah, Khaled Youssef ,  
Ahmed Elkaseer , Steffen Scholz , and Hoda Mohamed

**Abstract** The IoT solutions for health informatics are suffering from restriction of using one frequency which makes the network is unable to communicate via different frequencies. Also, this limitation of using a single frequency fixes a single communication range between nodes without the capability to vary the covering rang. This could consume high power if the system has to transmit data on long distance due to the need to use signal repeater node/s. This paper reports the development of a new heterogeneous design of IoT network via unsymmetrical frequencies in order to sense, process, exchange and visualize two vital signs. The sensing and processing phases are performed via a convenient design of noninvasive vital data acquisition nods. These data acquisition nodes of vital signs are integrated into an embedded system with the IoT nodes in order to provide effective, accurate and real-time health monitoring for vital signs. The design of IoT broker node enables real-time analysis and concatenation of two vital signs. In addition, the broker facilitates the communication between nodes to each other over multi-frequencies in order to cover variant distances and thus to optimize the usage of power. Moreover, the proposed software of the IoT broker is able to address run-time issues of network nodes in real time without the need to reset the whole network.

---

M. Salem (✉) · I. El-Maddah · H. Mohamed  
Faculty of Engineering, Ain Shams University, Cairo, Egypt  
e-mail: [g16091591@eng.asu.edu.eg](mailto:g16091591@eng.asu.edu.eg)

K. Youssef  
Faculty of Navigation Science and Space Technology, BSU, Beni-Suef, Egypt

A. Elkaseer · S. Scholz  
Institute for Automation and Applied Informatics, Karlsruhe Institute of Technology, Karlsruhe, Germany

A. Elkaseer  
Faculty of Engineering, Port Said University, 42526 Port Said, Egypt

© The Editor(s) (if applicable) and The Author(s), under exclusive license to Springer Nature Singapore Pte Ltd. 2021

S. G. Scholz et al. (eds.), *Sustainable Design and Manufacturing 2020*, Smart Innovation, Systems and Technologies 200, [https://doi.org/10.1007/978-981-15-8131-1\\_30](https://doi.org/10.1007/978-981-15-8131-1_30)

## 1 Introduction

Nowadays, there is an enormous transfiguration in healthcare systems due to the newly advent technologies such as Internet of things (IoT), bio-sensing, noninvasive sensing, mobile application, cloud computing, etc. [1]. Existing healthcare systems are not structured to serve adequately the growing needs of life expectancy. Thus, the human vital data sensing and visualization still has many challenges that has not been addressed yet. Consequently, there must be an adaptable, customized and usable IoT solution for health care. Vital data acquisition is considered one of the main components in healthcare system which provides care for the elderly, children and patients permanently. In particular, vital data acquisition is defined as the sensing, acquiring and processing of bio-signals in order to interpret these signals into vital information for disease diagnosing [1, 2]. In healthcare solution, after acquiring the vital signs, the IoT sends the vital signs between sub-system components and cloud computing, and thus IoT technology is considered an outstanding algorithm in providing healthcare services. In particular, the development of the sensors in vital data acquisition based on IoT integration enables to collect effective data from patients in order to analyze it for diagnoses and taking decisions accordingly [2]. Whereas, the IoT provides full communication between sub-system components [3, 4] in hospitals and real-time communication between patients and doctors in order to enable remote healthcare monitoring, diagnosis and guidance in medical treatment. The development of healthcare solutions via IoT algorithm enables acquiring a remote full picture of the patient's health status.

Different attempts have been made to integrate IoT to vital data acquisition. Mainetti et al. developed a IoT solution that can aggregate the biomedical information from various sensors in order to send it to a remote server machine [5]. This solution is able to send notifications/messages to caregivers or doctors. In particular, the data is aggregated by smart sensors and analyzed in order to carry out the vital information. The development was carried out through two levels. Firstly, the data was collected through different sensors via a communication technique based on Bluetooth Low Energy (BLE). Secondly, the data was analyzed in order to extract the information and send it via the gateway using Wi-Fi technology. The implementation of the gateway services was developed via an embedded Linux kit, which is Raspberry Pi. The developed solution was found effective and customizable. However, the developed approach was restricted to develop a prototype with a big size without a study about the power consuming and size of the applicable wearable device. Also, the usage of embedded Linux platform was capable to make a large number of tasks due to it is high processing power, but the authors minimized these tasks to perform gateway services only. Moreover, the vital data was exchanged via BLE without capability to integrate with different physical layer for sensing node. The vital signs is able to send/receive in range of BLE covering distance only. In another study in [6], the proposed solution allows doctor and patient to communicate wherever the patient is such as at home, at manufacturers and at schools. The design is as follows; firstly, body area network (BAN) that includes smart sensors which can be worn

by patients. Secondly, personal area network (PAN) that distributes sensors in the environment of the smart space. Thirdly, portable medical terminal (PMT) that is wearable by patients to detected state. The usage of the developed smart gateway allows an exchange of data through the whole sub-system components via a cloud server. The cloud server collects data from different resources and synchronizes it in the exchanging process. The solution was effective to provide real-time communication with the doctors, and the approach enables real-time sensing for vital signs. However, the design of sensing node is fully invasive, so the patient has to wear the developed wearable sensors. Also, the exchange of data was restricted to small distance because it was accessing the gateway via the mobile phone network, and a methodology to cover long distances was not considered.

However, in a recent study in [7], authors developed an epidermal temperature sensor for patient with an convenient integration with wireless antenna in order to provide real-time vital data to the cloud computing. This approach calculates the human body temperate. However, the proposed method is still invasive where the sensor has to be attached to human body, and the processing unit is remote. In another study, Li et al. developed a user-friendly body temperature technique [8]. The solution provides real-time body temperature sensing via embedded sensors in the pillow. The sensors were connected to the broker node via Bluetooth low energy (BLE). The author utilized a mobile application that acts as a broker in order to access the gateway via Wi-Fi or 4G network. The mobile concatenates the vital data from different temperature sensors and calculates the vital features using fuzzy logic control algorithm. The solution is very comfortable in using and consuming low power usage. However, the technique was restricted to be utilized during sleeping. Also, the authors did not mention the capabilities of integration with other IoT network in different frequencies.

Based on recent advances in vital data acquisition and Internet of things in health-care informatics, one can say that noninvasive vital data acquisition still has many challenges to address. Moreover, the Internet of things in health informatics is still limited to cover different distances using different frequencies, multiple bandwidths for transmission/receiving and integration with noninvasive data acquisition. In this context, this paper aims to design and develop a heterogonous IoT network based on a convenient communication algorithm. This design enables the IoT nodes to communicate with each other via multi-frequencies in order to cover variant distances and optimize the consumption of power. Also, the author extended the previously developed IoT algorithm for heart rate in [1] to be able to sense human body temperature (BT) data via a noninvasive method.

Following this introduction, the proposed IoT design is presented, and the results are discussed followed by conclusions and future prospects.



## 2 Heterogeneous IoT Network

The architecture of the proposed heterogeneous IoT network is shown in Fig. 1, which was designed in four nodes with the ability to enable communication via two frequencies 2.4 GHz and 433 MHz. The heart rate (HR) data acquisition node and the visualization node transmit/receive data over 433 MHz frequency band. However, the body temperature (BT) data acquisition node transmits data over 2.4 GHz frequency band. Finally, the broker node transmits and receives vital data over 2.4 and 433 GHz frequencies bands. The BT node and HR node sense, extract and process the vital data via full noninvasive algorithms and send the vital features to the IoT broker. Then, the IoT broker analyzes these data and sends the analyzed data to the cloud computing and the visualization node.

### 2.1 IoT Broker Node

Figure 2 shows the heterogeneous structure of the IoT broker node. The broker node performs the communication with all solution nodes, and the broker architecture supports communications with other nodes. In particular, the broker receives the HR reading via LoRa module with frequency 433 MHz and receives the BT values via Wi-Fi module with frequency 2.4 GHz. After that, the broker sends the vital data to the visualization node via LoRa module with 433 MHz frequency band. Moreover, the ESP32 concatenates the vital data frame with a communication protocols in order

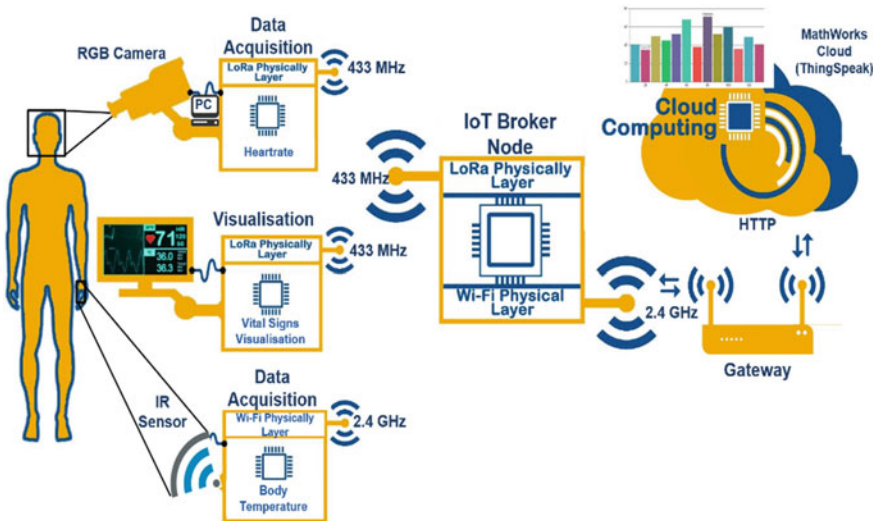
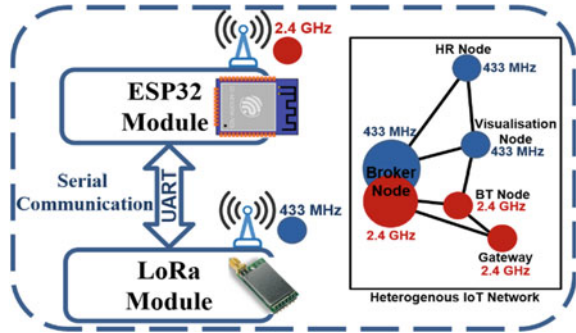


Fig. 1 Architecture of the heterogeneous IoT design with two vital signs (modified form [1])

**Fig. 2** Proposed heterogeneous architecture of broker node



to send it to the cloud computing. In Fig. 2 (heterogenous IoT network), the blue node refers to the communication network working at 433 MHz frequency, and the red node refers to 2.4 GHz frequency nodes. The broker can transmit/receive data over all nodes in the IoT architecture without a restriction to a specific frequency. This structure enables adding more nodes and enables transmitting data to different distances. Whereas, the ESP32 can cover a distance range about 30 m, and the LoRa can cover a distance up to 1.5 km.

The finite-state machine of the broker node is shown in Fig. 3. The process starts from the initial state, where the peripherals are initialized such as PORT, UART and SPI. Then, the broker connects to Wi-Fi and sets the LoRa in a normal mode (normal mode enables transmitting and receiving data). After that, the broker will be in a vital mesh communication state. In this state, the broker receives the body temperature vital data by establishing a communication session with the body temperature node via Wi-Fi on frequency 2.4 GHz on port 1000 and receives the heart rate vital data

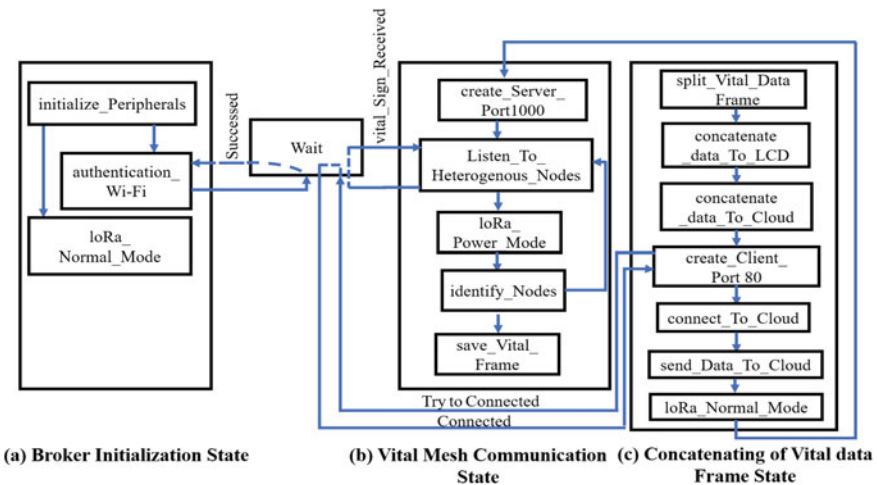


**Fig. 3** Finite-state machine of the broker node

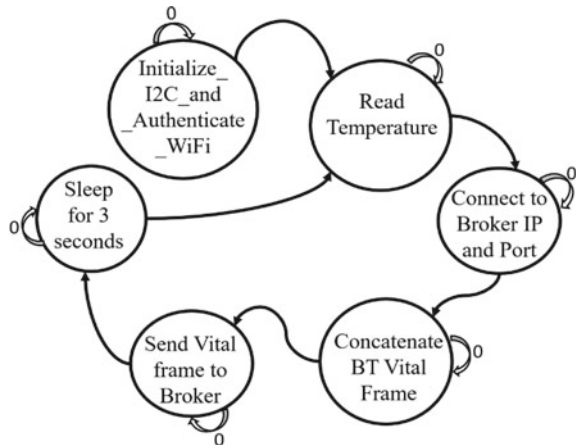
form heart rate node using LoRa on frequency 433 MHz. The broker identifies the connected nodes and saves all the vital features in a frame. Finally, this frame will be processed with specific ID which is called (Main1) and sends the processed frame to the visualization node via LoRa module on frequency 433 MHz. Moreover, the broker establishes a communication session with the gateway via Wi-Fi on frequency 2.4 GHz on port 80 and concatenates the vital frame in a POST request of HTTP in order to send the data to the MathWorks cloud computing.

## 2.2 Body Temperature Node

The body temperature vital sign is extracted by infrared IR sensor, and the received signal of IR sensor is processed via an embedded software which is developed for ESP32 module. Whereas, the temperature sensor is utilized to extract the body temperature vital data via a noninvasive methodology. The IR sensor sends/interfaces the sensed temperature to the ESP32 controller via inter-integrated circuit (I2C) communication bus with data rate 400 kHz. After, that, the ESP32 analyzes the received signal and interprets it into numeric values, where this interpreted signal (numeric values) refers to the human body temperature (BT) in Celsius degree. Then, the ESP32 sends the interpreted signal to the broker node (main controller) over 2.4 GHz frequency band.

The finite-state machine of the temperature node is shown in Fig. 4. The initial state starts the inter-integrated circuit (I2C) bus in order to enable the interface with the body temperature sensor. After that, the node receives/reads the sensed body temperature from the sensor and saves it in a buffer. Then, the node transmits the temperature data to the broker over 2.4 GHz frequency by creating client socket in order to communicate with the broker via TCP/IP on port 1000. As soon as the node concatenates the frame of temperature value and establishes socket communication

**Fig. 4** Finite-state machine of the body temperature data acquisition node



with the broker, the node will set in sleep mode for 3 s in order to optimize the power usage (Fig. 4).

### 3 Results

The BT node was validated on three volunteers in order to find the average of the sensed BT to calculate the quality and the error of the algorithm. During validation, the room temperature was around 27 °C. With the first volunteer, the average of the sensed BT from the head was 38.9 °C and from the finger was 23.2 °C. Also, with the second volunteer, the average of the sensed BT from the head was 36.8 °C and from the finger was 20.2 °C. With the third volunteer, the average of the sensed BT from the head was 36.3 °C and from the finger was around 25.1 °C. The results show that, the error of the algorithm is  $\pm 0.5$ – $3.5$  on sensing temperature from head and around  $-16$  °C on sensing from the finger. The average BT of 18 reading is 37.2 °C. The results show that, the error of the algorithm is reduced when there are a number of readings.

In order to validate the algorithm, the above values were captured from serial monitoring of body temperature node during the debugging phase (see Fig. 5). Whereas, the vital BT frame is printed on the serial monitoring terminal of the body temperature BT node. This validation was built by serial communication of (BT) node with 112500 baud rates to a PC terminal. After sending the BT frame to the broker as shown in Fig. 7, the BT node will be in sleep mode in order to optimize the power of

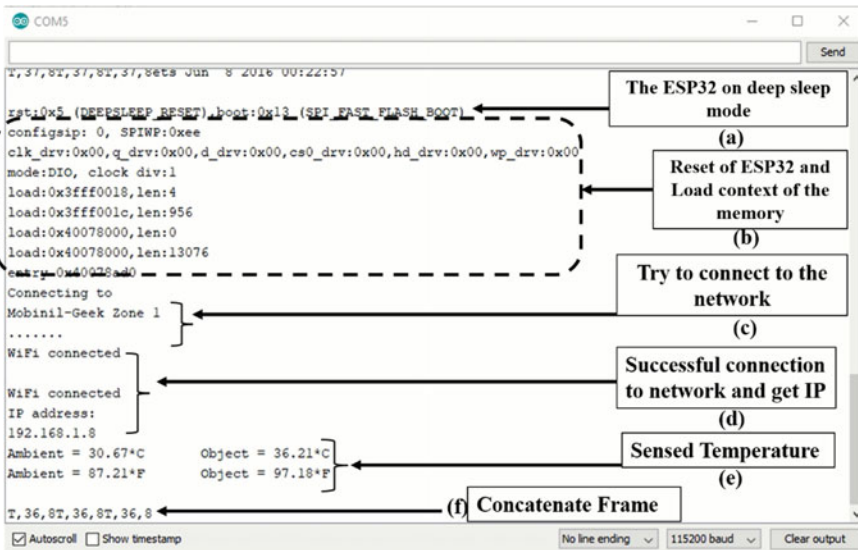


Fig. 5 Validation of body temperature (BT) node via serial monitoring

**Table 1** Developed IoT BT node in comparison with related work

Features	Developed BT algorithm	Miozzi et al. algorithm [7]	Li et al. algorithm [8]
Processing unit and platform	ESP32 with Wi-Fi	Microcontroller and RFID	Sensors with an embedded system
Method of sensing	Fully noninvasive	Semi-noninvasive	Semi-noninvasive
Using	Any place	In hospitals and clinics	In homes during sleeping
Update the IoT physical layer	Can be updated to BLE	Cannot be updated	Cannot be updated

the sensing node (see Fig. 5a). Then, the ESP32 will be reset in order to recover from the sleep mode to the normal mode (see Fig. 5b). After that, bootloader will load the code from the memory. After that, as shown in Fig. 5c, d, the ESP32 connects to the network of 2.4 GHz and get an IP. Then, the node will sense the BT and the environment in Celsius and Fahrenheit, as shown Fig. 5e. Finally, the node concatenates the vital frame and sends it to the broker node (see Fig. 5f) and sets the node to sleep mode again. The sensed temperature and the frame of body temperature vital sign are as follows; “T” points out to the ID of the frame, “36” refers to the temperature in Celsius, and “8” points out to the maximum throughput of the temperature node.

Table 1 shows the features of the developed body temperature sensing algorithm in comparison with related works. The advantages of the proposed algorithm are as follows; the development of the algorithm is very cheap, and it was around 350 LE. Also, the development node can be updated to send the vital sign on the BLE of ESP32. Moreover, the algorithm senses, processes and extracts the temperature in real time. The algorithm can work fully noninvasive but from short distance to the head.

The heterogeneous IoT broker performs communication with two different frequencies where the developed IoT broker node has the LoRa antenna with 433 MHz frequency band and the ESP32 antenna with 2.4 GHz frequency band. This design enables communication with two frequency bands and enables communication with two distance ranges, i.e., 30 m for the ESP32 range and 1.5 km for the LoRa. In particular, the integration between the ESP32 and the LoRa enables sending data over different bandwidths and different power consumptions. The broker can be utilized to select the suitable physical layer (ESP32 or LoRa) in order to rationalize consumption of power and resources. Figure 6 shows the captures of serial monitoring for the IoT broker node over different bandwidths. Whereas, Fig. 6a shows the communication frame with cloud computer via HTTP. The frame consists of three fields are as follows; field 1 for HR, field 2 for BT and field 3 for alarm of abnormal HR. The validation of receiving vital data from different frequencies is shown in Fig. 6b, c. However, Fig. 6c shows the socket communication session. Table 2 shows the developed IoT broker node in comparison with related works.

Figure 7a shows the visualization of BPM vital data on the cloud computing. Also, Fig. 7b shows the visualization of body temperature vital data on the cloud

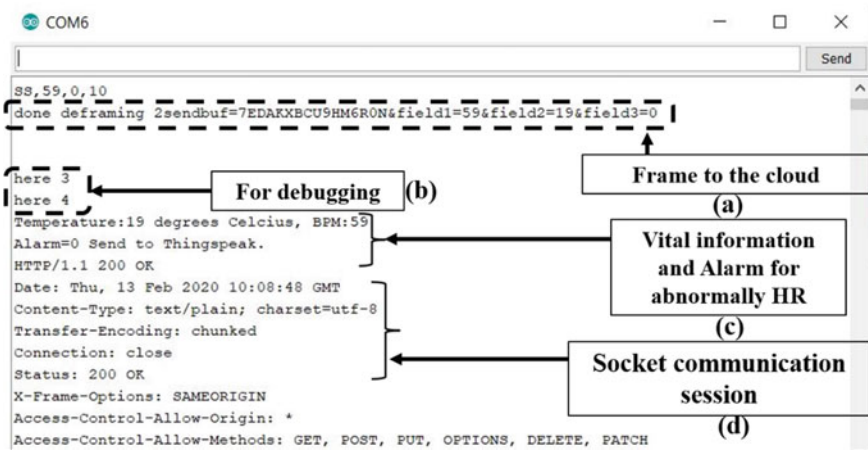


Fig. 6 Validation of IoT broker node during debugging phase

Table 2 Developed IoT broker in comparison with related work

Features	Developed IoT broker	Salama et al. IoT broker [4]	Mainetti et al. IoT broker [5]
Type of physical layer	Dual payload LoRa and Wi-Fi	Single payload Wi-Fi	Dual payload BLE and Wi-Fi
Utilization of physical layer (IoT module)	Both of the physical layers (ESP32 and Wi-Fi) are used to communicate with node. Moreover, Wi-Fi is used to access the gateway.	Wi-Fi is used for concatenate data form sensors and to access gateway.	BLE is used for concatenate vital data form sensors, and Wi-Fi is used for access gateway only.
Covering distance and bandwidth	30 m for 2.4 GHz and 1.5 km for 433 MHz	30 m for 2.4 GHz	100 m
Development method	Event based	RTOS	Embedded Linux

computing. However, Fig. 7c shows the alarm of abnormal BPM of a heart rate. These charts of Fig. 7a–c were captured during the testing phase. It is clear that, the three fields of the POST request are shown in chart of field 1, field 2 and field 3. The alarm is set high in case of low heart rate where it was less than 50 BPM in time 11:05 to 11:15 and in time 11:00 (see Fig. 7a–c). These results show the ability of the broker to handle the multi-vital signs and alarm in real time to the cloud computing.



Fig. 7 Vital data visualization on the cloud computing

## 4 Conclusion and Future Work

This paper reports on the development of heterogonous IoT network for dual-frequency (2.4 GHz and 433 MHz) communication and integrated into two nodes of noninvasive vital data acquisition. Also, a heterogeneous IoT broker was developed via an embedded system. The experimental results show that, the IoT broker can communicate to complex IoT nodes with different frequencies (2.4 GHz and 433 MHz) and to the cloud computing in real time without latency.

In addition, the results revealed that body temperature can be sensed via IR without a need to a high cost application. However, the experimental results showed that the IR body temperature found to be affected by the environment temperature, especially if it is very low/high, and thus it is recommended to use the IR sensing in a controlled room temperature. The error of the developed algorithm in room temperature is  $\pm 0.5$ – $3.5$  °C. Also, the error was calculated from 18 different readings. The average error of their readings is  $\pm 0.15$  °C.

For future work, it is planned to cover the design and the implementation of more than dual frequencies and to cover a remote memory node/s to save vital data in case of a drop-off connection to cloud computing. Moreover, it is recommended to cover a large number of vital signs such as inspiration and blood pressure.

## References

1. Salem, M., El-Maddah, I., Youssef, K., Mohamed, H.: Internet of things solution for non-invasive vital data acquisition: a step towards smart healthcare system, in sustainable design and manufacturing, KES-SDM, pp. 387–397. Springer, Singapore (2019)
2. Dias, D., Cunha, J.P.: Wearable health devices—vital sign monitoring, systems and technologies in the sensors, vol. 18, p. 2414 (2018)
3. Elkaseer, A., Salama, M., Ali, H., Scholz, S.: Approaches to a practical implementation of industry 4.0. In: The 11th International Conference on ACHI, Italy, pp. 141–146 (2018)
4. Salama, M., Elkaseer, A., Saied, M., Ali, H., Scholz, S.: Industrial internet of things solution for real-time monitoring of the additive manufacturing process. In: Proceedings of 39th International Conference on ISAT 2018, pp. 355–365. Springer International Publishing, Cham (2019)
5. Mainetti, L., Manco, L., Patrono, L., Secco, A., Sergi, I., Vergallo, R.: An ambient assisted living system for elderly assistance applications. In: 2016 IEEE 27th Annual International Symposium on PIMRC, pp. 1–6 (2016)
6. Korzun, D.G., Nikolaevskiy, I., Gurtov, A.: Service intelligence support for medical sensor networks in personalized mobile health systems. In: Internet of Things, Smart Spaces, and Next Generation Networks and Systems, pp. 116–127. Springer International Publishing, Cham (2015)
7. Miozzi, C., Amendola, S., Bergamini, A., Marrocco, G.: Reliability of a re-usable wireless epidermal temperature sensor in real conditions. In: IEEE 14<sup>th</sup> International Conference on Wearable and Implantable Body Sensor Networks (BSN), pp. 95–98 (2017)
8. Li, S., Chiu, C.: A smart pillow for health sensing system based on temperature and humidity sensors. *Sensors* **18**, 3664, (2018)



# Sustainability Assessment of Rapid Sand Mould Making Using Multi-criteria Decision-Making Mapping



Emanuele Pagone , Prateek Saxena , Michail Papanikolaou ,  
Konstantinos Salonitis , and Mark Jolly 

**Abstract** Capabilities of additive manufacturing (AM) for rapid tooling are well known in recent times. Rapid sand moulds are advantageous over traditional sand moulds in terms of cost, manufacturing time, flexibility, etc. This paper identifies metrics related to mould manufacturing and categorises them into four categories (cost, time, quality and environmental sustainability). A methodology based on the deterministic Technique for Order of Preference by Similarity to Ideal Solution (TOPSIS) multi-criteria decision-making algorithm is used to map at high resolution the influence of such categories on to the decision-making space when comparing AM with conventional sand mould making. Results show that AM is almost always clearly advantageous overall (excluding some very limited corner cases) for the examined case.

## 1 Introduction

Sand casting finds its importance in producing near-net-shape complex geometries. In a traditional sand casting process, hot molten metal is poured in a sand mould and is left to cool down at the room temperature. The molten metal solidifies and the casting is obtained. The pouring process can be manual, semi-automated or fully automated. The flow velocity of molten metal should be controlled to avoid any turbulence and to maintain high casting quality. The sand castings typically have low cooling rates because of the insulation provided by the sand surrounding the molten metal. This is advantageous particularly for shaping hard-to-machine materials [1]. The internal shape of the part is obtained by making use of a core which is placed inside the mould cavity. The cores and patterns are produced by skilled foundrymen [2]; thus, the accuracy of the tooling is dependent upon the skill set of artisans. The moulds for sand castings are expendable, i.e. they are temporary and not reusable moulds. One mould can only be used for producing one casting. Consequently, in order to

---

E. Pagone (✉) · P. Saxena · M. Papanikolaou · K. Salonitis · M. Jolly  
School of Aerospace, Transport and Manufacturing, Sustainable Manufacturing Systems Centre,  
Cranfield University, Bedfordshire MK43 0AL, UK  
e-mail: [e.pagone@cranfield.ac.uk](mailto:e.pagone@cranfield.ac.uk)

obtain repeatability in castings, moulds should be manufactured with high precision and accuracy. Furthermore, mould manufacturing is not only labour intensive but also time consuming. Gravity sand casting process finds its application in casting engine blocks. In the current work, we confine ourselves to the mould manufacturing process for gravity sand casting only.

Additive manufacturing (AM), commonly referred to as 3D printing, has emerged as a robust and rapid tooling technique in recent years [3]. However, its implementation in sand casting operations is not well explored yet. AM as per NF ISO/ASTM 52900 can be defined as “*the process of joining materials to make parts from 3D model data, usually layer upon layer, as opposed to subtractive manufacturing and formative manufacturing methodologies*”. The expendable mould making process using 3D printing is economical [4] and much faster [5, 6] than conventional mould making techniques. Also, the process is suitable for a wide range of materials used for mould making in sand casting process [5, 6]. For smaller production volumes, pattern making is rather expensive. As the pattern must be removed to create a cavity, this sometimes limits the geometry to be produced from conventional sand casting [7]. Several researchers have highlighted the importance and advantages of rapid sand casting over traditional sand casting [8–10]. However, a robust decision framework has never been implemented in the past to identify the scenarios in which one mould manufacturing method is advantageous over the other, according to authors’ best knowledge.

The work done in this paper identifies critical metrics related to mould sustainability, cost, quality and time required to produce one mould. The metrics are then categorised into four groups, and different scenarios are evaluated. A methodology based on multi-criteria decision analysis assigns a pre-determined importance (i.e. weight) to each category of metrics and determines objectively which process is to be preferred in a particular scenario. From a sustainability perspective, such approach also helps to select a cleaner manufacturing process at the same time critically evaluating the overall performance of the rapid sand casting process.

## 2 Sand Mould Manufacturing Process

### 2.1 Conventional Sand Moulds

In sand casting processes, a sand mould serves as a tool, forming an internal cavity for pouring in and solidifying the molten metal. In parts, such as engine blocks where a complex internal geometry is desired, a secondary tool element known as “core” is used. Cores are fabricated using silica sand, and a resin or binder is used to bind and cure the core. Cores are sometimes coated and baked before use.

Mould making is typically a machining process that involves energy consumption. The specific mould making energy ( $SEC_m$ ) for the process is 0.16 MJ/Kg [11]. Similarly, the specific core manufacturing energy ( $SEC_c$ ) has been found to be equal

to 0.51 MJ/Kg [11]. If  $w_m$  and  $w_c$  represent the weight of sand utilised for mould making and core making, respectively, then the total energy consumption ( $E_c$ ) in conventional mould and core production can be evaluated from Eq. 1.

$$E_c(\text{MJ}) = (\text{SEC}_m w_m) + (\text{SEC}_c w_c) \tag{1}$$

The CO<sub>2</sub> emissions for generating heat using grid electricity (also referred to as carbon intensity) are assumed to be 325 g CO<sub>2</sub>/KWh. More realistic data at any instant can be obtained from [12]. The overall CO<sub>2</sub> emissions can thus be evaluated from Eq. 2.

$$\text{CO}_{2,c}(\text{kgCO}_2) = \frac{325}{3600} * E_c(\text{MJ}) \tag{2}$$

### 2.2 Rapid Sand Moulds

One of the 3D printing technologies utilised for printing sand moulds is binder jetting. The process is capable of fabricating an optimised mould design with identical engineering competence and 33% lighter than the usual component [10].

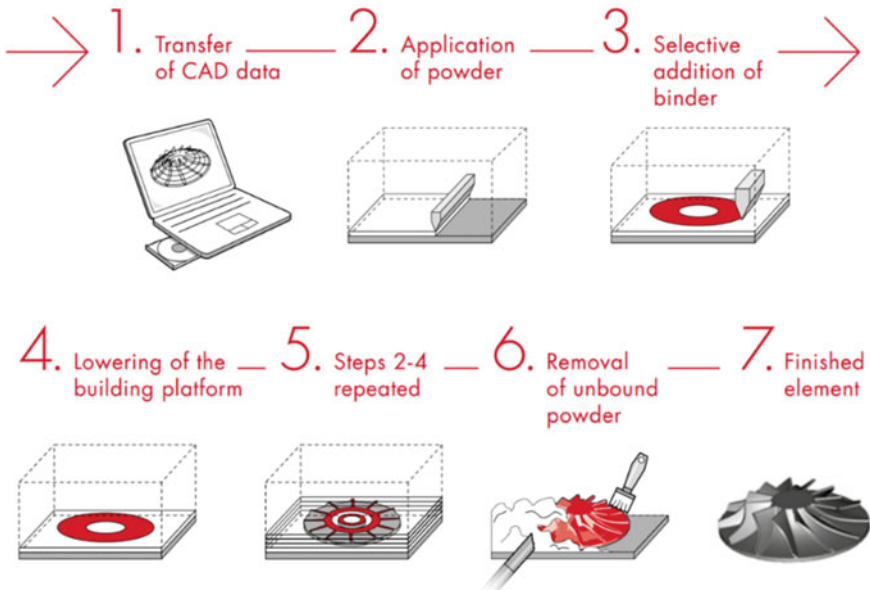


Fig. 1 Fabrication of sand moulds from binder jetting (Image adapted from [17])

The manufacturing process is carried out in seven steps (Fig. 1). A CAD model is first prepared using a standard CAD software, and subsequently, the model is then fed to the 3D printing machine. A re-coater spreads a layer of sand on the build platform. The inkjet head then sprays the binder droplets forming a layer. The build platform is lowered, and the process is repeated to fabricate the next layer. The process continues till the desired part is produced. Unbound sand is then removed using pressurised air or a brush, and the finished part is then obtained from the machine. In certain cases, an additional post-curing operation is carried out to enhance the strength of parts. The mould can then be utilised in sand casting operation. Utilisation of 3D printed moulds in energy-efficient sand casting processes such as CRIMSON has the potential to produce defect-free castings and at the same time reduce the energy consumption of the casting process [13–16].

Energy consumption for mould and core manufacturing depends on the printer specifications. There are several 3D printers available commercially with machine power ranging from 5000 to 10,300 W. For the current study, a VX500 Voxeljet printer has been considered. The maximum machine power for the printer is 10,300 W with a build (maximum) speed of  $3 \times 10^{-6} \text{ m}^3/\text{s}$ . The specific energy consumption ( $\text{SEC}_{\text{m,c}}$ ) for manufacturing the sand mould and a core with density  $1738 \text{ kg}/\text{m}^3$  is  $1.08 \text{ MJ}/\text{kg}$  [9]. Thus, the total energy consumption ( $E_{3\text{D}}$ ) in 3D printing of sand mould and core can be evaluated from Eq. 3. The corresponding  $\text{CO}_2$  emissions can be obtained from Eq. 4 (analogous to Eq. 2).

$$E_{3\text{D}}(\text{MJ}) = \text{SEC}_{\text{m,c}}(w_{\text{m}} + w_{\text{c}}) \quad (3)$$

$$\text{CO}_{2,3\text{D}}(\text{kg}_{\text{CO}_2}) = \frac{325}{3600} * E_{3\text{D}} (\text{MJ}) \quad (4)$$

### 3 Process Selection for Mould Manufacturing

The influence of multiple criteria such as environmental sustainability, quality, cost and production time in formulating a decision-making approach for optimal process selection is presented in this section. Metrics influencing the sand mould and their effect on the casting quality are considered. The positive or negative impact on the mould making process is identified for each quantity (see Table 1). The effect of increasing the quantity identifies its impact.

#### 3.1 Environmental Sustainability

Sand casting is one of the most energy-intensive manufacturing processes. Equations (1)–(4) can be used to evaluate the total energy consumption in mould making

**Table 1** Selected process metrics for expendable mould manufacturing

Quantity	Impact	Category
Total sand used in mould making ( $w_m$ )	Negative	Environmental sustainability
Total sand used in core making ( $w_c$ )	Negative	Environmental sustainability
Casting weight ( $w_{cast}$ )	Negative	Environmental sustainability
CO <sub>2</sub> emissions (CO <sub>2</sub> )	Negative	Environmental sustainability
Total energy consumption in mould making ( $E$ )	Negative	Environmental sustainability
Tensile strength of mould ( $\sigma_t$ )	Positive	Quality
Surface roughness of casting ( $R_a$ )	Negative	Quality
Porosity of casting	Negative	Quality
Compressive strength of casting ( $\sigma_c$ )	Positive	Quality
Hardness of casting (HV)	Positive	Quality
Cost of one mould	Negative	Cost
Mould making time	Negative	Time

and the corresponding CO<sub>2</sub> emissions. Material data for sand used in fabricating the mould and the core are adapted from Hawaldar and Zhang [8]. The authors fabricated the mould for manufacturing a pump bowl. The core and the mould were manufactured using a VX500 3D printer. The authors reported that the total mass of utilised sand ( $w_m$ ) in the conventional and 3D printing processes was equal to 301 kg and 90 kg, respectively. The mass of sand used for manufacturing the core ( $w_c$ ) was 7.7 kg (conventional) and 3.3 kg (3D printed). The casting mass ( $w_{cast}$ ) for the two moulds was found to be 34 kg (conventional) and 23 kg (3D printed).

Substituting  $w_m$  and  $w_c$  in Eq. (1) and (3), the total energy required to manufacture mould using the two mentioned processes is  $E_c = 52.08$  MJ and  $E_{3D} = 110.36$  MJ respectively. By substituting the two energy values in Eqs. (2) and (4), the CO<sub>2</sub> emissions for the two processes can be evaluated: CO<sub>2,c</sub> = 4.70 kgCO<sub>2</sub> and CO<sub>2,3D</sub> = 9.96 kgCO<sub>2</sub>.

### 3.2 Quality

Quality can be evaluated in terms of the quality of the parts produced from the two moulds (conventional and 3D printed sand mould). The strength of the mould itself can be an influencing factor from the mould perspective. Material data for the quality metric have been adapted from Snelling et al. [18]. Sand used for 3D printing is commercially available 3D powder, ViriCast™, from Viridis 3D. The 3D printed mould allows castings to be produced up to maximum of 1454.4 °C. Five tensile testing specimens were printed and cured at 204.4 °C for 5 h. Standard tensile testing apparatus was used to identify the tensile strength of the 3D printed dog-bone and compared against the conventional no-bake foundry sand mould. The mean tensile

**Table 2** Tooling cost for mould manufacturing [17]

Quantity	3D printed moulds		Conventional moulds
	$t_{\text{lead}} = 5$ days	$t_{\text{lead}} = 21$ days	$t_{\text{lead}} = 4-6$ weeks
1	€898	€410	€3600
5	€3080	€1428	€3684
10	€5490	€2525	€3789
50	€22,275	€10,300	€4628

strength ( $\sigma_t$ ) for the 3D printed part and the no-bake foundry sand mould were reported to be 0.16 MPa and 0.56 MPa, respectively. A356 alloy was then cast using the moulds from the two processes, and other characteristics were then identified.

Roughness average ( $R_a$ ) for the 3D printed moulds and no-bake sand moulds was reported to be 13.62  $\mu\text{m}$  and 12.17  $\mu\text{m}$ , respectively. The average density of two castings was found to be identical and equal to 2.61  $\text{g}/\text{cm}^3$ , and thus, density was excluded from the current analysis. Castings produced from 3D printed moulds were more porous compared to those produced from no-bake moulds. Average porosity was found to be 1.13 and 0.65% in 3D printed moulds and no-bake moulds, respectively. The Vickers hardness value of two moulds was 92.7 HV (3D printed) and 82.1 HV (no-bake mould). The metal cylinders were also tested for compressive strength, and the reported values were 170.8 MPa (3D printed) and 165 MPa (no-bake mould).

### 3.3 Cost

Cost is another important criterion for decision making. It typically involves material, labour, equipment, energy and manufacturing costs. For simplicity, all these costs can be referred to as tooling cost. The economics of 3D printed moulds is dependent on the lead time ( $t_{\text{lead}}$ ) and number of parts [8]. Depending on both factors, 3D printed moulds are capable of saving up to 75% of the mould manufacturing cost [17]. Table 2 shows the costs in mould manufacturing from the two processes. In the current study, cost for small production volumes (one part) with  $t_{\text{lead}} = 21$  days is considered.

### 3.4 Time

Time accounts for the total time spent for mould making, core making and fettling time. As 3D printing does not require patterns to be produced, time spent in making patterns is excluded from the current study. Fettling time refers to the time spent in removing risers, runners and feeder head after dismantling the mould by breaking in

conventional mould manufacturing. The data for calculating the time spent in two mould making processes have been adapted from [8].

### 3.5 Multiple-Criteria Decision Analysis Mapping Through Weighting

The combination of multiple, conflicting criteria in order to make an objective decision among a number of alternative options, is a sub-discipline of operations research called multi-criteria decision analysis (MCDA). Several MCDA methods have been developed over the past decades, and among them, the Technique for Order of Preference by Similarity to Ideal Solution (TOPSIS) has attracted significant attention for its ability to correctly compare criteria with different scales and inter-dependencies. Moreover, TOPSIS can take into account of compensatory trade-offs and combine qualitative and quantitative data [19]. TOPSIS applies weights to each criterion (initially normalised) to reflect their importance for the decision maker and then identifies a positive (i.e. best) and negative (i.e. worst) ideal solution. Finally, a score  $s^-$  is calculated to rank the alternatives considering their closeness to the mentioned ideal solutions. Higher scores imply a better choice [20].

In a previous work by the authors, TOPSIS has been combined with an algorithm capable of automatically mapping the decision-making space at high-resolution [21]. This can be accomplished categorising the criteria (that are considered equally important within each category) and applying an ordinal and combinatorial study of weight distributions to the categories. Four weight distributions laws with self-explanatory names (called “uniform”, “halving”, “quadratic” and “first two”) have been selected to satisfactorily describe the decision-making space (Fig. 2) [21].

Such methodology is used in this study to map the decision-making space of conventional mould making in comparison with an AM process.

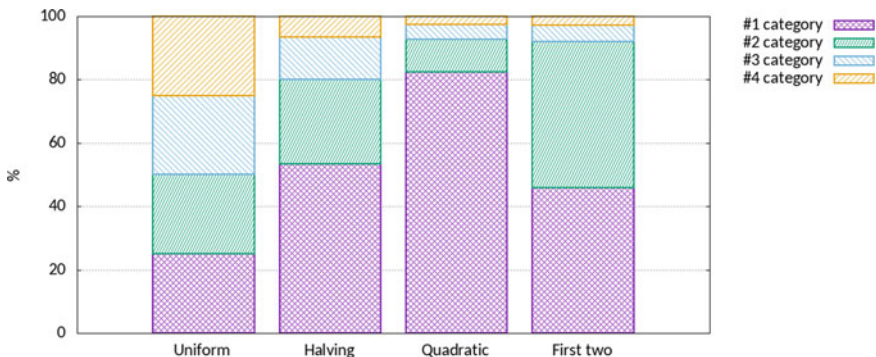


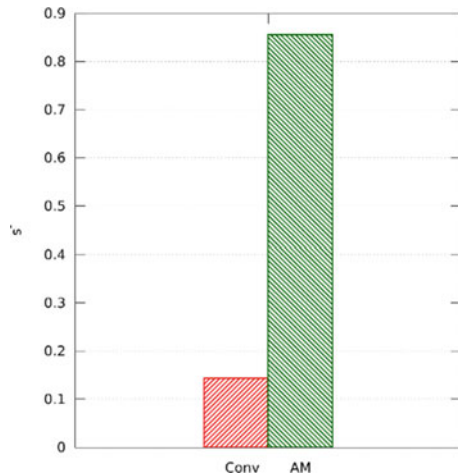
Fig. 2 Weight distribution laws applied to the TOPSIS method for the categories of criteria [21]

## 4 Results and Discussion

When categories are combined and they are considered equally important for the decision maker, AM clearly appears to be the best choice overall, showing a significant advantage over conventional mould making (Fig. 3). The maps showing the ordinal combinatorial study with different weight distributions (“halving”, “quadratic” and “first two” of Fig. 2) are presented in Fig. 4 identifying each case with the sequence of initial letters for each category (i.e. “e”: environmental sustainability, “t”: time, “q”: quality, “c”: cost). The position of the relevant letter in the sequence indicates the ranking of each category to set its weight.

The maps show a clear dominance of the AM option in almost every case. However, it is interesting that conventional mould making becomes (by a small margin) a better choice when quality is considered to be the most important characteristic according to the decision maker (“quadratic” weight distribution law cases starting with “q” in Fig. 4). Furthermore, another interesting aspect exposed by the high-resolution mapping is a few isolated, corner cases when there is no clear preference between the two options, i.e. when environmental sustainability and quality are the only two important categories (“first two” weight distribution law cases starting with “eq” or “qe” in Fig. 4). For these cases, it would be interesting to amplify the differences between alternatives using the criteria entropy of information [21] to obtain a clearer ranking.

**Fig. 3** Overall TOPSIS score  $s^-$  of conventional (“Conv”) and additive manufacturing (“AM”) sand mould making when all categories are equally important (“uniform” weight distribution law of Fig. 3)





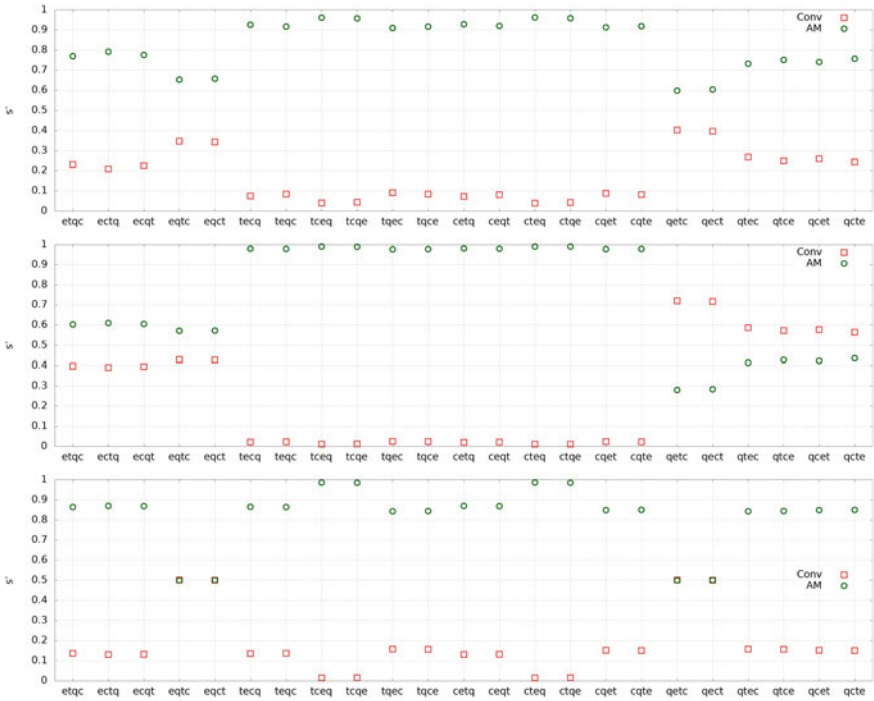


**Fig. 4** Overall TOPSIS score  $s^-$  of conventional (“Conv”) and additive manufacturing (“AM”) sand mould making with “halving” (top), “quadratic” (centre) and “first two” (bottom) weight distributions (as defined in Fig. 3). The importance of categories is represented by the position of its initial letter (i.e. “e”: environmental sustainability, “t”: time, “q”: quality, “c”: cost)

## 5 Conclusions

Sand casting is a well-established shaping process for manufacturing complex geometries. Additive manufacturing (AM) techniques for rapid tooling have seen a significant development in recent times, but their application in printing expendable moulds for sand castings is rather new. The AM printing process is known to be economical and faster than conventional mould making technique. However, there remains a gap in assessing the sustainability of rapid sand casting moulds. This paper establishes a robust sustainability assessment approach to compute key manufacturing quantities (in the categories of cost, time, quality and environmental sustainability) and combines them using a multi-criteria decision analysis tool able to map at high-resolution decision-making space. Results show that in many cases, AM is the best choice and identifies a few isolated cases where there is no clear better option between the two (i.e. when both environmental sustainability and quality are the only two most important categories for the decision maker) or when conventional mould making is to be preferred (i.e. when quality is the only major desired characteristic). It can be concluded that, in general, AM mould making is overall more

desirable over conventional techniques for producing single mould part. The comparative assessment of medium and large production volumes, including sustainability metrics, can be addressed in future works.

**Acknowledgements** The authors would like to thank the UK Engineering and Physical Sciences Research Council (EPSRC) for their support in the project “Energy Resilient Manufacturing 2: Small is Beautiful Phase 2 (SIB 2)” (EP/P012272/1).

## References

1. DeGarmo, E.P., Black, J.T., Kohser, R.A.: *Materials and Processes in Manufacturing*, 9th edn. Wiley, New York (2003)
2. Chua, C.K., Chou, S.M., Wong, T.S.: A study of the state-of-the-art rapid prototyping technologies. *Int. J. Adv. Manuf. Technol.* **14**(2), 146–152 (1998)
3. Levy, G.N., Schindel, R., Kruth, J.P.: Rapid manufacturing and rapid tooling with layer manufacturing (LM) technologies, state of the art and future perspectives. *CIRP Ann. Manuf. Technol.* **52**(2), 589–609 (2003)
4. Munish, C.: Rapid casting solutions: a review. *Rapid Prototyp. J.* **17**(5), 328–350 (2011)
5. Dimitry, D.M.: Advances in three dimensional printing—state of the art and future perspectives. *Rapid Prototyp. J.* **12**(3), 136–147 (2006)
6. Gill, S.S., Kaplas, M.: Comparative study of 3D printing technologies for rapid casting of aluminium alloy. *Mater. Manuf. Process.* **24**(12), 1405–1411 (2009)
7. Sama, S.R., Badamo, T., Lynch, P., Manogharan, G.: Novel sprue designs in metal casting via 3D sand-printing. *Addit. Manuf.* **25**, 563–578 (2019)
8. Hawaldar, N., Zhang, J.: A comparative study of fabrication of sand casting mold using additive manufacturing and conventional process. *Int. J. Adv. Manuf. Technol.* **97**(1), 1037–1045 (2018)
9. Sivarupan, T., Upadhyay, M., Ali, Y., El Mansori, M., Dargusch, M.S.: Reduced consumption of materials and hazardous chemicals for energy efficient production of metal parts through 3D printing of sand molds. *J. Clean. Prod.* **224**, 411–420 (2019)
10. Upadhyay, M., Sivarupan, T., El Mansori, M.: 3D printing for rapid sand casting—a review. *J. Manuf. Process.* **29**, 211–220 (2017)
11. Design, G.: CES Edupack Database. Granta Design, Cambridge (2016)
12. ICAX: Carbon Emissions Calculator. [Online]. Available [https://www.icax.co.uk/Carbon\\_Emissions\\_Calculator.html](https://www.icax.co.uk/Carbon_Emissions_Calculator.html). Accessed 01 Feb 2020
13. Papanikolaou, M., Saxena, P., Pagone, E., Salonitis, K., Jolly, M.R.: Optimisation of the filling Process in counter-gravity casting. In: *IOP Conference Series: Materials Science and Engineering* (2020)
14. Pagone, E., Salonitis, K., Jolly, M.: Energy and material efficiency metrics in foundries. *Procedia Manuf.* **21**, 421–428 (2018)
15. Salonitis, K., Jolly, M.R., Zeng, B., Mehrabi, H.: Improvements in energy consumption and environmental impact by novel single shot melting process for casting. *J. Clean. Prod.* **137**, 1532–1542 (2016)
16. Saxena, P., Papanikolaou, M., Pagone, E., Salonitis, K., Jolly, M.R.: *Digital manufacturing for Foundries 4.0*. Light Met. (2020)
17. Voxeljet: 3D printing save up to 75% in sand casting costs (2019). [Online]. Available <https://www.voxeljet.com/branchen/cases/3d-druck-spart-bis-zu-75-an-kosten-im-sandguss/>. Accessed 09 Sept 2019
18. Snelling, D., et al.: The effects of 3D printed molds on metal castings. In: *Proceedings of the Solid Freeform Fabrication Symposium*, pp. 827–845 (2013)

19. Triantaphyllou, E., Shu, B., Sanchez, S.N., Ray, T.: Multi-criteria decision making: an operations research approach. *Encycl. Electr. Electron. Eng.* **15**, 175–186 (1998)
20. Hwang, C.-L., Lai, Y.-J., Liu, T.-Y.: A new approach for multiple objective decision making. *Comput. Oper. Res.* **20**(8), 889–899 (1993)
21. Pagone, E., Salonitis, K., Jolly, M.: Automatically weighted high-resolution mapping of multi-criteria decision analysis for sustainable manufacturing systems. *J. Clean. Prod.* **257**, article no. 120272 (2020)

# NeoPalea: Compostable Composite Material for Packaging Applications



Leonardo Conti , Federico Rotini , Matteo Barbari , Marco Togni ,  
and Giuseppe Rossi 

**Abstract** The problem of packaging waste is deeply felt at international level, because each year hundreds of millions of tons of packaging are produced. While significant improvements have been made in the recycling of metal, wood, paper and cardboard packaging, plastic packaging still represents an open issue. The EU implemented regulatory actions to manage packaging and packaging waste by defining short-to-medium-term targets in terms of recycling rate. In such a context, the paper deals with an innovative composite material dedicated to the production of tertiary packaging, named NeoPalea. The proposed material is based on a combination of natural fibers and biodegradable biopolymers. It was prototyped to verify the performance as a potential substitute of the polymers currently used for packaging. The preliminary results obtained are encouraging.

## 1 Introduction

The packaging deriving from fossil sources continues to be the dominant solutions despite the growing concerns about the environmental impact due to large volumes

---

L. Conti · M. Barbari · M. Togni · G. Rossi

Dipartimento di Scienze e Tecnologie Agrarie, Alimentari, Ambientali e Forestali - Università degli Studi di Firenze, Piazzale delle Cascine, 18, 50144 Florence, Italy

e-mail: [leonardo.conti@unifi.it](mailto:leonardo.conti@unifi.it)

M. Barbari

e-mail: [matteo.barbari@unifi.it](mailto:matteo.barbari@unifi.it)

M. Togni

e-mail: [marco.togni@unifi.it](mailto:marco.togni@unifi.it)

G. Rossi

e-mail: [giuseppe.rossi@unifi.it](mailto:giuseppe.rossi@unifi.it)

F. Rotini (✉)

Dipartimento di Ingegneria Industriale, Università degli Studi di Firenze, via di S. Marta 3, 50139 Florence, Italy

e-mail: [federico.rotini@unifi.it](mailto:federico.rotini@unifi.it)

of material, high-energy consumption of the processes and landfill treatment of waste [1]. Approximately one-third of the plastic materials produced worldwide are used for packaging, equal to about 100 million tons; in fact, in industrialized Western countries, 50% of consumer goods have plastic packaging [2]. In Europe, 70 million tons of packaging waste were produced in 2016 and approximately 16.7 million tons of these were plastic waste [3]. Even though in recent years, the packaging recycling performance in the EU has increased significantly with homogeneous trends for nearly all Member States, standing at around 67% released for consumption, less than 30% of plastic waste is sent for recycling [4]. This means that 95% of the economic value of plastic packaging (between 70 and 105 billion euro at year) is lost after a very short lifecycle [5].

In such a context, the development of sustainable materials in the packaging sector, deriving from renewable resources, has received increasing attention as well as becoming a growing need, thus promoting an alternative use of natural resources with the aim of reducing landfill disposal problems [6]. Unlike synthetic polymers, biodegradable polymers (like cellulose, polysaccharides, proteins, etc.) are derived from the use of renewable raw materials (biomass in general, etc.), and as they can undergo physical, chemical, thermal or biological decomposition, they are therefore potentially suitable for inclusion in a composting process, both at a domestic scale and in specific plants [7]. Accordingly, this paper illustrates an innovative sustainable material made of straw and bioplastic, named NeoPalea, the related production process, the tests carried out for a preliminary characterization, and the results obtained. This information is used to discuss the potential of the material as an alternative to the production of tertiary packaging.

The content of the paper is organized as follows. Section 2 introduces the rationale behind the research and the related objectives. Section 3 describes NeoPalea and provides an overview of the production process. Section 4 introduces the tests conducted for the preliminary characterization of the new material, while the obtained results are presented in Sect. 5. Eventually, Sect. 6 discusses the outcomes and presents the conclusion.

## 2 Motivations Behind the Research and Specific Objectives

The most widespread paradigms to reduce the environmental impact of waste rely on the recycling of materials. However, in reference to plastics, it is necessary to specify that:

- The materials are not always recyclable.
- Transformations of materials in industrial processes might impact on recyclability, by transforming the materials into something not necessarily recyclable.
- The materials cannot be recycled for an infinite number of times.

- Although the recycling of material allows to radically reduce the cost of the environmental impact due to waste, recycling processes have costs that negatively impact on the competitiveness of products into market.
- Recycling processes have an environmental impact themselves.

A potential alternative to recycling is represented by compostable goods, as they could be easily transformed into something else by exploiting a natural disintegration process that is sustainable and eco-friendly by definition. This trend is witnessed also by the European Commission, which is particularly interested in innovative materials that are fully biodegradable and are harmless for the environment and ecosystems. Indeed, the state of art presents several composite materials that comprise straw or other fibrous materials, and binders for producing goods. For instance, in [8] a pulp obtained by the combination of straw with a binder is investigated as solution for manufacturing packaging elements.

Furthermore, several literature contributions fall in the field of patents, where the topics related to biodegradable materials are gaining even more interest for many applications. The patent [9] presents a structural board where a number of layers form hot-pressed straw and isocyanate resin works as binding agent. In [10], a brick tiles made of bamboo and straw is shown, hot-compressed and cooled. Patent [11] deals with a method for producing brick tiles and prefabricated components with stalks of various species, weeds and an adhesive with a base of polyurethane foam. The patent [12] presents blocks constituted by rice straw and isocyanate adhesives for the construction of walls of buildings. In [13], a machine is presented for beating, mixing with additives, laying and pressing fibrous materials to produce building blocks. The binder used is an adhesive or alternatively a cement (mortar, etc.). Eventually, known from the old patent [14] is a heat-shrinking system that comprises a layer of straw for the production of building blocks.

These, and other systems of the same type, present several limits, especially in relation to the production of elements for structural use (as those involved also in the packaging sector). In particular, they suffer from the following critical aspects:

- None of the systems of a known type envisages the production of elements made of exclusively compostable materials.
- The systems of a known type envisage a step of compression of fibrous materials of natural origin, but these processes do not confer to the elements the capacity to support loads. Consequently, the manufactured product has poor structural characteristics.

In such a context, the specific objective of the research was focused on the definition of a structural material fully compostable, which could be adopted for manufacturing a product (or parts of it) in order to substitute the plastics (or other materials) having greater environmental impact.

### 3 NeoPalea

The material here proposed is made of two main components, i.e., cereal straw and bioplastic. Here in the following, it is described together with the motivations that led the authors to consider straw and bioplastic as key components.

#### 3.1 *Straw and Bioplastic: Why?*

Straw is currently considered a waste material of the cereal supply chain, it has little reuse for agronomic or zootechnical needs, and this has led to a contraction of the market, with fluctuating economic prices and modest prospects of convenience in the collection and post-harvest phases. Alternative applications to the agro-zootechnical ones could involve the use of straw as a building material [15] or for energy purposes, to produce/cogenerate heat and electricity or to manufacture biofuels for the transportation sector [16]. However, in both sectors, there is not an effective or consolidated production chain. In Europe, the area cultivated with cereals is about 82 million hectares with an annual cereal production of 480 million tons [17]. Estimating an average productivity coefficient of 3 tons/ha, the amount of straw produced each year is about 2.1 billion tons; this creates a large amount of residues that are sometimes left directly on the field, in order not to become an additional cost for cereal companies. One of the objectives of the research is to valorize a by-product of the cereal sector, transforming it from a waste into a renewable resource in a continuous cycle, available in large quantities and on a broad scale.

Among the bioplastics, those considered for the scope are the natural polymers, meaning those based on polysaccharides, such as starch and cellulose, which are currently the most widely used on the market. They are extracted from renewable agricultural resources (corn, potato, tapioca, rice, sugar cane, etc.) characterized on the basis of the technical report on bioplastics CEN/TR 15392/2010. The 2017 estimates specify 0.82 million ha (0.02% of the world's agricultural area, equivalent to 5 billion ha) of land invested solely for cultivating wood cellulose feedstock for the production of 2.05 million tons of bioplastics [18]. These data demonstrate the lack of competition in exploiting the soil for the production of foodstuffs and the production of bioplastics, despite the market growth anticipated in the next five years [2].

More specifically, among the bioplastic materials available on the market, the choice for prototype development has fallen on Mater-Bi: a biodegradable and compostable bioplastic that complies with EN 13432-2002, produced from corn starch by Novamont S.p.A. and used as a single or multilayer film with variable thicknesses (20–40  $\mu\text{m}$ ). In addition to Mater-Bi, in the last few years other biodegradable materials emerged in the market, which find application in various packaging sectors and could represent potential alternatives for the considered application.

### 3.2 Manufacturing Process

The key feature of the composite material and the related production process lies in the possibility of obtaining precompressed products, made of straw in a state of compression (between 1 and 13 N/mm<sup>2</sup>), inserted inside closed cells, all contained within a shell. Cells and shells are in a state of tension and made of Mater-Bi (or other biopolymers). The straw, the cells and the shell are configured to maintain a permanent state of coaction, with the fibrous organic material permanently compressed and the bioplastic shell permanently in tension. The composite material maintains the internal tensions, compression and traction, each in one of the component materials. The straw is in the form of stems, neither the fibrous material nor the bioplastics are subjected to treatments with chemical additives during the production phases, and the procedure is carried out without the use of water. All individual components are compostable according to EN 13432 standard.

The product-forming cycle (Fig. 1) begins with a plurality of bundles of straw arranged in parallel with each bundle wrapped in a sheet of Mater-Bi to form elementary cylinders. They are then compressed into a mold by means of a piston. In such a way, the straw spreads the fibers in all directions.

With the fibrous material in a state of compression, the process entails a heating phase up to approximately 80 °C, carried out by high-frequency electromagnetic radiation generators. They are arranged to obtain a uniform diffusion of the electromagnetic waves inside the mass of material contained in the mold. The heating phase takes place in such a way that the temperature reached is sufficient to make the bioplastic material melt but without altering the physical/mechanical characteristics of the fibrous organic material. At the end of the heating phase, by maintaining the piston in the final position reached, and therefore with the fibrous material in a compression condition, a forced cooling or spontaneous cooling step is performed until solidification of the bioplastic material and subsequent extraction of the finished product.

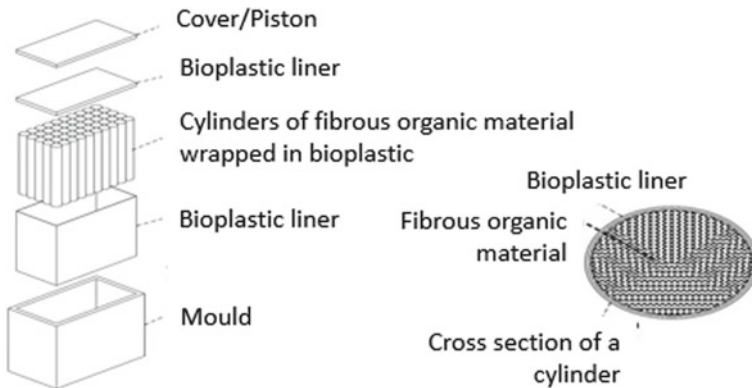
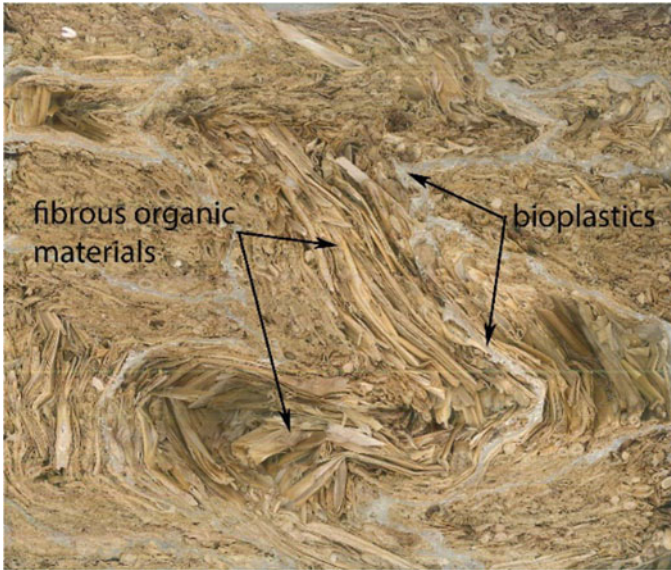


Fig. 1 Process for manufacturing a product with the proposed material





**Fig. 2** Cross section of a block prototype. It is possible to observe the particular disposition of the fibrous material and the closed cells of bioplastic material

As regards the mold preparation, this should be with a shape and size corresponding to the desired shape and size of the finished product and it must be made of a permeable material that is non-reactive to microwaves. The mold should also be of the removable type, in order to facilitate the extraction of the finished product.

As illustrative application of the process described above, a block prototype was manufactured (Fig. 2), which has an extended alveolar structure inside. It consists of a three-directional reticulum of Mater-Bi formed by a set of closed cells connected one to the other and to the external shell, in which the bioplastic material constituting the outer shell and the walls of the cells adhere to the adjacent fibrous material.

Therefore, at the end of the molding process, the straw consists of fibrous stems without any single preferential orientation but instead arranged in all directions. Advantageously, the lack of a preferred direction confers cutting resistance to the product in all directions. It is worth noting that the material lends itself to being adapted to various uses, not only packaging (see Sect. 6).

## 4 Characterization of the New Material

In reference to what stated in Sect. 2, some tests have been conducted to verify the properties/features that the authors deemed useful for several applications, especially in the packaging sector:

- Manufacturability of different shapes: verification of the usability of the material for producing products with different shapes.
- Mechanical characterization: verification of the mechanical behavior under compression and deflection loads.
- Compostability: preliminary evaluation of the compostability properties.

The objective of the manufacturability test was focused on the verification of the material's capability to fill the mold according to different shapes. The test has been performed by producing three prototypes through the process described in the previous section. The considered geometries were defined according to the applications the material could have in the field of packaging, i.e., panels and elements having circular or angular shapes.

The mechanical characterization was performed to find out the elastic modulus of the compressed material. Four parallelepiped-shaped specimens with a square base measuring  $160 \times 160$  mm and 100 mm high, and a density of about  $150 \text{ kg/m}^3$ , were manufactured through the process described in Sect. 3. They were subjected to compression, with loading conditions in the elastic field in the same direction as they were pressed during the production phase. The loading procedure consisted of the application of increasing weights until reaching the total load of about 40 kPa, with the test repeated three times for each specimen.

A second preliminary mechanical characterization was performed to determine the static elastic deflection modulus. Three thin square specimens,  $160 \times 160$  mm in size and 40 mm in height, and density of about  $148 \text{ kg/m}^3$ , were subjected to deflection with a single central load in the elastic range, in a perpendicular direction to that of the pressing during production. The specimens were placed on two movable supports to guarantee the isostaticity of the configuration at a fixed distance. They were loaded into the center by means of a rocker arm, with weights increasing gradually, up to a maximum load of 76 kPa.

Both the elastic moduli have been obtained by applying the standard definitions available in literature [19] to the experimental data.

Eventually, the compostability of the material has been verified through the bio-oxidation process operated by the aerobic microorganisms present in the *Eisenia foetida*, i.e., the earthworm, which is gaining even more interest especially for in house composting practices. Indeed, as acknowledged in literature [20], such a process has lower costs, does not require mechanical systems to turn over the material, requires lesser human involvement, lesser time, and provides a final product, i.e., the vermicompost, that is odorless, stabilized, nutritious and abundant of enzymes and phytohormones.

## 5 Results

Figure 3 shows the prototypes obtained by the manufacturability tests conducted on the three different shapes selected for the proof. During the production process of



**Fig. 3** Two different prototypes: angular element (a) and panel (b). The material had performed properly, according to the shape of the mold

the prototypes, the required energy resources were those foreseen by the process model without significant variations depending on the manufactured shapes. As it is possible to observe, the shapes have been obtained with a satisfactory performance, in reference to the capability of the material to fill the mold, without internal voids and preserving the internal structure of the material described in Sect. 3.

The results of the compression tests have demonstrated that the first load cycle entails a settling of the material, whereas the second and third cycles show an almost total recovery of the deformation and a much higher elastic modulus than that of the first test. The elastic moduli are almost homogeneous, with an average value of around  $2 \text{ N/mm}^2$  (1.93). The three specimens subjected to static deflection showed an elastic modulus similar to that of the compressed specimens. The elasticity is different in the two directions of the plane with a ratio of between 1.45 and 2.19. The maximum elastic modulus is  $7 \text{ N/mm}^2$ , the minimum  $1.2 \text{ N/mm}^2$ , with high variability. Within the same test, the ratio between the best elastic modulus obtained in one direction and the other in the perpendicular direction is between 1.5 and more than 2. The variability in general and a sort of anisotropy of each specimen could depend on the lack of uniformity in the arrangement of straw and bioplastics.

Eventually, Fig. 4 shows the results of the vermicomposting process, verified after 10 and 70 days, respectively; both the colonies provided the same outputs. As it is possible to observe, although it was just a preliminary test, the outcomes are encouraging since the material after 70 days has been digested almost totally (Table 1).



**Fig. 4** Outcomes of the vermicomposting tests: **a** result after 10 days and **b** after 70 days

**Table 1** Summary of the mechanical characterization tests

E	Measuring unit	1	2	3	4
E1–1st cycle	N/mm <sup>2</sup>	1.11	1.08	0.93	0.97
E2–2nd cycle	N/mm <sup>2</sup>	1.80	2.10	1.92	1.96
E3–3rd cycle	N/mm <sup>2</sup>	1.68	2.10	1.90	1.98
Mean E2-3	N/mm <sup>2</sup>	1.74	2.10	1.91	1.97
MoE	Measuring unit	1	2	3	Average
Best	N/mm <sup>2</sup>	2.54	7.04	1.90	3.83
Worst	N/mm <sup>2</sup>	1.75	3.21	1.20	2.06
Best/Worst	–	1.45	2.19	1.57	1.40

## 6 Discussion and Conclusion

In reference to the state of the art presented in Sect. 2, NeoPalea has a density similar to the material [8], but it presents better structural performance. Indeed, the precompressed state generated through the manufacturing process allows to obtain an improved stiffness. Furthermore, NeoPalea presents mechanical characteristics that outperform those of EPS, although the density of the latter is five times lesser. However, by acting on the pressure parameter during the production process, the density of the material can be managed to obtain a good compromise between the weight of the final product and the required mechanical characteristics. Therefore, the characterization of the relationships among pressure, density and mechanical characteristics of the final product becomes a crucial investigation activity to gain knowledge to design packaging made of NeoPalea. In addition, as the material is a composite material, its mechanical behavior strongly depends also on the spatial orientation/disposition of matrix and organic fibers, which thus become important design parameters to be investigated, still preserving the manufacturability of packaging through the process described in Sect. 3. Therefore, the mechanical characterization of NeoPalea is a strategic research activity for its industrialization in order to

develop models to assist the design process of packaging for instance through virtual prototyping techniques specifically dedicated.

Eventually both tests, one related to the manufacturability of different shapes and the other one referred to vermicomposting, have produced encouraging results.

NeoPalea, as well as its production process, manages to perfectly reconcile the strategy that facilitates the achievement of the European goals. This material, in addition to the use of a waste product from an agricultural supply chain, does not undergo any treatment with degrading chemicals during the production process, and the use of water is virtually excluded throughout the entire process. The material produced, after being placed on the market and terminating its function, has a highly sustainable end-of-life expectancy as, for instance, it can be converted into compost.

Although this research has focused on the technological aspects characterizing the prototypes made in the laboratory, it is necessary to continue the characterization of NeoPalea to identify future applications, in contexts different from the packaging sector. Use is also desirable in the furnishing sector, for instance, in disposable/composite exhibition installations, in the production of food crate (fruit and fish), as structural building materials biobased, and in the manufacturing of artifacts that are currently made of plastic materials. Moreover, a further step forward in the research is the determination of the environmental performance of the material and its entire industrial process.

Eventually, tests will be conducted using fibers different from straw but always identifiable as waste of other supply chains. Examples are the use of swamp reeds from the cleaning out of canals and ditches, the use of urban pruning discards and the use of marine plants (like the “*Posidonia Oceanica*” which represents a waste for several seaside countries). The advantage of being able to pack organic material together with thermo-melting biopolymers will surely provide applications with wide margins of flexibility in terms of organic materials to be used.

## References

1. Weale, A., Pridham, G., Cini, M., Porter, Dimitrios Konstadakopoulos, M., Flynn, B.: Packaging and packaging waste. In: Environmental Governance in Europe: An Ever Closer Ecological Union. <https://doi.org/10.1093/acprof> (2010)
2. E.V., E.B.: BIOPLASTICS facts and figures (2018)
3. Dahlbo, H., Poliakova, V., Mylläri, V., Sahimaa, O., Anderson, R.: Recycling potential of post-consumer plastic packaging waste in Finland. *Waste Manage.* (2018). <https://doi.org/10.1016/j.wasman.2017.10.033>
4. Rigamonti, L., Ferreira, S., Grosso, M., Marques, R.C.: Economic-financial analysis of the Italian packaging waste management system from a local authority’s perspective. *J. Clean. Prod.* **87**, 533–541 (2015). <https://doi.org/10.1016/j.jclepro.2014.10.069>
5. Ellen MacArthur Foundation: The new plastics economy: rethinking the future of plastics. Ellen MacArthur Found. <https://doi.org/10.1103/Physrevb.74.035409> (2016)
6. Babalis, A., Ntintakis, I., Chaidas, D., Makris, A.: Design and development of innovative packaging for agricultural products. *Procedia Technol.* **8**, 575–579 (2013). <https://doi.org/10.1016/j.protcy.2013.11.082>

7. Meeks, D., Hottle, T., Bilec, M.M., Landis, A.E.: Compostable biopolymer use in the real world: Stakeholder interviews to better understand the motivations and realities of use and disposal in the US. *Resour. Conserv. Recycl.* **105**, 134–142 (2015). <https://doi.org/10.1016/j.resconrec.2015.10.022>
8. Curling, S.F., Laffin, N., Davies, G.M., Ormondroyd, G.A., Elias, R.M.: Feasibility of using straw in a strong, thin, pulp moulded packaging material. *Ind. Crops Prod.* **97**, 395–400 (2017)
9. Shezhang, G.: Oriented structural straw board and preparation method. China patent CN 103448107A, 3 Dec 2013
10. Yongli, G., Haitao, L., Shuheng, L., Jingwen, S., Shiwen, S., Qisheng, Z.: Bamboo scrimber straw brick, bamboo laminated wood straw brick and preparing method thereof. China patent CN 103538138A, 29 Jan 2014
11. Kelin, M.: Method for producing bricks and prefabricated parts used for building by utilizing weeds and crop straw. China patent CN 102328336A, 25 Jan 2012
12. Ruskey, J.A.: Culm blocks. United States patent US 6951080B2, 4 April 2005
13. Eagan, S.A., Eagan T.G.: Process and apparatus for forming a building block. United States patent US 5507988A, 16 April 1996
14. Charriere, J.J.: Composite article comprising a central core wrapped in a cover, and its uses. European Patent EP 0345125A1, 6 Dec 1989
15. Pritchard, M.B., Pitts, A.: Evaluation of strawbale building: Benefits and risks. *Archit. Sci. Rev.* (2006). <https://doi.org/10.3763/asre.2006.4949>
16. Cherubini, F., Ulgiati, S.: Crop residues as raw materials for biorefinery systems—A LCA case study. *Appl. Energy* (2010). <https://doi.org/10.1016/j.apenergy.2009.08.024>
17. FAO: FAO Cereal Supply and Demand Brief. Food and Agriculture Organization of the United Nations (FAO) (2017)
18. Brodin, M., Vallejos, M., Opedal, M.T., Area, M.C., Chinga-Carrasco, G.: Lignocellulosics as sustainable resources for production of bioplastics—a review. *J. Clean. Prod.* (2018). <https://doi.org/10.1016/j.jclepro.2017.05.209>
19. Hartsuijker, C., Welleman, J.: *Engineering Mechanics*, vol. 2. Springer, Berlin (2001). ISBN 978-1-4020-4123-5
20. Masciandaro, G., Bianchi, V., Macci, C., Peruzzi, E., Doni, S., Ceccanti, B., Iannelli, T.: Ecological and agronomical perspectives of vermicompost utilization in Mediterranean Agro-ecosystems. *Dyn. Soil Dyn. Plant* **4**, 76–82 (2010)

# Using FFF and Topology Optimisation to Increase Crushing Strength in Equestrian Helmets



Shwe Soe, Michael Robinson, Khaled Giasin, Rhosslyn Adams,  
Tony Palkowski, and Peter Theobald

**Abstract** International standards ensure that equestrian helmets achieve high performance. Recently, one such standard (PAS 015) was revised to include a lateral deformation requirement, ensuring helmets can withstand the potential crushing forces associated with equestrian. This increased performance needs to be achieved against a minimal mass penalty, which is an important consumer consideration. This paper explores how shell design optimisation can improve crush resistance, validated using additive manufacturing and mechanical testing. This approach achieved a 73% increase in crush force, for only an 11% mass increase.

## 1 Introduction

Helmet design has remained relatively static since the 1970s [1], broadly consisting of a foam liner, polymer shell and comfort foam. The foam liner is the main energy absorbing component, separated from the head by a layer of comfort foam. The polymer shell distributes load to the underlying liner. Both the shell and the liner contribute to crushing strength, an important test within equestrian to protect again a horse rolling on a rider.

---

The original version of this chapter was revised: The author's name has been updated from "Khaled Gaisin" to "Khaled Giasin". The correction to this chapter is available at [https://doi.org/10.1007/978-981-15-8131-1\\_50](https://doi.org/10.1007/978-981-15-8131-1_50)

---

S. Soe · M. Robinson (✉) · K. Giasin · R. Adams · P. Theobald  
Cardiff University, Cardiff CF243AA, UK  
e-mail: [RobinsonM12@cardiff.ac.uk](mailto:RobinsonM12@cardiff.ac.uk)

S. Soe  
University of the West of England, Bristol, UK

K. Giasin  
University of Portsmouth, Portsmouth, UK

T. Palkowski  
Champion Manufacturing, Cardiff, UK

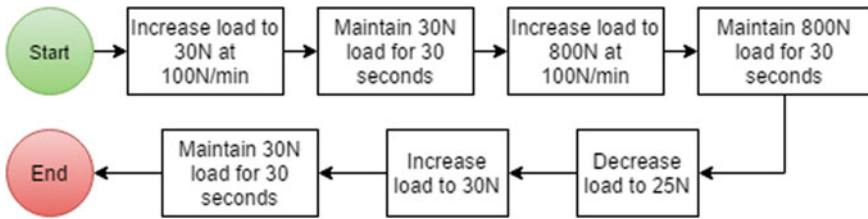


Fig. 1 PAS 015 lateral deformation (crushing) test protocol

The helmet sector is now fast-evolving, driven by an increased public awareness of head health that is encouraging manufacturers to produce new designs and features that offer enhanced protection [2, 3]. In equestrianism, the Publicly Available Specification (PAS) PAS015:2011 [4] has recently been updated to include enhanced crushing performance (Fig. 1), which creates new design challenges and commercial opportunities.

This study aims to achieve this increased crush resistance by evolving the existing shell design, at minimal mass penalty.

## 2 Materials and Methods

### 2.1 Existing Baseline Helmet

An existing injection moulded equestrian helmet shell was mechanically assessed to establish baseline performance, independent of other components. Two flat platens were used to achieve 30 mm helmet shell deflection (Fig. 2).

Additionally, this baseline shell was evaluated (S-Scan Ltd; Materialise) to determine the internal and external geometry and, thus, the wall thickness (~2–2.5 mm)

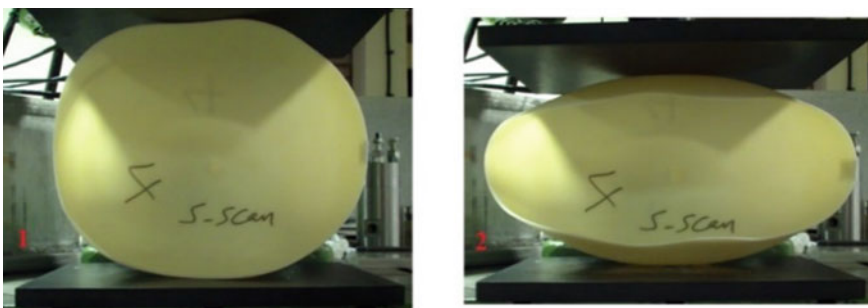


Fig. 2 Exemplar lateral deformation of the helmet shell



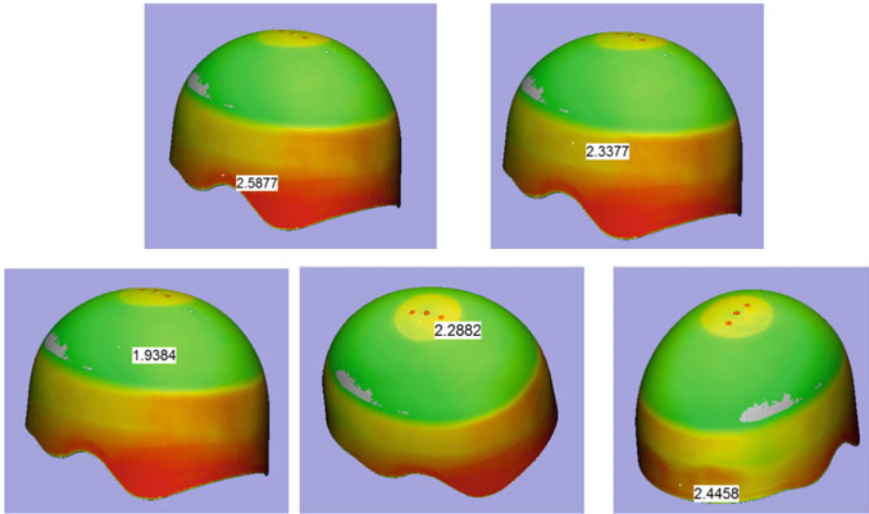


Fig. 3 Localised shell wall thickness

(Fig. 3). This scanned data was subsequently used to generate CAD geometry, for topology optimisation and additive manufacturing.

### 2.2 ABS Modelling

An ABS constitutive model was developed to enable computational analysis. The moulded baseline shell was manufactured from PA-709 (CHIMEI), with raw quasi-static tensile testing data used to capture the elasto-plastic behaviour and to develop the ABS material model within Abaqus.

Computational analysis of the shell geometry revealed that modelling stress-softening behaviour (Fig. 4a) resulted in comparable performance to perfectly elasto-

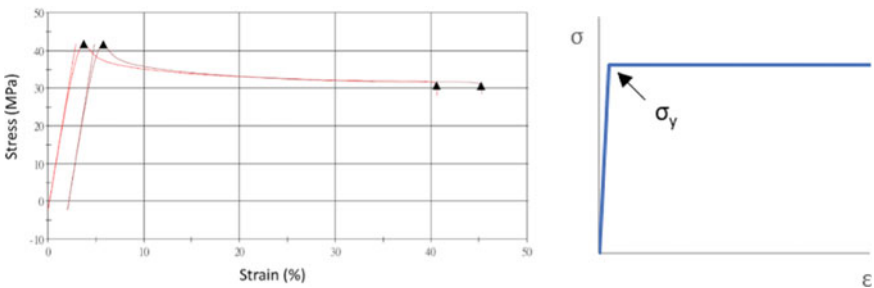


Fig. 4 ABS material. a Tensile testing data, b elasto-plastic material model

**Table 1** Properties extracted from diagram and general ABS properties, used in following simulation

Mass density	Young's modulus	Yield failure stress	Poisson's ratio
1 g/cm <sup>3</sup>	2.6 GPa	40 MPa	0.4

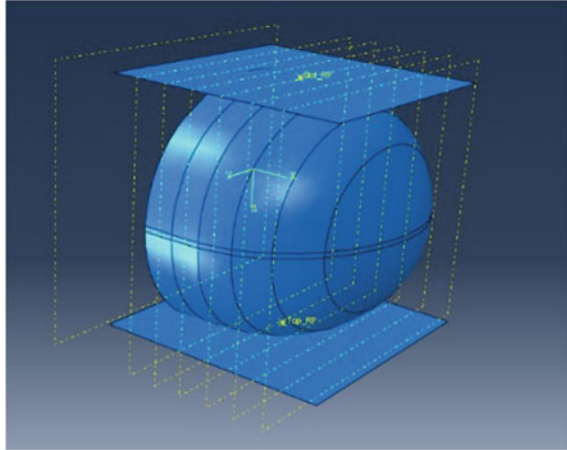
plastic behaviour (Fig. 4b). This is likely due to the relatively low internal strains experienced by the deforming shell, resulting in minimal plastic deformation; hence, to reduce computational expense, a simplified perfectly elasto-plastic model was used in the following work (Table 1).

### 2.3 Topological Optimisation

Major challenges are faced when increasing helmet stiffness, given the need for minimal mass whilst retaining the intrinsic shell geometry. One of the main tasks was to identify the precise shell region to be thickened, such that the overall stiffness could be increased with minimal additional material. Two structural optimisation approaches were considered to achieve this aim: parametric optimisation (PO) and topology optimisation (TO). PO required the helmet shell to be manually 'split' into several distinct regions, from crown to edge. Each region was then incrementally assigned minimum to maximum thickness, whilst other regions remain constant. Whilst this approach provided a clear understanding of each change, the number of iterations was computationally expensive. By comparison, TO is a faster and more effective route for structural optimisation. This study utilised the TO options within the Abaqus FEA solver, specifically the sizing optimisation, to optimise shell thickness [5, 6].

Sizing optimisation starts with a finite element model generated by topology optimisation. The first sizing optimisation step was to split the shell model into six equally spaced regions, from crown to edge. This allowed the whole shell to be selected as a design area, where the design variables (thickness of each region) could be assigned with minimum (0.5 mm) to maximum thickness (3 mm). The design responses (strain energy and weight) were assigned as inputs for this optimisation study. Objective functions were used to define the optimisation, with reduction of strain energy to yield maximum stiffness. A design constraint was also imposed, to control the weight limit. The remaining set-up included a parallel set of upper and lower rigid plates, with the shell geometry sandwiched between them. The bottom plate was fixed in place, and the top plate was deflected 30 mm towards it, to replicate the axial compression observed during mechanical testing. A fine quadrilateral mesh was applied to the shell, and a surface-to-surface contact was specified. A maximum of 25 design cycles was then set to achieve a converged solution (Fig. 5).

**Fig. 5** FEA topology optimisation modelling in Abaqus software: the shell is split into sections



## 2.4 ABS Validation Using Additive Manufacturing

In addition to a full-size shell (used for topology optimisation and final validation), a half-scale shell was also produced. This step was taken to improve confidence in the computational analysis; as the full-size shell encountered manufacturing issues that could affect the validation process.

Fused filament fabrication (FFF) AM ABS material performance was validated against the moulded ABS grade, using a half-scale (MakerBot) shell and then a full-scale (Leapfrog) validation derived from the above CAD data. This shell was selectively thickened to produce digital models for additive manufacture, with two separate constant thicknesses assigned to the crown and sides of the helmet. For scaled validation, these two thicknesses formed the entirety of the helmet, resulting in a distinct ridge. For full-size manufacture, a region was assigned between the crown and sides, allowing for a smooth transition between the two thicknesses.

The validation simulation for both scaled and full-size helmets was performed using solid continuum elements. Mechanical testing was performed as per PAS015:2011 (Fig. 6). For the full-size shell, this was performed to 30 mm, whilst the deformation was halved (15 mm) for the scaled shells.

The scaled shell was simplified to ease printing, by flattening the lower edge of the shell (Fig. 7). By scaling and simplifying this shell, most of the issues that arise during FFF printing were eliminated, allowing for a side-by-side comparison between mechanical testing and simulation.

Whilst support structures were used during the manufacture of the full-size helmet shell, due to its scale cracks and minor inter-layer failures occurred, highlighting overhang issues. Cyanoacrylate was selectively applied to ensure these did not cause premature shell failure.

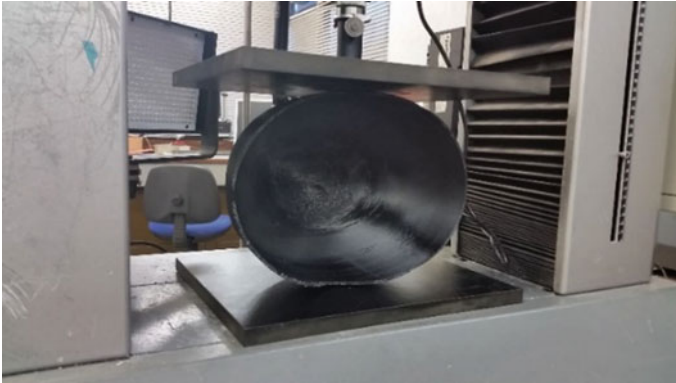


**Fig. 6** PAS015:2011 compression testing of full-scale ABS AM shell



**Fig. 7** Successfully printed scaled models: 2 mm overall thickness (left) and 4 mm edge thickened (right)

### 3 Results and Discussion

#### 3.1 Topological Optimisation

Topological optimisation results are presented in Fig. 8, demonstrating the varying target levels of force and displacement.

Examining Fig. 8, a clear trend of increased thickness around the base of the shell and lower thickness at the crown of the shell can be observed. It was found that the crown region required a minimum thickness of 0.5 mm to remain effective, whilst the edge region consistently increased to the maximum 3 mm thickness.

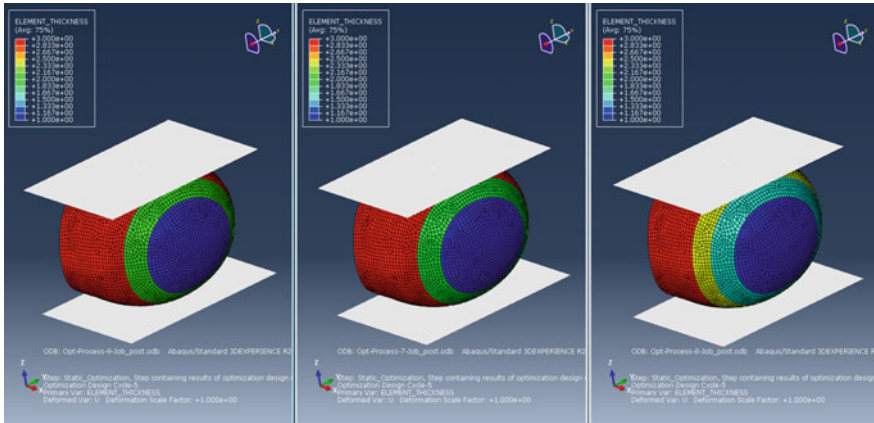


**Fig. 8** Optimised shell results when compressed to 20 mm or 150 N, 16 mm or 100 N, 10 mm or 50 N respectively

### 3.2 AM ABS Validation

Shell optimisation for crushing strength can be achieved by increasing shell side thickness and decreasing crown region thickness (Sect. 3.1). Whilst this would optimise the shell for crushing strength, there are secondary implications from reducing the thickness of the crown region (e.g. penetration resistance reduction, load distribution from impacts, etc.). Therefore, the 2 mm crown thickness of the moulded ABS shell was adopted as the crown thickness, to ensure compliance with secondary requirements (e.g. penetration resistance).

For the scaled shells, a 2 mm constant thickness was investigated, plus a combination of a 2 mm crown thickness of and a 4 mm edge thickness. For the full-size shell, the crown thickness was set to 2 mm, the edge thickness was set to 3 mm, and the transition region switched linearly between the two thicknesses.

#### Scale-Model Validation

The mechanical and computational compression of the scaled shells is shown in Fig. 9.

Doubling the rim thickness increased the shell’s compressive stiffness, with the force required to achieve a 30 mm deflection increasing from 133 to 563 N. High agreement is evident between FEA and experimental results for both simulation, with the constant thickness model reporting an ~8.9% difference in peak load, whilst only a 1.4% difference when comparing data for the thickened shell. This provided justification that FFF was appropriate for producing a full-size helmet shell.

#### Full-Size Helmet Shell

The results of the computational and mechanical compression of the full-size helmet shell are presented in Fig. 10.

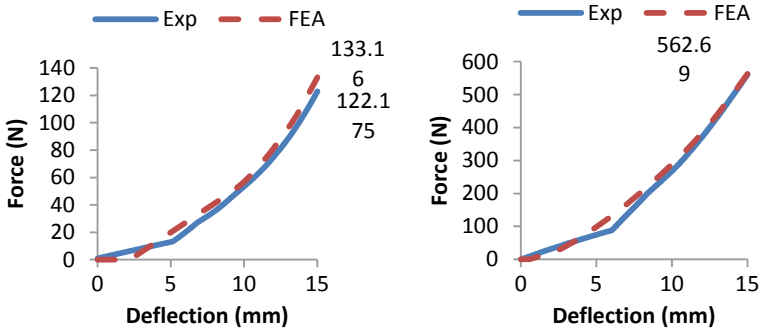


Fig. 9 FEA and experimental results of scaled shells. a 2 mm constant, b 4 mm edge thickened

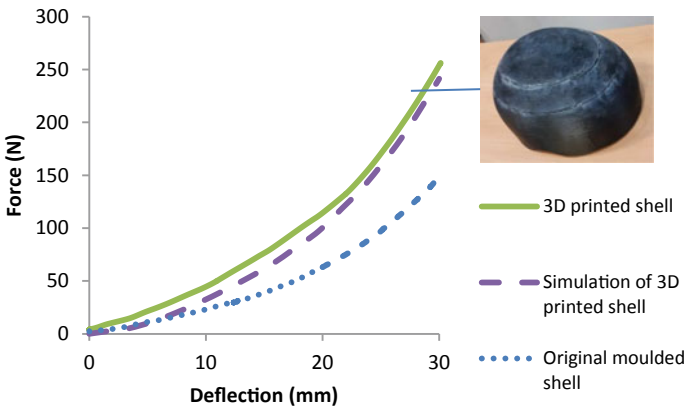


Fig. 10 Full-scale shell and simulated validation

Examining Fig. 10, the simulated and mechanical testing of the 3D printed shell are in good agreement. Whilst the simulation initially underpredicts the mechanical testing, the two curves begin to align with increased deflection, with a minor (6.2%) difference in peak stress.

The optimised shell is significantly stiffer (+73% peak compressive force) when comparing its mechanical response to that of the original moulded shell, whilst incurring only an 11% mass penalty. The cyanoacrylate could potentially affect the performance of the helmet, although the close correlation between simulated and mechanical compression indicates that this increase is driven by shell stiffness alteration.

## 4 Conclusion

This study has investigated the potential to achieve a significant increase in peak compressive force (73%), with only a modest mass penalty (11%). This serves as a platform for future work, highlighting a potential region for efficient reinforcement.

**Acknowledgements** The authors would like to acknowledge ASTUTE 2020 (Advanced Sustainable Manufacturing Technologies) operation part-funded by the European Regional Development Fund (ERDF) through the Welsh Government. This project was run in collaboration with Champion manufacturing and DB mouldings.

## References

1. Fernandes, F., De Sousa, R.A.: Motorcycle helmets—a state of the art review. *Accid. Anal. Prev.* **56**, 1–21 (2013)
2. Omalu, B.I., et al.: Chronic traumatic encephalopathy in a National Football League player. *Neurosurgery* **57**(1), 128–134 (2005) (discussion 128–134)
3. Omalu, B.I., et al.: Chronic traumatic encephalopathy in a national football league player: part II. *Neurosurgery* **59**(5), 1086–1093 (2006)
4. BSI, PAS015:2011: Helmets for equestrian use, in British Standards Institution, London, BSI (2011)
5. Svanberg, K.: The method of moving asymptotes—a new method for structural optimisation. *Int. J. Numer. Meth. Eng.* **24**(2), 359–373 (1987)
6. Assistance, S.U.: Abaqus Optimisation Techniques (2019)

# Polish Public Transport Fire Safety Study



R. Dobrzyńska 

**Abstract** An increase in the number of passenger cars on Polish roads causes, among others, traffic difficulties, increased noise level and atmospheric air pollution. The solution to these problems may be an increase of public transport in the share of the passenger transport. Factors that can affect the decision to opt out of passenger cars for public transport may be economic, environmental, but they also include greater safety, including fire safety. Statistical data indicate that fires of passenger cars in Poland constitute over 80% of the number of fires of all means of transport, while fires of means of public transport constitute approx. 3%. Fire safety of means of transport depends largely on the properties of combustible materials constituting structural elements and furnishing. Requirements and criteria for material assessment are specified in standards and legal acts. They depend on the type of transport. So there are different requirements for coaches and different ones for trains or passenger ships. Findings of flammability tests of public transport furnishing indicate that not all materials can meet the requirements of fire safety regulations and incorrectly selected may pose a threat to the health and life of people in the vehicle.

## 1 Introduction

Statistical data indicate that fires of means of transport, the number of which is increasing year by year, are a large problem in Poland. Table 1 shows the number of fires in Poland in the years 2010–2019 which took place in individual types of transport means intended for transporting people. It should be noted that fires of passenger cars constitute the largest share—about 80% in the number of fires of transport means [1].

The high number of fires of passenger cars suggests an increase of the share of public transport in passenger transport. Planes and means of water transport are among the safest means from the point of view of fire safety. However, the selection

---

R. Dobrzyńska (✉)

Faculty of Maritime Technology and Transport, West Pomeranian University of Technology in Szczecin, al. Piastów 41, 71-065 Szczecin, Poland  
e-mail: [renata.dobrzynska@zut.edu.pl](mailto:renata.dobrzynska@zut.edu.pl)

© The Editor(s) (if applicable) and The Author(s), under exclusive license to Springer Nature Singapore Pte Ltd. 2021

S. G. Scholz et al. (eds.), *Sustainable Design and Manufacturing 2020*, Smart Innovation, Systems and Technologies 200, [https://doi.org/10.1007/978-981-15-8131-1\\_34](https://doi.org/10.1007/978-981-15-8131-1_34)



**Table 1** Number of fires in Poland in the years 2010–2019 in transport means intended for transporting people

	Types of transport means	Year											
		2010	2011	2012	2013	2014	2015	2016	2017	2018	2019		
		The number of fires											
Road	Motorcycles	81	88	86	100	119	105	109	113	146	133		
	Coaches, trolley buses	240	207	219	191	182	178	165	177	181	189		
	Passenger cars, car trailers	7072	6938	6726	6337	6796	6980	7525	7904	8500	8338		
Railway	Passenger trains	66	55	41	26	31	26	28	24	27	27		
Aircraft	Passenger planes	0	0	0	0	2	0	0	0	1	1		
	Tourist, agricultural, sports and sanitary aircraft, including helicopters, gliders, hang-gliders	2	3	2	2	2	2	4	3	4	1		
Marine	Passenger ships, ferries	3	0	0	1	0	1	2	0	0	12		
Inland sailing	Yachts, fishing boats, cutters	11	10	17	13	6	4	10	9	12	5		
	Passenger ships, ferries	0	2	0	0	0	1	0	0	0	0		
	Yachts, sailboats, boats	8	3	13	10	9	9	10	8	11	17		
Others	Trams	30	22	24	15	13	18	9	15	14	18		
	Metro	–	0	0	1	2	0	1	0	0	1		

of the appropriate means of public transport depends on a lot of factors, including its availability, length of the route, necessary changes, travel costs, etc. Therefore, buses and trains are used most often.

The bus fire is very dynamic. Most often, it ends with a complete burning down of the vehicle. An example may be the coach fire which burnt down completely on 9 October 2018 in the region of Dobrojewo. Fifty-five children and five carers were travelling on the coach. The coach driver, after noticing the smoke coming out of the engine compartment, stopped the vehicle and ordered an evacuation. Then he tried to put out the fire with his own fire extinguisher but the flames were too large to be extinguished. When fire engines arrived, most of the bus was already in flames. The fire also moved to the part of the forest where the bus stood. Fortunately, the firefighters put out the fire [2].

Fires of passenger trains are usually not so dramatic. In recent years in Poland, the so-called small fires were the most often, the flames were put out with fire extinguishers, the wagons were equipped with, and there were no fatalities.

## **2 Requirements Regarding the Combustion Properties of Interior Furnishing Materials Used in Public Transport**

Fire safety of means of transport depends largely on the combustion properties of materials constituting structural elements and furnishing. These properties include, inter alia: ignitability, smoke formation, toxicity of thermal decomposition products and burning of these materials, intensity of heat release, rate of flame spread on the material surface. Both the course of the fire and the safety of people in the burning vehicle depend on these characteristics of materials. There are materials available in the market that can slow down the course of fire or can cause its growth, posing a direct threat to people's health and life.

In Poland, the criteria for the selection of structural and furnishing materials are specified in the relevant regulations. The requirements for materials in terms of fire safety are already known at the design stage. These requirements depend on the means of public transport, the material to be used, and its function. So there are different requirements for materials used on ships, and different for products intended for passenger trains or coaches. There are different combustion properties for structural materials, and different for finishing and furnishing materials.

In the case of ships or other objects located at sea, the requirements for materials used on them are determined, inter alia, by the International Convention for the Safety of Life at Sea SOLAS [3] and Directive 2014/90/EU of the European Parliament and of the Council [4], abbreviated as MED Directive, which applies to marine equipment listed in Appendix A1 of Directive 2015/559 [5], installed on new or existing conventional ships flying the flag of a Member State of the European Union, when this equipment is first placed or replaced with a new one. Requirements of these

documents for equipment materials used on ships along with research methods and assessment criteria are presented in Table 2. The research methods and assessment

**Table 2** Requirements for equipment materials used on ships along with research methods and assessment criteria

Type material	Test methods	Criteria
1.	IMO Res. MSC.307(88)-(2010 FTP Code), Annex 1, Part 2	Toxicity: The average value of the maximum value of the gas concentration measured at each test shall not exceed the following limits: CO—1450 ppm, HCl—600 ppm, HF—600 ppm, NO <sub>x</sub> —350 ppm, HBr—600 ppm, HCN—140 ppm, SO <sub>2</sub> —120 ppm (200 ppm for floor coverings)  Smoke: An average ( $D_m$ ) of the maximum specific optical density of smoke ( $D_s \max$ ) of three tests: $D_m < 200$ for materials used as surface of bulkheads, linings or ceilings; $D_m < 400$ for materials used as primary deck coverings; $D_m < 500$ for materials used as floor coverings; $D_m < 400$ for plastic pipes
	IMO Res. MSC.307(88)-(2010 FTP Code), Annex 1, Part 5	Floor coverings; CFE $\geq 7 \text{ kW/m}^2$ , $Q_{sb} \geq 0,25 \text{ MJ/m}^2$ , $Q_p \leq 10 \text{ kW}$ , $Q_t \leq 2 \text{ MJ}$  Bulkhead, wall and ceiling linings: CFE $\geq 20 \text{ kW/m}^2$ , $Q_{sb} \geq 1.5 \text{ MJ/m}^2$ , $Q_p \leq 4 \text{ kW}$ , $Q_t \leq 0.7 \text{ MJ}$
	ISO 1716	Maximum gross calorific value shall not exceed $45 \text{ MJ/m}^2$
2.	IMO Res. MSC.307(88)-(2010 FTP Code), Annex 1, Part 7	An after-flame time greater than 5 s for any of the 10 or more specimens; burn through, to any edge; ignition of cotton wool below the specimen; an average char length in excess of 150 mm; observed in any specimens tested by either surface or edge ignition; and the occurrence of a surface flash propagating more than 100 mm from the point of ignition with or without charring of the base fabric
3.	IMO Res. MSC.307(88)-(2010 FTP Code), Annex 1, Part 8	Progressive smouldering or flaming of the upholstery components any time within 1 h of the placement of the cigarette; flames, afterglow; smoking or smouldering for more than 120 s of the removal of the burner tube

(continued)

**Table 2** (continued)

Type material	Test methods	Criteria
4.	IMO Res. MSC.307(88)-(2010 FTP Code), Annex 1, Part 9	Production externally detectable amounts of smoke, heat or glowing after a period of 1 h following the application of the ignition source; escalating combustion behaviour so that it is unsafe to continue the test and requires forcible extinction; smouldering to the extremities of the specimen, to either side or to the full thickness of the specimen; flames, afterglow, smoking or smouldering for more than 120 s of the removal of the burner tube

$D_m$  specific optical density of smoke;  $CFE$  Critical flux at extinguishment;  $Q_{sb}$  Heat for sustained burning;  $Q_p$  Total heat release;  $Q_i$  Peak heat release rate

Type materials: 1. Surface materials and floor coverings with low flamespread characteristics (a) decorative veneers, (b) paint systems, (c) floor coverings, (d) pipe insulation covers, (e) adhesives used in the construction of “A”, “B” & “C” class divisions, (f) combustible ducts membrane; (2) Draperies, curtains, and other suspended textile materials and films; (3) Upholstered furniture; 4. Bedding component

criteria are described in the International Code for Application of Fire Test Procedures (2010 FTP Code) [6].

Requirements for structural and furnishing materials used in the railway industry are specified in PN-EN 45545-2 + A1:2015-12 [7]. It indicates research methods, according to which fire tests should be carried out, and material assessment criteria. Requirements for selected types of furnishing materials for railway wagons are presented in Table 3. These criteria refer to the hazard level, where HL1 means the lowest hazard and HL3 the highest.

The requirements for materials constituting the furnishing for road public transport are rather small in terms of fire safety (Table 4). They are specified in UNECE Regulation No. 118 in Appendices 6–8 [8]. However, they only apply to vehicles of category M<sub>3</sub>, class II and III, i.e. vehicles with a maximum mass exceeding 5 tonnes, transporting more than 22 passengers and not intended for transporting standing passengers and for use in the city (city buses). Conducting tests according to Regulations 118 is mandatory for the purposes of the approval of vehicles of category M<sub>3</sub>, class II and III. For other categories of vehicles used for passenger transport (M<sub>1</sub>, M<sub>2</sub>, M<sub>3</sub> class I), there are no requirements regarding combustion properties of the furnishing materials.

It is worth noting that materials that are used to furnish accommodation and service spaces on ships: hung curtains, drapes, upholstered furniture, mattresses and bedding components must meet only the requirements for resistance to small sources of ignition, such as a burner flame or a cigarette. They are not subjected to testing for the release of toxic combustion products or smoke formation. And these factors mainly determine the threat to the lives of people in the fire zone and

the effectiveness of evacuation. Tests have shown that when burning upholstered systems consisting of polyurethane fabrics and foams, excessive amounts of carbon, hydrogen cyanide and hydrogen chloride monoxides are released, concentrations of which exceed considerably the concentration limits and may cause loss of health and life of people who are in their vicinity during a fire [9–11].

The criteria for selection of materials for the furnishing of passenger trains seem to be the most severe. They include several fire properties of materials, including smoke

**Table 3** Requirements for selected types of furnishing materials for railway wagons

Type material	Requirement	Methods	Parameter and unit	Criteria			
				Maximum or minimum	HL1	HL2	HL3
1.	R1	ISO 5658-2	CFE, kW m <sup>-2</sup>	Min.	20 <sup>a</sup>	20 <sup>a</sup>	20 <sup>a</sup>
		ISO 5660-1: 50 kW m <sup>-2</sup>	MARHE, kW m <sup>-2</sup>	Max.	a	90	60
		EN ISO 5659-2: 50 kW m <sup>-2</sup>	D <sub>s</sub> (4), –	Max.	600	300	150
		EN ISO 5659-2: 50 kW m <sup>-2</sup>	VOF4, min	Max.	1200	600	300
		EN ISO 5659-2: 50 kW m <sup>-2</sup>	CIT <sub>G</sub> , –	Max.	1.2	0.9	0.75
2.	R18	ISO 9705-2	MARHE, kW	Max.	75	50	20
		ISO 9705-2	RHR peak, kW	Max.	350	350	350
3.	R20	EN ISO 12952-2	After burning time s	Max.	10	10	10
		ISO 5660-1: 25 kW m <sup>-2</sup>	MARHE, kW m <sup>-2</sup>	Max.	50	50	50
		EN ISO 5659-2: 25 kW m <sup>-2</sup>	D <sub>s</sub> max., –	Max.	200	200	200
		EN ISO 5659-2: 25 kW m <sup>-2</sup>	CIT <sub>G</sub> , –	Max.	0.75	0.75	0.75
4.	R21	ISO 5660-1: 25 kW m <sup>-2</sup>	MARHE, kW m <sup>-2</sup>	Max.	75	50	50
		EN ISO 5659-2: 25 kW m <sup>-2</sup>	D <sub>s</sub> max., –	Max.	300	300	200

(continued)

**Table 3** (continued)

Type material	Requirement	Methods	Parameter and unit	Criteria			
				Maximum or minimum	HL1	HL2	HL3
		EN ISO 5659-2: 25 kW m <sup>-2</sup>	CIT <sub>G</sub> , –	Max.	1.2	0.9	0.75

*CFE* Critical Flux at Extinguishment; *MARHE* maximum average rate of heat emission; *D<sub>s</sub>(4)* the optical density in the test chamber 4 min into the test multiplied by a factor; *VOF4* cumulative value of specific optical densities in the first 4 min of the test; *CIT<sub>G</sub>* Conventional Index of Toxicity; *RHR* maximum average heat release rate; *D<sub>s</sub> max.* maximum optical density in the test chamber

<sup>a</sup>If flaming droplets/particles are reported during the test ISO 5658-2, or for the special case of materials which do not ignite in ISO 5658-2 and are additionally reported as unclassifiable, the following requirements shall be added: Test to the requirements of EN ISO 11925-2 with 30 s flame application

The acceptance requirements are: flame spread <150 mm within 60 s and no burning droplets/particles

Type materials: 1. Curtains and sunblind in passenger area and staff area, staff compartments

Tables, folding tables downward facing surface; 2. Complete passenger seats; 3. Loose upholstery items for seats, couchettes, and beds; 4. Upholstery for passenger seats and head rest, Armrests for passenger seats, Mattresses

formation and toxicity of combustion products. However, materials that meet the standard requirements do not have to ensure fire safety. Toxicity tests are carried out in a chamber with a defined volume. During the tests, the concentration of gases released during thermal decomposition and burning is measured in the chamber. However, the chamber is an integrator circuit. Toxic fire hazard cannot be determined on the basis of the concentration values measured in the measuring chamber because the measured concentrations do not refer to either the surface or the mass of the material being tested. Therefore, the emission of fumes will be different even for samples with the same composition, but of different thicknesses, and thus of a different mass. The results of such tests are therefore not useful for quantitative assessment of toxic hazards during thermal decomposition and burning of furnishing materials.

The fulfilment of flammability requirements by materials in accordance with UNECE Regulation No. 118 may not guarantee the fire safety of people on the coach. The cause of the fire may have a large impact on the course of the rescue operation. If a fire is due to a technical defect and it is detected quickly enough and the driver stops the vehicle immediately, the passengers will leave the coach safely without any damage to their health. The situation can get complicated if the fire occurs, for example, as a result of falling out of the road, collision with another vehicle or an element of the infrastructure. Passengers due to injuries caused by an accident will not be able to leave the vehicle by themselves. Then, the burning coach will be a deadly trap for them.

**Table 4** Requirements for materials acc. Regulation No. 118

Material	Test method	Measured parameter	Criteria
<p>(a) Material(s) and composite material(s) installed in a horizontal position in the interior compartment; and</p> <p>(b) Insulation material(s) installed in a horizontal position in the engine compartment and any separate heating compartment</p>	Regulation No. 118 Annex 6	Horizontal burning rate $B$	Taking the worst test results into account, $B < 100$ mm/minu or if the flame extinguishes before reaching the last measuring point
<p>(a) Material(s) and composite material(s) installed more than 500 mm above the seat cushion and in the roof of the vehicle</p> <p>(b) Insulation material(s) installed in the engine compartment and any separate heating compartment</p>	Regulation No. 118 Annex 7	Melting behaviour	Taking the worst test results into account, no drop is formed which ignites the cotton wool
<p>(a) Material(s) and composite material(s) installed in a vertical position in the interior compartment</p> <p>(b) Insulation material(s) installed in a vertical position in the engine compartment and any separate heating compartment</p>	Regulation No. 118 Annex 8	Vertical burning rate $V_i$	Taking the worst test results into account $V_i < 100$ mm/min or if the flame extinguishes before the destruction of one of the first marker threads occurred

### 3 Flammability Tests of Interior Furnishing Materials Used in Coaches

Fire statistics indicate that among all means of public transport, the majority of fires occurred on buses. Therefore, materials available in the Polish market, which due to their properties could be useful for the production of coach seats, were selected for testing flammable properties. Seats are the main furnishing of the vehicle. Considering that polyurethane foam and the material of the backrest and seat cover, the main materials included in the coach seat, plastics such as: acrylonitrile butadiene styrene (ABS) copolymer, flame retardant acrylonitrile butadiene styrene (ABS FR) copolymer, polycarbonate/acrylonitrile-butadiene-styrene composite (PC/ABS), polypropylene (PP), flame-retardant polypropylene (PP FR), polyamide 6 (PA6) as well as wood-based MDF board and polyurethane foams (PU1 and PU2) were tested. Plastic samples were 3 mm thick, MDF board 9 mm thick, polyurethane foams 13 mm thick.

Due to trade secrets, the names of products and their composition have been classified. Only the type of material tested is disclosed, whereas, e.g. the sample code: "PU1" means that the sample is a polyurethane foam with a different composition and density than the "PU2" polyurethane foam. During the tests, the fusibility and vertical burning rate of the tested materials were determined. Tests of the horizontal burning rate have been omitted due to the provision of Regulation No. 118 stating that if the materials meet the requirements for vertical burning rate, they also meet the requirements for the horizontal burning rate. The conformity of the flammable properties of the tested materials with the requirements of UNECE Regulation No. 118 determining the possibility of using these materials in the coach as furnishing was assessed on the basis of the obtained test results.

#### 3.1 Testing of Material Fusibility

Material fusibility is an important property that affects the possibility of spreading flames. The resulting falling of drops may ignite other adjacent materials or severely burn people, e.g. when falling onto exposed skin.

The research methodology is specified in Appendix 7 to UNECE Regulation No. 118 [8].

During the tests, it is observed whether there will be precipitation igniting cotton wool. The final result of the test shall be the worst result obtained when testing four material samples. The final results of the fusibility tests of selected materials are presented in Table 5.

Only polypropylene, among the materials tested, does not meet the requirements, and due to fire safety, it cannot be used in coaches.



**Table 5** Final results of the fusibility tests of selected materials

Tested material	ABS	AB FR	PC/ABS	PP	PP FR	PA6	MDF	PU1	PU2
Drop is formed which ignites the cotton wool	No	No	No	Yes	No	No	No	No	No
Meeting the requirements of Annex 7 Regulation No. 118	Yes	Yes	Yes	No	Yes	Yes	Yes	Yes	Yes

### 3.2 *Testing the Vertical Burning Rate of Materials*

The vertical burning rate depends on the burning time of the materials installed vertically. As for the bus, these are mainly seat backrests. From the point of view of fire safety, it would be best if the seats were constructed of self-extinguishing or fire slow-spreading materials.

Tests on the vertical burning rate of materials are carried out in accordance with the procedure described in Appendix 8 to UNECE Regulation No. 118 [8]. During the tests, three times are measured, from the application of the flame to the burning of the next marker threads. On their basis, vertical burning rates of  $V_1$ ,  $V_2$  and  $V_3$  materials are determined. The final result of the test shall be the worst result obtained for one of the three tested samples of the same material type. The final results of the vertical burning rate test of selected materials are presented in Table 6.

Based on the obtained test results, it was found that not all of the tested materials meet the requirements for products constituting coach furnishing. After applying the burner for 15 s, the polypropylene sample was burning quite intensively, but the vertical burning rate was not over 100 mm/min. However, the vertical burning rate of the ABS sample was 205 mm/min. This means that if such material was used for a 70 cm high backrest cover, it would burn out within less than 4 min in actual fire conditions. It is worth noting that such an intensely burning material releases a lot of heat, which may cause thermal decomposition of adjacent materials and accelerate their burning. It can be noticed that the vertical burning rate of the ABS FR sample was larger than ABS but the sample was not completely burnt. The sample extinguished itself, and the length of the burnt material section was 365 mm, i.e. below the height of the second and third marker threads. The reason for burning out of marker threads was a very high flame, not the material burning rate.

The difference in the vertical burning rate of polyurethane foams may be due to their different composition and density. The reference to the actual fire conditions of the values of the vertical burning rate of polyurethane foams, designated during the laboratory tests is very difficult due to the thickness of the samples. The test samples should be up to 13 mm thick, while the foams used in the seat and backrest of the coach seat are usually thicker. Therefore, the burning process can also take place deep into the foam, which can affect the vertical burning rate. Only full-scale tests can show the burning process of the entire seat.

On the basis of the obtained test results, it was found that five out of the materials tested met the requirements of Appendices to UNECE Regulation 118, therefore they could be used as an element of coach furnishing (Table 7) after fulfilling the other approval requirements such as strength ones.

**Table 6** Test results of determined vertical burning rate of materials

	ABS	ABS FR	PC/ABS	PP	PP FR	PA6	MDF	PU1	PU2
The flame time used, s	15	15	15	15	15	15	15	15	15
$t_1$ , s	112	100	–	270	256	261	–	–	9
$t_2$ , s	143	123	–	398	327	615	–	–	15
$t_3$ , s	158	145	–	443	357	824	–	–	18
Burning time of the sample, s	306	310	18	580	575	1030	226	15	41
Length of sample burn, mm	560	365	70	560	560	560	235	140	560
Burning drops	Yes	Yes	No	Yes	Yes	Yes	No	No	Yes
$V_1$ , mm/min	129	144	0	53	56	55	0	0	1600
$V_2$ , mm/min	164	190	0	59	72	38	0	0	1560
$V_3$ , mm/min	205	223	0	73	91	39	0	0	1800
Meeting the requirements of Annex 8 Regulation No. 118	No	No	Yes	Yes	Yes	Yes	Yes	Yes	No

$t_1$  Time from the start of the application of the igniting flame to the severance of one of the first marker threads;  $t_2$  time from the start of the application of the igniting flame to the severance of one the second marker threads;  $t_3$  time from the start of the application of the igniting flame to the severance of one the third marker threads;  $V_1$ ,  $V_2$ ,  $V_3$  the burning rate

**Table 7** Fulfilling the requirements of Regulation No. 118 by the materials tested

	ABS	ABS FR	PC/ABS	PP	PP FR	PA6	MDF	PU1	PU1
Meeting the requirements of Annex 7	Yes	Yes	Yes	No	Yes	Yes	Yes	Yes	Yes
Meeting the requirements of Annex 8 Regulation No. 118	No	No	Yes	Yes	Yes	Yes	Yes	Yes	No
Meeting the requirements of Regulation No. 118	No	No	Yes	No	Yes	Yes	Yes	Yes	No

## 4 Conclusion

Combustible materials that constitute furnishing of means of transport may pose a threat to the health and life of people staying in them during a fire. There are specific requirements and criteria for their selection, but these are basically qualitative criteria. The results of tests of materials made with the recommended methods allow to determine the fire properties of materials, e.g. to determine whether they are easily flammable or inflammable, whether they spread flames over their surface quickly or slowly, whether they emit very toxic combustion products, etc. However, they make no reference to a specific object—its cubature, specificity, evacuation conditions, etc. Therefore, they are not reliable when determining the fire risk of an object. They can even mislead the user who will treat materials that meet the requirements of the regulations and standards as safe. Meanwhile, meeting certain assessment criteria by the material does not mean that this material is resistant to fire. It only means that in determined test conditions, it meets the agreed criteria. Of course, the requirements of standards and legal acts for materials are minimum requirements, they do not mean that manufacturers cannot produce their products with much better properties. However, this usually involves higher production costs.

The selection of materials will effectively influence the fire safety of public transport vehicles when the risk assessment of rooms during a fire will take into account not only qualitative but also quantitative criteria set for actual conditions.

## References

1. Statistical data KG PSP: [http://www.straz.gov.pl/panstwowa\\_straz\\_pozarna/interwencje\\_psp](http://www.straz.gov.pl/panstwowa_straz_pozarna/interwencje_psp), 30 Jan 2020
2. <https://gazetalubuska.pl/pozar-autokaru-z-dziecmi-kolo-miejscowosci-dobrojewo-w-powiecie-miedzyrzeczkim-pojazd-doszczetnie-splonal-kierowca-ewakuowal/ga/13560993/zd/31613723#wiadomosci>, 14 Jan 2020
3. International Convention for the Safety of Life at Sea SOLAS, IMO
4. Directive 2014/90/EU of the European Parliament and of the Council of 23 July 2014 on marine equipment and repealing Council Directive 96/98/EC. Off. J. Eur. Union L 257, 28 Aug 2014
5. Commission Directive (EU) 2015/559 of 9 April 2015 amending Council Directive 96/98/EC on marine equipment Text with EEA relevance. Off. J. Eur. Union L 95, 10 April 2015
6. Code for Application of Fire Test Procedures (FTP 2010 Code), FTP 2010, IMO Resolution MSC.307(88)
7. PN-EN 45545-2 + A1:2015-12 Railway applications: Fire protection on railway vehicles. Requirements for fire behaviour of materials and components
8. Regulation No. 118 of the Economic Commission for Europe of the United Nations (UNECE)—Uniform technical prescriptions concerning the burning behaviour and/or the capability to repel fuel or lubricant of materials used in the construction of certain categories of motor vehicles [2015/622]. Off. J. Eur. Union L 102, 21 April 2015
9. Dobrzyńska, R.: Toksyczność produktów rozkładu termicznego i spalania pianek poliuretanowych stosowanych do wyrobu mebli tapicerowanych. *Bezpieczeństwo i Technika Pożarnicza* **28**(4), 53–58 (2012)

10. Dobrzyńska R.: Wpływ toksyczności produktów rozkładu termicznego i spalania materiałów wyposażenia wnętrza na warunki bezpiecznej ewakuacji, *Prace Naukowe Akademii im. Jana Długosza w Częstochowie. Technika, Informatyka, Inżynieria Bezpieczeństwa*, T. **2**, 13–21 (2014)
11. Dobrzyńska, R.: Selection of outfitting and decorative materials for ship living accommodations from the point of view of toxic hazard in the initial phase of fire. *Polish Maritime Res.* **16**(2), 72–74 (2009)

# The Effect of Heat Treatment of AlSi<sub>10</sub>Mg on the Energy Absorption Performance of Surface-Based Structures



Michael Robinson, Quanquan Han, Heng Gu, Shwe Soe, and Rossitza Setchi

**Abstract** Additive Manufacturing of cellular lattice structures offers opportunities to fine-tune the mechanical response by altering geometric variables. It is known that heat treatment cycles provide an effective way of altering mechanical properties while relieving residual stress. By exploiting the combined influence of these two variables, this study demonstrates the possibility of optimising energy absorption in AlSi<sub>10</sub>Mg honeycomb lattice structures, manufactured using selective laser melting. This finding indicates that heat treatment and powder quality have a significant influence on the mechanical response of the honeycomb. Additionally, this highlights the opportunity to establish an energy absorption diagram, via mapping the relative performance of variable lattice geometries and heat treatment cycles. At the same time, the consistency of powder quality can be tightly controlled.

## 1 Introduction

There is an ongoing interest in the use of aluminium and its alloys in the aerospace and automotive sectors, due to its combination of high specific strength and low density [1–4]. AlSi<sub>10</sub>Mg is one of these alloys, traditionally used for casting, with good weldability thanks to its near-eutectic Al and Si composition [5]. In addition, the inclusion of Mg causes Mg<sub>2</sub>Si precipitates to form upon heat treatment, resulting in hardening of the alloy [6].

Heat treatment of AlSi<sub>10</sub>Mg has been shown to affect mechanical properties, particularly strength and ductility [7, 8]. However, exploiting these benefits can be challenging when using traditional manufacturing techniques (e.g. casting), due to

---

M. Robinson (✉) · Q. Han · H. Gu · S. Soe · R. Setchi  
Cardiff University, Cardiff, UK  
e-mail: [RobinsonM12@cardiff.ac.uk](mailto:RobinsonM12@cardiff.ac.uk)

Q. Han  
Shandong University, Jinan, China

S. Soe  
University of the West of England, Bristol, UK

inherent geometric limitations. Additive manufacturing (AM) is a developing manufacturing technology, which has been shown to be suitable for the fabrication of complex structures with tunable mechanical performance [9]. This ability to selectively alter functional performance, during post-processing, raises an opportunity to develop structures with improved energy absorption performance.

While the effect of heat-treating AlSi<sub>10</sub>Mg cellular structures has been investigated [10], this work focused on a strut-based structure. Such structures have high initial stiffness. However, they are buckling dominated, leading to high internal strains. This is evidenced by the failure observed, even in structures heat-treated to increase ductility [10]. Surface-based honeycomb structures have been investigated by the authors, with low internal strains recorded in the range of  $\pm 0.3$  at densification [9]. Therefore, surface-based structures are potentially more applicable to the relatively low ductility observed in metallic materials. Additionally, re-entrant structures have demonstrated excellent energy absorption capacity [11].

## 2 Materials and Methods

This study explores the use of a novel re-entrant honeycomb structure. By exploiting the low internal strains of surface-based structures, and re-entrant geometry, a structure with potential for high energy absorption was realised (Fig. 1).

The re-entrant honeycomb (Fig. 1) was created with a wall thickness of 0.75 mm, a cell width of 10 mm and an overall nominal height of 20 mm. The resultant relative density of the structure was 0.137 g/cm<sup>3</sup>. An extrusion angle of 15° was employed to achieve a re-entrant structure. Further opportunities to explore the variants of

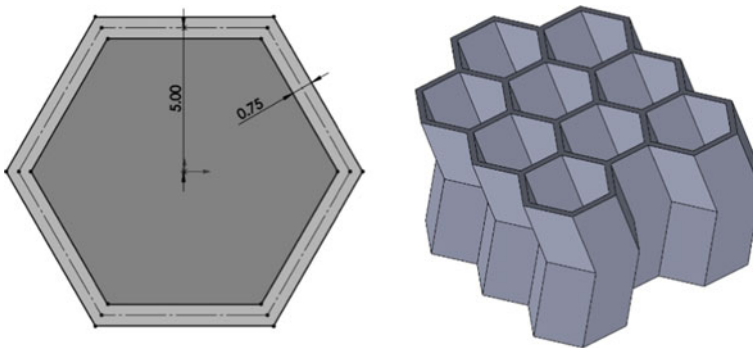


**Fig. 1** Re-entrant honeycomb geometry used in this work



**Table 1** Chemical composition of AlSi<sub>10</sub>Mg

Element	Mass (%)	Element	Mass (%)
Aluminium	Balance	Zinc	<0.10
Silicon	9.00–11.00	Manganese	<0.10
Magnesium	0.25–0.45	Nickel	<0.05
Iron	<0.25	Copper	<0.05
Nitrogen	<0.20	Lead	<0.02
Oxygen	<0.20	Tin	<0.02
Titanium	<0.15		

this structure include different shaped honeycombs (square, pentagon, octagon); cell width; cell height; wall thickness; re-entrant angles.

### Powder

Previous work has been undertaken by the authors exploring the effect of heat treating on the mechanical performance of AlSi<sub>10</sub>Mg components, made of virgin powder [12]. These results were used as a point of comparison against recycled powder in this study. The same build strategy adopted in this previous testing was again adopted here, to ensure that the only variable was the re-cyclability of the powder. The recycled powder was re-used approximately ten times before this study. Based on the powder morphology inspection, the recycled powder was less spherical and coated by partially melted particles compared to virgin powder. These drawbacks were expected to degrade the mechanical properties of the as-fabricated component. The chemical composition of AlSi<sub>10</sub>Mg is displayed in Table 1.

### Machine and Build Strategy

The build layout can be seen in Fig. 2. A Renishaw AM250 (Renishaw plc, Wotton-under-Edge, Gloucestershire, UK) SLM system, employing a modulated ytterbium fibre laser with a wavelength of 1071 nm, was used to fabricate honeycomb and tensile specimens. The processing parameters were laser power 200 W; hatching spacing 130 μm; powder layer thickness 25 μm; laser scanning speed 500 mm/s. A chessboard scanning strategy was employed for this study. The rotation angle between each adjacent layer was set to 67° to eliminate the chance of scan lines repeating themselves directly on top of one another, thus creating poor material properties.

### Heat Treatment

One re-entrant honeycomb structure and one tensile bar were subjected to the same heat treatment cycle as the virgin components [12] (550 °C for 2 h, followed by furnace cooling), as shown in Fig. 3.

All mechanical experimentation was performed using a Z100 (Zwick, Germany) electro-mechanical uniaxial testing machine, at a constant speed of 1 mm/min. Additionally, a CAM028 (iMetrum, UK) non-contact video extensometer was used to collect strain data for tensile testing.

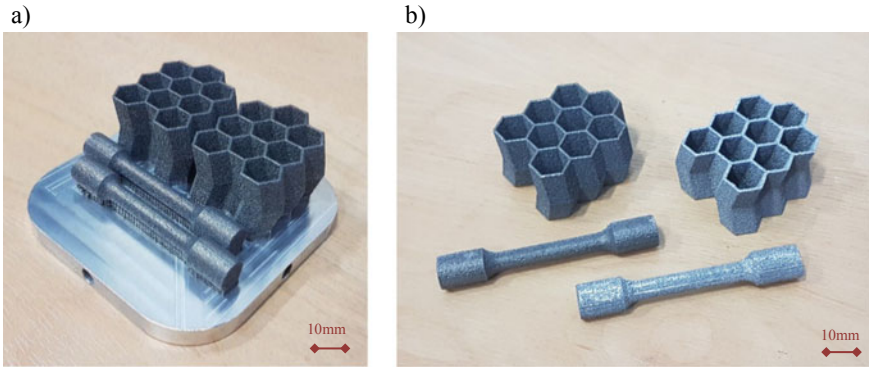
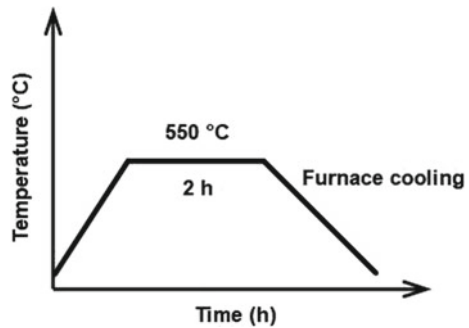


**Fig. 2** Re-entrant honeycombs and tensile bars tested in this study. **a** Build layout, **b** as-built (left-most) and heat-treated (right-most) specimens

**Fig. 3** Schematic of heat treatment



### 3 Results and Discussion

#### 3.1 Tensile Response

It was found that the ductility of the as-built recycled material was significantly reduced (to ~40% that of virgin material), while the peak stress (before the failure of the recycled specimen—0.08) was only reduced to 78% virgin material. Comparatively, the ductility of the treated material was reduced to a similar level (~40% of virgin), while the peak stress, at a strain equivalent to the point of failure for the recycled specimen (0.26), was reduced to only ~90%. These findings highlight how powder quality affected tensile strength, ultimately influencing mechanical properties (Fig. 4).

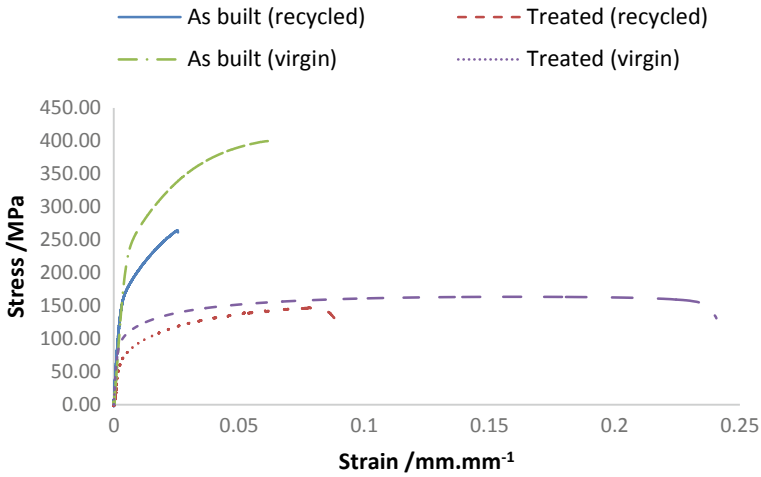


Fig. 4 Tensile testing data for as-built and heat-treated bars

### 3.2 Re-entrant Honeycomb Response

At  $\epsilon = 0.75$ , the compressive force generated by the treated honeycomb is equivalent to its first peak in force. The energy absorbed by the treated honeycomb up to this strain was  $8.95 \text{ MJ/m}^3$ , 205% that absorbed by the as-built honeycomb at failure ( $4.36 \text{ MJ/m}^3$ ). This increase in absorbed energy was also achieved at only 44% of the peak force of the as-built honeycomb (20.6 MPa vs. 46.7 MPa) (Fig. 5).

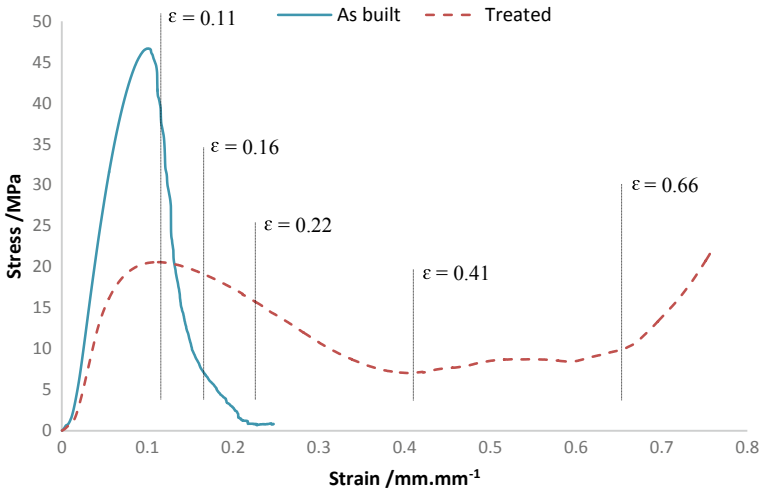
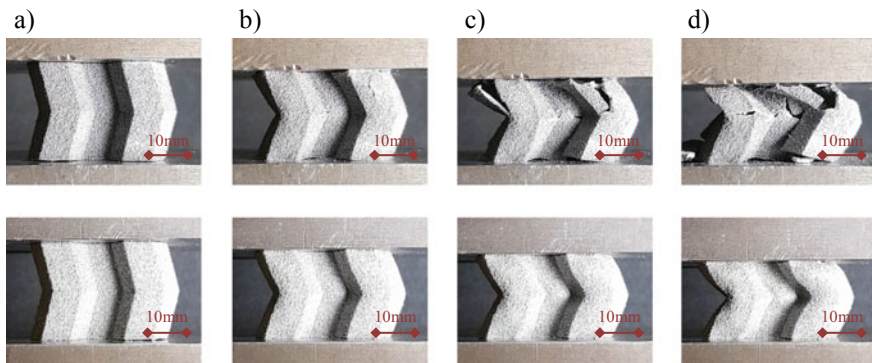


Fig. 5 Compressive response of re-entrant honeycomb, with and without heat treatment

During initial deformation of the as-built honeycomb (to  $\epsilon = 0.11$ ), the compression was uniform and appeared only to involve bending of the cell walls. However, as  $\epsilon$  exceeded 0.11, cracks propagated throughout the honeycomb. Then, as  $\epsilon$  reached 0.16, these fractured fragments were forcefully expelled from the main honeycomb geometry, significantly reducing the remaining material between the compression platens. This expulsion resulted in the compressive stress reducing from 46.7 to 0.8 MPa, over  $\epsilon = 0.11$  to 0.24. At equivalent strains, when compared to the as-built honeycomb, the treated one deforms with little visual damage (Fig. 6). However, evidence of cracks in the treated specimen become apparent at higher strains, with a clear fracture emerging by  $\epsilon = 0.41$  (Fig. 7a).

The localised fracture of as-built honeycomb can be correlated with the as-built tensile response. The strain that the honeycomb component was exposed to during compression far exceeded its tolerance level, leading to premature failure and an unfavourable energy absorption response. By comparison, the treated honeycomb



**Fig. 6** Comparison of compressive loading of as-built (upper images) and treated (lower images) re-entrant honeycombs, **a**  $\epsilon = 0$ , **b**  $\epsilon = 0.11$ , **c**  $\epsilon = 0.16$ , **d**  $\epsilon = 0.22$

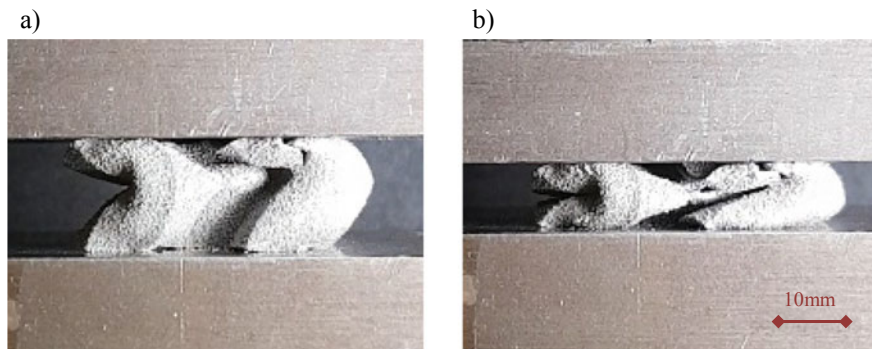


**Fig. 7** Further compressive loading of treated re-entrant honeycomb, **a**  $\epsilon = 0.41$ , **b**  $\epsilon = 0.66$

experienced localised fracture at a much later stage of compression ( $\varepsilon = 0.41$ ), followed by symmetrical bending with respect to the folded angle ( $\varepsilon = 0.66$ ).

Low peak stress in the heat-treated honeycomb, followed by a relatively long plateau region until densification ( $\varepsilon = 0.75$ ), indicates that heat treatment significantly improved energy absorption performance. While this is promising, a reduction in stress over the plateau region should not exist in an ideal energy absorption material. As indicated in Sect. 2, future geometric alterations to honeycomb variants will allow this drop in stress to be addressed.

## 4 Conclusion

AlSi<sub>10</sub>Mg tensile test components produced from recycled powder demonstrated a notable reduction in peak stress, and a far more significant decrease in ductility, when compared to virgin material. By exploiting surface-based re-entrant structures, this reduction in ductility was accounted for, allowing a functional structure to be built with the recycled material.

This work demonstrates how AlSi<sub>10</sub>Mg powder can be re-utilised to produce functional cellular structures. Additionally, material testing data is presented to inform the design and engineering of future structures, using recycled powder.

**Acknowledgements** The authors would like to acknowledge ASTUTE 2020 (Advanced Sustainable Manufacturing Technologies) operation part-funded by the European Regional Development Fund (ERDF) through the Welsh Government. This work emerged from collaborative ASTUTE projects runs separately with Continental Teves and Airbus.

## References

1. Çam, G., Koçak, M.: Progress in joining of advanced materials. *Int. Mater. Rev.* **43**(1), 1–44 (1998)
2. Han, Q., Geng, Y., Setchi, R., Lacan, F., Gu, D., Evans, S.L.: Macro and nanoscale wear behaviour of Al-Al<sub>2</sub>O<sub>3</sub> nanocomposites fabricated by selective laser melting. *Compos. B Eng.* **127**, 26–35 (2017)
3. Wong, M, Tsopanos, S, Sutcliffe, C.J., Owen, I.: Selective laser melting of heat transfer devices. *Rapid Prototyping J.* (2007)
4. Han, Q., Gu, H., Soe, S., Setchi, R., Lacan, F., Hill, J.: Manufacturability of AlSi<sub>10</sub>Mg overhang structures fabricated by laser powder bed fusion. *Mater. Des.* **160**, 1080–1095 (2018)
5. Read N., Wang, W., Essa, K., Attallah, M.M.: Selective laser melting of AlSi<sub>10</sub>Mg alloy: process optimisation and mechanical properties development. *Mater. Design (1980–2015)* **65**, 417–424 (2015)
6. Thijs, L., Kempen, K., Kruth, J.-P., Van Humbeeck, J.: Fine-structured aluminium products with controllable texture by selective laser melting of pre-alloyed AlSi<sub>10</sub>Mg powder. *Acta Mater.* **61**(5), 1809–1819 (2013)

7. Iturrioz, A., Gil, E., Petite, M., Garciandia, F., Mancisidor, A., San, Sebastian M.: Selective laser melting of AlSi<sub>10</sub>Mg alloy: influence of heat treatment condition on mechanical properties and microstructure. *Welding World* **62**(4), 885–892 (2018)
8. Li, W., Li, S., Liu, J., Zhang, A., Zhou, Y., Wei, Q., Yan, C., Shi, Y.: Effect of heat treatment on AlSi<sub>10</sub>Mg alloy fabricated by selective laser melting: Microstructure evolution, mechanical properties and fracture mechanism. *Mater. Sci. Eng. A* **663**, 116–125 (2016)
9. Robinson, M., Soe, S., Johnston, R., Adams, R., Hanna, B., Burek, R., McShane, G., Celeghini, R., Alves, M., Theobald, P.: Mechanical characterisation of additively manufactured elastomeric structures for variable strain rate applications. *Add. Manuf.* **27**, 398–407 (2019)
10. Suzuki, A., Sekizawa, K., Liu, M., Takata, N., Kobashi, M.: Effects of heat treatments on compressive deformation behaviors of lattice-structured AlSi<sub>10</sub>Mg alloy fabricated by selective laser melting. *Adv. Eng. Mater.* **21**(10), 1900571 (2019)
11. Adams, R., Soe, S.P., Santiago, R., Robinson, M., Hanna, B., McShane, G., Alves, M., Burek, R., Theobald, P.: A novel pathway for efficient characterisation of additively manufactured thermoplastic elastomers. *Mater. Des.* **180**, 107917 (2019)
12. Han, Q., Jiao, Y.: Effect of heat treatment and laser surface remelting on AlSi<sub>10</sub>Mg alloy fabricated by selective laser melting. *Int. J. Adv. Manuf. Technol.* **102**(9–12), 3315–3324 (2019)

# Blockchain-Enabled ESG Reporting Framework for Sustainable Supply Chain



Xinlai Liu, Haoye Wu, Wei Wu, Yelin Fu, and George Q. Huang

**Abstract** Nowadays sustainability has received global attention in supply chain. To evaluate the sustainability level, environmental, social, and governance (ESG) reporting is widely adopted especially for the listed companies. However, due to the lack of data authentication, consistency, and transparency, the ESG-based sustainability evaluation is still inadequate. To address those challenges, this paper proposes a blockchain-based ESG reporting framework for facilitating the sustainability evaluation of listed company. Firstly, a fact-telling blockchain gateway is designed to facilitate the raw data authentication issues. It plays the role of light node to transfer the data of smart infrastructure/devices to the blockchain network, which satisfies both privacy and transparency. Secondly, a versioning smart contract mechanism is developed to verify the consistency between the raw data and the final ESG report. Thirdly, a token-based sustainability evaluation mechanism is used to evaluate the behaviors of listed company in the sustainable supply chain. The discussion analyzes the benefits and potential obstacles of utilizing the proposed framework in the ESG reporting preparation, generation, and publication. The results of this study contribute a reliable approach to facilitate the sustainability-level evaluation of listed company.

## 1 Introduction

Nowadays sustainability has received globally attention in supply chain. By increasing the sustainability level, the enterprises (especially listed companies) not just achieve the cost savings, but also improve the reputation for sustainability investment. As an important sustainability evaluation method, environmental, social, and governance (ESG) reporting is widely used to assess non-financial performance of companies [1]. Take Hong Kong Exchange as an example, the annual exposure of ESG report is regarded as an obligation for more than 2000 listed companies under the principle of “Comply or Explain” [2].

---

X. Liu · H. Wu · W. Wu · Y. Fu · G. Q. Huang (✉)  
The University of Hong Kong, 08544 Hong Kong, China  
e-mail: [gquang@hku.hk](mailto:gquang@hku.hk)

To generate an ESG report for a listed company, it typically includes three stages: report preparation, report generation, and report publication. To make a clear understating, here, we used a collaborative company focusing on textile supply chain and logistics, which is listed on Hong Kong Exchange, as shown in Fig. 1. In the stage of report preparation, the textile company needs to prepare the raw data both from its internal and from its upstream and downstream stakeholders, based on the standards of government ESG requirements. In the stage of report generation, the company usually needs to cooperate with a professional service company to produce a qualified ESG report. In the stage of report publication, the external stakeholders, such as investors, NGOs, and Hong Kong Exchange, could evaluate the company’s sustainability level through the disclosed ESG reporting. According to our investigation, the cost per ESG report is from 0.3 million HKD to 1.5 million HKD. The annual market value of ESG reporting is from 703.8 million HKD to 3654 million HKD. Therefore, both listed companies and ESG professional service providers have strong requirements for the cutting-edge technologies to further upgrade their ESG-related activities.

However, it still has some challenges to generate a trustable, consistent and transparent ESG report. The first challenge is the authentication of ESG raw data in report preparation stage. The raw data, such as the electricity usage, wastewater, and green gas emission, are usually collected and sent manually from listed company and its upstream and downstream cooperators. It can hardly be evaluated its authentication in the report preparation stage. The second challenge is the inconsistency concerns between the ESG data and final ESG report in report generation stage. It leads to an inconsistent and less trustable ESG report, which does harm to the listed company. The third challenge is the less-transparency concerns between the ESG report and

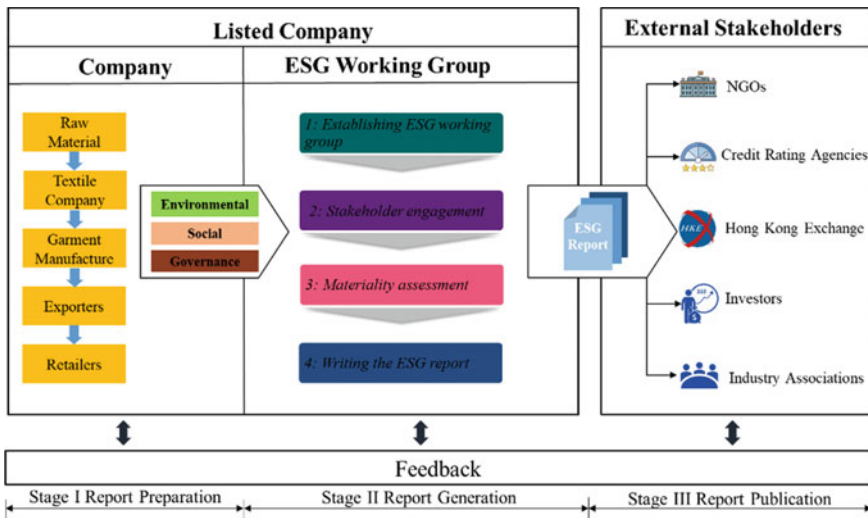


Fig. 1 ESG reporting processes of a textile company



ESG standards in the report publication stage. For example, the listed company could expose less items than the ESG standards for hiding the disadvantage aspects in ESG reporting. It jeopardizes the transparency of the report to stakeholders, such as the regulators, NGOs, and investors. To sum up, these collaborating companies face three key challenges involving the ESG reporting: authentication, consistency, and transparency.

To address the three challenges, this paper proposes a blockchain-enabled ESG reporting framework with the help of IoT and cloud technologies. This paper focuses on three key fundamental infrastructure and services, including fact-telling blockchain gateway, versioning smart contract, and blockchain-based issuing mechanism, along the stages of report preparation, report generation, and report publication. To our best knowledge, such blockchain-based integrated solutions for ESG reporting cannot be found on both academia and industry. In addition, including fact-telling blockchain gateway, versioning smart contract, and blockchain-based issuing mechanism that have been proposed through the research will be adapted for building such a total solution.

The rest of this paper is organized as follows. Section 2 presents the technical architecture of the blockchain-enabled ESG reporting framework. Section 3 describes its three key components. In Sect. 4, we present the discussions. In Sect. 5, we briefly summarize this research and present the future direction.

## 2 Overview of Blockchain-Enabled ESG Reporting

The overall of blockchain-enabled ESG reporting is illustrated in Fig. 2, aiming at achieving the future vision of trustable and highly efficient ESG reporting

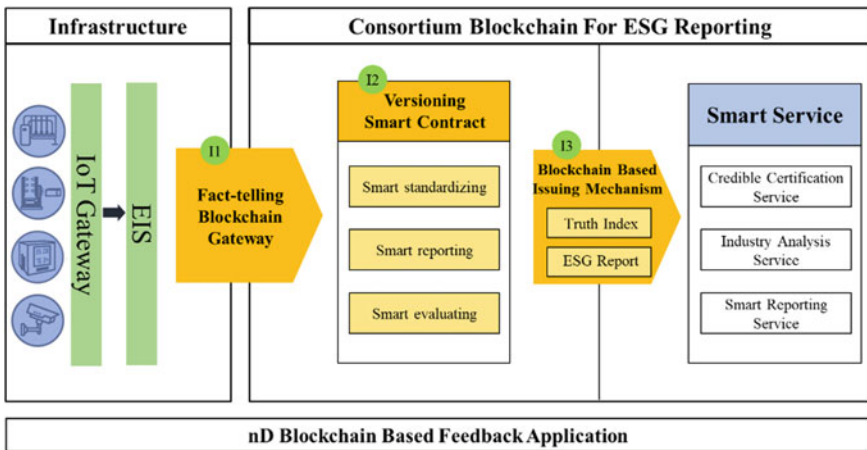


Fig. 2 Overview of blockchain-enabled ESG reporting platform

through blockchain technology and smart contract. It is especially proposed to enable an innovative blockchain-enabled conceptual design and scientific prototype in the ESG reporting, including three key innovations, marked as “I1—fact-telling blockchain gateway,” “I2—versioning smart contract,” and “I3—blockchain-based issuing mechanism.”

At the left of the architecture, it is a well-packaged IoT-enabled fundamental infrastructures, which is the information communication technology and sensory enabler to support the trustable and efficient ESG reporting services. It is an integration of multiple technologies in both software and hardware to enable physical asset with intelligent reasoning, sensible, and interactable capabilities and aims to support the data collection services across every phase of ESG reporting [3, 4]. The IoT gateway technology was introduced by previous research [5–7], to provide an all-in-one solution for managing and capturing real-time data, especially the environmental data, which is generated from RFID/auto-ID devices and preprocessing data locally.

Fact-telling blockchain gateway is newly introduced in this research to form the innovative blockchain-enabled fundamental infrastructure for ESG reporting preparation stage. It works as a lightweight node of blockchain platform with two key functions: data hub and fact-level evaluation. On the one hand, it is the core technologies to manage the ESG data collecting devices (e.g., smart glove smart glasses, and smart boxes) for listed company’s information capturing, which will be developed and applied in this project to coordinate and facilitate smart assets and devices. On the other hand, blockchain gateway provides a fact-telling mechanism for evaluating the fact-level of ESG raw data, which will be further explained in later section.

The versioning smart contract, as the core innovation in consortium blockchain, is used for the report generation stage. It has three key features, namely multi-consensus, smart execution, and flexible version mechanism. It facilitates the coordination and execution of ESG reporting processes, operations, and scheduling of different groups of resources to fulfill targeted tasks. Through this, the generation of ESG report can be made smart and highly efficient through equipped with flexible parameter setup, multi-party negotiation & agreement, and linked with services on the consortium. Notably, the typical utilization of versioning smart contract in ESG report generation includes smart standardizing, smart reporting, and smart evaluating, which will be discussed in details below. Compared with the traditional manual report generation, the versioning smart contract-based solution provides an automatic, flexible, and reliable ESG reporting generation process. Therefore, it is expected to achieve the greatest return in cost-saving, highly efficient report generation in every procedure of ESG report industry, and to enable the best possible services to stakeholders.

In the right of the architecture, it is the blockchain-based issuing mechanism, which is proposed to solve the less-transparency problems in ESG report publication. In the stage of report publication, the blockchain-based issuing mechanism is designed to achieve more transparent and trustable ESG report issuing mechanism for stakeholders, like investors, NGOs, and HKEX. It has two key components, fact index and ESG report issuing. Here, fact index refers to the summary of token-based

data authentication index, token-based data consistency index, and token-based transparency index. It can be calculated by advanced decision analytics, such as the AHP and VIKOR. [8]. Through the blockchain-based issuing mechanism, different stakeholders can get the own preferred services, including credible certification service for listed companies, industry analysis service for investors, and smart reporting service for professional agencies.

### 3 The Key Components of Blockchain-Enabled ESG Framework

#### 3.1 Fact-Telling Blockchain Gateway

Blockchain gateway (BG) is an overall middleware solution to collect, process, and analyze ESG data derived from enterprises and link to the blockchain. Each blockchain gateway works as an entrance node of the blockchain network. As shown in Fig. 3, BG is basically comprised by two main parts, hosted hardware and software. In the hardware aspect, it actually provides a running environment for software with basic computing and communication capacity. A plenty of hardware products could

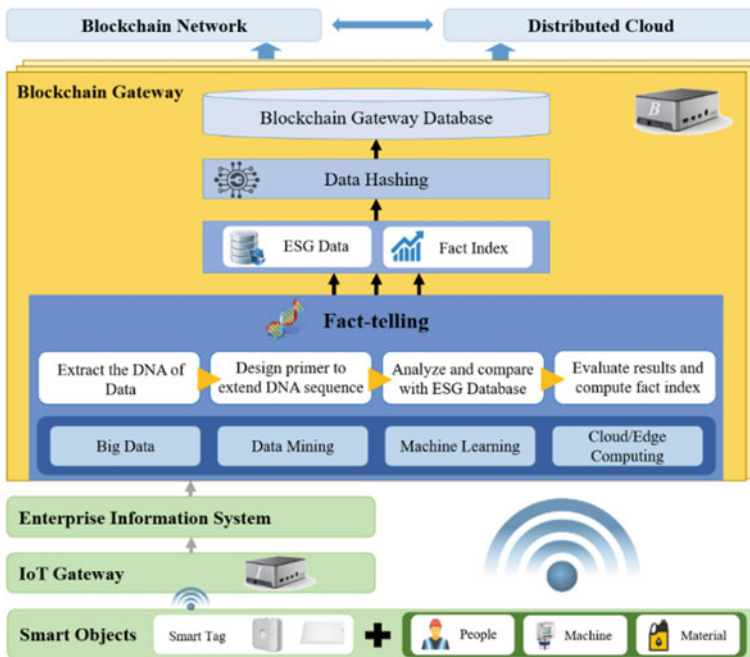


Fig. 3 Mechanism for fact-telling blockchain gateway

be qualified for BW, including smartphones, smart base stations, and smart wearables that could support open operating systems. Usually, this hardware not only has some integrated functions such as abundant sensors, GPS, and camera, but also possesses multiple types of wired or wireless communication interfaces including network port (RJ45), OTG port, cellular network, Wi-Fi, and Bluetooth. These interfaces endow BG with the ability to integrate with and centrally manage more peripheral devices such as smart wearables, assistive tools, and special sensors. In the software aspect, four key functions are enabled. (1) connects (wired or wirelessly), hosts, and provides a specific channel to collect data from the enterprise information system or smart objects; (2) computes an index to reflect how much the ESG data accords with the fact by applying the fact-telling mechanism that we developed; (3) hashes the ESG data and fact index to a unique identification circulating in the blockchain via the cryptology techniques; and (4) uploads the hashed data to the blockchain network and original data to distributed cloud for backup.

The fact-telling mechanism is developed to quantify reliability of the ESG data provided by companies. The fact index is used to assess the authenticity of the whole ESG report data. Here, how to realize fact-telling is motivated by biological practices identifying one kind of species via DNA. It is obvious that every species has its own specific characteristics in DNA for distinction, and their DNA is not likely to be changed after birth. Exclusive rules or algorithms are devised to process the DNA of data, making it unified and comparable. Notably, there are two ways of analyzing preprocessed data to clarify its difference and similarity. One is to compare the current data with the standard data from the database under the same condition. The other is to compare the data collected in one company with others at the same duration for the same measurement.

### 3.2 *Versioning Smart Contract*

Versioning smart contract is another important innovation in this paper. As envisaged by Ethereum blockchain, a smart contract enforces a relationship with cryptographic code [9]. They are programs that execute exactly as they are set up to by their creators. Characterized two key features are multi-party agreement and self-execution [10]. However, ESG industry exists many dynamic demands, such as the changes of threshold of sustainability level, updates of weight of different ESG data parameters, and even the turnover of the contract parties. Therefore, a more flexible smart contract mechanism is proposed, namely versioning smart contract. As seen in Fig. 4, the concept of versioning smart contract is presented from technological perspective and commercial perspective.

From a technological perspective, it introduces the basic method of generating a versioning smart contract, as follows:

Step 1: *“Initialize” refers to write a Register contract.*

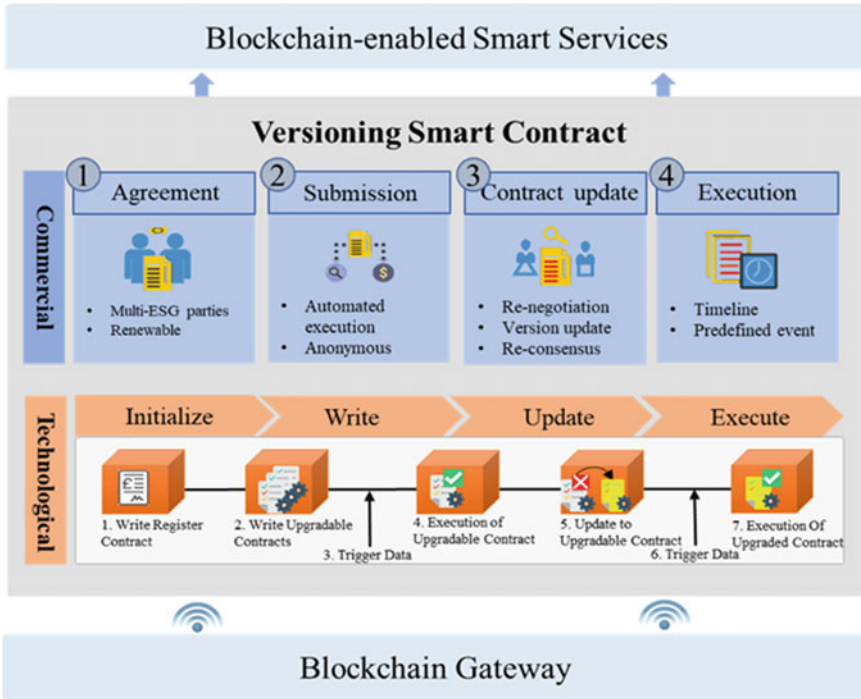


Fig. 4 Concept mechanism of version smart contract

- Step 2: “Write” means to generate all other upgradable contracts with constructors requiring Register’s address;
- Step 3: deploy Register giving to its constructor data—all other upgradable contract from step 2;
- Step 4: deploy new version of “upgradable” contract with same address of Register and disable/kill old version of “upgradable” contract;
- Step 5: register address of the new version of “upgradable” contract in the Register.

From a commercial perspective, the achievement process of versioning smart contract includes agreement, submission, contract update, and execution. It plays a key role in providing an approach to fulfill the dynamic demands for the ESG stakeholders. Here, we list three typical scenarios of the dynamic demands in ESG industry.

In the first scenario, the business activities of a specific company could be changeable. For example, a listed company formerly focused on textile manufacturing industry, then expanded/change its business into textile transportation. It will definitely pose new ESG requirements for the listed company.

In the second scenario, the standards of ESG report from HKEX could be dynamic, in terms of an old attribute value, or newly increased attributes. This always happens considering the constantly updated environment threats and challenges.

In the third scenario, there are many listed companies in HKEX from the same industry. They are distributed geographically. One might locate in Vietnam; another might locate in mainland China. The standards of ESG criteria for the above companies could be varied, due to the local policies and/or laws. Therefore, based on the dynamic business environments, we are envisaging that versioning smart contract could provide a flexible contract mode.

### ***3.3 Blockchain-Based Issuing Mechanism***

Once the professional company completes ESG reporting and uploads it to the blockchain, corresponding fact index tokens, which indicates how much this report is created based on the fact, will be granted. The fact index token adopts a fuzzy description, including excellent, good, and poor. It is aimed to avoid ranking and inter-comparison but still motivate enterprises to do better. Both the ESG report and fact index tokens are issued to certain stakeholders who own the permission of approaching, which is monitored by the account management of the whole chain.

The fact index tokens consist of three components, namely fact token, consistency token, and transparency token. They are weighted to sum up to get the final index, depending on the level of importance and influence. First, the fact token is aimed at awarding the authenticity of raw data devoted to ESG, which is calculated in the fact-telling blockchain gateway. Second, the consistency token refers to a reward for how much the ESG report proposed by the professional agency keeps in accordance with the raw data offered by the enterprise. For example, the service provider may intend to ignore some information which defaces the total performance. Or some may fabricate a value to beautify the index on purpose. Those behaviors are against the fact and also not expected for stakeholders, like investors. So accordingly, the consistency token will be decreased. Techniques in data mining, such as outlier detection and classification, will be applied to go through all the data displayed in the ESG report and compare it with original data provided. Third, the transparency token specifies the disclosure degree of ESG report submitted to the blockchain relative to the official requirement listed by the government. For instance, the company is required to uncover the amount of emitted gas, liquid waste, and solid waste in their ESG report, and however, in the submitted report, the solid emissions are not exposed without any explanations. In this case, the system will consider this report is not complete or conceals some facts and thus grant fewer transparency token to it. To attain the final fact index tokens, kinds of fuzzy methods can be used to weight those three tokens computed above, as shown in Fig. 5.

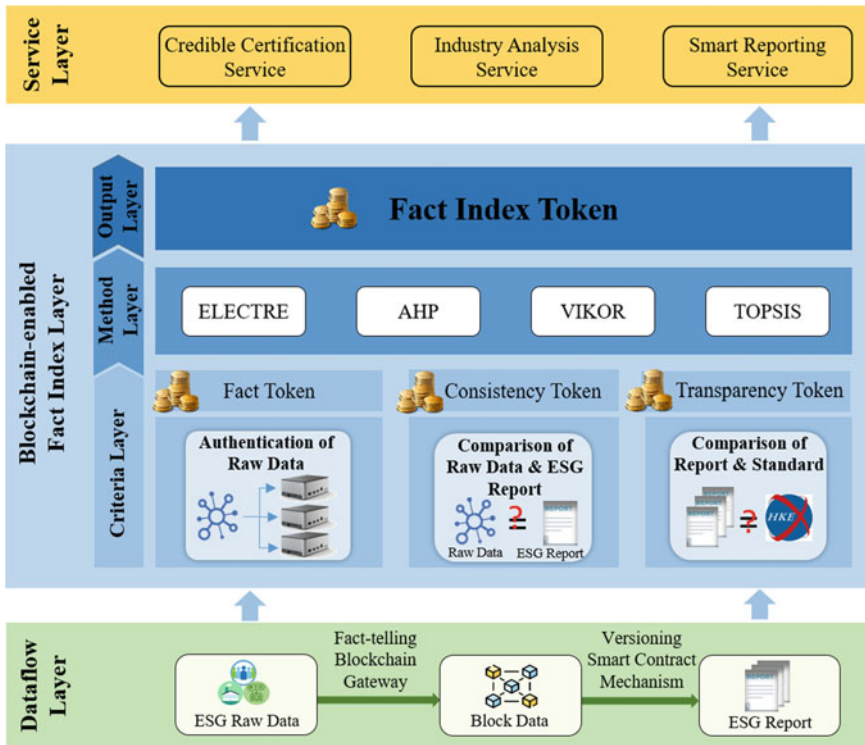


Fig. 5 Mechanism of blockchain-based issuing

## 4 Discussion

The rising awareness of sustainability has increased the demands for evaluation of non-financial performance, including environmental, social, and governance aspects. However, the traditional ESG reporting approach relies on paper-based manual work. It not only costs a lot time and manpower, but also has less reliable reporting processes. Therefore, the listed companies and ESG professional service providers are facing significant challenges to upgrade the ESG reporting industry, so as to satisfy the guideline provided by the HKEX and meet the market demands from various stakeholders, including investors, NGOs, associations. This paper proposed to enable an innovative blockchain-enabled conceptual framework in the ESG reporting with the help of IoT technologies. It is envisaging to have the following benefits:

Firstly, the blockchain-based framework will result in significant improvements in the ESG reporting quality, consistent, efficiency, and transparency. In particular, by means of the blockchain platform and related technologies, listed companies will provide more credible data, ESG professional service providers will issue the ESG report in a more efficient manner, and the external stakeholders, including investors, NGOs, associations, will refer to the ESG reporting in a more transparent way.

Secondly, the use of initial project deliverables will significantly improve the competitiveness of the ESG reporting business in general. It is expected that the collaborative companies would be able to reduce the overall direct costs and improve their competitiveness through efficiency and reputation gains.

Thirdly, the blockchain-enabled approach not only extends the capability of ESG reporting industry significantly, but also provides an interoperable platform to integrate and coordinate other fragmented information systems uses in different stages and occasions associated with the ESG business. It improves the decision mechanism and streamlines the reporting process for better managing the report preparation, report generation, and report publication.

However, there are also some potential obstacles to conduct this work. On the one hand, some ESG raw data might be sensitive to the listed companies. It is natural that they are unwilling to put all the raw data to a whole transparent blockchain system. Therefore, it is necessary to achieve the tradeoff between transparency and privacy. On the other hand, the use of proposed approach might not be in accordance with the interests of professional ESG service providers since it simplifies ESG reporting procedures and reduces the thresholds of conducting this business.

## 5 Conclusion and Future Direction

This paper proposed a blockchain-enabled framework to facilitate the ESG reporting industry. A suite of core technologies is presented to form the foundation for developing a total solution. Firstly, the concept of fact-telling blockchain gateway is developed to quantify the fact probability of ESG data. It provides a promising solution to address the data authentication issues at the stage of report preparation. Secondly, versioning smart contract mechanism is firstly proposed to meet dynamic service demands among multiple parties at the stage of report generation. Thirdly, the mechanism of token-based ESG report issuing is established to attain the fact index and publish the ESG reports at the stage of report publication. It helps the professional ESG service agencies provide a reliable and transparent sustainability report along with its fact index.

Further researches are necessary to conduct as following aspects. On one hand, an important aspect is blockchain-based ESG data management and analytics. As numerous ESG data are collected from deployed smart devices, how to use historical and real-time ESG data to support sustainability evaluation and autonomous decision-making is to be considered. On the other hand, it is very worthy to explore how to achieve high performance of the blockchain system connecting with numerous smart devices. It directly influences the usability and scalability of the system.

**Acknowledgements** This work should thank Mr. Kai Kan and Dr. David Leung for the valuable suggestions.



## References

1. Chen, J.: Environmental, social, and governance (ESG) criteria. Investopedia. <https://www.investopedia.com/terms/e/environmental-social-and-governance-esg-criteria.asp>. Last accessed 5 Feb 2020
2. Consultation paper review of the environmental, social and governance reporting guide and related listing rules. <https://www.hkex.com.hk/-/media/HKEX-Market/News/Market-Consultations/2016-Present/May-2019-Review-of-ESG-Guide/Consultation-Paper/cp201905.pdf>. Last accessed 2019
3. Xu, G., Huang, G.Q., Fang, J.: Cloud asset for urban flood control. *Adv. Eng. Inform.* **29**(3), 355–365 (2015)
4. Qiu, X., Luo, H., Xu, G., Zhong, R., Huang, G.Q.: Physical assets and service sharing for IoT-enabled supply hub in industrial park (SHIP). *Int. J. Prod. Econ.* **159**, 4–15 (2015)
5. Zhang, Y., Qu, T., Ho, O.K., Huang, G.Q.: Agent-based smart gateway for RFID-enabled real-time wireless manufacturing. *Int. J. Prod. Res.* **49**(5), 1337–1352 (2011)
6. Huang, G.Q., Qu, T., Fang, M.J., Bramley, A.N.: RFID-enabled gateway product service system for collaborative manufacturing alliances. *CIRP Ann.* **60**(1), 465–468 (2011)
7. Fang, J., Qu, T., Li, Z., Xu, G., Huang, G.Q.: Agent-based gateway operating system for RFID-enabled ubiquitous manufacturing enterprise. *Robot. Comput. Integr. Manuf.* **29**(4), 222–231 (2013)
8. Awasthi, A., Govindan, K., Gold, S.: Multi-tier sustainable global supplier selection using a fuzzy AHP-VIKOR based approach. *Int. J. Prod. Econ.* **195**, 106–117 (2018)
9. Farrell, S., Machin, H., Hinchliffe, R.: Lost and found in smart contract translation—considerations in transitioning to automation in legal architecture. In *UNCITRAL, modernizing international trade law to support innovation and sustainable development*. In: Proceedings of the Congress of the United Nations Commission on International Trade Law, Macau, vol. 4, pp. 95–104 (2017)
10. Xu, R., Chen, Y., Blasch, E., Chen, G.: Blendcac: a smart contract enabled decentralized capability-based access control mechanism for the IoT. *Computers* **7**(3), 39 (2018)

# Low-Sulphur Marine Fuels—Panacea or a New Threat?



Agnieszka Ubowska and Renata Dobrzyńska

**Abstract** As a result of increasing air pollution, global actions have been taken to improve air quality. One of these measures is the reduction of  $\text{SO}_x$  emission from ships. This group of transport means has used (until the end of 2019) fuel with a maximum sulphur content of up to 3.5%. The article describes fuels with low sulphur content currently approved for use (with sulphur content below 0.5 and 0.1% for Emission Control Area). This amount is 500 times greater than the permissible sulphur content in car fuel (up to 3500 times greater by the end of 2019). Low-sulphur marine fuels include blend fuels the use of which raises doubts. What threats does their use pose? The most significant problems associated with limiting the sulphur content of marine fuel have already been identified. These include the incompatibility and instability described in the article. Are there any others? The publication is an attempt to resolve this issue.

## 1 Introduction

Although sulphur oxides are pollutants with the greatest reduction in emissions within the European Union (Fig. 1) [1], they still cause a problem. According to the World Health Organization, annually 4.2 million people die prematurely from ambient air pollution [2].

The main source of  $\text{SO}_x$  is the combustion of sulphur-containing fuels, i.e., all types of coal and oil.  $\text{SO}_x$  emission factors for each fuel can be calculated from Eq. 1.

$$\Phi = (1 - r) \cdot \frac{S}{H} \quad (1)$$

where:  $\Phi$ —fuel emission factor,  $S$ —sulphur content of the fuel,  $H$ —thermal content of the fuel,  $r$ —mass fraction of sulphur retained in the ash [3].

---

A. Ubowska (✉) · R. Dobrzyńska  
West Pomeranian University of Technology in Szczecin, Al. Piastow 41, 71-065 Szczecin, Poland  
e-mail: [agnieszka.ubowska@zut.edu.pl](mailto:agnieszka.ubowska@zut.edu.pl)

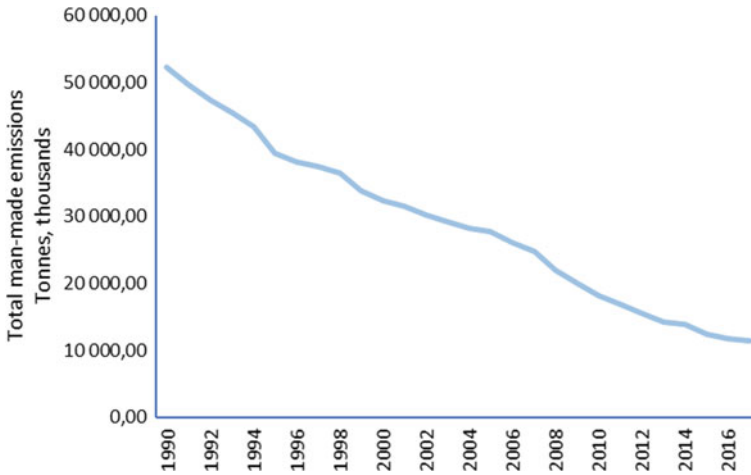


Fig. 1 OECD sulphur oxides emission in 1990–2016 [1]

Table 1 SO<sub>x</sub> emission factors (for power plants) [3]

Energy source	Sulphur content (% of fuel weight)	Thermal content (MJ/kg)	SO <sub>x</sub> emission factor (g/GJ)
Residual fuel oil	3	43	1395
Distillate fuel oil	0.3	45	135
Natural Gas	0.002	51	1

For liquids and gaseous fuels  $r$  is assumed to be zero. SO<sub>x</sub> emission factors for selected fuels are presented in Table 1.

The higher the sulphur content of the fuel, the greater the SO<sub>x</sub> emission. The fuels used until now in maritime transport were characterized by a much higher sulphur content than those used in road transport (the sulphur content of fuels used in trucks or passenger cars must not exceed 0.001%). To improve air quality and protect the environment, the maximum sulphur content of marine fuels was reduced outside the SECA zone (Sulphur Emission Control Areas) to 0.5% m/m (mass by mass) from 3.5% (on January 1, 2020), according to MARPOL 73/78 (the International Convention for the Prevention of Pollution from Ships, 1973 as modified by the Protocol of 1978) (Fig. 2) [4].

SECA zone includes the Baltic Sea area (as defined in regulation 1.11.2 of Annex I), the North Sea (as defined in regulation 5(1)(f) of Annex V); and any other sea area, including port areas, designated by the Organization in accordance with the criteria and procedures set forth in appendix III to Annex VI [4]. To meet the requirements for sulphur oxide reduction, some flag States have accepted and approved exhaust gas cleaning systems (scrubbers). From the 1st of March 2020, only vessels with

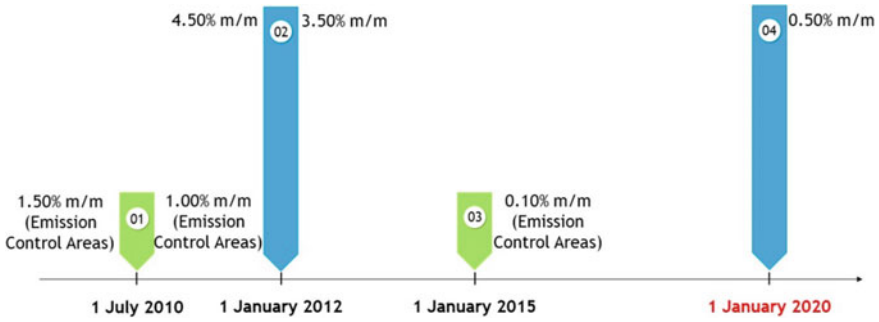


Fig. 2 Maximum sulphur content of fuel oil used on board ships [4]

SO<sub>x</sub> scrubbers are allowed to carry fuel with sulphur content higher than 0.50% in their fuel tanks.

## 2 Marine Fuels

The amendment to the regulations on limiting sulphur content has resulted in the following categories of marine fuel [5, 6]:

- Distillate marine fuels (DM),
- Residual marine fuels (RM),
- Ultra-low sulphur fuel oil (ULSFO), sulphur max 0.10%:
  - (a) ULSFO-RM ultra-low sulphur fuel oil, residual properties (heating required),
  - (b) ULSFO-DM ultra-low sulphur fuel oil, distillate properties (no heating required),
- Very-low sulphur fuel oil (VLSFO), sulphur max 0.50%:
  - (a) VLSFO-RM very-low sulphur fuel oil, residual properties (heating required),
  - (b) VLSFO-DM very-low sulphur fuel oil, distillate properties (no heating required),
- Low-sulphur fuel oil (LSFO), sulphur max 1.00%, (heating required),
- High-sulphur fuel oil (HSFO), sulphur above 1.00% (m/m), (heating required),
- other like LNG or biofuels.

ULSFO are mostly neat distillates, but also hybrids—gas oil blended with residual oil. This type of fuel works well with standard engine configurations, however, it may require operational changes (e.g., resulting from relatively low viscosity levels of distillates) [7]. An example of relatively low viscosity, low-density fuel oil with good ignition properties is Shell’s ULSFO (Table 2), designed to be utilized by engines rated to use ISO 8217 residual fuels [8].

**Table 2** Shell's ULSFO properties [9]

Properties	Value
Density (kg/m <sup>3</sup> )	790–910
Viscosity at 50 °C (mm <sup>2</sup> /s)	10–60
CCAI	800
Sulphur (mass %)	<0.1
Flash (°C)	>60
Hydrogen sulphide (mg/kg)	<2
Acid number (mg KOH/g)	<0.5
Total sediment accelerated (mass %)	0.01–0.05
Total sediment potential (mass %)	0.01–0.05
Carbon residue (mass %)	2
Pour point (°C)	18
Water (vol.%)	0.05
Ash (mass %)	0.01

Very-low sulphur fuel oil is the fuel obtained by blending suitable residual refineries products with low sulphur distillates (Table 3). These blends can contain up to 40% residue. Still, their sulphur content is below the 0.50% threshold [7]. They can potentially be hypersensitive to mixing with other fuels on board. The 0.50%-sulphur fuel is the most widely used group of fuels. There are more and more commercial products on the market, which requires much greater attention to aspects of storage, handling, treatment and combustion.

**Table 3** DMA (marine-distillate class A) fuel properties [10]

Properties	Value
Density at 15 °C (max.) (kg/m <sup>3</sup> )	890
Viscosity at 40 °C (mm <sup>2</sup> /s)	2–6
Cetane index (min.)	40
Sulphur (max.) (mass %)	1
Flash (min.) (°C)	60
Hydrogen sulphide (max.) (mg/kg)	2
Acid number (max.) (mg KOH/g)	0.5
Carbon residue (max.) (mass %)	0.3
<i>Pour point</i> (max.) (°C)	
Winter quality	–6
Summer quality	0
Water (max.) (vol.%)	–
Ash (max.) (mass %)	0.01
Lubricity (max.) (µm)	520

Low-sulphur fuel oil from 1 January 2020 can be used only on ships equipped with scrubbers. An example of the characteristics of such fuel is given in Table 3.

The industry uses marine gas oil (MGO) as a trade term, distinguishing between two types:

- LS MGO (sulphur content  $\leq 0.10\%$ )/ECA Fuel,
- HS MGO (sulphur content  $> 0.10\%$ )/Global Fuel.

Marine gas oil consists exclusively of distillates, usually of a blend of various distillates. Because of the lowest sulphur content, such fuel can be used in EU ports or Emission Control Areas, and marine gas oil is still one of the most preferred clean fuel used on ships. The properties of commercial HS MGO are listed in Table 4.

**Table 4** HS MGO properties [11]

Properties	Value
Density at 15 °C (max.) (kg/m <sup>3</sup> )	860
Viscosity at 40 °C (mm <sup>2</sup> /s)	1.5–6
Cetane index (min.)	50
Sulphur (max.) (mass %)	0.2
Flash (min.) (°C)	60
Carbon residue (max.) (mass %)	0.2
<i>Pour point</i> (max.) (°C)	
Winter quality	–6
Summer quality	0
Water (max.) (vol.%)	–
Ash (max.) (mass %)	0.01

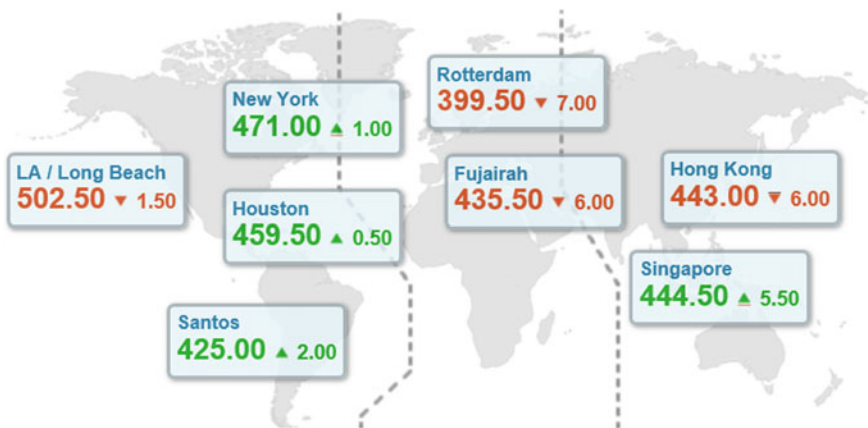


**Fig. 3** VLSFO prices, \$/mt (as of March 6, 2020) [12]



Fig. 4 MGO prices, \$/mt (as of March 6, 2020) [12]

Figures 3 and 4 show the prices of two most commonly used types of fuel, depending on the region of the world. Price differences between the ports are significant, and the MGO price reaches even 35% higher than VLSFO.

### 3 Fuel Properties Versus Ship's Technical Capabilities

Wide variability of fuel formulations resulted in differences in their properties, that is:

- viscosity,
- density,
- lubricity,
- cold flow densities,
- ignition quality.

Maritime companies have noticed a problem related to the properties of new fuel mixtures before the new regulations came into force. Particularly noteworthy is the study by MAN Energy Solutions [13]. In addition, the study of fuels indicates that the reduction of sulphur and aromatic hydrocarbons leads to a significant deterioration in the tribological properties of the fuel [14]. Typical problems that require attention include the storage conditions. Fuels that are not compatible should be stored separately. Particular care should also be given to the fuel cleaning process. The highest suitable temperature and the lowest possible flow in the separators should be used. This will ensure efficient cleaning and maximum removal of cat fines.

Fuel systems need to be flexible and simple, making the fuel changing easier. During fuel switching, temperature and viscosity should be monitored (max. 2 °C/min). Because the viscosity may vary from low distillate range to high residual

range, the engine's high-pressure fuel pumps must be able to operate on fuels with varying viscosities [13].

The recommended marine fuels should be characterized by minimum viscosity for distillate grades: 2 cSt at 40 °C and cat fines (Al + Si) content limited to 60 ppm.

### 3.1 Stability and Compatibility of Fuel

According to ISO 8217:2017, fuels must be stable. The stability of a fuel is defined in terms of its potential to change its condition during storage and use. As far as the residual marine fuel is concerned, its chemical composition depends upon the source of the crude oil and the manufacturing processes. The residual fuel, however, includes asphaltenes, resins and liquid hydrocarbons, generally referred to as asphaltenes [15]. This term covers a wide range of heavier hydrocarbon structures, the exact constituents being dependent on the crude source and choice of blend stocks.

If the asphaltenes cannot be retained in their suspended (colloidal) state, they will drop out as sludge (sticky and highly viscous), and the fuel becomes unstable (Fig. 5). Asphaltenes precipitation can be considered in three aspects:

- stability: the fuel as supplied,
- compatibility: the ability of two fuels forming a stable mix when commingled,
- stability reserve: a measure of the ability of an oil to maintain asphaltenes in a dispersed state and prevent flocculation of the asphaltenes [5].

Using unstable fuels on ships may result in:

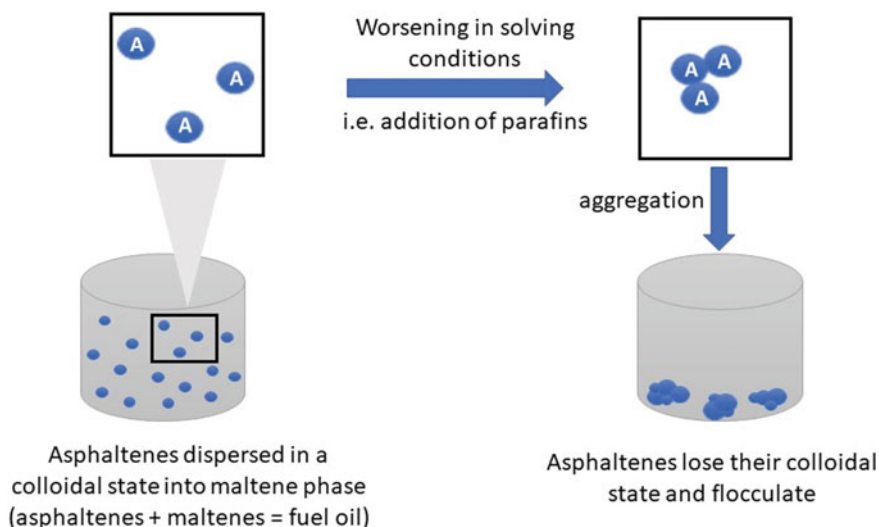


Fig. 5 Asphaltene precipitation process [5]



**Table 5** Typical fuel type characteristic, where high: ●●●●●●, low: ● [13]

Properties	General data	HSHFO	VLSFO (0.5%S)	DMA	ULSFO-RM	Parafinic type	Aromatic type
Sulphur (%)	0–3.5	Up to: ●●●●●●	●●	●	●	●●	●●
Density (kg/m <sup>3</sup> ) at 15 °C	800–1010	●●●●●●	●●●●●●	●	●●	●●	●●●●●●
Viscosity, cSt at 50 °C	2–700	●●●●●●	●●●●●●	●	●●	●●	●●●●●●
Pour point (°C)	–15 to +40	●●	●●	●	Up to: ●●●●●●	Up to: ●●●●●●	●●
Cat fines: Al + Si (ppm)	0–60–80 (++)	●●●●	up to: ●●●●●●	●	●●	●	Up to: ●●●●●●
Combustability	n.a.	●●●●	●●●●	●●●●●●	●●●●●●	●●●●●●	●●
Stability	n.a.	●●●●●●	●●●●●●	●●●●●●	●●●●●●	●●●●●●	●●●●●●
Compatibility (mixability)	n.a.	●●	●●	●●	●	●	●●●●

- clogging of filters, separators and pipes,
- overloaded fuel pumps,
- problems with ignition and combustion,
- permanent damage to pistons, piston rings and cylinder liners,
- shutdown of the main and auxiliary engines (in extreme cases) [13].

Compatibility, when referring to a blend of two fuels, means that the composition remains stable (i.e., precipitation process does not occur). Despite components being individually stable, the component fuels may still be incompatible. Incompatibility arises as a consequence of lack of stability reserve and changes to the solvency of the continuous phase for the asphaltenes [16].

To identify what kind of fuels are received by a port, its crew is equipped with tools like the Certificate of Quality (COQ) given by suppliers or a rough guideline in a tabular form (Table 5).

## 4 New Doubts Related to the Use of Low Sulphur Fuels

Incompatibility and stability are not the only doubts associated with the introduction of new marine fuels. Currently, most concerns are raised in relation to the blending of very-low sulphur fuels. Environmental protection organizations point out that the issue with this group of fuels is that it is a source of black carbon. According to MEPC 75/5/5, 'low-sulphur fuel blends created to comply with the 2020 sulphur cap contain high proportions of aromatic compounds, in a range between 70 and 95%. On

combustion, these fuels resulted in an increase in BC emissions of 10–85% compared to HFO and 67% to 145% compared to DMA (the highest quality distillate fuel, along with DMZ, that is normally supplied for marine)’ [17]. According to the global oil and gas industry association (IPECA) and International Bunker Industry Association (IBIA), these claims are based on flawed assumptions about the nature of the fuels that are expected to come on the market. VLSFO on average are more paraffinic in nature than the high-sulphur fuel oils that they are replacing [18]. The emerging doubts are not based on in-depth research. Nevertheless, consideration should be given to introducing new provisions to the MARPOL convention. IPECA and IBIA, taking into account environmental safety, suggest the following regulations should be considered:

- ‘amend MARPOL Annex VI to prohibit the use of low-sulphur heavy fuel oil blends that increase BC emissions; and
- adopt a resolution, covering the period up until the above restriction comes into effect, calling on all shipowners, charterers, Member States and fuel providers to observe a voluntary prohibition on the use of any marine fuel whose aromatic content is likely to lead to BC emissions greater than those commonly associated with distillate fuels’ [18].

## 5 Conclusions

For existing vessels, VLSFO is the best choice, since it does not require introducing technical changes (installing of exhaust gas cleaning systems). The advantage of VLSFO over MGO results from a significant price difference. The increasing number of fuel types, in particular their blends, can increase problems related to the incompatibility of mixtures. Different fuels should be segregated on board, and their tanks and fuel treatment lines should be designed to work independently to reduce the risk of instability and incompatibility that may occur when mixing two types of fuel.

The coming years will show if reducing the sulphur content of marine fuel reduced global sulphur oxide emissions. They will also allow to identify any problems that may arise. Supporting good practices, both among fuel suppliers and the crew, will enable the correct operation of fuel systems, minimizing any possible losses.

## References

1. Eurostat: Air pollution statistics—emission inventories. [https://ec.europa.eu/eurostat/statistics-explained/index.php?title=Air\\_pollution\\_statistics\\_-\\_emission\\_inventories&oldid=447076#Sulphur\\_oxides](https://ec.europa.eu/eurostat/statistics-explained/index.php?title=Air_pollution_statistics_-_emission_inventories&oldid=447076#Sulphur_oxides). Last accessed 3 Mar 2020
2. Schraufnagel, D.E., Balmes, J.R., Cowl, C.T., De Matteis, S.: Air pollution and noncommunicable diseases: a review by the Forum of International Respiratory Societies’ Environmental Committee, Part 1: the damaging effects of air pollution. *Chest* **155**(2), 409–416 (2019)

3. Complainville, Ch., Martins, J.O.: Organisation for Economic co-operation and development. Economics Department Working Papers No. 151. NO<sub>x</sub>/SO<sub>x</sub> Emissions and carbon abatement. OCDE/GD(94)125, Paris (1994)
4. IMO, Revised MARPOL Annex VI, MEPC 58/23/Add.1, Regulations for the prevention of air pollution from ships (2008)
5. CIMAC Guideline: Marine fuel handling in connection to stability and compatibility. 2019-01 (1st ed.)
6. IMO: Resolution MEPC.320(74), Guidelines for consistent implementation of the 0.50 sulphur limit under MARPOL Annex VI (2019)
7. Alfa Laval: Marine fuels in the low-sulphur era. <https://www.alfalaval.com/industries/marine-transportation/marine/oil-treatment/fuel-line/marine-fuels-in-the-low-sulphur-era/>. Last accessed 3 Mar 2020
8. ISO 8217:2017 Petroleum products - Fuels (class F) - Specifications of marine fuels
9. Shell Trading & Supply: Marine fuels. [https://www.shell.com/business-customers/marine/fuel/ulsfo/\\_jcr\\_content/par/textimage.stream/1473174550832/63227b468f3b14843b50e01f fec2d1af1f667bd2/typical-properties-shell-ulsfo.PDF](https://www.shell.com/business-customers/marine/fuel/ulsfo/_jcr_content/par/textimage.stream/1473174550832/63227b468f3b14843b50e01f fec2d1af1f667bd2/typical-properties-shell-ulsfo.PDF). Last accessed 3 Mar 2020
10. ExxonMobil: Marine distillate fuel. <https://www.exxonmobil.com/en-GQ/Commercial-Fuel/pds/GL-XX-ExxonMobil-Marine-Distillate-Fuel>. Last accessed 3 Mar 2020
11. Steaua Romana Refinery: [http://www.omnimpex.ro/texte/petroliere/engleza\\_07/MARINE%20%20GAS%20OIL%20\(MGO\).pdf](http://www.omnimpex.ro/texte/petroliere/engleza_07/MARINE%20%20GAS%20OIL%20(MGO).pdf). Last accessed 2 Mar 2020
12. World Bunker Prices: <https://shipandbunker.com>. Last accessed 6 Mar 2020
13. MAN Energy Solution: Detailed information on preparation and operation on fuels with maximum 0.50% sulphur, [http://www.tribocare.com/pdf/2020/man\\_2020\\_fuels.pdf](http://www.tribocare.com/pdf/2020/man_2020_fuels.pdf). Last accessed 2 Mar 2020
14. Szczepanek, M.: Biofuels as an alternative fuel for West Pomeranian fishing fleet. IOP Conf. Ser. J. Phys. Conf. Series 1172 (2019)
15. Mullins, O.: The asphaltenes. *Ann. Rev. Anal. Chem.* **4**, 393–418 (2011)
16. Joint Industry Guidance: The supply and use of 0.50%-sulphur marine fuel (2019)
17. MEPC 75/5/5: The need for urgent action to stop the use of blended very low sulphur fuels leading to increases in ship-source Black Carbon globally (FOEI, WWF, Pacific Environment and CSC)
18. MEPC 75/5/7: The nature of Very Low Sulphur Fuel Oils and their potential impact on Black Carbon emissions (IPIECA and IBIA)

# Effect of Build Bed Location on Density and Corrosion Properties of Additively Manufactured 17-4PH Stainless Steel



Rachel Johnson, I. S. Grech, N. Wint, and N. P. Lavery

**Abstract** Additive manufacture (AM) has revolutionized the manufacturing industry by developing a method of manufacture that allows for rapid prototyping, increased design freedom, and flexible production. Despite this, additively manufactured components exhibit a greater susceptibility to corrode. The corrosion properties of additively manufactured 17-4PH stainless steel (SS) are explored in this paper as a function of build bed location. A combination of advanced electrochemical techniques and density measurements has been used to determine this effect. All additively manufactured parts tested in this paper underwent corrosion via a localized pitting mechanism, and the degree of corrosion appears to be independent of build bed position. A key finding from this paper pertains to the variation in component density with build bed position, which is proposed to be related to the distance from powder distribution.

## 1 Introduction

### 1.1 Introduction and Literature Review

Additive manufacture (AM) involves the production of components on a layer-by-layer material deposition basis, offering the freedom to design net shapes of high specific strength out of a variety of metallic materials. A benefit of rapid prototyping processes, such as AM, is the ability to create complex 3D geometries that could not be traditionally manufactured [1]. This technology has a variety of uses within the

---

R. Johnson (✉)

College of Engineering, Swansea University, Swansea, UK

e-mail: [rachellouisejohnson@yahoo.co.uk](mailto:rachellouisejohnson@yahoo.co.uk)

I. S. Grech · N. P. Lavery

Future Manufacturing Research Institute, College of Engineering, Swansea University, Swansea, UK

I. S. Grech · N. Wint

Materials Research Centre, College of Engineering, Swansea University, Swansea, UK

© The Editor(s) (if applicable) and The Author(s), under exclusive license to Springer Nature Singapore Pte Ltd. 2021

S. G. Scholz et al. (eds.), *Sustainable Design and Manufacturing 2020*, Smart Innovation, Systems and Technologies 200, [https://doi.org/10.1007/978-981-15-8131-1\\_38](https://doi.org/10.1007/978-981-15-8131-1_38)

aerospace, automotive, and medical industries [1] making it a highly beneficial area for research.

Powder bed fusion (PBF) systems make use of a bed of powder in the build chamber which is melted layer by layer. A typical schematic for laser powder bed fusion (LPBF) has been included in Fig. 1 detailing the direction of laser orientation, gas flow, and powder distribution in relation to the build bed. In Fig. 1's schematic, the laser scans across the build bed to melt the powder and the direction of this defines the 'scan pattern.' 'Laser scan speed' determines the speed the beam moves at.

Point distance (PD), hatch spacing (HS), and exposure time (ET) that can also be altered to have an impact on finished components characteristics. Figure 2 defines PD and HS on a typical scan pattern, where light blue dots indicate the scan pattern of the laser beam. PD is the distance between the center of the laser beam spots; HS is the center-point distance between melt lines. ET is the period in which the laser is on, and the power is the chosen value for laser power.

Once solidified the melted layer is lowered and a new powder layer distributed on top. The manufacturing process typically takes place in an inert gas atmosphere, which fills or flows over the build bed [2]. Using inert gas is essential to the AM

Fig. 1 LPBF schematic

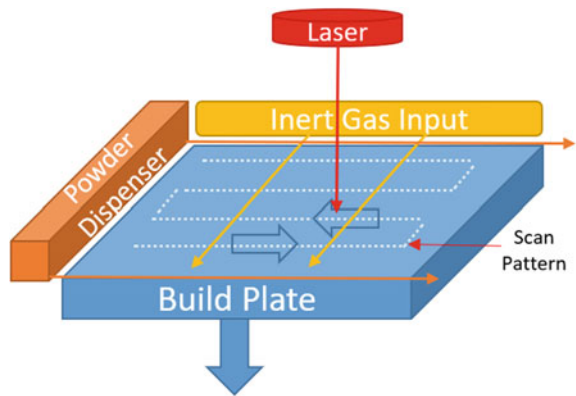
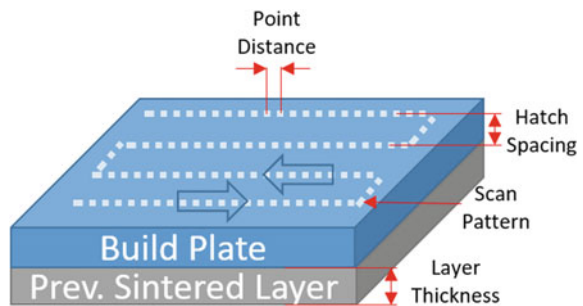


Fig. 2 Variable process parameters schematic



process, as metal powders can oxidize when exposed to air, particularly, at higher temperatures [3].

There are many process parameters that can be varied during LPBF, ultimately resulting in changes in the properties of the final component. Energy density, (1) [4], is a common metric used for defining properties of additively manufactured materials. Laser beam diameter is the size of the laser beam being used during the LPBF process.

$$\text{Energy Density} = \text{Laser Power}/(\text{Laser Scan Speed} * \text{Laser Beam Diameter}) \quad (1)$$

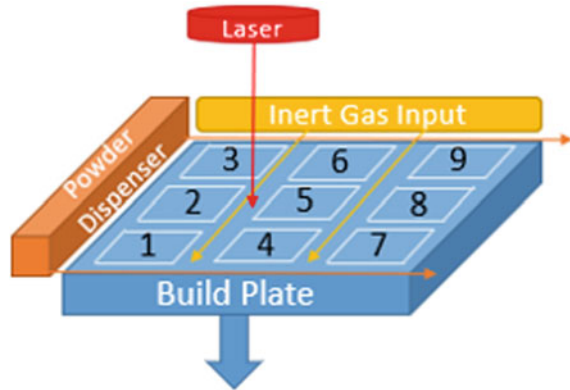
For AM components to be widely used in service, certain key properties and their performance must be understood. Corrosion performance may be more variable when compared to wrought material due to the higher prevalence of porosity in AM components. The susceptibility of AM components to corrode tends to increase with increasing porosity levels, and some porous printed parts have been shown to exhibit stable corrosion pit growth [5]. Corrosion can lead to a reduction in mechanical properties and eventual component failure. Notably, for use in low-pressure turbine blades, corrosion pits are common sites for fatigue crack initiation [6].

Much of the research conducted into the corrosion of AM components has found porosity to be a key indicator of corrosion susceptibility [5]. One such parameter which may affect the porosity, and therefore, the corrosion performance is the flow of inert gas within the build chamber. The flow of inert gas can spread dislodged spatter across the build bed onto previously melted areas which then become reheated due to this spatter [7]. This spatter can be further dislodged during the keyhole welding regime of the AM process. The keyhole welding regime is where the melt pool becomes far deeper and narrower, and a melt channel is formed around the laser beam. This results in a plume of gas being released from the part [8]. Philo et al. [9] created computational models to simulate gas flow which allows for characterization of spatter accumulation and visualization of fluid flow in the build chamber, accurately representing this particle expulsion. Additionally, Mindt et al. [10] developed a computational platform to enable the origin of several LPBF defects, such as spatter, to be explained.

Many research papers have evaluated the correlation between build parameters and resulting corrosion characteristics. However, with such an uptake of AM, it is important that all potential corrosion enablers are tested to evaluate performance and reliability. This research paper will focus on the novel investigation of corrosive behavior of LPBF 17-4PH SS with respect to build bed location and inert gas flow. Both density and electrochemical characteristics will be investigated as a function of build bed location. This work will be the starting point for the creation of a knowledge repository for optimized build bed location, to minimize corrosion of components built via LPBF.

**Table 1** AM 17-4PH SS chemical composition

Element AM	Iron	Chromium	Nickel	Copper	Manganese	Carbon	Si, Nb, Mo, N, O, P, S
Weight percentage	Balance	16–17	3.5–4.5	1 (max)	1 (max)	0.07 (max)	<1

**Fig. 3** 3 × 3 build bed array

## 2 Materials and Methodology

### 2.1 Materials

The chemical composition of the AM 17-4PH SS powder can be found in Table 1.

The Renishaw AM 400 was used for manufacture and was run in an argon atmosphere. The build bed was sectioned into 9 blocks, with a 3 × 3 alphabetical (A-I) cube array in each block, as shown in Figs. 3 and 4.

Build parameters varied between the alphabetical cubes, see Table 2, and these parameters were kept constant in each block. For example, cube 1.A will be produced using the same build parameters as cube 2.A, 3.A, etc. Volumetric energy density (VED) was calculated, and values above/below this were given to each cube.

### 2.2 Density Measurements

Density measurements were conducted using a One Attention Sigma 700/701 force tensiometer using Archimedes Principle. Cubes A, C, E, G, and I were tested as the extreme points in each block and were repeated three times. The mass of each cube was measured prior to and after being immersed in distilled water mixed with a surfactant. The change in mass was used to calculate percentage density of the AM cube using (2), and a porosity percentage of the AM component using (3). Finally,

**Fig. 4** Alphabetized cube array [11]



**Table 2** Build parameters for cubes A-I

Sample	Point distance (PD)	Hatch spacing (HS)	Exposure time (ET)	Power (W)	Energy density (J/mm <sup>3</sup> )
A	60	60	60	180	60
B	60	80	90	215	80.625
C	60	100	120	250	100
D	80	60	90	250	93.75
E	80	80	120	180	67.5
F	80	100	60	215	32.25
G	100	60	120	215	86
H	100	80	60	250	37.5
I	100	100	90	180	32.4

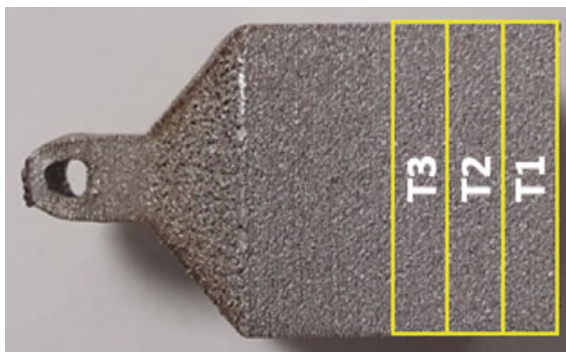
a percentage density was calculated using (4), comparing the density of theoretical conventionally manufactured (CM) density of 17-4PH SS, and the measured AM density of 17-4PH SS.

$$\rho_{AM\ Cube} = (\rho_{water} - (T_{water} - 20) * (0.00025)) \frac{M}{\Delta M} \tag{2}$$

$$Porosity = 100 * \left( 1 - \frac{\rho_{AM\ Cube}}{\rho_{Theoretical\ CM}} \right) \tag{3}$$

$$Density\ Comparison = 100 - Porosity \tag{4}$$



**Fig. 5** Cube slice sections

### 2.3 Potentiodynamic Scan

The cubes were cut into thin sections—T1 (final printed layer), T2, and T3, as shown in Fig. 5.

These samples were then mounted and polished to a 1  $\mu\text{m}$  mirror finish to keep appropriate consistency between samples. The samples were masked to reveal a smaller surface area and set up in a three electrode configurations consisting of a platinum counter electrode, a saturated calomel electrode (SCE), and working electrode which were immersed in a 1% NaCl electrolyte solution. A scan rate of 0.1667 mV/s was used. Prior to all scans, a 30-min electrolyte exposure allowed for electrode stabilization. The electrolyte was deaerated by sufficiently purging it with nitrogen, as was the surrounding atmosphere. Some scans were limited to one repeat due to sample surface defects.

## 3 Results

### 3.1 Density Measurements

Average density measurements were taken for each block to understand any general effect that builds bed location may have on density. Table 3 shows this in an arrangement reflecting the build bed gas flow and powder distribution. Lowest average

**Table 3** Average block density

Average build bed density (%)			
Block 1, 2, 3	98.90 ( <i>SD 1.26</i> )	99.81 ( <i>SD 1.61</i> )	99.90 ( <i>SD 1.69</i> )
Block 4, 5, 6	99.62 ( <i>SD 1.52</i> )	100.32 ( <i>SD 1.48</i> )	100.38 ( <i>SD 1.56</i> )
Block 7, 8, 9	97.43 ( <i>SD 3.16</i> )	98.69 ( <i>SD 2.41</i> )	96.50 ( <i>SD 2.48</i> )

**Table 4** Average density per cube showing build parameter impact

Cube	A	C	E	G	I
Av density (%)	99.93	100.40	100.50	98.79	95.85
Std dev	0.87	1.61	1.03	2.34	1.94

block density appears in blocks 7, 8, and 9 which were furthest away from powder distribution. The standard deviations (SD) are highest in blocks 7, 8, and 9.

Table 4 shows the average density for the cubes tested. Cube I’s parameters lead to the lowest density, and cube E’s parameters lead to the highest density.

Table 4 shows cube G with the greatest density variation between blocks which led to it being analyzed via potentiodynamic scans. Any findings here can be linked to build bed location as cube G has the same build parameters across the bed.

### 3.2 Potentiodynamic Scans

The highest/lowest density values for cube G were used in these scans—3.G and 9.G, respectively. Tables 5, 6, 7, 8, 9, and 10 document the data from these scans including pitting potential ( $E_{pit}$ ) and repassivation potential ( $E_{prot}$ ).  $E_{pit}$  is the potential at which the sample begins stable pit growth on the forward scan [12].  $E_{prot}$  is the potential whereby any active pits formed will repassivate on the reverse scan [12], however, this point may not always occur if, for example, pits were never formed or if the samples never repassivate. Both the  $E_{pit}$  and  $E_{prot}$  voltage (V) and current density

**Table 5** 3.GT1 potentiodynamic scan data, including repeats

Sample	$E_{pit}$ (V versus SCE)	$E_{pit}$ current density (A/cm <sup>2</sup> )	$E_{prot}$ (V versus SCE)	$E_{prot}$ current density (A/cm <sup>2</sup> )	$E_{pit}-E_{prot}$ (V)
3.GT1-1	0.006	3.26E-6	/	/	/
3.GT1-2	0.019	6.70E-5	-0.125	5.79E-5	0.144
3.GT1-3	0.021	1.10E-6	/	/	/
Std dev	0.007	3.06E-5	/	/	/

**Table 6** 3.GT2 potentiodynamic scan data, including repeats

Sample	$E_{pit}$ (V versus SCE)	$E_{pit}$ current density (A/cm <sup>2</sup> )	$E_{prot}$ (V versus SCE)	$E_{prot}$ current density (A/cm <sup>2</sup> )	$E_{pit}-E_{prot}$ (V)
3.GT2-1	0.053	2.11E-5	/	/	/
3.GT2-2	0.389	3.93E-7	/	/	/
3.GT2-3	0.117	2.96E-7	/	/	/
Std Dev	0.146	9.78E-6	/	/	/

**Table 7** 3.GT3 potentiodynamic scan data, including repeats

Sample	$E_{\text{pit}}$ (V versus SCE)	$E_{\text{pit}}$ current density ( $\text{A}/\text{cm}^2$ )	$E_{\text{prot}}$ (V versus SCE)	$E_{\text{prot}}$ current density ( $\text{A}/\text{cm}^2$ )	$E_{\text{pit}} - E_{\text{prot}}$ (V)
3.GT3-1	0.023	2.39E-4	-0.061	3.15E-4	0.084
3.GT3-2	0.060	6.67E-6	-0.140	2.50E-6	0.200
3.GT3-3	0.105	1.71E-3	-0.020	1.26E-3	0.125
Std dev	0.034	7.54E-4	0.050	5.35E-4	0.048

**Table 8** 9.GT1 potentiodynamic scan data, including repeats

Sample	$E_{\text{pit}}$ (V versus SCE)	$E_{\text{pit}}$ current density ( $\text{A}/\text{cm}^2$ )	$E_{\text{prot}}$ (V versus SCE)	$E_{\text{prot}}$ current density ( $\text{A}/\text{cm}^2$ )	$E_{\text{pit}} - E_{\text{prot}}$ (V)
9.GT1-1	0.022	3.14E-5	-0.300	1.63E-6	0.322
9.GT1-2	0.026	1.40E-5	-0.268	5.11E-5	0.294
Std Dev	0.002	8.70E-6	0.016	2.47E-5	0.014

**Table 9** 9.GT2 potentiodynamic scan data, including repeats

Sample	$E_{\text{pit}}$ (V versus SCE)	$E_{\text{pit}}$ current density ( $\text{A}/\text{cm}^2$ )	$E_{\text{prot}}$ (V versus SCE)	$E_{\text{prot}}$ current density ( $\text{A}/\text{cm}^2$ )	$E_{\text{pit}} - E_{\text{prot}}$ (V)
9.GT2-1	0.018	5.11E-6	/	/	/
9.GT2-2	0.089	2.38E-6	/	/	/
Std dev	0.036	1.37E-6	/	/	/

**Table 10** 9.GT3 potentiodynamic scan data, including repeats

Sample	$E_{\text{pit}}$ (V versus SCE)	$E_{\text{pit}}$ current density ( $\text{A}/\text{cm}^2$ )	$E_{\text{prot}}$ (V versus SCE)	$E_{\text{prot}}$ current density ( $\text{A}/\text{cm}^2$ )	$E_{\text{pit}} - E_{\text{prot}}$ (V)
9.GT3-1	0.057	3.61E-6	/	/	/
9.GT3-2	0.083	2.57E-4	-0.265	6.08E-5	0.348
9.GT3-3	0.085	1.42E-3	-0.144	5.34E-4	0.229
Std dev	0.013	6.16E-4	0.061	2.37E-4	0.060

( $\text{A}/\text{cm}^2$ ) values have been included in Tables 5, 6, 7, 8, 9, and 10 as well as the difference in these values.

### 4 Discussion

Using Table 3 as an indicator of density variation across the build bed, the lowest density percentages were located in the blocks 1, 4, 7, 8, and 9. These five blocks are positioned at the furthest point away from gas flow and powder distribution. This suggests that this positioning may have a negative impact on density properties, and therefore, indicate porosity differences, of AM parts build with the same VED. This lower density value could be due to dislodged spatter negatively impacting nearby parts. When setting up a build, the manufacturer must be aware of the potential issues caused by spatter and place parts accordingly. More specifically, for the parts printed in the blocks further away from the powder distribution, there could be an insufficient spread of powder. This could be mitigated by fine-tuning build parameters to increase powder dosage, or by using a powder with better flow.

Cube I exhibited the lowest density percentages compared to cube E with the highest density percentages, however, this may be attributed to the build parameters for these cubes rather than the build bed location. Table 5 shows the average density percentages for cubes A, C, E, G, and I clearly showing this trend.

Tables 5, 6, 7, 8, 9, and 10 show the data gathered from potentiodynamic scans of all samples, including pitting potential, repassivation potential, current densities at both these points, and the difference between  $E_{pit}$  and  $E_{prot}$ . Figures 7, 8, 9, 10, and 11 show this potentiodynamic scan data represented as voltage versus SCE (V) against current density ( $A/cm^2$ ) graphs. Figure 6 shows porosity against the  $E_{pit}$  voltages for all samples and slices, and sample of scans conducted are displayed in Figs. 7, 8, 9, 10, and 11. Figure 6 shows the variation in pitting potential for cube 3.G is far greater than that for cube 9.G. As cube 3.G is closer to the powder distribution, this suggests that there is a higher variability in pitting potential when components are printed closer to the powder distribution. For this to be determined as a pattern, additional tests will be essential.

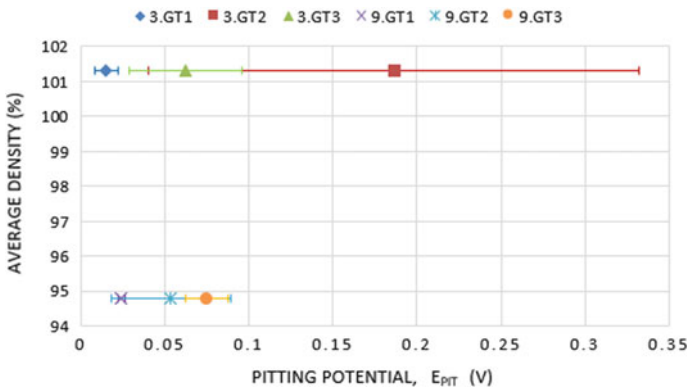


Fig. 6 Average density versus pitting potential

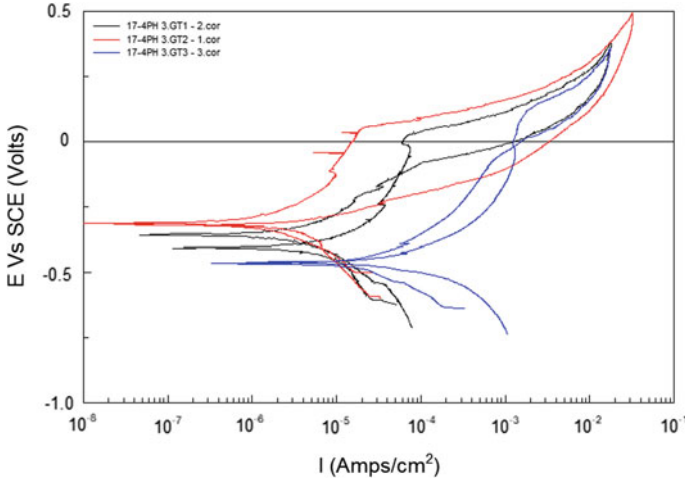


Fig. 7 Scan data for cube 3.GT1, T2, T3

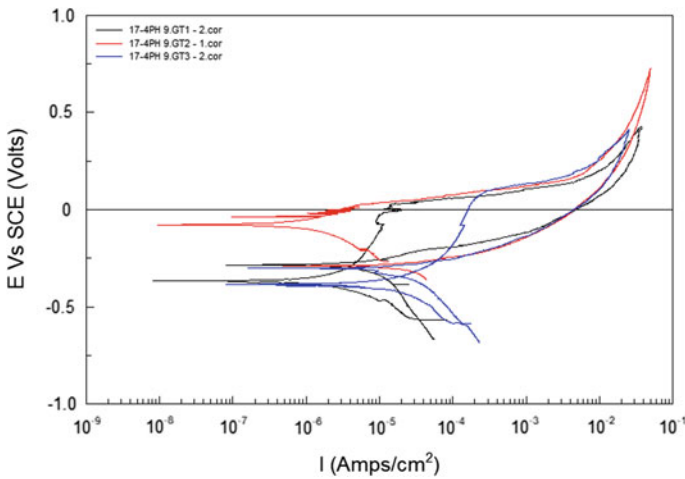


Fig. 8 Scan data for cube 9.GT1, T2, T3

Figure 7 shows the potentiodynamic scans for cube 3.G at all slice intervals, T1, T2, and T3. There is an increase in  $E_{pit}$  voltage as the depth into the sample increases—T1 being the surface of the cube and T3 being closer to the center of the cube. Despite this, the variation in this data is too great to draw any significant conclusions from. Each sample exhibits a differing size hysteresis loop, and Table 6 shows none of the 3.GT2 samples repassivate. The  $E_{prot}$  values do not exhibit any significant relationship.

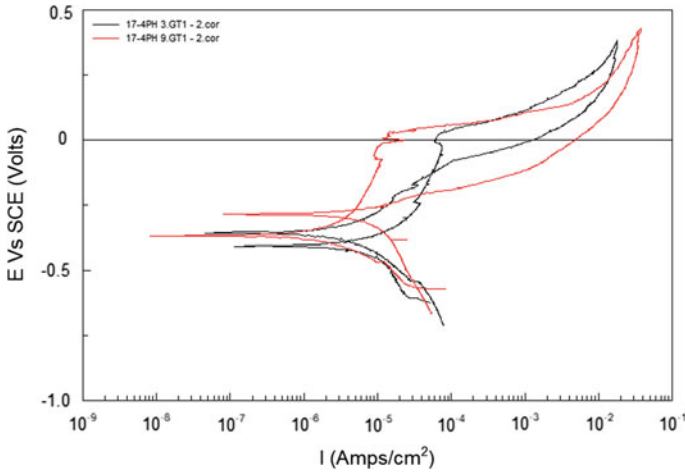


Fig. 9 Scan data for cube 3.GT1 and 9.GT1

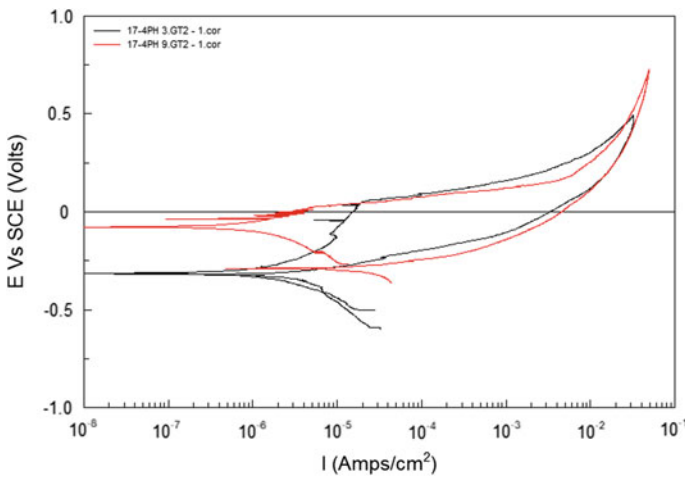
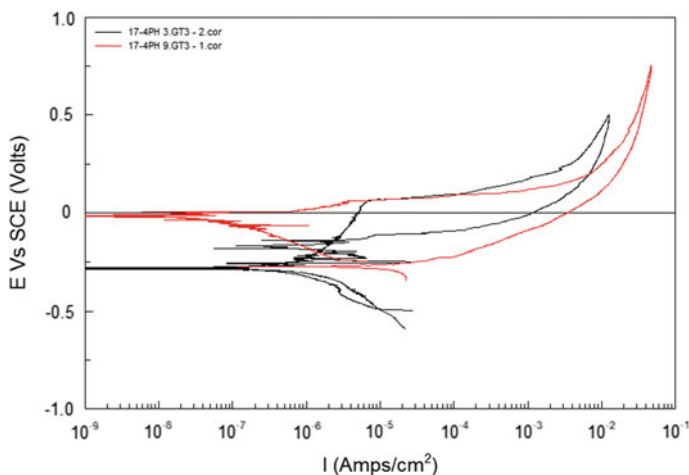


Fig. 10 Scan data for cube 3.GT2 and 9.GT2

Similarly, Fig. 8 shows the potentiodynamic scan data for cube 9.G at T1, T2, and T3. Here, the  $E_{pit}$  voltage values are all similar, 0.026, 0.018, and 0.083 V versus SCE for slice T1, T2, and T3, respectively; yet, they exhibit no trend based on depth into the cube suggesting the trend seen for cube 3.G was coincidental and not reproducible. This demonstrates that there is a large variation in printed parts due to the random nature of porosity distribution, even parts with high densities. For the samples as shown in Fig. 8, only the 9.GT1-2 and 9.GT3-2 repassivated and the  $E_{prot}$  values for the repassivation voltage and current densities are very similar. The  $E_{prot}$  voltages and current densities exhibit a standard deviation of  $1.5E-3$  and  $4.85E-6$ , respectively,



**Fig. 11** Scan data for cube 3.GT3 and 9.GT3

demonstrating very closely matched data points. This similarity in data is not reflected by the 3.G sample. Furthermore, for all the 9.G samples that repassivated, the  $E_{\text{pit}} - E_{\text{prot}}$  values are significantly larger than those for the 3.G samples as shown in Tables 5, 6, and 7. This suggests that cube 9.G may experience greater passive film disruption and therefore difficulty restoring the passive film [12]. This passive film disruption could be influenced by build bed location, cube 9.G could experience far greater spatter causing irregularities in the passive layer due to additional heat input from the spatter particles. This disruption could also be related to powder distribution as cube 9.G is situated at a far greater distance from the powder spread than cube 3.G.

From Fig. 9, Tables 5 and 8 show pitting potential occurs at very similar voltages for samples 3.GT1-2 and 9.GT1-2, 0.019, and 0.026 V versus SCE, respectively. The  $E_{\text{pit}} - E_{\text{prot}}$  value is larger in the 9.GT1-2 sample compared to the 3.GT1-2 sample. The hysteresis loops are vastly different, 9.GT1-2 having the larger loop, suggesting cube 9.G experiences a greater passive film disruption compared to cube 3.G.

From Tables 6 and 9, the  $E_{\text{pit}}$  voltages for samples 3.GT2-1 and 9.GT2-1 were seen to be 0.053 and 0.018 V versus SCE, respectively, and  $2.11\text{E}-5$  and  $5.11\text{E}-6$  A/cm<sup>2</sup>. While this data presented is similar, and it is not repeatable. Cube 3.GT2's  $E_{\text{pit}}$  voltage had the greatest standard deviation for any cube tested at 0.146. No relationship can be drawn here between the  $E_{\text{prot}}$  values or  $E_{\text{pit}} - E_{\text{prot}}$  as both the samples do not repassivate.

Figure 11 shows the potentiodynamic scan data for samples 3.GT3-2 and 9.GT3-1, which follows the trend of  $E_{\text{pit}}$  values for both samples being similar. The  $E_{\text{pit}}$  voltage values for samples 3.GT3-2 and 9.GT3-1 are 0.06 and 0.057 V versus SCE, respectively, and  $6.67\text{E}-6$  and  $3.61\text{E}-6$  A/cm<sup>2</sup> for current density values. No link can be drawn between the hysteresis loops as only the 3.GT3-2 sample repassivates.

It is noted that none of the sample slices exhibited clear regions of metastable pit growth. With no clear region of metastable pit growth this could suggest that once localized corrosion has initiated, pitting immediately follows. If this were to happen, there would be little chance of repassivation for the AM parts where comparatively the conventionally manufactured parts could repassivate.

## 5 Conclusion

Parts printed at a greater distance from powder distribution will exhibit reduced density due to insufficient powder spread. There is a link between pitting potential ( $E_{pit}$ ) and build bed location. Parts printed further away from powder distribution will exhibit larger hysteresis loops, and therefore greater passive film disruption. The printed cubes exhibit a significant lack of uniform porosity through the depth of the cube irrespective of build bed location.

## 6 Future Consideration

Future work should consider how porosity distribution varies across build bed, specifically variation in size, volume, aspect ratio, and porosity distribution. As 17-4PH SS is a heat-treatable alloy, research could explore how different heat treatments affect porosity, and whether this process could improve corrosion performance. It should be expected that changes in microstructure would occur from heat treatment. Heat treatment cycles could include vacuum heat treating or hot isostatic pressing (HIP).

**Acknowledgements** The author would like to acknowledge the enthusiasm and support of Dr. Natalie Wint, Professor Nicholas Lavery, and Iwan Grech of Swansea University. Their passion, guidance, and expertise imparted throughout this project were vital to its completion.

## References

1. Hague, R., Campbell, I., Dickens, P.: Implications on design of rapid manufacturing. Proc IMechE, Part C: J Mech. Eng. Sci. **217**, 25–30 (2003)
2. Sander, G., Tan, J., Balan, P., Gharbi, O., Feenstra, D., Singer, L., et al.: Corrosion of additively manufactured alloys: a review. Corrosion **74**(12), 1318–1350 (2018)
3. Sames, W., List, F., Pannala, S., Dehoff, R., Babu, S.: The metallurgy and processing science of metal additive manufacturing. Int. Mater. Rev. **61**(5), 315–360 (2016)
4. Guo, Q., Zhao, C., Qu, M., Xiong, L., Escano, L., Hojjatzadeh, S., et al.: In-situ characterization and quantification of melt pool variation under constant input energy density in laser powder bed fusion additive manufacturing process. Addit. Manuf. **28**, 600–609 (2019)
5. Örnek, C.: Additive manufacturing—a general corrosion perspective. Corros. Eng. Sci. Tech. **53**(7), 531–535 (2018)



6. Schönbauer, B., Stanzl-Tschegg, S., Perlega, A., Salzman, R., Rieger, N., Turnbull, A., et al.: The influence of corrosion pits on the fatigue life of 17-4PH steam turbine blade steel. *Eng. Fract. Mech.* **147**, 158–175 (2015)
7. Sutton, A., Kriewall, C., Leu, M., Newkirk, J., Brown, B.: Characterization of laser spatter and condensate generated during the selective laser melting of 304L stainless steel powder. *Addit. Manuf.* **31**, 100904 (2020)
8. Zhang, M., Chen, G., Zhou, Y., Li, S., Deng, H.: Observation of spatter formation mechanisms in high-power fiber laser welding of thick plate. *Appl. Surf. Sci.* **280**, 868–875 (2013)
9. Philo, A., Butcher, D., Sillars, S., Sutcliffe, C., Sienz, J., Brown, S. et al.: CFD Modeling and Simulation in Materials Processing 2018, A Multiphase CFD Model for the Prediction of Particulate Accumulation in a Laser Powder Bed Fusion Process. [S.l.]. Springer (2018)
10. Mindt, H., Desmaison, O., Megahed, M., Peralta, A., Neumann, J.: Modeling of powder bed manufacturing defects. *J. Mater. Eng. Perform.* **27**(1):32–43 (2017). GUID=5867ead0780943f3bea1b9301c4628e8&ckck=1
11. Grech, I.: Corrosion performance of additively manufactured invar and 17-4PH. In: Presentation presented at Solid Freeform Fabrication Symposium; Texas (2019)
12. Esmailzadeh, S., Aliofkhaezai, M., Sarlak, H.: Interpretation of cyclic potentiodynamic polarization test results for study of corrosion behavior of metals: a review. *Prot. Metals Phys. Chem. Surf.* **54**(5), 976–989 (2018)

# Control Systems Architecture with a Predictive Identification Model in Digital Ecosystems



Alexander Suleykin and Natalya Bakhtadze

**Abstract** The paper describes basic architectural principals and main control system components using predictive identification models in digital ecosystems. We introduce the architecture for both Time-Driven and Batch-Driven and Alert-Driven modes for configuration of predictive identification models. In our work we discussed the main principals of Digital Ecosystems architecture with Alert-Driven control based on Associative search methods, regarding the main architectural components of each Ecosystem layer and its requirements for stability, reliability and scalability of such systems. In addition, the method of a predictive model development based on Data Mining approach with Associative Search is presented.

## 1 Introduction

Today, the global transformation of commercial production features the switch from hi-tech to digital industry. The popularity of cloud services, additive technologies, IoT, RFID technologies, digital twins, and big data analysis is increasing. Control technologies enabling time savings in decision-making, project implementation and products bringing to market are widely used. Cluster networking with horizontal linkages are predominant. A clear trend is the conversion of branch and intersectoral digital platforms into digital ecosystems enabling new business models, innovations and higher competitiveness [1].

Digital ecosystem means a distributed sociotechnical system featuring adaptive-ness, self-organization, and stability, whose subjects (such as automated systems and economic actors) compete and collaborate for knowledge exchange during the system's evolution [2]. A digital ecosystem operates on the basis of the computer network infrastructure using intelligent control technologies, such as multi-agent technologies [3].

---

A. Suleykin (✉) · N. Bakhtadze

V.a. Trapeznikov Institute of Control Sciences of the Russian Academy of Science, 65  
Profsoyuznaya Street, Moscow 117997, Russia

e-mail: [aless.sull@mail.ru](mailto:aless.sull@mail.ru)

© The Editor(s) (if applicable) and The Author(s), under exclusive license to Springer  
Nature Singapore Pte Ltd. 2021

S. G. Scholz et al. (eds.), *Sustainable Design and Manufacturing 2020*, Smart Innovation,  
Systems and Technologies 200, [https://doi.org/10.1007/978-981-15-8131-1\\_39](https://doi.org/10.1007/978-981-15-8131-1_39)

In the recent 30 years, the model predictive control [4] became the most common control technology for complex large-dimensional processes with nonlinearities, long dead times, and interacting variables. Its key element is a predeveloped mathematical model which is implanted in the control loop. The model is addressed in real time for a plant dynamics forecast which is further used for calculating new control actions.

Tightening requirements to control speed, accuracy, and effectiveness in uncertainty conditions under a wide range of process disturbances highlight the limitation of traditional approaches to the synthesis of automatic control systems. Data mining-based models show the highest potential. Such models with real-time tuning opportunities use the patterns extracted from historical and current data. These patterns form the essence of the term inductive knowledge [5]. To develop an effective process management system within the Digital Ecosystem, a detailed analysis of the functioning and interaction of all systems at all levels of production management is required in order to adequately form the architecture of control models in digital ecosystems, both in Time-Driven and Batch-Driven and Alert-Driven modes. In this paper, we present an approach and architecture for the creation of Digital Ecosystems with control systems engine for industrial complexes based on processing and intellectual analysis of big data and Alert-Driven predictive models.

## 2 Related Work

There are many works presented the Event-Triggered Control for different types of systems. So, in [6] authors present an approach to event triggered model predictive control for discrete-time linear systems. It is shown that the event triggered implementation, in stationarity, is able to keep the state in an explicitly computable set given by the disturbance bound and the event threshold. In [7] it is proposed an event-based sampling policy to implement a constraint-tightening, robust MPC method. The proposed policy enjoys a computationally tractable design and is applicable to perturbed, linear time-invariant systems with polytopic constraints. Authors showed that the triggering mechanism is suitable for plants with no centralized sensory node as the triggering mechanism can be evaluated locally at each individual sensor.

In [8] authors discussed real-time control communication issues and in [9] a finite-horizon linear-quadratic optimal control problem regarded, where only a limited number of control messages are allowed for sending from the controller to the actuator. To restrict the number of control actions computed and transmitted by the controller, authors employ a threshold-based event-triggering mechanism that decides whether or not a control message needs to be calculated and delivered.

In researched related work authors discussed mostly the application of Event-Triggered control for different types of processes, efficiency of their algorithms and provided different simulation results to prove their concepts, stability of the models, the need for application of Event-Triggered approach for control and its benefits. In contrast, in our research we present the concepts of Digital Ecosystems architecture with Alert-Driven intelligent model predictive control. This approach

base on a development of an intelligent real-time predictive models. Corresponding methods named the Associative Search ones use the Knowledge base and clustering techniques for model design at every fixed point in time. The main architectural components of each Ecosystem layer are proposed as well as their requirements for stability, reliability and scalability of such systems.

### 3 Digital Ecosystem Agents and Common Architectural Elements

The full complex production system consists of different levels of data aggregations, transformations and decision making. Each level can be represented using Digital Agent (DA), and all Agents of the system with their interactions between each other and the external environment are Digital Ecosystem. In our research, the Digital Ecosystem for production processes or Energy industry consists of 4 Agents, which represent the autonomous, reliable, scalable, stable and fault-tolerant entity. Each Agent can be represented by subagents and so on, until there is achieved enough abstraction level for some particular use case. The architecture of control systems for a complex plant, which can include industrial production or an electric power system with predictive models that can be configured in real time, should be based on a multi-agent principle [10, 11]. For electric power systems, we can conceptually describe the architecture of such a “typical” network agent as an element of the digital ecosystem:

1. The first level is the equipment of power systems. This level can include substations, power lines, energy distribution centers, etc. At this level, a large amount of data is generated, which is processed and transmitted for analysis to higher levels of the architecture.
2. The second is the level of measurements in real time (Real-time measurements). This level includes measuring systems, as well as parameters and position sensors, which are either elements of the equipment itself, protection and automation systems, or are made in the form of separate measuring systems. Sources of primary information reflect the current state of the equipment of the power unit of electric power systems. Measurements are carried out by various types of sensors: electrical, mechanical, electrochemical, pressure, temperature, radiation, etc. In addition to equipment related to the power circuit, the state of secondary protection and automation systems is monitored: starting and switching relays, blocking systems, protection and automation settings. The sources of primary information also include the measuring part of the systems of commercial and technical accounting and measurement units of parameters recorded by the equipment for recording emergency events.
3. The level of messaging (Message-Oriented Middleware—MoM) is the collection of all data from sensors on one cluster (server group) for a specific autonomous control system (agent)—substation, distribution center, electrical installation,

etc. At this level, it is necessary to separate all data from sensors by streams and provide access to these streams depending on the availability of rights to access measurements. Countless numbers of data consumers—various models, systems, other agents, and other possible interested parties in the consumption of measurement data at a higher level—can be connected to a single message (measurement) flow. Measurement collection should be organized using a special class of messaging systems, which can be characterized as productive, unlimited horizontally scalable, fault tolerant, and reliable. Next, we consider in more detail the architecture of control systems for Time-Driven and Batch-Driven and Alert-Driven configuration modes for the predictive identification model.

#### **4 Control System Architecture for Time-Driven and Batch-Driven Identification Circuit**

Time-Driven and Batch-Driven creation of predictive models is carried out for production control subsystems that do not require real-time mode. Such systems include, in particular, subsystems related to the ERP level. Time-Driven and Batch-Driven Identification Circuit (Offline Identification—OI) should consist of four large subsystems:

- (1) The subsystem of cold data is the main subsystem for storing real data on the functioning of the production system obtained from sensors. It is assumed that all data will be stored on disk in distributed mode, which will provide faster access to data if necessary. If it is needed to retrain the model more often (for example, once every few minutes), then it will be necessary to use solutions with quick access to data—such as column databases, Key-Value, etc. This level is a constantly updated knowledge base for subsequent training and retraining forecast management models. This subsystem should have the characteristics of fault tolerance of data storage, horizontal scalability and distribution.
- (2) The forecasting subsystem serves as the foundation for the formation of control actions.
- (3) Modeling subsystem—here the model is retrained based on the new input data of the real system. Retraining of the model is carried out on the basis of Batch-Driven or Time-Driven approaches. In the first approach, the trigger for retraining is to replenish the knowledge base by a certain number of records or a certain increase in the amount of data (batch). When Time-driven training takes place at pre-configured time intervals (usually from several hours to several days or weeks). After the basic forecasting model has been changed, it is “seamlessly” integrated into the forecasting subsystem, replacing the outdated model.
- (4) Feedback subsystem—directly transfers the control action generated by the regulator (in accordance with the adjusted model) to the object. Feedback data should also be archived and subsequently used to increase the efficiency of forecast models, allowing to find hidden (deep) dependencies in the data (deep learning).

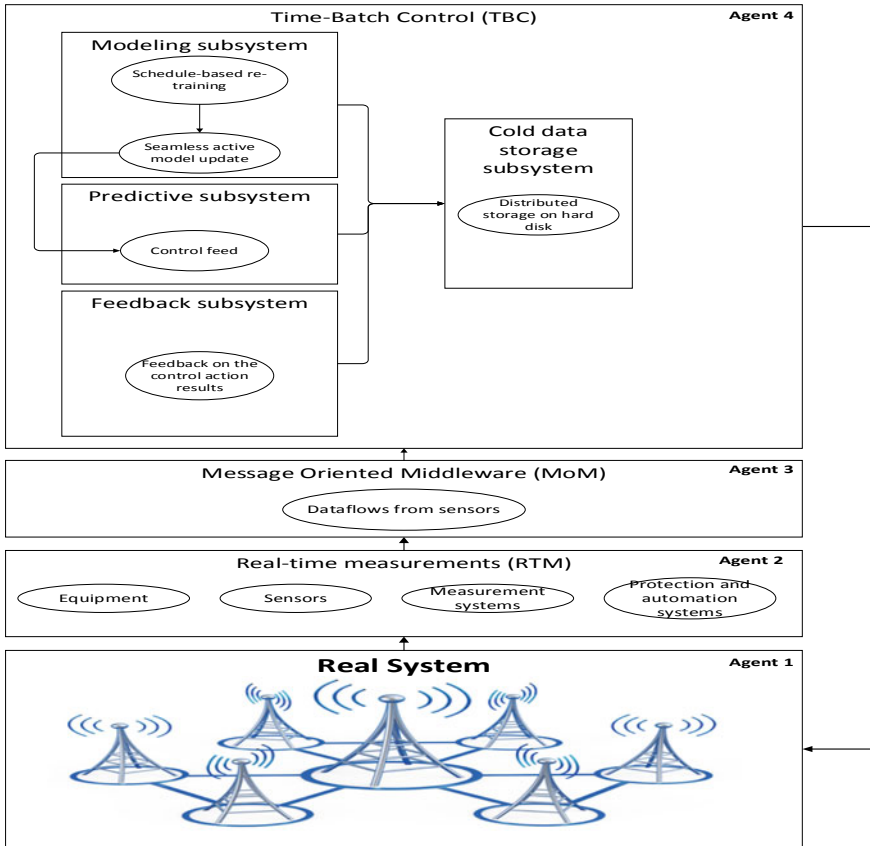


Fig. 1 Time-Driven and Batch-Driven mode for Identification model

Figure 1 shows the architecture of the Time-Driven and Batch-Driven mode.

### 5 Alert-Driven Predictive Models

Alert-Driven identification should be carried out in process control systems (SCADA, DCS) and operational process control (MES). Their main goal is to provide retraining of the model not at strictly defined time intervals (as is done in accordance with the MPC principle—model predictive control), but only if it is necessary to retrain the model—at certain input values.

The Alert-Driven authentication layer should consist of the following subsystems:

- (1) The subsystem of “hot” data—all classes of systems and databases that provide quick access to data for reading and writing. These classes of systems include

NoSQL databases of the Key-value type, In memory databases, timeseries databases and column-oriented databases. Databases of this class must be fault tolerant, horizontally scalable and provide the fastest access to data for reading and writing. This subsystem is necessary for the possibility of retraining models online (or near real time), providing quick access to data. In essence, this is the Online Knowledge Base (OKB), which is formed by accumulating input from a real system. All data from the real system are stored in the online storage system, after which they serve as a source for retraining the model in cases where it is necessary.

- (2) The monitoring subsystem is necessary for the analysis of incoming data flows (input vectors) at a specific time period and signaling if necessary, that at a certain point in time for a given vector of inputs, this model (for example, linear) ceases to satisfactorily predict the output at a given value of the control action. In other words, instead of the traditional model update, the alert principle of model update (Alert-Driven) is applied. All information received is also archived, replenishing the knowledge base—for the subsequent stages of model training.
- (3) The forecasting subsystem makes a forecast of the output (output) and the corresponding parameters of the system model based on the incoming data stream and the working model in a specific time period.
- (4) Alert-Driven modeling subsystem—the main subsystem for maintaining the relevance of the control model based on incoming data streams. In this subsystem, a retraining of the control model in real time (or near real-time) should occur in cases where a signal has arrived about the need for retraining from the monitoring subsystem. Next, a new training of the model in real-time mode takes place, occurring in memory (In Memory) based on quick access to data in the storage subsystem. Based on virtualization technologies, it is possible to dynamically increase the allocated RAM for retraining the model, if necessary, while containerization will allow to separate this subsystem into an independent ecosystem agent for more efficient management of this agent—dynamically allocating the required amount of RAM or memory for storage, if necessary. When the model is retrained, it is necessary to make a “seamless” update of the main model with zero downtime of the active control model. Retrained models enter the prediction subsystem, providing a “seamless” update of active agent.
- (5) The feedback subsystem directly supplies the control action to the control object. This subsystem, in turn, is necessary for the possibility of collecting statistics on the results of applying the current active control model and the subsequent enrichment of the knowledge base for the ability to improve the quality of model creation.

It is also necessary to list the requirements for technologies for retraining the model:

- (a) in memory computing—the ability to perform all calculations in RAM without accessing the hard drive to increase the speed of recalculation of the new model;

- (b) distribution—the ability to perform distributed calculations on a cluster if necessary, depending on the amount of data in the online storage subsystem;
- (c) fault tolerance—in the event of failure of one cluster node, the system must be operational and do not lose the ability to continue recalculating the model;
- (d) the presence of specialized built-in libraries for machine learning—the ability to recalculate the model itself using ready-made solutions;
- (e) horizontal scalability—the ability, if necessary, to increase the performance of model by not only dynamically increasing the RAM and CPU using virtualization tools but also by adding new servers to the cluster.

Figure 2 depicts the Identification model architecture for Alert-Driven mode.

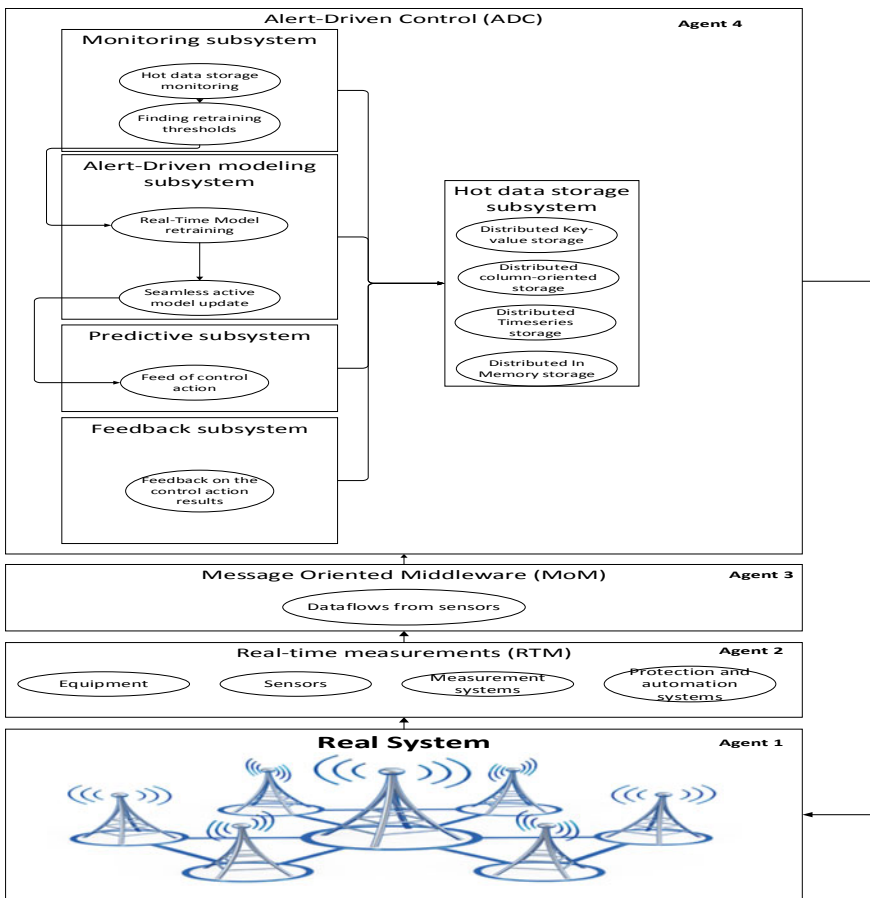


Fig. 2 Alert-Driven mode for Identification model



## 6 Predictive Models Development

It is proposed to develop models based on the knowledge bases and data mining methods as predictive models for systems with an alert control principle. The models described below not only demonstrate high accuracy for various control objects but also the methods of their construction demonstrate very high performance due to the use of clustering techniques.

Regardless of whether the models are retrained offline or online, the models are retrained based on data mining. To identify a variety of nonlinear production processes, associative search methods [12, 13] have demonstrated high efficiency. Algorithms based on knowledge revealed from process history (inductive knowledge, persistently enriched) implement an intelligent approach to construct identification models. The intelligence is applying knowledge (*Knowledge Based*) revealed from historical data on the basis of their analysis (*Data Mining*).

The process of knowledge processing in the intelligent system is reduced to recovering (associative search of) *knowledge* over its fragment. Meanwhile, the *knowledge* may be interpreted as associative connections between *images*. As an image, we will use “sets of indicators,” that are components of input vectors, input variables. The criterion of closeness between images may be formulated in very different manners. In the most general case, it may be a logic function, the predicate. In a particular case, when sets of indicators are vectors in  $n$ -dimensional space, the criterion of closeness may be a distance in this space.

The associative search process may be implemented either as a process of recovering the image over partially given indicators (or recovering a knowledge fragment under the conditions of incomplete information; as a rule, just this process is simulated in different models of the associative memory), or as a process of searching other images that are associatively connected with the given one, respecting to other time instants. In [12], an approach to form the support of decision making on the control is proposed, based on dynamic modeling the associative search procedure. Results of adoption of the associative search algorithms developed by the authors applied for industrial processes of the chemical and petroleum manufacturing, processes of control in intelligent power networks (smart grids), trading processes, transport logistic processes. The method of the *associative search* consists in creating *virtual* predicting models. The method assumes constructing predicting model of a dynamic plant, being new under each  $t$ , by use of a set of history data (“associations”) formed at the stage of learning and adaptively corrected in accordance to certain criteria, rather than approximating real process in the time. Within the present context, linear dynamic model is of the form:

$$y_N = \sum_{i=1}^m a_i y_{N-i} + \sum_{j=1}^{r_s} \sum_{s=1}^S b_{j,s} x_{N-j,s}, \forall j = \overline{1, N}, \quad (1)$$

where:  $y_N$  is the prediction of the plant output at the time instant  $N$ ,  $x_N$  is the vector of input actions,  $m$  is the memory depth in the output,  $r_s$  is the memory depth in the

input,  $S$  is the dimension of the input vectors,  $a_i$  and  $b_{j,s}$  are the tuned coefficient, meanwhile  $x_{N-j,s}$  is selected disregarding the order of the chronological decreasing and has been referred as the *associative pulse*.

Let us note that this model is not classical regression one: there are selected certain inputs in accordance to a certain criterion, rather than all chronological “tail.” The algorithm of deriving the virtual model consists in constructing at each time instant an approximating hypersurface of the space of input vectors and single-dimensional outputs. To construct a virtual model, corresponding to a certain time instant, from the archive, there are selected input vectors being in a certain sense close to the current input vector. Again, by use of classical (non-recursive) least squares (LS) method, there is determined the output value (modeled signal) in the next time instant. Meanwhile, each point of the global nonlinear surface of the regression is formed in the result of using linear “local” models, in each new time instant. Unlikely to classical regression models, for each fixed time instant from the process history, there are selected input vectors being close to the current input vector in the sense of a certain criterion (rather than the chronological sequence as it is done in regression models). Thus, in Eq. (1)  $r_s$  is the number of vectors from the archive (from the time instant 1 to the time instant  $N$ ), selected in accordance to the *associative search criterion*. At each time segment  $[N - 1, N]$ , there is selected a certain set of  $r_s$  vectors,  $1 \leq r_s \leq N$ . Under the assumptions that the input actions meet the Gauss–Markov conditions, the estimates obtained via the LS method are unbiased and statistically effective. To study the dynamics of non-stationary processes, associative search algorithms in the frequency domain were proposed using wavelet analysis [14]. In [15], the conditions for the approach of parameter values to critical boundaries are presented, including, using these methods, a possible approximation to the stability boundaries and transition to chaotic dynamics is predicted. The system approach to the investigation of multi-agent systems is effectively exemplified in representation of such objects as *multimodal* ones. Their multimodality appears both in the decomposition of the production process into independent stages (phases) and in the study of various operation modes as control objects.

In both cases, the extended state vector  $[x_{k1}^1 \dots x_{km}^1 \dots x_{kM}^1 \dots x_{k1}^s \dots x_{km}^s \dots x_{kM}^s \dots x_{k1}^S \dots x_{km}^S \dots x_{kM}^S]$  is used to describe the plant where the index  $k$  denotes a time point of discrete system operation,  $s$  is the number of mode (step, phase),  $m$  is the number of the input vector’s component. Values of some components of the state vector for various modes may be constant, in particular, zero. The operability of multi-agent systems can be treated as their stability with a multi-agent system being considered as a complex dynamical system [15]. The paper presents the techniques ensuring the stability of a multi-agent relay transportation control system as of a non-stationary dynamical system.

## 7 Conclusion

In this paper, we have proposed to use different architecture principles for application Identification models in digital ecosystems. According to the use case, Time-Driven and Batch-Driven, or Alert-Driven approaches for retraining the Identification model should be used. While Time-Driven and Batch-Driven mode is carrying out at particular periods of time or after predefined amount of input data (batch), Alert-Driven mode for retraining the model is occurring only after special signals that came from the monitoring subsystem. All defined subsystems, in essence, are agents in our multi-agent environment (digital ecosystem), where these agents are dwelling as a totally autonomous entity. The proposed requirements for such systems architecture rely on stability, reliability, and scalability of components.

A predictive model for the system is developed on the base of intelligent algorithms using associative search methods, which have already shown the high efficiency in forecasting and can be used as a core engine for prediction and retraining the model. The proposed architecture is sustainable and follows the concept of environmental sustainability through the main properties of each architectural element and its reliability. In essence, subsystems are reliable and fault tolerant with automatic failover of any compute node. At the same time, a robust predictive algorithm based on system production knowledge and learning will quickly respond to a changing situation. In accordance to the forecast, an adequate control recommendation will be created. Therefore, a devastating environmental impact on production facilities or nature is excluded. The authors suggest further research in the synthesis of model predictive control algorithms for digital ecosystems based on the models of the proposed type.

It is planned to regard the problem of data fusion, investigate the Digital Twins capabilities; add external ecosystem as a part of current architecture and describe its role; deeper analyze predictive subsystem and ensure sustainable digital ecosystem development.

## References

1. Chang, E., West, M.: Digital ecosystems: a next generation of the collaborative environment. In: Proceedings of 20th International Conference on Information Integration and Web-based Applications and Services (iiWAS 2006), pp. 3–24 (2006)
2. Dong, H., Hussain, F.K., E. Chang.: An integrative view of the concept of digital ecosystem. In: Proceedings of the Third International Conference on Networking and Services. Washington, DC, USA, IEEE Computer Society, pp. 42–44 (2007)
3. Senyo, P.K., Liu, K., Effah, J.: Understanding behaviour patterns of multi-agents in digital business ecosystems: an organisational semiotics inspired framework. In: In book: Advances in Human Factors, Business Management and Society. Springer, Cham (2018). [https://doi.org/10.1007/978-3-319-94709-9\\_21](https://doi.org/10.1007/978-3-319-94709-9_21)
4. Qin, S.J., Badgwell, T.A.: MPC. 4th generation. MPC. Fig. 1 Approximate genealogy of linear MPC algorithms. *Contr. Eng. Pract.* **11**, 733–764 (2003)
5. Vapnik, V.N.: *Statistical Learning Theory*. Wiley, New York (1998)

6. Lehmann, D., Henriksson, E., Johansson, K.: Event-triggered model predictive control of discrete-time linear systems subject to disturbances. In: 2013 European Control Conference, ECC 2013, pp. 1156–1161 (2013). <https://doi.org/10.23919/ecc.2013.6669580>
7. Sharifi, A., Bregman, S., Esfahani, P., Keviczky, T.: A Decentralized Event-Based Approach for Robust Model Predictive Control (2018)
8. Baillieul, J., Antsaklis, P.J.: Control and communication challenges in networked real-time systems. *Proc. IEEE* **95**, 9–28 (2007)
9. Demirel, B., Ghadimi, E., Quevedo, D., Johansson, M.: Optimal control of linear systems with limited control actions: Threshold-based event-triggered control. *IEEE Trans Contr Netw Syst* (2017). <https://doi.org/10.1109/tcns.2017.2701003>
10. Bakhtadze, N., Lototsky, V., Yadykin, I., Maximov, E.: Multi-agent technologies in stability control of multimodal large-scale energy network. *IFAC-PapersOnLine* **7**(1), 1067–1072 (2013)
11. Bakhtadze, N., Lototsky, V., Yadykin, I., Sakrutina, E.: Multi-agent approach to design of multimodal intelligent immune system for smart grid. *IFAC-PapersOnLine* **7**(1), 1164–1169 (2013)
12. Bakhtadze, N., Kulba, V., Lototsky, V., Maximov, E.: Identification-based approach to soft sensors design. In: Proceedings of IFAC Workshop of Intelligent Manufacturing Systems. Alicante, Spain, pp. 86–92 (2007)
13. Bakhtadze, N., Sacrutina, E., Jharko, E.: Predictive associative search models in variable structure control systems. *WSEAS Trans. Mathem.* **15**, 407–419 (2016)
14. Bakhtadze, N., Sacrutina, E.: Applying the multi-scale wavelet-transform to the identification of non-linear time-varying plants. *IFAC-PapersOnLine* **49**(12), 1927–1932 (2016)
15. Georgé, J.-P.: Making self-organizing adaptive multi-agent systems work—towards the engineering of emergent multi-agent systems. In: Bergenti, F., Gleizes, M.-P., Zambonelli, F. (eds.) *Methodologies and Software Engineering for Agent Systems*, pp. 321–340. Springer, New York (2004)

# Research on the Green Evaluation System of Manufacturing Process



Pengcheng Yan, Gang Zhao, Na Zhang, Xin Huang, Xiaolong Luo, and Shujun Yu

**Abstract** In view of the current domestic most of the problems of “three highs” iron and steel enterprise, to comprehensive multi-level evaluation of iron and steel enterprise, contribution rate of the resources and the environment, this paper proposes a process for manufacturing iron and steel enterprise based on gray correlation analysis method of the green evaluation method, to systematically study the greening level of iron and steel enterprise. First, according to the manufacturing process of iron and steel enterprises, a multi-level green evaluation index system is established, and then the actual production data in the enterprise is processed using the gray correlation analysis method to obtain the optimal values and build a matrix. According to the gray system theory, the gray correlation coefficient matrix is calculated, and finally according to the size of the correlation, green sex compared to the enterprise. In this paper, an example is applied to make an empirical study on this method. The results show that this method is effective and can provide an objective scientific basis for the green evaluation of iron and steel enterprises.

---

P. Yan

Key Laboratory of Metallurgical Equipment and Control Technology of Ministry of Education, Wuhan University of Science and Technology, 430081 Wuhan Hubei, China

G. Zhao

Hubei Key Laboratory of Mechanical Transmission and Manufacturing Engineering, Wuhan University of Science and Technology, 430081 Wuhan Hubei, China

N. Zhang (✉) · X. Huang · X. Luo

Wuhan Boiler Group Valve Co., Ltd., 430223 Wuhan Hubei, China  
e-mail: [404957525@qq.com](mailto:404957525@qq.com)

S. Yu (✉)

Evergande School of Management, Wuhan University of Science and Technology, 430081 Wuhan Hubei, China  
e-mail: [yushujun@wust.edu.cn](mailto:yushujun@wust.edu.cn)

## 1 Introduction

The steel manufacturing industry is characterized by multiple inputs and multiple outputs, with a long production cycle and a large consumption of resources and energy. Steel manufacturing life cycle process will consume a lot of material resources and produce a lot of waste and pollutants. Currently, the negative impact of steel enterprises on the environment exceeds 10% of the total industrial volume [1]. To solve these problems, this paper introduces the gray correlation analysis method, based on the manufacturing process of iron and steel enterprises to study system of green, in order to explore some of the problems existing in the iron and steel enterprises in the production process. Its production process is analyzed and improved, and for the green evaluation of the manufacturing process in iron and steel enterprises to provide effective reference.

Under the circumstance that the reduction of resources, energy, and ecological problems has attracted much attention, many scholars have studied and built an evaluation system related to the environmental performance and industrial planning of steel enterprises [2–4] and carried out systematic green analysis and evaluation of steel enterprises from the perspective of ecological industry. However, taking the manufacturing process of steel enterprises as the starting point, the utilization and recycling of resources and energy, the treatment of wastes and pollutants, the negative impact on the environment as a whole, and the research on the establishment of a multi-level evaluation index system are not much. According to the production data of three steel enterprises, Zhao [5] evaluated and analyzed the green index by using the radar chart statistical method. Through experimental research, Min [6] established the evaluation model of equipment-related time, performance, cost, resources, environmental evaluation index system, and data envelope method. Yang [7] conducted a comprehensive study on the environmental performance of typical steel enterprises on the basis of establishing the basic theory of multi-factor environmental ecological assessment system. Through the research and analysis of the above scholars, it is found that most of the evaluation results and the actual situation there is a gap. Based on the gray system theory, the gray correlation analysis method compares the correlation degree of the evaluation objects according to the similarity or difference degree between the evaluation factors from a quantitative perspective. This method is not only simple and feasible, but also better overcomes the shortcomings of traditional greenness evaluation of steel enterprises [8] and improves the accuracy of greenness evaluation of steel enterprises. In this paper, based on the gray correlation method, the evaluation index system matrix is established to analyze the greenness of four steel enterprises and calculate their correlation degree. So as to evaluate the greenness of enterprises and make intelligent judgment to a certain extent, so as to realize the greenness analysis of steel enterprises and improve the greenness level of steel enterprises.

## 2 The Research Methods

Gray correlation analysis is a new systematic evaluation method used to compare and judge the pros and cons of different schemes [9]. First of all, the optimal index was found among the indexes of many evaluation schemes, and all the optimal indexes and scheme indexes were summarized to obtain the gray correlation coefficient matrix. Then, all the indexes were normalized, and the similarity degree between the evaluation scheme and the optimal scheme was compared, analyzed, and calculated, and the similarity degree was used as the judgment criterion of the correlation degree.

The mathematical model of gray relational analysis is as follows:

$$R = E \times W \tag{1}$$

where  $R = (r_j, I = 1, 2, \dots, m)$  is the result vector of comprehensive judgment of  $m$  objects being evaluated;  $W (w_j = 1, 2, \dots, n)$  is the weight distribution vector of  $n$  evaluation indicators:

$$\sum_{j=1}^{n=1} w_j = 1 \tag{2}$$

$E$  is the judgment matrix of each index:

$$E = \begin{bmatrix} \varepsilon_1(1) & \varepsilon_1(2) & \dots & \varepsilon_1(m) \\ \varepsilon_2(1) & \varepsilon_2(2) & \dots & \varepsilon_2(m) \\ \dots & \dots & \dots & \dots \\ \varepsilon_m(1) & \varepsilon_m(2) & \dots & \varepsilon_m(m) \end{bmatrix} \tag{3}$$

At last, the correlation degree  $R$  is judged and sorted, according to the advantages and disadvantages of the scheme.

### 2.1 Determine the Optimal Index $F^*$

Set:

$$F^* = \{j_1^*, j_2^*, \dots, j_n^*\} \tag{4}$$

Type,  $j_k^* (k = 1, 2, \dots, n)$  is the optimal value of the KTH index. In practice, the optimal value may have two possible situations: (1) the larger the value, the better; (2) the smaller the value, the better. Then, the optimal value is calculated according to the actual situation. At the same time, when selecting the optimal value, factors

such as feasibility, cost, and benefit should be taken into account, and the evaluation results should be in line with the reality to the maximum extent.

After selecting the optimal index value, matrix  $D$  can be constructed:

$$D = \begin{bmatrix} j_1^* & j_1^* & \dots & j_n^* \\ j_1^1 & j_2^1 & \dots & j_n^1 \\ \dots & \dots & \dots & \dots \\ j_1^m & j_2^m & \dots & j_n^m \end{bmatrix} \tag{5}$$

where  $j_k^*$  is the actual data of indicator  $k$  in scheme  $i$ .

### 2.2 Normalization of Index Values

Because of the differences among the evaluation indexes, it is impossible to analyze them directly. In order to make the analysis, results have high feasibility, each initial index is normalized. Let  $[j_{k1}, j_{k2}]$  be the change interval of the KTH index, where  $j_{k1}$  and  $j_{k2}$  are the lower limit and upper limit, respectively, in the above interval in all schemes. Then, the following formula can be used to normalize the initial value in the above formula:

$$C_k^i \in (0, 1) \tag{6}$$

The bigger, the better type:

$$C_k^i = \frac{j_k^j - j_{k1}}{j_{k2} - j_{k1}} (i = 1, 2, \dots, m; k = 1, 2, \dots, n) \tag{7}$$

The smaller, the better type:

$$C_k^i = \frac{j_{k2} - j_k^j}{j_{k2} - j_{k1}} (i = 1, 2, \dots, m; k = 1, 2, \dots, n) \tag{8}$$

So  $D$  goes to  $C$

$$C = \begin{bmatrix} C_1^* & C_2^* & \dots & C_n^* \\ C_1^1 & C_2^1 & \dots & C_n^1 \\ \dots & \dots & \dots & \dots \\ C_1^m & C_2^m & \dots & C_n^m \end{bmatrix} \tag{9}$$



### 2.3 Gray Relational Coefficient Matrix

Will  $\{C^*\} = \{C_1 \text{ and } C_2^*, \dots, C_n^*\}$  as the reference sequence,  $\{C\} = \{C_{1i}, C_{2i}, \dots, C_{ni}\}$  as the standard sequence, then the correlation coefficient of the index  $k$  of scheme  $I$  and its optimal index are calculated, namely:

$$\varepsilon_i(k) = \frac{\min_i \min_k |C_k^* - C_k^i| + \rho \max_i \max_k |C_k^* - C_k^i|}{|C_k^* - C_k^i| + \rho \max_i \max_k |C_k^* - C_k^i|} \tag{10}$$

where  $\rho \in [0, 1]$ , generally take  $\rho = 0.5$ .

### 2.4 Calculate the Correlation Degree of Each Index

From the formula of  $I(k)$ ,  $E$  can be obtained as follows:  $R = E \times w$ , that is:

$$r_i = \sum_{k=1}^n W(k) \times \varepsilon_i(k) \tag{11}$$

The calculated correlation degree result  $r_i$  is sorted according to the size. If the calculated value of the scheme is larger, it means that it is closer to the optimal scheme. According to the advantages and disadvantages of the degree of the program order, the best program is very intuitive.

## 3 Construct the Green Evaluation Index System

Due to the complexity of steel life cycle manufacturing process, the establishment of a systematic green evaluation index system for steel enterprises needs to consider many factors. We should not only improve the utilization of resources and energy in the manufacturing process, but also reduce the negative impact on the ecological environment. The green evaluation indexes of steel enterprises can be summarized as follows: water consumption ( $C_1$ ), energy consumption ( $C_2$ - $C_6$ ), resource consumption ( $C_7$ - $C_{11}$ ), liquid consumption ( $C_{12}$ - $C_{15}$ ), gas consumption ( $C_{16}$ - $C_{21}$ ), and solid consumption ( $C_{22}$ - $C_{24}$ ). Based on the characteristics of the production process of iron and steel enterprises, specific performance indicators reflect the energy and resource utilization of enterprises and the impact of emissions on the ecosystem [10]. The construction of green evaluation index system of iron and steel enterprises is shown in Table 1.

According to the value of the data, the green evaluation index can be divided into two types: the bigger the better, and the smaller the better. The value of each

**Table 1** Green evaluation indicators score of three iron and steel enterprises

Index term	A iron and steel enterprises	B iron and steel enterprises	C iron and steel enterprises	D iron and steel enterprises
(C <sub>1</sub> ) new amount of water per ton of steel	3.632	3.773	3.982	4.011
(C <sub>2</sub> ) energy consumption in coking process of ton steel	123.313	108.000	120.230	128.330
(C <sub>3</sub> ) energy consumption in sintering process of ton steel	54.180	55.540	51.870	56.560
(C <sub>4</sub> ) energy consumption in pelletizing process of ton steel	30.75	25.002	20.02	22.620
(C <sub>5</sub> ) energy consumption in iron smelting process per ton steel	417.51	430.32	387.45	420.330
(C <sub>6</sub> ) energy consumption in steelmaking process of ton steel converter	500	508	487	501
(C <sub>7</sub> ) fuel ratio of blast furnace	294.390	321.41	348.09	350.213
(C <sub>8</sub> ) blast furnace coke ratio	160.633	166.08	158.99	157.221
(C <sub>9</sub> ) coal ratio of blast furnace	36.181	45.09	41.87	43.78
(C <sub>10</sub> ) the ratio of two energy generation to total electricity consumption.	2.542	2.841	1.874	2.050
(C <sub>11</sub> ) tons of iron ore consumption	10.003	15.301	42.74.	30.822
(C <sub>12</sub> ) discharge of waste water per ton of steel	1.510	1.493	1.712	1.631

(continued)

**Table 1** (continued)

Index term	A iron and steel enterprises	B iron and steel enterprises	C iron and steel enterprises	D iron and steel enterprises
(C <sub>13</sub> ) reutilization rate of production water	97.400	97.600	96.800	96.300
(C <sub>14</sub> ) COD emissions per ton of steel	0.0411	0.0733	0.0884	0.0852
(C <sub>15</sub> ) ammonia nitrogen emissions per ton of steel	0.0081	0.0072	0.0124	0.0103
(C <sub>16</sub> ) SO <sub>2</sub> emissions per ton of steel	1.411	1.721	0.972	1.122
(C <sub>17</sub> ) NO <sub>x</sub> (NO <sub>2</sub> ) emission per ton steel	1.1	1.5	0.76	1.36
(C <sub>18</sub> ) CO <sub>2</sub> emissions per ton of steel	1.91	2.03	1.89	2.01
(C <sub>19</sub> ) utilization rate of blast furnace gas	97.9	98.3	97.2	97.8
(C <sub>20</sub> ) utilization ratio of coke oven gas	97.110	99.302	95.611	97.222
(C <sub>21</sub> ) heat recovery of converter gas in ton steel	25	29	19	21
(C <sub>22</sub> ) recovery and utilization of iron dust (mud)	99.	100	100	98
(C <sub>22</sub> ) recovery and utilization of iron dust (mud)	99	100	99	97
(C <sub>24</sub> ) utilization ratio of converter slag	98	100	92	94

indicator will have stable dynamic changes under the actual production conditions of the enterprise, and most of the data will fluctuate up and down within a specified value range. In order to ensure the reliability of the green evaluation results, it is necessary to process the indicator data. Take a group of actual data of a single index of an enterprise in a certain month for research. Through MATLAB, the data were processed to obtain the actual fitting curve  $g(x)$  of a single index in the manufacturing process. According to the definition of integral, set the integrand function as  $g(x)$ , the curve of the integral function corresponds to the maximum and minimum values of the  $x$ -coordinate (number of days), as the upper and lower limits of the integral, and the integral gets a result (that is, the area of the fitted curve). Then, divide the integral result by the difference between the upper and lower limits of the interval to get the result as the judgment value of the evaluation index.

$$\frac{\int_{x_b}^{x_a} g(x)dx}{x_a - x_b} = H \quad (12)$$

where  $g(x)$  is the fitting curve,  $x_a$  is the first day of a month,  $x_b$  is the last day of the same month, and  $H$  is the judgment value of green level of a single indicator.

## 4 Case Analysis

In this paper, four representative iron and steel enterprises are selected and their greenness level is analyzed with the gray correlation analysis method. Firstly, the actual data related to their production are selected, and then the actual data are calculated after the above processing, as shown in Table 1.

According to the actual index values of the four enterprises, the gray correlation coefficient method is applied to evaluate their greenness. The main process is as follows:

- A. The evaluation index system matrix  $D$  is established. According to the data in Table 1, for each specific index (reserved to two decimal places). From the data of each enterprise to be evaluated, an optimal index is selected in turn, among which indexes C11, C19, C20, C21, C22, C23, and C24 are the larger and the better, and the remaining indexes are the smaller and the better, as shown in Eq. (13).

$$D = \begin{bmatrix} 3.63 & 108.00 & 51.87 & 20.02 & 387.45 & 487 \\ 3.63 & 123.31 & 54.18 & 30.75 & 417.51 & 500 \\ 3.77 & 108.00 & 55.54 & 25 & 430.32 & 508 \\ 3.98 & 120.23 & 51.87 & 20.02 & 387.45 & 487 \\ 4.01 & 128.33 & 56.56 & 22.62 & 420.33 & 501 \end{bmatrix}$$

$$\begin{matrix}
 294.39 & 157.22 & 36.18 & 1.87 & 42.74 & 1.49 \\
 294.39 & 160.63 & 36.18 & 2.54 & 10 & 1.50 \\
 321.41 & 166.08 & 45.09 & 2.84 & 15.3 & 1.49 \\
 348.09 & 158.99 & 41.87 & 1.87 & 42.74 & 1.71 \\
 350.21 & 157.22 & 43.78 & 2.05 & 30.82 & 1.63 \\
 \\
 96.3 & 0.041 & 0.007 & 0.97 & 0.76 & 1.89 \\
 97.4 & 0.041 & 0.008 & 1.41 & 1.1 & 1.91 \\
 97.6 & 0.073 & 0.007 & 1.72 & 1.5 & 2.03 \\
 96.8 & 0.088 & 0.012 & 0.97 & 0.76 & 1.89 \\
 96.3 & 0.085 & 0.010 & 1.12 & 1.36 & 2.01 \\
 \\
 98.3 & 99.30 & 29 & 100 & 100 & 100 \\
 97.9 & 97.11 & 25 & 99 & 99 & 98 \\
 98.3 & 99.30 & 29 & 100 & 100 & 100 \\
 97.2 & 95.61 & 19 & 100 & 99 & 92 \\
 97.8 & 97.22 & 21 & 98 & 97 & 94
 \end{matrix} \quad (13)$$

B. According to Eqs. (7) and (8), the evaluation indicator matrix is normalized, as shown in Eq. (14):

$$C = \begin{bmatrix}
 1 & 1 & 1 & 1 & 1 & 1 \\
 1 & 0.25 & 0.51 & 0 & 0.30 & 0.38 \\
 0.63 & 1 & 0.22 & 0.54 & 0 & 0 \\
 0.08 & 0.40 & 1 & 1 & 1 & 1 \\
 0 & 0 & 0 & 0.76 & 0.23 & 0.33 \\
 \\
 1 & 1 & 1 & 1 & 1 & 1 \\
 1 & 0.62 & 1 & 0.31 & 0 & 0.91 \\
 0.52 & 0 & 0 & 0 & 0.16 & 1 \\
 0.04 & 0.80 & 0.36 & 1 & 1 & 0 \\
 0 & 1 & 0.15 & 0.81 & 0.64 & 0.36 \\
 \\
 1 & 1 & 1 & 1 & 1 & 1 \\
 0.15 & 1 & 0.2 & 0.41 & 0.54 & 0.86 \\
 0 & 0.32 & 1 & 0 & 0 & 0 \\
 0.38 & 0 & 0 & 1 & 1 & 1 \\
 1 & 0.06 & 0.6 & 0.8 & 0.19 & 0.14 \\
 \\
 1 & 1 & 1 & 1 & 1 & 1 \\
 0.64 & 0.41 & 0.6 & 0.5 & 0.67 & 0.75 \\
 1 & 1 & 1 & 1 & 1 & 1 \\
 0 & 0 & 0 & 1 & 0.67 & 0 \\
 0.55 & 0.44 & 0.2 & 0 & 0 & 0.5
 \end{bmatrix} \quad (14)$$

C. By calculating the correlation coefficient matrix, formula (15) is obtained according to the gray system theory.

$$E = \begin{bmatrix} 1 & 0.4 & 0.51 & 0.33 & 0.42 & 0.54 \\ 0.57 & 1 & 0.39 & 0.52 & 0.33 & 0.33 \\ 0.35 & 0.45 & 1 & 1 & 1 & 1 \\ 0.33 & 0.33 & 0.33 & 0.68 & 0.39 & 0.43 \\ & 1 & 0.57 & 1 & 0.62 & 0.33 & 0.85 \\ & 0.51 & 0.33 & 0.33 & 0.33 & 0.37 & 1 \\ & 0.34 & 0.71 & 0.44 & 1 & 1 & 0.33 \\ & 0.33 & 1 & 0.37 & 0.72 & 0.58 & 0.44 \\ & 0.37 & 1 & 0.38 & 0.46 & 0.52 & 0.78 \\ & 0.33 & 0.42 & 1 & 1 & 0.33 & 0.33 \\ & 0.33 & 0.33 & 0.33 & 1 & 1 & 0.33 \\ & 1 & 0.35 & 0.56 & 0.38 & 0.66 & 0.37 \\ & 0.58 & 0.46 & 0.56 & 0.5 & 0.60 & 0.67 \\ & 1 & 1 & 1 & 1 & 1 & 1 \\ & 0.33 & 0.33 & 0.33 & 1 & 0.60 & 0.33 \\ & 0.53 & 0.47 & 0.38 & 0.33 & 0.33 & 0.5 \end{bmatrix} \tag{15}$$

D. To enterprise’s green evaluation and suggestion, the weight of each index in the set values is equal. By type (11), all the practical scheme and ideal scheme, in the correlation value of  $r_A = 0.6021$ ,  $r_B = 0.6425$ ,  $r_C = 0.6567$ , and  $r_D = 0.4913$ .

The order shows green for enterprise C, B, A, D, the quality of green indicators in every enterprise can judge according to the correlation coefficient (type), the correlation coefficient, the greater the greening level of the enterprise, the better.

Four iron and steel enterprises were systematically evaluated by the gray relational analysis method according to the evaluation results and the relative trend of each enterprise in each index in the gray relational matrix. Accordingly, the following suggestions are proposed to the four steel enterprises:

- (1) The greenness of enterprise A is poor, but all indexes are evenly distributed, so the greenness level of all indexes can be improved synchronously from the system level.
- (2) Enterprise B and C higher green on the whole, its advantage lies in resource consumption and energy consumption, but its disadvantage is that the gas consumption. The enterprise should consider how to reduce consumption in the steel manufacturing process to improve enterprise’s green, how to improve the recycle of resource and energy, to achieve green energy conservation and emissions reduction targets;
- (3) The greenness of enterprise D is the worst. Except for the comparative advantages of indicators C8 and C13, other green evaluation indicators are all inferior, so the greenness level should be greatly improved on the whole.

## 5 Conclusion

This article takes the manufacturing process of iron and steel enterprises as the starting point and uses the gray correlation analysis method as the basis to establish a green evaluation index system to analyze and evaluate the greenness of iron and steel enterprises. The difference from previous evaluation methods is that the green evaluation of steel companies is regarded as a gray system. When evaluating multiple evaluation indicators, these evaluation indicators constitute a discrete scheme in the correlation of multi-factor evaluation indicators. The sample is within a certain range, and the correlation between each index item and the optimal index item can be used to better reflect the correlation of each index, so as to provide an effective reference for the level of greening among enterprises.

The above research shows that the advantage of the gray correlation analysis method lies in that: due to the large amount of index data for the evaluation and analysis of the greenness of iron and steel enterprises, the gray correlation analysis method is used to ensure the accuracy, scientificity, and objectivity of the evaluation results. To a large extent, avoid the bias caused by people's randomness, inclination, and subjectivity, and analyze the level of greening among steel companies, which is conducive to improving steel companies' awareness of their own greenness. Make reasonable decisions based on the actual situation to maximize the economic and social benefits of the enterprise.

**Acknowledgements** This work is financially supported by National Natural Science Foundation of China (Grant No. 51675388).

## References

1. Zhao, Gang, Zhang, Hua, Zhang, Guangjun, Guo, Liming: Morphology and coupling of environmental boundaries in an iron and steel industrial system for modelling metabolic behaviours of mass and energy. *J. Clean. Prod.* **100**(8), 247–261 (2015)
2. Zhao, Gang, Zhang, Xiang, Fang, Cheng, Ruan, Dan, Wang, Yanan: Systemic boundaries in industrial systems: a new concept defined to improve LCA for metallurgical and manufacturing systems. *J. Clean. Prod.* **187**, 717–729 (2018)
3. Yan, J., Song, Y., Liang, B.: A research on the iron and Steel Enterprise'S Competitiveness based on principal component analysis—using Tangshan Iron and Steel Group Co. Ltd. as an example. In: *Second International Conference on Intelligent System Design and Engineering Application*. IEEE Computer Society, pp. 756–759 (2012)
4. Zhao, G., Gao, X., Yang, S., Duan, J., Hu, J., Guo, X., Wang, Z.: A mechanism model for accurately estimating carbon emissions on a micro scale of the steel industrial system. *ISIJ Int.* **59**(2), 381–390 (2019)
5. Zhao, G., Dan, R., Qiang, W.: Quantitative evaluation of the greenness of steel enterprises oriented to manufacturing process. *Mach. Des. Manuf.* **z1**, 157–164 (2019)
6. Min, Z., Lei, W., Wang, G.F. et al: A relative green degree evaluation model for equipments of iron and steel enterprises. *International conference on management and service science IEEE* pp. 1–6 (2011)

7. Yang, H.-J., Zhang, T.-X., Peng, J.-F.: Environmental performance evaluation of steel enterprises based on abrupt progression method. *Value Eng.* **9**, 1–3 (2014)
8. Deng, J.-L.: Overview of grey system. *World Sci* **7**, 1–5 (1983)
9. Xuerui, T., Julong, D., Liu, S., Hongxing, P.: Multi-stratummedical grey relational theory and its application research. In: *Proceedings of the IEEE International Conference on Systems, Man and Cybernetics, Montréal, Canada, 7–10 Oct IEEE (2007)*
10. Deng, L.-J., Xia, J.-H.: Application of radar graph analysis in comprehensive evaluation of potato variety characteristics. *Agric. Sci. GuiZhou* **41**(7), 59–62 (2013)



# A Life Cycle Comprehensive Cost-Based Method for Active Remanufacturing Time Prediction



Xin Yao, Hua Zhang, Wei Yan, and Zhigang Jiang

**Abstract** In order to solve the problems of low-process efficiency and high remanufacturing cost caused by uncertainty of service time and damage degree of mechanical and electrical products, a prediction method for active remanufacturing timing of mechanical and electrical products oriented to full life cycle comprehensive cost is proposed. Firstly, based on the analysis of service characteristics of mechanical and electrical products, the concept of comprehensive cost of mechanical and electrical products including three dimensions of energy cost, environmental impact cost and economic cost is proposed. Secondly, based on the life cycle approach, the prediction model of active remanufacturing time is established by analyzing the impact of products on comprehensive cost in different stages of the life cycle. Thirdly, the multi-objective problem is transformed into a single-objective problem by linear weighting method to find the optimal solution which is the best time for active remanufacturing of products. Finally, the research and analysis of a certain type of engine have verified the effectiveness and feasibility of the above method.

## 1 Induction

As one of the significant components of green manufacturing, remanufacturing has been widely used for its advanced repair and transformation technology of energy conservation and environmental protection for waste products [1]. Since the invalidation forms of retired products are uneven, the process programs of enterprises in

---

X. Yao

Key Laboratory of Metallurgical Equipment and Control Technology of Ministry of Education, Wuhan University of Science and Technology, Wuhan Hubei 430081, China

H. Zhang (✉)

Hubei Key Laboratory of Mechanical Transmission and Manufacturing Engineering, Wuhan University of Science and Technology, Wuhan Hubei 430081, China  
e-mail: [zhanghua403@163.com](mailto:zhanghua403@163.com)

W. Yan · Z. Jiang

Academy of Green Manufacturing Engineering, Wuhan University of Science and Technology, Wuhan Hubei 430081, China

© The Editor(s) (if applicable) and The Author(s), under exclusive license to Springer Nature Singapore Pte Ltd. 2021

S. G. Scholz et al. (eds.), *Sustainable Design and Manufacturing 2020*, Smart Innovation, Systems and Technologies 200, [https://doi.org/10.1007/978-981-15-8131-1\\_41](https://doi.org/10.1007/978-981-15-8131-1_41)

remanufacturing vary greatly, which makes it difficult to form the optimal input–output ratio [2]. In order to solve the contradiction, The concept of active remanufacturing arises at the historic moment, which remanufactures the product before it is retired, makes it have the best performance, energy saving, high efficiency, low investment and environmental protection in the whole life cycle and effectively prolongs the service life and value of product. As a prerequisite for remanufacturing, active remanufacturing timing prediction has become a hot research topic at this stage.

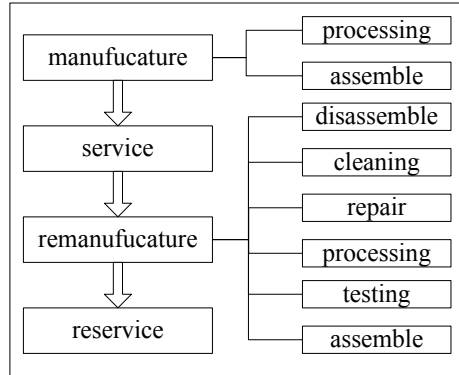
Many scholars have done research on the prediction of active remanufacturing time: The evolution of product service properties with time is analyzed, and a model is established to effectively solve the uncertainty of blank in remanufacturing by Ke et al. [3]. The product environment and the cost index are analyzed, and the decision model of the active remanufacturing time is established, respectively, to get the optimal time by Xiang et al. [4]. Reliability is used to characterize the decline characteristics of products during the service period, and the optimal time for active remanufacturing of products based on reliability analysis is obtained by Chen et al. [5]. The time domain of active remanufacturing considering environmental impact based on replacement theory is determined by Liu et al. [6]. The time of active remanufacturing was determined by establishing energy consumption—time model of product life cycle by Ke et al. [7]. However, the product level is often focused, while the failure type and failure degree of parts are neglected in these methods, which makes it difficult to accurately predict the time of active remanufacturing. In addition, the impact on the active remanufacturing time is only considered for a single factor such as energy consumption or environment in these literatures, which makes it hard to predict the time from the perspective of the overall life cycle.

## 2 Problem of Boundary

Active remanufacturing is the technology of actively remanufacturing a product during its service life, within the time predicted by its performance evolution law [8]. Because of the relevance of different life cycle stages of a product, the analysis of changes in the factors that affect the product's active remanufacturing timing needs to start with the life cycle perspective, the product life cycle system boundary as shown in Fig. 1.

Therefore, an annual average comprehensive cost evaluation model is developed by researching and analyzing the deductive laws of energy cost, environmental impact cost and economic cost at each stage of the product life cycle. The minimum annual comprehensive cost is taken as the goal to predict the active.

**Fig. 1** Product life cycle system boundary



### 3 Prediction Model

Each influencing factor is analyzed and quantified in each stage of the product life cycle, and an active remanufacturing timing prediction model for the comprehensive cost of the product is established. Generally, there are little differences in energy consumption, environmental emissions and costs of same products during the manufacturing stage, which can be regarded as constant; after the product is remanufactured, it is no different even better than the new product, and the service environment is the same; in this study, the energy consumption cost, environmental emission cost and economic cost of the service phase and the re-service phase are approximated.

#### 3.1 Energy Cost

Product life cycle energy requirements include electricity, oil, gas, coal, etc. Assuming a total of types, the energy consumption is calculated as follows:

$$E_i = A_i + \int_0^{t_a} f_i(t)dt + (B_i + g_i(t)) + \int_0^{t_b} f_i(t)dt \tag{1}$$

where  $A_i$  is the  $i$ th energy consumption in the manufacturing stage;  $\int_0^{t_a} f_i(t)dt$  and  $\int_0^{t_b} f_i(t)dt$  are the  $i$ th energy consumption during service and re-service;  $f_i(t)$  is the transform function for  $i$ th energy consumption with service/re-service time  $t_a/t_b$ ;  $B_i + g_i(t)$  is the  $i$ th energy consumption during remanufacturing;  $B_i$  is the  $i$ th energy consumption required for the product during disassembly, cleaning, repair, processing, testing and assembly, and it is considered constant because it is independent of time;  $g_i(t)$  is the  $i$ th energy consumption during product repair step.

Every energy source has a different price in the market, and the energy cost of the product is:

$$C_E = \sum_{i=1}^n E_i \times \gamma_i \tag{2}$$

where  $\gamma_i$  is the equivalent factor per unit of  $i$ th energy (e.g., the unit of electricity is “yuan/kWh”).

### 3.2 Environmental Impact Cost

Aiming at the connection between the environmental impact and cost of the mechanical and electrical product life cycle, the concept of willingness to pay was adopted to represent the degree of environmental pollution by environmental impact cost [9] (Fig. 2).

The environmental impact emissions include Co, Co<sub>2</sub>, CH<sub>4</sub>, SO<sub>2</sub>, No<sub>x</sub>, etc. If the product has  $m$  kinds of environmental impact emissions, the amount of  $j$ th emissions is:

$$W_j = X_j + \int_0^{t_a} V_j(t)dt + (Y_j + u_j(t)) + \int_0^{t_b} V_j(t)dt \tag{3}$$

where  $X_j$  is the  $j$ th emissions during manufacture;  $\int_0^{t_a} V_j(t)dt$  and  $\int_0^{t_b} V(t)dt$  are the  $j$ th emissions during service and re-service;  $V_j(t)$  is the function of  $j$ th emission;  $Y_j + u_j(t)$  is the  $j$ th emissions during remanufacturing;  $u_j(t)$  is the  $j$ th emissions during product repair step;  $Y_j$  is the  $j$ th emissions from other steps.

- (1) According to life cycle approach, in this study, the environmental impacts are classified into five categories: global warming potential (GWP), human health potential (HHP), acidification potential (AP), eutrophication potential (EP) and photochemical ozone formation potential (POFP) [10].
- (2) After characterization, the value of environmental impact  $s$  in the product life cycle is obtained:

$$W_s = W_j \times \alpha_{js} \tag{4}$$

where  $\alpha_{js}$  is the characterization factor for the  $s$  impact of substance  $j$  on the environment.

- (3) The society’s willingness to pay for the environmental degradation caused by products is:

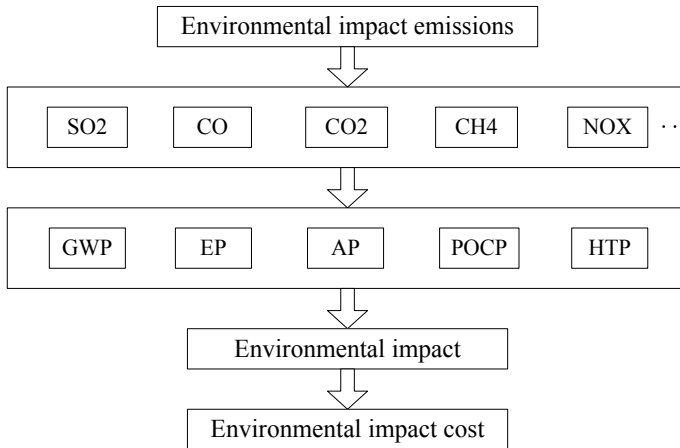


Fig. 2 Product environmental impact cost

$$C_W = \sum_{s=1}^5 (W_s \times \beta_s) \tag{5}$$

where  $\beta_s$  is the compensation weight factor for unit environmental impact  $s$ . The environmental impact weight factor of POFP, GWP, EP, AP and HHP was 0.875, 1.2, 10.8, 15.2 and 98.5.

### 3.3 Economic Cost

Product life cycle economic cost can be obtained by the following formula:

$$C_C = \sum ma + C_r + \delta(t) + \sum b \cdot m(t) + \delta(t) \tag{6}$$

where costs in the manufacturing phase include raw material prices  $\sum ma$  and management fees  $C_r$ ;  $m$  and  $a$  are the quality and unit price of the raw materials;  $\delta(t)$  is cost in the service/re-service phase, which is mainly from maintenance;  $\sum b \cdot m(t)$  is the cost of remanufacturing phase;  $m(t)$  and  $b$  are the quality and unit price of the repair materials.

### 3.4 Multi-objective Decision Making

It is a conventional and effective strategy to turn a multi-objective problem into a single-objective solution. Depending on the importance of each goal, appropriate

weights are assigned, then its linear combination is optimized, and the optimal solution is used as the solution to the problem. This is the linear weighting method [11].

According to the above analysis, the average annual energy consumption cost, average annual environmental impact cost and average annual economic cost of the objective function that affects the decision-making problem of active remanufacturing timing can be expressed as:

$$f_E(t) = \frac{C_E}{t} \quad f_W(t) = \frac{C_W}{t} \quad f_C(t) = \frac{C_C}{t} \quad (7)$$

According to the importance of each objective function, different weights are assigned to the objective function. The weight distribution has a direct impact on the objectivity of the optimization result, which depends on the strength of the relatively important factors required by the enterprise. The weight coefficients corresponding to each objective function are  $\omega_k (k = 1, 2, 3)$ , where  $\omega_k > 0$ ,  $\sum_{k=1}^3 \omega_k = 1$ , and selection methods are: expert scoring method, tolerance method, etc. Based on this, the evaluation function is constructed as follows:

$$F(t) = \omega_1 f_E(t) + \omega_2 f_W(t) + \omega_3 f_C(t) \quad (8)$$

Solving single-objective optimization problems:

$$\begin{cases} F(t) \rightarrow \min \\ 0 < t < t_{\max} \end{cases} \quad (9)$$

Since this is a nonlinear programming problem, the linprog function is used in MATLAB, when  $t = t_r$ , and the average annual comprehensive product cost is the smallest, which is the best time for product active remanufacturing.

## 4 Case

A certain type of engine with a rated speed of 2200 r/min was selected, for example analysis to predict its active remanufacturing timing.

### 4.1 Engine Energy Cost

- (1) The energy consumption list of the main components collected during the engine manufacturing stage is shown in Table 1. Checking the current market prices can be obtained: coal 0.7 yuan/kg, crude oil 4.2 yuan/kg, natural gas 2.5 yuan/m<sup>3</sup>,

**Table 1** Energy consumption in manufacturing stage of main parts

Main parts	Coal (kg)	Crude oil (kg)	Natural gas (m <sup>3</sup> )	Electricity (kWh)
Crankshaft	822.97	64.89	29.87	1557.70
Connecting rod	168.90	13.29	6.12	517.84
Cylinder liner	18.38	5.04	2.32	166.61
Cylinder block	2186.18	140.57	7.27	6500.58
Cylinder head	1003.30	64.51	3.34	2898.25
Piston	26.34	2.37	5.40	2362.40

electricity 1.3 yuan/kWh. The energy cost of the engine manufacturing stage is 22,428.959 yuan.

- (2) Degradation of engine performance during service stage is mainly due to cylinder wear [12]. The energy consumption caused by this in 1–5 years is 5500.01, 15978.95, 33215.32, 54398.91, 82001.13 kWh. While consuming electrical energy, extra diesel is consumed. It is known that the current market price of diesel is 6.38 yuan/L. Fitting the data can obtain the energy cost of the engine during the service phase as follows:

$$C_{E_2} = 3057.04t^2 + 3057.04t \tag{10}$$

- (3) In the remanufacturing of the engine, the electric energy of replacing the piston and cylinder liner with new parts is 75.20 kWh, the main consideration is the remanufacturing energy consumption of other major components (crankshaft laser spraying nickel–cadmium alloy for surface repair; connecting rod small head hole replacement bushing, honing, large head hole nano-brush nickel plating, etc.). Among them, the energy required for the repair process is shown in Table 2, and the remaining process energy consumption is 50.03 kWh. The energy cost of the engine remanufacturing phase is obtained by fitting the collected data:

$$C_{E_3} = 34.41t + 373.269 \tag{11}$$

The engine life cycle energy cost is as follows:

**Table 2** Energy consumption of repair process (kWh)

Time (year)	Crankshaft	Connecting rod	Cylinder block	Cylinder head
1	8.64	7.94	17.85	161.91
2	17.27	15.87	35.71	161.91
3	25.89	23.83	53.55	161.91
4	34.54	31.77	71.42	161.91
5	43.17	39.71	161.92	161.91

$$C_E = 3057.04t^2 + 3091.45t + 22802.23 \tag{12}$$

### 4.2 Engine Environmental Impact Cost

- (1) The emissions from coal, diesel, etc., used in the engine manufacturing stage are CH<sub>4</sub>, CO<sub>2</sub>, SO<sub>2</sub>, CO, NO<sub>x</sub>, CH<sub>4</sub>, etc., as shown in Table 3.
- (2) The pollutants caused by the electric power consumed by the engine and diesel during the service phase are as follows:

$$W_{uj} = \begin{bmatrix} \text{CO} \\ \text{CO}_2 \\ \text{SO}_2 \\ \text{NO}_x \\ \text{CH}_4 \end{bmatrix} = \begin{bmatrix} 26.10t^2 + 26.10t \\ 758.39t^2 + 758.39t \\ 2.39 \times 10^{-2}t^2 + 2.39 \times 10^{-2}t \\ 2.22t^2 + 2.22t \\ 1.41 \times 10^{-2}t^2 + 1.41 \times 10^{-2}t \end{bmatrix} \tag{13}$$

- (3) Remanufacturing phase is mainly indirect pollutant emissions caused by electricity:

$$W_{rmj} = \begin{bmatrix} \text{CO} \\ \text{CO}_2 \\ \text{SO}_2 \\ \text{NO}_x \\ \text{CH}_4 \end{bmatrix} = \begin{bmatrix} 1.21t + 84.56 \\ 487.63t + 374.49 \\ 46.24t + 1300.87 \\ 2.92t + 1064.35 \\ 0.83t + 1103.77 \end{bmatrix} \tag{14}$$

When calculating the environmental impact of the engine, the environmental impact caused by the production unit’s electrical energy, diesel, etc., was taken from the CLCD. According to the model established above, social compensation willingness to produce per liter of diesel is taken as an example, various environmental impact compensation weight factors are determined, and the environmental impact cost per liter of diesel is obtained. The final cost of the environmental impact of the engine life cycle is acquired in the same way:

**Table 3** Environmental impact list of main parts in manufacturing stage (kg)

Emissions	Crankshaft	Connecting rod	Cylinder block/head	Cylinder liner	Total
CO	0.055	0.011	0.310	0.103	0.469
CO <sub>2</sub>	232.78	47.69	1353.2	28.11	1661.7
SO <sub>2</sub>	0.575	0.118	3.649	0.085	4.427
NO <sub>x</sub>	0.301	0.062	2.472	0.072	2.907
CH <sub>4</sub>	0.492	0.101	3.513	0.080	4.186



$$C_W = 441.92t^2 + 466.82t + 6982.7 \quad (15)$$

### 4.3 Engine Economic Cost

- (1) In the manufacturing stage, 353.6kg cast iron (3.2 yuan /kg), 126.4kg steel (3.9yuan/kg) and 3kg silicon–aluminium alloy (30yuan/kg) were consumed, and the management cost is 1200 yuan, which totals 2833.48 yuan.
- (2) The economic cost of the engine service phase is mainly the cost of maintenance, which is mainly related to performance degradation such as cylinder wear. From this, the economic cost of the engine service phase is as follows:

$$C_u = 330t^2 + 330t \quad (16)$$

- (3) The economic cost of engine remanufacturing phase includes: replacement cost of piston and cylinder liner (56.5 yuan), nickel–cadmium alloy and nickel purchase cost. At present, the market nickel is about 90 yuan/kg, and nickel–cadmium alloy is 129 yuan/kg. The economic cost of engine remanufacturing phase is as follows:

$$C_W = 441.92t^2 + 466.82t + 6982.7 \quad (17)$$

The economic cost of the engine life cycle can be expressed as:

$$C_W = 441.92t^2 + 466.82t + 6982.7 \quad (18)$$

### 4.4 Engine Active Remanufacturing Timing Forecast

From what has been discussed above, the average annual energy consumption, environmental impact and economic cost of the engine's life cycle are obtained:

$$\begin{aligned} f_E(t) &= 3057.04t + 3091.45 + 22802.23/t \\ f_W(t) &= 441.92t + 466.82 + 6982.7/t \\ f_C(t) &= 330t + 559.35 + 3036.38/t \end{aligned} \quad (19)$$

Let  $\omega_k = 1/3$ , and the evaluation function is as follows:

$$F(t) = 3828.96t + 4116.8 + 32821.31/t \quad (20)$$

Currently, the service life of the engine is at most 10 years, and it means that  $t_{\max} = 10$ :

$$\begin{cases} F(t) \rightarrow \min \\ 0 < t < 10 \end{cases} \quad (21)$$

When  $t = 2.93$  in MATLAB,  $F(t)$  is solved to the minimum, which is the optimal time for active remanufacturing of the engine.

## 5 Conclusions

Aiming the uncertainty of each component of the product during remanufacturing and its associated characteristics at various stages of the life cycle, the concept of life cycle comprehensive costs including energy costs, environmental impact costs and economic costs was proposed. An active remanufacturing timing prediction model of the average annual product cost was established, and the solution method is presented. Taking a certain type of engine as an example, the effectiveness of this method is proved. This method can make up for the shortcomings of focusing on product levels and single angles in the existing literature and has broad application prospects.

**Acknowledgements** This work is financially supported by National Natural Science Foundation of China (Grant No. 51675388).

## References

1. Bensmain, Y., Dahane, M., Bennekrouf, M., et al.: Preventive remanufacturing planning of production equipment under operational and imperfect maintenance constraints: a hybrid genetic algorithm based approach. *Reliab. Eng. Syst. Saf.* **185**, 546–566 (2019)
2. Song, S., Wang, W., Ke, Q.: Optimization design of predecisional remanufacturing based on structure coupling matrix. *Comput. Integr. Manuf. Syst.* **23**(4), 744–752 (2017)
3. Ke, Q., Wang, H., Liu, G., Song, S.: Timing decision-making analysis method for proactive remanufacturing based on performance parameters. *China Mech. Eng.* **27**(14), 1899–1904 (2016)
4. Qin, X., Hua, Z., Zhigang, J., et al.: A decision-making method for active remanufacturing time based on environmental and economic indicators. *Int. J. Online Biomed. Eng.* **12**(12), 32–37 (2016)
5. Le, Chen, et al.: Timing decision-making method of engine blades for predecisional remanufacturing based on reliability analysis. *Front. Mech. Eng.* **14**(4), 412–421 (2019)
6. Liu, Z., Afrinaldi, F., Zhang, H.C., et al.: Exploring optimal timing for remanufacturing based on replacement theory. *CIRP Ann. Manuf. Tech.* **65**(1), 447–450 (2016)
7. Ke, Q., Wang, H., Song, S., et al.: A timing decision-making method for product and its key components in proactive remanufacturing. *Procedia Cirp* **48**, 182–187 (2016)
8. Gao, W., Li, T., Peng, S.T., et al.: Optimal timing and recycling operation mode for electro-mechanical products active remanufacturing. *Front. Eng. Manag.* **3**(02), 21–28+90–91 (2016)

9. Zhao, G., Zhang, H., Zhang, G., Guo, L.: Morphology and coupling of environmental boundaries in an iron and steel industrial system for modelling metabolic behaviours of mass and energy. *J. Clean. Prod.* **100**(8), 247–261 (2015)
10. Chen, Q., Zhe, Z., Lan, W., et al.: Identifying miRNA-disease association based on integrating miRNA topological similarity and functional similarity. *Quant. Biol.* **7**(3), 202–209 (2019)
11. Zhao, G., Zhang, X., Fang, C., Ruan, D., Wang, Y.: Systemic boundaries in industrial systems: a new concept defined to improve LCA for metallurgical and manufacturing systems. *J. Clean. Prod.* **187**, 717–729 (2018)
12. Zhao, G., Gao, X., Yang, S., Duan, J., Hu, J., Guo, X., Wang, Z.: A mechanism model for accurately estimating carbon emissions on a micro scale of the steel industrial system. *ISIJ Int.* **59**(2), 381–390 (2019)

# Analysis of Coal Gas Resource Utilization and Energy Flow View Model in Iron and Steel Enterprises



Xiao Li, Gang Zhao, Qi Zhou, Pengcheng Yan, Xiong Liu, and Shujun Yu

**Abstract** During the production and operation of iron and steel enterprises, a large amount of very important by-product gas resources such as blast furnace gas, coke oven gas and Linz–Donawitz process gas are produced. In order to realize the efficient use value of gas resources, focus on two aspects of its comprehensive utilization and optimization methods. Firstly, according to the different characteristics of by-production gas in iron and steel enterprises at present, the optimal use way is analyzed to promote the conversion of by-production gas from the main fuel utilization (or even direct emission) to the moderate resource utilization, so as to realize the improvement of comprehensive utilization rate. Secondly, according to the characteristics of gas energy flow system, an energy flow view description model is established and the linear optimization model of gas energy flow density is given; then, the feasibility of the optimized method is verified by simulation with actual data of a steel plant.

## 1 Introduction

Since the 1990s, China's steel industry has developed very rapidly [1], and now it has firmly established itself as the world's largest steel country. With the increasingly broad and indispensable application of steel materials in daily life, China's crude steel production has always been in a state of continuous growth. The iron and steel industry is a pillar industry capable of rapid development of China's national economy, but at the same time the energy consumption of the iron and steel industry

---

X. Li

Key Laboratory of Metallurgical Equipment and Control Technology of Ministry of Education, Wuhan University of Science and Technology, Wuhan Hubei 430081, China

G. Zhao · Q. Zhou · P. Yan · X. Liu

Hubei Key Laboratory of Mechanical Transmission and Manufacturing Engineering, Wuhan University of Science and Technology, Wuhan Hubei 430081, China

S. Yu (✉)

Evergrande School of Management, Wuhan University of Science and Technology, Wuhan Hubei 430081, China

e-mail: [yushujun@wust.edu.cn](mailto:yushujun@wust.edu.cn)

© The Editor(s) (if applicable) and The Author(s), under exclusive license to Springer Nature Singapore Pte Ltd. 2021

S. G. Scholz et al. (eds.), *Sustainable Design and Manufacturing 2020*, Smart Innovation, Systems and Technologies 200, [https://doi.org/10.1007/978-981-15-8131-1\\_42](https://doi.org/10.1007/978-981-15-8131-1_42)

accounts for about 15% of the country's total energy consumption [2]. It is a typical high-input, high-energy and high-polluting industry. Therefore, in combination with China's basic national policy of saving resources and protecting the environment, taking the green manufacturing route [3], it is of great significance to achieve its energy saving and emission reduction. In the industrial processes of iron and steel enterprises [4], about 60% of the coal resources consumed are converted into three by-product gas resources: blast furnace gas (BFG), coke oven gas (COG) and Linz–Donawitz process gas (LDG). Its output and consumption are almost accompanied by the entire steel manufacturing process, and it is the most important secondary energy source for steel companies, accounting for about 40% of the company's total energy consumption. The utilization level of by-product gas in iron and steel enterprises is related to the energy utilization level of the enterprise and plays an important role in the balance and regulation of the enterprise energy system [5]. Therefore, in order to improve the comprehensive utilization rate of by-product gas resources, resource utilization is used to reduce the large-scale gas release phenomenon, so as to maximize the use of gas resources and maximize the production benefits [6]. Simultaneously, establishing a gas energy flow view model to describe the overall gas system, an optimized function model of the gas energy flow density is given, the energy flow density value of the gas system is optimized and analyzed to verify the feasibility of the results, and it is of great significance to steel companies even looking at the energy conservation and emission reduction of the overall industrial area.

## 2 Comprehensive Utilization of By-Product Gas

Blast furnace gas, coke oven gas and Linz–Donawitz process gas, these iron and steel industry by-product gases are mainly composed of  $H_2$ , CO,  $CO_2$ ,  $N_2$ ,  $CH_4$ ,  $O_2$  and so on, and the specific constituent volumes of each component are shown in Table 1. Due to the different composition ratios of the various components, the characteristics of the three types of gas are greatly different. The total output of by-product gas in China's steel mills is very huge, some of which are toxic and corrosive. Random dispersal will cause waste of resources and also easily affect the environment. Therefore, according to the characteristics of different gases, the best

**Table 1** Source, composition, calorific value and output of three kinds of gas

Gas type	Source	The composition ratio of the component (%)							Calorific value/ (KJ/m <sup>3</sup> )
		H <sub>2</sub>	CO	CO <sub>2</sub>	N <sub>2</sub>	CH <sub>4</sub>	O <sub>2</sub>	C <sub>m</sub> H <sub>n</sub>	
BFG	Ironmaking	1.3–3.0	23–27	15–19	55–60	0.2–0.5	0.2–0.4	–	3000–3800
COG	Coking	55–60	5–8	1.5–3.0	3–7	23–27	0.3–0.8	2–4	8800–16,000
LDG	Steelmaking	0.5–2.0	50–70	10–25	10–20	–	0.3–0.8	0.2–0.6	6300–8400

utilization path is allocated and material conversion is performed to realize partial resource utilization in order to improve the comprehensive utilization rate.

## 2.1 Blast Furnace Gas

BFG is a by-product produced by the blast furnace ironmaking process. China's blast furnace gas can produce more than 1.2 trillion cubic meters per year with a huge output. Because the main flammable component is CO, which accounts for about 25%, and the non-flammable gas CO<sub>2</sub> and NO<sub>2</sub> content reaches 75%, resulting in a lower heating value of BFG and a relatively low combustion temperature. However, it can still meet the gas or steam temperature required by the heat engine, and its use value can be enhanced through the following channels:

### (1) Enrichment technology and separation and extraction of carbon dioxide

In view of the low proportion of effective combustion component CO in BFG, if some common innocuous gases CO<sub>2</sub> and N<sub>2</sub> are removed, the CO can be enriched to 70–80%, so that the heating value is increased to 8000–10,000 kJ/m<sup>3</sup>, which can be used to replace the use of purchased energy such as coke oven gas or natural gas. Simultaneously, CO<sub>2</sub> has a wide range of applications in industrial production [7]. Using its physical and chemical properties, it can be used in food preservation, low-temperature extraction, and metal processing, medical, inorganic chemical and other production fields [8]. Therefore, the removed CO<sub>2</sub> and N<sub>2</sub> mixed gas can be separated to extract carbon dioxide. Under the background of huge annual output of BFG, there will be a considerable amount of CO<sub>2</sub> extraction. In China's active CO<sub>2</sub> consumption market, it can bring an additional economic benefit, and not only can reduce CO<sub>2</sub> emissions, but also can promote sustainable industrial development and social environmental protection.

### (2) Gas–steam combined cycle power generation [9] (CCPG)

After mixing the blast furnace gas with the desulfurized coke oven gas and air, it is combusted in the combustion chamber of a steam turbine, and the high-temperature and high-pressure flue gas generated by the combustion is used to push the turbine unit for work and power generation. Simultaneously, the high-temperature gas discharged from the turbine unit is introduced into the waste heat boiler to generate high-temperature and high-pressure steam, which promotes the steam turbine to perform work and generate electricity. CCPG thermoelectric conversion efficiency can be nearly 10% higher than conventional boiler generators, reaching more than 45%, which greatly reduces the cost of power generation and has good energy-saving effects, and economic and environmental benefits.

### (3) Regenerative combustion technology

Regenerative combustion technology is a kind of energy-saving and environmental protection technology with great development potential. It recovers the waste heat of the flue gas through the heat storage body, so that the combustion medium can be preheated to 800–1100 °C; then, the BFG, which was originally insufficient in combustion temperature, can be used as the fuel for the rolling furnace. Simultaneously, the regenerative heating furnace achieves high-temperature lean oxygen combustion during the combustion process due to the jet of the combustion medium and the cigarette smoke, and the  $\text{NO}_x$  concentration is also significantly reduced during the combustion process, which not only achieves the efficient comprehensive utilization of BFG, but also reduces environmental protection row.

## 2.2 Coke Oven Gas

COG is a by-product produced when coking coal is used in high-temperature coking to produce coke and tar. China produces more than 150 billion cubic meters of coke oven gas each year, and its output is relatively stable; the main combustible components are  $\text{H}_2$  (approximately 58%) and  $\text{CH}_4$  (approximately 25%), which are high calorific value gas fuels. The theoretical combustion temperature can reach 2150 °C. With the wide application of thermal storage technology, low calorific value gas can replace the use of COG, which can save a large amount of surplus COG, which is used for the resource utilization of gas.

### (1) Manufacture of hydrogen by COG

China's current industrial hydrogen production is mainly based on natural gas, petroleum and coal, compressed natural gas and water vapor are mixed and reacted at high temperatures [10]. The  $\text{H}_2$  content in COG has reached 58%. As a raw material for hydrogen production, just remove the impurity gas according to the current gas treatment process, and then use pressure swing adsorption and other technologies to obtain hydrogen with a purity of 99.99%, which is a very good raw material for hydrogen production. After the extraction of hydrogen, the main flammable gas is about 60%  $\text{CH}_4$ , which increased the calorific value by about 60%. Wang Haifeng [11] concluded that COG hydrogen production is more economical by comparing the technical process of hydrogen production from natural gas and COG hydrogen production. It can bring huge social and economic benefits in response to China's material energy shortage, improvement of the ecological environment and ecological transformation of the steel industry.

### (2) COG directly reduces iron oxide

Excellent reducing gases  $\text{H}_2$  and  $\text{CO}$  can be obtained by oxygen-catalyzing pyrolysis of  $\text{CH}_4$  in COG, so that the proportion of  $\text{H}_2$  and  $\text{CO}$  in COG can reach 95%. The production of sponge iron through a gas-based shaft furnace promotes the combined process of blast furnace–direct-reduced iron shaft furnace [11], which can greatly

reduce the consumption of coking coal and coke resources, which is an important resource utilization approach.

### **2.3 Linz–Donawitz Process Gas**

LDG is a by-product gas produced by converter oxygen-blowing steelmaking. Due to the uneven amount of LDG generated during the smelting process, the large change in the content of the component causes the calorific value to fluctuate greatly and the risk is high. LDG will be sprayed together with a large amount of high-temperature iron oxide dust during the production process, and it needs to be cooled and dusted before being put into use. The main flammable component of LDG is CO (approximately 63%), which belongs to a higher heating value fuel. It can be mixed with BFG and COG and can also be used in steelmaking baking instead of COG or natural gas. LDG can be utilized in the following two ways.

#### (1) Active lime production

LDG can be used instead of traditional coke and pulverized coal as a fuel for the production of limestone. Its calorific value is moderate. Compared with BFG and COG, it is very suitable for the production needs of gas-fired lime pits. Fuel for producing low-sulfur lime for steelmaking. This technology is now very mature, and some domestic steel companies have been put into use and achieved considerable economic benefits.

#### (2) Chemical production

The content of LDG (high-quality basic chemical raw materials) can reach up to 75%, so it can be used for pressure swing adsorption purification to produce high-value chemical products such as methanol and ammonia, and it can also be directly used in methanol. The content of CO and CO<sub>2</sub> in LDG can reach 80%, and it is used to make carbon for methanol production from coke oven gas to improve the hydrogen-to-carbon ratio of synthesis gas, thereby increasing the methanol conversion rate. Liu and Zhang [12] compared the two coal gases to methanol processes. The results are shown in Table 2.

## **3 Modeling of Gas Energy Flow View in Iron and Steel Enterprises**

The occurrence, consumption, storage and transportation of by-product gas in iron and steel enterprises have become a more complex system due to the composition of the gas energy flow system including a number of different processes, production units and work equipment. Correspondingly have the following characteristics:



**Table 2** Comparison of production processes for methanol production

Name	COG pure oxygen conversion to methanol	COG supplemented with LDG pure oxygen conversion to methanol	LDG with COG for hydrogen extraction to methanol
LDG utilization	No use	Partial use	All use
Syngas hydrogen-to-carbon ratio	2.58	2.05–2.1	2.05–2.1
Input costs	Medium	High	Low
Operability	Difficult	Difficult	Easy
Safety	Medium	Medium	High
Energy consumption	Medium	Low	Low

### (1) Flowability

Due to the occurrence, consumption, storage and transportation of gas, each process, production unit and work equipment in the gas energy flow system are interconnected to form a process, which needs to be represented by certain graphics.

### (2) Dynamic

The production, consumption, storage and transportation of the gas system are a simultaneous and continuous dynamic system. For example, the gas consumption in each process will cause the gas output to change with the gas volume in the storage and transportation system; therefore, its dynamic performance is the flow of gas resources, and it needs to be able to model and express the flow process.

The energy flow view model is based on the target energy as the center of view. It provides a clear description of the ins and outs of the entire energy, its coming process or processes, the consumed processes and the imbalance amount, which is helpful for a deeper understanding of the energy consumption of steel companies [13]. Enterprise energy consumption. Therefore, the energy flow view model is used to clearly describe the specific source and destination of gas in iron and steel enterprises. Simultaneously, feedback settings are added to make the model have certain adjustment capabilities. The specific model is as follows:

The directions of the three-colored arrows in Fig. 1 represent the specific source flows of the three by-product gases. The feedback instruction indicates that the information on the gas storage in the gas storage is fed back to the purchased gas instruction.

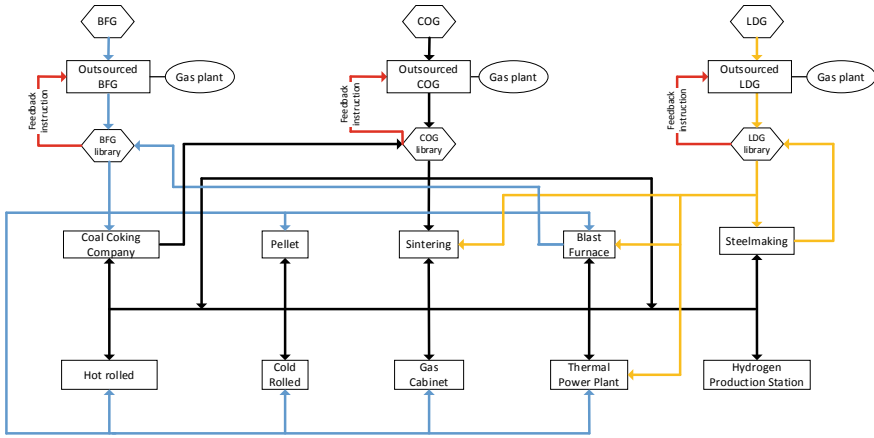


Fig. 1 Energy flow view of the gas system of a steel company

## 4 Energy Flow Density Optimization

### 4.1 Optimization Model

The utilization level of by-product gas corresponds to the energy utilization level of the enterprise, and it also plays a certain role in balancing and regulating the energy system of the enterprise. According to the energy flow view model of the gas system, a kind of gas energy flow density index is defined, which represents the heating value contained in a unit volume of the gas system, and a linear optimization model of the gas energy flow density is obtained for simulation analysis.

Define gas energy flow density function:

$$N = \frac{\sum_{\alpha=1}^S q_{\alpha}}{\frac{\sum_{\alpha=1}^S E_{\alpha}(\text{BFG})}{a_{\text{BFG}}} + \frac{\sum_{\alpha=1}^S F_{\alpha}(\text{COG})}{b_{\text{COG}}} + \frac{\sum_{\alpha=1}^S G_{\alpha}(\text{LDG})}{c_{\text{LDG}}}} \quad (1)$$

Among them,  $S$  is the number of users of the gas use process in the iron and steel enterprise;  $q_{\alpha}$  is the heat value (unit: GJ) consumed by unit user  $\alpha$  in a single time;  $a_{\text{BFG}}, b_{\text{COG}}, c_{\text{LDG}}$  represent three calorific values per unit volume of gas (unit: GJ/km<sup>3</sup>);  $E_{\alpha}(\text{BFG}), F_{\alpha}(\text{COG}), G_{\alpha}(\text{LDG})$  represent three calorific values of gas (unit: GJ).

It is known that the heat value consumed by a user in a single process per unit time is a fixed value, and the molecular formula  $\sum_{\alpha=1}^S q_{\alpha}$  of the gas energy flow density function is a fixed value. Therefore, in order to ensure the maximum energy flow density  $N$ , only the objective function needs to be defined as:

$$\min f = \frac{\sum_{\alpha=1}^S E_{\alpha(\text{BFG})}}{a_{\text{BFG}}} + \frac{\sum_{\alpha=1}^S F_{\alpha(\text{COG})}}{b_{\text{COG}}} + \frac{\sum_{\alpha=1}^S G_{\alpha(\text{LDG})}}{c_{\text{LDG}}} \tag{2}$$

Set constraints:

Assuming that the three by-product gas productions are  $X_{\text{BFG}}$ ,  $Y_{\text{COG}}$  and  $Z_{\text{LDG}}$  (unit: CJ) in a unit time, the total gas consumption should be less than the total gas production:

$$\sum_{\alpha=1}^S E_{\alpha(\text{BFG})} \leq X_{\text{BFG}}, \sum_{\alpha=1}^S F_{\alpha(\text{COG})} \leq Y_{\text{COG}}, \sum_{\alpha=1}^S G_{\alpha(\text{LDG})} \leq Z_{\text{LDG}} \tag{3}$$

The sum of the calorific value of the three types of gas allocated to the user of a single process per unit time should be equal to the total consumption per unit time of the process:

$$q_{\alpha} = E_{\alpha(\text{BFG})} + F_{\alpha(\text{COG})} + G_{\alpha(\text{LDG})} \tag{4}$$

Define that the density of gas energy flow consumed by a single process user in a unit time according to process constraints should be greater than the historical minimum  $m_{\alpha}$  (unit GJ/km<sup>3</sup>), which should meet:

$$\frac{E_{\alpha(\text{BFG})} + F_{\alpha(\text{COG})} + G_{\alpha(\text{LDG})}}{\frac{E_{\alpha(\text{BFG})}}{a_{\text{BFG}}} + \frac{F_{\alpha(\text{COG})}}{b_{\text{COG}}} + \frac{G_{\alpha(\text{LDG})}}{c_{\text{LDG}}}} \geq m_{\alpha} \tag{5}$$

Simplified to the following form:

$$\left(\frac{m_{\alpha}}{a_{\text{BFG}}} - 1\right)E_{\alpha\text{BFG}} + \left(\frac{m_{\alpha}}{b_{\text{COG}}} - 1\right)F_{\alpha\text{COG}} + \left(\frac{m_{\alpha}}{c_{\text{LDG}}} - 1\right)G_{\alpha\text{LDG}} \leq 0 \tag{6}$$

A linear optimization model for gas energy flow density in iron and steel enterprises can be obtained.

### 4.2 Optimization–Simulation Example

By querying the daily energy analysis reports of a steel company for two consecutive months, 60 sets of daily production data of steel companies were obtained, and the data were used to calculate the known fixed values in the above optimization function, select the average value of the data from two consecutive days as a group, set a total of 30 groups of data and apply the linprog function in the optimization toolbox of MATLAB. The comparison between the optimized energy flow density linear curve

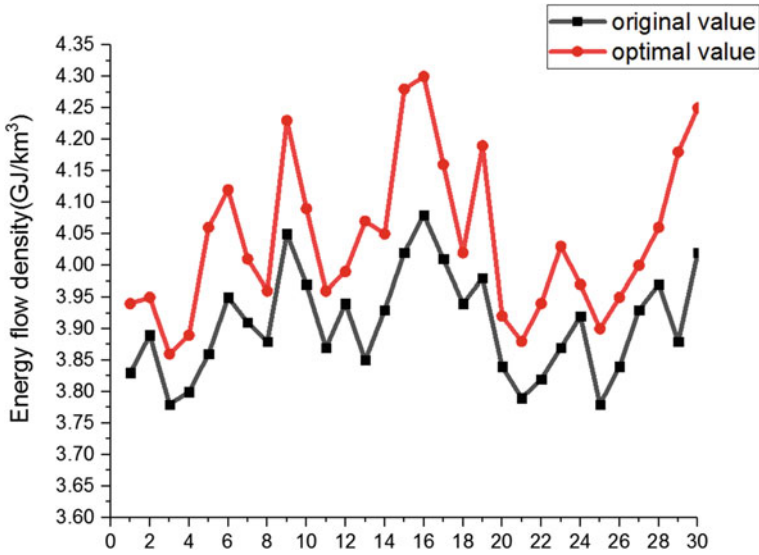


Fig. 2 Comparison before and after energy flow density optimization

obtained from the simulation and the original data energy flow density curve is shown below (Fig. 2):

Through the optimization results, it can be found that the optimized energy flow density increased by 7.73% compared to the original data, the smallest was 1.27%, and the average improvement was 3.41%.

## 5 Conclusion

- (1) For the by-product gas of iron and steel enterprises is currently mainly used for fueling or even directly released, resulting in waste of resources and environmental pollution, based on the differences in characteristics caused by the different composition ratios of the three types of gas, the best way to use by-product gas was discussed, and part of the by-product gas in iron and steel enterprises was transformed from fueling to appropriate resource utilization to maximize the use value of by-product gas resources, while also having good economic and environmental benefits, to achieve a win-win situation.
- (2) The use of gas almost runs through the whole process of steel production, and the gas energy flow is related to all processes and key stations, which is the most important subsystem of the energy system of steel enterprises. The existing researches lack the description of the whole structure and behavior of the gas energy flow system, so according to the characteristics of gas energy flow system, this paper establishes the view model of gas energy flow from the

perspective of gas energy and describes the flow path of the whole gas clearly. In view of the gas dispersion problem, based on the overall understanding of the energy flow view model, the energy flow density index is put forward, and the optimization function is constructed to obtain the linear optimization model of gas energy flow density. The simulation results of the gas energy flow system of a certain iron and steel enterprise show that the model has certain application value, and indicate that there are still some problems in the current energy flow system of the enterprise, which can provide certain guidance and theoretical basis for its optimization and adjustment in the future.

**Acknowledgements** This work is financially supported by National Natural Science Foundation of China (Grant No. 51675388).

## References

1. Zhao, G., Zhang, H., Zhang, G., Guo, L.: Morphology and coupling of environmental boundaries in an iron and steel industrial system for modelling metabolic behaviours of mass and energy. *J. Clean. Prod.* **100**(8), 247–261 (2015)
2. Zhang, C.-X., Shangguan, F.-Q., Hu, C.-Q., et al.: Steel process structure and its impact on CO<sub>2</sub> emission. *Iron Steel* **45**(5), 1–6 (2010)
3. Jiang, Z.-G., Zhang, H.: Study on index system of multi-objective decision-making for production process oriented green manufacturing enterprise. *Machin. Des. Manuf.* **8**, 232–234 (2008)
4. Zhao, G., Zhang, X., Fang, C., Ruan, D., Wang, Y.: Systemic boundaries in industrial systems: a new concept defined to improve LCA for metallurgical and manufacturing systems. *J. Clean. Prod.* **187**, 717–729 (2018)
5. Hu, J.-J., Xie G.-W.: Analysis of reasonable utilization of gas resources in iron and steel enterprise. *Energy Metallurg. Ind.* **3**, 3 (2015)
6. Zhang, Q.: Study on reasonable utilization and optimizing distribution of gases fuel in iron and steel complex. Northeastern, Shenyang (in Chinese) (2008)
7. Zhao, G., Gao, X., Yang, S., Duan, J., Hu, J., Guo, X., Wang, Z.: A mechanism model for accurately estimating carbon emissions on a micro scale of the steel industrial system. *ISIJ Int.* **59**(2), 381–390 (2019)
8. Liu, H., Wang, W., Wei, X.-M., Huang, Y., Liu, G.-Q.: Research progress of utilization of industrial by-product gas. *Mod. Chem. Ind.* **36**(04), 46–52 (2016)
9. Zhang, Q., Cai, J.-J., Wu, F.-Z., Pang, X.-L., Ge, H.: Utilization of blast furnace in metallurgical industry. *Ind. Furn.* **01**, 9–12 (2007)
10. Guo, H.: Comprehensive optimized utilization of oil and gas resources in refinery enterprises. South China University of Technology, Guang dong (2006). <https://doi.org/10.7666/d.y990436>
11. Wang, H.-F., Zhang, C.-X., Hu, C.-Q., Qi, Y.-H.: Important development trends of coke oven gas utilization in steel plant. *J. Iron Steel Res.* **03**, 1–12 (2008)
12. Liu, J.-X., Zhang, P.-H.: Methanol product from COG and LDG. *Fuel Chem. Process.* **4401**, 51–52 (2013)
13. Zhao, F.: Research and application of energy consumption modeling method in iron and steel enterprises. Tong Ji University, Shanghai (2011). <https://doi.org/10.7666/d.y2012221>

# Lightweight Design of Valve Body Structure Based on Numerical Simulation



Qi Zhou, Gang Zhao, Xin Huang, Na Zhang, and Xiaolong Luo

**Abstract** In order to save costs and protect resources, and improve the green level of valve body design, a numerical design method was used to lightweight the valve body structure for an electric gate valve being developed by S Company. The original square valve body structure was designed as a cylindrical structure. SolidWorks was used to model the valve body structure in three dimensions. The flow simulation was used to perform flow path extraction and flow field analysis on the valve body. Fluid–structure interaction analysis was performed on the optimized valve body, and mechanical performance analysis was performed. The analysis results show that the mass of the valve body is reduced by 728 kg, the optimization rate is 20.8%, the allowable stress requirements are met, and the lightweight design of the valve body is OK.

## 1 Introduction

“Made in China 2025” adheres to sustainable development as an important focus of building a manufacturing power, strengthens the promotion and application of energy-saving and environmental protection technologies, processes and equipment, and comprehensively promotes clean production. Developing a circular economy, improving the efficiency of resource recovery and utilization, building a green manufacturing system and taking the path of ecological civilization are all inevitable trends in China and the world. S Company incorporated the concept of green manufacturing into the design and manufacturing process of the valve to achieve the goals of energy

---

Q. Zhou · X. Huang (✉)

Key Laboratory of Metallurgical Equipment and Control Technology of Ministry of Education, Wuhan University of Science and Technology, Wuhan Hubei 430081, China  
e-mail: [vincentlvy@163.com](mailto:vincentlvy@163.com)

G. Zhao

Hubei Key Laboratory of Mechanical Transmission and Manufacturing Engineering, Wuhan University of Science and Technology, Wuhan Hubei 430081, China

N. Zhang · X. Luo

Wuhan Boiler Group Valve Co. Ltd., Wuhan Hubei 430223, China

© The Editor(s) (if applicable) and The Author(s), under exclusive license to Springer Nature Singapore Pte Ltd. 2021

S. G. Scholz et al. (eds.), *Sustainable Design and Manufacturing 2020*, Smart Innovation, Systems and Technologies 200, [https://doi.org/10.1007/978-981-15-8131-1\\_43](https://doi.org/10.1007/978-981-15-8131-1_43)

saving and emission reduction [1] and low carbon production. Green manufacturing is the embodiment of sustainable development strategy in manufacturing industry. It is committed to improving the coordination between human technological innovation, productivity development and ecological environment, which is in line with the theme of the times. Therefore, the implementation of green manufacturing is an effective way to achieve energy saving and emission reduction in traditional manufacturing [2]. “Lightweight” becomes a role as an important part of green manufacturing. Therefore, it is important to design a lightweight body.

For the lightweight design of the valve body and its flow field, temperature field and mechanical performance analysis, many scientists have done a lot of researches on it. Zhao studied the shape and coupling of environmental boundaries in the steel industry system, used to simulate the metabolic behavior of mass and energy, and reasonably explain the relationship between process and environmental protection [3]. Zhao studied industrial system boundaries to improve metallurgical and manufacturing systems by LCA [4] that provides a systematic approach to lightweight design; Ma used a finite element software to carry out a lightweight design of the four-way valve structure [5] and experimentally demonstrated the low-temperature pressure resistance; Zhu et al. studied a lightweight valve body based on SLM technology [6], which can form complex structure valve body, but the strength of the valve body is not OK, and the materials that can be used are difficult to produce; Wang et al. modeled the valve body three-dimensionally based on the fluid volume method and analyzed its temperature field under the combined effect of temperature and high-temperature gas in the cylinder, and coke deposits are continuously generated and accumulated around the nozzle outlet [7]. Lv takes a certain type of roadheader multi-way valve as the research object and used ANSYS to analyze the strength of the valve body with an ideal structure and the valve body with a casting defect structure under different pressures. With the increase of pouring temperature, the maximum porosity at the shrinkage of the casting first increases and then remains unchanged; when the pouring temperature is constant, the maximum porosity at the shrinkage of the casting appears first as the pouring time increases. Decrease and then increase rapidly and keep the same law [8]. Ma has studied the influence of valve body clearance on the internal flow field distribution of the valve body. It can be seen that the simplified processing cannot be performed when the valve body performance is accurately predicted. The influence of the clearance on the valve body performance and internal flow field distribution must be considered [9]. Yi made a mechanical analysis of the valve body of the CD-GF drilling ball valve. Studies have shown that the tensile load is the main factor affecting the strength of the valve body [10]. Lei has studied the influence of heat treatment process on the structure and performance of the valve body. The research shows that the efficient matching of pressure and flow, as much as possible to improve the dynamic response, reduce the lift pressure difference, and improve the control accuracy have become the focus of research in the industry [11].

It can be known from the above studies that all the researches are only for lightweight design of valves and small-caliber valves under normal temperature and

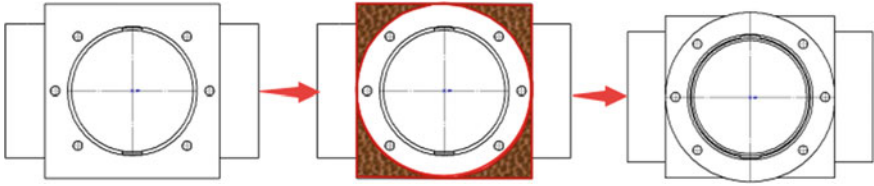


**Fig. 1** Valve body optimization path

low-pressure conditions. However, the lightweight design of high-temperature, high-pressure, large-caliber valves has not been studied in depth, and research is blank. Therefore, this paper uses theoretical analysis and numerical simulation to carry out lightweight design for large-caliber electric gate valves.

This paper first analyzes the flow field distribution of the valve body structure. Secondly, the flow field and stress distribution of the cylindrical valve body after structural optimization were analyzed under the same working conditions, including thermal stress analysis and static stress analysis. Finally, the analysis results are compared. The valve body structure that meets the original strength requirements and is beautiful and light in weight is obtained, and the goal of green and lightweight valve bodies is achieved. In this paper, the optimized path of the electric gate valve body is shown in Fig. 1. The cube structure on the upper part of the valve body is transformed into a cylindrical structure, and the strength analysis of the optimized structure is performed.

## 2 The Research Methods

In this paper, after a simple analysis of the valve body’s working condition, it is obtained that the Reyro number of the fluid in the valve body is much greater than 2300. Therefore, a turbulence model is used in the fluid analysis and an elastic mechanics model is selected in the static stress analysis.

Elasticity is a discipline that seeks the physical quantities of displacement, stress and strain produced by elastic deformation bodies under certain constraints. The theoretical model used in this paper is the stress–strain equation. For an isotropic, uniform, continuous valve body, the valve body must meet the generalized Hook’s law:

$$\left. \begin{aligned}
 \sigma_x &= \frac{1}{E} [\sigma_x - \mu(\sigma_y + \sigma_z)] \\
 \sigma_y &= \frac{1}{E} [\sigma_y - \mu(\sigma_x + \sigma_z)] \\
 \sigma_z &= \frac{1}{E} [\sigma_z - \mu(\sigma_x + \sigma_y)] \\
 \gamma_{xy} &= \frac{1}{G} \tau_{xy} \\
 \gamma_{yz} &= \frac{1}{G} \tau_{yz} \\
 \gamma_{xz} &= \frac{1}{G} \tau_{xz}
 \end{aligned} \right\} \tag{1}$$



in which  $E$  is the elastic modulus,  $G$  is the shear modulus,  $\mu$  is Poisson's ratio,  $\sigma$  is the normal stress and  $\gamma$  is the shear stress.

And

$$G = \frac{E}{2(1 + \mu)}.$$

The fluid can be considered as a continuous distribution of particles, and time is used to measure the change of particles in three dimensions. In the analysis model, each physical quantity (speed, pressure, density) of the fluid is analyzed as a function of the three-dimensional space position vector and time. According to the needs of practical problems, this paper chooses the standard  $k - \varepsilon$  model. The  $k - \varepsilon$  turbulence model in Cartesian coordinate system is divided into two continuity equations, the turbulence energy equation and the energy dissipation rate equation.

The turbulent flow energy  $K$  equation is:

$$\frac{\partial}{\partial t}(\rho K) + \frac{\partial}{\partial x_j}(\rho K \overline{\mu_j}) \frac{\partial}{\partial x_j} \left[ \left( \mu + \frac{\mu_t}{\sigma_k} \right) \frac{\partial K}{\partial x_j} \right] + P_K + G_b - \rho \varepsilon - Y_M \quad (2)$$

The energy dissipation  $\varepsilon$  equation is:

$$\frac{\partial}{\partial t}(\rho \varepsilon) + \frac{\partial}{\partial x_j}(\rho \varepsilon \overline{\mu_j}) = \frac{\partial}{\partial x_j} \left[ \left( \mu + \frac{\mu_t}{\sigma_\varepsilon} \right) \frac{\partial \varepsilon}{\partial x_j} \right] + C_{\varepsilon 1} \frac{\varepsilon}{k} P_k + C_{\varepsilon 1} \frac{\varepsilon}{k} C_{\varepsilon 3} G_b - C_{\varepsilon 2} \rho \frac{\varepsilon^2}{k} \quad (3)$$

In the  $K$  equation:  $P_k$  is the turbulent kinetic energy generation term;  $G_b$  is the buoyancy generation term;  $-\rho \varepsilon$  is the dissipation term;  $Y_M$  is the compressible correction term.

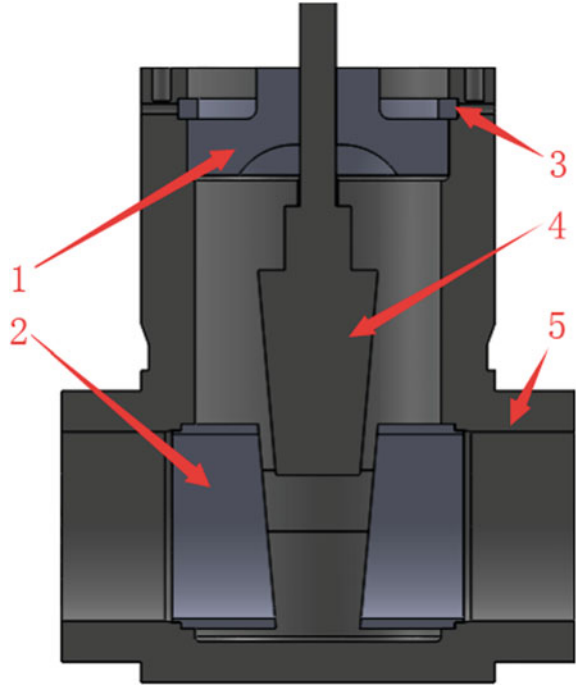
### 3 Modeling Analysis

The 3D solid model and the stress numerical analysis model are established to analyze optimized valve body safety in this paper.

#### 3.1 Physical Model

Models of the valve body, valve seat, pressure equalizing ring, packing chamber and valve disk of the gate valve were established using SolidWorks 3D modeling software, as shown in Fig. 2.

**Fig. 2** 3D model of electric gate valve



The valve body and the valve seat are welded. The pressure equalizing ring has no frictional contact with the valve body, and the packing chamber and the pressure equalizing ring have no frictional contact.

In the figure, 1 is a packing chamber, 2—a valve seat, 3—a pressure equalizing ring, 4—a valve disk and a valve stem (in order to simplify the model), and 5—a valve body.

### 3.2 Numerical Analysis Model

Through the previous theoretical calculations, the theoretical model for numerical analysis has been determined. For fluid analysis, a standard  $k - \epsilon$  turbulence model is used in this paper. For static stress analysis, a general static stress analysis model is directly selected. And finally, fluid–structure coupling calculation is performed. Fluid analysis before static stress analysis. Firstly, the three-dimensional model of the gate valve is imported into the analysis software. In order to establish the fluid area and solid area separately, it is necessary to ensure that the valve body cavity is closed. Therefore, before the parameter setting, the two ends of the valve body are closed. In Eqs. (2) and (3),  $\rho$  is density.  $\epsilon$  is turbulent dissipation rate. PK is the turbulent kinetic energy generation term.  $G_b$  is the buoyancy generation term. –

$\rho\varepsilon$  is the dissipation term. YM is the compressible correction term and value query literature [12]. Material is forged alloy steel F91, and material parameters are shown in Table 1.

### Meshing

Import the valve body in the saved *.x\_b* file format into the workbench. Select solid material F91, and mesh the model in the flow simulation module. For static stress analysis, it is a steady-state analysis. The type of mesh is not very high. For the convenience of calculation, this paper uses the simplest tetrahedral mesh. The results are shown in Fig. 3.

**Table 1** Material properties of forged alloy steel F91

Density (kg/m <sup>3</sup> )	Elastic modulus (GPa)	Yield strength (MPa, 550 °C)	Poisson's ratio
7700	210	212	0.3
Expansion (/K 10 <sup>-6</sup> )	Thermal conductivity (W/(m*K))	Specific heat (J/(kg*K))	Allowable value [13]
12.5	38	440	107 MPa

**Fig. 3** Meshing of the model

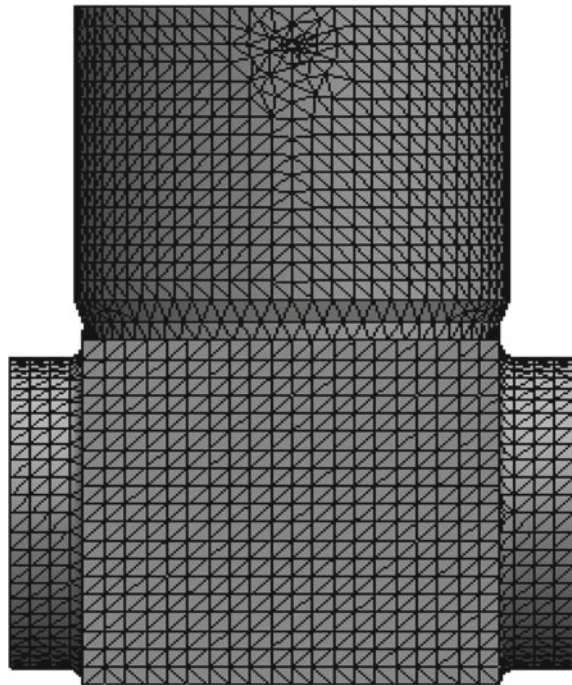


**Table 2** Parameters of valve body working conditions

Body parameters		Working parameter	
Nominal size	DN500	Design pressure	14 MPa
Body material	F91	Working temperature	550 °C
Processing form	Forging	Working medium	High-temperature gas
Allowable stress	$[\sigma] = 107 \text{ MPa (550 °C)}$	Working pressure	10.6 MPa

**Boundary Conditions**

The fluid simulation boundary is set as the mass flow inlet according to the actual situation. The inlet temperature and pressure are in the initial state when high-temperature steam enters; that is, the inlet temperature is 550 °C and the inlet pressure is 14 MPa. Because the gate valve is mainly used for opening and closing, there is almost no pressure drop, so the outlet boundary is set as the pressure boundary, the size is 14 MPa, and the temperature is 550 °C. The initial conditions set the inner temperature of the valve body to 550 °C and the pressure to 14 MPa, as shown in Table 2. And import the results of fluid analysis into the stress analysis module for stress–fluid–structure interaction analysis. For the analysis load, according to the actual working status of the valve body, the inlet and outlet ends of the valve body are bolted to other pipelines. In order to simplify the analysis model, the ends of the inlet and outlet are set as surface fixed constraints during static analysis, and the other areas are all free-end connections.

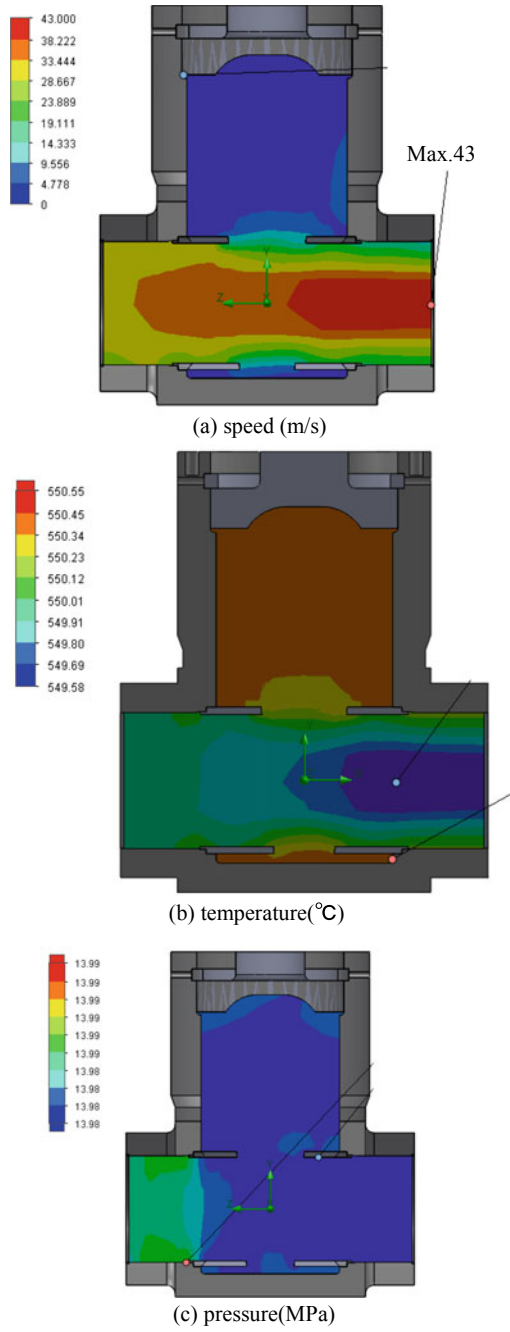
**4 Results and Analysis**

From the previous numerical simulation calculations, this paper has obtained simulation data on fluid velocity, temperature, static pressure and static stress simulation data on the valve body before and after optimization. The data will be analyzed and discussed below.

**4.1 Fluid Simulation Results**

The purpose of fluid simulation is to numerically simulate the working conditions of the gate valve in order to provide a reliable working load for stress simulation. Figure 4a shows the cloud diagram of the speed change of the high-temperature steam flowing through the valve body, Fig. 4b shows the cloud diagram of the temperature change when the high-temperature steam flows through the valve body, and Fig. 4c shows the static pressure display cloud diagram of the high-temperature steam in the valve body. As shown in Fig. 4a, the speed of the steam near the filling chamber and the bottom of the valve body is very small and almost stationary, while the speed of

Fig. 4 Fluid analysis results



the passage of the valve body is very large, reaching a maximum value of 43 m/s near the outlet. As shown in Fig. 4b, the temperature of the high-temperature steam in the valve body is basically maintained at about 550 °C, and it floats up and down by 0.5 °C. The minimum value is 549.5 °C in the area with a large flow velocity near the outlet; the maximum value is 550.3 °C in the area with a small flow velocity near the packing chamber and the bottom. As shown in Fig. 4c, the pressure change in the valve body is small, with only a small pressure loss. It fluctuates in the range of almost 14 MPa (i.e., design pressure). The maximum value is 14 MPa where the valve seat is raised, and the minimum value is 13.9 MPa where the valve seat is dropped.

The analysis shows that the temperature and pressure changes in the valve body are small, and both are within the range of working conditions. When the temperature is uniformly distributed, the thermal stress of the system is very small, and analysis can be omitted. Only the static strength at the operating temperature needs to be analyzed, and the internal pressure can be used as the input load for the static strength analysis.

### 4.2 Stress Analysis Results

As a basis for comparison before and after optimization, the properties of the valve body before optimization must be analyzed before the analysis of the circular valve body. Figure 5a shows the combined stress cloud diagram of the valve body before optimization, and Fig. 5b shows the Y-direction shear stress cloud diagram of the valve body before optimization. Figure 5c shows the Z-direction shear stress cloud diagram of the ZX plane of the front valve body, and Fig. 5d shows the Z-direction shear stress cloud diagram of the ZX plane of the front valve body.

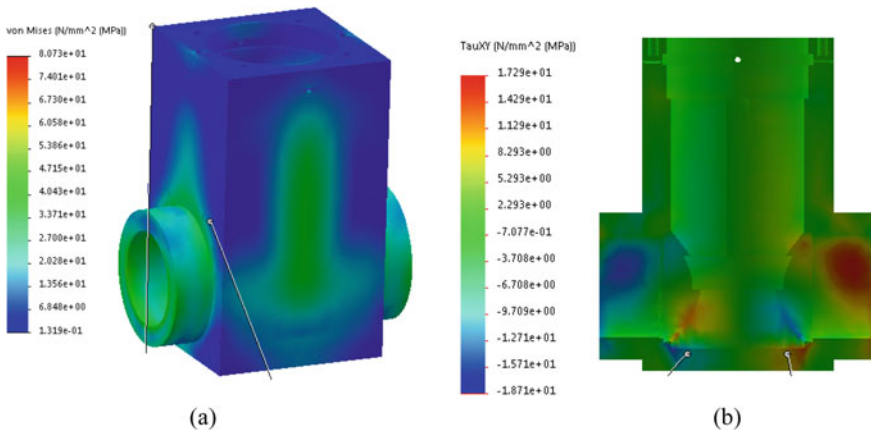


Fig. 5 Results of stress analysis before optimization

As shown in Fig. 5a, the maximum stress value of the valve body before optimization is 80.7 MPa, and the position where it appears is at the sharp corner of the valve seat. As shown in Fig. 5b, the maximum *Y* shear resistance of the optimized front valve body is 17.2 MPa, which is symmetrically distributed at the valve seat junction. As shown in Fig. 6a, the maximum stress value of the valve body after optimization is 98.7 MPa, and the position where it appears is at the sharp corner of the valve seat. As shown in Fig. 6b, the maximum *X*-shear of the valve body after optimization is 27.6 MPa, which is almost symmetrically distributed at the valve seat junction.

The analysis shows that the main stress of the valve body after optimization is still derived from the *Z* normal stress, and the maximum value reaches 98.7 MPa, which is much larger than the other directions. The maximum shear is mainly *Z* shear stress, and the maximum is 27.6 MPa. Obviously, the stress in each direction does not change much, and the maximum increment is 5 MPa. And the stress is still concentrated at the interface between the high-speed inner wall and the valve seat. It can be seen from the cloud diagram that the temperature and pressure changes of high-temperature steam when flowing through the valve body are not obvious. Both are in the operating range of 550 °C and 14 MPa, and the speed quickly flows through the valve body in the high-speed area of the circulation area. It can be seen that steam passes quickly through the valve body. The upper part of the valve body does not flow into the steam. For the low-speed area, the steam flows in when it does not reach the working conditions. When it reaches the working conditions, it only flows slowly at a very small speed, which is consistent with the actual situation.

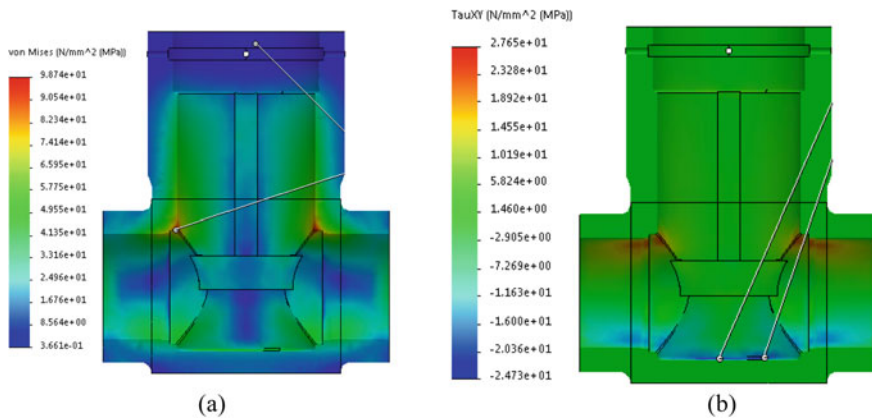


Fig. 6 Results of stress analysis after optimization

**Table 3** Comparison of valve body attributes before and after optimizations

	After optimization	Before optimization	Increments	Optimization rate
Mass(kg)	2760	3488	-728	+20.8%
Max. combined stress (MPa)	98.7	80.7	+10.0	Safety
Max. shear stress (MPa)	27.6	17.2	+10.4	Safety

### 4.3 Comparative Analysis Results

According to the above stress cloud diagram simulation data, the specific simulation result parameters of the optimized valve body before and after optimization are obtained, and the specific attribute changes of the valve body before and after optimization are obtained by sorting the results. Lightweight valve comparison of attributes before and after volume optimization is easily shown in Table 3. As can be seen in Table 3, the mass of the valve body is reduced by 728 kg, the optimization rate is 20.8%, and the maximum stress is less than 107 MPa, which meets the design requirements.

## 5 Conclusion

This article theoretically plans an optimized route, removes some materials on the valve body and changes the square valve body head to a cylindrical valve body head. As far as materials are concerned, the mass of the valve body is reduced by 728 kg, and the optimization rate is 20.8%. In terms of strength check, this paper first analyzes the fluid of the valve body and analyzes the temperature, flow rate and pressure of the high-temperature steam in the valve body. It is obtained that the maximum position of the flow velocity is near the exit, which is basically about 40 m/s, and the maximum value reaches 43 m/s, which meets the requirements of relevant national standards; the temperature and pressure are basically maintained at 550 °C and 14 MPa. For the static stress analysis, it is found that the stress at the sharp corners is large, but all are less than the allowable stress value of the material that is 107 MPa, which is considered safe. Therefore, the optimized valve body not only is beautiful and light in weight, but also does not reduce the strength requirements of the valve body; that is, it achieves the purpose of weight reduction under the condition of meeting the strength requirements.

In the process of lightweight research, this paper has shortcomings, and some laws have been found in the simulation process. These are the following suggestions: (1) The study found that the places with high stress are mainly distributed at the sharp corners of the inner wall and the valve seat protruding the location of the runner. The reason for the analysis is that there is a step behind the valve seat welded to the valve



body, which hinders the flow of high-temperature steam and generates a large impact, which increases the stress of the valve body. In view of this problem, the suggestion proposed in this article is to make a slope at the inlet of the valve seat flow passage so that high-temperature steam can pass through the valve body with low resistance and reduce impact. (2) When the temperature fluctuates, the thermal stress increases [14]. Therefore, the prerequisite for reducing thermal stress is uniform temperature distribution. In order to reduce the impact of thermal stress on the service life of the valve body, this article recommends that the necessary thermal insulation measures must be taken for the valve body during work to avoid additional temperature thermal stress.

**Acknowledgements** This work is financially supported by National Natural Science Foundation of China (Grant No. 51675388).

## References

1. Lu, F., Cao, H., Zhang, H.: Theory and Technology of Green Manufacturing. Science Press, Beijing (2005)
2. Zhang, H., Jiang, Z.: Theory and Practice of Green Manufacturing System Engineering. Science Press, Beijing (2005)
3. Zhao, G., Zhang, H., Zhang, G., Guo, L.: Morphology and coupling of environmental boundaries in an iron and steel industrial system for modelling metabolic behaviours of mass and energy. *J. Clean. Prod.* **100**(8), 247–261 (2015)
4. Zhao, G., Zhang, X., Fang, C., Ruan, D., Wang, Y.: Systemic boundaries in industrial systems: A new concept defined to improve LCA for metallurgical and manufacturing systems. *J. Clean. Prod.* **26**(187), 717–729 (2018)
5. Ma, S., Wang, X.: Research on lightweight design technology of large-capacity refrigeration four-way valve. *Mach. Tool Hydraul.* **46**(22), 45–50 (2018)
6. Zhu, Y., Zhang, L.: Lightweight directional valve body and directional valve based on SLM technology (2019), CN201910491655.6
7. Wang, X., Zhao, W., Li, B.: Temperature field analysis of injector needle valve body based on fluid-solid coupling. *Veh. Eng.* **1**(5), 74–79 (2019)
8. Lv, W.: Analysis on influence of multiway valves defects of roadheader for structural strength of valve body based on ANSYS. *Coal Mine Mach.* **40**(12), 91–93 (2019)
9. Ma, G., Ji, J., Yao, D.: Effects of valve clearance on valve performance and internal flow field distribution. *J. Drain. Irrig. Machin. Eng.* **37**(11), 960–966 (2019)
10. Yi, X., Yao, Z., Zhou, Y.: Analysis of mechanical properties of CD-GF type drilling ball valve body. *China Petrol. Machin.* **47**(9), 23–29 (2019)
11. Lei, X., Zhao, L., Yan, S.: The effect of heat treatment on the microstructure and the properties of ductile iron valve housing. *Hydro-Pneumat. Seal.* **39**(4), 90–93 (2019)
12. Ding, X., Jiao, N.: Fluid Simulation Computing from Entry to Mastery. Tsinghua University Press, Beijing (2014)
13. NB/T47010-2017. People's Republic of China Energy Industry Standard
14. Li, Y., Li, N., Yan, J.: Heat transfer characteristics of a new ceiling radiant cooling panel with uniform temperature distribution in the surface. *J. Civil Archit. Environm. Eng.* **36**(5), 16–22 (2014)
15. Li, Y., Li, N., Yan, J.: Heat transfer characteristics of a new ceiling radiant cooling panel with uniform temperature distribution in the surface. *J. Civil Archit. Environ. Eng.* **36**(5), 16–22 (2014)

# Research on Quantitative Evaluation of Green Property of Iron and Steel Enterprises Based on BP Neural Network



Junsong Xiao, Gang Zhao, and Pengcheng Yan

**Abstract** To objectively evaluate the resource efficiency and environmental impact of iron and steel enterprises, it is necessary to comprehensively evaluate the greenness of their manufacturing process. In this paper, based on the green evaluation index of iron and steel enterprises, a two-level green evaluation system derived from the manufacturing process is established, and a green evaluation and prediction model of the manufacturing process are established. Firstly, the data in the actual production process of iron and steel enterprises are normalized. The first 75% of the data is taken as the training set, and the last 25% as the test set. Then, the data set is imported into the constructed BP neural network for training. Finally, through the analysis of the training results, it can simulate the experts to evaluate the diagnosis and predict the optimized manufacturing process.

## 1 Introduction

In the process of building a community with a shared future for mankind, the issue of environmental protection has drawn the attention of people from all walks of life. Nowadays, China's industrialization and modernization process is speeding up. The rapid development of the steel industry not only improves the development speed of China's economy, but also causes pollution and damage to China's natural ecological environment and social environment.

It can be considered that green manufacturing is one of the main driving forces of sustainable industrial development [1], and iron and steel enterprises should take optimizing the manufacturing process, comprehensive utilization of resources, and reduction of pollutant emissions as their mission. As a heavy industry with high

---

J. Xiao · G. Zhao (✉)

Key Laboratory of Metallurgical Equipment and Control Technology of Ministry of Education, Wuhan University of Science and Technology, Wuhan, Hubei 430081, China  
e-mail: [jasonzhao@wust.edu.cn](mailto:jasonzhao@wust.edu.cn)

P. Yan

Hubei Key Laboratory of Mechanical Transmission and Manufacturing Engineering, Wuhan University of Science and Technology, Wuhan, Hubei 430081, China

© The Editor(s) (if applicable) and The Author(s), under exclusive license to Springer Nature Singapore Pte Ltd. 2021

S. G. Scholz et al. (eds.), *Sustainable Design and Manufacturing 2020*, Smart Innovation, Systems and Technologies 200, [https://doi.org/10.1007/978-981-15-8131-1\\_44](https://doi.org/10.1007/978-981-15-8131-1_44)

energy consumption, high emission, and high pollution [2], it is very necessary for the government or the enterprises themselves to conduct green evaluation on their manufacturing process.

In the field of green evaluation, many scholars have put forward some evaluation index systems of iron and steel enterprises. For example, literature [3] established the evaluation index system of green supply chain management performance of iron and steel enterprises and studied the green supply chain management system of the four major iron and steel enterprises. Literature [4] designed the evaluation index system of the eco-efficiency of iron and steel enterprises and provided suggestions for improving the eco-efficiency of enterprises. Literature [5] established the planning scenario of sustainable development by constructing the iron and steel industry EIA index system and analyzing a plan with the improved analytic hierarchy process (AHP) fuzzy comprehensive evaluation model.

But for the quantitative evaluation on the steel manufacturing process, and the improved model is still lack of related research, considering the green evaluation index system of iron and steel enterprise index, distinct features, combined with the analytic hierarchy process (AHP), first proposed the BP neural network is applied to the green evaluation system of iron and steel enterprise. It reflects the current iron and steel enterprise greenness by the study of specific quantifiable indicators and predict the improved comprehensive evaluation. For work-related personnel, they can know and improve timely the plan of the enterprise and reduce the effects of decision lag. Neural network is widely used in many fields, such as pattern recognition, automatic control, signal processing, and decision support [6].

## **2 Construction of Green Evaluation Index System**

### ***2.1 Establishment Principles of the Index System***

In establishing an evaluation index system of green, we must hold to systematic, typicality, concise, and practical, which can be quantified, such as principles. By analyzing the relationship between the systematic features of the manufacturing process itself and the external environment analysis, in view of this overall goal, the level analysis of the comprehensive evaluation index system of the green manufacturing process is further expanded, and the perfect goal and scientific index system are established.

By combining the specific environment of iron and steel enterprises in our country at present and using the more mature green evaluation index system of iron and steel manufacturing for reference, a scientific, reasonable, and comprehensive evaluation index system is finally formed.

## **2.2 Establishment of the Model**

In this paper, the most commonly used system analysis method called the analytic hierarchy process (AHP) is used to analyze the comprehensive evaluation index system of green building projects.

The basic idea is to focus on the iron and steel manufacturing process through the indicators, namely material—material resources, water—water, energy conservation—energy consumption, emission reduction—gas, liquid, solid emissions, and to expand.

After the comprehensive analysis of each sub-target, the sub-index of each sub-target lower layer, namely the determination of the criterion layer, is selected based on the standards required by the relevant standards of the steel industry. Specific evaluation indicators are given in Table 1.

## **3 Green Evaluation Model Based on Neural Network**

### **3.1 Working Principle of BP Neural Network**

The neural model is designed to simulate the structure of biological neurons and simulate the information processing mechanism of the human brain. Structurally, the BP network has an input layer, a hidden layer, and an output layer.

In essence, the BP algorithm takes the network error as the objective function and uses the gradient descent method to calculate the minimum value of the objective function.

The connection weight of the hidden layer to the output layer indicates that how these characteristics affect the output result. For example, if a certain feature has a greater impact on an output, the weight of connecting them will be larger. The process of backpropagation is like this: Each node in the output layer will get an error. The output layer propagates the error back as the input layer does. The output layer is first obtained, and then, the output layer is transmitted to the hidden layer according to the connection weight [7]. As shown in Fig. 1, it is the basic structure diagram of the BP neural network.

### **3.2 The Construction of the Neural Network**

According to the actual situation of the green evaluation system of iron and steel enterprises, the influence factors of the bottom layer are explored with the method of the analytic hierarchy process (AHP), and the green evaluation of the system is divided into two levels [8].

The BP neural network model is designed as follows.

**Table 1** Evaluation index and number

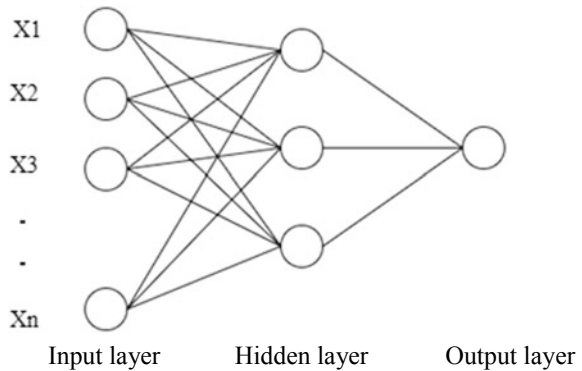
The total target	Points target	Points target layer	Quantification of indicators
Comprehensive evaluation of manufacturing process greenness	Material resource B1	Consumption of iron ore X1	Iron ore consumption for 1 ton steel production
		Scrap factor X2	Qualified ratio of scrap quantity to crude steel
	Water resources B2	New water volume per ton of steel X3	New water consumption for 1 ton steel production
	Energy consumption B3	Energy consumption in coking process X4	Energy consumption to produce 1 ton of coke
		Energy consumption of sintering process X5	Energy consumption to produce 1 ton of sinter
		Pellet process energy consumption X6	Energy consumption to produce one ton of pellet iron ore
		Energy consumption in iron making process X7	Energy consumption to produce 1 ton of pig iron
		Energy consumption of converter steelmaking process X8	Energy consumption to produce 1 ton of steel
		Blast furnace fuel ratio X9	The amount of fuel used to produce one ton of pig iron
		Residual heat recovery X10	Power generation generated by using residual heat and pressure
	Liquid discharge B4	Wastewater discharge per ton of steel X11	Wastewater discharged from the production of 1 ton of steel
		COD emission per ton of steel X12	Cod amount (water pollution) discharged from production of 1 ton steel
		Ammonia nitrogen emission per ton of steel x13	NH <sub>3</sub> /NH <sub>4</sub> <sup>+</sup> content in 1 ton of molten steel produced

(continued)

**Table 1** (continued)

The total target	Points target	Points target layer	Quantification of indicators
	Gas discharge B5	SO <sub>2</sub> emission per ton of steel X14	1 ton of SO <sub>2</sub> produced
		NO <sub>x</sub> emission per ton of steel X15	Production of NO <sub>2</sub> emitted by 1 ton
		CO <sub>2</sub> emission per ton of steel X16	1 ton of CO <sub>2</sub> produced
	Solid discharge B6	Recovery rate of iron sludge X17	Ratio of recycled iron sludge to total iron sludge produced
		Utilization rate of blast furnace slag X18	Ratio of recycled blast furnace slag to total blast furnace slag produced
		Converter slag utilization rate X19	Converter slag utilization

**Fig. 1** Basic structure diagram of the BP neural network



Firstly, determine the number of cells in the input layer.

There are 19 sub-indexes in the green evaluation index system of iron and steel enterprises, namely X1, X2, X3, X4, X5, X6, X7, X8, X9, X10, X11, X12, X13, X14, X15, X16, X17, X18, and X19. According to the six sub-target layers, the criterion layer of one sub-target B2 contains only one index X3, so it is considered separately. The number of units in the input layer of the other five sub-target layers is 2, 7, 3, 3, and 3.

Secondly, the hidden layer is designed. Hidden layer neurons number associated with the complexity of the various indices contain rules, it cannot be calculated directly with the calculation method of science or directly decided, according to the experience, contains two layers BP neural network can be said all of the logical relationship, to improve the accuracy of the evaluation results, need to pass data test

to determine. According to the test, the number of hidden layers in 5 sub-target layers is 2, 3, 2, 2, and 2 layers [9].

Finally, the output layer is designed. The output layer is the number of network training, the accuracy, the prediction value of the model.

### 3.3 Training and Testing of Neural Network

To enrich the training data, the data of M enterprise in 4 years and 16 quarters were collected, as well as the comprehensive evaluation of M enterprise in these 16 quarters by the industry expert system. Among them, the data of the first 12 quarters is used as the training set and the data of the last 4 quarters as the test set. If the error between the output result of the test set and the result given by the expert system is less than 2% [10], then the neural network can realize the green evaluation of the manufacturing process.

To train the model well, it is necessary to normalize the data by mapping the original data and transforming it according to Formula (1). For example, the transformation of index X1 and X2 in the first quarter is given in Table 2. See Tables 3, 4, 5, and 6 for other data after transformation. Tables 3, 4, 5, and 6 list only the first four quarters and the last four quarters.

$$y_i = 1 - \frac{|X_i - X_{ij}|}{X_{ij}} \tag{1}$$

In Tables 3 and 4, Da and Db are the score values of the experts on the index of material resources and energy consumption. Data import training BP neural network model, the output of hidden layers with higher speed of convergence of relu excitation function, network training is completed, through the quarter from 13 to 16 to test the accuracy-test sets of data, and accuracy calculation formula for Formula (2), five groups of secondary index model of training results accuracy such as Table 7.

$$R = \frac{|P - Z|}{Z} \cdot 100\% \tag{2}$$

where *R* is the accuracy, *P* is the predicted value of the model, and *Z* is the score of experts.

**Table 2** Conversion example

	Original value $X_i$	Reference value $X_{ij}$	After transformation $y_i$
X1	1.67024	1.6	0.9561
X2	37.62297	42.7	0.8811

**Table 3** First four quarters of training data of material resources and energy consumption

Quarter	X1	X2	Da	X4	X5	X6	X7	X8	X9	X10	Db
1	0.9561	0.8811	0.9327	0.9581	0.9120	0.9079	0.9781	0.9765	0.9527	0.9191	0.9557
2	0.9792	0.8572	0.921	0.9096	0.9278	0.9087	0.9551	0.9409	0.8578	0.9749	0.9306
3	0.9521	0.8337	0.8984	0.9469	0.9520	0.9109	0.9581	0.9269	0.9628	0.8184	0.9311
4	0.9645	0.9611	0.9645	0.9561	0.9231	0.9242	0.9199	0.9546	0.8860	0.8718	0.9261



**Table 4** Last four quarters of training data of material resources and energy consumption

Quarter	X1	X2	Da	X4	X5	X6	X7	X8	X9	X10	Db
13	0.9323	0.9535	–	0.9540	0.9880	0.9465	0.9231	0.9240	0.9959	0.9864	–
14	0.9910	0.9487	–	0.9121	0.9802	0.9564	0.9833	0.9148	0.9790	0.9363	–
15	0.9403	0.9040	–	0.9457	0.9434	0.9325	0.9725	0.9238	0.9690	0.9848	–
16	0.9275	0.9878	–	0.9784	0.9137	0.9202	0.9971	0.9737	0.8513	0.9390	–

In Tables 5 and 6, Dc, Dd, and De are, respectively, the score values of the experts on the liquid, gas, and solid emission indexes

### 3.4 Steel Enterprises Green Rating Results

The model training of the criterion layer index was carried out above, and the accuracy of the result exceeded 98%, so the accuracy requirement was met. Now the BP neural network was used to train and predict the scoring of the data of the sub-target layer, and the green comprehensive evaluation result of the manufacturing process was finally obtained.

In Table 8, the training and prediction of initial data is given. In the table,  $P$  means four quarters average accuracy.

However, the computer cannot recognize the evaluation level, so it is necessary to vectorize the level. The corresponding vector is shown in Table 9.

For the output vector of  $4 * 1$ , if the result vector is (0.0952, 0.9538, 0.0384, 0.0021), the main element closest to 1 is taken, that is, the evaluation is good.

The results of the trained network for the next four quarters are given in Table 10. The table lists only the average accuracy.

The results are consistent with the expert evaluation. From the prediction results of the neural network, the green index evaluation and prediction of iron and steel enterprises can be well realized by using the neural network.

## 4 Conclusion

By optimizing the relative value of the manufacturing process and substituting it into the model, the optimized green index can be predicted well. By comparing the evaluation results given by experts, BP neural network can well evaluate and predict the green index of the manufacturing process. In this study, the use of intelligent technology is conducive to the objective evaluation of the green of manufacturing enterprises.

**Table 5** First four quarters of training data of liquid, gas, and solid discharge

Quarter	X11	X12	X13	Dc	X14	X15	X16	Dd	X17	X18	X19	De
1	0.8673	0.8882	0.8570	0.8809	0.9563	0.7844	0.9719	0.8829	0.8278	0.8127	0.9158	0.8480
2	0.9861	0.9839	0.8212	0.9448	0.8295	0.7550	0.8024	0.7884	0.8505	0.8408	0.8452	0.8365
3	0.9663	0.9222	0.8817	0.9312	0.8556	0.8047	0.8847	0.8396	0.8921	0.9348	0.9057	0.9196
4	0.9251	0.8628	0.8845	0.8877	0.8435	0.8042	0.8661	0.8421	0.9768	0.8780	0.8982	0.9301

**Table 6** Last four quarters of training data of liquid, gas, and solid discharge

Quarter	X11	X12	X13	Dc	X14	X15	X16	Dd	X17	X18	X19	De
13	0.9515	0.8864	0.8271	–	0.8771	0.8538	0.9551	–	0.9676	0.8905	0.7971	–
14	0.9314	0.8961	0.9231	–	0.8977	0.9396	0.8224	–	0.9822	0.9312	0.8675	–
15	0.9481	0.9169	0.8172	–	0.9378	0.8044	0.8541	–	0.8266	0.8453	0.8481	–
16	0.9417	0.9353	0.8700	–	0.8013	0.8607	0.8007	–	0.9185	0.8123	0.7137	–

**Table 7** Prediction accuracy of BP neural network

Title	Content				
Points target layer	Da	Db	Dc	Dd	De
Average accuracy (%)	99.54	98.70	99.19	99.13	99.32

**Table 8** Initial data of training and prediction

Quarter	B1	B2	B3	B4	B5	B6	Grade
1	0.932	0.973	0.955	0.880	0.882	0.848	Good
2	0.921	0.9912	0.9306	0.9448	0.7884	0.8365	Low
3	0.8984	0.9859	0.9311	0.9312	0.8396	0.9196	Good
4	0.9645	0.9239	0.9261	0.8877	0.8421	0.9301	Good
5	0.8794	0.845	0.9234	0.8807	0.85	0.8493	Low
6	0.9595	0.8134	0.9179	0.9378	0.8662	0.9111	Satisfactory
7	0.9716	0.9045	0.9571	0.8652	0.8725	0.9444	Good
8	0.9149	0.8022	0.9504	0.8618	0.8157	0.8875	Low
9	0.9635	0.8019	0.933	0.8559	0.8595	0.9171	Satisfactory
10	0.9083	0.9724	0.9198	0.8165	0.8627	0.8214	Low
11	0.9927	0.9529	0.9231	0.9367	0.8537	0.8434	Good
12	0.9948	0.9249	0.9238	0.8739	0.8608	0.9388	Good
13	0.9453	0.9999	0.9628	0.8784	0.8981	0.9067	Excellent
14	0.9685	0.9639	0.9506	0.912	0.907	0.9329	Good
15	0.9531	0.9469	0.9303	0.9156	0.8212	0.8289	Low
16	0.9199	0.8386	0.9489	0.8914	0.8603	0.8448	Satisfactory

**Table 9** Level vector representation

Grade	Vector representation			
Excellent	1	0	0	0
Excellent	0	1	0	0
Satisfactory	0	0	1	0
Low	0	0	0	1

**Table 10** Test sets prediction results

Quarter	Prediction results	Main element	Grade
13	(0.8538, 0.1032, 0.0354, 0.0013)	(1, 0, 0, 0)	Excellent
14	(0.3421, 0.8904, 0.3354, 0.0198)	(0, 1, 0, 0)	Good
15	(0.0189, 0.1612, 0.2253, 0.7311)	(0, 0, 0, 1)	Low
16	(0.0324, 0.2063, 0.8344, 0.1364)	(0, 0, 1, 0)	Satisfactory

**Acknowledgements** This work is financially supported by National Natural Science Foundation of China (Grant No. 51775392).

## References

1. Zhao, G., Zhang, H., Zhang, G., Guo, L.: Morphology and coupling of environmental boundaries in an iron and steel industrial system for modeling metabolic behaviors of mass and energy. *J. Clean. Prod.* **100**(8), 247–261 (2015)
2. Zhao, G.: Systemic boundaries in industrial systems: A new concept defined to improve LCA for metallurgical. *J. Clean. Prod.* **187**, 717–729 (2018)
3. Yan, J., Song, Y., Liang, B.: A research on the iron and steel enterprise's competitiveness based on principal component analysis—using Tangshan Iron and Steel Group Co. Ltd as an example. In: Second International Conference on Intelligent System Design and Engineering Application, pp. 756–759. IEEE Computer Society (2012)
4. Zhao, G., Gao, X., Yang, S., Duan, J.: A mechanism model for accurately estimating carbon emissions on a micro-scale of the steel industrial system. *ISIJ Int. (Iron Steel Inst. Japan)* **59**(2), 381–390 (2019)
5. Zhao, G., Dan, R.: Quantitative evaluation of the greenness of steel enterprises oriented to the manufacturing process. *Mach. Des. Manuf.* **z1**, 157–160, 164 (2019)
6. Min, Z., Lei, W., Wang, G.F., et al.: A Relative Green Degree Evaluation Model for Equipments of Iron and Steel Enterprises, pp. 1–6. IEEE, New York (2011)
7. Hong-Juan, Y., Tian-Xia, Z., Jin-Fang, P.: Environmental performance evaluation of steel enterprises based on abrupt progression method. *Value Eng.* **9**, 1–3 (2014)
8. Ju-Long, D.: Overview of grey system. *World Sci.* **7**, 1–5 (1983)
9. Li, G.: A novel feature extraction method for machine learning based on surface electromyography. *Neural Comput. Appl.* **31**(12), 9013–9022 (2019)
10. Lu-Jun, D., Jin-Hui, X.: Application of radar graph analysis in comprehensive evaluation of potato variety characteristics. *Agric. Sci. GuiZhou* **41**(7), 59–62 (2013)

# Research on Green Design of Valve Products Based on Response Surface Method



Xiong Liu, Gang Zhao, Xiao-long Luo, Na Zhang, and Xin Huang

**Abstract** In order to realize the green design requirement of 550 mm gate valve in a valve system of an enterprise, the response surface method was used to optimize the body structure by single factor objective. Body wall thickness, height of stiffener, and thickness of stiffener as the objective factor, gate parameterized model is set up, using the finite element analysis software to optimize the former body strength that is numerically simulated, and based on DOE target optimization design for the parameters of optimized body coupling analysis, get the body by the maximum equivalent stress is 103 MPa. The results show that the strength of the improved valve body can apply to the requirements of the actual working condition, and the consumption of raw materials of the product is greatly reduced compared with the original design, which meets the requirements of the green design of valve products.

## 1 Introduction

Since green manufacturing was listed as one of the five major projects in the Made in China 2025 plan, China has been advocating the concept of sustainable development and following the path of ecological civilization. Green design is a brand new design concept, which is different from the traditional people-oriented idea. In the design process, resources utilization, energy consumption, and environmental protection are emphasized, which is the inevitable trend of the future manufacturing industry transformation and upgrading [1–4].

---

X. Liu

Key Laboratory of Metallurgical Equipment and Control Technology of Ministry of Education, Wuhan University of Science and Technology, Wuhan, Hubei 430081, China

G. Zhao

Hubei Key Laboratory of Mechanical Transmission and Manufacturing Engineering, Wuhan University of Science and Technology, Wuhan, Hubei 430081, China

X. Luo (✉) · N. Zhang · X. Huang

Wuhan Boiler Group Valve Co., Ltd, Wuhan, Hubei 430223, China

e-mail: [694332305@qq.com](mailto:694332305@qq.com)

Valve manufacturing is an indispensable part of China's manufacturing industry, but China's valve industry started late, relatively backward development, gate valve design technology innovation, process optimization, equipment management, and other aspects of the world's top level is still a big gap [5]. In the traditional gate valve design process, the designers seldom consider the environmental issues such as resource consumption and ecological pollution, which is obviously contrary to the concept of green design and manufacturing. In recent years, the research on gate valve structure analysis and optimization direction is also increasing. According to the shortcomings of previous gate valve design methods, LI proposed the equivalent stress classification design approach [6]. Liu proposed a gate valve runner optimization method based on numerical simulation analysis of the flow behavior of fluid flow in gate valves [7]. Luo calculated the stress distribution of the valve body under high pressure load and cut the thickness of the valve wall to obtain the gate valve structure meeting the strength requirements [8]. Shang effectively reduced the deformation of valve body by optimizing the layout of reinforcing rib position [9].

However, most of the electric gate valve structure lightweight by reducing the wall thickness size, applying the pressure in the valve body to calculate the equivalent stress, has not formed a standard and effective valve products green design system. Based on response surface method, this paper conducts green design and research on an electric gate valve of an enterprise and reveals the law of the maximum equivalent stress distribution of each design parameter, which can provide an effective reference method for the green design of mechanical products of the enterprise.

## 2 Methods and Theories

### 2.1 Response Surface Method

Response surface method is a statistical method to find the optimal solution in a certain range. It considers the random errors of events, including experimental design, model building, and response analysis, polynomial function fitting, and searching for the optimal solution. Based on the response of each factor, the best experimental condition can be found by the response value [10].

The design of response surface requires that the horizontal range of factors should be considered reasonably, otherwise the results obtained by this method are not representative and cannot get better optimization results. Therefore, detailed theoretical knowledge is needed to determine a reasonable range of experimental data when selecting factor levels. By designing different structural parameters of gate valve on response surface, the response value under each factor is obtained, and then, the fitting equation is obtained by nonlinear fitting method. Generally, quadratic polynomials are obtained through the interaction between each factor, higher-order polynomials

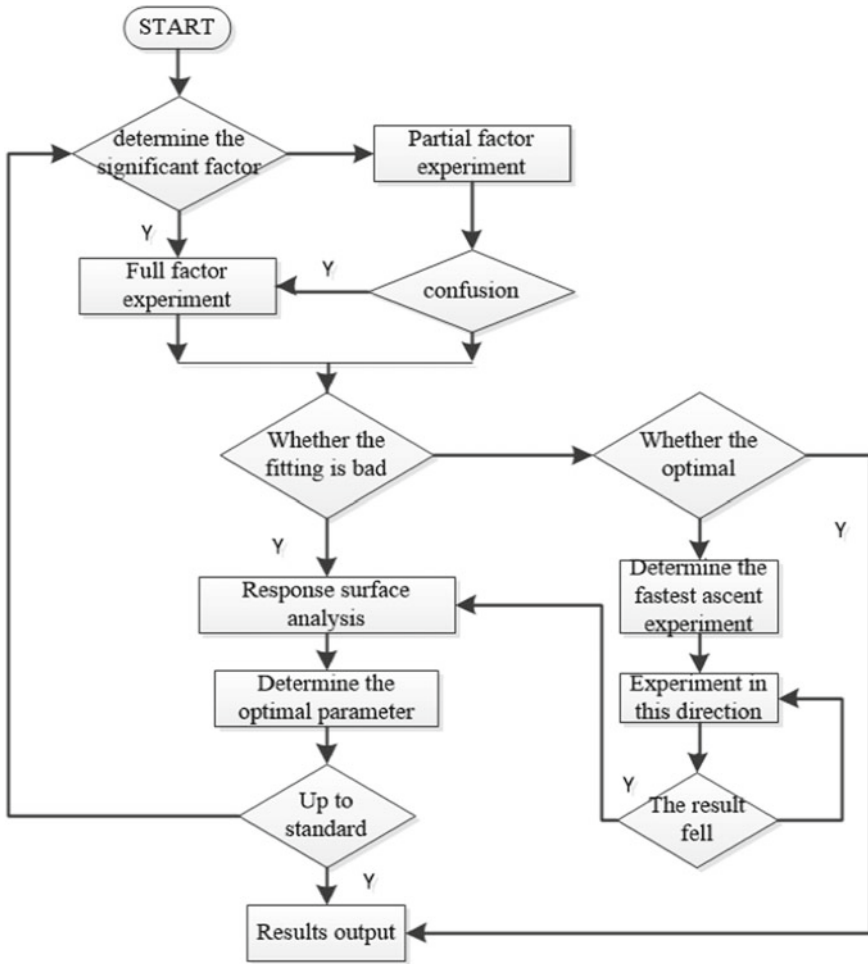


Fig. 1 Response surface analysis flow

are used in complex relationships, and response surface graph and objective optimization value are obtained through fitting simulation. The response surface analysis flow is shown in Fig. 1.

## 2.2 Coupling Calculation Theory

The actual engineering field is generally composed of multiple physical fields, and a single field can hardly exist. Fluid–solid coupling is divided into unidirectional coupling and bidirectional coupling. Unidirectional coupling usually does not

consider the effect of the solid domain on the fluid domain, while bidirectional coupling requires the simultaneous existence of two computational domains. The lightweight of the electric gate valve focuses on the analysis of the solid field, so the unidirectional fluid–solid coupling is chosen as the simulation method [11]. Due to the interaction between the fluid inside the electric gate valve and the inner cavity, the variables of the flow channel and the inner cavity of the valve body are equal, which can be expressed as the following parametric equation:

$$\begin{aligned} n \cdot \tau_f &= n \tau_s \\ l_f &= l_s \\ v_f &= v_s \end{aligned} \quad (1)$$

Formula:  $\tau_f$ ,  $\tau_s$  are the stress of flow passage and valve body,  $l_f$ ,  $l_s$  are the amount of flow passage and valve body movement, and  $v_f$ ,  $v_s$  are flow channel and valve body speed.

According to Eq. (1), the flow path of electric gate valve is numerically simulated in computer. After the calculation, the pressure field result of the flow channel outer wall is imported into the coupling surface of the valve body.

### 3 Finite Element Analysis and Result Discussion

#### 3.1 Pretreatment Setting

The established 3D model was imported into the design model (DM), and the flow channel in the gate valve was extracted with fill function to distinguish two different calculation areas. Using free mesh division method, the span center angle is set as fine, the relevant center parameters are set as fine, and the slip degree is set as high. The total number of valve body model division units is 159,947, and the total number of flow channel model division units is 120,150. The meshing model is shown in Fig. 2.

##### (1) Flow field

The fluid flow medium in the flow channel of the electric gate valve is high-temperature steam, and the maximum flow rate in the working condition is no more than 50 m/s, which belongs to the low-speed flow process. Since the performance parameters (such as speed, pressure, and density) of the low-speed steam basically do not change during the flow process and can be approximately equal to a constant, the gate valve runner medium is simulated as an incompressible fluid. The boundary conditions of the model are: the velocity inlet is adopted, the size is 42 m/s, and the temperature is 540 °C. Adopting pressure outlet, the design pressure of electric gate valve is 10.5 MPa. The surface of the fluid region is set as no slip, that is, the velocity component in each direction is 0.

##### (1) Structure field



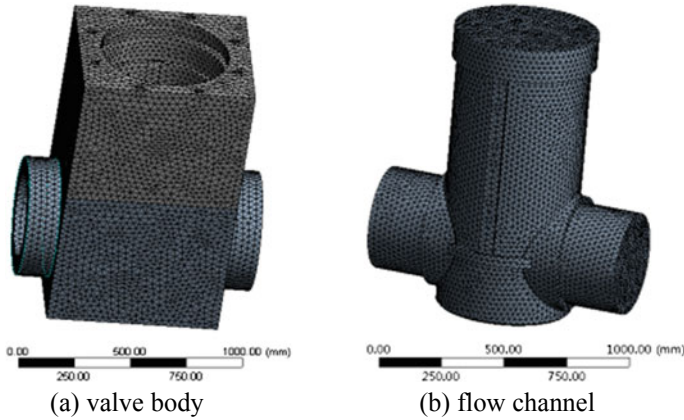


**Fig. 2** Grid division of the structure

Electric gate valve for special equipment, according to the actual needs of the choice of good mechanical properties of alloy forged steel F91 (10Cr9Mo1VNbN) as the material of electric gate valve. Its mass characteristics include: mass density of 7780 kg/m<sup>3</sup>, elastic modulus of 212 GPa, Poisson’s ratio of 0.29, setting the interface between the fluid domain and the solid domain as the coupling surface.

### 3.2 The Numerical Simulation

Numerical simulation was carried out on computer, and the velocity vector and pressure distribution of the coupling surface in the fluid region were obtained through post-processing, as shown in Fig. 3.

We can know from figure (a) that the horizontal high-temperature steam flows in a relatively stable direction, with a small range of velocity variation from the inlet to the outlet. The velocity of the main channel is basically maintained at 42 m/s, and the maximum velocity is 49.95 m/s. However, there is an obvious difference between the velocity of the vertical orifice and that of the horizontal orifice, which indicates that the optimization of the vertical structure of the valve body has little influence on the pressure loss of the orifice during the operation of the valve system. According to figure (b), the pressure value of the fluid–solid coupling surface is basically maintained at 10.5 MPa, and the pressure is stable at all points of the flow passage. The pressure loss of the airflow at the intersection of the medium passage hole is small and can be ignored. The maximum pressure at the edge of the valve body bend is 10.52 MPa.

The coupling analysis of fluid domain and solid domain is constructed, the pressure output calculated in the fluid domain is taken as the input load in the solid domain, and then, the distribution of stress value of the valve body is obtained. The

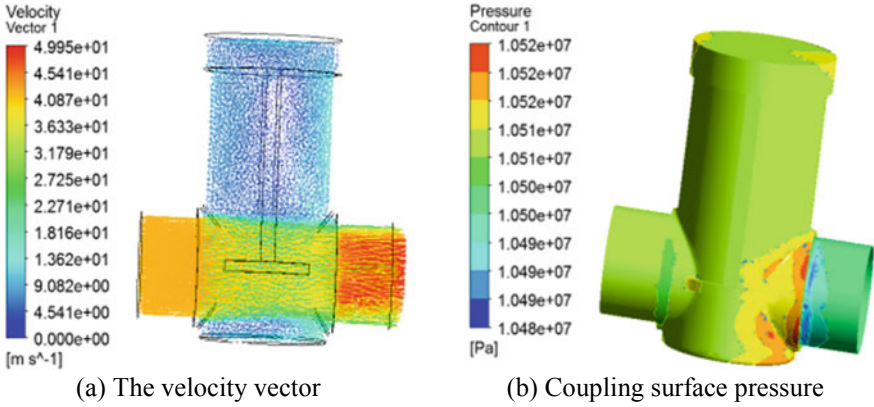
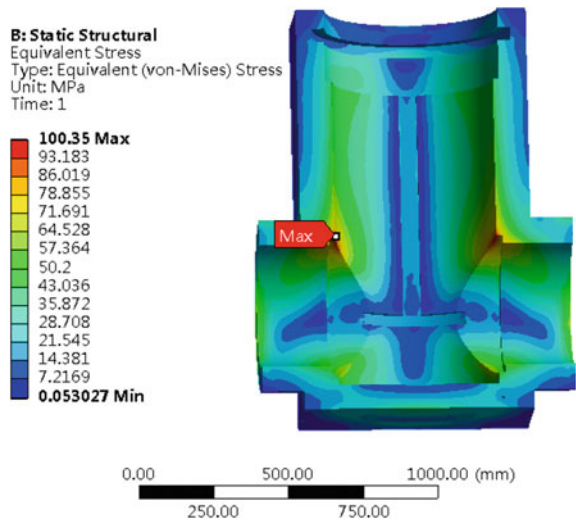


Fig. 3 Numerical simulation results of flow channel

Fig. 4 Stress distribution of valve body before optimization



maximum stress point is at the edge where the flow passage intersects, and the size is 100.35 MPa, as shown in Fig. 4.

## 4 Green Design and Optimization

### (1) Optimization mathematical model

From Fig. 4, it can be seen that the equivalent stress value on the upper part of the valve body is small, within the allowable stress range of the material, except

for the large equivalent stress value at the junction of the gate valve’s inner cavity. Therefore, for this part of the weight reduction optimization, determine the transverse and longitudinal reinforcement size and distribution, in order to meet the strength requirements of the gate valve body. Since the design of electric gate valve must meet the requirements of safety and economic cost at the same time, this paper adopts the design of exploration optimization design module in Workbench. By setting the change interval of the initial value and the definition of the objective function, the optimal group of solutions (that is, the critical extreme value of the objective function) are obtained by automatically searching within the value interval. The wall thickness  $h_0$ , width  $w_1, w_2$ , and height  $l_1$  and  $l_2$  of transverse and longitudinal stiffeners at the upper part of the valve body are selected as design variables, and this value of  $[\sigma]$  is the constraint condition ( $[\sigma]$  is the allowable stress value), and the total weight  $M$  (Kg) of the valve body is the objective function. The following lightweight design mathematical model () is established:

$$\left\{ \begin{array}{l} \text{s.t.} \left\{ \begin{array}{l} 65 \leq h_0 \leq 95 \\ 10 \leq l_1 \leq 40 \\ 40 \leq l_2 \leq 60 \\ 15 \leq w_1 \leq 25 \\ 15 \leq w_2 \leq 25 \\ \sigma \leq [\sigma] \\ \min M \end{array} \right. \end{array} \right. \quad (2)$$

(2) Response factor scope

The upper and lower boundaries of design parameters are set in the DOE interface, and the specific parameters are given in Table 1, and the screening method algorithm is selected to automatically search for optimization [12], with a total of 100 sample points.

(3) Response factor scope

After the design point is updated, the optimization results of gate valve parameters are obtained through several iterations. Figure 5 is the local influence factor diagram of each design variable on the total weight and the maximum equivalent stress of

**Table 1** Main design variables of electric gate valve body

Design variables	Initial value	Scope	Physical meaning
$h_0$	80	65–95	Upper body wall thickness
$l_1$	50	40–60	Transverse stiffener height
$l_2$	25	10–40	Longitudinal stiffener height
$w_1$	20	15–25	Transverse reinforcement width
$w_2$	20	15–25	Longitudinal reinforcement width

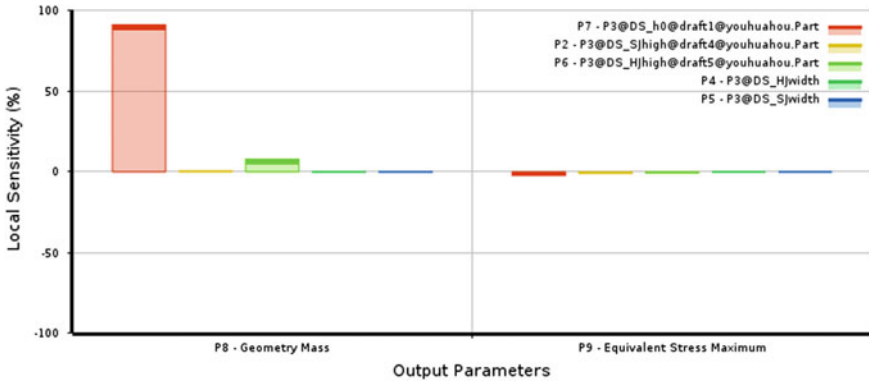


Fig. 5 Influence factors of design variables on the objective function

the valve body. It can be seen from the figure that the wall thickness of the upper part of the valve body  $h_0$  has the greatest influence on the total weight. The width  $l_1$  and wall thickness  $h_0$  of transverse stiffener have great influence on the maximum equivalent stress of valve body.

Figure 6a shows the response diagram of the wall thickness  $h_0$  and the width of transverse reinforcing rib  $w_1$  on the upper part of the valve body to the regular distribution of the total weight. It can be seen from the figure that the wall thickness of the valve body decreases with the decrease of  $h_0$  and the total weight  $M$ , but the strength level of the valve body decreases obviously, and the safety performance cannot be guaranteed. Figure 6b shows the response of design variables  $h_0$  and  $w_1$  to the law distribution of the maximum equivalent stress. It can be seen from the figure that the larger the value of wall thickness  $h_0$  and transverse reinforcement  $w_1$ , the smaller the maximum equivalent stress. But at a certain point, the change is no longer apparent.

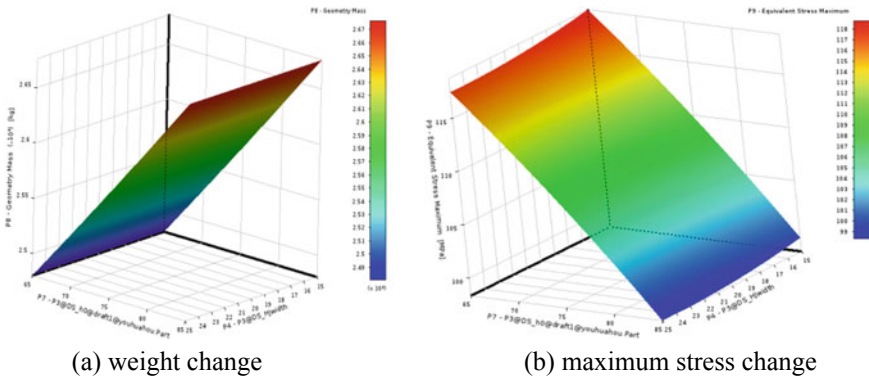
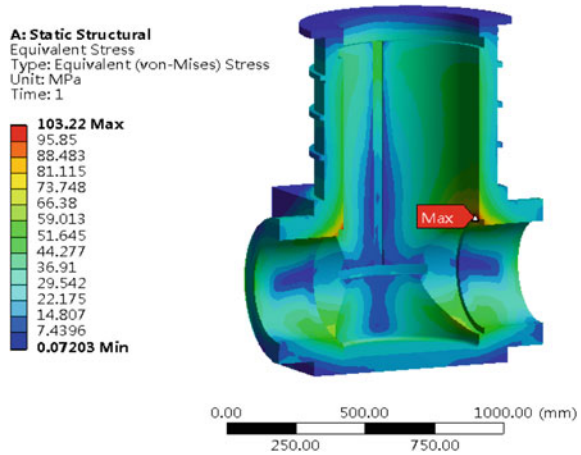


Fig. 6 Response of  $h_0$  and  $w_1$  to weight and stress change of valve body

**Fig. 7** Equivalent stress distribution of valve body



After comprehensive consideration,  $h_0 = 66.792$  mm,  $l_1 = 46.860$  mm,  $l_2 = 31.579$  mm,  $w_1 = 18.617$  mm, and  $w_2 = 15.629$  mm are selected as the final size.

The combination of the best parameters of the designed valve body was passed back to the Workbench-integrated analysis module to analyze the valve body. The analysis results are shown in Fig. 7.

Figure 7 shows that the maximum equivalent stress of the valve body after structural optimization is 103.22 MPa, which is less than the allowable stress of the material, and the structural strength meets the requirements.

From Table 2, we can realize the comparative analysis of valve body parameters before optimization and after roundness optimization. The valve body wall thickness  $h_0$  is reduced from 80 to 68 mm, and the wall thickness is reduced by 16%. The difference of maximum equivalent stress of valve body before and after optimization is small, which can meet the strength requirement. At the same time, the total weight of the electric gate valve is reduced from 3488 to 2579 kg. The lightweight effect is obvious, in line with the requirements of green design.

**Table 2** Comparison of valve body parameters before and after optimization

Parameter	$h_0$ (mm)	$l_1$ (mm)	$l_2$ (mm)	$w_1$ (mm)	$w_2$ (mm)	$\sigma_{max}$ (mm)	$M$ (kg)
Before	80	50	25	20	20	100.3	3488
After	67.79	46.86	31.58	18.62	15.63	103.2	2579.3
Roundness	68	47	32	19	16	103	2579

## 5 Conclusion

In this study, taking DN550 series electric gate valve of an enterprise as an example, with its valve body structure green design as the goal, based on the response surface method to optimize the design, the following conclusions are obtained:

- (1) The numerical simulation method can be used to more accurately understand the actual working condition of the valve body. According to the stress cloud diagram of valve body structure, the stress value of the whole part of the valve body is smaller, and the stress distribution of valve body structure is more uniform after optimization. The maximum equivalent stress occurs at the intersection of the valve body and the horizontal channel, causing fatigue damage to the internal structure of the valve body.
- (2) The relationship between wall thickness, transverse and longitudinal reinforcement size, and maximum equivalent stress on the upper body of electric gate valve was designed by response surface method. In the target range, the maximum equivalent stress of valve body increases with the increase of design parameters and the maximum equivalent stress tend to be stable after reaching the critical value. The total weight of valve body is reduced by 26% after optimization, which greatly reduces the material cost.
- (3) Green design and manufacturing is the focus of future research on manufacturing industry. The research on the lightweight green design method for manufacturing products can greatly reduce the resource consumption of enterprises and have a positive impact on ecological environment protection.

**Acknowledgements** This research is supported by the National Natural Science Foundation of China (Grant No. 51775392).

## References

1. Zhang, H., Huang, C., Li, R.: Super short-process green manufacturing method and energy consumption analysis of micro casting forging and milling for high performance parts. *China Mech. Eng.* **029**(021), 2553–2558 (2018)
2. Zhao, G., Zhang, H., Zhang, G., Guo, L.: Morphology and coupling of environmental boundaries in an iron and steel industrial system for modelling metabolic behaviours of mass and energy. *J. Clean. Prod.* **100**(8), 247–261 (2015)
3. Zhao, G., Zhang, X., Fang, C., Ruan, D., Wang, Y.: Systemic boundaries in industrial systems: a new concept defined to improve LCA for metallurgical and manufacturing systems. *J. Clean. Prod.* **187**, 717–729 (2018)
4. Zhao, G., Gao, X., Yang, S., Duan, J., Hu, J., Guo, X., Wang, Z.: A mechanism model for accurately estimating carbon emissions on a micro scale of the steel industrial system. *ISIJ Int. (Iron Steel Inst. Jpn)* **59**(2), 381–390 (2019)
5. Liu, W., Yang, S., Peng M.-Y., Wang, Y.: Research status and localization of underground safety valve at home and abroad. *J. Southwest Petrol. Univ.* **40**(3), 164–174 (2018)

6. Li, M., Zeng, Y.-Y., Wu, W., Zhou, S.Z.: Stress classification and strength assessment of 3000 m deep water gate valve. *Mech. Des. Manuf.* **7**, 96–99 (2016)
7. Liu, P., Liu, Y., Huang, Z., Cai, B., Sun, Q., Wei, X., Xin, C.: Design optimization for subsea gate valve based on combined analyses of fluid characteristics and sensitivity. *J. Petrol. Sci. Eng.* **182** (2019)
8. Xiao-Ling, L., Jun-Bing, Z.: Valve body stress analysis and structure optimization of high pressure gate valves. *Chem. Eng. Mach.* **45**(5), 633–635 (2018)
9. Shan, Y., Zhou, G., Li, P.: Finite element analysis and optimum design of deformation of valve body of low pressure gate valve with large diameter. *Valve* **1**, 20–22 (2017)
10. Liao, B., Sun, B., Li, Y.: Sealing reliability modeling of aviation seal based on interval uncertainty method and multidimensional response surface. *Chin. J. Aeronaut.* **32**, 9 (2019)
11. Kong, F.-Y., Chen, H., Wang, T., Su, X.: Analysis of pump body strength based on fluid-solid coupling of decompression tower bottom pump. *J. Mech. Eng.* **49**(2), 159–164 (2013)
12. Yuan, Y., Wang, Z., Zhang, Z.: The study of bridge girder lightening based on DOE and Wolf algorithm. *Mech. Des. Manuf.* **11**, 186–189 (2018)

# Integrated Electronic Systems for Acquisition of Customers for Transport and Logistics Services



A. Wiktorowska-Jasik , L. Filina-Dawidowicz , A. Cernova-Bickova, D. Możdrzeń , and D. Bickovs

**Abstract** Nowadays different electronic systems are used to acquire customers for transport and logistics services. The article aims to analyze these systems and examine the opinions of transport and logistics company owners concerning the possibilities of using integrated tools. Its primary objective was an attempt at obtaining an answer to the questions that concerned, among others: the impact of integrated electronic systems on processes related to customer acquisition, and the main benefits that the companies may derive from use of freight exchange services. To this end the selected freight exchanges were characterized. The survey questionnaire was developed, that was applied to marketing research among those owners of TSL companies, that use the services of freight exchange platforms in Latvia. The research revealed that owners of transport companies were willing to adopt the use of integrated electronic systems in the process of customer acquisition. The selected functions of such systems were also determined, with the preferences of their potential users.

## 1 Introductions

Contemporary TSL market is characterized by strong competition, which forces every company to undertake numerous actions, with the main objective of not just its presence in the market, but foremostly, the increase in its profits and market share. Nowadays, one of the significant activities undertaken by companies in the TSL sector is the implementation and use of IT systems, suites and applications, improving the course of each of the logistics processes. Tools of this type are also applied to successfully acquire customers for transport and logistics services.

---

A. Wiktorowska-Jasik · L. Filina-Dawidowicz (✉) · D. Możdrzeń  
West Pomeranian University of Technology, al. Piastów 41, 71-065 Szczecin, Poland  
e-mail: [Ludmila.filina@zut.edu.pl](mailto:Ludmila.filina@zut.edu.pl)

A. Cernova-Bickova  
A'Tuin Ltd., Maskavas Street 258 k-1-53, 1063 Riga, Latvia

D. Bickovs  
Latvian Maritime Academy, Flotes Street 12 k-1, 1016 Riga, Latvia



One of the basic activities, implemented to search for orders, is the use of services of freight exchanges. The application use in the transport management processes has increased significantly over the past twenty years. It is currently estimated that over 100 freight exchanges operate in Europe alone [20]. Electronic freight exchanges are the basic tools used by forwarding companies. They support the process of optimizing flows throughout the entire logistics chain by coordinating and cooperating the activities of suppliers, customers and other entities and contribute to the sustainable development of supply chains.

The variety of existing and emerging electronic systems means, that transport companies can select different solutions that may differ in their functionality. This requires their acquaintance with the specifics and efficiency of each and every too. Against this background, the trend of creating integrated electronic systems based on IT tools is also observed.

The analysis of available subject literature demonstrated that issues related to the description of electronic freight exchanges were subject to only a rather selective description. The need to systematize the singular information was noticed, especially in the aspect of applying integrated electronic systems, and above all to support it with practical research carried out among actual users of these systems.

Therefore, the article aims to analyze the tools applied to acquire customers for cargo freight services, and investigate the opinions of owners of transport companies concerning the potential for use of integrated tools. The case study of the Latvian market has been considered and a survey among transport companies was carried out.

## 2 Literature Analysis

Modern IT systems have become an indispensable tool in the freight forwarder's operations. Managing the vehicle fleet is getting more and more difficult. The increased competition on the forwarding services market requires constant improvement of quality as well as constantly providing new offers. Moreover, there is a growing number of customers, who require forwarders to be fast in their actions, as well as expect to receive flexible and comprehensive services. The contemporary standard for operation of forwarder is the use of freight exchanges. The facilitate daily operations in the organization of transport processes, allow for international contacts to be established, as well as grant access to free cargo, enabling their users to find inexpensive freight rates for every destination. These systems allow transport companies to find their customers and limit the number of empty runs, thus maximizing companies' profits. There are many electronic freight exchanges on the European transport services markets. They enable their users to find freights and manage their transport fleets. Freight exchanges have become the specific institutions regulating logistics processes. This means that programs are used mainly to improve the efficiency of transport processes, as well as to increase safety and the degree of environmental protection [21, 23].

Freight exchanges form the modern transaction platforms for companies from the TSL sector. Currently the freight exchange is a virtual market for exchange of information between carriers and forwarders. It is a place where one can find additional orders, while reducing transport costs, and filling the free cargo space with freight. For the participants of the transport market the electronic freight exchanges are significant, as these offer quick market insight, as they can serve as a tool for quick valuation of freights at a given moment. This is so, as the request for quotes is not sent to a single transport company, but to several thousand transport companies offering transport services [4, 19].

As far subject literature is considered the issues of customer acquisition systems application for the transport services market is typically narrowed down to the systems offered by the major exchange operators, and in particular those of the electronic freight exchanges [9]. The approach toward defining the freight exchanges also failed to adopt an unanimous solution. This may result from the extensive scope of operation of freight exchanges. Modern exchanges are no longer just a type of virtual market, where transactions are concluded, but they also offer a number of additional services. Using the exchanges one can search for the most beneficial solution of haulage of freight, or find a freight matching the vehicle fleet of the respective company. In addition, freight exchanges offer their users a number of services accelerating and securing the conclusion of transactions, e.g., defining a road map, text messengers or the possibility of debt collection, etc. Nowadays, exchanges are used as a marketing tool in penetrating new markets, allowing the parties to get to know their future contractor. For this reason, it is believed that the operation of freight exchanges is complex and covers many different areas of their functioning [2].

The publications describing freight exchanges emphasize the benefits that the enterprises, which use their services, may obtain. These benefits include, among others [16]:

- access to the pan-European freight market,
- the ability to develop e-CMR among EU and non-EU countries,
- the ability to use the freight exchange as a platform for collection of transport orders and customer communication,
- facilitation of effective control of all dispatchers working within the logistics system,
- time savings, which result from the possibility of simultaneous communication with several or even a dozen potential contractors,
- the ability to manage all freights and to direct freight information to specific recipients,
- reduction of costs of fuel and vehicle maintenance, resulting from reduction in the number of empty runs, reduction of CO<sub>2</sub> emissions,
- global freight management possibilities, which result from the fact that all information required is collected in a single system, etc.

Subject literature also devotes significant attention to the importance of information technologies in supply chain management [1, 15, 24]. It analyzes methods and models of integrated supply chain network design [13, 17, 18]. These models

include, among others, reliability, varying numbers of suppliers and buyers of goods [14]. This approach to the analyzed subject field stems mainly from the fact that in the recent decades an intense development of ICT was observed, including technologies dedicated for the transport industry. These changes brought about a significant alteration in the functioning model of this market [12, 23, 26]. The way of obtaining and handling orders has been changed, which led many companies to transfer their activities to electronic markets. These include freight exchanges, which nowadays play a significant role in establishment of business contacts.

The issues of integrated customer acquisition systems application on the transport services market were not widely described in the subject literature. Most of the available positions relate to intelligent transport systems, whose task is to combine information technology with transport infrastructure and vehicles [4, 6, 8, 11, 20]. In general, they are treated as instruments for improving the efficiency and safety of transport leading to its sustainable development [3, 7, 10].

Subject literature analysis proved that in the abundance of available research data concerning the functioning of electronic systems and tools for support of acquisition of transport companies' customers, the issue of applying integrated IT solutions was only described in general, and this knowledge still requires its further systematization.

### **3 Selected Electronic Systems Supporting the Acquisition of Road Haulage Customers**

There are currently many freight exchanges operating on the global market. The most valued and prominent operators of electronic freight exchange services, at least in Europe, include in particular: Trans.eu, TimoCom, Wtransnet, Transporeon Group, etc. Most of these systems were created during the last two decades, and they are characterized by the free access to their services.

Trans.eu, for example, is a Polish company founded in 2004. Every day, it serves over 200,000 users, who place or query offers for transport of goods and vehicles [19]. Its owner and operator is the Logintrans company, based in Wrocław. The centers of this exchange are located in: Vilnius, Lithuania (coordinating its activities in Latvia, Lithuania and Estonia), Lauenau, Germany (Germany, Austria, Switzerland), Antwerp, Belgium (United Kingdom, Spain, Italy, Ireland, Sweden) and Bratislava, Slovakia (Slovakia, Czech Republic, Hungary). This exchange also offers instant messaging services, which is used to provide service information, and allow the transactions to be concluded. It is characterized by high speed of transactions service. In addition, it has a number of solutions enabling, for example, the assessment of contractors and the level of transaction risk (the so-called TransRisk index). To facilitate that assessment the exchange secured its access to the Register of Transport Debtors. Trans.eu also offers the TransTask index, which makes it easier for a transport company to manage its employees. The main benefit is the quick and efficient transmission of information to drivers. Moreover, Trans.eu enables creating

of transport orders for the transactions concluded with use of the exchange. This service is provided using TransOrder application, which facilitates the operations of freight forwarders. The Trans.eu system allows monitoring of drivers' tasks, thus making it an important tool for transport management.

The German TimoCom is another exchange operator that brings together more than 100,000 international users, who offer free cargo spaces and competitive freight rates [20]. The exchange allows freight forwarders to eliminate the time-consuming search for a suitable haulage company for carrying out a specific order. This largely improves the process of searching for transport orders in the contracted logistics market. It is worth emphasizing that TimoCom program was translated into more than 20 European languages, making it easier for clients to use its services. This solution significantly facilitates cooperation of business partners.

Wtransnet is another example of a company operating as an electronic freight exchange. The basic direction of development of this operator is management of technology platforms to ensure a high level of profitability and transaction security. User access process at Wtransnet is very restrictive, and companies providing there their services are systematically monitored. As a result, it is one of the safer exchanges, where the most recognizable companies in the transport sector operate. Wtransnet offers services in three different segments: real-time offer queries, establishing long-term cooperation between carriers and forwarders, and searching for companies to perform contracts [25].

Also Transporeon Group, which provides cloud-based logistics services, has become one of the most significant entities in the electronic freight exchange market. It is an innovative platform formed to manage freight rates and optimize transport processes. Transporeon enables the creation of a network of the most experienced consignors, suppliers, sellers, consignees and carriers in the world. It allows for reduction in the number of empty trucks and an increase in the transparency of transport processes [22].

Cargo.It is an example of an exchange that is mainly used by transport, forwarding and trade companies from the Baltic States, Russia, Belarus, Ukraine and Kazakhstan. It is a free freight exchange that works on the basis of a website and is intended for those who offer transport, and loads to haul. Its customers are predominantly companies from the manufacturing and commercial sectors, forwarders, etc. This exchange offers loads mainly from Lithuania, Latvia, Estonia, Western Europe and Russia. Every day, approximately 7000–8000 new cargo offers and 10,000–12,000 offers of transport services are placed in its database. This exchange has more than 15,000 forwarding and transport companies permanently registered [5].

## 4 Methodology

The article attempts to answer the following research questions:

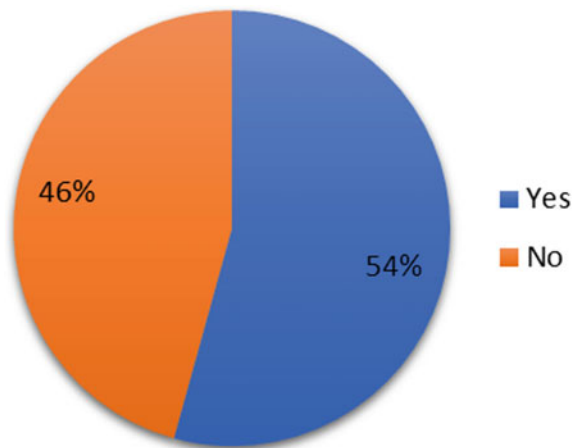
- what is the impact of integrated electronic systems on customer acquisition processes?
- what are the main benefits that the companies may attain by using the services of freight exchanges?
- which exchanges are the most significant in the process of acquiring customers and supporting the operations of transport and logistics companies?

The analysis of available subject literature was carried out to acquire the necessary data needed to conduct the research. Survey was used as a tool that made it possible to reach the opinions of users of freight exchanges. The survey covered transport and logistics companies located in Latvia. After elaborating the questions, the electronic survey form was activated from 21/02/2019 to 16/04/2019. The survey was sent to 465 transport and logistics companies operating in the Latvian TSL sector. 35 companies participated in the survey. Then the filled surveys were analyzed and conclusions were formulated. This allowed us to acquire research results relating to the impact of exchanges on the operation of enterprises from the transport and logistics industry.

## 5 Research Results

The results of the survey revealed the opinions of transport and logistics companies concerning integrated electronic systems. Respondents were asked whether they used electronic systems to acquire cargo freight customers. Figure 1 presents the percentage of analyzed companies that used electronic systems to acquire customers. Over half (54%) of the surveyed companies apply such systems, proving their familiarization with those, and the need to acquire customers by means of electronic systems. 46% of companies did not use such systems, and their operations are most likely based on cooperation with regular customers.

**Fig. 1** Answers to the question “Does your company use electronic systems to acquire cargo freight customers?”



Respondents using the electronic systems were further asked to indicate the system they use to acquire customers (Fig. 2). It was possible to mark several answers. Companies used different systems to acquire their customers. In Latvia three systems attracted the largest frequency of answers, followed by the option “Other”: Cargo.lt (was used by 14 companies), TimoCom (13 companies), and Trans.eu (12 companies). Five companies also apply other electronic tools to acquire customers.

Answering next question, representatives of surveyed transport companies expressed a decisive demand for use of a new integrated electronic system for customer acquisition (94% of respondents) (Fig. 3). It should be emphasized that transport and logistics companies notice the benefits of applying this type of systems, as this option was also marked by these companies that have not yet used electronic systems. Only 6% (2 companies) were reluctant to use the new, potential system,

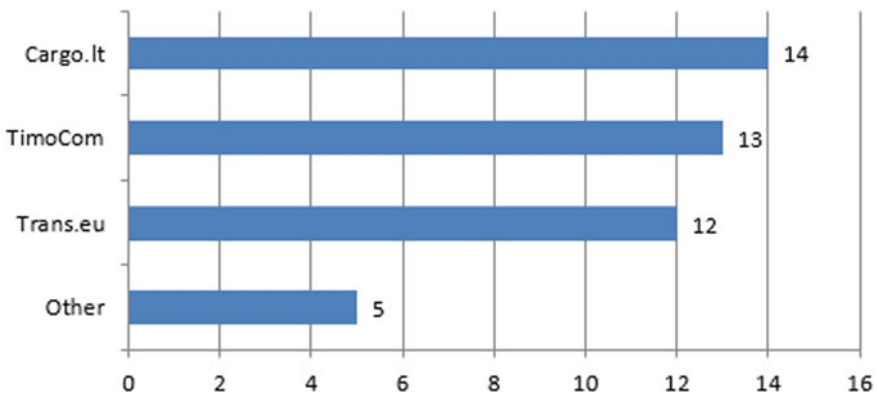
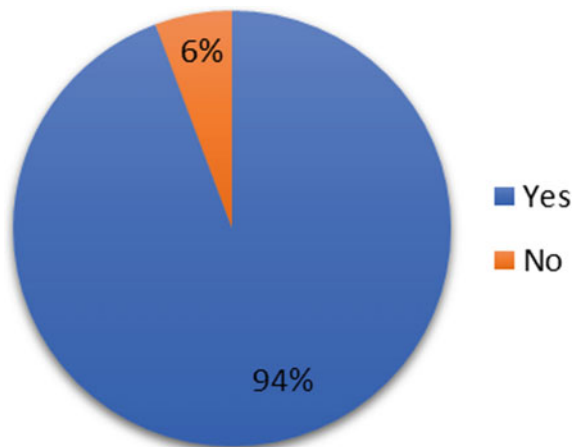


Fig. 2 Answers to the question “What electronic systems does your company apply to acquire customers?” (number of responses)

Fig. 3 Answers to the question “Would your company like to apply a new, integrated electronic system for acquisition of cargo freight customers?”



which may form a further proof of their plans to continue cooperation with their permanent customers.

The next question in the survey questionnaire concerned aspects that should be improved in the existing electronic systems (Fig. 4). The majority of respondents believe that these platforms should be free of charge (32 out of 35 responses), up-to-date, equipped with a user-friendly interface (31 responses) and that the platform should be also made available to the drivers of HGVs (26 responses). Other responses concerned aspects of the reliability of this type of systems, and the possibility of reliable and quick customer verification.

The last question in the survey concerned the person within the company, who was responsible for implementation of modern tools (systems, applications, software) (Fig. 5). In the majority of the surveyed companies this decision was reserved for the business owner (26 of 35 responses). The decision-makers also included persons in charge of transport management (5 responses). Other entities indicated by

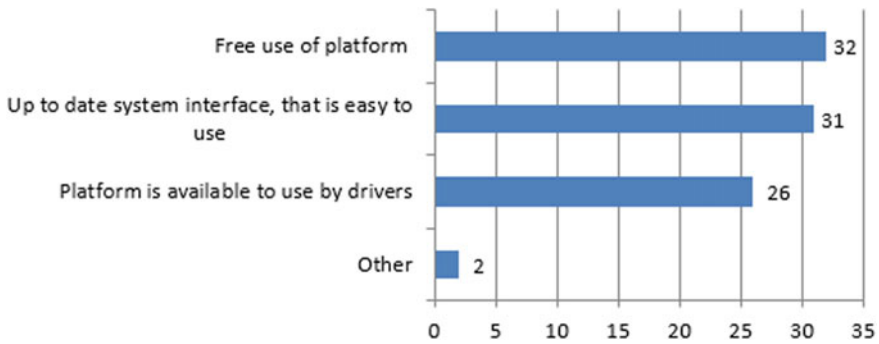


Fig. 4 Answers to the question “What can be improved in the existing electronic systems?” (number of responses)

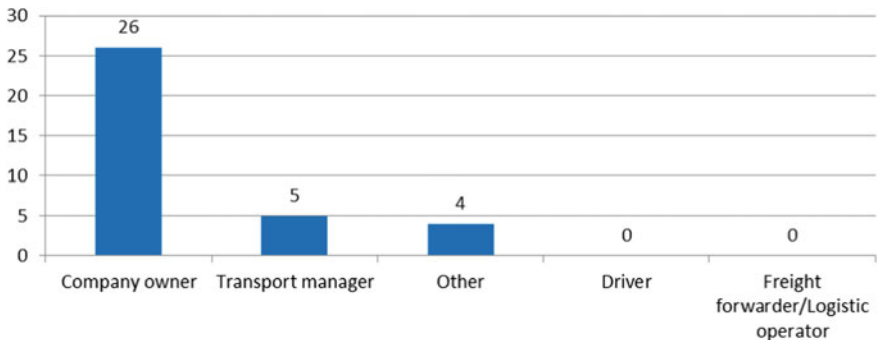


Fig. 5 Answers to the question “Who, in your company, is responsible for making the decisions to implement modern tools (systems, applications, software) to improve the organization of transport processes?” (number of responses)

the respondents, as responsible for reaching decisions in this regard, are the management board, project manager or IT technicians (4 of total number of responses). Other options (drivers, forwarders or logistic operators) were not indicated as having influence on this type of decisions in the company.

Conducted research results proved that transport and logistics companies are interested to use integrated electronic systems and see the possible advantages of its implementation.

## 6 Conclusions

The study of the impact of integrated electronic systems on the customer acquisition processes in transport and logistics companies demonstrated that freight exchanges significantly influence their operations. The companies notice the benefits of using the services of such systems, and express their will to cooperate with them. This demonstrates the significance of freight exchanges for the activities of transport and logistics companies, as well as sustainable development of transport.

The opinions of owners of TSL companies active in the Latvian market have been examined. These companies use mainly the Cargo.lt, TimoCom and Trans.eu systems. The main benefits the companies expect from using integrated electronic systems are primarily the acquisition of new customers, as well as savings (it is expected that the use of integrated electronic systems will be free of charge). These systems should also be reliable and include the access for drivers thereto. It should be stated that further extension of the functionality of these systems is also expected. Customers wish to have various options available in a single place, including the possibility for verification of contractor. Nevertheless, decisions regarding the application of these systems usually belong to the business owners.

It should be noted, however, that the conducted research only covered the Latvian market. Therefore, further research will be required in other countries, using similar systems, which will allow us to compare the achieved results. For the authors of the present publication it will constitute a direction for further research.

**Acknowledgements** The article was based on research carried out under the project entitled “RTF – Using ferry real time information to optimize intermodal transport chains in the Baltic Sea Region” performed within Interreg BSR program.

## References

1. Adamczewski, P.: Informatyczne wspomaganie łańcucha logistycznego. Wydawnictwo AE, Poznań (2001)
2. Bartczak, K., Barańska, A.: Wpływ giełd transportowych na funkcjonowanie przedsiębiorstw z branży logistycznej. *Logistyka* **1**, 163–172 (2016)



3. Blaik, P.: *Logistyka. Koncepcja integrowanego zarządzania*. PWE, Warszawa (2010)
4. Bohács, G., Frikker, I., Kovács, G.: Intermodal logistics processes supported by electronic freight and warehouse exchanges. *Transp. Telecommun.* **14**(3), 206–213 (2013)
5. Cargo.lt Homepage. <https://www.cargo.lt>. Last accessed 09 March 2020
6. Fuks, K., Kawa, A., Pierański, B.: Adaptation of social network analysis to electronic freight exchange. In: Barbucha D., Nguyen N., Batubara J. (eds.) *New Trends in Intelligent Information and Database Systems. Studies in Computational Intelligence*, vol. 598. Springer, Cham, pp. 151–159 (2015)
7. Gillis, T.: *Securing the Borderless Network: Security for the Web 2.0*. Word, 1st edn. Cisco Press (2011)
8. Kamiński, T.: *Wybrane zagadnienia Inteligentnych Systemów Transportowych*. Oficyna Wydawnicza Politechniki Warszawskiej, Warszawa (2019)
9. Kawa, A.: Elektroniczna giełda transportowa jako podmiot sektora usług logistycznych. *Prace Naukowe Uniwersytetu Ekonomicznego we Wrocławiu* **355**, 79–87 (2012)
10. Kępa, L., Tomasik, P., Dobrzyński, S.: *Bezpieczeństwo systemu e-commerce*. Helion, Gliwice (2012)
11. Koźlak, A.: Inteligentne systemy transportowe jako instrument poprawy efektywności transport. *Logistyka* **2** (2008)
12. Kurose, J., Ross, K.: *Sieci komputerowe. Ujęcie całościowe*. Helion, Gliwice (2018)
13. Lemmens, S., Decouttere, C., Vandaele, N., Bernuzzi, M.: A review of integrated supply chain network design models: Key issues for vaccine supply chains. *Chem. Eng. Res. Des.* **109**, 366–384 (2016)
14. Linn, Y.K., Yeh, C.T., Huang, C.F.: Reliability assessment of a multistate freight network for perishable merchandise with multiple suppliers and buyers. *Int. J. Syst. Sci.* **48**(1), 74–83 (2017)
15. Nath, T., Standing, C.: Drivers of information technology use in the supply chain. *J. Syst. Inf. Technol.* **12**(1), 70–84 (2010)
16. Romanow, P.: *Nowe technologie w branży logistyczno-spedycyjnej*. Wydawnictwo Ecorys, Warszawa (2013)
17. Santos, A.M.P., Salvador, R., Guedes, S.C.: A dynamic view of the socioeconomic significance of ports. *Maritime Econ. Logistics* **20**(2), 169–189 (2018)
18. Semenov, I.N., Filina-Dawidowicz, L.: Topology-based approach to the modernization of transport and logistics systems with hybrid architecture. Part 1. Proof-of-Concept study. *Archiv. Transp.* **43**(3), 105–124 (2017)
19. Sosnowski, J., Nowakowski, Ł.: *Elektroniczne giełdy transportowe*. Difin Warszawa (2015)
20. Sosnowski, J., Nowakowski, Ł.: *Systemy elektroniczne w transporcie drogowym*. Difin Warszawa (2018)
21. Starkowski, D., Grzybowska, K.: Zasady i warunki wykorzystania zintegrowanych narzędzi informatycznych przez przewoźników drogowych i spedycyjnych w obszarze wspomagających pracę spedytora w planowaniu operacji transportowej z wykorzystaniem giełdy transportowej Timocom Soft - Und Hardware GmbH. Część 1. *Autobusy: Technika, Eksploatacja, Systemy Transportowe* **17**(6), 1758–1765 (2016)
22. Transporeon Homepage. <https://www.transporeon.com/pl>. Last accessed 09 March 2020
23. Woźniak, W., Kielec, R., Siąsiadek, M., Wojnarowski, T.: A functional analysis of selected transport exchanges and tendering platforms in the transport orders market. In: *Proceedings of the 31st International Business Information Management Association Conference, IBIMA, Italy* (2018)
24. Wrong, Ch.W.Y., Kee-hung, Lai., Cheng, T.C.E.: Value of information integration to supply chain management: roles of internal and external contingencies. *J. Manage. Inf. Syst.* **28**(3), 161–200 (2011)
25. Wtransnet Homepage. <https://www.wtransnet.com>. Last accessed 09 March 2020
26. Zubkov, V., Sirina, N., Amelchenko, O.: Information technologies in the area of intersectoral transportation. In: Murgul V., Pasetti M. (eds.) *International Scientific Conference Energy Management of Municipal Facilities and Sustainable Energy Technologies EMMFT 2018. EMMFT-2018. Advances in Intelligent Systems and Computing*, vol. 982. Springer, Cham (2018)

# Mechanical Performance of Polylactic Acid from Sustainable Screw-Based 3D Printing



Paolo Minetola , Luca Fontana, Rossella Arrigo , Giulio Malucelli ,  
and Luca Iuliano 

**Abstract** Screw-extrusion-based 3D printing or fused granular fabrication (FGF) is a less widespread variant of filament-based 3D printing for polymers. An FGF printer can be fed directly from polymer granules for improved sustainability. Shorter manufacturing routes and the potential of using recycled pellets from waste plastics are key features of FGF in the circular economy framework. A modified version of a standard Prusa i3 plus printer, which was equipped with a Mahor screw extruder, is used to test the mechanical performance of polylactic acid (PLA) processed with different layer infill and printing speed. Rheological and thermal analyses are carried out to characterise the material. The energy consumption of the FGF printer was measured during the fabrication of Dumbbell specimens. Tensile test results are consistent with other investigations presented in the literature. A higher printing speed promotes FGF eco-efficiency without a detrimental effect on the material strength, whereas lower printing speed should be preferred for increased material stiffness.

---

P. Minetola (✉) · L. Fontana · L. Iuliano  
Department of Management and Production Engineering (DIGEP), Politecnico di Torino, Corso  
Duca degli Abruzzi 24, 10129 Turin, Italy  
e-mail: [paolo.minetola@polito.it](mailto:paolo.minetola@polito.it)

L. Fontana  
e-mail: [luca.fontana@polito.it](mailto:luca.fontana@polito.it)

L. Iuliano  
e-mail: [luca.iuliano@polito.it](mailto:luca.iuliano@polito.it)

R. Arrigo · G. Malucelli  
Department of Applied Science and Technology (DISAT), Politecnico di Torino, Corso Duca  
degli Abruzzi 24, 10129 Turin, Italy  
e-mail: [rossella.arrigo@polito.it](mailto:rossella.arrigo@polito.it)

G. Malucelli  
e-mail: [giulio.malucelli@polito.it](mailto:giulio.malucelli@polito.it)

P. Minetola · L. Iuliano  
Integrated Additive Manufacturing Centre (IAM@PoliTO), Politecnico di Torino, Corso Duca  
degli Abruzzi 24, 10129 Turin, Italy

## 1 Introduction

After the expiration of Stratasys key patent for fused deposition modelling (FDM) technology in 2009, a wide number of low-cost 3D printers for fused filament fabrication (FFF) has been developed and is available in the market. FDM and FFF processes are more popularly named as 3D printing, and the feedstock is a thermoplastic filament that is melted, extruded and deposited over the print bed layer wise [1].

Despite the wide diffusion and popularity of 3D printing that is favoured by a relatively low cost of materials and machine, the need to fabricate the semi-finished product of the polymeric filament introduces inefficiencies in the sustainability of 3D printed product life cycle. Rather than using polymeric pellets for manufacturing the filament, the granules can be directly used as feedstock for 3D printing. This alternative involves the elimination of the filament production step throughout the manufacturing route of 3D printed products and enables easier recycling of 3D printing scraps [2]. Therefore, the resources are exploited with more efficiency for the same goal of layered manufacturing. No energy is wasted in the filament fabrication step, and the raw thermoplastic does not undergo partial processing that can adversely affect material properties because of the thermal cycles and phase transformations.

Moreover, filament manufacturing requires narrow dimensional tolerances to avoid issues of bucking, slippage or blocking of the material in the feeding system of the 3D printer [3]. The filament is wound onto spools for storage purposes and the first portion of it is subjected to higher mechanical stress because of the smaller winding radius around the spool support. As a consequence, especially for less ductile polymers, the last part of the filament that is unwound from the spool breaks into fragile pieces and cannot be used for 3D printing.

Another disadvantage of conventional 3D printing is the limited range of thermoplastic polymers that are commercially available as filament feedstock. From the economic point of view, 3D printed filaments are sold at a price that is five to ten times higher than that of raw plastic.

To overcome the aforementioned shortcomings, the use of 3D printers with a modified extrusion head, which can be fed with thermoplastic granules like in traditional injection moulding, has been proposed in the literature. Pellet additive manufacturing (PAM), fused pellet manufacturing or modelling (FPM) and fused granular fabrication (FGF) are the names used to refer to the pellet-extrusion process for layered manufacturing. The advantages of FGF over FFF rely on the continuous automatic feed of the 3D printer with a broader range of thermoplastic granules that can be mixed in the extruder, reduced thermal degradation of the polymer during printing, and the opportunity to use plastic wastes within the circular economy perspective.

Among industrial AM systems, one of the few machines that can be fed with pellets is the Arburg freeformer. However, in the Arburg plastic freeforming (APF) process, the plasticating screw is used to prepare the molten material, whose droplet deposition in the layer is dosed through a piezoelectric nozzle [4].

Two types of FGF have been proposed and investigated in the literature. The first type employs a plunger-based system like a syringe. For example, Volpato et al. used a piston to extrude polypropylene (PP) granules that were molten in a heated reservoir [5]. Conversely, more researchers have developed or used a screw-based extrusion head for continuous feeding of the 3D printer.

Reddy et al. studied the influence of main FGF process parameters on the product strength and surface finish [6]. Valkenaers et al. designed a screw extrusion system and presented some results for polycaprolactone (PCL) with a 0.2 mm nozzle [7]. Tseng et al. designed and developed a temperature-controlled screw extruder for PEEK (polyether ether ketone) [8], while a similar system with the addition of an automatic feeder was proposed by Whyman et al. [9]. Woern et al. investigated the potential to use recycled particles for four thermoplastics [10]. Similar research was conducted by Reich et al. for waste polycarbonate (PC) [11].

To further extend the application of the FGF technology to large part manufacturing, Liu et al. proposed an extrusion system with two stages to increase the machine capacity. A traditional plasticating unit for polymer extrusion is used in the first stage to feed a dosing extruder for printing in the second stage [12]. Nieto et al. demonstrated the use of a screw extruder for printing large acrylonitrile butadiene styrene (ABS) and PLA parts that were assembled to build toilets for the naval industry [13]. With the aid of a multiphysics modelling software, Wang et al. designed a screw-based extrusion system to be mounted on an industrial robot [14].

Byard et al. demonstrated the economic and environmental sustainability deriving from the use of FGF for large-scale products using Fab Labs as recycling centres for 3D printing waste [15].

In this paper, a modified version of a low-cost 3D printer is used for screw extrusion printing of PLA. The material viscosity is evaluated together with the thermal and mechanical properties for different layer infill and printing speeds. Finally, the energy consumption of the 3D printing system is measured for eco-efficiency considerations.

## 2 Materials and Methods

A description of the test equipment and testing procedures is provided in this section. The rheological behaviour of the PLA material was evaluated before printing to get the reference value of the viscosity to assess the capacity of the screw extruder. Differential scanning calorimetry (DSC) was used to determine the percentage of crystallinity and the thermal transitions of the 3D printed material, including the glass transition temperature ( $T_g$ ), crystallization temperature ( $T_c$ ), and melting temperature ( $T_m$ ). Tensile tests were carried out to evaluate the mechanical behaviour of the PLA processed by FGF.

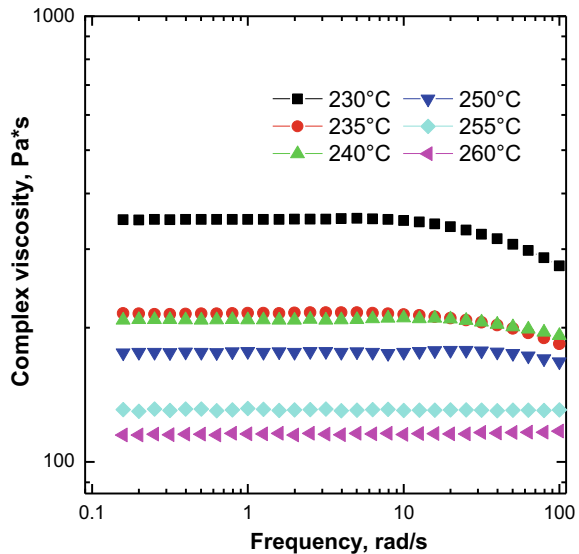
## 2.1 Viscosity of PLA Material

The pellets of natural PLA material were supplied by Mahor XYZ company, together with the pellet extruder. The granules, which are not perfectly spherical, have an average size of about 3.30 mm. The PLA pellets are sold at 8.80 €/kg, which is about half of the price of 1 kg spool of cheap coloured PLA.

The rheological behaviour of the Mahor PLA material was assessed with an ARES (TA Instrument, USA) strain-controlled rheometer in parallel plate geometry (plate diameter: 25 mm). Frequency scans were carried out from  $10^{-1}$  to  $10^2$  rad/s at different temperatures, under nitrogen atmosphere. The strain amplitude was selected for each sample in order to fall in the linear visco-elastic region. Prior to the measurements, PLA pellets were vacuum dried overnight at 70 °C.

Figure 1 reports the trend of complex viscosity as a function of frequency for the studied material at different temperatures. At the lowest tested temperature, PLA exhibit a Newtonian plateau in the low-frequency range, followed by a shear-thinning behaviour (characterised by a sharp decrease of the viscosity as a function of frequency) at higher frequency values. As expected, the Newtonian behaviour is progressively more pronounced as the temperature increases and covers the whole investigated frequency range at 260 °C. This behaviour can be attributed to the enhanced dynamics of PLA macromolecules at high temperature, with consequent anticipation of the macromolecular chain relaxation.

**Fig. 1** Viscosity curves for PLA material



## 2.2 DSC Analysis

DSC analyses were carried out using a QA1000 TA instrument apparatus (Waters Lc, USA). All the experiments were performed under dry nitrogen gas (20 mL/min) using samples of around 8 mg in sealed aluminium pans. The PLA material was tested with a heating ramp from 0 to 200 °C at 10 °C/min.

## 2.3 Tensile Tests

Tensile tests were carried out according to ASTM D638 guidelines (crosshead speed: 1 mm/min until 0.2% of deformation is reached and 10 mm/min up to sample break), using an Instron® 5966 dynamometer (Norwood, MA, USA). Dumbbell specimens of ASTM D638 type IV were 3D printed using different process parameters.

## 2.4 Screw-Based 3D Printer

A Prusa i3 Plus 3D printer was modified at Spazio Geco Fab Lab in Pavia (Italy) and equipped with a Mahor XYZ screw-based extruder for FGF technology and used for the production of the tensile samples of PLA material. Apart from the extrusion head, the power supply was replaced with a 400 W one to increase the heating capacity of the machine. The modified 3D printer can reach a maximum extrusion temperature of 290 °C and a maximum bed temperature of 90 °C. By this way, the potential of the Prusa printer was extended to process a wider range of polymers from pellets.

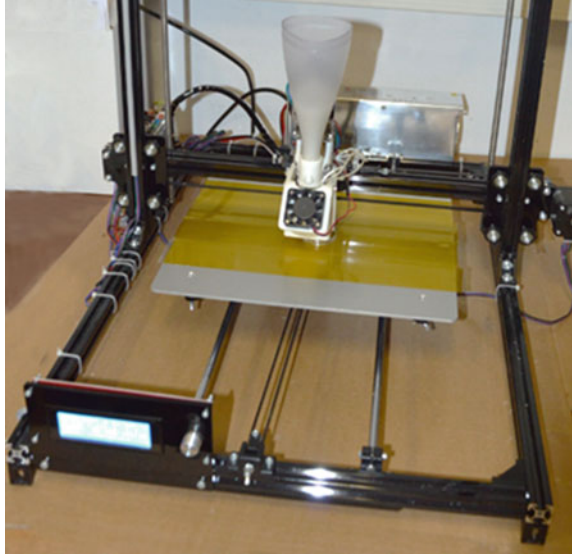
The hopper of the extruder is a self-replicated part as in other modified 3D printers [16], whereas the nozzle has a diameter of 0.8 mm. The cartesian structure and axis resolution of the original machine remains unchanged. Thus, the FGF printer (Fig. 2) has a positioning accuracy of 0.004 mm for the Z axis and 0.012 mm for X and Y axes over a working volume of 300 × 300 × 420 mm.

## 2.5 Slicing Software

Slic3r open software was used to slice the solid to layer (STL) model of the object and generate the standard ISO .gcode file with the print path of each layer. Within the software, the configuration of the machine was replicated from the standard Prusa i3.

Nevertheless, before printing the PLA tensile sample, a hollow test cube was printed to calibrate the machine configuration and the printing parameters as

**Fig. 2** Modified 3D printer with a Mahor extruder for FGF technology



suggested by Alexander et al. [2]. A Kapton ribbon tape (Fig. 2) was employed on the print bed to promote the adhesion of the first printing layer.

The test cube with an edge length of 20 mm and the thickness of 2 mm of the side walls was exploited for setting the optimal value of the parameter named extrusion multiplier in Slic3r software. The extrusion multiplier setting is particularly critical in the change of the type of extrusion head, since this parameter allows the fine tuning of the extrusion flow rate, which in the Mahor head is defined by the rotation speed of the coaxial screw.

Figure 3 shows the replicas of the test cubes printed for different values of the extrusion multiplier. With the fixed set of parameters of Table 1, the optimal value of the extrusion multiplier was 0.6. Lower values decrease the flow rate, and the mass of extruded and deposited material is insufficient. Conversely, for values of the extrusion multiplier setting higher than 0.6, the sidewalls of the test cube become too thick because an excess of PLA material is extruded (Fig. 3).

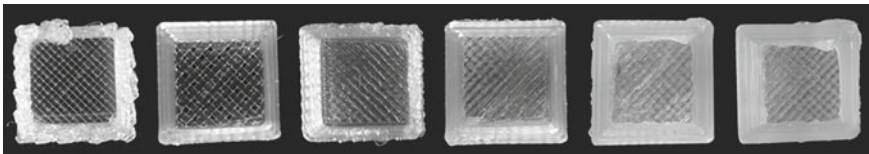
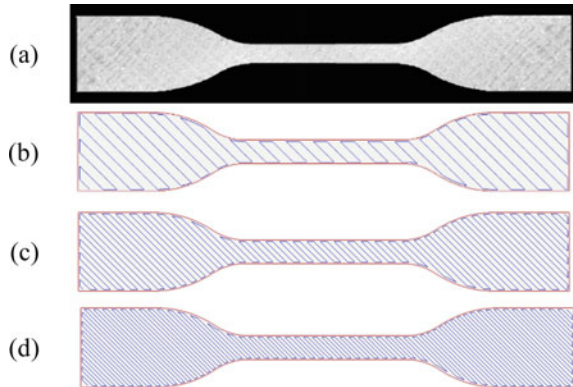


**Fig. 3** Test cubes printed for different values of the extrusion multiplier

**Table 1** Main parameters used in Slic3r software for printing

Parameter	Value	Parameter	Value
Layer height	0.3 mm	Fill pattern	Rectilinear
Extruder temperature	245 °C	Fill angle (referred to x axis)	-45°/+45°
First layer bed temperature	65 °C	Number of perimeters	1
Layer bed temperature	60 °C	Number of top solid layers	2
Extrusion multiplier	0.6	Number of bottom solid layers	2

**Fig. 4** Dumbbell specimen printed with 25% infill (a), print path for 25% infill (b), print path for 50% infill (c), print path for 75% infill (d)



### 3 Results

#### 3.1 Specimen Fabrication

A total of 18 Dumbbell specimens were fabricated with three levels of the infill of 25, 50 and 75% using the same parameters of the test cube (Table 1). The print path for the specimen in an intermediate layer is shown in Fig. 4. Three replicas were produced for each infill percentage, and each replica was 3D printed using two different speed sets for the extrusion head (Table 2).

#### 3.2 Specimen Characteristics

After 3D printing, the thickness of each specimen was measured with a centesimal micrometer, and the specimens were weighed using a Gibertini 1000HR-CM balance with a resolution of 0.01 g. The measures are reported in Table 3 along with the printing time and energy that was measured using a Meterk M34EU power meter plug.



**Table 2** Speeds of the extrusion head in the two printing sets

Parameter	High-speed printing set (mm/s)	Low-speed printing set (mm/s)
Perimeters	15	7.5
Infill (internal and top solid one)	15	7.5
Infill for solid and gaps	20	10
Bridges	30	15
Support material (skirt)	30	15
Speed for non-print moves	150	100
First layer speed	15	7.5

**Table 3** Measured characteristics of the tensile specimens

No.	Infill (%)	Print speed (mm/s)	Thickness (mm)	Weight (g)	Average thickness (mm)	Average weight (g)	Printing time (min)	Energy (kWh)
1	75	15	4.10	4.961	4.10	4.919	27	0.068
2	75	15	4.07	4.882				
3	75	15	4.12	4.915				
4	75	7.5	4.11	4.899	4.11	5.028	59	0.140
5	75	7.5	4.12	5.078				
6	75	7.5	4.11	5.107				
8	50	15	4.14	4.112	4.04	4.153	23	0.058
9	50	15	4.03	4.243				
12	50	15	3.95	4.105				
7	50	7.5	4.19	4.072	4.06	4.056	48	0.113
10	50	7.5	4.00	3.952				
11	50	7.5	4.00	4.143				
16	25	15	3.98	3.305	4.00	3.352	19	0.047
17	25	15	4.02	3.364				
18	25	15	4.01	3.388				
13	25	7.5	3.93	3.316	3.92	3.363	40	0.093
14	25	7.5	3.86	3.449				
15	25	7.5	3.98	3.325				

**Table 4** Results of the DSC analysis

	$T_g$ (°C)	$T_{cc}$ (°C)	$T_m$ (°C)	$\Delta H_{cc}$ (J/g)	$\Delta H_m$ (J/g)	$X_c$ (%)
Unprocessed PLA	62.9	112.4	177.8	27.1	30.8	3.9
PLA75%_15	63.9	101.7	178.4	34.9	57.5	24.3
PLA75%_7.5	64.2	100.7	178.0	37.9	58.3	21.9
PLA50%_15	65.0	104.2	179.7	37.4	51.0	14.6
PLA50%_7.5	64.9	102.7	179.3	38.3	52.5	15.3
PLA25%_15	64.6	106.7	178.9	31.9	47.0	16.2
PLA25%_7.5	64.6	104.3	179.2	36.7	50.2	14.5

### 3.3 Results of DSC Analysis

The main thermal properties collected during the second heating scan are reported in Table 4. All the produced samples show reduced  $T_{cc}$  values as compared to unprocessed PLA, indicating an enhanced crystallization ability of PLA macromolecules as a consequence of the 3D printing process.

The percentage of the crystalline phase is computed by Eq. 1.

$$X_c = \frac{\Delta H_m - \Delta H_{cc}}{\Delta H_m^0} \cdot 100 \quad (1)$$

where  $\Delta H_m^0 = 93$  J/g.

As far as the content of the crystalline phase is concerned, unprocessed PLA is almost amorphous, while the processed samples show higher crystallinity degrees, due to the orientation experienced by PLA chains during processing, which promotes the formation of crystalline structures.

### 3.4 Results of Tensile Testing

Table 5 collects the main mechanical properties, in terms of elastic module ( $E$ ), ultimate tensile strength (UTS) and elongation at break, of all investigated samples.

UTS and elongation at break are almost unaffected by the processing parameters, while higher elastic modulus values are observed for PLA samples processed with low printing speed.

**Table 5** Results of the tensile test: average values  $\pm$  standard deviation

Specimen	E (MPa)	UTS (MPa)	Elongation at break (%)
PLA75%_15	782.76 $\pm$ 135.04	23.03 $\pm$ 1.53	4.54 $\pm$ 0.48
PLA75%_7.5	1030.15 $\pm$ 199.41	24.81 $\pm$ 2.67	4.86 $\pm$ 0.30
PLA50%_15	773.07 $\pm$ 28.42	19.70 $\pm$ 1.64	4.62 $\pm$ 0.48
PLA50%_7.5	1079.26 $\pm$ 269.21	18.86 $\pm$ 1.71	4.22 $\pm$ 0.18
PLA25%_15	763.05 $\pm$ 208.44	19.03 $\pm$ 0.67	4.34 $\pm$ 0.36
PLA25%_7.5	1031.71 $\pm$ 174.16	19.64 $\pm$ 1.35	4.30 $\pm$ 0.52

## 4 Conclusions

In this paper, a screw extrusion FGF machine was used to test the performance of PLA material printed from pellet feedstock. The PLA granules were extruded at about 245 °C. Therefore, the Mahor extruder demonstrated good dosing capacity for a material viscosity of about 200 Pa·s (Fig. 1). This reference value, obtained by the rheological analysis of the PLA material, will be considered as a reference for future research activities involving the use of the same FGF printer with other thermoplastic pellets.

The results of the tensile tests for the printed PLA specimens, which were printed with different parameters, are consistent with previous results presented in the literature. When compared to the recent study of Wang et al. [17] for FFF printing, the higher layer thickness of the FGF specimens reduces the interlayer bonding strength.

The presence of air gaps increases as the infill percentage drops, so the higher UTS was obtained for the 75% infill with a beneficial effect of the higher crystallinity content, as evidenced by the DSC results. On the contrary, relevant differences in terms of UTS were not observed between the PLA specimens with 50% infill and those with 25% infill. The presence of two solid (100% infill) layers, on the top and bottom faces of the Dumbbell specimen for a total of 1.2 mm over the thickness of 4 mm, reduces the differences for lower percentages of the infill parameter.

Indications about an eco-efficient use of the modified FGF printer can be gathered by the comparison of the energy consumed for printing the different specimens to the actual strength obtained by tensile test results. As the value of UTS is not influenced by the printing speed, it is convenient to adopt higher printing speeds to complete the production in shorter times with related savings in terms of costs and energy. For every unit strength (MPa) of PLA material, about 0.01 MJ are consumed with the high-speed printing set of parameters, while around 0.02 MJ are necessary with the low-speed set. The highest eco-efficiency of 0.008 MJ/MPa is obtained in printing the specimen with 25% infill at 15 mm/s speed.

Further investigations are ongoing to identify the capacity of the modified screw-based 3D printer for processing other types of thermoplastics. Within the circular economy perspective, limitations of current screw design in printing recycled plastics should be investigated depending on the particle shape, size and distribution. The opportunity to create blends by mixing different polymers or additives directly in the GGF extruder will be taken into consideration as well.

## References

1. Calignano, F., et al.: Overview on additive manufacturing technologies. *Proc IEEE* **105**(4), 593–612 (2017). <https://doi.org/10.1109/JPROC.2016.2625098>
2. Alexandre, A., Cruz Sanchez, F.A., Boudaoud, H., Camargo, M., Pearce, J.M.: Mechanical properties of direct waste printing of polylactic acid with universal pellets extruder: comparison to fused filament fabrication on open-source desktop three-dimensional printers. *3D Print. Addit. Manuf.* (2020). <https://doi.org/10.1089/3dp.2019.0195>
3. Valkenaers, H., Vogeler, F., Voet, A., Kruth, J.-P.: Screw extrusion based 3D printing, a novel additive manufacturing technology. In: *International Conference on Competitive Manufacturing*, Stellenbosch, South Africa (2013)
4. Minetola, P., Calignano, F., Galati, M.: Comparing geometric tolerance capabilities of additive manufacturing systems for polymers. *Addit. Manuf.* **32**, 101103 (2020). <https://doi.org/10.1016/j.addma.2020.101103>
5. Volpato, N., Kretschek, D., Foggiatto, J., da Silva Cruz, C.G.: Experimental analysis of an extrusion system for additive manufacturing based on polymer pellets. *Int. J. Adv. Manuf. Technol.* **81**(9–12), 1519–1531 (2015). <https://doi.org/10.1007/s00170-015-7300-2>
6. Reddy, B., Reddy, N., Ghosh, A.: Fused deposition modelling using direct extrusion. *Virtual Phys. Protot.* **2**(1), 51–60 (2007). <https://doi.org/10.1080/17452750701336486>
7. Valkenaers, H., Vogeler, F., Ferraris, E., Voet, A., Kruth, J.-P.: A novel approach to additive manufacturing: screw extrusion 3D-printing. In: *Proceedings of the 10th International Conference on Multi-Material Micro Manufacture*, pp. 235–238 (2013)
8. Tseng, J.-W., Liu, C.-Y., Yen, Y.-K., Belkner, J., Bremicker, T., Liu, B.H., Sun, T.-J., Wang, A.-B.: Screw extrusion-based additive manufacturing of PEEK. *Mater. Des.* **140**, 209–221 (2018). <https://doi.org/10.1016/j.matdes.2017.11.032>
9. Whyman, S., Arif, K.M., Potgieter, J.: Design and development of an extrusion system for 3D printing biopolymer pellets. *Int. J. Adv. Manuf. Technol.* **96**(9–12), 3417–3428 (2018). <https://doi.org/10.1007/s00170-018-1843-y>
10. Woern, A.L., Byard, D.J., Oakley, R.B., Fiedler, M.J., Snabes, S.L., Pearce, J.M.: Fused particle fabrication 3-D printing: recycled materials' optimization and mechanical properties. *Materials* **11**(8), 1413 (2018). <https://doi.org/10.3390/ma11081413>
11. Reich, M.J., Woern, A.L., Tanikella, N.G., Pearce, J.M.: Mechanical properties and applications of recycled polycarbonate particle material extrusion-based additive manufacturing. *Materials* **12**(10), 1642 (2019). <https://doi.org/10.3390/ma12101642>
12. Liu, X., Chi, B., Jiao, Z., Tan, J., Liu, F., Yang, W.: A large-scale double-stage-screw 3D printer for fused deposition of plastic pellets. *J. Appl. Polym. Sci.* **134**(31), 45147 (2017). <https://doi.org/10.1002/app.45147>
13. Nieto, D.M., López, V.C., Molina, S.I.: Large-format polymeric pellet-based additive manufacturing for the naval industry. *Addit. Manuf.* **23**, 79–85 (2018). <https://doi.org/10.1016/j.addma.2018.07.012>
14. Wang, Z., Liu, R., Sparks, T., Liou, F.: Large-scale deposition system by an industrial robot (I): design of fused pellet modeling system and extrusion process analysis. *3D Print. Addit. Manuf.* **3**(1), 39–47 (2016). <https://doi.org/10.1089/3dp.2015.0029>

15. Byard, D.J., Woern, A.L., Oakley, R.B., Fiedler, M.J., Snabes, S.L., Pearce, J.M.: Green fab lab applications of large-area waste polymer-based additive manufacturing. *Addit. Manuf.* **27**, 515–525 (2019). <https://doi.org/10.1016/j.addma.2019.03.006>
16. Minetola, P., Galati, M.: A challenge for enhancing the dimensional accuracy of a low-cost 3D printer by means of self-replicated parts. *Addit. Manuf.* **22**, 256–264 (2018). <https://doi.org/10.1016/j.addma.2018.05.028>
17. Wang, S., Ma, Y., Deng, Z., Zhang, S., Cai, J.: Effects of fused deposition modeling process parameters on tensile, dynamic mechanical properties of 3D printed polylactic acid materials. *Polym. Test.* **86**, 106483 (2020). <https://doi.org/10.1016/j.polymertesting.2020.106483>

# Organization and Implementation of Intermodal Transport of Perishable Goods: Contemporary Problems of Forwarders



L. Filina-Dawidowicz  and S. Stankiewicz 

**Abstract** During performance of transport processes of perishable goods, forwarders may face different challenges and problems that could influence transportation efficiency. The objective of the article was to analyze the contemporary problems associated with the organization and implementation of perishable goods transportation involving intermodal transport technology. The case study of frozen goods transportation performed by freight forwarders operating in Poland was considered. The research was conducted using marketing research methods. The survey questionnaire was developed, and forwarders' opinions concerning the issues occurring during organization and implementation of transport process using road and maritime transport were analyzed. In the result of the conducted research, it was stated that transport of perishable goods is more challenging for forwarders than transport of other types of cargo. The most problematic is organization of transport within set time period. One of the biggest issues connected with implementation of maritime transport is securing of correct operation of the containers' refrigeration unit. Frequent traffic disturbances are seen to be main challenges for forwarders in road transport of goods. Results of the present research may be of interest for transport and forwarding companies that specialize in transport of perishable goods using intermodal transport technology, as well as their customers.

## 1 Introduction

Nowadays, the dynamic development of intermodal transport of perishable goods, including food and agricultural products, is observed [1, 2]. These cargo are transported in loading units (e.g., refrigerated containers) from their manufacturers to consumption locations over greater distances and require the securing of appropriate microclimate conditions in cargo space [3–5]. These conditions should be provided during the whole intermodal transport chain in order to keep the proper goods' quality [6, 7].

---

L. Filina-Dawidowicz (✉) · S. Stankiewicz  
West Pomeranian University of Technology, al. Piastów 41, 71-065 Szczecin, Poland  
e-mail: [ludmila.filina@zut.edu.pl](mailto:ludmila.filina@zut.edu.pl)

© The Editor(s) (if applicable) and The Author(s), under exclusive license to Springer Nature Singapore Pte Ltd. 2021  
S. G. Scholz et al. (eds.), *Sustainable Design and Manufacturing 2020*, Smart Innovation, Systems and Technologies 200, [https://doi.org/10.1007/978-981-15-8131-1\\_48](https://doi.org/10.1007/978-981-15-8131-1_48)

543

The increase in usage of intermodal transport for perishable goods is due to fact that it allows to assure fast cargo deliveries, increase the level of its safety, minimize costs, and improve operational activities (including handling operations) [1, 8, 9]. Its wide usage also influence the development of new concepts and technological solutions applied in intermodal freight transport, including transport of perishable goods, and affect taking action toward its sustainable development [1, 10, 11].

Cargo delivery using intermodal transport technology is usually arranged by forwarder or logistics operator who is in charge of organization and implementation of a number of necessary activities related to cargo movement. Even in case of well-planned and organized transport process, its implementation may bring about different undesirable events, which may affect additional costs, delays, and cargo quality losses. The potential occurrence of these events should be taken into account by forwarders already at the preparation stage of such kind of transport.

The objective of the article was to analyze contemporary problems faced by forwarders during organization and implementation of intermodal transport of perishable goods. Additionally, the research aimed to investigate the opinions of forwarders on their perception of potential issues concerning required activities. The case study of frozen goods transportation arranged by forwarders employed in companies located in Poland was considered. The survey questionnaire had been developed, and the opinions of forwarders regarding the issues of organization and implementation of transport process using road and maritime connections were analyzed and compared.

## **2 Activities Related to Intermodal Transport of Perishable Goods**

Intermodal transport of perishable goods is managed by forwarder or logistics operator, who is responsible for efficient and safe performance of cargo transport along the entire route from the consignor to the consignee. The transport process is dealing with a sequence of activities seen as a whole, aiming to deliver the cargo to the recipient. These activities can be divided into those occurring before cargo transportation (related to the planning and organizing of transport process), those occurring during the transportation (related to its implementation), and occurring after the transportation (related to transaction's finalization and settlement).

Proper planning and organizing of individual operations within the transport chain (Fig. 1) include i.a. selection of the transport route taking into account the locations of its dispatch and delivery, the provision of an appropriate loading unit and transport means, selection of cargo transshipment terminals for subsequent transport means, including the necessary reloading equipment and devices ensuring constant access to the electric power supply of container's refrigeration unit, signing haulage contracts with selected carriers, preparation and completion of documents accompanying the transport, etc. During that stage, forwarders assess the time of cargo delivery and costs

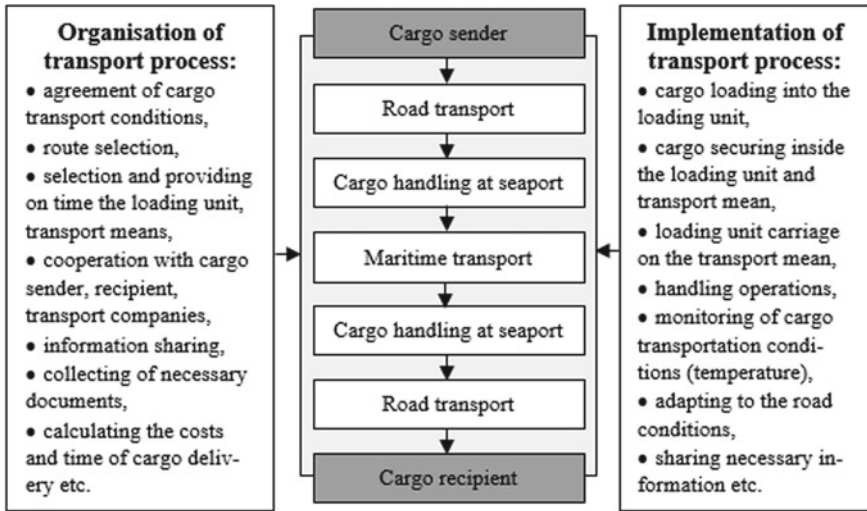


**Fig. 1** Selected activities taken during organizing and implementing of intermodal transport chain of perishable cargo

of transport process that allows to calculate the price proposal for the customer [8]. During organization of cargo transportation, forwarder faces the number of problems and challenges, one of which is organizing the process allowing to ensure a permanent connection of container’s refrigeration unit to power supply, which is needed to maintain the required conditions inside its cargo space [3].

The implementation of cargo transport process begins at the consignor’s warehouse, where immediately before loading the goods into the loading unit, a quantitative and qualitative inspection takes place, to confirm compliance of goods with the issued transport documentation. After completing the loading operations and approval of the documentation, the carrier receives the waybill. From this moment, both the carrier and the forwarder should be in constant contact with each other, as well as with other participants of the transport process, throughout the entire transport chain performed using different means of transport. Incorrect communication often leads to misunderstandings and delays in the execution of necessary actions. Therefore, it is important to assure efficient information flow between the parties, concerning i.a.: completed operations and goods inspections, customs clearances, current status of shipment, pickup and delivery dates, etc. Due to the specificity of perishable cargo, it should be transported quickly and delivered “just in time” according to the customers’ requirements [11] that may state the considerable challenge for the forwarder. The transport process ends with unloading the delivered goods at the consignee, issuing a receipt, verifying the goods, and settling the amounts due by the client to the forwarder, as well as by the forwarder to the carrier, who performed the transport.



On the basis of analyzed available subject literature, it can be stated that intermodal transport of perishable goods is constantly developing, striving to increase transport efficiency and reduce the risk associated therewith [12–14]. Actions taken to this end may have a positive impact on the development of international trade, including reducing the costs incurred by enterprises dealing with the organization and implementation of the transport of perishable goods [2, 4, 6]. Innovations in intermodal transport technologies, including intelligent solutions, are introduced to improve transport and logistics systems operation and enable sustainable transport development [1, 10, 15]. Despite these improvements, forwarders and logistics operators still face difficulties related to performance of transport processes.

Current literature pays attention to different problems occurred during perishable goods transportation. These problems deal i.a. with routing and fleet planning [16, 17], transport reliability [18], cargo quality degradation [3, 7], need to minimize transportation cost, and overtime to products delivery [8, 11]. Moreover, transport impact on the environment is analyzed [19], and the factors influencing sustainable intermodal freight transport systems are considered [9]. The attention is paid to operation of different nodes of intermodal transport chains, including intermodal terminals located in seaports and inland [20–23]. It should be noted that in available literature mainly, individual problems occurred during organization and implementation of intermodal transport are analyzed.

Wide number of literature positions discusses risk factors occurring during perishable cargo transportation, including food products, within logistics chains [12–14]. These analyses consider particular nodes functioning [3], as well as implication of different transport technologies during cargo transportation within the supply chains [24]. Cause–effect relationships in particular situations are analyzed that are mostly related to implementation of transport processes [12, 24].

Following conducted analysis of the available subject literature, it should be concluded that the contemporary problems faced by forwarders during organization and implementation of transport processes for perishable goods were analyzed to the small extent. Therefore, it is reasonable to analyze and compare forwarders' opinions on these issues.

### 3 Methodology

After conducting subject literature analysis and interviews with representatives of forwarders, the survey questionnaire was developed, and the survey among the representatives of forwarders was carried out. The questionnaire was divided into two parts. The first part contained general questions concerning the person completing the survey, while the second part—questions related to issues connected with transport of perishable goods. The survey was prepared in an electronic version in Polish and contained questions regarding difficulties and problems occurring during the organization and implementation of transport process of perishable goods—in particular frozen cargo.

The electronic survey was then sent, in January 2020, to 30 selected companies operating in Poland involved in organizing and monitoring intermodal transport of cargoes, including perishable goods. 23 people returned the completed survey questionnaires. Then, the achieved results were analyzed and compared, and the appropriate conclusions have been drawn.

## 4 Research Results

### 4.1 *Identification of Problems Related to Transport of Perishable Goods*

As a result of the research, the problematic areas have been identified that may occur during organization and implementation of intermodal transport of perishable goods. The developed set of issues was consulted with managers of transport companies and forwarders.

Among the problems occurring during the organization of the perishable goods transport, issues have been identified related to:

- ensuring conditions of cargo transportation,
- arrangement of transportation at the lowest possible cost,
- organization of reloading operations at the transshipment terminal,
- completion and correct filling of the required documentation accompanying the transport,
- organization (providing on time) of an appropriate transport means and person operating the vehicle (e.g., driver),
- organization (providing on time) of an appropriate loading unit,
- cooperation with the cargo sender or recipient,
- cooperation with the carrier,
- communication between participants of cargo transport,
- organization of transport within set time period,
- planning the transport route, etc.

In addition, the problems occurring at the stage of cargo transportation implementation have been considered, and issues that arise during maritime and road transportation of cargo were identified related to:

- the need to ensure continuity of the cargo cooling/freezing process,
- inadequate securing of cargo inside transport mean,
- infrastructure constraints (e.g., insufficient road quality and density, etc.),
- traffic disruption (e.g., congestion at the port entrance, road accidents, etc.),
- vehicles' malfunctions/failures,
- improper operation of container refrigeration unit,
- adverse weather conditions,

- incorrect information exchange (e.g., with the ship, driver, etc.).

The identified problems were assessed by representatives of forwarders employed in Polish transport companies organizing and implementing international transport of frozen cargo.

## 4.2 *Survey Results Analysis*

The respondents were first asked to reply to general questions concerning the respondent. Among 23 forwarders who completed the survey, there were 11 men (accounting for 48% of the sample), and 12 women (52% of respondents). The vast majority of respondents were forwarders aged 25–40, followed by people between 41 and 55 years old and then by those under 25 years. There were no representatives of the 55+ group completing the survey. The questionnaire was filled by forwarders, among whom a separate group of FCL forwarders was distinguished, constituting 39% of respondents, and those without specifying a specialization (61%). The largest group formed respondents with 5–15 years of professional experience (43% of respondents), followed by the group of respondents with less than 5 years of experience (39%) and 16–25 years of professional seniority (14%). Only one person with more than 25 years of experience completed the survey. The activities of enterprises employing persons who took part in the survey cover mainly Europe (96% of respondents indicated this option) and, to a lesser extent, Asia (35%). Other continents (e.g., Africa, North and South America, Australia, and New Zealand) also were mentioned among the areas of transport companies activity by 30% of respondents.

After answering the general questions, the respondents proceeded to the second part of the questionnaire concerning the issues that may arise during the organization and implementation of intermodal transport of perishable goods.

In order to determine the specifics of the companies represented by the respondents, they were asked about the share of serviced orders that involved handling perishable goods, in the company's overall turnover. In case of 70% of respondents, the share of perishable goods in the total number of orders handled by the company was below 25%, which proves that these enterprises also deal with other cargo types. 22% of interviewed forwarders indicated that their companies service 25–75% of perishable cargo, and only 8% of respondents worked in companies servicing more than 75% of orders related to perishable goods.

The respondents were asked to assess the level of difficulty related to the organization and implementation of frozen cargo transport, compared to other cargo types on a five-point Likert scale, where 1 meant no difficulties, and 5—considerable difficulties. The respondents rated the level of difficulty associated with the organization of the transport of perishable loads as medium (Fig. 2). 39% of forwarders rated this level at 2 points, and 35% of respondents at 3 points, which means that this type of cargo require special attention in organizing its transport. The mean score of these grades was 2.78 points and standard deviation—0.93.

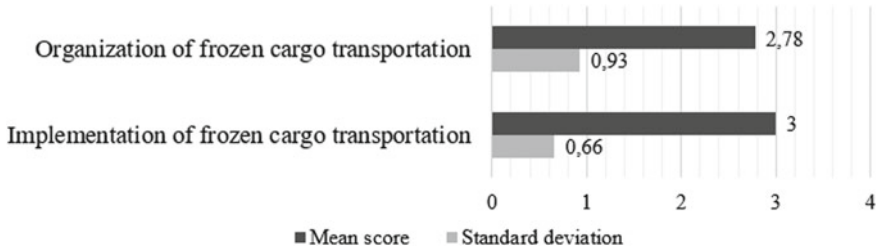


**Fig. 2** Mean scores and standard deviations of answers to the question: “How do you assess the level of difficulty associated with the organization and implementation of frozen goods transport, as compared to other types of cargo?”

Similarly, the difficulty associated with the implementation of perishable cargo transport was assessed as medium. The average rating was 3 and standard deviation—0.66 (57% of respondents rated it at 3 points). It should be noted that when assessing the difficulties associated with the organization of cargo transportation, the opinions of the respondents were more divided than it was in case of assessing the difficulties associated with the cargo transport itself. This may be due to the forwarders’ different level of experience and challenges faced during agreement of cargo transport details. The delivery of goods, including the occurrence of certain adverse events, frequently depends on the planning and organization of particular activities. Moreover, it should be highlighted that mean score of assessments put by FCL forwarders’ group was 3.56 points for transport process organization and 3.33 points for its implementation.

Respondents were also asked about the problems that may occur during the organization of frozen cargo transport, and rated selected issues on a scale of 1–5, where 1 meant that the issue was not significant, and 5—that it had significant impact (Fig. 3). The analysis covered 11 previously identified issues. The majority of respondents

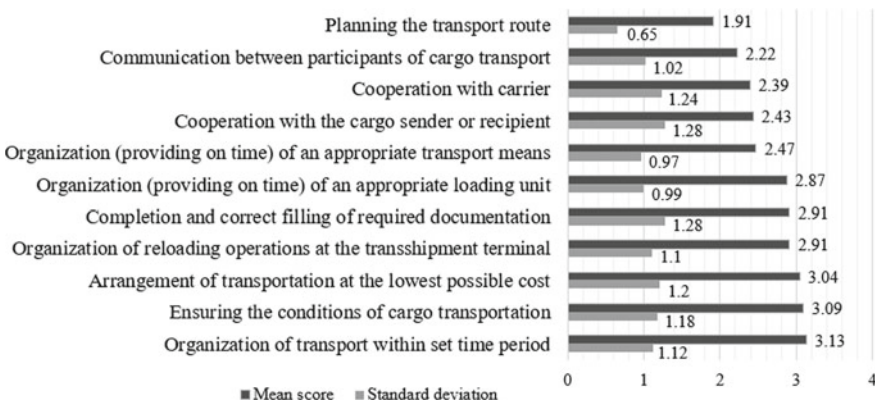


**Fig. 3** Mean scores and standard deviations of answers to the question: “What issues take place during organizing the transport of frozen cargo?”

assessed the problems at an average level (with mean scores between 1.91 and 3.13 points). The main problems faced by forwarders at the stage of the organization of perishable goods transport concern the arrangement of processes within the set time period, activities related to ensuring the conditions necessary for frozen cargo transportation, as well as organization of transport process at the lowest possible costs. The planning of transport route was indicated by respondents as the least problematic. It should be noted that FCL forwarders gave the higher ratings to the problems with completion of necessary documentation and problems with assurance on time the loading unit.

The next two questions concerned the problems occurring during intermodal transport of frozen cargo using road and maritime transport. The respondents were asked to rate the respective issues identified on five-point Likert scale, where 1 meant that the issue was not significant, and 5 that it had significant impact. Research covered eight identified issues.

Analyzing respondents' answers (Fig. 4), it could be stated that during road transport of frozen cargo, the most significant problems are caused by i.a.: traffic disturbances (e.g., congestion, road accidents, etc.), inadequate securing of cargo, malfunctions of vehicle, and container's refrigeration unit. Adverse weather conditions and erroneous exchange of information with the driver were listed as the least significant ones.

The same issues were assessed by respondents in regard to maritime transport implementation (Fig. 5). On the basis of the answers analysis, it could be stated that the biggest problems are associated with improper operation of the container's refrigerating unit and inadequate securing of cargo inside transport mean.

The problem of the least significance occurring in maritime transport of frozen cargo from the forwarder's viewpoint deals with infrastructure constraints (e.g., insufficient ports' infrastructure, etc.). FLC forwarders pointed out the same problems as the most and least important during implementation of goods delivery using road and maritime transport.

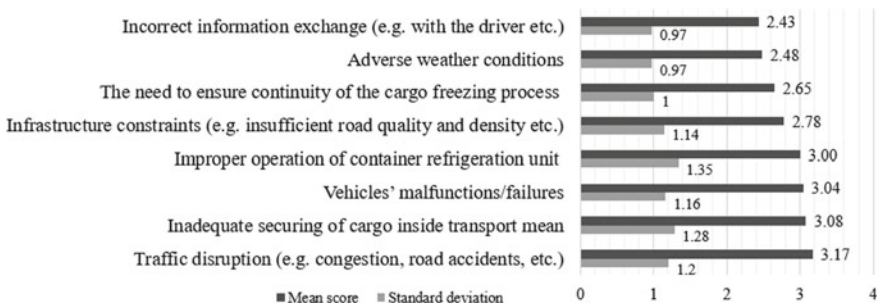


**Fig. 4** Mean scores and average deviations of answers to the question: “What issues take place during implementing the road transport of frozen cargo?”

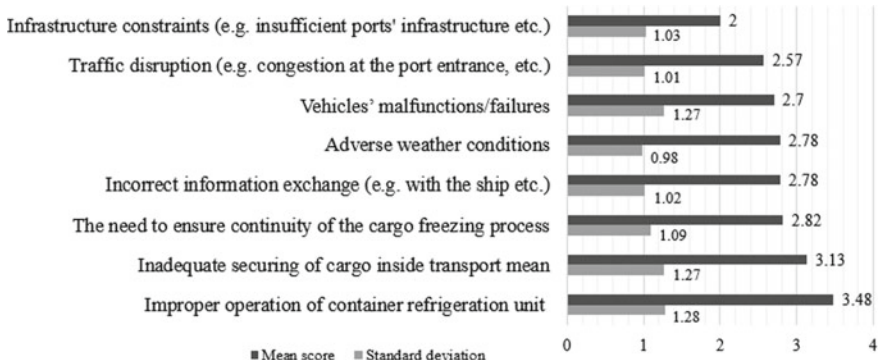


**Fig. 5** Mean scores and average deviations of answers to the question “What issues take place during implementing maritime transport of frozen cargo?”

## 5 Conclusions

The article presents the results of analysis of selected problems and difficulties faced by forwarders operating in Poland, associated with organization and implementation of intermodal transport of perishable goods.

Based on the conducted research results, it can be concluded that according to forwarders’ opinions, transport of perishable cargo requires more care than the transport of other cargo types. Forwarders’ consider that implementation of transport process is more demanding than its organization. When organizing frozen cargo transport, the significant challenges deal with arrangement of operations within set time period and ensuring conditions of cargo transport. Road transport is more dependent on the traffic situation (e.g., congestions, accidents on the road, etc.). In turn, during maritime transport performance, main issues deal with ensuring the proper operation of the container’ refrigeration unit throughout the entire sea voyage. Research results point out the problematic area of activities implemented by forwarders that influence efficient performance of transport process.

Further directions of our research will cover the analysis of risk factors influencing perishable cargo transport using intermodal transport technology, as well as quantitative and qualitative assessment of this risk. Presented research results may be interesting not only for forwarders and transport companies specializing in cargo transport, but also for their customers, allowing them to be aware of the problems faced by intermodal transport companies in their pursuit of performing the transport processes and sustainable transport development.

## References

1. Bontekoning, Y., Priemus, H.: Breakthrough innovations in intermodal freight transport. *Transp. Plann. Tech.* **27**, 335–345 (2004)
2. Menesatti, P., Pallottino, F., De Prisco, N., Ruggeri Laderchi, D.: Intermodal versus conventional logistic of refrigerated products: a case study from Southern to Northern Europe. *Agric. Eng. Int. CIGR J.* 81–88 (2014)
3. Filina, L., Filin, S.: An analysis of influence of lack of the electricity supply to reefer containers serviced at sea ports on storing conditions of cargoes contained in them. *Polish Marit. Res.* **4**, 96–102 (2008)
4. Pérez-Mesa, J.C., García-Barranco, M.C., Piedra-Muñoz, L., Galdeano-Gómez, E.: Transport as a limiting factor for the growth of Spanish agri-food exports. *Res. Transp. Econ.* **78**, 100756 (2019)
5. Łokietek, T., Jaszczak, S., Nikończuk, P.: Optimization of control system for modified configuration of a refrigeration unit. *Proc. Comput. Sci.* **159**, 2522–2532 (2019)
6. Rodrigue, J.-P.: *Reefers in North American Cold Chain Logistics: Evidence from Western Canadian Supply Chains*. University of Calgary, The Van Horne Institute (2014)
7. Rong, A., Akkerman, R., Grunow, M.: An optimization approach for managing fresh food quality throughout the supply chain. *Int. J. Prod. Econ.* **131**(1), 421–429 (2011)
8. Abbassi, A., Alaoui, A.E., Boukachour, J.: Modelling and solving a bi-objective intermodal transport problem of agricultural products. *Int. J. Ind. Eng. Comput.* **9**(4), 439–460 (2018)
9. Kumar, A., Anbanandam, R.: Analyzing interrelationships and prioritising the factors influencing sustainable intermodal freight transport system: as grey-DANP approach. *J. Clean. Prod.* **252**, 119769 (2020)
10. Jedermann, R., Nicometo, M., Uysal, I., Lang, W.: Reducing food losses by intelligent food logistics. *Philos. Trans. Royal Soc. A* **372**, 1–20 (2014)
11. Lukinskiy, V., Lukinskiy, V., Merkurjev, Y.: Modelling of transport operations in supply chains in obedience to “just-in-time” conception. *Transport* **33**(5), 1162–1172 (2018)
12. Convertino, M., Liang, S.: Probabilistic supply chain risk model for food safety. *Planet@Risk* **2**(3), 191–195 (2014)
13. Diabat, A., Govindan, K., Panicke, V.V.: Supply chain risk management and its mitigation in a food industry. *Int. J. Prod. Res.* **50**(11), 3039–3050 (2012)
14. Zimon, D., Madzfk, P.: Standardized management systems and risk management in the supply chain. *Int. J. Qual. Reliab. Manag.* **37**(2), 305–327 (2019)
15. Semenov, I.N., Filina-Dawidowicz, L.: Topology-based approach to the modernization of transport and logistics systems with hybrid architecture. Part I. Proof-of-concept study. *Arch. Transp.* **43**(3), 105–124 (2017)
16. Baykasoğlu, A., Subulan, K., Taşan, A.S., Dudaklı, N.: A review of fleet planning problems in single and multimodal transportation systems. *Transp. A: Transp. Sci.* **15**(2), 631–697 (2019)
17. Prasolenko, O., Burko, D., Tolmachov, I., Gyulyev, N., Galkin, A., Lobashov, O.: Creating safer routing for urban freight transportation. *Transp. Res. Proc.* **39**, 417–427 (2019)
18. Dullaert, W., Zamparini, L.: The impact of lead time reliability in freight transport: a logistics assessment of transport economics findings. *Transp. Res. Part E: Logist. Transp. Rev.* **49**(1), 190–200 (2013)
19. Ma, Q., Wang, W., Peng, Y., Song, X.: An optimization approach to the intermodal transportation network in fruit cold chain, considering cost, quality degradation and carbon dioxide footprint. *Polish Marit. Res.* **25**(1), 61–69 (2018)
20. Brzeziński, M., Pyza, D.: Designing of transshipment terminals for selected intermodal transport systems. *Adv. Intell. Syst. Comput.* **1032**, 52–62 (2020)
21. Fan, Y., Behdani, B., Bloemhof-Ruwaard, J., Zuidwijk, R.: Flow consolidation in hinterland container transport: an analysis for perishable and dry cargo. *Transp. Res. Part E: Logist. Transp. Rev.* **130**, 128–160 (2019)

22. Filina-Dawidowicz, L., Gajewska, T.: Customer satisfaction in the field of comprehensive service of refrigerated containers in seaports. *Period. Polytech. Transp. Eng.* **46**(3), 151–157 (2018)
23. Kostrzewski, M., Kostrzewski, A.: Analysis of operations upon entry into intermodal freight terminals. *Appl. Sci.* **9**(12), 2558 (2019)
24. Zelikov, V.A., Akopova, E.S., Pilivanova, E.K., Popova, L.K.: Model of management of the risk component of intermodal transport: information and communication technologies of transport logistics. *Adv. Intell. Syst. Comput.* **726**, 668–675 (2019)



# Analysis of Electric Power Consumption by the Heat Pump Used in the Spray Booth



Piotr Nikończuk  and Wojciech Tuchowski 

**Abstract** The paint shop is one of the most energy-consuming locations in the cars production process. The highest energy consumption in paint shops is related to heating the exchanged air. Currently, recuperators are used to recover waste heat in paint booths. The values of the temperature change coefficient in the recuperators are so low that the temperature of the air discharged into the atmosphere behind the recuperators is still positive. This happens even for negative outside air temperatures. There are solutions for installing heat pumps for spray booths used for heat recovery or dehumidification. The paper presents a quick method of assessment of electric power consumed by heat pump working in spray booth. The proposed method enables preliminary estimation of electric power consumption by the heat pump and further estimation of the energy efficiency of the entire spray booth. It is based on a simplified model containing an equation averaging the energy efficiency of air heat pumps.

## 1 Introduction

The paint shop is one of the most energy-consuming locations in the cars production process [1]. Energy consumption in the paint shop is related to painting equipment [2], compressed air preparation [3] and ventilation systems [4, 5]. The highest energy consumption in paint shops is related to heating the exchanged air. This also applies to paint shops of collision repair and vehicle renovation. Currently, recuperators are used to recover waste heat in paint booths. Usually that are cross- or rotary-recuperators. Cross-recuperators are not resistant to the formation of overspray deposits, and this problem is described in [6, 7]. The mathematical model of sediment formation in the cross-flow recuperator and the results of simulation are presented in [8], and also a model of the recuperator's reliability in the spray booth is also presented [9]. Dedicated solutions of the countercurrent recuperator [10] were also proposed. The temperature distribution analysis [11] and data from experiments from real object indicate that values of the temperature change coefficient in the recuperators are

---

P. Nikończuk (✉) · W. Tuchowski  
West Pomeranian University of Technology Szczecin, al. Piastow 17, 70-110 Szczecin, Poland  
e-mail: [piotr.nikonczuk@zut.edu.pl](mailto:piotr.nikonczuk@zut.edu.pl)

so low that the temperature of the air discharged into the atmosphere behind the recuperators is still positive. This happens even for negative outside air temperatures.

There are many unconventional applications of heat pumps, among others in district heating [12] or at petrol stations [13]. At positive air temperatures, high efficiency indexes of *coefficient of performance* (COP) are maintained by air heat pumps [14]. The use of heat pump enables the next step of acquiring waste heat from the air after the heat exchanger [15]. The recovered heat can be used to heat the air in the spray booth, accumulated, or transferred for other uses, e.g., space heating or hot water preparation. Accumulated heat can be used for later use in the work of a spray booth. In addition, the heat pump in the spray booth can be used to cool the air in hot summers and dehumidify the air, especially when the booth works in drying mode. The heat from cooling the air can be accumulated and/or used for other purposes.

There are solutions for installing heat pumps for spray booths used for heat recovery or dehumidification. However, these solutions do not combine both of these functions. In addition, they do not provide for heat accumulation, use of heat from other alternative heat sources, or heat transfer to other consumers. The heat pumps are not installed together with the recuperators. The solution presented below can be used both in spray booths with or without a recuperator.

Figure 1 presents a conceptual solution for using the heat pump in a spray booth. The heat pump is part of the heat exchange device. Individual modes of operation of the heat exchange device allow for recovery, accumulation, use of heat for other purposes, and obtaining heat from an alternative source of heat, e.g., solar.

List of markings in Figs. 2 and 3: 1—compressor, 2a—heat exchanger in the air supply duct, 2b—heat exchanger in the exhaust duct, 2c—heat exchanger in the exhaust duct after the recuperator, 3—air supply duct, 4—exhaust duct, 5—heat accumulator, 6a—lower heat exchanger in a heat accumulator, 6b—upper heat exchanger in a heat accumulator, 6c—heat exchanger in a heat accumulator for alternative heat sources, 8—alternative heat source, 9—heat exchanger transferring heat for other use, 10—recuperator, 11—ceiling air supply filter, 12—exhaust filter, 13—Pre-filter, 14—supply fan, 15—exhaust fan, 16—working chamber, 19—expansion valve, 20—space above the ceiling filter (plenum), 21—burner with heat exchanger, 22a—damper in the air supply duct, 22b—recirculation damper, 23—heat exchange device module.

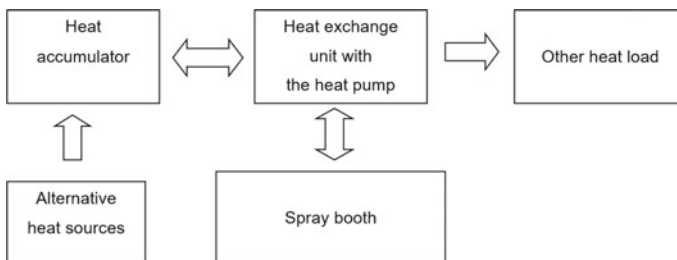


**Fig. 1** Conceptual solution for using a heat pump



In this concept, the heat exchangers may contain refrigerant or indirect heat carriers in the form of water or glycol. The best values of COP for heat pumps are obtained when the refrigerant is used directly in heat exchangers. However, due to the destructive effect of refrigerants on the atmosphere, for large installations, it is necessary to use indirect heat carriers for safety. The intermediate heat carrier transfers heat to the refrigerant in the evaporator, and the refrigerant releases heat to the intermediate carrier in the condenser. Intermediate carriers that release heat in the evaporator and receive heat in the condenser are in independent circuits.

The proposed solution allows to obtain the following functionalities:

- recovery of waste heat from the ejected air,
- heating fresh air,
- heat accumulation,
- cooling fresh air during the summer,
- air drying in recirculation during drying mode,
- use and accumulation of heat from other sources, e.g., solar panels,
- using the heat recovered from the cabin for other purposes, e.g., heating rooms or domestic hot water,
- heating fresh air with heat from the accumulator without using a heat pump while recovering waste heat from the exhaust air from the spray booth.

The above functionality allows for rational, associated waste management not only in the spray booth, but at the paint shop level. The recovered or accumulated heat can be used in the further operation of the spray booth or for other purposes, e.g., domestic hot water or space heating. Other heat demand may also be considered, but the expected medium temperature must be taken into account, and at higher COP, expected temperatures may change. This allows a significant reduction of energy consumption.

Figure 2 shows a painting booth equipped with a recuperator and a heat pump, working in painting mode. In order to recover heat from the removed air behind the recuperator, a heat exchanger 2c was placed in the launcher's duct. The heat exchanger 2b is located behind the exhaust filter in the floor, and its task is to cool and dehumidify the air in drying mode.

In the heat exchange device module 23 shown in Fig. 2, the heat pump and its equipment are included. Figure 3 presents a schematic of the refrigerant and intermediate heat transfer circuits during the selected operation mode of spray booth.

Due to the negative impact of refrigerants on the environment [16], indirect heat carriers were used, and the volume proportion of refrigerant was minimized. In the painting mode, the intermediate heat carrier receives heat from the removed air in the heat exchanger 2c, located in the exhaust duct after the cross-recuperator 10. Then, in the exchanger 18 acting as an evaporator, it transfers heat to the refrigerant. The compressed refrigerant in the heat exchanger 19 acting as a condenser transfers heat to the intermediate heat carrier. An indirect heat carrier heats the heated air in the exchanger 2b, located in the plenum of the spray booth.

The next part of the article focuses on the analysis of the energy efficiency and electric power consumption of heat pump used in refinishing spray booth.

There are models of changing the temperature and humidity in the paint booth [17], energy consumption [18], optimization of temperature control [19], and minimizing fuel consumption [20].

## 2 The Analysis of Electric Power Consumption

For heat pumps, manufacturers very often specify the COP coefficient. This factor is also called the energy efficiency factor. The efficiency factor describes the relationship of the supplied electric power  $P_{el}$  to the useful, heat power  $Q_N$  given by the heat pump

$$\text{COP} = \frac{\frac{dQ_N}{dt}}{P_{el}} \quad (1)$$

where:

COP      energy efficiency [-]  
 $dQ_N/dt$     total useful power [W],  
 $P_{el}$         consumed electric power [W]

The COP efficiency ratio depends on the temperature difference between the lower and upper heat sources. For modern heat pumps, a balance circuit applies at a constant temperature in the upper heat source  $T_k = 308$  [K] and a degree of circuit excellence equal to 0.5. The comparative cycle is described by the following equation:

$$\text{COP} = 0.5 * \frac{T_k}{T_k - T_0} \quad (2)$$

where:

$T_k$     temperature of upper heat source [K],  
 $T_0$     temperature of lower heat source [K],

assuming

$$\Delta T_k = T_k - T_0 \quad (3)$$

Energy efficiency indicator is equal:

$$\text{COP} = \frac{T_k}{\Delta T_k} \quad (4)$$

Actual COP energy efficiency indicators provided by air heat pump manufacturers differ from the comparative cycle. The values of these indicators vary for different heat pumps from different manufacturers. These differences result from the

use of different refrigerants, different construction elements of heat pumps and heat exchangers, etc. Based on the analysis of information provided by heat pump manufacturers, the average energy efficiency can be described by the following relationship [2]:

$$\text{COP} = 49.3 * \Delta T_k^{-0.777} \tag{5}$$

Figure 4 presents graphs of the COP dependence on the temperature difference according to Eq. (2) for the comparative circuit and Eq. (5) averaging the COP of real heat pumps [2].

Knowing the demand for useful heat output  $Q_N$  and the temperature difference  $\Delta T_k$ , the electrical power  $P_{el}$  consumed by the heat pump can be calculated:

$$P_{el} = \frac{\frac{dQ_N}{dt}}{\text{COP}} \tag{6}$$

Substituting COP relationship described by Eq. (5) into Eq. (6) is obtained

$$P_{el} = \frac{\frac{dQ_N}{dt}}{49.3 \Delta T_k^{-0.777}} \tag{7}$$

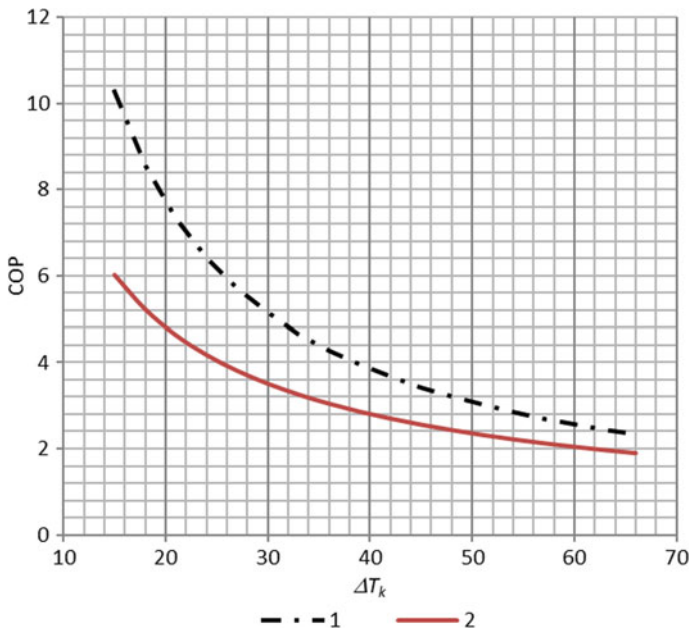


Fig. 4 COP indicators for heat pumps, 1—comparison index according to Eq. (2), 2—average COP values for real heat pumps according to Eq. (5)

It should be taken into account that the *COP* coefficient values provided by the manufacturers refer to the temperature difference  $\Delta T_k$  for the media on the evaporator and condenser. If other indirect heat carriers also take part in the heat pump operation, the calculation of the energy efficiency index should take into account the temperature changes at individual stages. When using an intermediate heat carrier in the lower source, a temperature difference  $\Delta T_k^d$  will appear between the temperature of the heat source  $T_0^z$  and the temperature on the evaporator  $T_0$ . Electric power can be calculated from the formula:

$$P_{el} = \frac{\frac{dQ_N}{dt}}{49.3(\Delta T_k + \Delta T_k^d)^{-0.777}} \quad (8)$$

### 3 Summary

The presented analysis concerns the electricity consumption of the heat pump in the spray booth. The proposed method enables preliminary estimation of electric power consumption by the heat pump and further estimation of the energy efficiency of the entire spray booth. It is based on a simplified model containing an equation averaging the energy efficiency of air heat pumps [21]. The COP of a heat pump depends on many parameters related to its structural elements and the refrigerant used [22]. However, this is only a small part of the topic of waste heat recovery in paint booths and its storage and management. Many works also show the effectiveness of heat recovery in recuperators and heat pumps. Therefore, each individual solution requires a separate approach and identification of real object dynamics, for example, using genetic algorithms [23]. Control systems also play an important role, as well as their proper selection based on well-identified object dynamics. Accurate knowledge of the heat pump's dynamics along with the entire spray booth installation makes it possible to improve the control quality of the entire spray booth. The currently used programmable controllers enable quick reconfiguration of the control algorithm [19] and reconfiguration of the heat pump [24].

### References

1. Giampieri, A., Ling-Chin, J., Ma, Z., Smallbone, A., Roskilly, A.P.: A review of the current automotive manufacturing practice from an energy perspective. *Appl. Energy* **261**, 1–29 (2020)
2. Zakrzewski, B., Złoczowska, E., Tuchowski, W.: Efektywność powietrznych pomp ciepła. *Chłodnictwo* **4**, 14–20 (2013)
3. Adamkiewicz, A., Nikończuk, P.: Waste heat recovery from the air preparation room in a paint shop. *Arch. Thermodyn.* **40**(3), 229–241 (2019). <https://doi.org/10.24425/ather.2019.130003>
4. Li, J., Uttarwar, R.G.: Huang Y (2013) CFD-based modeling and design for energy-efficient VOC emission reduction in surface coating systems. *Clean Tech. Environm. Policy* **15**(6), 1023–1032 (2013)

5. Ogonowski, Z.: Drying control system for spray booth with optimization of fuel consumption. *Appl. Energy* **88**(5), 1586–1595 (2011)
6. Nikończuk, P.: Preliminary modeling of overspray particles sedimentation at heat recovery unit in spray booth. *Maint. Reliab. (Eksploatacja i Niezawodność)* **20**(3), 387–393 (2018)
7. Nikończuk, P.: Study of heat recovery in spray booths. *Metal Finish.* **111**(6), 37–39 (2013)
8. McGinness, M.: A novel new approach to VOC and HAP emission control. In: Twenty-Second National Industrial Energy Technology Conference, Houston, TX, 5–6 April, 2000
9. Nikończuk, P.: Preliminary analysis of heat recovery efficiency decrease in paint spray booths. *Trans. Inst. Metal Finish.* **92**(5), 235–237 (2014). <https://doi.org/10.17531/ein.2020.2.9>
10. Nikończuk, P., Rosochacki, W.: The concept of reliability measure of recuperator in spray booth. *Maint. Reliab. (Eksploatacja i Niezawodność)* **22**(2), 265–271 (2020). <https://doi.org/10.17531/ein.2020.2.9>
11. Królikowski, T., Nikończuk, P.: Finding temperature distribution at heat recovery unit using genetic algorithms. *Proc. Comput. Sci.* **112**, 2382–2390 (2017)
12. Kurtz-Orecka, K., Tuchowski, W.: Combined heat pump-district heating network energy source. *E3S Web of Conferences* (2018)
13. Kurtz-Orecka, K., Tuchowski, W.: Energy efficiency of renewables to cover energy demands of petrol station buildings. In: Ball P., Huaccho Huatuco L., Howlett R., Setchi R. (eds) *Sustainable Design and Manufacturing. KES-SDM 2019. Smart Innovation, Systems and Technologies*, vol 155. Springer, Singapore (2019)
14. Rohdin, P., Johansson, M., Löfberg, J., Ottosson, M.: Energy Efficient Process Ventilation in Paint Shops in the Car Industry—Experiences and An Evaluation of a Fullscale Implementation at Saab Automobile in Sweden, Ventilation (2012). <http://hv.diva-portal.org/smash/get/diva2:565542/fulltext01.pdf>
15. Nikończuk, P., Zakrzewski, B.: Device for exchanging air with heat recovery, especially in spray booths. Patent EP2684613
16. Staffel, I.: A Review of Domestic Heat Pump Coefficient of Performance. [http://www.academia.edu/2300785/A\\_review\\_of\\_domestic\\_heat\\_pumps](http://www.academia.edu/2300785/A_review_of_domestic_heat_pumps)
17. Alt, S., Sawodny, O.: Model-based temperature and humidity control of paint booth HVAC systems. *IEEE International Conference on Mechatronics (ICM)*, pp. 160–165 (2015)
18. Feng, L., Meaers, L.: Analysis of HVAC energy in automotive paint shop. In: *ASME 2015 International Manufacturing Science and Engineering Conference, Materials; Biomanufacturing; Properties, Applications and Systems; Sustainable Manufacturing*, vol. 2. Charlotte, North Carolina, USA, June 8–12, 2015, MSEC2015-9281
19. Jaszczak, S., Nikończuk, P.: Synthesis of spray booth control software in programmable controller. *Przegląd Elektrotechniczny* **11**(1), 182–185 (2015). <https://doi.org/10.15199/48.2015.11.44>
20. Nikończuk, P., Zakrzewski, B.: The spray booth with heat recovery. Patent EP15461560
21. Tuchowski, W., Kurtz-Orecka, K.: The impact of refrigerants on the efficiency of automotive air-conditioning system. In: Ball, P., Huaccho Huatuco, L., Howlett, R., Setchi, R. (eds) *Sustainable Design and Manufacturing. KES-SDM 2019. Smart Innovation, Systems and Technologies*, vol 155. Springer, Singapore (2019)
22. Tuchowski, W., Kurtz-Orecka, K.: The influence of refrigerants used in air-conditioning systems in motor vehicles on the environment. In: Ball, P., Huaccho Huatuco, L., Howlett, R., Setchi, R. (eds) *Sustainable Design and Manufacturing 2019. KES-SDM. Smart Innovation, Systems and Technologies*, vol 155. Springer, Singapore (2019)
23. Jaszczak, S., Nikończuk, P.: Identification of the plant dynamic using genetic algorithms. In: *IEEE 21st International Conference on Methods and Models in Automation and Robotics—MMAR* (2016). <https://doi.org/10.1109/mmar.2016.7575189>
24. Łokietek, T., Jaszczak, S., Nikończuk, P.: Optimization of control system for modified configuration of a refrigeration unit. *Proc. Comput. Sci.* **159**, 2522–2532 (2019)



# Correction to: Using FFF and Topology Optimisation to Increase Crushing Strength in Equestrian Helmets



Shwe Soe, Michael Robinson, Khaled Giasin, Rhosslyn Adams,  
Tony Palkowski, and Peter Theobald

**Correction to:**  
**Chapter “Using FFF and Topology Optimisation to Increase Crushing Strength in Equestrian Helmets” in:**  
**S. G. Scholz et al. (eds.), *Sustainable Design and Manufacturing 2020*, Smart Innovation, Systems and Technologies 200,**  
[https://doi.org/10.1007/978-981-15-8131-1\\_33](https://doi.org/10.1007/978-981-15-8131-1_33)

In the original version of the book, the author name has been updated from “Khaled Gaisin” to “Khaled Giasin” in the Chapter “Using FFF and topology optimisation to increase crushing strength in equestrian helmets”. The chapter and book have been updated with the changes.

---

The updated version of this chapter can be found at  
[https://doi.org/10.1007/978-981-15-8131-1\\_33](https://doi.org/10.1007/978-981-15-8131-1_33)

© The Editor(s) (if applicable) and The Author(s), under exclusive license to Springer Nature Singapore Pte Ltd. 2021  
S. G. Scholz et al. (eds.), *Sustainable Design and Manufacturing 2020*, Smart Innovation, Systems and Technologies 200  
[https://doi.org/10.1007/978-981-15-8131-1\\_50](https://doi.org/10.1007/978-981-15-8131-1_50)

# Author Index

## A

Accorsi, Riccardo, 161  
Adams, Rhosslyn, 369  
Akkaladevi, Sharath Chandra, 261  
Aleksander, Bak, 93  
Amarasinghe, Ranjith, 107  
Andrzej, Blazejewski, 53, 93  
Antomarioni, Sara, 61  
Arrigo, Rossella, 531  
Artan, Deniz, 319

## B

Bakhtadze, Natalya, 439  
Baokun, Han, 107  
Barbari, Matteo, 357  
Bari Di, Giulia, 307  
Bevilacqua, Maurizio, 61  
Bickovs, D., 521  
Boeva, Veselka, 27  
Borgianni, Yuri, 1  
Bortolini, Marco, 161, 183, 193  
Botti, Lucia, 183

## C

Cernova-Bickova, A., 521  
Charles, Amal, 297  
Chen, Wei, 227  
Chen, Xiaobo, 13  
Chen, Yang, 41  
Cholewa, Mariusz, 71, 119  
Ciarapica, Filippo Emanuele, 61  
Conti, Leonardo, 357

## D

Dobrzyńska, Renata, 379, 415  
Dorner, Manuel, 149

## E

Elkaseer, Ahmed, 285, 297, 333  
El-Maddah, Islam, 333  
Ergen, Esin, 319  
Evans, I., 273

## F

Fauth, Janin, 307  
Fayne, Audrey, 205  
Feng, Qixiang, 173, 251  
Ferrari, Emilio, 183  
Filina-Dawidowicz, L., 521, 543  
Fleig, Claus, 149  
Fontana, Luca, 531  
Fu, Yelin, 403

## G

Gaberščik, Carla, 205  
Gaisin, Khaled, 369  
Galizia, Francesco Gabriele, 161, 183, 193  
Gamberi, Mauro, 193  
Gao, Jie, 227  
Grech, I. S., 425  
Griffiths, C. A., 239, 273  
Gualano, Francesco, 161, 193  
Gu, Dongdong, 227  
Gu, Heng, 395

## H

Hallstedt, Sophie I., 27

Han, Quanquan, 215, 251, 395  
 Helman, Joanna, 71, 119  
 Hofmann, Michael, 261  
 Huaccho Huatuco, Luisa, 41  
 Huang, George Q., 403  
 Huang, Xin, 451, 485, 509

**I**

Iuliano, Luca, 531

**J**

Jayasundara, Chathura, 107  
 Jerzy, Zuchniewicz, 53, 81, 93  
 Jiang, Zhigang, 463  
 Johnson, Rachel, 239, 273, 425  
 Jolly, Mark, 345  
 Junk, Stefan, 149

**K**

Kazimierz, Kamiński, 81  
 Kirby, M. J., 239  
 Krause-Juettler, Grit, 119  
 Kwok, Sze Yin, 27

**L**

Lavery, N. P., 425  
 Lee, Jacquetta, 13  
 Liu, Xinlai, 403  
 Liu, Xiong, 475, 509  
 Liu, Ying, 173  
 Li, Xiao, 475  
 Luo, Xiao-long, 451, 485, 509

**M**

Maccioni, Lorenzo, 1  
 Ma, Chenglong, 227  
 Malucelli, Giulio, 531  
 Marquardt, Clarissa, 307  
 Ma, Shuai, 173, 251  
 Minetola, Paolo, 531  
 Mitchell, Sinéad, 205  
 Mohamed, Hoda, 333  
 Molasy, Mateusz, 71, 119  
 Mora, Cristina, 183  
 Moshiri, Mandaná, 297  
 Możdrzeń, D., 521  
 Mudugamuwa, Amith, 107  
 Müller, Tobias, 285

**N**

Naldi, Ludovica Diletta, 193  
 Nikończuk, Piotr, 555

**O**

Oliani, Marcella, 161

**P**

Pagone, Emanuele, 345  
 Palkowski, Tony, 369  
 Papanikolaou, Michail, 345  
 Paweł, Znaczkó, 81  
 Pekok, Mulla, 215  
 Pichler, Andreas, 261  
 Piotr, Zmuda Trzebiatowski, 53, 93  
 Plasch, Matthias, 261

**R**

Rabsch, Dominik, 285  
 Raule, Nicola, 307  
 Rees, A., 239, 273  
 Remigiusz, Knitter, 53, 93  
 Robinson, Michael, 369, 395  
 Ronco, Johanna Lisa, 307  
 Rosienkiewicz, Maria, 71, 119  
 Rossi, Giuseppe, 357  
 Rotini, Federico, 357  
 Russo, Davide, 129, 139  
 Ryan, Michael, 215

**S**

Salem, Mahmoud, 297, 333  
 Salonitis, Konstantinos, 345  
 Saxena, Prateek, 345  
 Scholz, Steffen G., 285, 297, 307, 333  
 Setchi, Rossitza, 173, 215, 227, 251, 395  
 Soe, Shwe, 369, 395  
 Song, Jun, 173, 251  
 Song, Yingjie, 227  
 Spreafico, Christian, 129, 139  
 Spreafico, Matteo, 129  
 Stankiewicz, S., 543  
 Suleykin, Alexander, 439

**T**

Tang, Qian, 173, 251  
 Tekce, Isilay, 319  
 Theobald, Peter, 369  
 Togni, Marco, 357  
 Tomasz, Krolikowski, 53, 93

Tuchowski, Wojciech, [555](#)

**U**

Ubowska, Agnieszka, [415](#)

**W**

Wiktorowska-Jasik, A., [521](#)

Wint, N., [425](#)

Wögerer, Christian, [261](#)

Wu, Haoye, [403](#)

Wu, Wei, [403](#)

**X**

Xiao, Junsong, [497](#)

**Y**

Yan, Pengcheng, [451](#), [475](#), [497](#)

Yan, Wei, [463](#)

Yao, Xin, [463](#)

Youssef, Khaled, [333](#)

Yu, Shujun, [451](#), [475](#)

**Z**

Zhang, Hua, [463](#)

Zhang, Na, [451](#), [485](#), [509](#)

Zhao, Gang, [451](#), [475](#), [485](#), [497](#), [509](#)

Zhou, Qi, [475](#), [485](#)